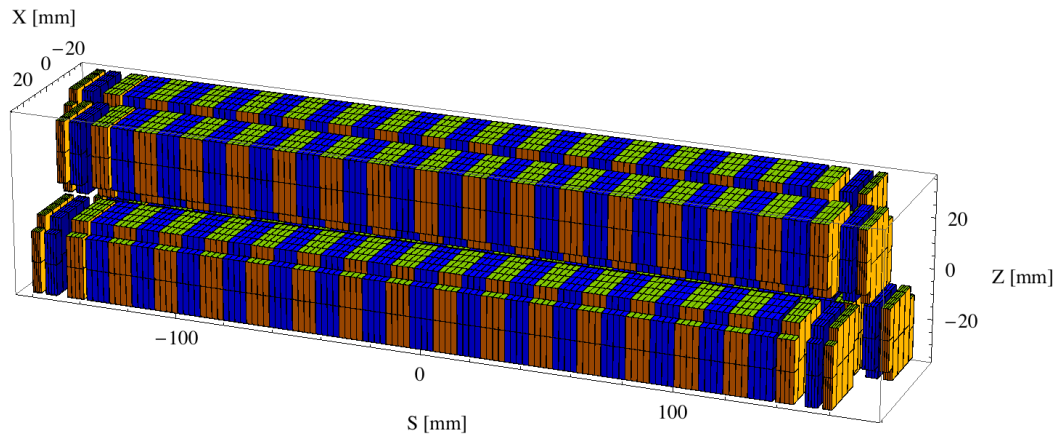


Elliptically Polarising Undulators with 11 mm Magnetic Gap at the MAX IV 3 GeV Ring

Erik Wallén*

9 Dec 2010



*Email: erik.wallén@maxlab.lu.se, Telephone +46 46 222 33 56, Address: E. Wallén, MAX-lab, Box 118, SE-22100 Lund, Sweden

Contents

1	Introduction	4
2	Undulator models	4
2.1	The elliptically polaraising undulator epu38gap11	5
2.1.1	Modes of operation in the elliptically polaraising undulator epu38gap11 . .	5
2.1.2	Magnet model of the elliptically polaraising undulator epu38gap11Plan . .	6
2.1.3	Analysis of the magnetic field of the epu38gap11Plan ID	6
2.1.4	Synchrotron radiation from the epu38gap11Plan ID	6
2.1.5	Magnet model of the elliptically polaraising undulator epu38gap11Heli . .	18
2.1.6	Analysis of the magnetic field of the epu38gap11Heli ID	18
2.1.7	Synchrotron radiation from the epu38gap11Heli ID	22
2.1.8	Magnet model of the elliptically polaraising undulator epu38gap11Incl . .	30
2.1.9	Analysis of the magnetic field of the epu38gap11Incl ID	30
2.1.10	Synchrotron radiation from the epu38gap11Incl ID	31
2.1.11	Magnet model of the elliptically polaraising undulator epu38gap11Vert . .	43
2.1.12	Analysis of the magnetic field of the epu38gap11Vert ID	43
2.1.13	Synchrotron radiation from the epu38gap11Vert ID	45
2.2	The elliptically polaraising undulator epu43p6gap11	56
2.2.1	Modes of operation in the elliptically polaraising undulator epu43p6gap11	56
2.2.2	Magnet model of the elliptically polaraising undulator epu43p6gap11Plan	57
2.2.3	Analysis of the magnetic field of the epu43p6gap11Plan ID	57
2.2.4	Synchrotron radiation from the epu43p6gap11Plan ID	57
2.2.5	Magnet model of the elliptically polaraising undulator epu43p6gap11Heli	69
2.2.6	Analysis of the magnetic field of the epu43p6gap11Heli ID	69
2.2.7	Synchrotron radiation from the epu43p6gap11Heli ID	73
2.2.8	Magnet model of the elliptically polaraising undulator epu43p6gap11Incl .	81
2.2.9	Analysis of the magnetic field of the epu43p6gap11Incl ID	81
2.2.10	Synchrotron radiation from the epu43p6gap11Incl ID	82
2.2.11	Magnet model of the elliptically polaraising undulator epu43p6gap11Vert	94
2.2.12	Analysis of the magnetic field of the epu43p6gap11Vert ID	94
2.2.13	Synchrotron radiation from the epu43p6gap11Vert ID	96
2.3	The elliptically polaraising undulator epu48gap11	107
2.3.1	Modes of operation in the elliptically polaraising undulator epu48gap11 .	107
2.3.2	Magnet model of the elliptically polaraising undulator epu48gap11Plan .	108
2.3.3	Analysis of the magnetic field of the epu48gap11Plan ID	108
2.3.4	Synchrotron radiation from the epu48gap11Plan ID	108
2.3.5	Magnet model of the elliptically polaraising undulator epu48gap11Heli . .	120
2.3.6	Analysis of the magnetic field of the epu48gap11Heli ID	120
2.3.7	Synchrotron radiation from the epu48gap11Heli ID	124
2.3.8	Magnet model of the elliptically polaraising undulator epu48gap11Incl . .	132
2.3.9	Analysis of the magnetic field of the epu48gap11Incl ID	132
2.3.10	Synchrotron radiation from the epu48gap11Incl ID	133
2.3.11	Magnet model of the elliptically polaraising undulator epu48gap11Vert . .	145
2.3.12	Analysis of the magnetic field of the epu48gap11Vert ID	145
2.3.13	Synchrotron radiation from the epu48gap11Vert ID	147
2.4	The elliptically polaraising undulator epu53gap11	158
2.4.1	Modes of operation in the elliptically polaraising undulator epu53gap11 .	158
2.4.2	Magnet model of the elliptically polaraising undulator epu53gap11Plan .	159
2.4.3	Analysis of the magnetic field of the epu53gap11Plan ID	159
2.4.4	Synchrotron radiation from the epu53gap11Plan ID	159

2.4.5	Magnet model of the elliptically polaraising undulator epu53gap11Heli . .	171
2.4.6	Analysis of the magnetic field of the epu53gap11Heli ID	171
2.4.7	Synchrotron radiation from the epu53gap11Heli ID	175
2.4.8	Magnet model of the elliptically polaraising undulator epu53gap11Incl . .	183
2.4.9	Analysis of the magnetic field of the epu53gap11Incl ID	183
2.4.10	Synchrotron radiation from the epu53gap11Incl ID	184
2.4.11	Magnet model of the elliptically polaraising undulator epu53gap11Vert . .	196
2.4.12	Analysis of the magnetic field of the epu53gap11Vert ID	196
2.4.13	Synchrotron radiation from the epu53gap11Vert ID	198
2.5	The elliptically polaraising undulator epu53p6gap11	209
2.5.1	Modes of operation in the elliptically polaraising undulator epu53p6gap11	209
2.5.2	Magnet model of the elliptically polaraising undulator epu53p6gap11Plan	210
2.5.3	Analysis of the magnetic field of the epu53p6gap11Plan ID	210
2.5.4	Synchrotron radiation from the epu53p6gap11Plan ID	210
2.5.5	Magnet model of the elliptically polaraising undulator epu53p6gap11Heli	222
2.5.6	Analysis of the magnetic field of the epu53p6gap11Heli ID	222
2.5.7	Synchrotron radiation from the epu53p6gap11Heli ID	226
2.5.8	Magnet model of the elliptically polaraising undulator epu53p6gap11Incl .	234
2.5.9	Analysis of the magnetic field of the epu53p6gap11Incl ID	234
2.5.10	Synchrotron radiation from the epu53p6gap11Incl ID	235
2.5.11	Magnet model of the elliptically polaraising undulator epu53p6gap11Vert	247
2.5.12	Analysis of the magnetic field of the epu53p6gap11Vert ID	247
2.5.13	Synchrotron radiation from the epu53p6gap11Vert ID	249
2.6	The elliptically polaraising undulator epu58gap11	260
2.6.1	Modes of operation in the elliptically polaraising undulator epu58gap11 .	260
2.6.2	Magnet model of the elliptically polaraising undulator epu58gap11Plan .	261
2.6.3	Analysis of the magnetic field of the epu58gap11Plan ID	261
2.6.4	Synchrotron radiation from the epu58gap11Plan ID	261
2.6.5	Magnet model of the elliptically polaraising undulator epu58gap11Heli . .	273
2.6.6	Analysis of the magnetic field of the epu58gap11Heli ID	273
2.6.7	Synchrotron radiation from the epu58gap11Heli ID	277
2.6.8	Magnet model of the elliptically polaraising undulator epu58gap11Incl . .	285
2.6.9	Analysis of the magnetic field of the epu58gap11Incl ID	285
2.6.10	Synchrotron radiation from the epu58gap11Incl ID	289
2.6.11	Magnet model of the elliptically polaraising undulator epu58gap11Vert . .	297
2.6.12	Analysis of the magnetic field of the epu58gap11Vert ID	297
2.6.13	Synchrotron radiation from the epu58gap11Vert ID	299
List of Tables		312
List of Figures		329

Table 1: Beam parameters in the middle of the straight sections of the MAX IV 3 GeV Ring [1]

Beam Energy	3.0	GeV
Beam Current	500	mA
Energy Spread (rms)	0.0010	
Horizontal Beta Function	9.00	m
Horizontal Emittance	0.263	nmrad
Vertical Beta Function	4.80	m
Vertical Emittance	0.008	nmrad
σ_h rms horizontal beam size	48.65	μm
$\sigma_{h'}$ rms horizontal beam divergence	5.406	μrad
σ_v rms vertical beam size	6.197	μm
$\sigma_{v'}$ rms vertical beam divergence	1.291	μrad

1 Introduction

This report describes elliptically polarising undulators with a magnetic gap of 11 mm that may be installed on the MAX IV 3 GeV ring [1].

The modelling assumes that there is a straight section length of 4 m available for the insertion devices.

The modelling also assumes that the minimum magnetic gap of the elliptically polarising undulators is 11 mm, which is larger than the assumed 9 mm magnetic gap in the two earlier reports about insertion devices for the MAX IV 3 GeV ring. The publication dates for the two earlier reports are 22 Sep 2009 and 15 Feb 2010 and the reports can be found at [2]. The two earlier reports contains detailed explanations of synchrotron radiation calculations and also accelerator physics calculations of e.g. tune shifts.

The elliptically polarising undulators described in this report will induce strong dynamic multipoles for the stored beam. The dynamic multipoles have to be compensated for in order to obtain a long lifetime and high injection efficiency. The compensation for the dynamic multipoles will be done with current strips between the magnet blocks of the elliptically polarising undulators and the accelerator vacuum chamber. The current strips are assumed to require 1.4 mm of vertical aperture. The vertical dimension of the straight section vacuum chamber is hence assumed to be 9 mm, which also gives a 0.6 mm clearance between the magnets of the elliptically polarising undulators and the vacuum chamber with current strips.

The beam parameters in the middle of the straight sections the 3 GeV MAX-IV storage ring are given in Table 1 [1].

2 Undulator models

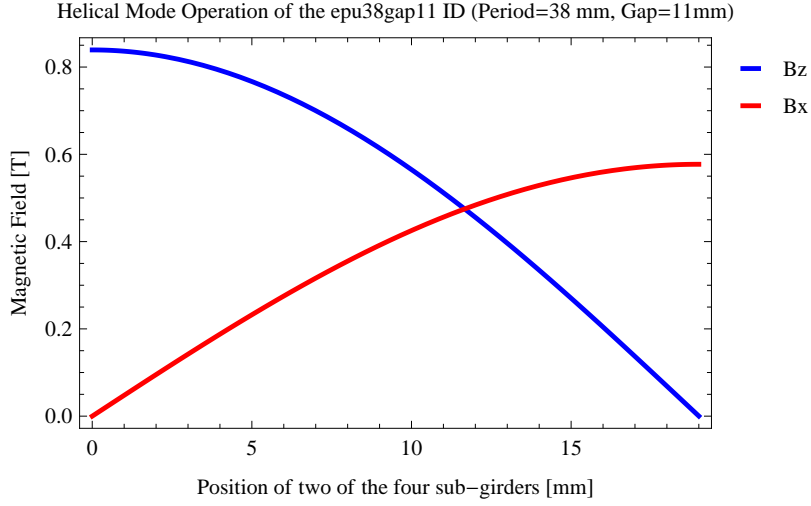


Figure 1: Vertical and horizontal magnetic field for the the epu38gap11 ID when operating in the helical mode for different positions for two of the four sub-girders

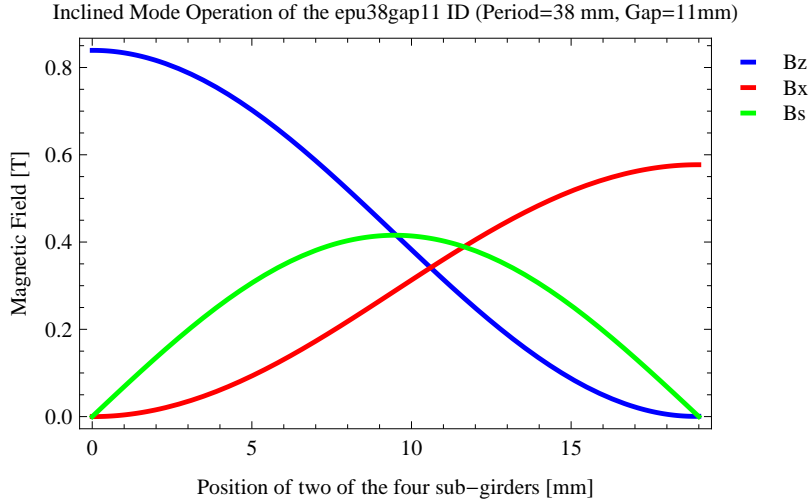


Figure 2: Vertical, horizontal, and longitudinal magnetic field for the the epu38gap11 ID when operating in the inclined mode for different positions for two of the four sub-girders

2.1 The elliptically polarising undulator epu38gap11

2.1.1 Modes of operation in the elliptically polarising undulator epu38gap11

Horizontal polarisation of the emitted synchrotron radiation from the epu38gap11 ID (Period=38 mm, Gap=11mm) is found in the planar mode when there is no movement of the sub-girders.

Circular polarisation is found in the elliptical mode of operation for a symmetric sub-grider movement of 11.666 mm. Figure 1 shows the vertical and horizontal magnetic field for the epu38gap11 ID when operating in the helical mode.

45 degree polarisation is found in the inclined mode of operation for an assymetric sub-grider movement of 10.6 mm. Figure 2 shows the vertical and horizontal magnetic field for the epu38gap11 ID when operating in the inclined mode.

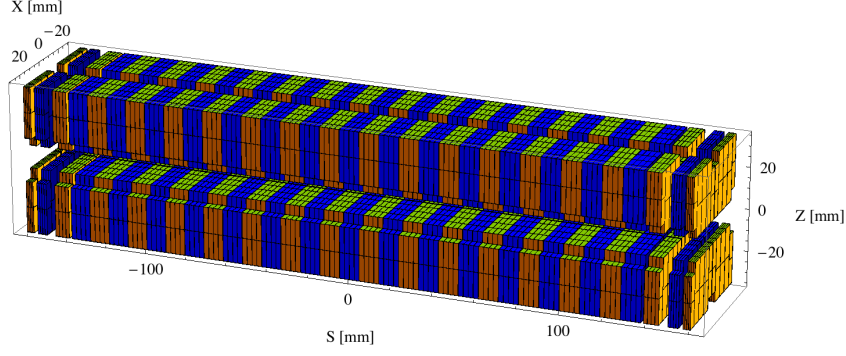


Figure 3: Magnetic model of the epu38gap11Plan ID. The ID has been modelled with Radia [3]

The following sub-sections will cover four different situations: The epu38gap11 operating in the planar mode for horizontal polarisation (epu38gap11Plan); The epu38gap11 operating in the helical mode for circular polarisation (epu38gap11Heli), the epu38gap11 operating in the inclined mode for 45 degree polarisation (epu38gap11Incl); and The epu38gap11 operating in the vertical mode for vertical polarisation (epu38gap11Vert).

2.1.2 Magnet model of the elliptically polarising undulator epu38gap11Plan

The Radia [3] magnet model of the epu38gap11Plan ID is shown in Figure 3. The length of the magnet model is 320.976 mm. The magnetic material in the model is NdFeb with a remanence of 1.28 T, a material similar to VACODYM 776 TP from Vacuumschmelze. Blocks with vertical magnetisation are blue and blocks with horizontal magnetisation are yellow. The block size is $30 \times 30 \times 9.5 \text{ mm}^3$ and there is a 5. mm cut-out in two of the corners of the blocks. The total length of the epu38gap11Plan ID is 3930.98 mm.

2.1.3 Analysis of the magnetic field of the epu38gap11Plan ID

The effective magnetic fields on axis and the fundamental photon energy of the epu38gap11Plan ID are shown in Table 2. The higher harmonic contents in the magnetic field of an elliptically polarising undulator made of permanent magnets is negligible and the effective field has about the same strength as the peak field.

2.1.4 Synchrotron radiation from the epu38gap11Plan ID

The power map of the emitted synchrotron radiation by the epu38gap11Plan ID, assuming a 0.5 A filament beam with an energy of 3 GeV and undulator properties of the synchrotron radiation, is shown in Figure 7. The on-axis power density is 37.256 kW/mrad^2

A map of the degree of linear polarisation of the fundamental harmonic of the synchrotron radiation emitted by the epu38gap11Plan ID over the angle of observation is shown in Figure 8.

A map of the degree of 45 degree polarisation of the fundamental harmonic of the synchrotron radiation emitted by the epu38gap11Plan ID over the angle of observation is shown in Figure 9.

Table 2: Effective Fields on axis and Fundamental Photon Energy of the epu38gap11Plan ID

Undulator Period	38	mm
Undulator Gap	11	mm
Undulator Mode	Planar	
Undulator Phase	0.000	mm
Vertical Peak Field	0.833	T
Effective Vertical Field	0.839	T
Kx (from vert. field)	2.978	
Horizontal Peak Field:	0.000	T
Effective Horizontal Field	0.000	T
Kz (from hor. field)	0.000	
Photon Energy, Harm.1	0.414	keV
Emitted Power	7.878	kW
Total Length	3931.0	mm

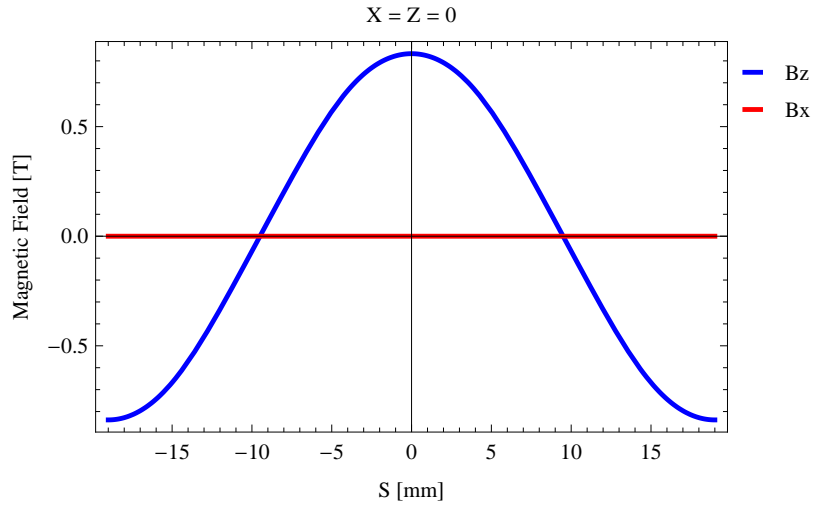


Figure 4: Vertical magnetic field in a central pole of the epu38gap11Plan ID along the ID axis, $X = Z = 0$

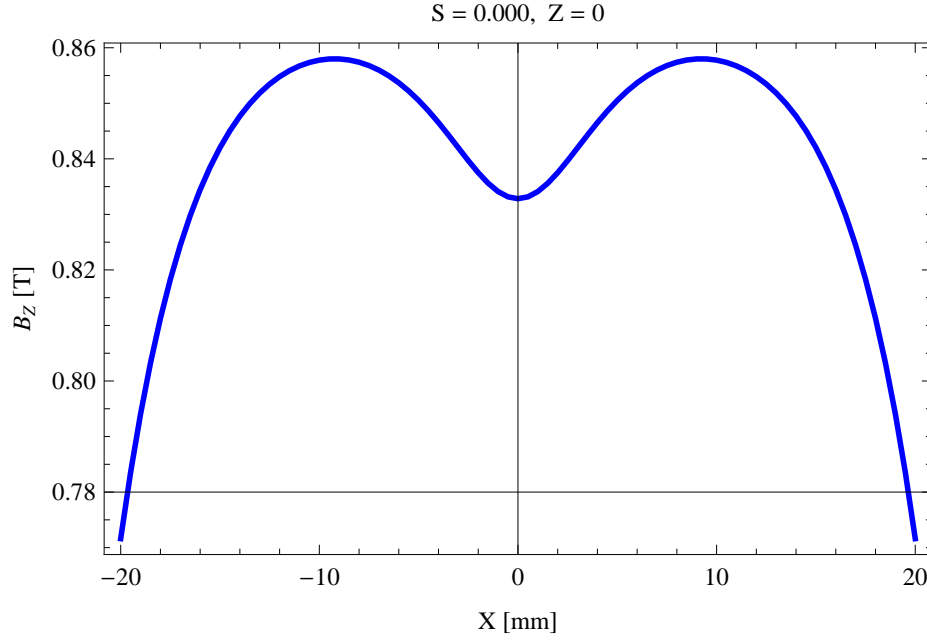


Figure 5: Vertical magnetic field in a central pole of the epu38gap11Plan ID along the horizontally transverse direction to the ID axis, $S = 0.000, Z = 0$

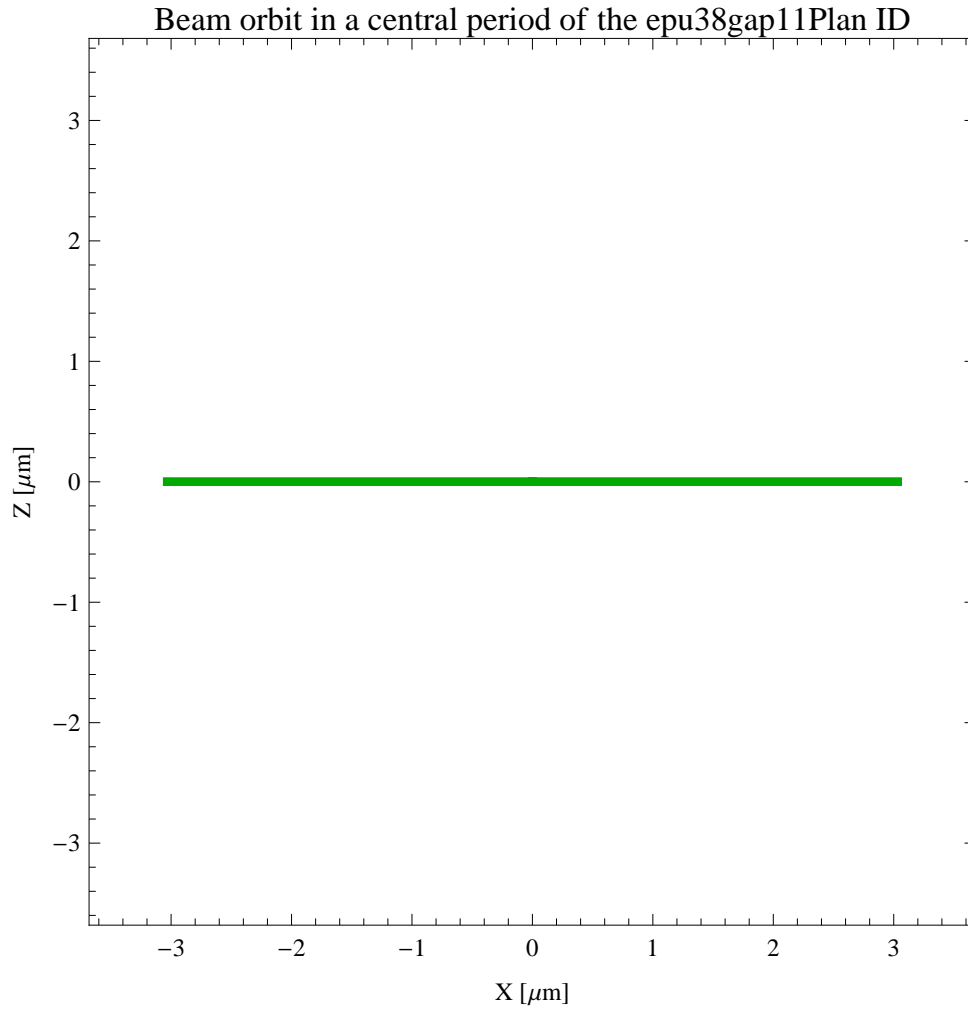


Figure 6: The beam orbit of the electron beam through a central period of the epu38gap11Plan ID

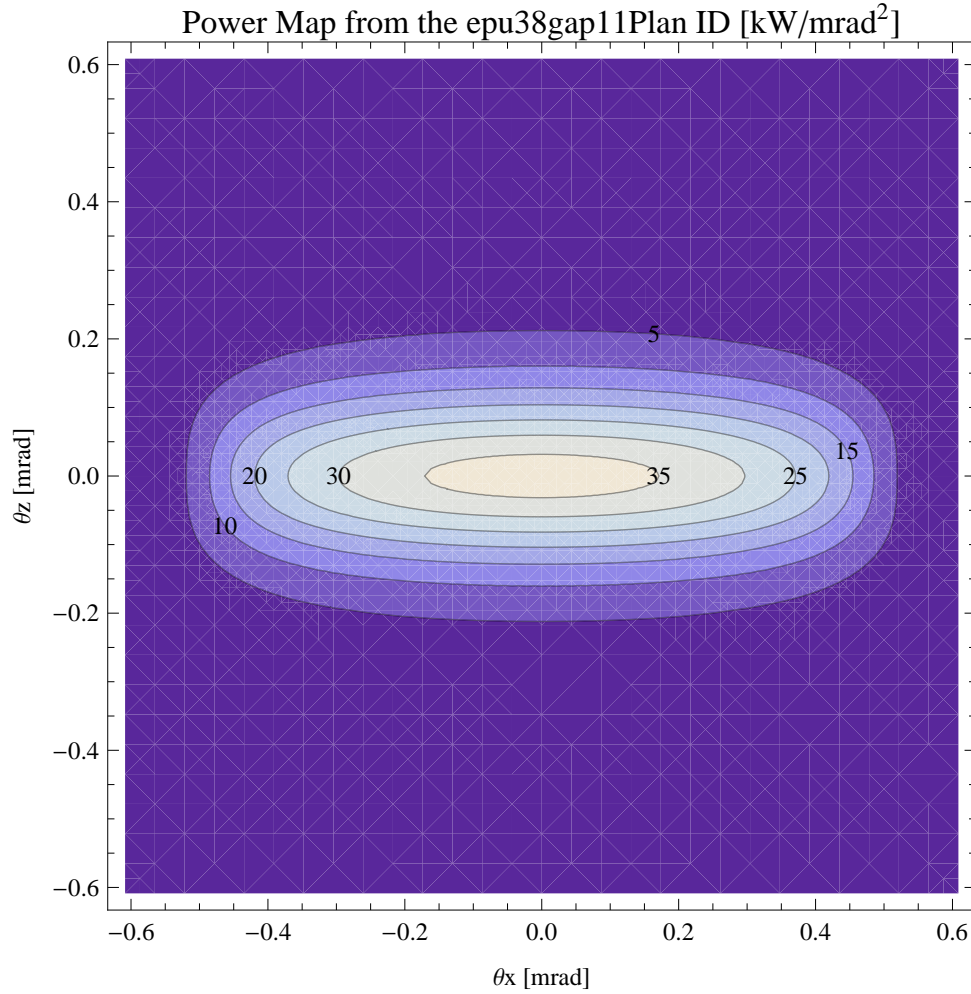


Figure 7: Map of the power distribution of the emitted synchrotron radiation by the epu38gap11Plan ID

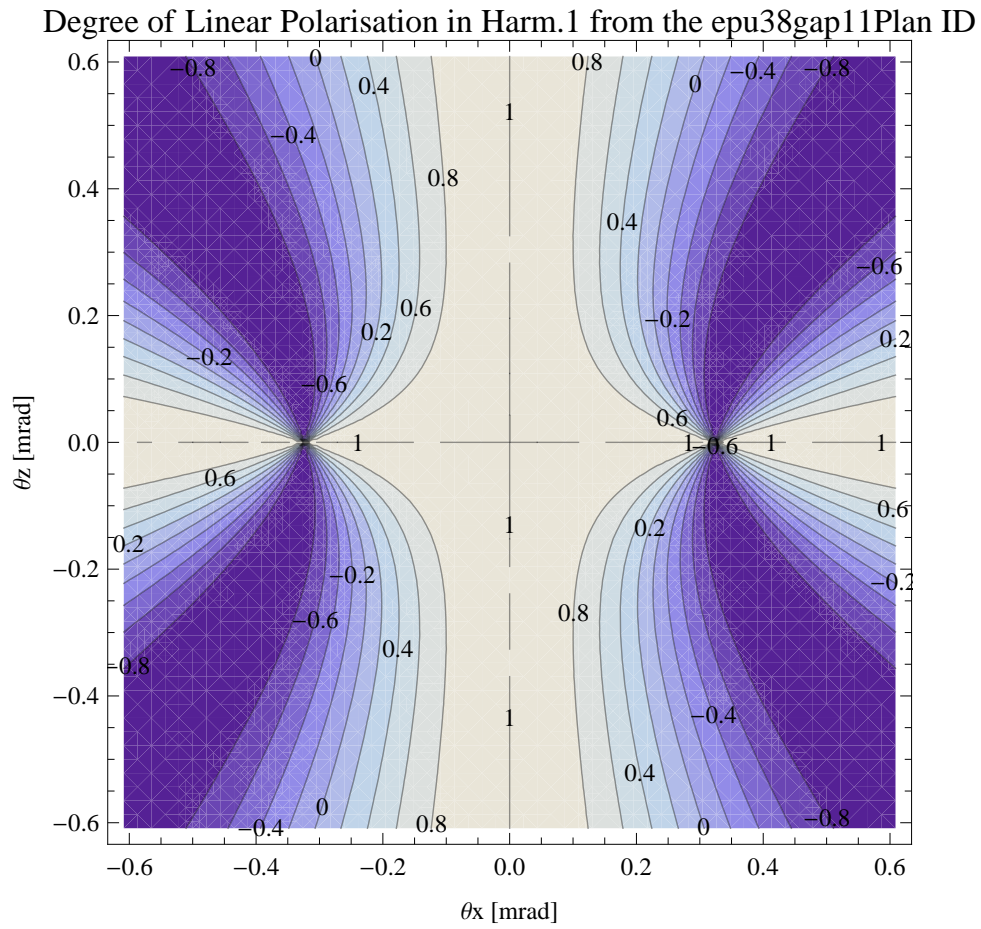


Figure 8: Map of linear polarisation in the fundamental harmonic of the synchrotron radiation emitted by the epu38gap11Plan ID

Degree of 45 degree Polarisation in Harm.1 from the epu38gap11Plan ID

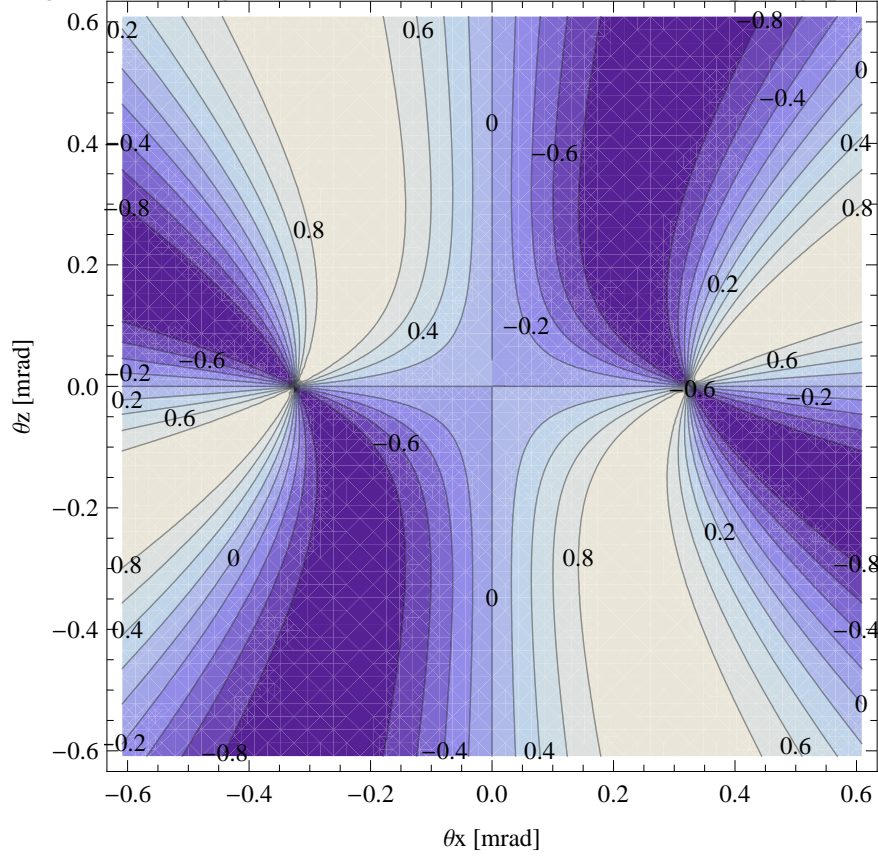


Figure 9: Map of 45 degree polarisation in the fundamental harmonic of the synchrotron radiation emitted by the epu38gap11Plan ID

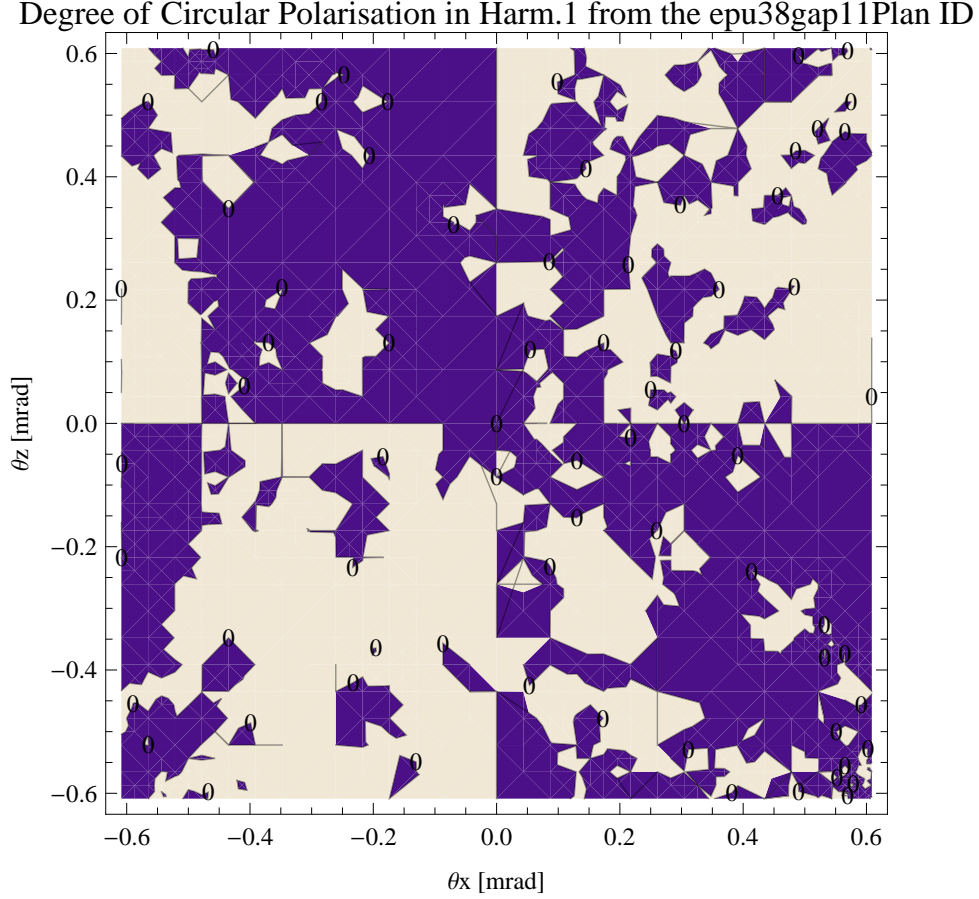


Figure 10: Map of circular polarisation in the fundamental harmonic of the synchrotron radiation emitted by the epu38gap11Plan ID

A map of the degree of circular polarisation of the fundamental harmonic of the synchrotron radiation emitted by the epu38gap11Plan ID over the angle of observation is shown in Figure 10.

The on axis brilliance at peak energy and the angular spectral flux from the epu38gap11Plan ID have been calculated with the given beam parameters, which are 0.5 A of stored current, $\beta_H = 9$ m, $\varepsilon_H = 0.263$ nmrad, $\beta_V = 4.8$ m, $\varepsilon_V = 8$. pmrad, and an energy spread of 0.001.

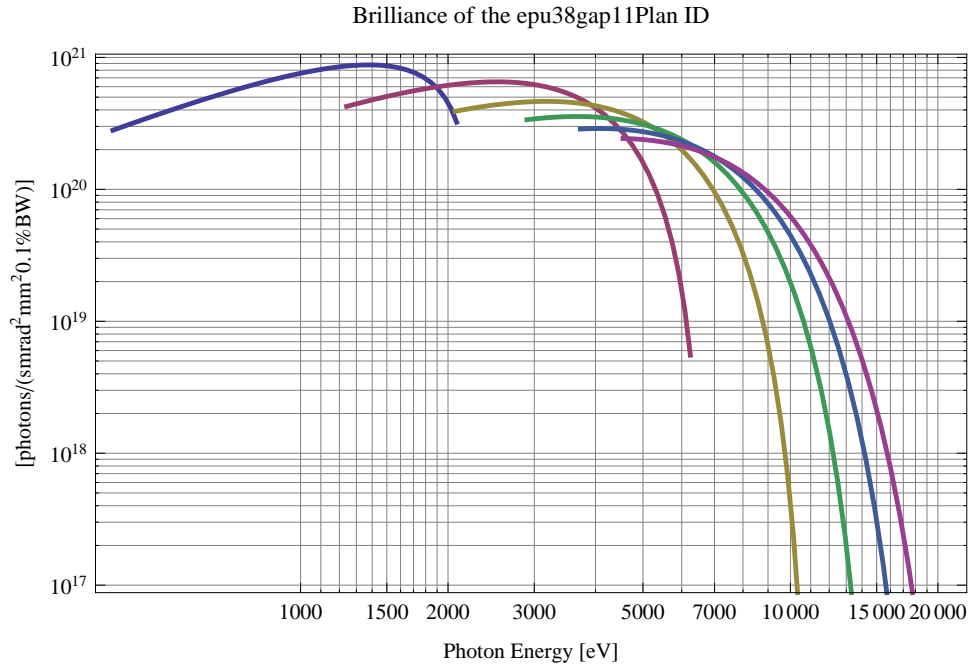


Figure 11: The brilliance at peak energy of the synchrotron radiation emitted by the epu38gap11Plan ID

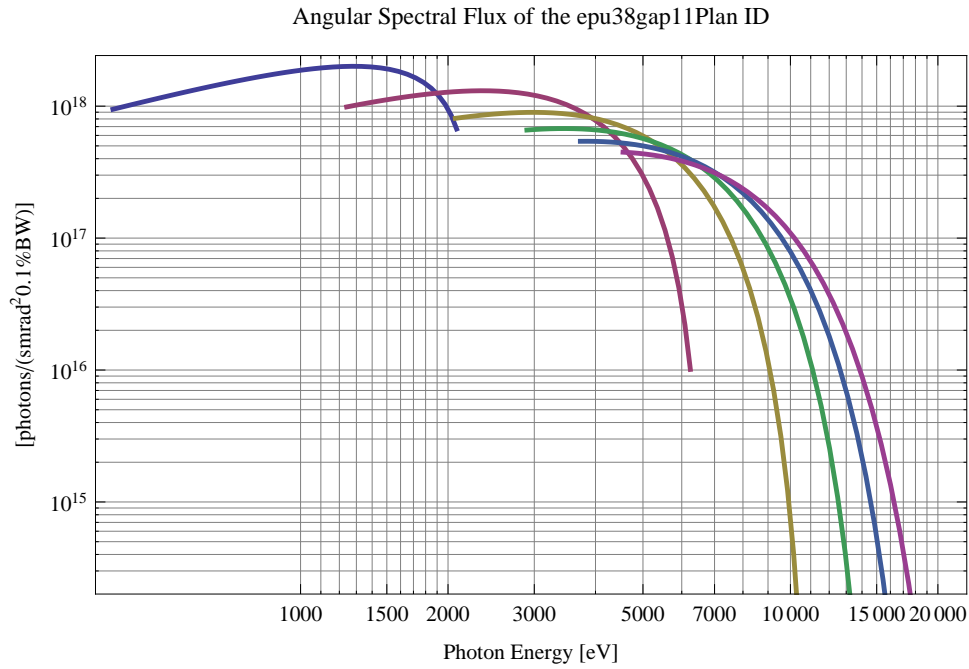


Figure 12: The angular spectral flux of the synchrotron radiation emitted by the epu38gap11Plan ID

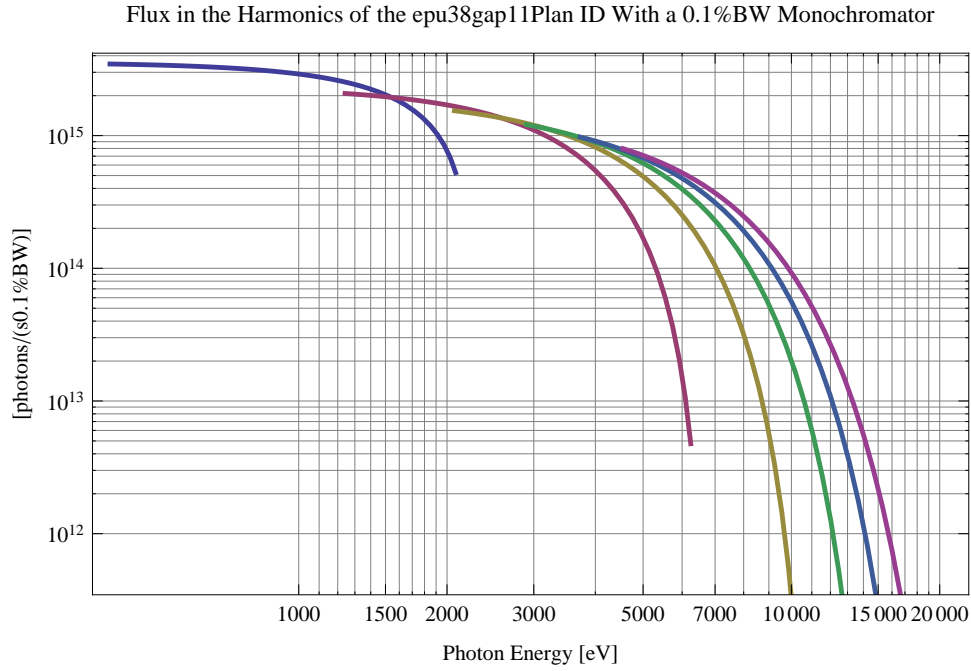


Figure 13: The flux of photons in the harmonics of the emitted synchrotron radiation from the epu38gap11Plan ID using a 0.1%BW monochromator

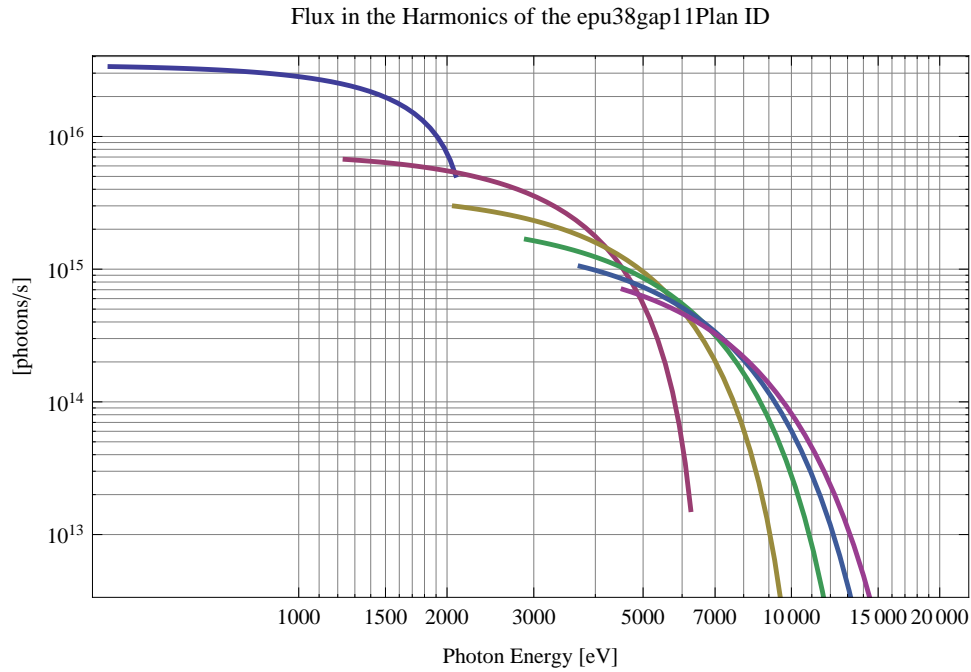


Figure 14: The flux of photons in the harmonics of the emitted synchrotron radiation from the epu38gap11Plan ID

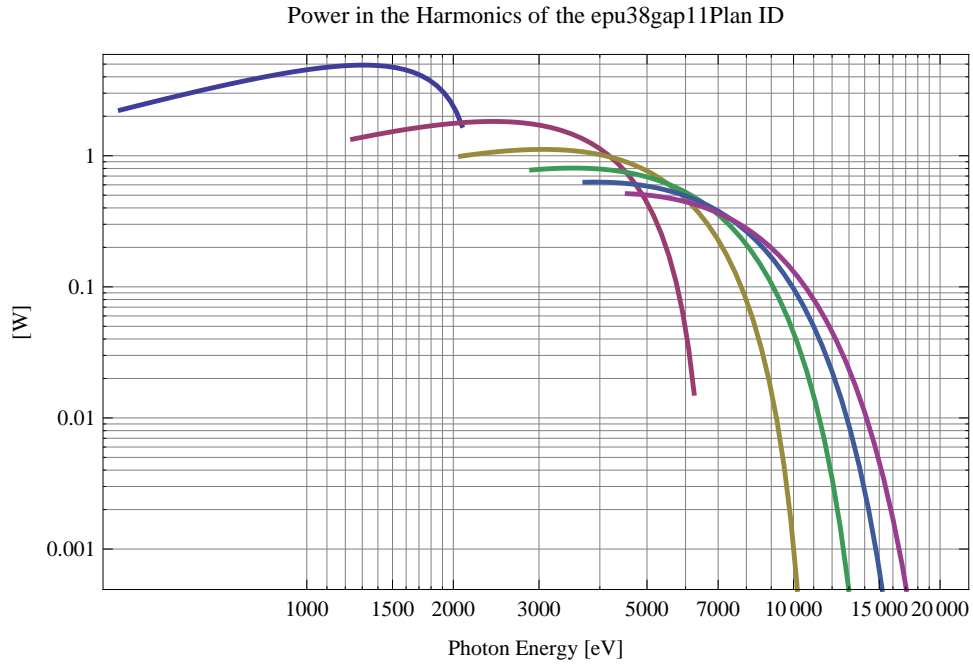


Figure 15: The power in the harmonics of the emitted synchrotron radiation from the epu38gap11Plan ID

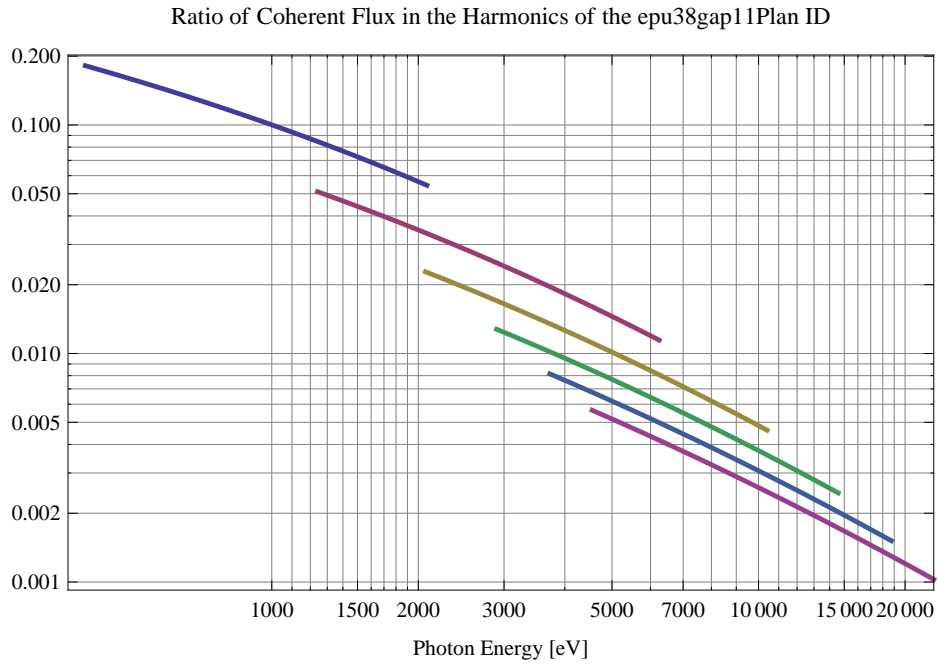


Figure 16: The ratio of coherent flux in the harmonics of the emitted synchrotron radiation from the epu38gap11Plan ID

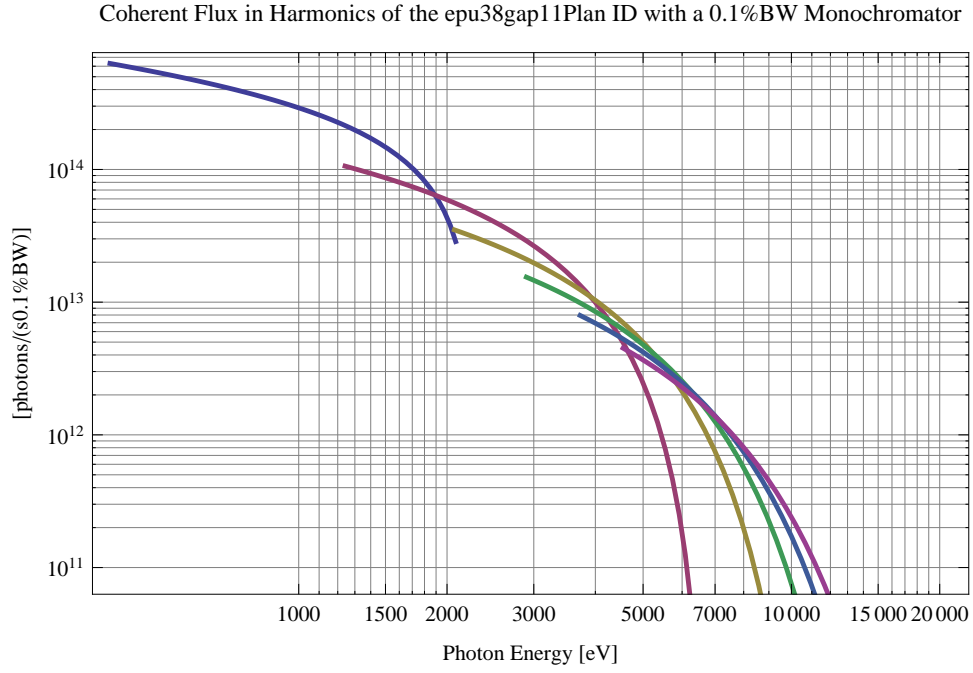


Figure 17: The coherent flux in the harmonics of the epu38gap11Plan ID using a 0.1%BW Monochromator

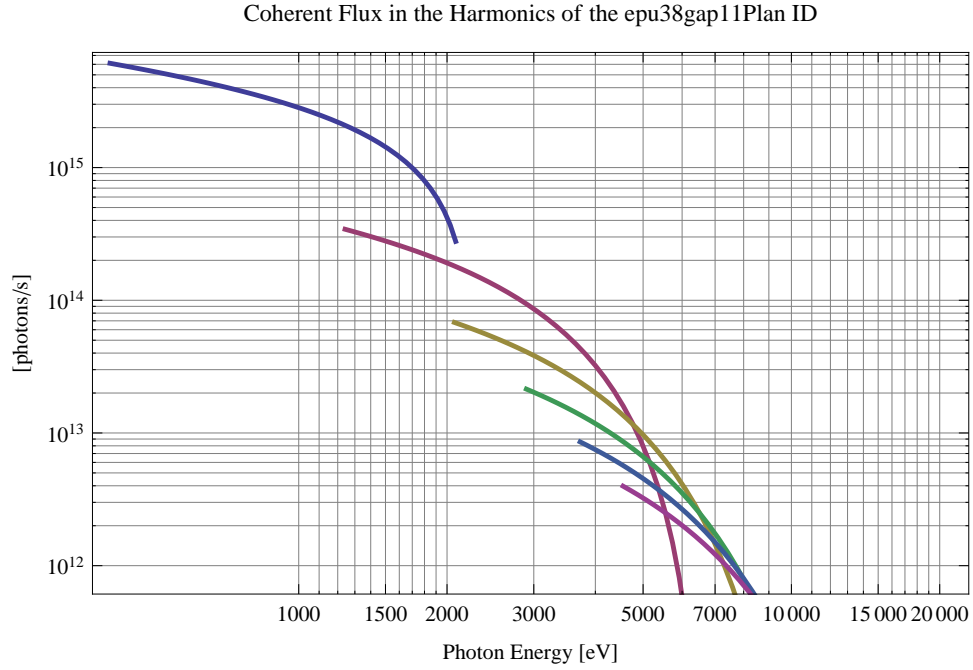


Figure 18: The coherent flux in the harmonics of the epu38gap11Plan ID

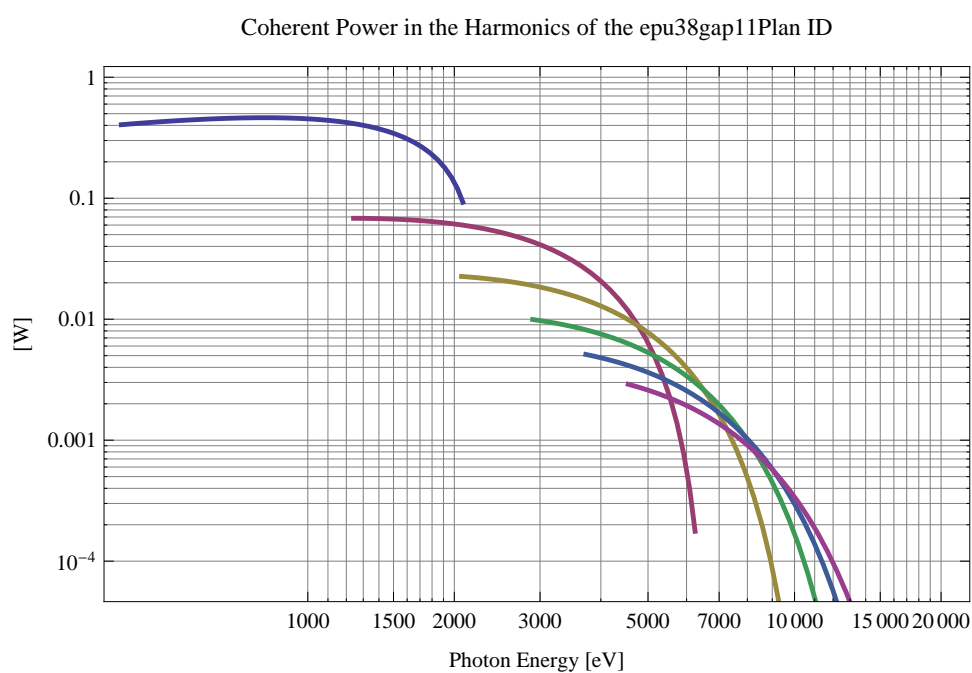


Figure 19: The power of coherent synchrotron radiation in the harmonics of the epu38gap11Plan ID

The brilliance at peak energy and the angular spectral flux density from the epu38gap11Plan ID for different harmonics at maximum K-value (2.978) are given in Table 3 and for minimum K-value (0.400) these values are given in Table 4.

Table 3: The brilliance at peak energy and the angular spectral flux density from the epu38gap11Plan ID for different harmonics at maximum K-value (2.978)

Harmonic	Photon Energy [eV]	Brilliance [Ph./ (smrad ² mrads ² 0.1%BW)]	Angular Spectral Flux [Ph./ (smrad ² 0.1%BW)]
1	413.934	2.81×10^{20}	9.47×10^{17}
3	1241.8	4.25×10^{20}	9.87×10^{17}
5	2069.67	3.91×10^{20}	8.08×10^{17}
7	2897.54	3.37×10^{20}	6.59×10^{17}
9	3725.41	2.87×10^{20}	5.41×10^{17}
11	4553.28	2.43×10^{20}	4.48×10^{17}

Table 4: The brilliance at peak energy and the angular spectral flux density from the epu38gap11Plan ID for different harmonics at minimum K-value (0.4)

Harmonic	Photon Energy [eV]	Brilliance [Ph./ (smrad ² mrads ² 0.1%BW)]	Angular Spectral Flux [Ph./ (smrad ² 0.1%BW)]
1	2082.54	3.23×10^{20}	6.72×10^{17}
3	6247.63	5.54×10^{18}	1.01×10^{16}
5	10412.7	6.1×10^{16}	1.09×10^{14}
7	14577.8	6.35×10^{14}	1.12×10^{12}
9	18742.9	6.5×10^{12}	1.15×10^{10}
11	22908.	6.62×10^{10}	1.17×10^8

2.1.5 Magnet model of the elliptically polarising undulator epu38gap11Heli

The Radia [3] magnet model of the epu38gap11Heli ID is shown in Figure 20. The length of the magnet model is 320.976 mm. The magnetic material in the model is NdFeb with a remanence of 1.28 T, a material similar to VACODYM 776 TP from Vacuumschmelze. Blocks with vertical magnetisation are blue and blocks with horizontal magnetisation are yellow. The block size is 30.x30.x9.5 mm³ and there is a 5. mm cut-out in two of the corners of the blocks. The total length of the epu38gap11Heli ID is 3930.98 mm.

2.1.6 Analysis of the magnetic field of the epu38gap11Heli ID

The effective magnetic fields on axis and the fundamental photon energy of the epu38gap11Heli ID are shown in Table 5. The higher harmonic contents in the magnetic field of an elliptically polarising undulator made of permanent magnets is negligible and the effective field has about the same strength as the peak field.

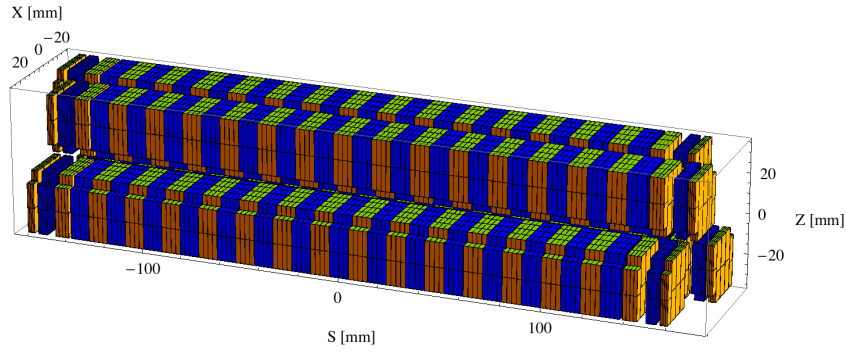


Figure 20: Magnetic model of the epu38gap11Heli ID. The ID has been modelled with Radia [3]

Table 5: Effective Fields on axis and Fundamental Photon Energy of the epu38gap11Heli ID

Undulator Period	38	mm
Undulator Gap	11	mm
Undulator Mode	Helical	
Undulator Phase	11.666	mm
Vertical Peak Field	0.472	T
Effective Vertical Field	0.475	T
Kx (from vert. field)	1.686	
Horizontal Peak Field:	0.476	T
Effective Horizontal Field	0.475	T
Kz (from hor. field)	1.686	
Photon Energy, Harm.1	0.586	keV
Emitted Power	5.050	kW
Total Length	3931.0	mm

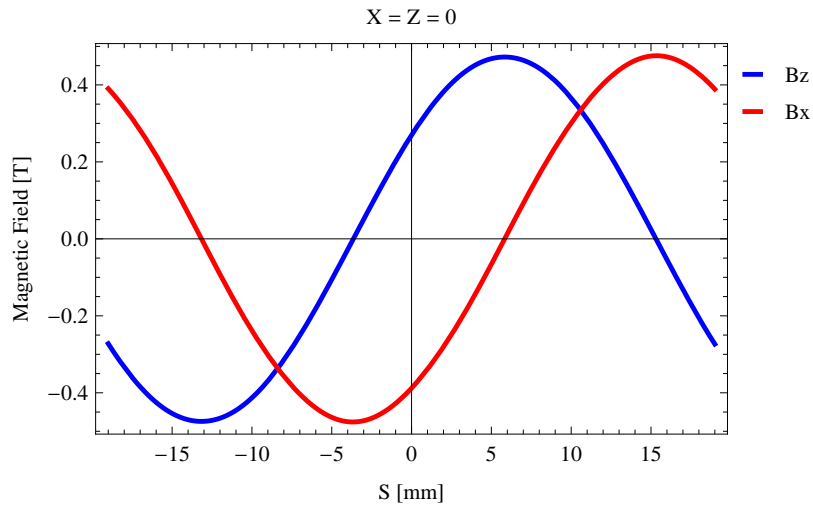


Figure 21: Vertical magnetic field in a central pole of the epu38gap11Heli ID along the ID axis, $X = Z = 0$

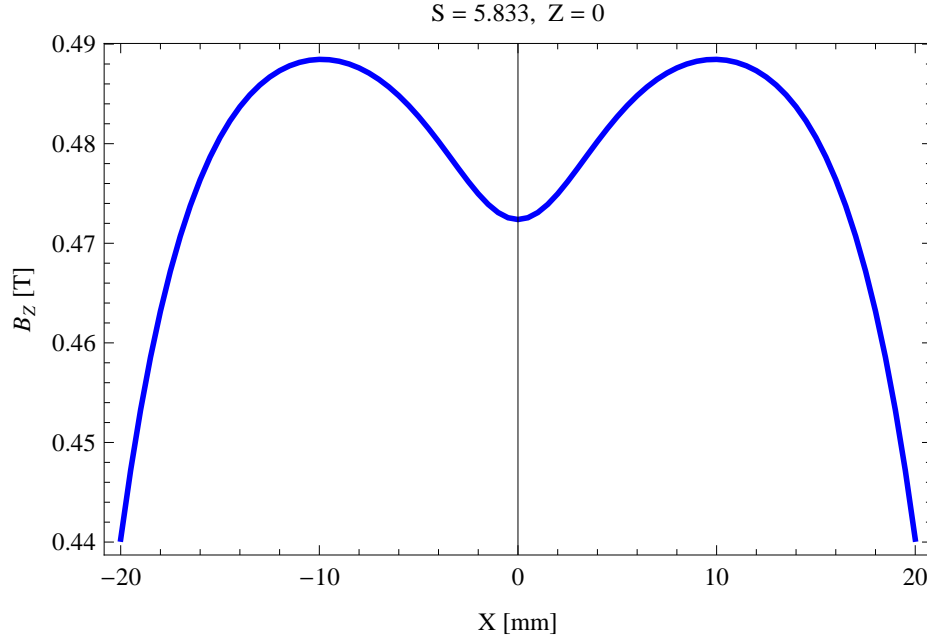


Figure 22: Vertical magnetic field in a central pole of the epu38gap11Heli ID along the horizontally transverse direction to the ID axis, $S = 5.833$, $Z = 0$

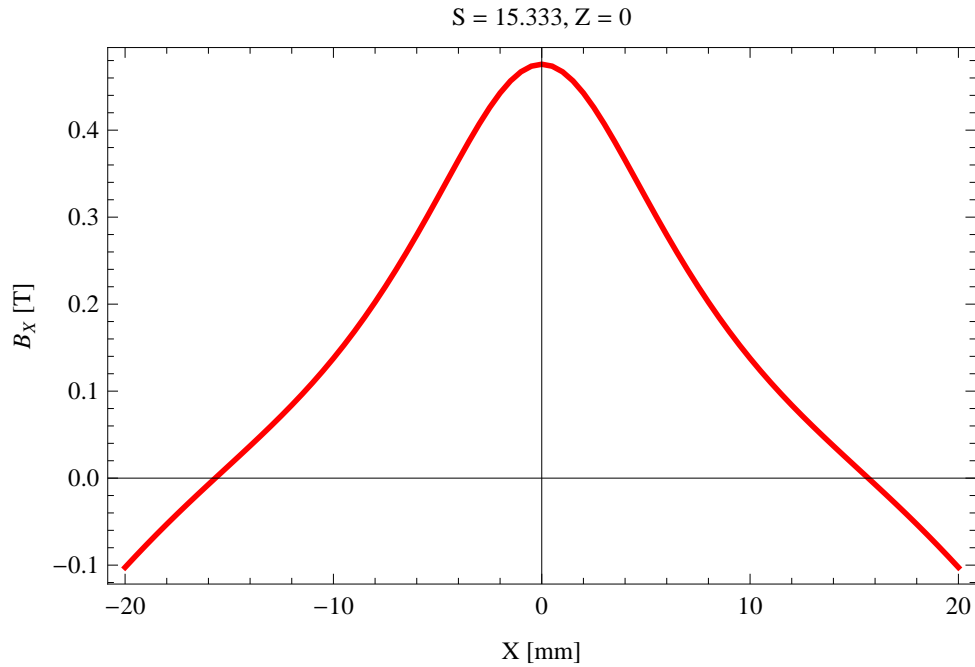


Figure 23: Horizontal magnetic field in a central pole of the epu38gap11Heli ID along the horizontally transverse direction to the ID axis, $S = 15.333$, $Z = 0$

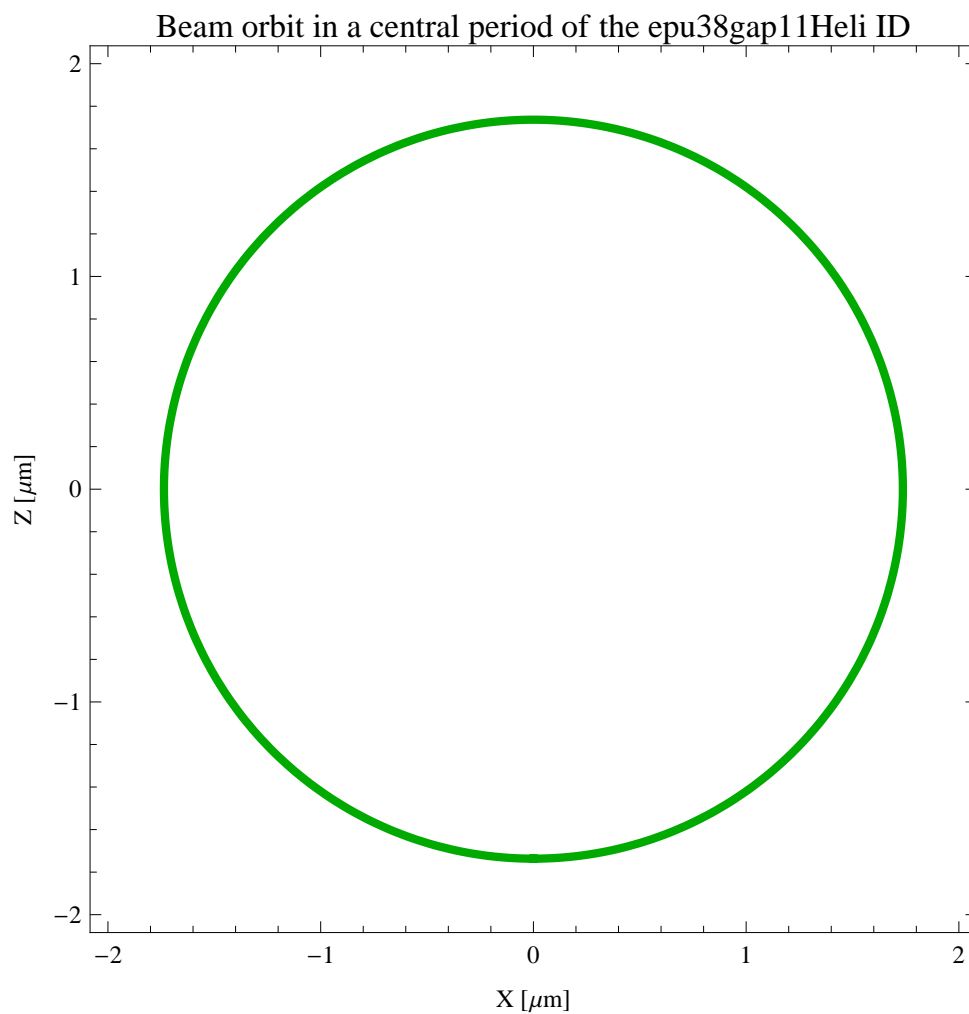


Figure 24: The beam orbit of the electron beam through a central period of the epu38gap11Heli ID

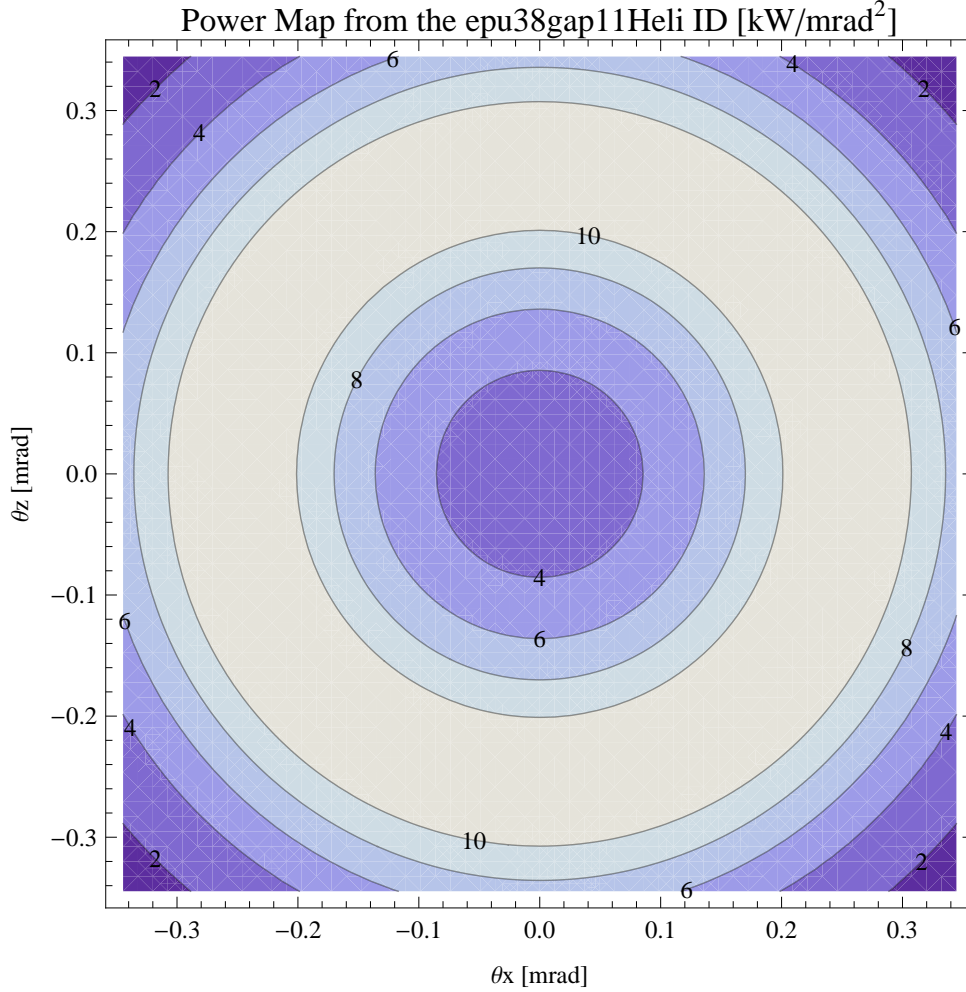


Figure 25: Map of the power distribution of the emitted synchrotron radiation by the epu38gap11Heli ID

2.1.7 Synchrotron radiation from the epu38gap11Heli ID

The power map of the emitted synchrotron radiation by the epu38gap11Heli ID, assuming a 0.5 A filament beam with an energy of 3 GeV and undulator properties of the synchrotron radiation, is shown in Figure 25. The on-axis power density is 2.891 kW/mrad²

A map of the degree of linear polarisation of the fundamental harmonic of the synchrotron radiation emitted by the epu38gap11Heli ID over the angle of observation is shown in Figure 26.

A map of the degree of 45 degree polarisation of the fundamental harmonic of the synchrotron radiation emitted by the epu38gap11Heli ID over the angle of observation is shown in Figure 27.

A map of the degree of circular polarisation of the fundamental harmonic of the synchrotron radiation emitted by the epu38gap11Heli ID over the angle of observation is shown in Figure 28.

The on axis brilliance at peak energy and the angular spectral flux from the epu38gap11Heli ID have been calculated with the given beam parameters, which are 0.5 A of stored current, $\beta_H = 9$ m, $\varepsilon_H = 0.263$ nrad, $\beta_V = 4.8$ m, $\varepsilon_V = 8$. pmrad, and an energy spread of 0.001.

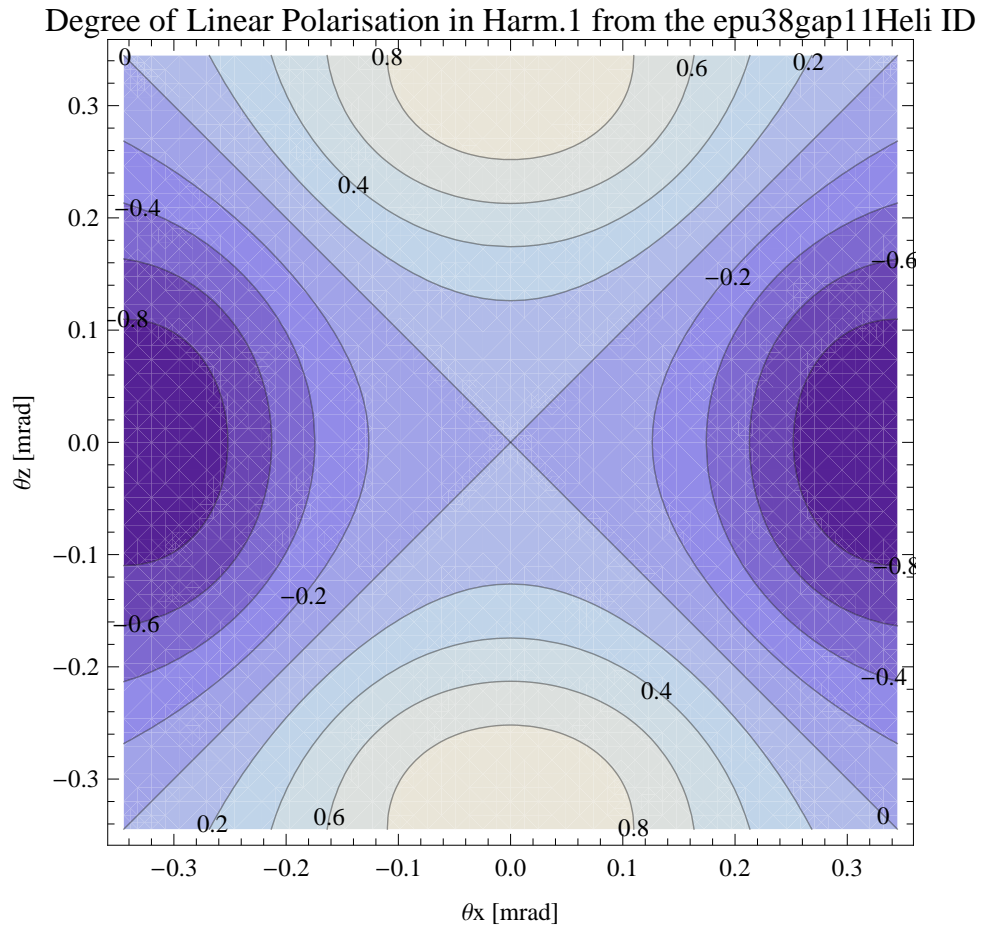


Figure 26: Map of linear polarisation in the fundamental harmonic of the synchrotron radiation emitted by the epu38gap11Heli ID

Degree of 45 degree Polarisation in Harm.1 from the epu38gap11Heli ID

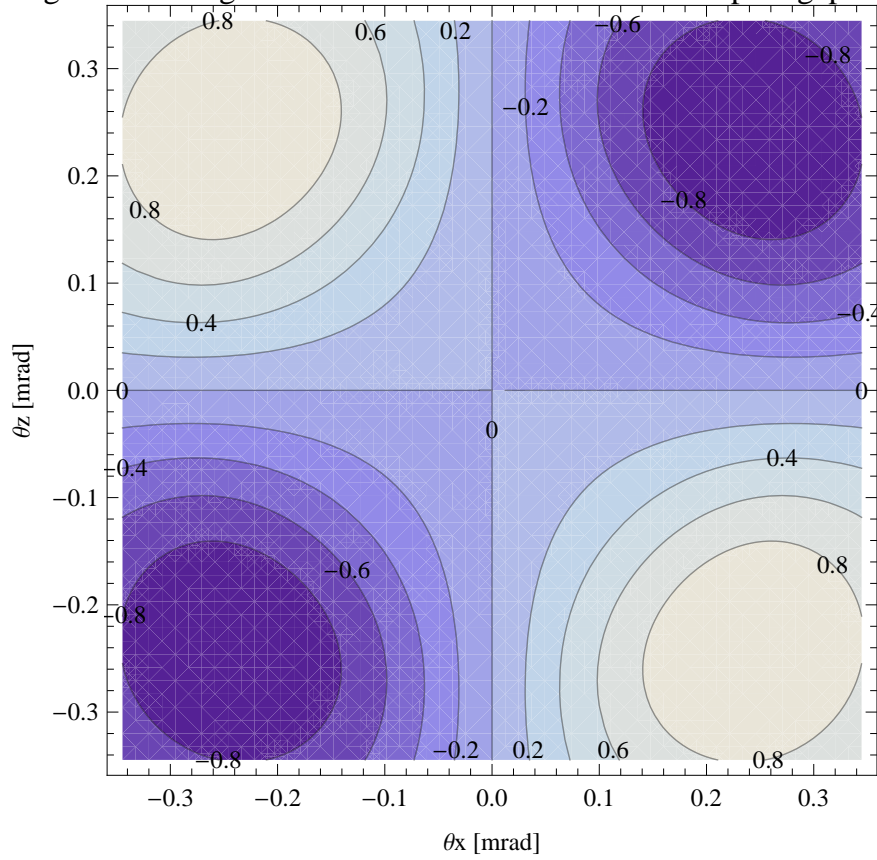


Figure 27: Map of 45 degree polarisation in the fundamental harmonic of the synchrotron radiation emitted by the epu38gap11Heli ID

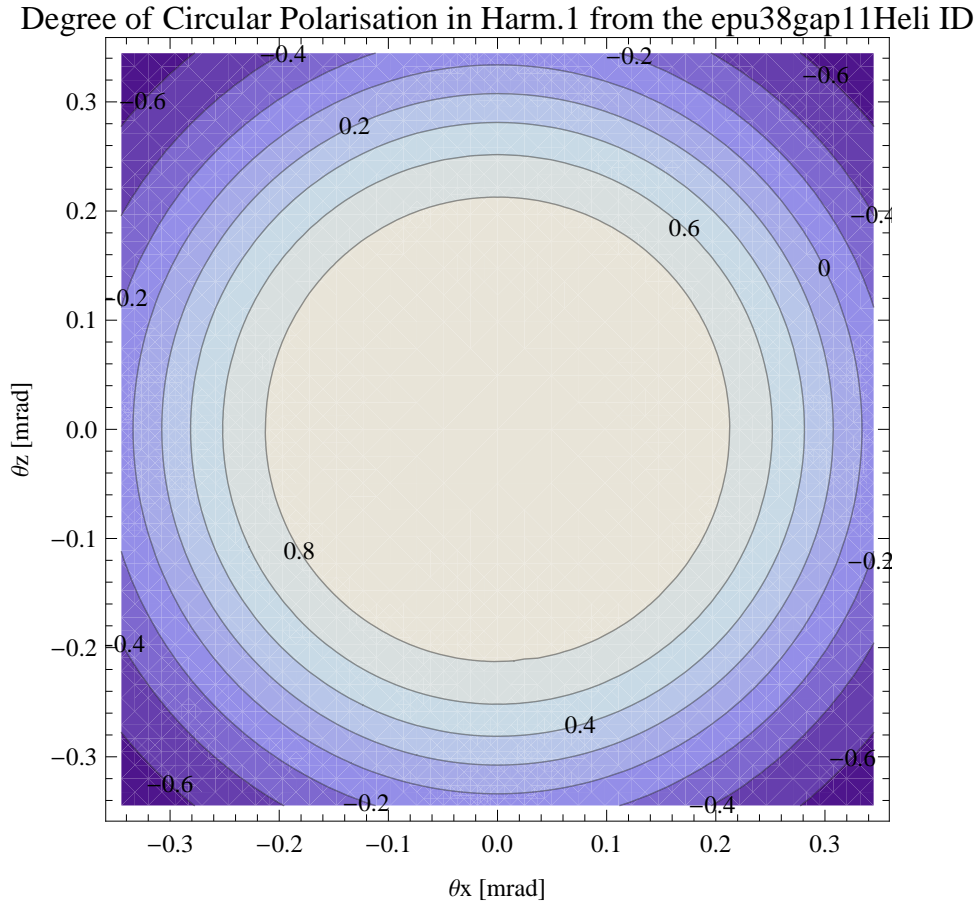


Figure 28: Map of circular polarisation in the fundamental harmonic of the synchrotron radiation emitted by the epu38gap11Heli ID

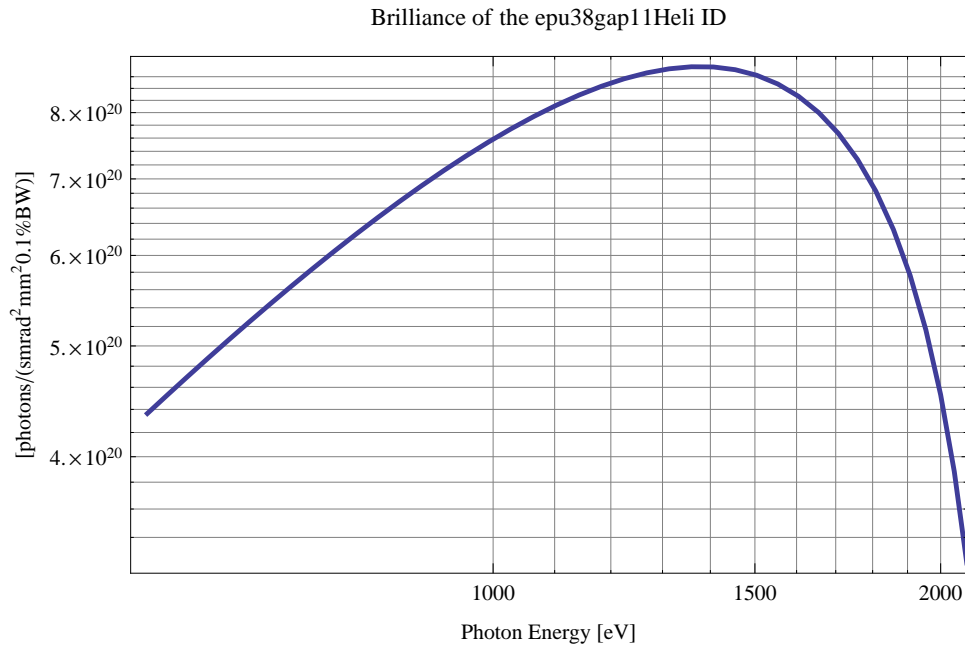


Figure 29: The brilliance at peak energy of the synchrotron radiation emitted by the epu38gap11Heli ID

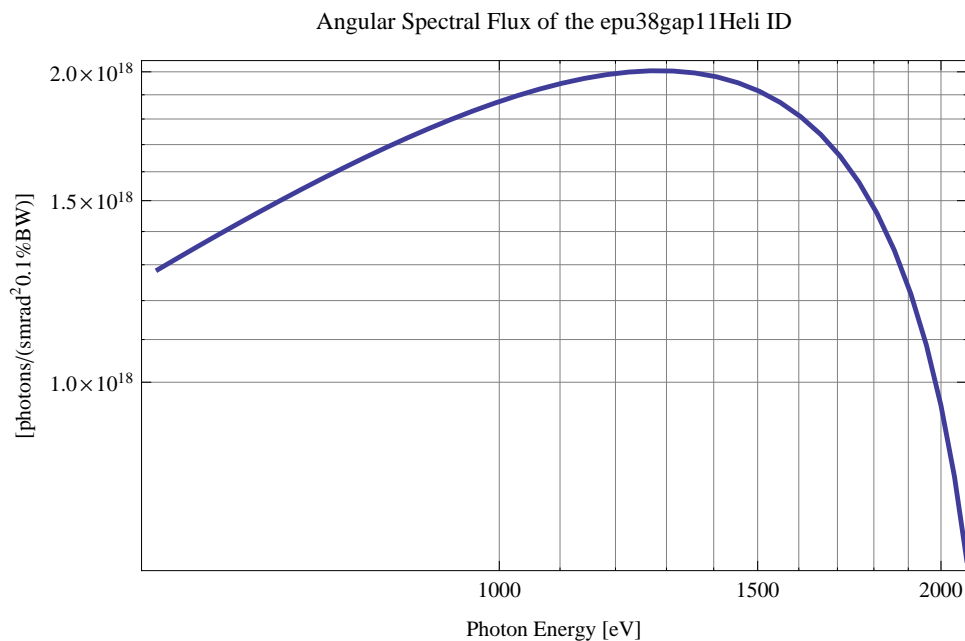


Figure 30: The angular spectral flux of the synchrotron radiation emitted by the epu38gap11Heli ID

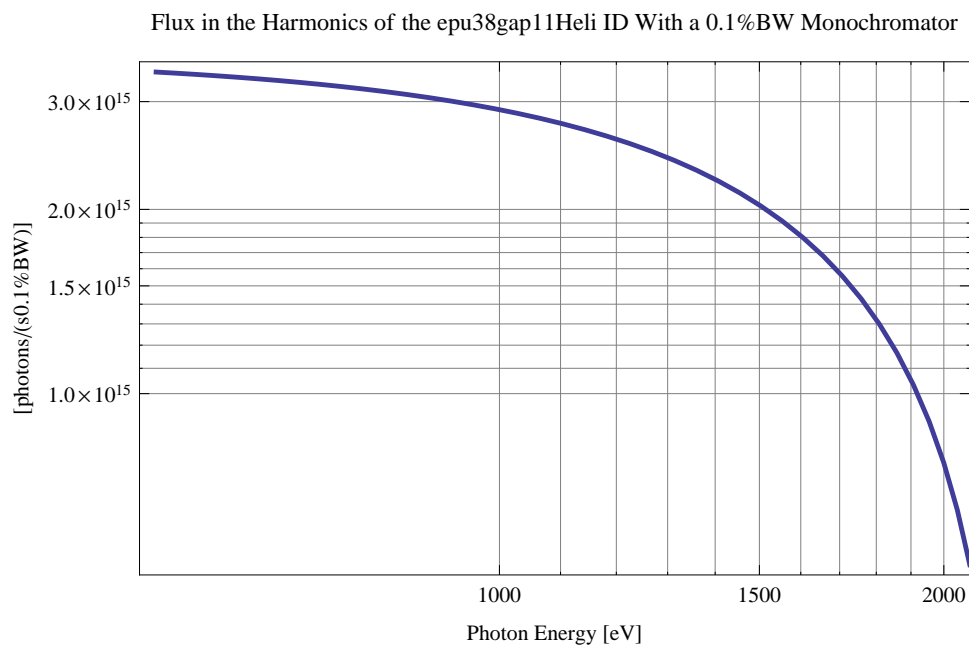


Figure 31: The flux of photons in the harmonics of the emitted synchrotron radiation from the epu38gap11Heli ID using a 0.1% BW monochromator

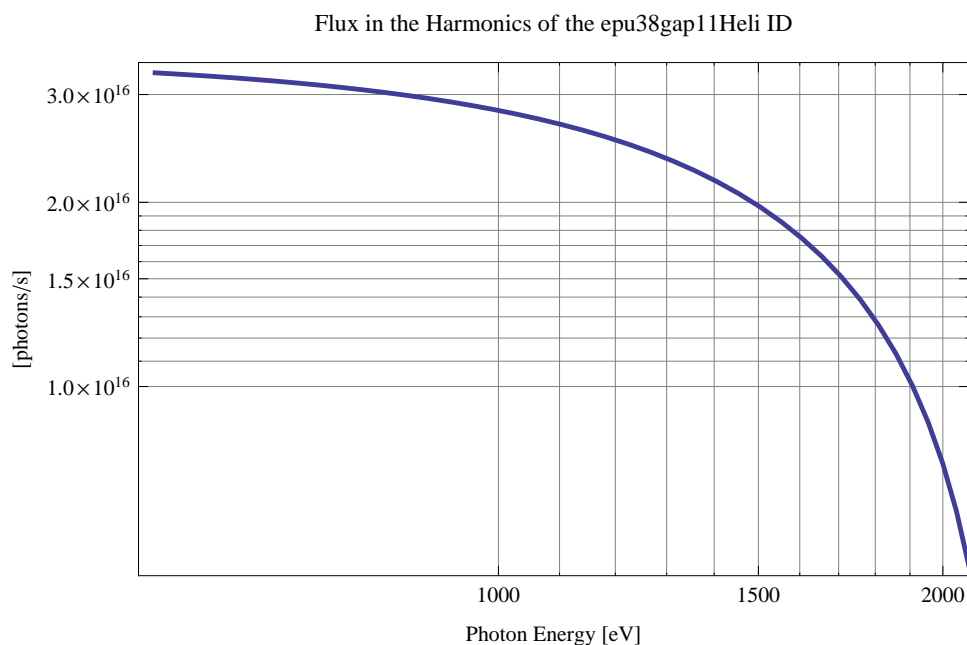


Figure 32: The flux of photons in the harmonics of the emitted synchrotron radiation from the epu38gap11Heli ID

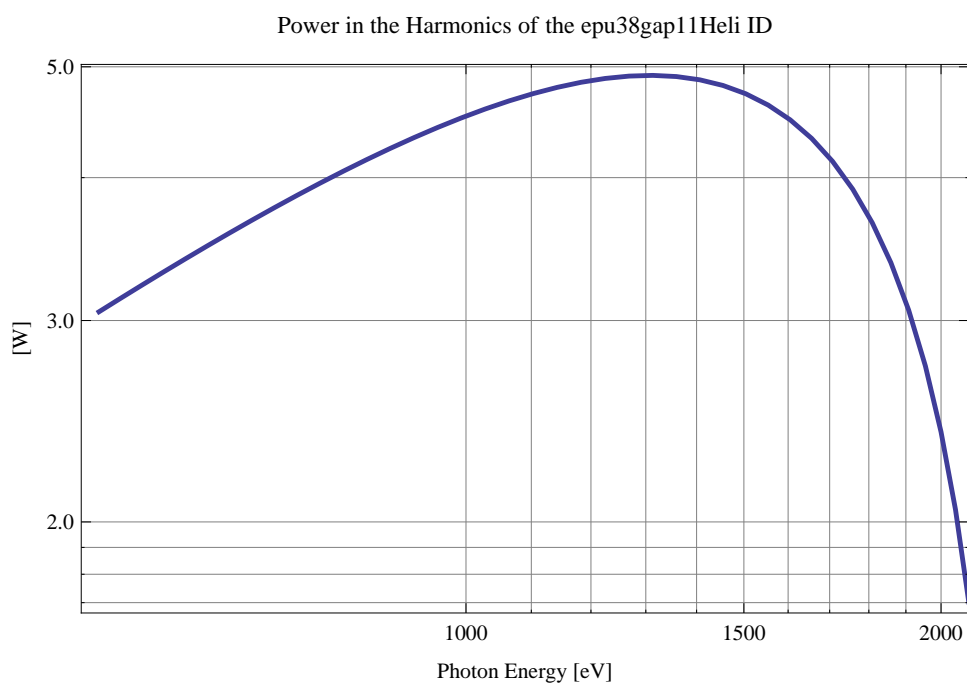


Figure 33: The power in the harmonics of the emitted synchrotron radiation from the epu38gap11Heli ID

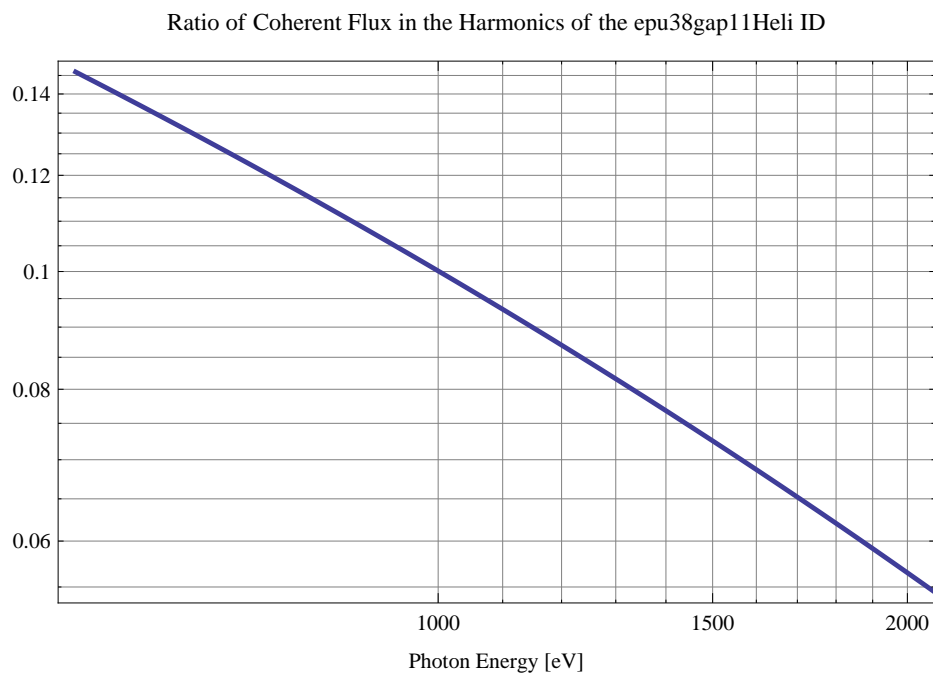


Figure 34: The ratio of coherent flux in the harmonics of the emitted synchrotron radiation from the epu38gap11Heli ID

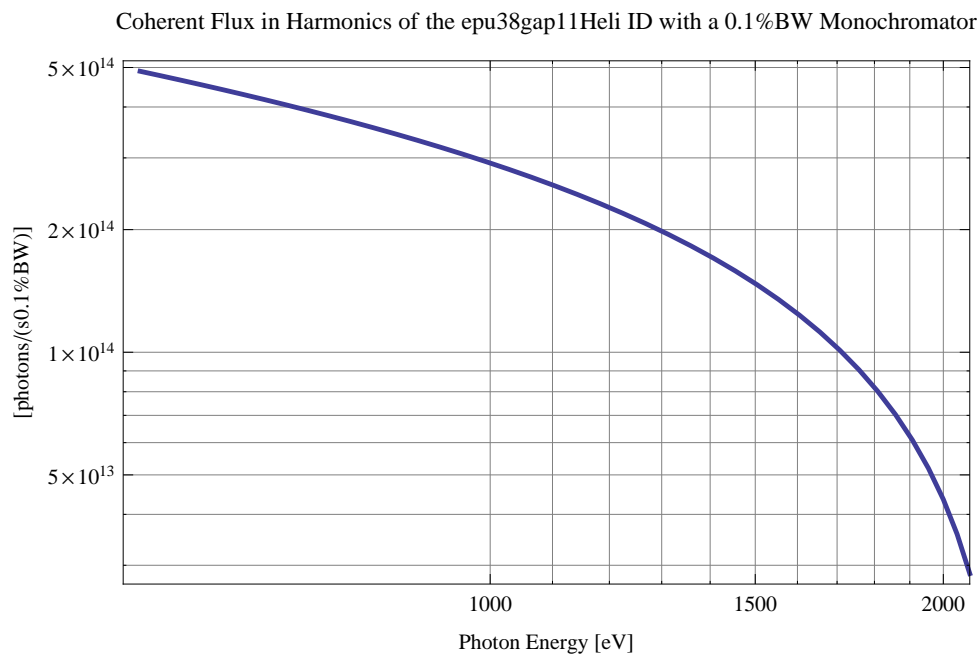


Figure 35: The coherent flux in the harmonics of the epu38gap11Heli ID using a 0.1%BW Monochromator

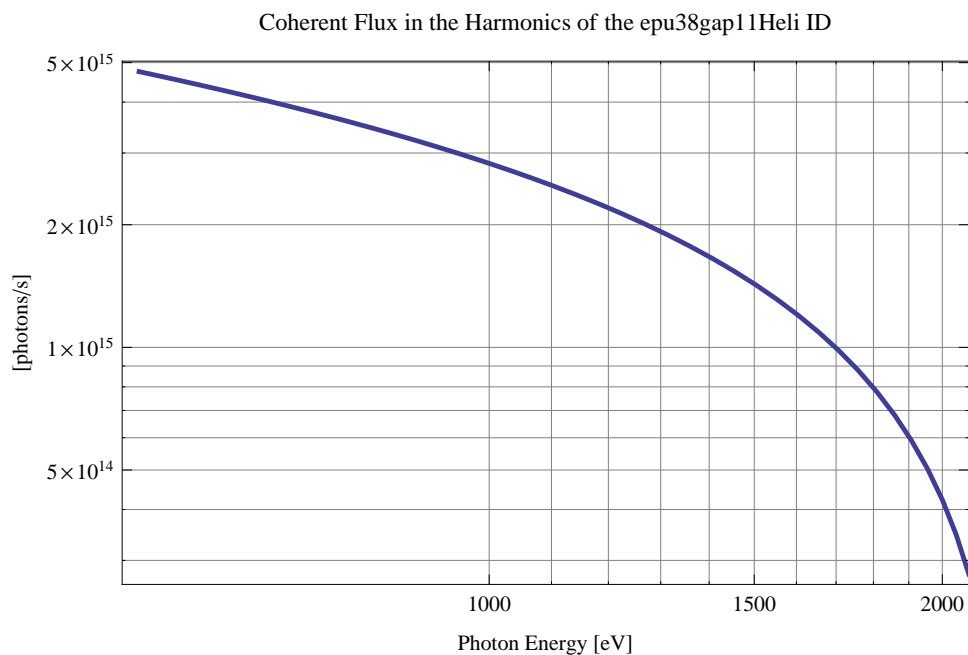


Figure 36: The coherent flux in the harmonics of the epu38gap11Heli ID

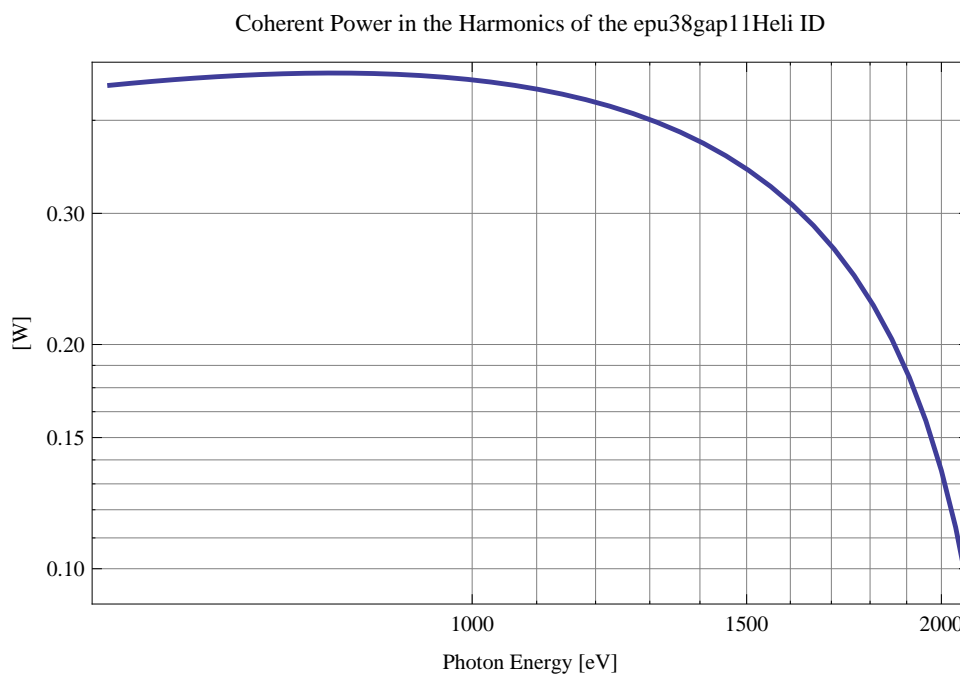


Figure 37: The power of coherent synchrotron radiation in the harmonics of the epu38gap11Heli ID

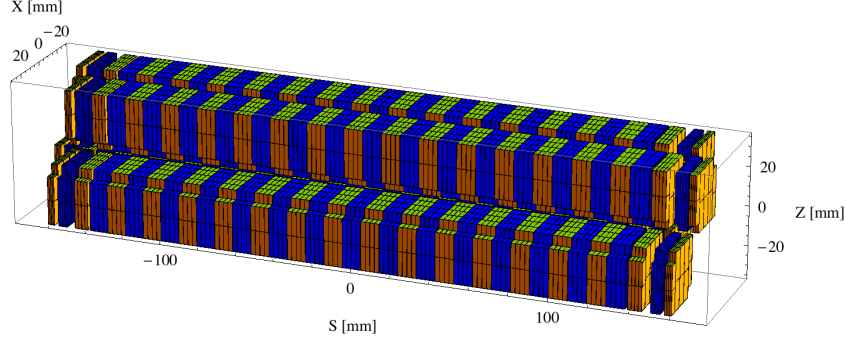


Figure 38: Magnetic model of the epu38gap11Incl ID. The ID has been modelled with Radia [3]

The brilliance at peak energy and the angular spectral flux density from the epu38gap11Heli ID for different harmonics at maximum K-value (2.384) are given in Table 6 and for minimum K-value (0.400) these values are given in Table 7.

Table 6: The brilliance at peak energy and the angular spectral flux density from the epu38gap11Heli ID for different harmonics at maximum K-value (2.384)

Harmonic	Photon Energy [eV]	Brilliance [Ph./ (smrad ² mrad ² 0.1% BW)]	Angular Spectral Flux [Ph./ (smrad ² 0.1% BW)]
1	585.387	4.36×10^{20}	1.29×10^{18}

Table 7: The brilliance at peak energy and the angular spectral flux density from the epu38gap11Heli ID for different harmonics at minimum K-value (0.4)

Harmonic	Photon Energy [eV]	Brilliance [Ph./ (smrad ² mrad ² 0.1% BW)]	Angular Spectral Flux [Ph./ (smrad ² 0.1% BW)]
1	2082.54	3.23×10^{20}	6.72×10^{17}

2.1.8 Magnet model of the elliptically polarising undulator epu38gap11Incl

The Radia [3] magnet model of the epu38gap11Incl ID is shown in Figure 38. The length of the magnet model is 320.976 mm. The magnetic material in the model is NdFeb with a remanence of 1.28 T, a material similar to VACODYM 776 TP from Vacuumschmelze. Blocks with vertical magnetisation are blue and blocks with horizontal magnetisation are yellow. The block size is 30.x30.x9.5 mm³ and there is a 5. mm cut-out in two of the corners of the blocks. The total length of the epu38gap11Incl ID is 3930.98 mm.

2.1.9 Analysis of the magnetic field of the epu38gap11Incl ID

The effective magnetic fields on axis and the fundamental photon energy of the epu38gap11Incl ID are shown in Table 8. The higher harmonic contents in the magnetic field of an elliptically

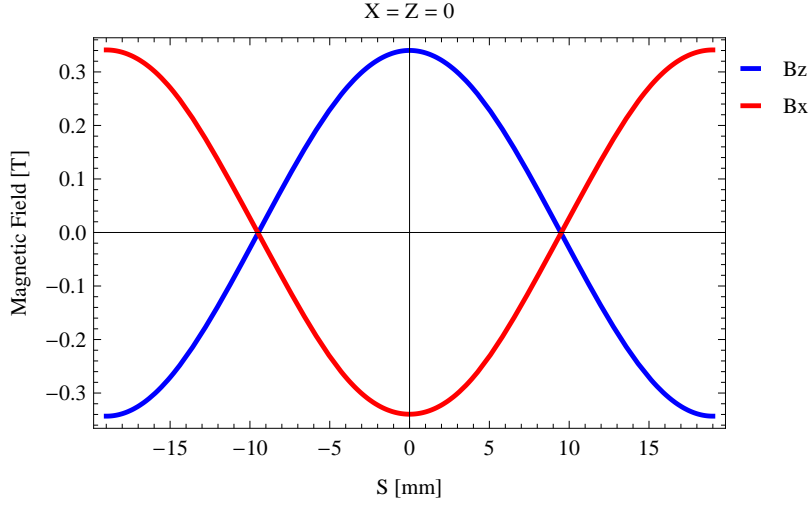


Figure 39: Vertical magnetic field in a central pole of the epu38gap11Incl ID along the ID axis, $X = Z = 0$

polarising undulator made of permanent magnets is negligible and the effective field has about the same strength as the peak field.

Table 8: Effective Fields on axis and Fundamental Photon Energy of the epu38gap11Incl ID

Undulator Period	38	mm
Undulator Gap	11	mm
Undulator Mode	Inclined	
Undulator Phase	10.600	mm
Vertical Peak Field	0.340	T
Effective Vertical Field	0.341	T
Kx (from vert. field)	1.210	
Horizontal Peak Field:	-0.340	T
Effective Horizontal Field	0.341	T
Kz (from hor. field)	1.210	
Photon Energy, Harm.1	0.913	keV
Emitted Power	2.603	kW
Total Length	3931.0	mm

2.1.10 Synchrotron radiation from the epu38gap11Incl ID

The power map of the emitted synchrotron radiation by the epu38gap11Incl ID, assuming a 0.5 A filament beam with an energy of 3 GeV and undulator properties of the synchrotron radiation, is shown in Figure 43. The on-axis power density is 21.080 kW/mrad²

A map of the degree of linear polarisation of the fundamental harmonic of the synchrotron radiation emitted by the epu38gap11Incl ID over the angle of observation is shown in Figure 44.

A map of the degree of 45 degree polarisation of the fundamental harmonic of the synchrotron radiation emitted by the epu38gap11Incl ID over the angle of observation is shown in Figure 45.

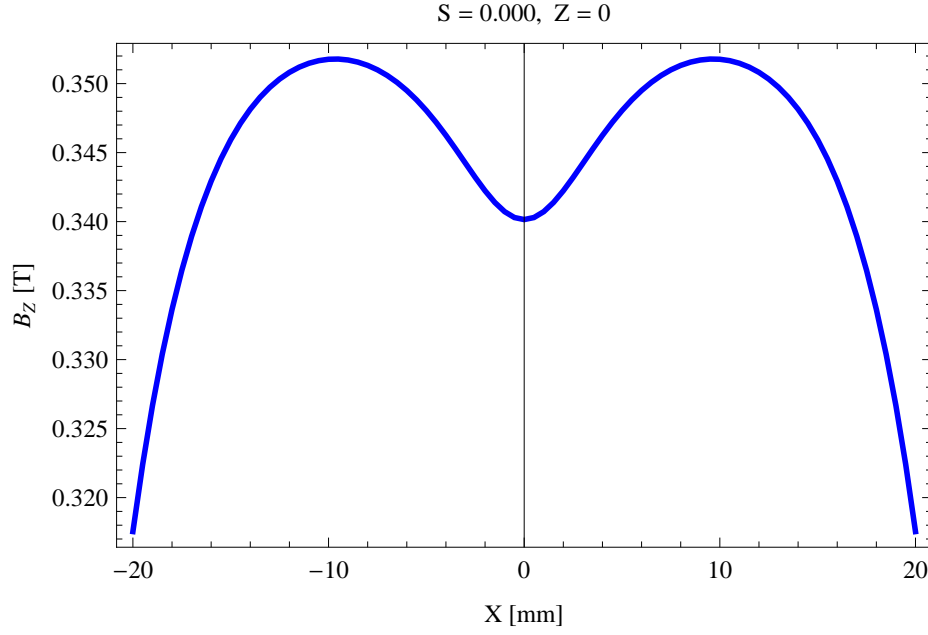


Figure 40: Vertical magnetic field in a central pole of the epu38gap11Incl ID along the horizontally transverse direction to the ID axis, $S = 0.000, Z = 0$

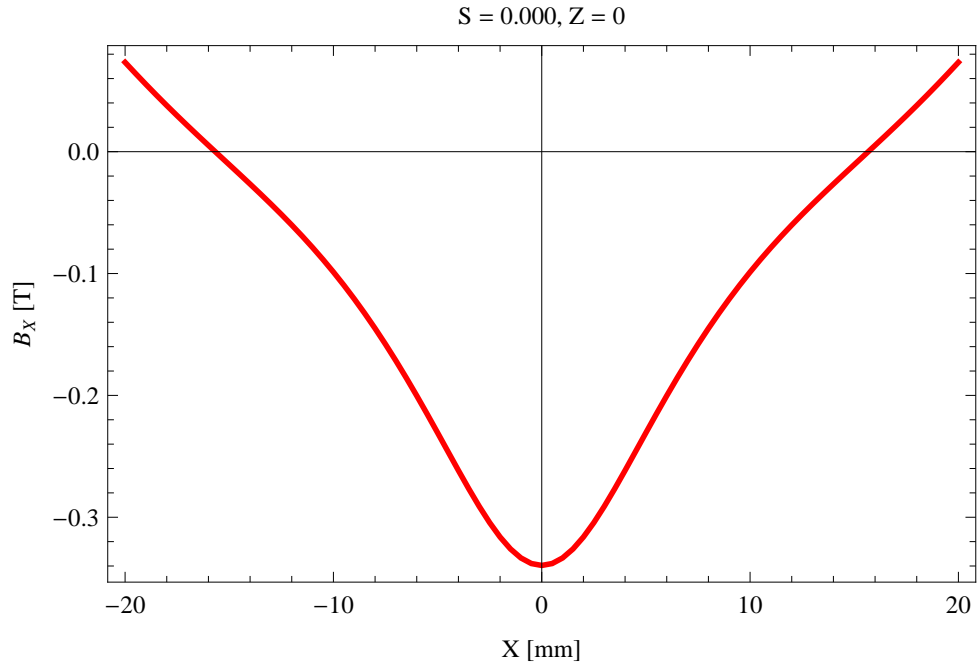


Figure 41: Horizontal magnetic field in a central pole of the epu38gap11Incl ID along the horizontally transverse direction to the ID axis, $S = 0.000, Z = 0$

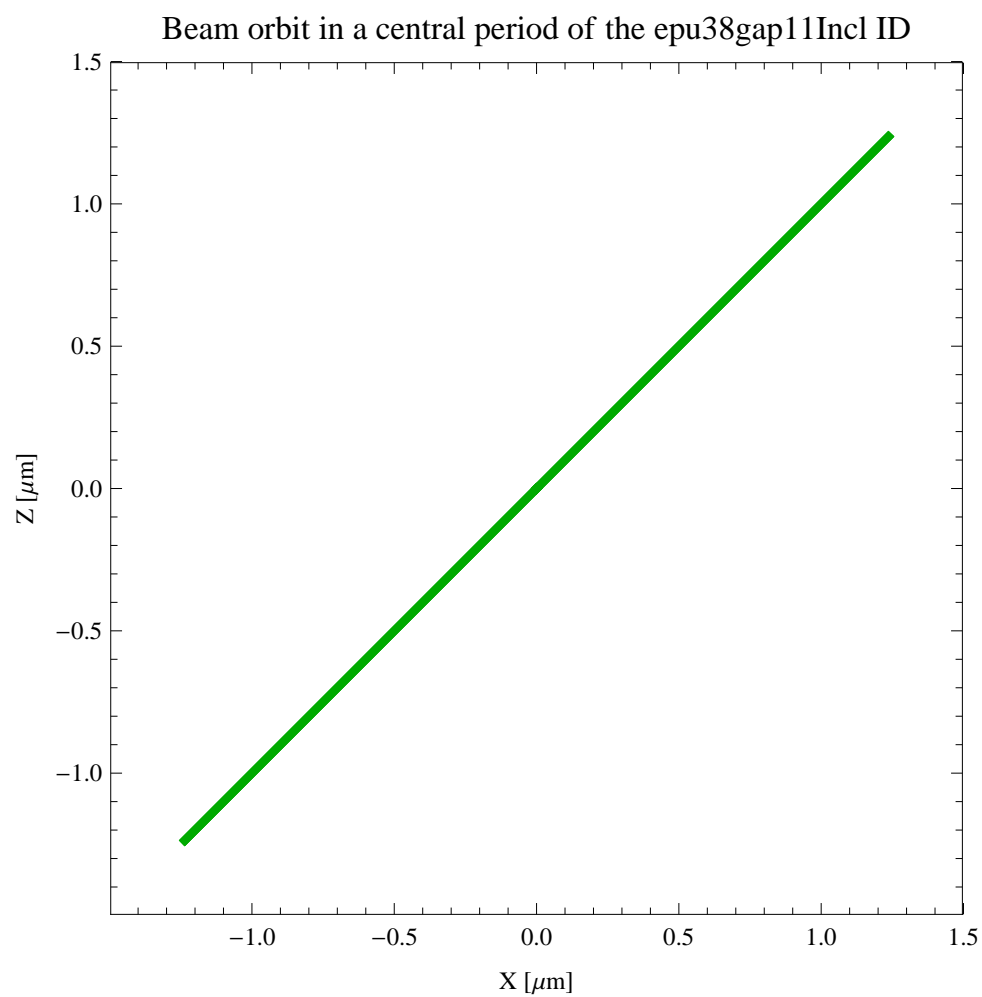


Figure 42: The beam orbit of the electron beam through a central period of the epu38gap11Incl ID

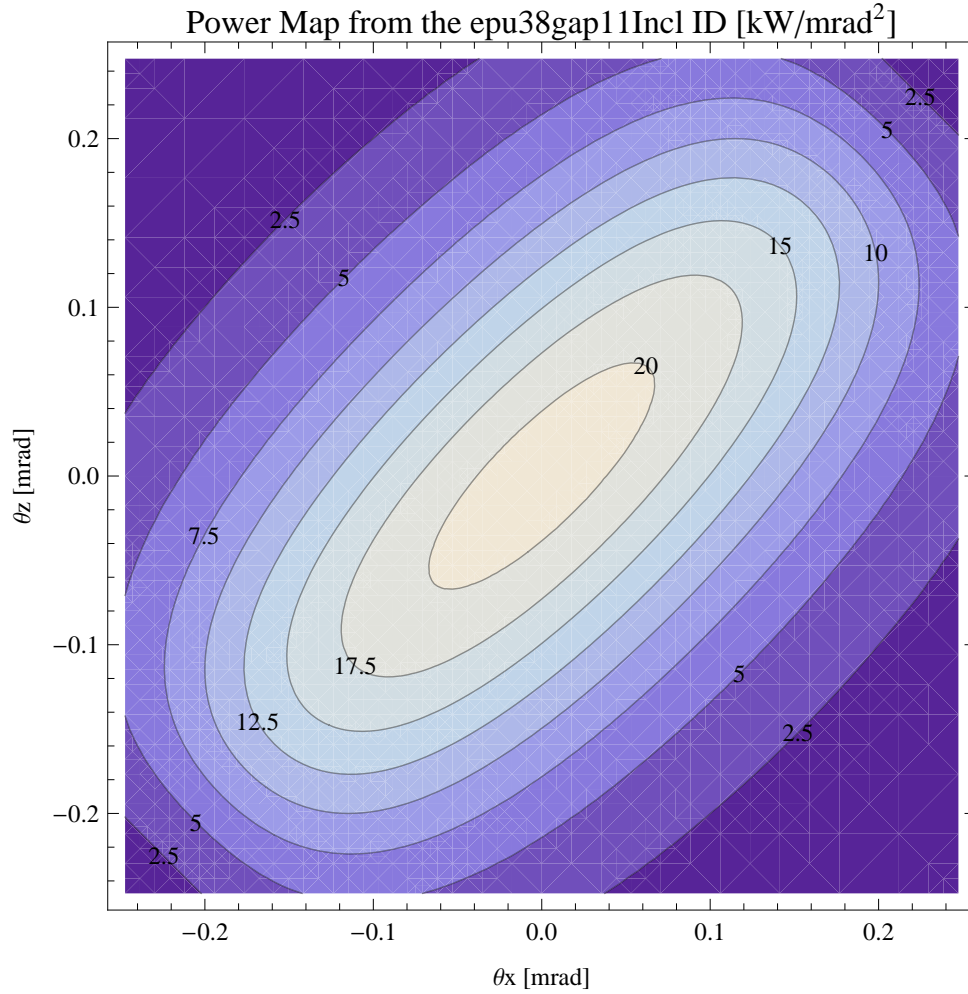


Figure 43: Map of the power distribution of the emitted synchrotron radiation by the epu38gap11Incl ID

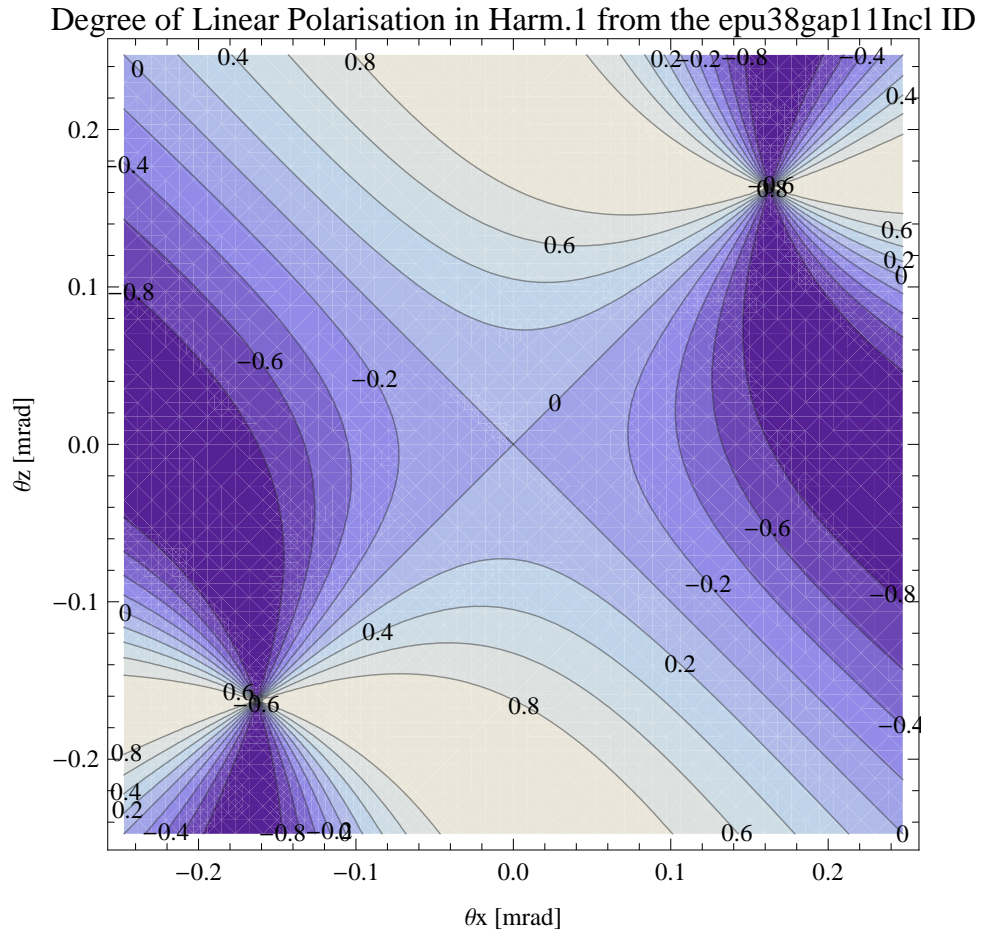


Figure 44: Map of linear polarisation in the fundamental harmonic of the synchrotron radiation emitted by the epu38gap11Incl ID

Degree of 45 degree Polarisation in Harm.1 from the epu38gap11Incl ID

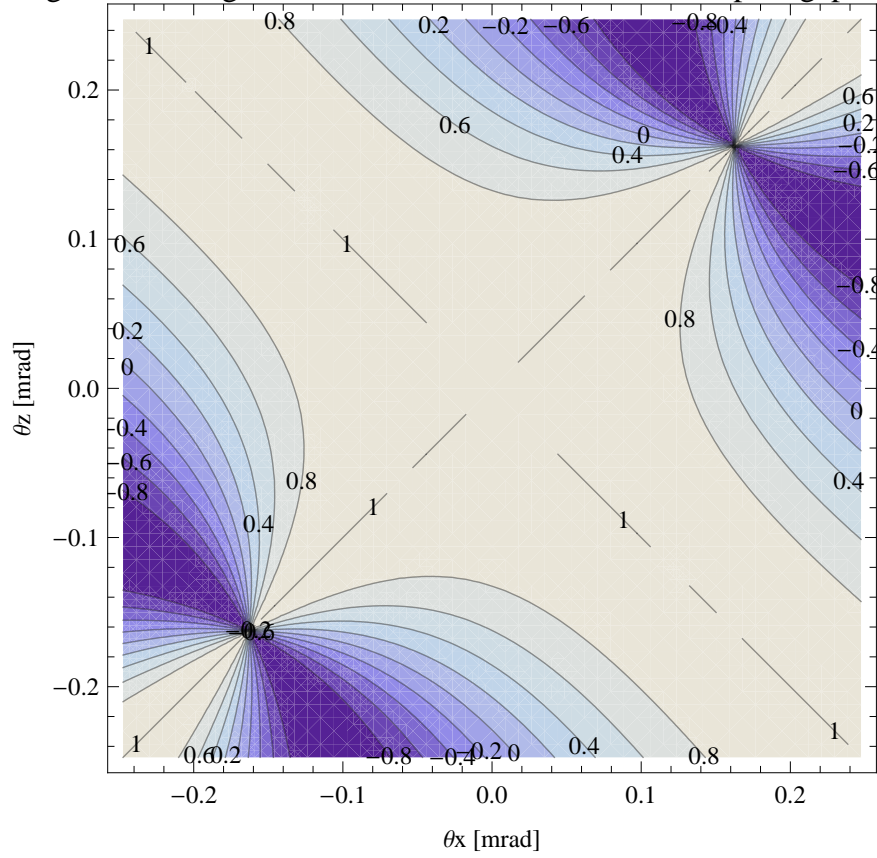


Figure 45: Map of 45 degree polarisation in the fundamental harmonic of the synchrotron radiation emitted by the epu38gap11Incl ID

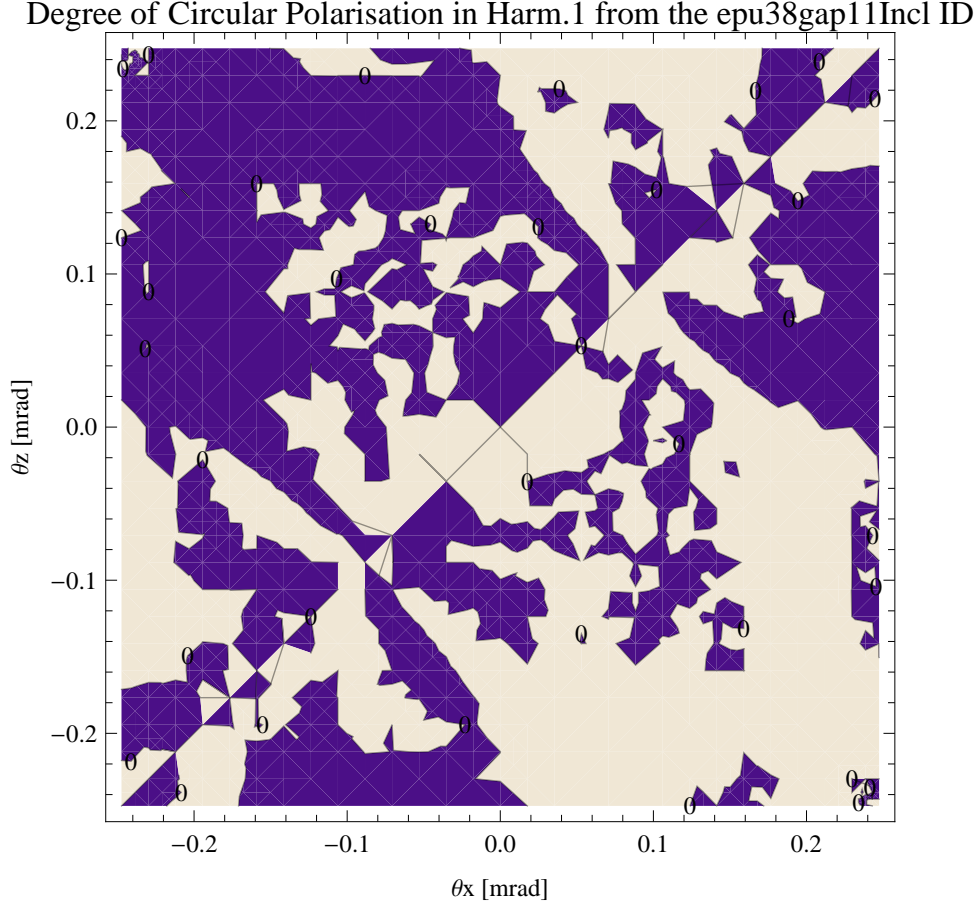


Figure 46: Map of circular polarisation in the fundamental harmonic of the synchrotron radiation emitted by the epu38gap11Incl ID

A map of the degree of circular polarisation of the fundamental harmonic of the synchrotron radiation emitted by the epu38gap11Incl ID over the angle of observation is shown in Figure 46.

The on axis brilliance at peak energy and the angular spectral flux from the epu38gap11Incl ID have been calculated with the given beam parameters, which are 0.5 A of stored current, $\beta_H = 9$ m, $\varepsilon_H = 0.263$ nmrad, $\beta_V = 4.8$ m, $\varepsilon_V = 8$ pmrad, and an energy spread of 0.001.

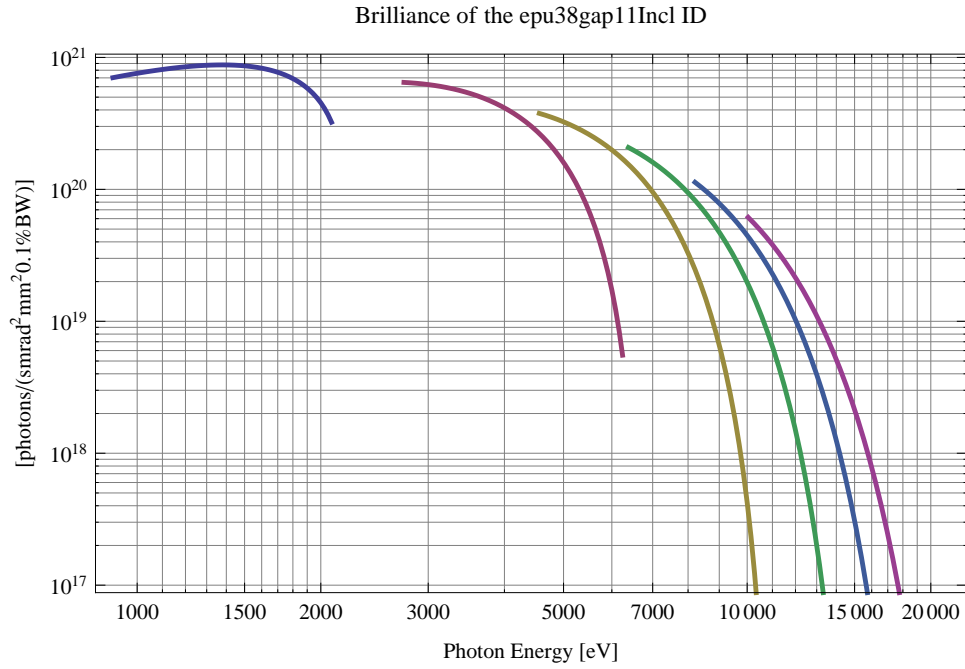


Figure 47: The brilliance at peak energy of the synchrotron radiation emitted by the epu38gap11Incl ID

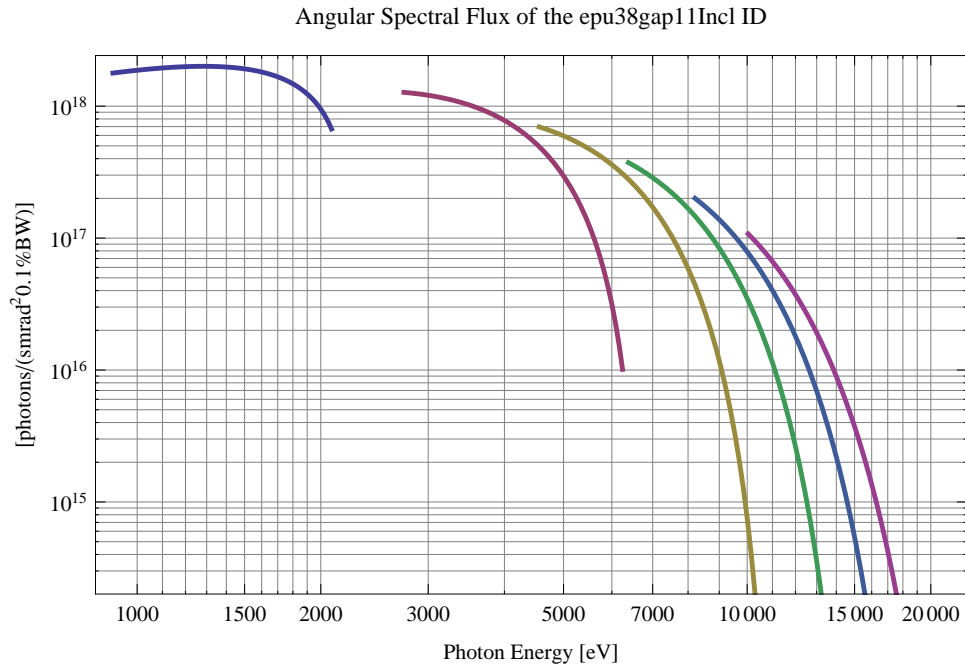


Figure 48: The angular spectral flux of the synchrotron radiation emitted by the epu38gap11Incl ID

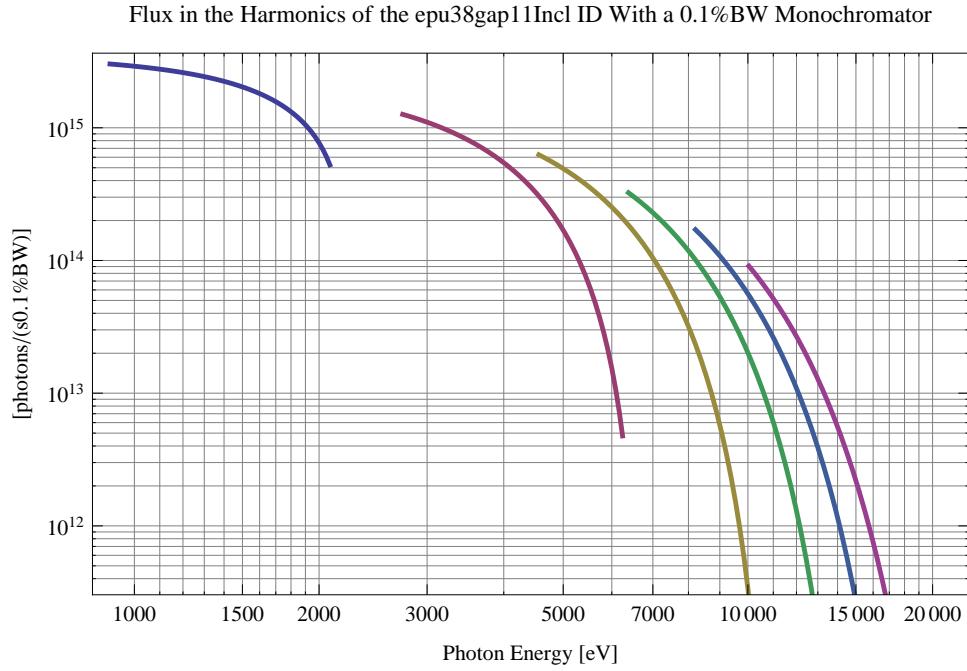


Figure 49: The flux of photons in the harmonics of the emitted synchrotron radiation from the epu38gap11Incl ID using a 0.1%BW monochromator

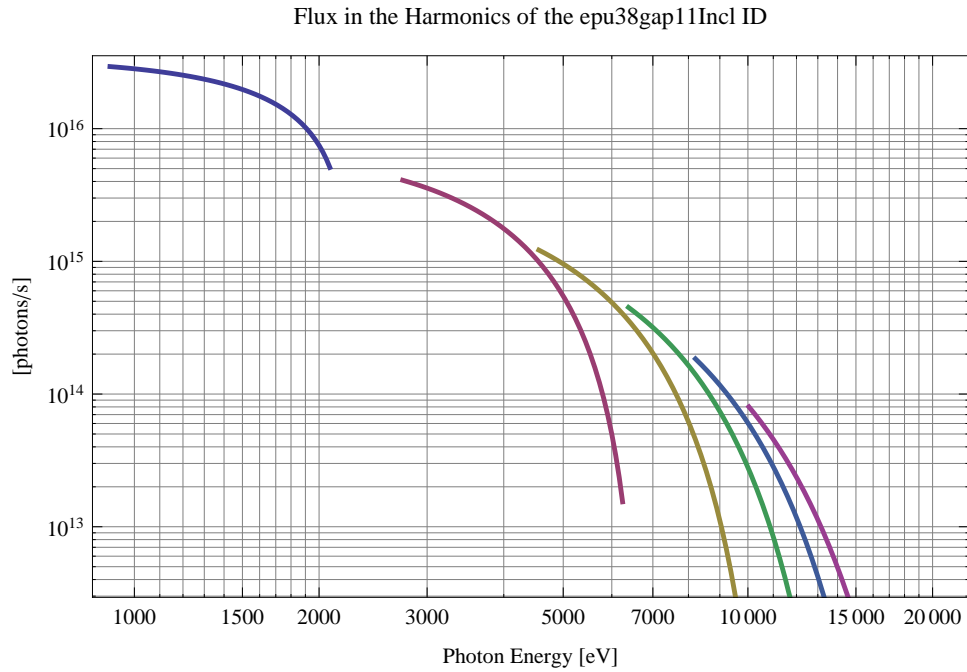


Figure 50: The flux of photons in the harmonics of the emitted synchrotron radiation from the epu38gap11Incl ID

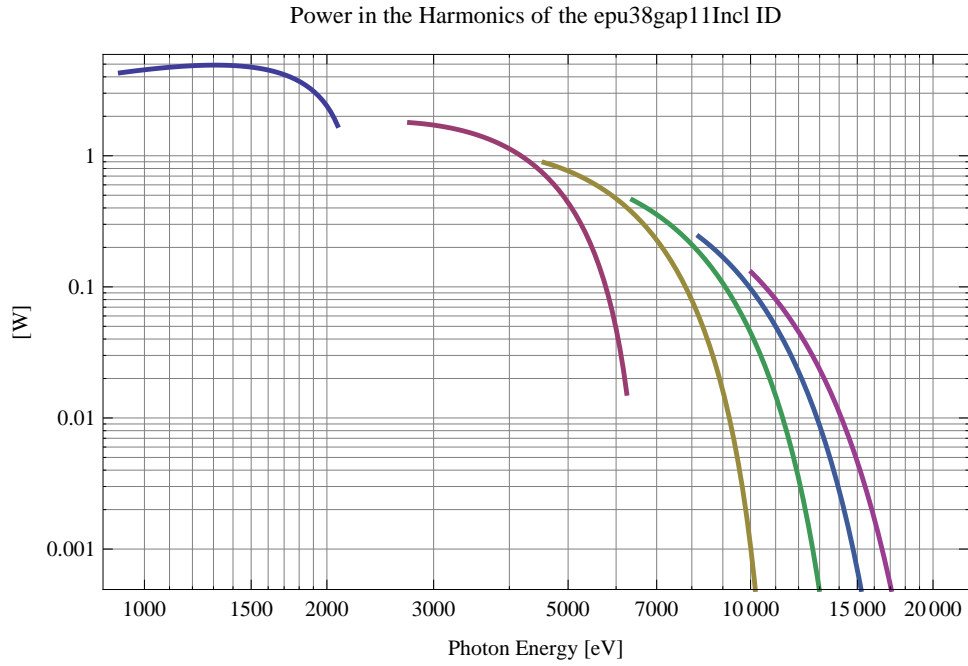


Figure 51: The power in the harmonics of the emitted synchrotron radiation from the epu38gap11Incl ID

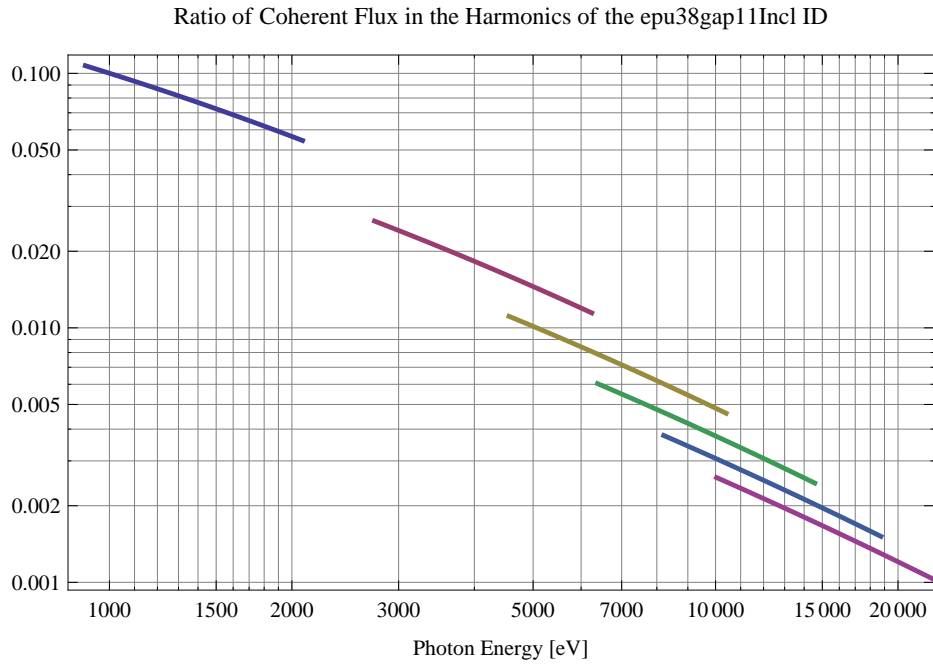


Figure 52: The ratio of coherent flux in the harmonics of the emitted synchrotron radiation from the epu38gap11Incl ID

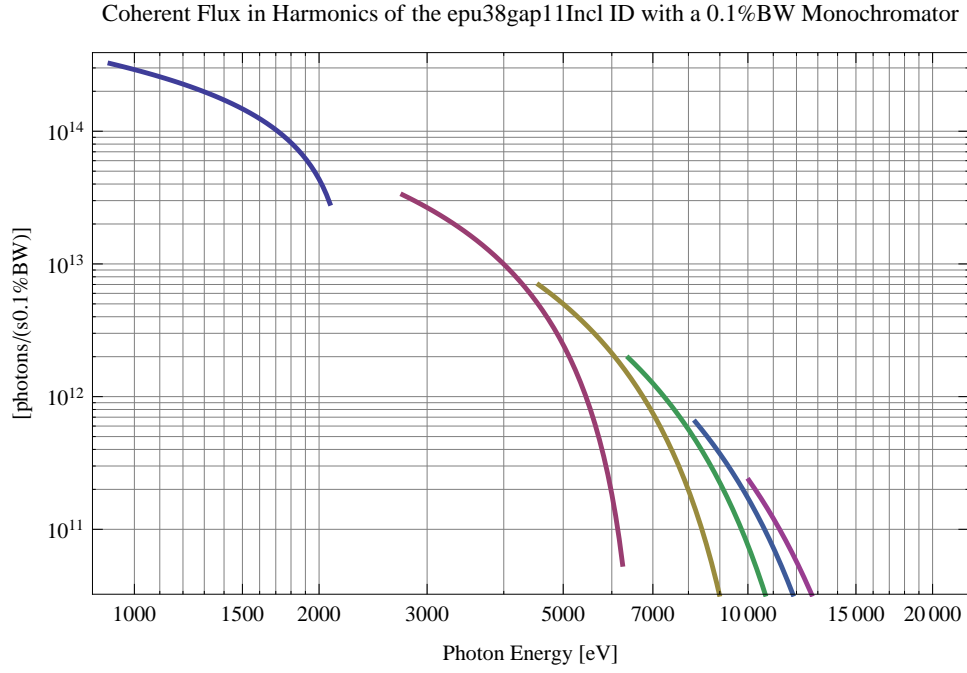


Figure 53: The coherent flux in the harmonics of the epu38gap11Incl ID using a 0.1%BW Monochromator

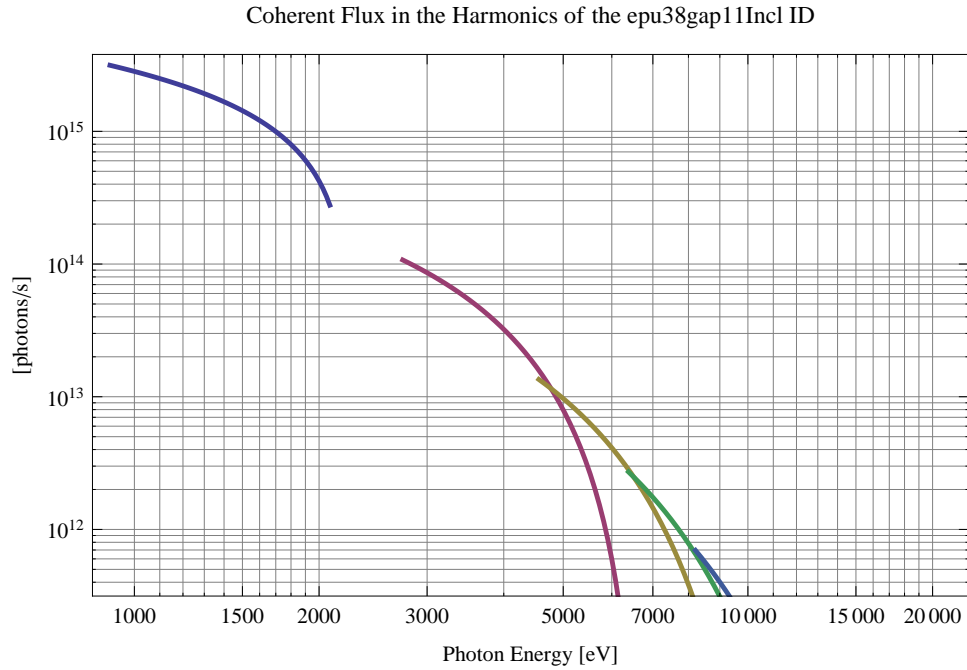


Figure 54: The coherent flux in the harmonics of the epu38gap11Incl ID

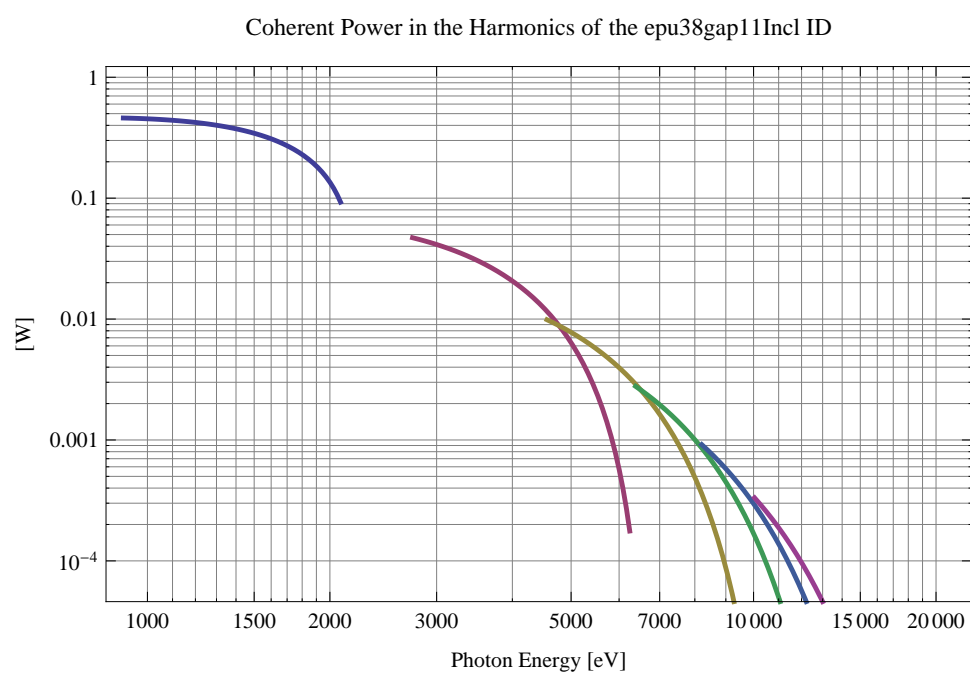


Figure 55: The power of coherent synchrotron radiation in the harmonics of the epu38gap11Incl ID

The brilliance at peak energy and the angular spectral flux density from the epu38gap11Incl ID for different harmonics at maximum K-value (1.712) are given in Table 9 and for minimum K-value (0.400) these values are given in Table 10.

Table 9: The brilliance at peak energy and the angular spectral flux density from the epu38gap11Incl ID for different harmonics at maximum K-value (1.712)

Harmonic	Photon Energy [eV]	Brilliance [Ph./ (smrad ² mrad ² 0.1% BW)]	Angular Spectral Flux [Ph./ (smrad ² 0.1% BW)]
1	912.518	7.02×10^{20}	1.78×10^{18}
3	2737.55	6.47×10^{20}	1.27×10^{18}
5	4562.59	3.77×10^{20}	6.96×10^{17}
7	6387.62	2.08×10^{20}	3.73×10^{17}
9	8212.66	1.13×10^{20}	$2. \times 10^{17}$
11	10037.7	6.14×10^{19}	1.08×10^{17}

Table 10: The brilliance at peak energy and the angular spectral flux density from the epu38gap11Incl ID for different harmonics at minimum K-value (0.4)

Harmonic	Photon Energy [eV]	Brilliance [Ph./ (smrad ² mrad ² 0.1% BW)]	Angular Spectral Flux [Ph./ (smrad ² 0.1% BW)]
1	2082.54	3.23×10^{20}	6.72×10^{17}
3	6247.63	5.54×10^{18}	1.01×10^{16}
5	10412.7	6.1×10^{16}	1.09×10^{14}
7	14577.8	6.35×10^{14}	1.12×10^{12}
9	18742.9	6.5×10^{12}	1.15×10^{10}
11	22908.	6.62×10^{10}	1.17×10^8

2.1.11 Magnet model of the elliptically polarising undulator epu38gap11Vert

The Radia [3] magnet model of the epu38gap11Vert ID is shown in Figure 56. The length of the magnet model is 320.976 mm. The magnetic material in the model is NdFeb with a remanence of 1.28 T, a material similar to VACODYM 776 TP from Vacuumschmelze. Blocks with vertical magnetisation are blue and blocks with horizontal magnetisation are yellow. The block size is 30.x30.x9.5 mm³ and there is a 5. mm cut-out in two of the corners of the blocks. The total length of the epu38gap11Vert ID is 3930.98 mm.

2.1.12 Analysis of the magnetic field of the epu38gap11Vert ID

The effective magnetic fields on axis and the fundamental photon energy of the epu38gap11Vert ID are shown in Table 11. The higher harmonic contents in the magnetic field of an elliptically polarising undulator made of permanent magnets is negligible and the effective field has about the same strength as the peak field.

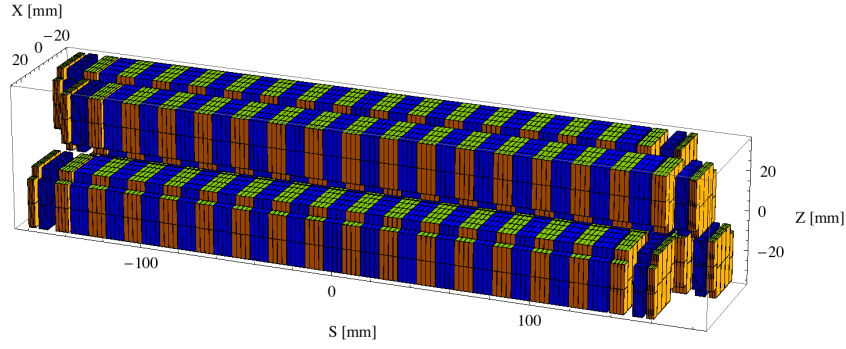


Figure 56: Magnetic model of the epu38gap11Vert ID. The ID has been modelled with Radia [3]

Table 11: Effective Fields on axis and Fundamental Photon Energy of the epu38gap11Vert ID

Undulator Period	38	mm
Undulator Gap	11	mm
Undulator Mode	Vertical	
Undulator Phase	19.000	mm
Vertical Peak Field	-0.001	T
Effective Vertical Field	0.000	T
Kx (from vert. field)	0.000	
Horizontal Peak Field:	0.577	T
Effective Horizontal Field	0.577	T
Kz (from hor. field)	2.048	
Photon Energy, Harm.1	0.727	keV
Emitted Power	3.726	kW
Total Length	3931.0	mm

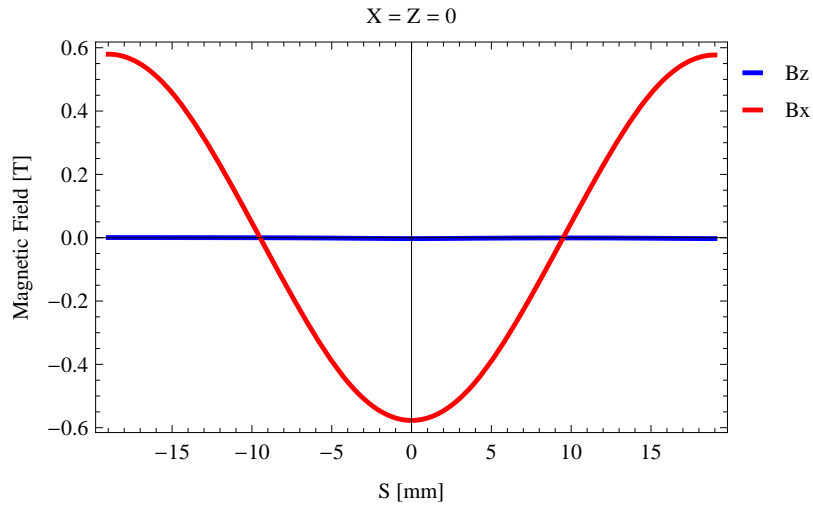


Figure 57: Vertical magnetic field in a central pole of the epu38gap11Vert ID along the ID axis, $X = Z = 0$

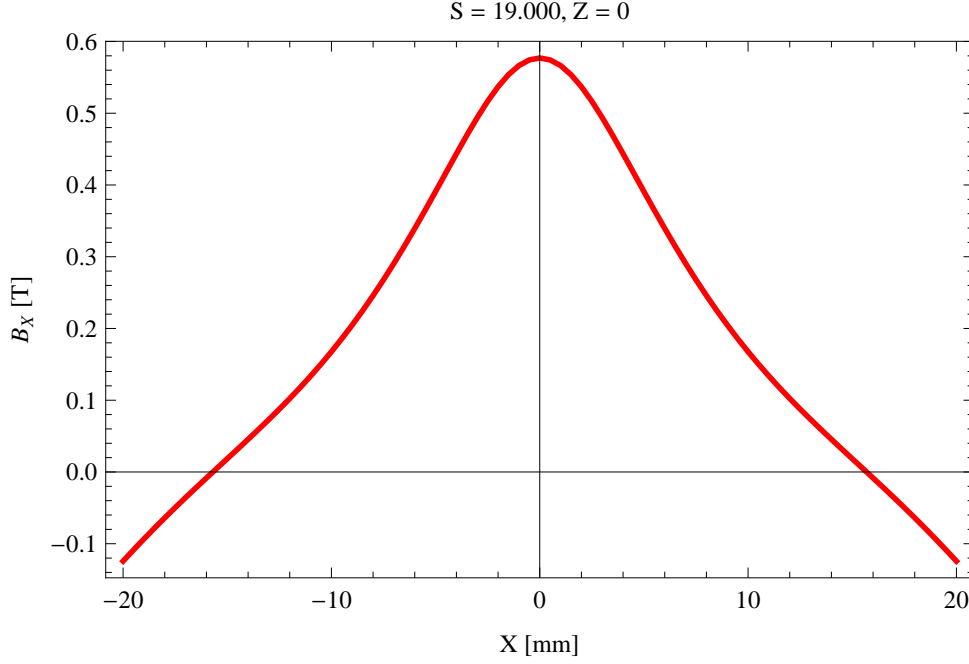


Figure 58: Horizontal magnetic field in a central pole of the epu38gap11Vert ID along the horizontally transverse direction to the ID axis, $S = 19.000$, $Z = 0$

2.1.13 Synchrotron radiation from the epu38gap11Vert ID

The power map of the emitted synchrotron radiation by the epu38gap11Vert ID, assuming a 0.5 A filament beam with an energy of 3 GeV and undulator properties of the synchrotron radiation, is shown in Figure 60. The on-axis power density is 25.385 kW/mrad²

A map of the degree of linear polarisation of the fundamental harmonic of the synchrotron radiation emitted by the epu38gap11Vert ID over the angle of observation is shown in Figure 61.

A map of the degree of 45 degree polarisation of the fundamental harmonic of the synchrotron radiation emitted by the epu38gap11Vert ID over the angle of observation is shown in Figure 62.

A map of the degree of circular polarisation of the fundamental harmonic of the synchrotron radiation emitted by the epu38gap11Vert ID over the angle of observation is shown in Figure 63.

The on axis brilliance at peak energy and the angular spectral flux from the epu38gap11Vert ID have been calculated with the given beam parameters, which are 0.5 A of stored current, $\beta_H = 9$ m, $\varepsilon_H = 0.263$ nmrad, $\beta_V = 4.8$ m, $\varepsilon_V = 8$ pmrad, and an energy spread of 0.001.

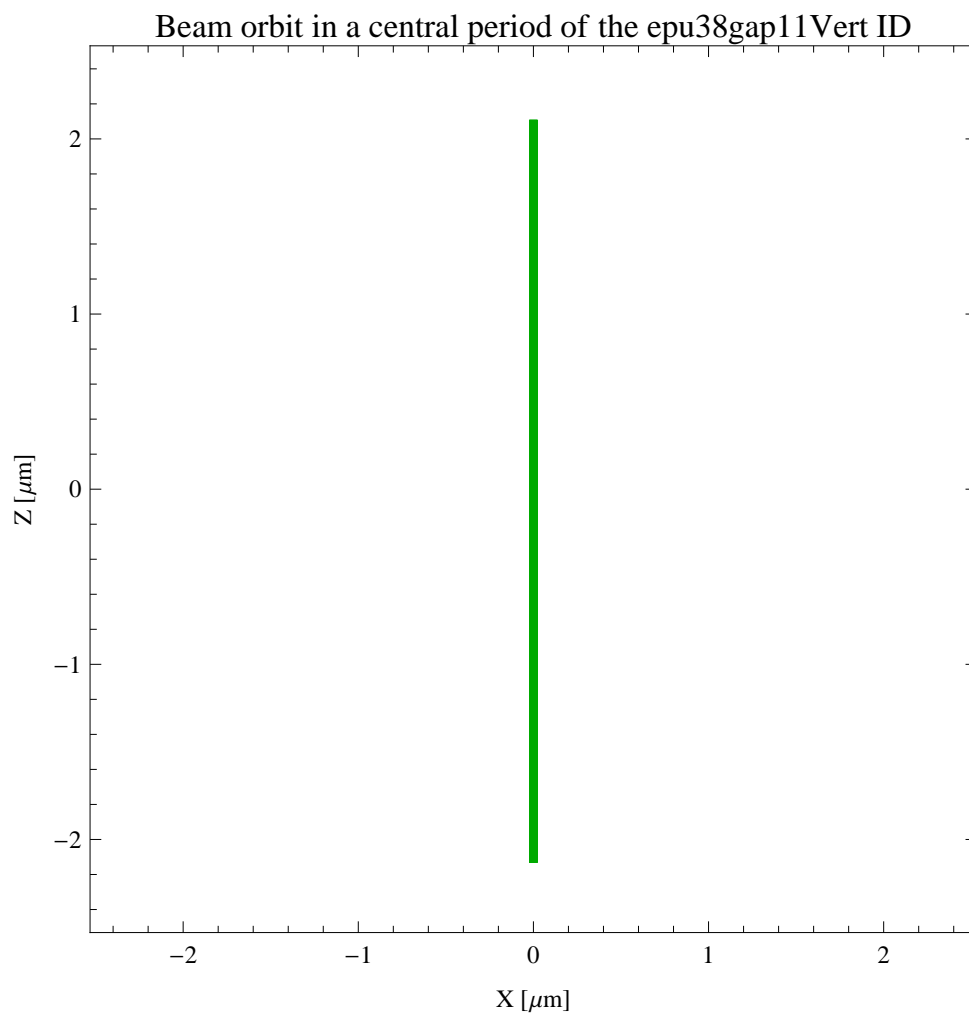


Figure 59: The beam orbit of the electron beam through a central period of the epu38gap11Vert ID

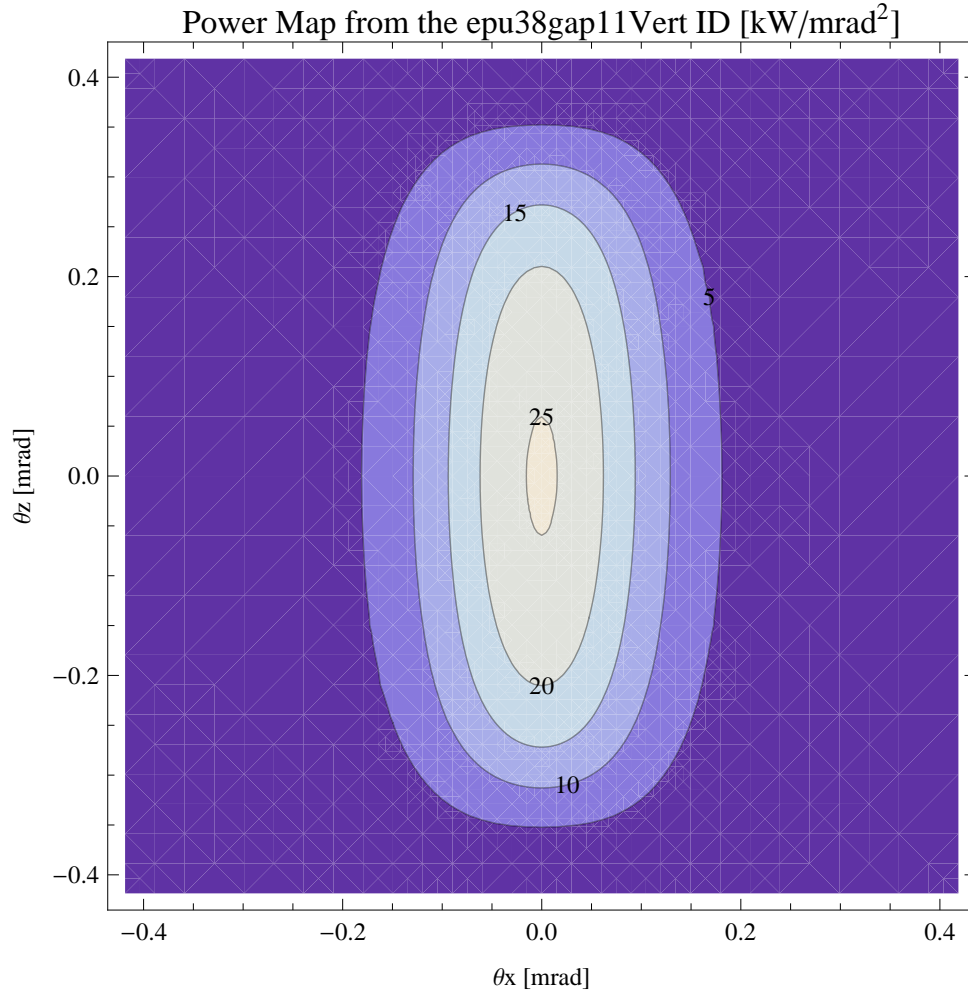


Figure 60: Map of the power distribution of the emitted synchrotron radiation by the epu38gap11Vert ID

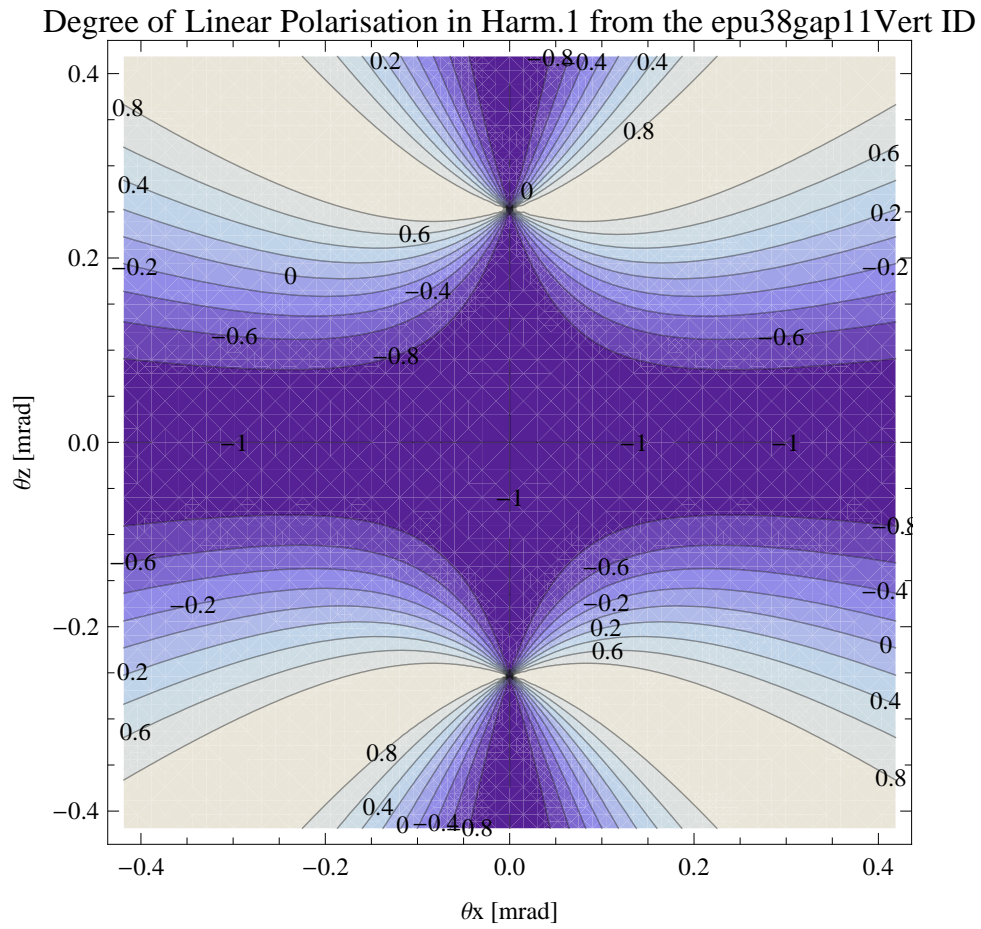


Figure 61: Map of linear polarisation in the fundamental harmonic of the synchrotron radiation emitted by the epu38gap11Vert ID

Degree of 45 degree Polarisation in Harm.1 from the epu38gap11Vert ID

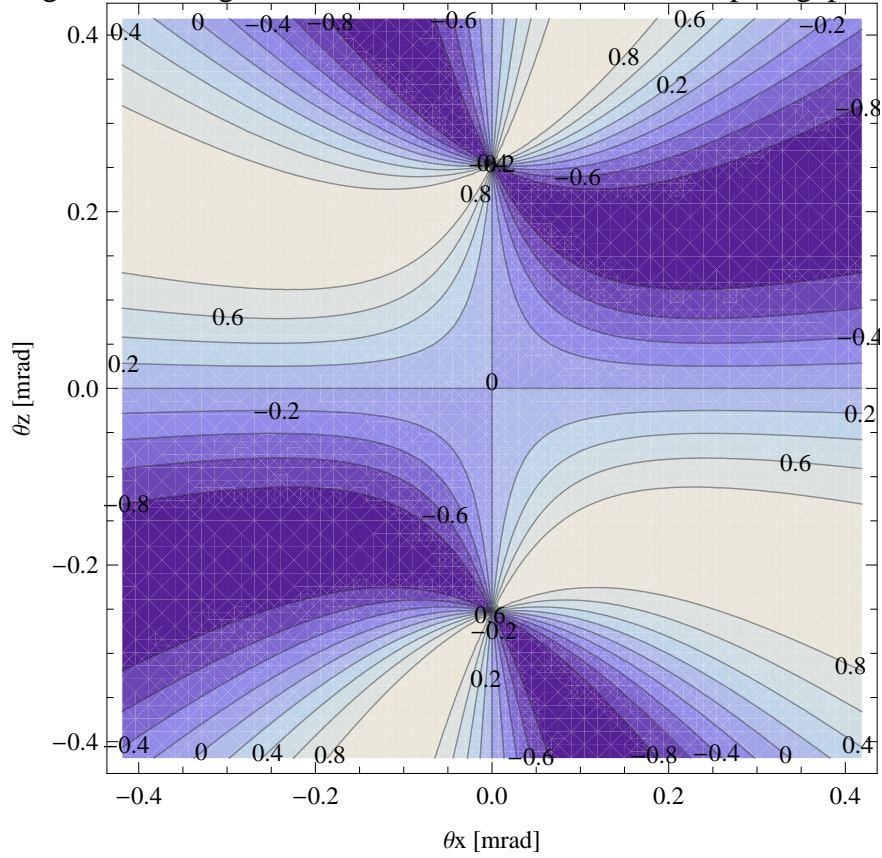


Figure 62: Map of 45 degree polarisation in the fundamental harmonic of the synchrotron radiation emitted by the epu38gap11Vert ID

Degree of Circular Polarisation in Harm.1 from the epu38gap11Vert ID

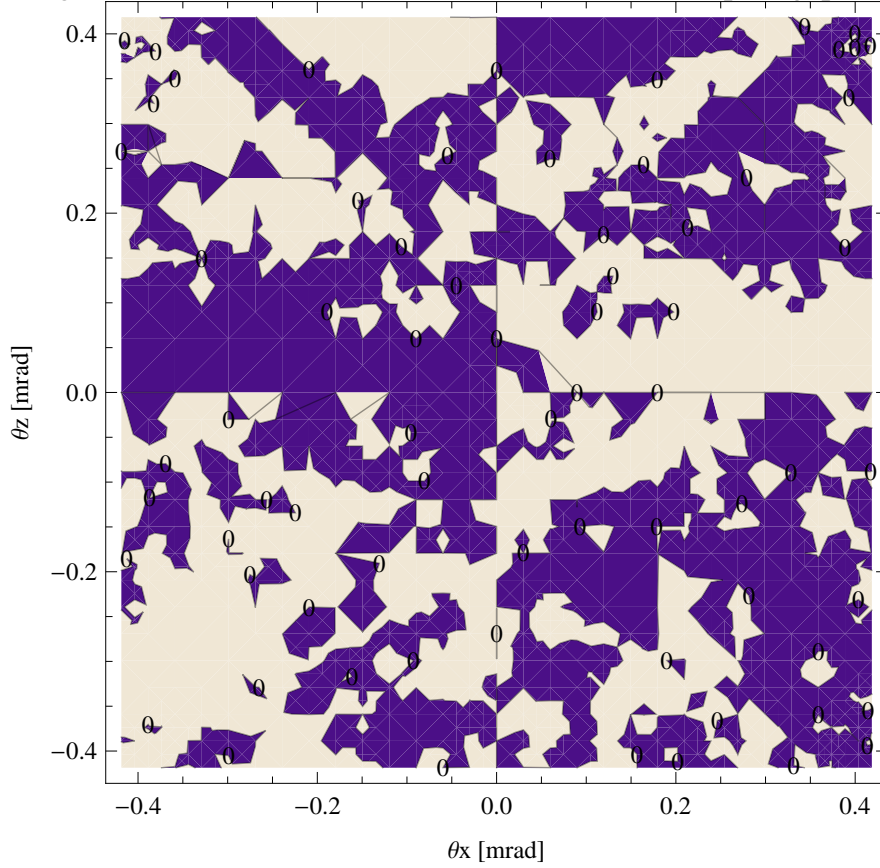


Figure 63: Map of circular polarisation in the fundamental harmonic of the synchrotron radiation emitted by the epu38gap11Vert ID

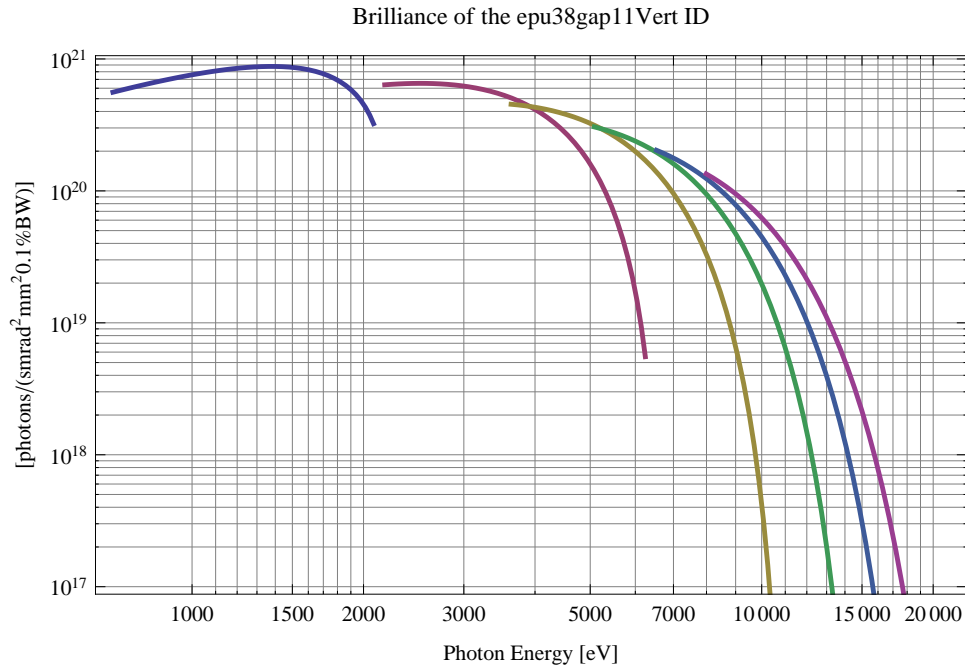


Figure 64: The brilliance at peak energy of the synchrotron radiation emitted by the epu38gap11Vert ID

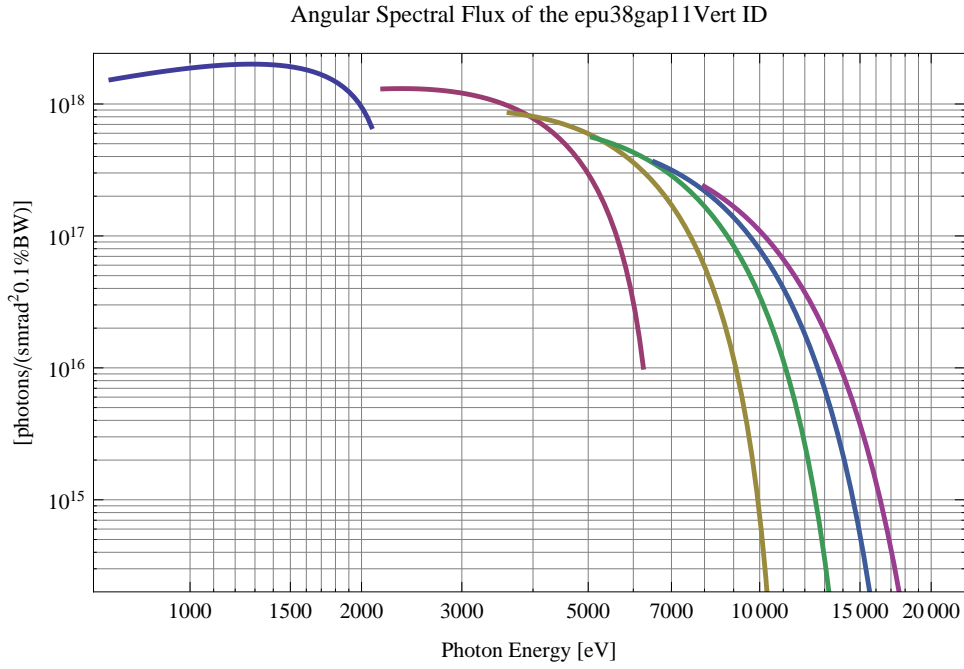


Figure 65: The angular spectral flux of the synchrotron radiation emitted by the epu38gap11Vert ID

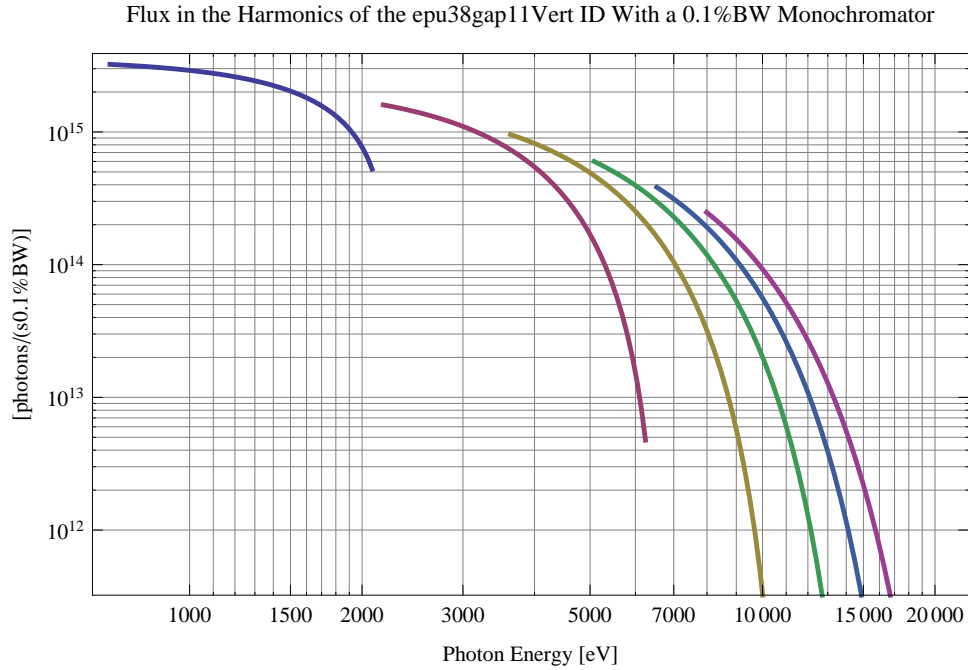


Figure 66: The flux of photons in the harmonics of the emitted synchrotron radiation from the epu38gap11Vert ID using a 0.1% BW monochromator

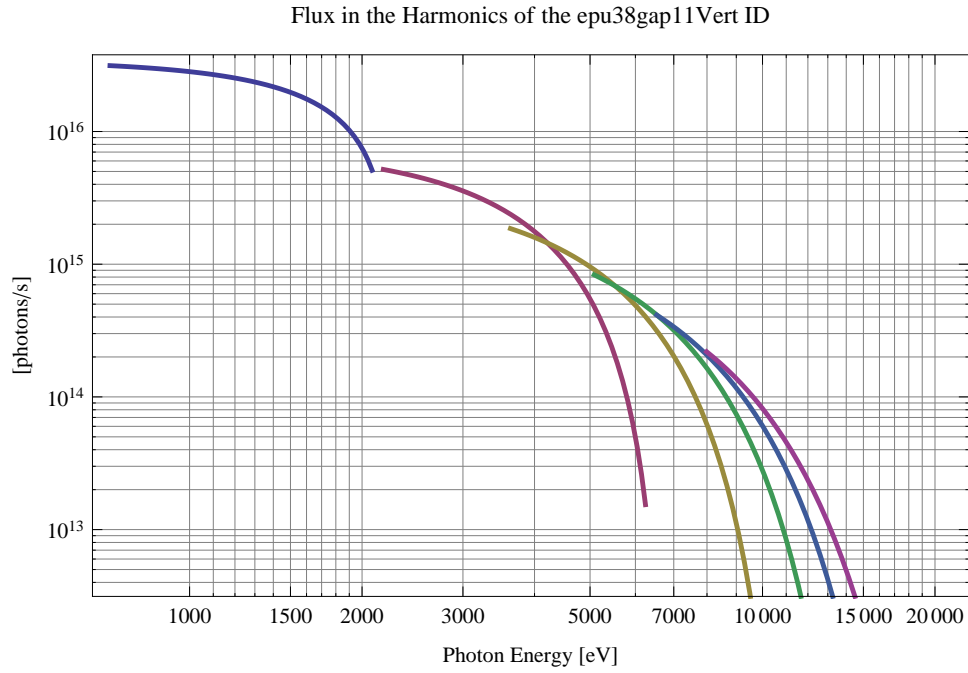


Figure 67: The flux of photons in the harmonics of the emitted synchrotron radiation from the epu38gap11Vert ID

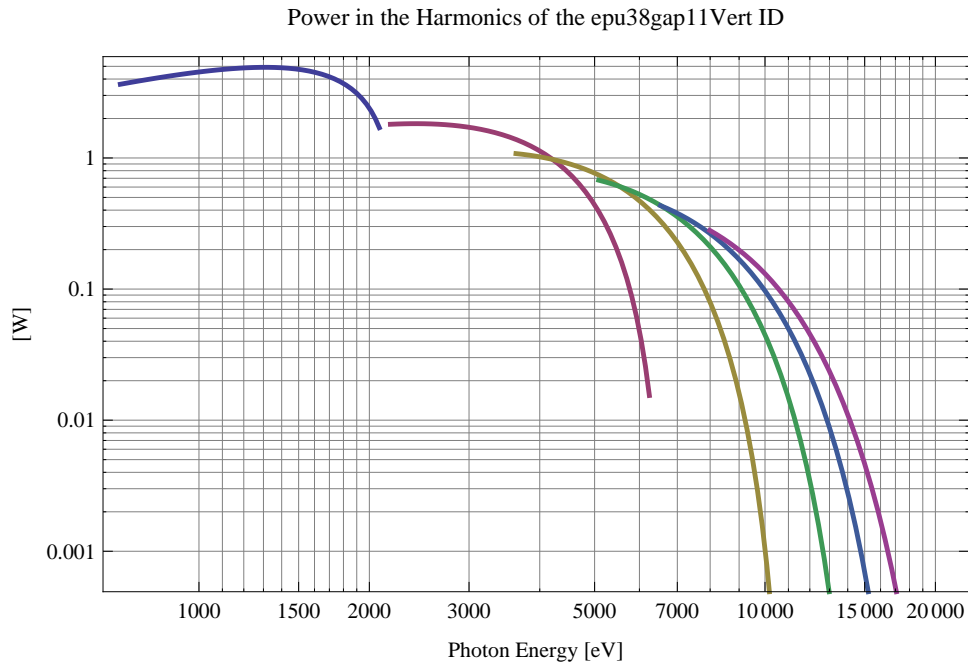


Figure 68: The power in the harmonics of the emitted synchrotron radiation from the epu38gap11Vert ID

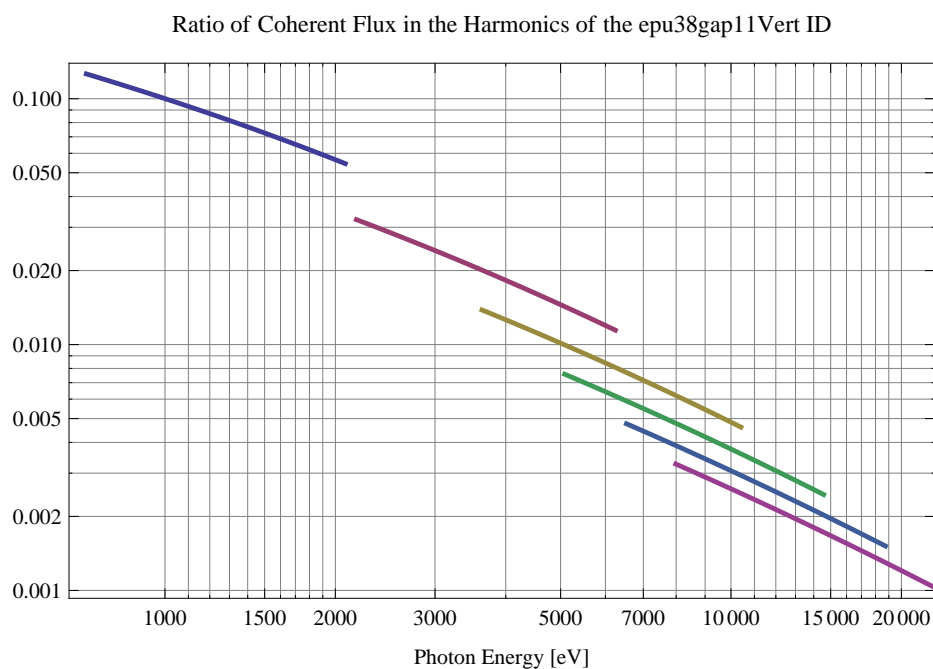


Figure 69: The ratio of coherent flux in the harmonics of the emitted synchrotron radiation from the epu38gap11Vert ID

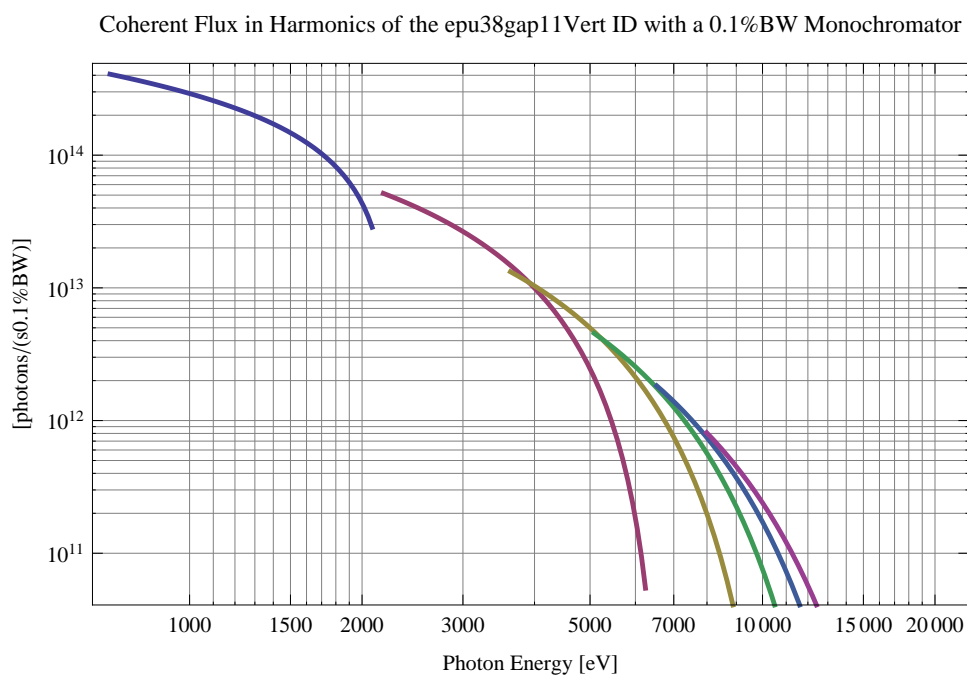


Figure 70: The coherent flux in the harmonics of the epu38gap11Vert ID using a 0.1%BW Monochromator

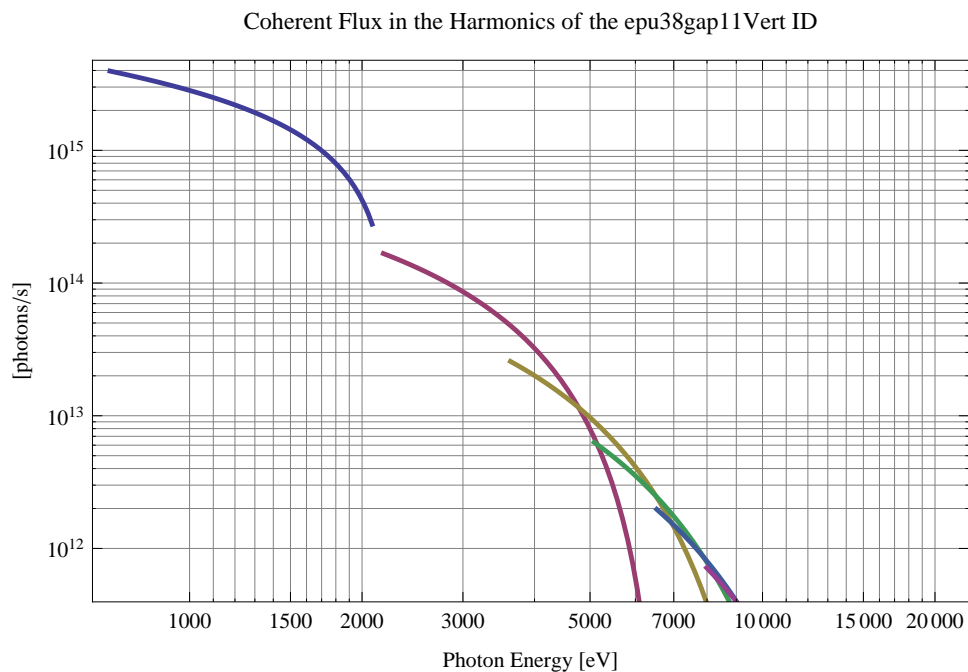


Figure 71: The coherent flux in the harmonics of the epu38gap11Vert ID

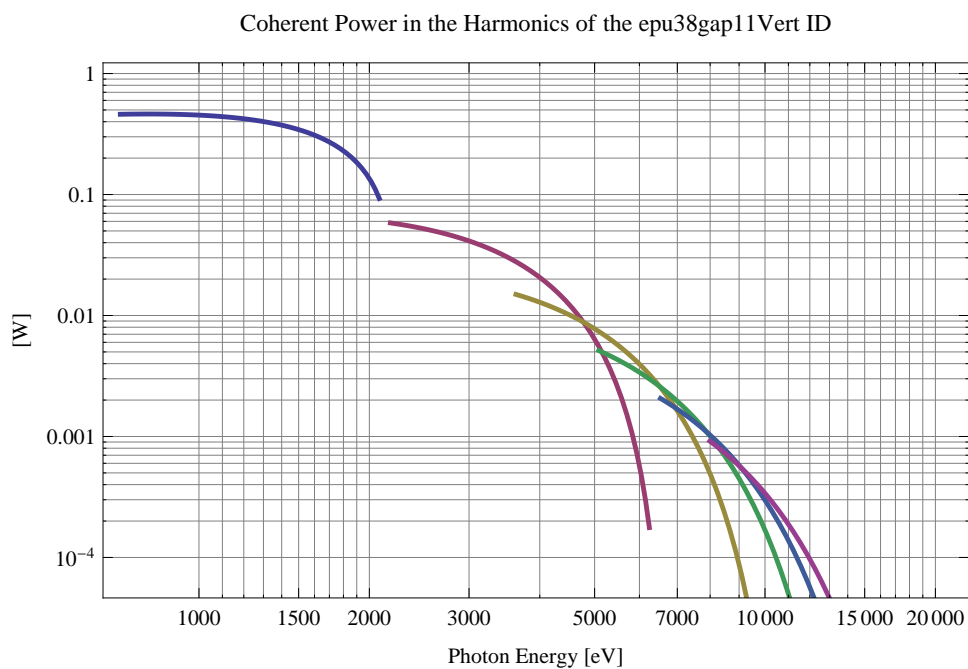


Figure 72: The power of coherent synchrotron radiation in the harmonics of the epu38gap11Vert ID

The brilliance at peak energy and the angular spectral flux density from the epu38gap11Vert ID for different harmonics at maximum K-value (2.048) are given in Table 12 and for minimum K-value (0.400) these values are given in Table 13.

Table 12: The brilliance at peak energy and the angular spectral flux density from the epu38gap11Vert ID for different harmonics at maximum K-value (2.048)

Harmonic	Photon Energy [eV]	Brilliance [Ph./ (smrad ² mrad ² 0.1% BW)]	Angular Spectral Flux [Ph./ (smrad ² 0.1% BW)]
1	726.252	5.59×10^{20}	1.53×10^{18}
3	2178.76	6.37×10^{20}	1.3×10^{18}
5	3631.26	4.54×10^{20}	8.58×10^{17}
7	5083.76	3.05×10^{20}	5.58×10^{17}
9	6536.27	2.03×10^{20}	3.64×10^{17}
11	7988.77	1.35×10^{20}	2.38×10^{17}

Table 13: The brilliance at peak energy and the angular spectral flux density from the epu38gap11Vert ID for different harmonics at minimum K-value (0.4)

Harmonic	Photon Energy [eV]	Brilliance [Ph./ (smrad ² mrad ² 0.1% BW)]	Angular Spectral Flux [Ph./ (smrad ² 0.1% BW)]
1	2082.54	3.23×10^{20}	6.72×10^{17}
3	6247.63	5.54×10^{18}	1.01×10^{16}
5	10412.7	6.1×10^{16}	1.09×10^{14}
7	14577.8	6.35×10^{14}	1.12×10^{12}
9	18742.9	6.5×10^{12}	1.15×10^{10}
11	22908.	6.62×10^{10}	1.17×10^8

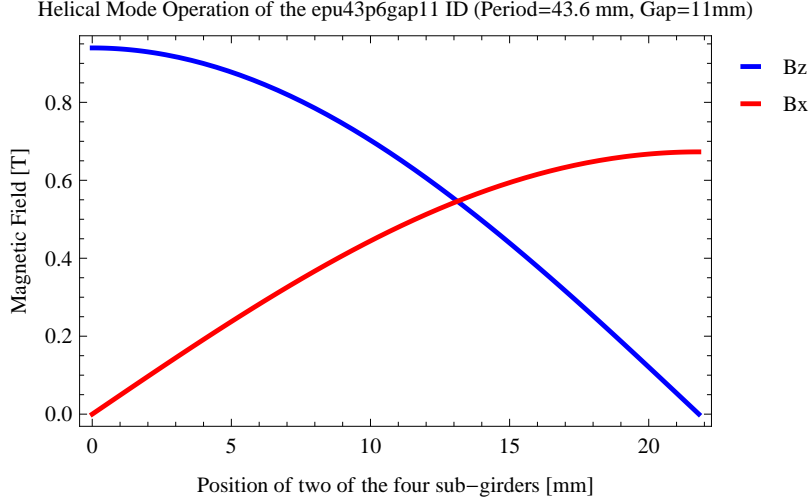


Figure 73: Vertical and horizontal magnetic field for the the epu43p6gap11 ID when operating in the helical mode for different positions for two of the four sub-girders

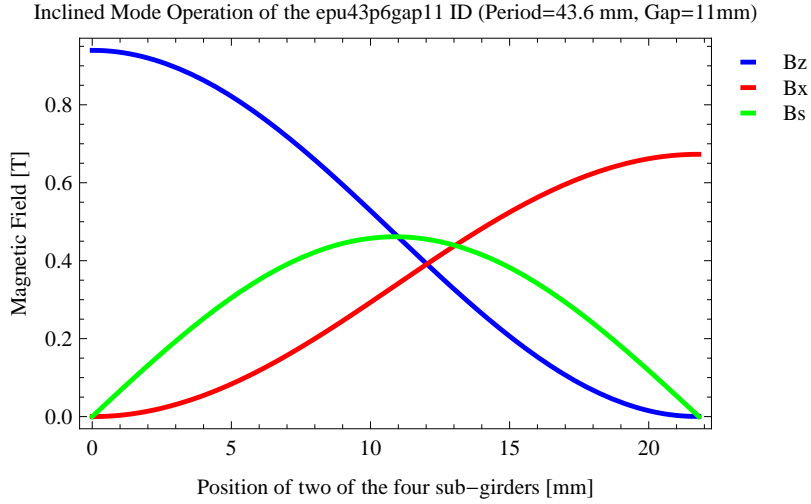


Figure 74: Vertical, horizontal, and longitudinal magnetic field for the the epu43p6gap11 ID when operating in the inclined mode for different positions for two of the four sub-girders

2.2 The elliptically polarising undulator epu43p6gap11

2.2.1 Modes of operation in the elliptically polarising undulator epu43p6gap11

Horizontal polarisation of the emitted synchrotron radiation from the epu43p6gap11 ID (Period=43.6 mm, Gap=11mm) is found in the planar mode when there is no movement of the sub-girders.

Circular polarisation is found in the elliptical mode of operation for a symmetric sub-grider movement of 13.1256 mm. Figure 73 shows the vertical and horizontal magnetic field for the epu43p6gap11 ID when operating in the helical mode.

45 degree polarisation is found in the inclined mode of operation for an assymetric sub-grider movement of 12.0267 mm. Figure 74 shows the vertical and horizontal magnetic field for the epu43p6gap11 ID when operating in the inclined mode.

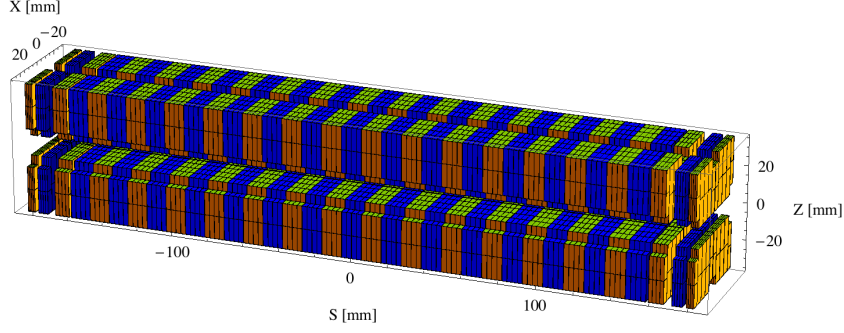


Figure 75: Magnetic model of the epu43p6gap11Plan ID. The ID has been modelled with Radia [3]

The following sub-sections will cover four different situations: The epu43p6gap11 operating in the planar mode for horizontal polarisation (epu43p6gap11Plan); The epu43p6gap11 operating in the helical mode for circular polarisation (epu43p6gap11Heli), the epu43p6gap11 operating in the inclined mode for 45 degree polarisation (epu43p6gap11Incl); and The epu43p6gap11 operating in the vertical mode for vertical polarisation (epu43p6gap11Vert).

2.2.2 Magnet model of the elliptically polarising undulator epu43p6gap11Plan

The Radia [3] magnet model of the epu43p6gap11Plan ID is shown in Figure 75. The length of the magnet model is 366.067 mm. The magnetic material in the model is NdFeb with a remanence of 1.28 T, a material similar to VACODYM 776 TP from Vacuumschmelze. Blocks with vertical magnetisation are blue and blocks with horizontal magnetisation are yellow. The block size is $30 \times 30 \times 10.9 \text{ mm}^3$ and there is a 5. mm cut-out in two of the corners of the blocks. The total length of the epu43p6gap11Plan ID is 3941.27 mm.

2.2.3 Analysis of the magnetic field of the epu43p6gap11Plan ID

The effective magnetic fields on axis and the fundamental photon energy of the epu43p6gap11Plan ID are shown in Table 14. The higher harmonic contents in the magnetic field of an elliptically polarising undulator made of permanent magnets is negligible and the effective field has about the same strength as the peak field.

2.2.4 Synchrotron radiation from the epu43p6gap11Plan ID

The power map of the emitted synchrotron radiation by the epu43p6gap11Plan ID, assuming a 0.5 A filament beam with an energy of 3 GeV and undulator properties of the synchrotron radiation, is shown in Figure 79. The on-axis power density is 36.551 kW/mrad^2

A map of the degree of linear polarisation of the fundamental harmonic of the synchrotron radiation emitted by the epu43p6gap11Plan ID over the angle of observation is shown in Figure 80.

A map of the degree of 45 degree polarisation of the fundamental harmonic of the synchrotron radiation emitted by the epu43p6gap11Plan ID over the angle of observation is shown in Figure 81.

Table 14: Effective Fields on axis and Fundamental Photon Energy of the epu43p6gap11Plan ID

Undulator Period	43.6	mm
Undulator Gap	11	mm
Undulator Mode	Planar	
Undulator Phase	0.000	mm
Vertical Peak Field	0.930	T
Effective Vertical Field	0.940	T
Kx (from vert. field)	3.828	
Horizontal Peak Field:	0.000	T
Effective Horizontal Field	0.000	T
Kz (from hor. field)	0.000	
Photon Energy, Harm.1	0.236	keV
Emitted Power	9.915	kW
Total Length	3941.3	mm

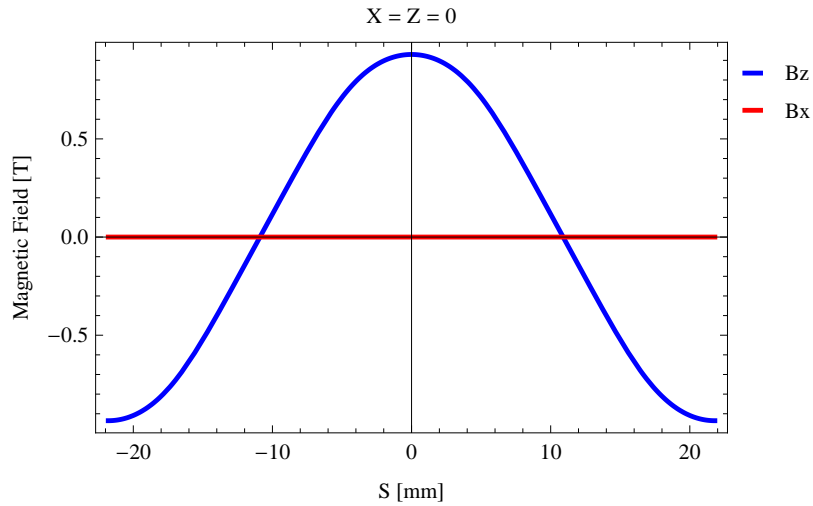


Figure 76: Vertical magnetic field in a central pole of the epu43p6gap11Plan ID along the ID axis, $X = Z = 0$

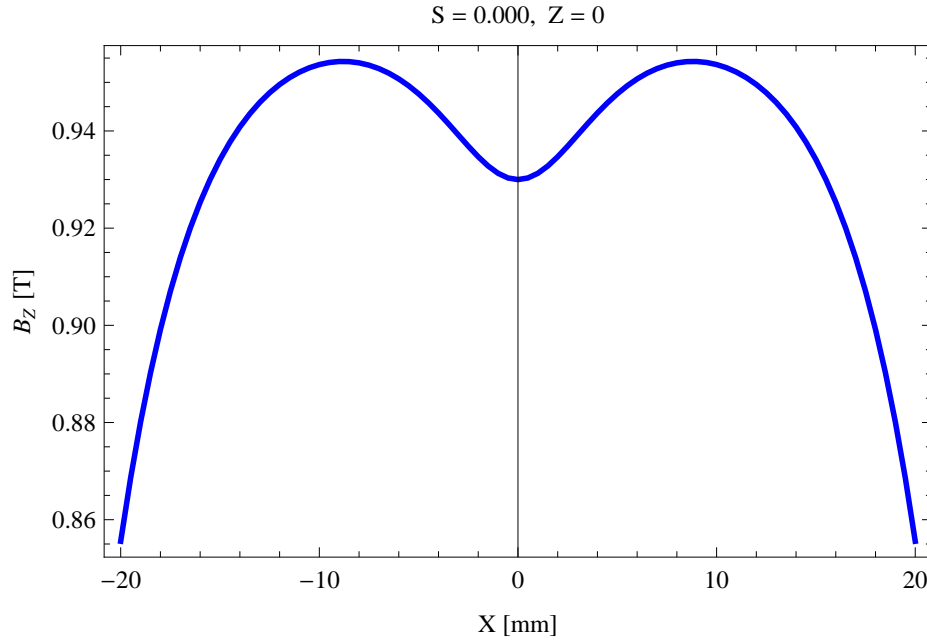


Figure 77: Vertical magnetic field in a central pole of the epu43p6gap11Plan ID along the horizontally transverse direction to the ID axis, $S = 0.000, Z = 0$

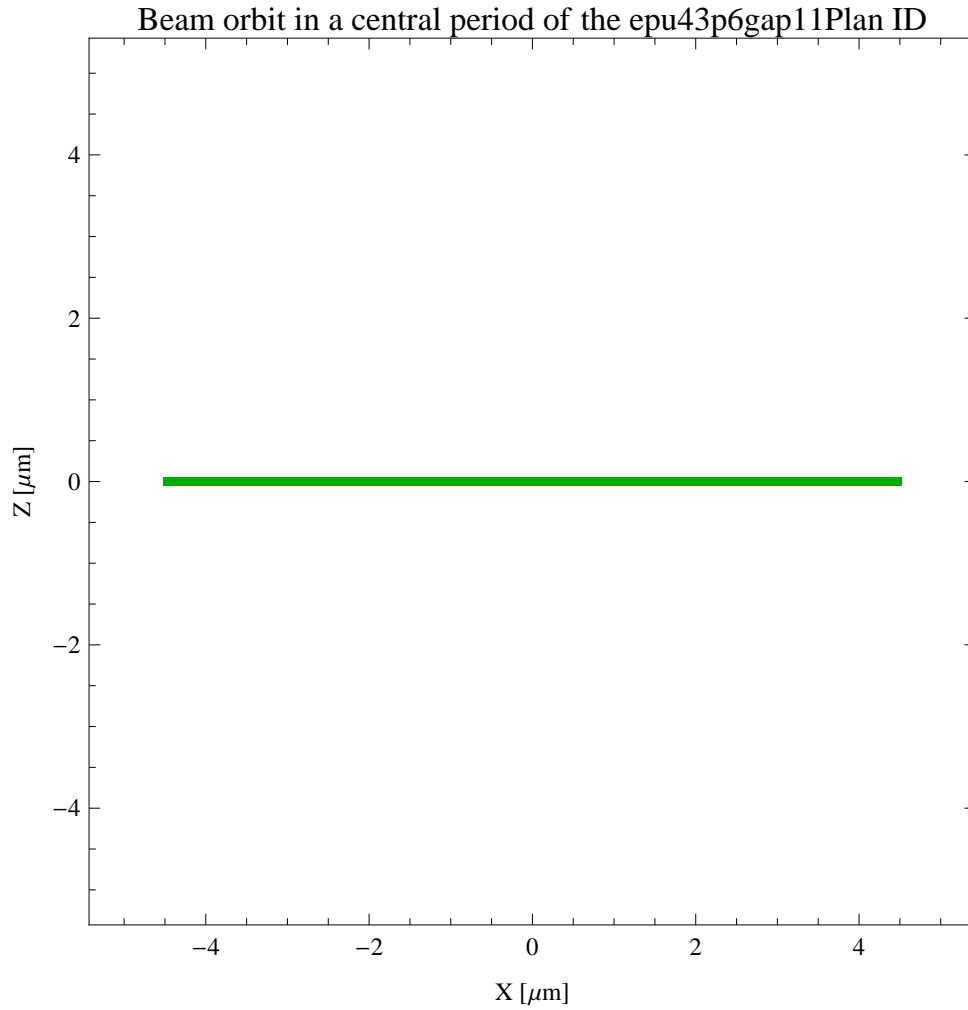


Figure 78: The beam orbit of the electron beam through a central period of the epu43p6gap11Plan ID

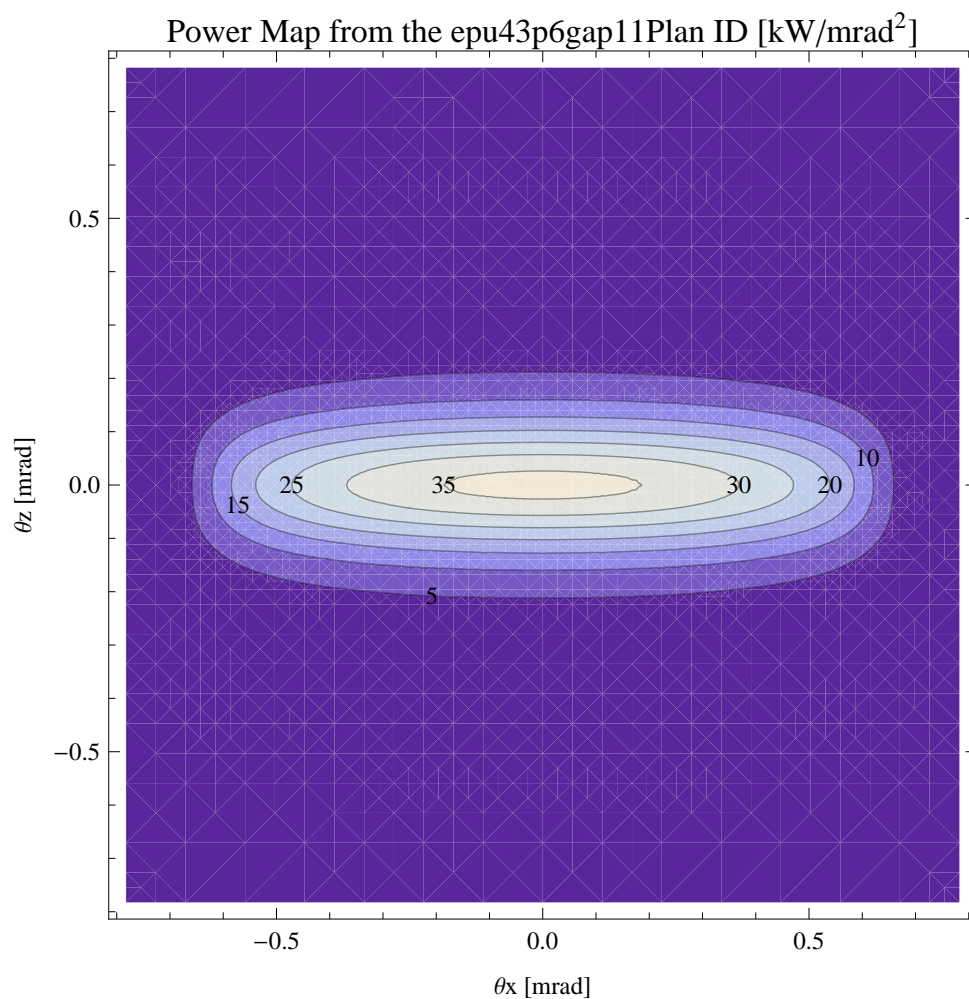


Figure 79: Map of the power distribution of the emitted synchrotron radiation by the epu43p6gap11Plan ID

Degree of Linear Polarisation in Harm.1 from the epu43p6gap11Plan ID

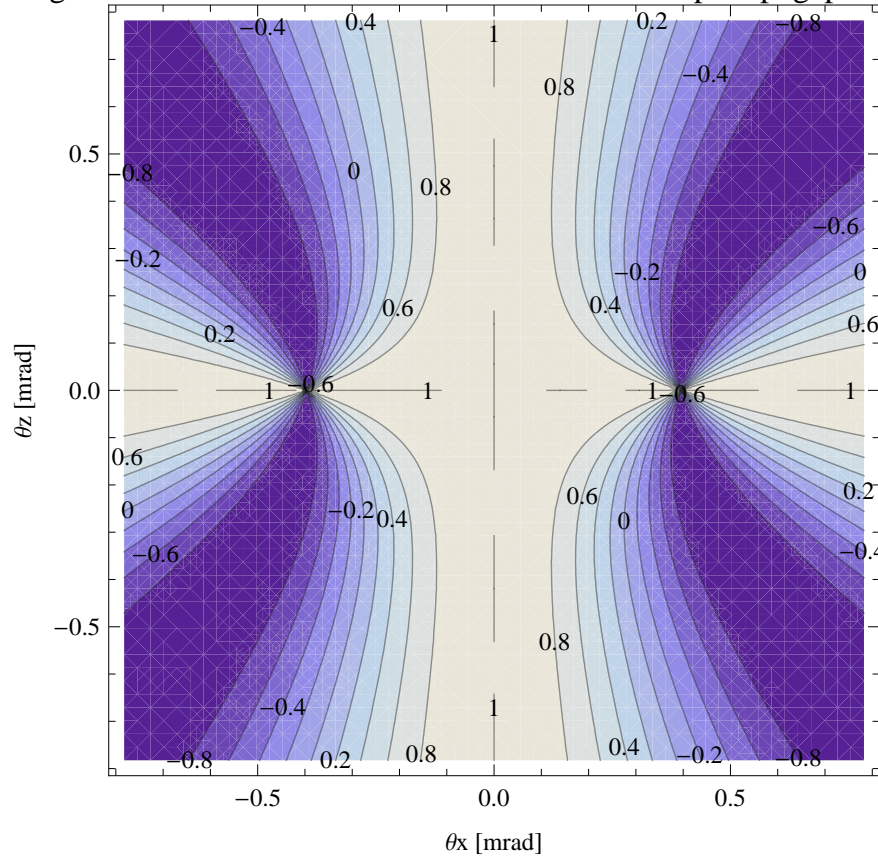


Figure 80: Map of linear polarisation in the fundamental harmonic of the synchrotron radiation emitted by the epu43p6gap11Plan ID

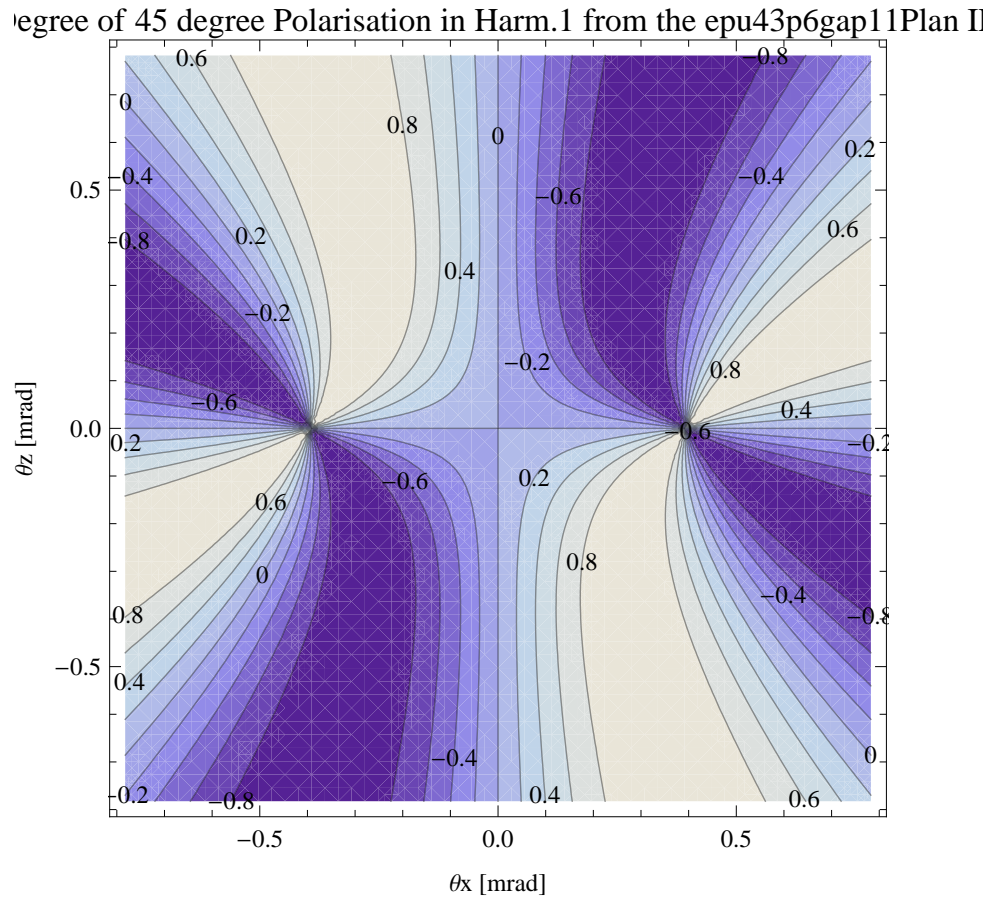


Figure 81: Map of 45 degree polarisation in the fundamental harmonic of the synchrotron radiation emitted by the epu43p6gap11Plan ID

Degree of Circular Polarisation in Harm.1 from the epu43p6gap11Plan II

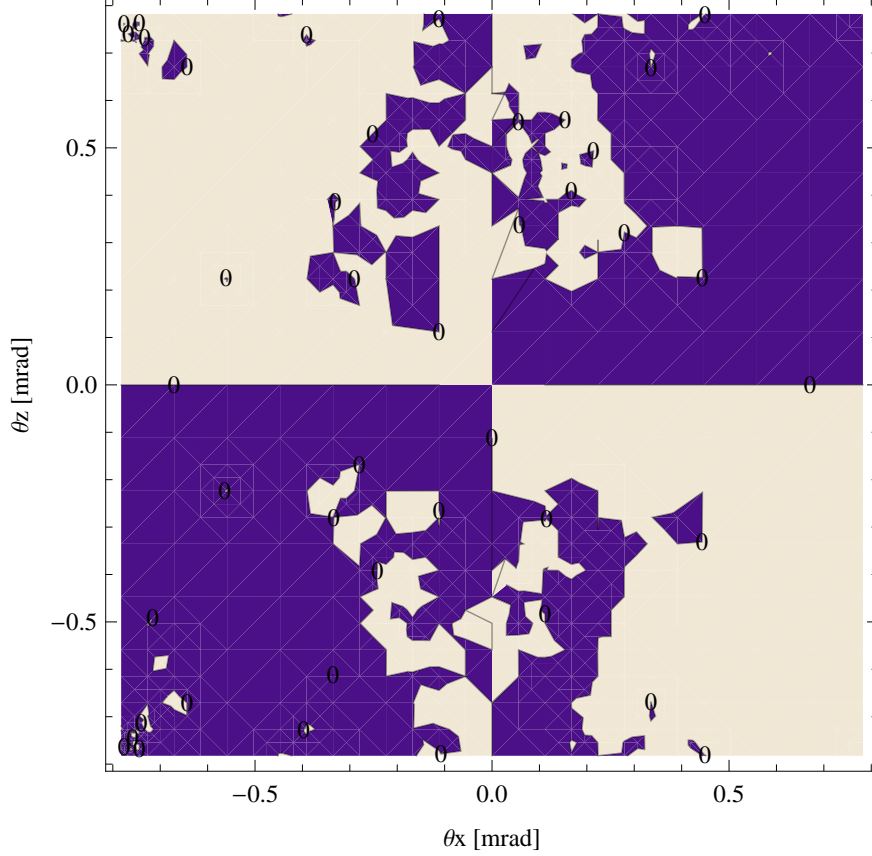


Figure 82: Map of circular polarisation in the fundamental harmonic of the synchrotron radiation emitted by the epu43p6gap11Plan ID

A map of the degree of circular polarisation of the fundamental harmonic of the synchrotron radiation emitted by the epu43p6gap11Plan ID over the angle of observation is shown in Figure 82.

The on axis brilliance at peak energy and the angular spectral flux from the epu43p6gap11Plan ID have been calculated with the given beam parameters, which are 0.5 A of stored current, $\beta_H = 9$ m, $\varepsilon_H = 0.263$ nmrad, $\beta_V = 4.8$ m, $\varepsilon_V = 8$. pmrad, and an energy spread of 0.001.

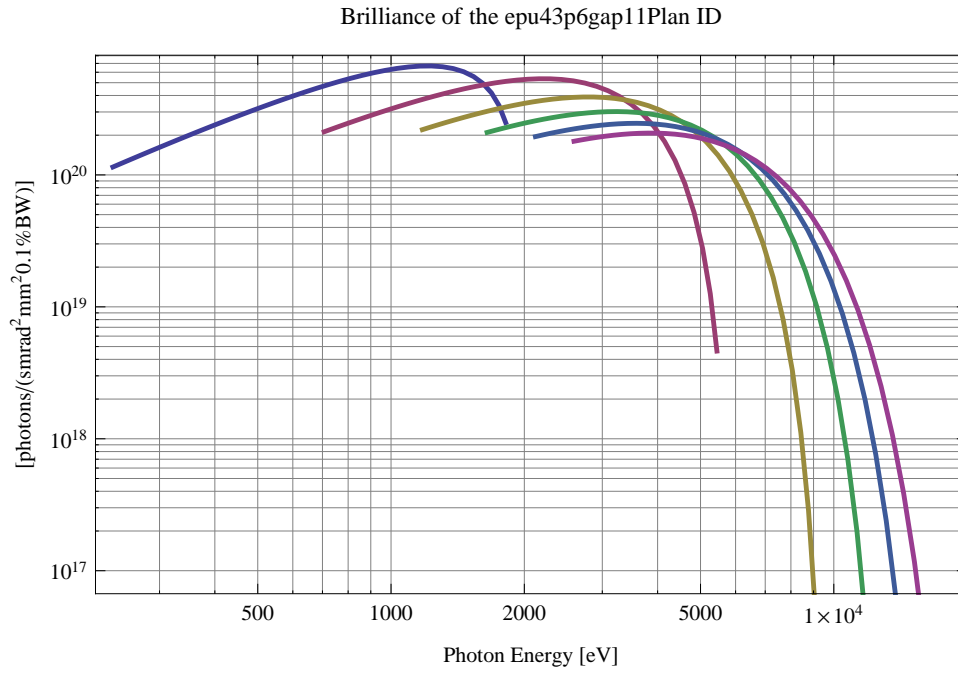


Figure 83: The brilliance at peak energy of the synchrotron radiation emitted by the epu43p6gap11Plan ID

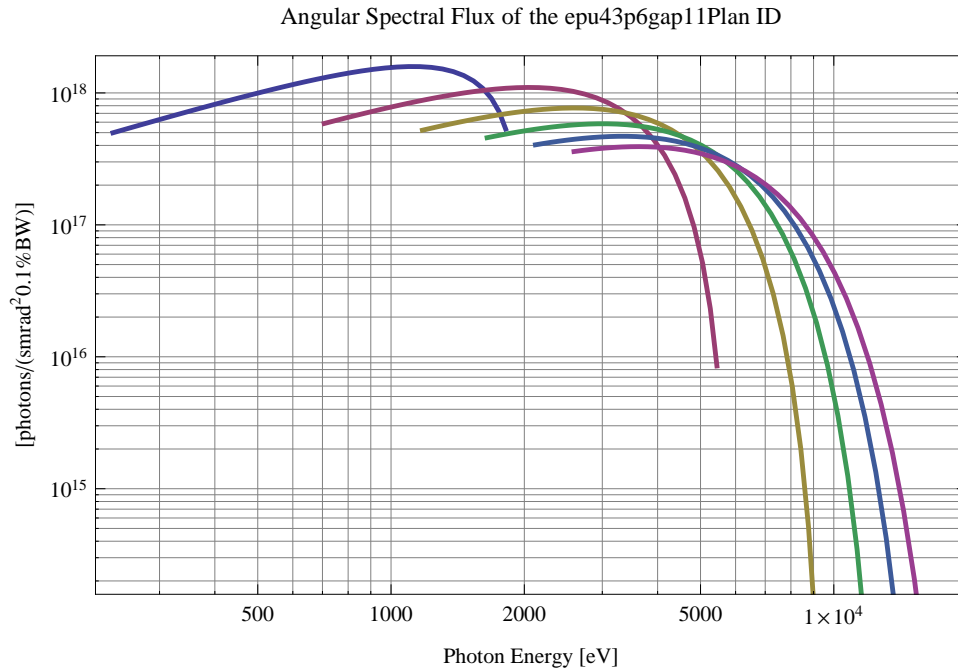


Figure 84: The angular spectral flux of the synchrotron radiation emitted by the epu43p6gap11Plan ID

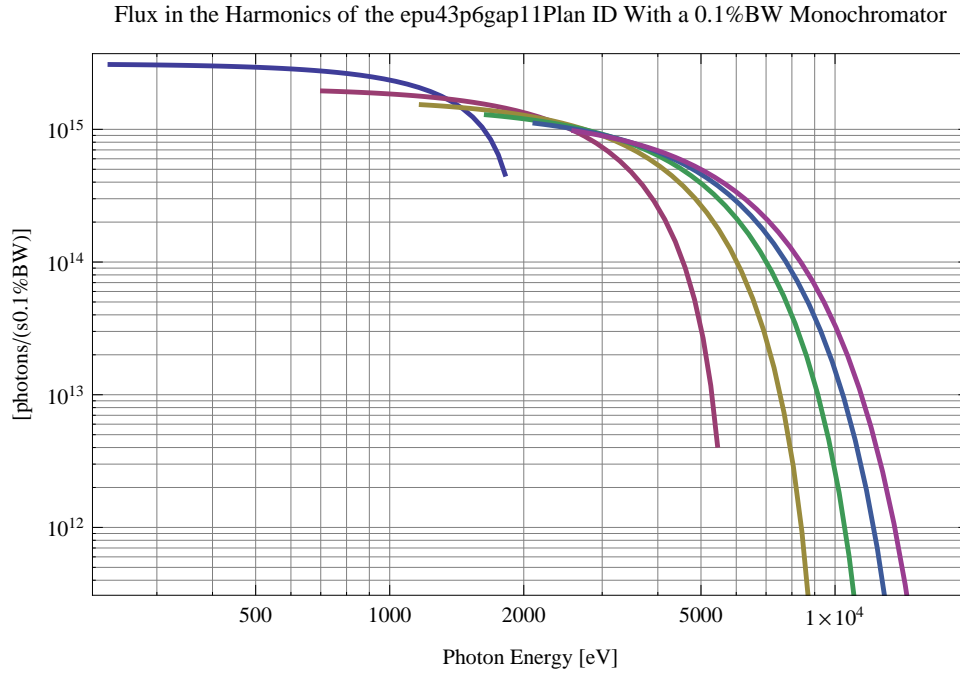


Figure 85: The flux of photons in the harmonics of the emitted synchrotron radiation from the epu43p6gap11Plan ID using a 0.1%BW monochromator

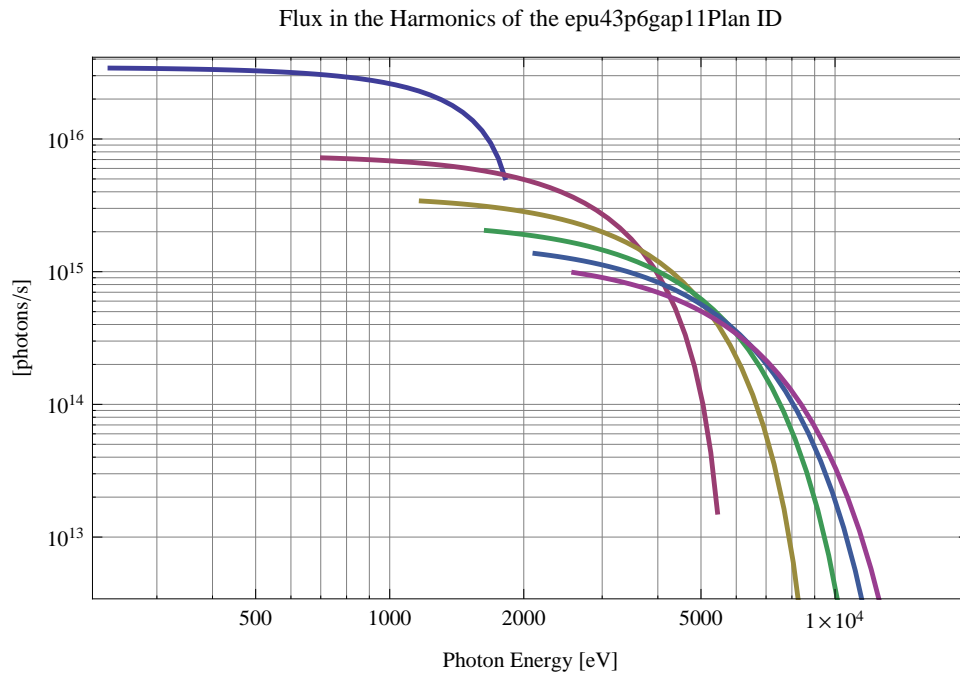


Figure 86: The flux of photons in the harmonics of the emitted synchrotron radiation from the epu43p6gap11Plan ID

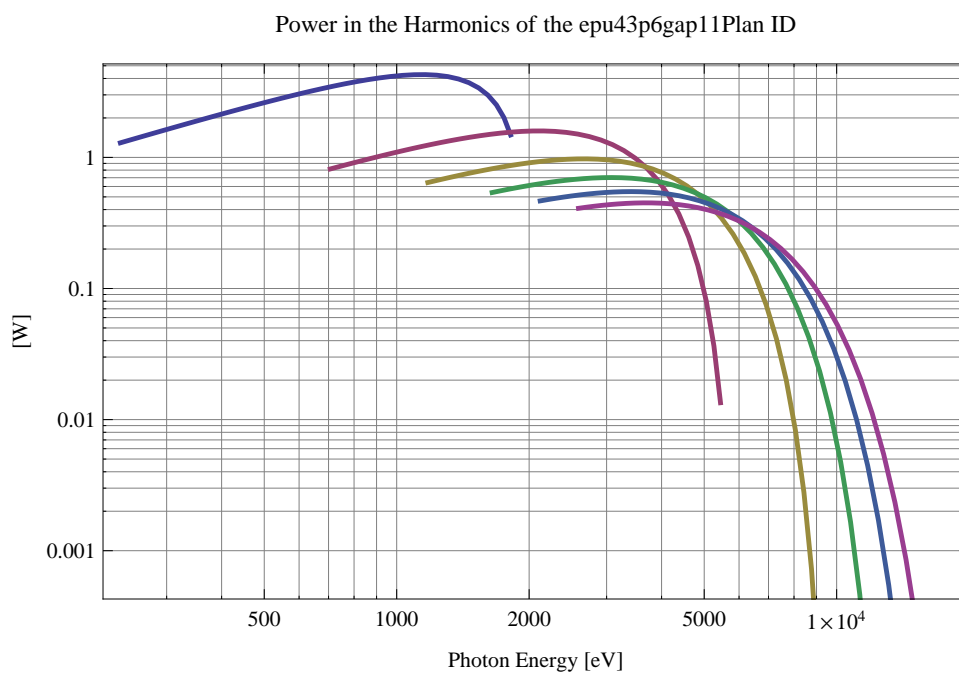


Figure 87: The power in the harmonics of the emitted synchrotron radiation from the epu43p6gap11Plan ID

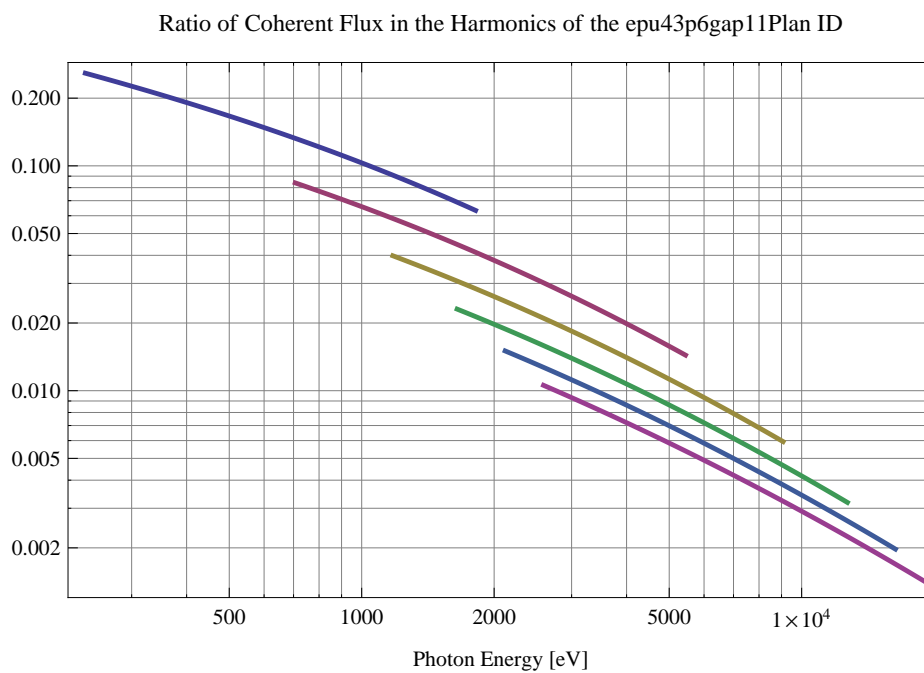


Figure 88: The ratio of coherent flux in the harmonics of the emitted synchrotron radiation from the epu43p6gap11Plan ID

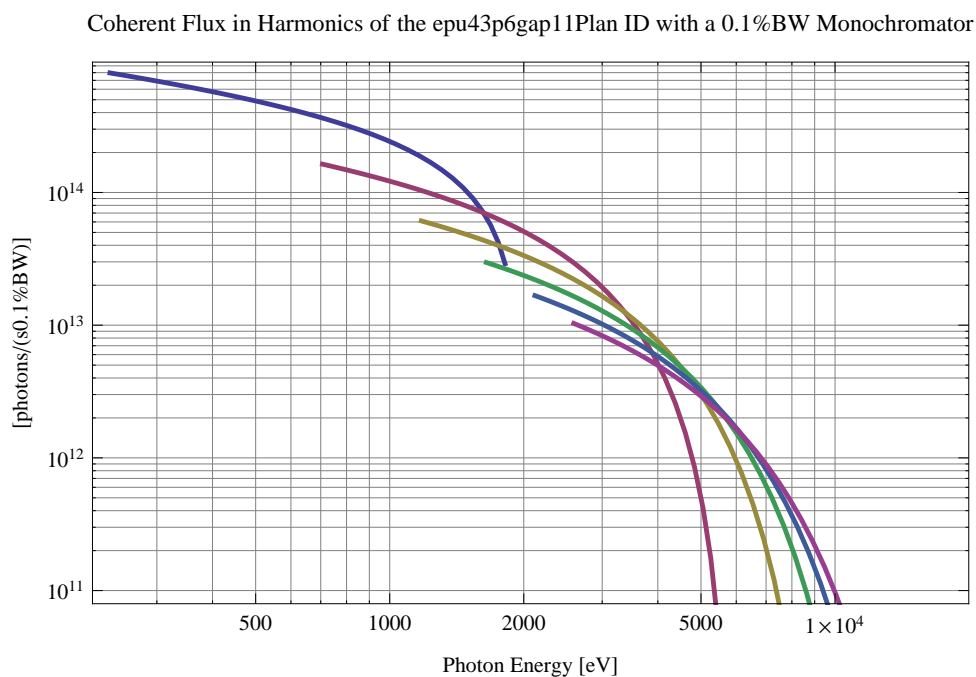


Figure 89: The coherent flux in the harmonics of the epu43p6gap11Plan ID using a 0.1%BW Monochromator

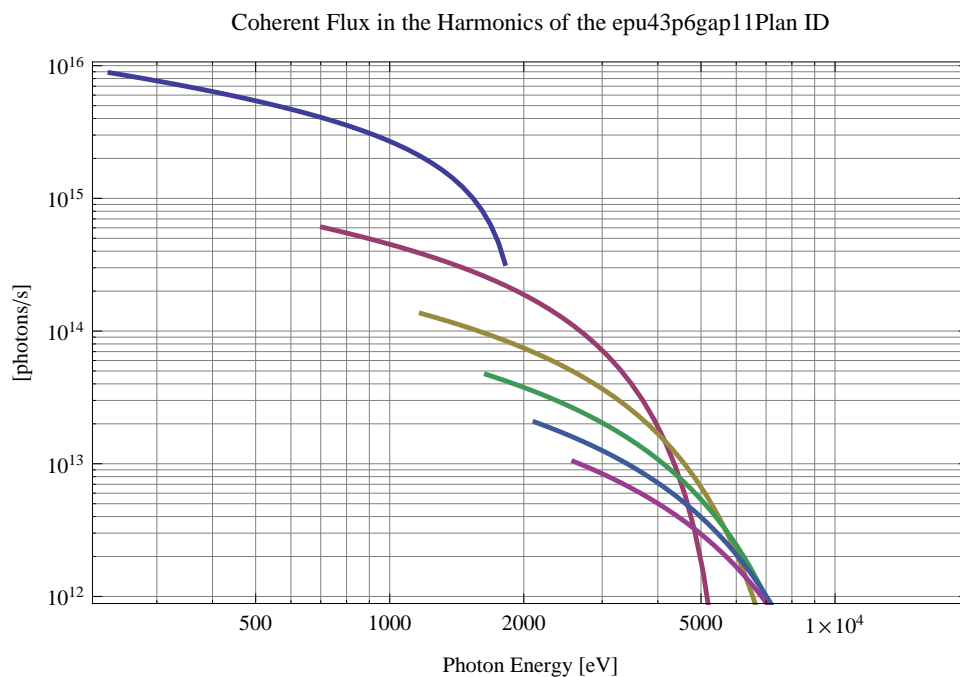


Figure 90: The coherent flux in the harmonics of the epu43p6gap11Plan ID

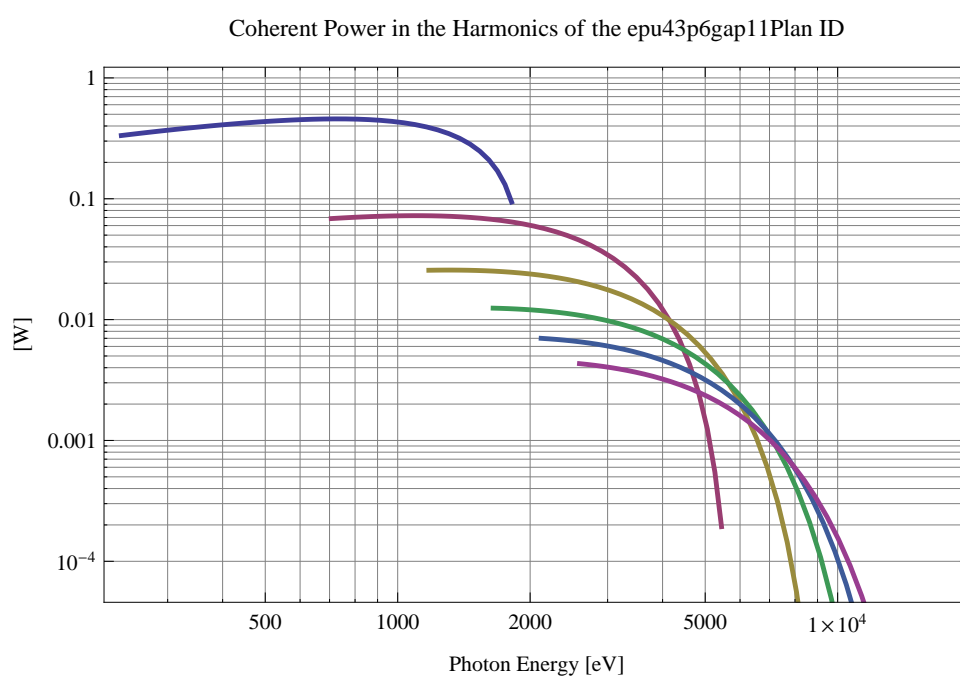


Figure 91: The power of coherent synchrotron radiation in the harmonics of the epu43p6gap11Plan ID

The brilliance at peak energy and the angular spectral flux density from the epu43p6gap11Plan ID for different harmonics at maximum K-value (3.828) are given in Table 15 and for minimum K-value (0.400) these values are given in Table 16.

Table 15: The brilliance at peak energy and the angular spectral flux density from the epu43p6gap11Plan ID for different harmonics at maximum K-value (3.828)

Harmonic	Photon Energy [eV]	Brilliance [Ph./((smrad ² mrads ² 0.1%BW))]	Angular Spectral Flux [Ph./((smrad ² 0.1%BW))]
1	235.427	1.15×10^{20}	4.99×10^{17}
3	706.281	2.12×10^{20}	5.86×10^{17}
5	1177.13	2.2×10^{20}	5.21×10^{17}
7	1647.99	2.1×10^{20}	4.58×10^{17}
9	2118.84	1.95×10^{20}	4.04×10^{17}
11	2589.7	1.8×10^{20}	3.59×10^{17}

Table 16: The brilliance at peak energy and the angular spectral flux density from the epu43p6gap11Plan ID for different harmonics at minimum K-value (0.4)

Harmonic	Photon Energy [eV]	Brilliance [Ph./((smrad ² mrads ² 0.1%BW))]	Angular Spectral Flux [Ph./((smrad ² 0.1%BW))]
1	1815.06	2.49×10^{20}	5.33×10^{17}
3	5445.18	4.62×10^{18}	8.52×10^{15}
5	9075.31	5.21×10^{16}	9.34×10^{13}
7	12705.4	5.46×10^{14}	9.71×10^{11}
9	16335.5	5.62×10^{12}	9.94×10^9
11	19965.7	5.74×10^{10}	1.01×10^8

2.2.5 Magnet model of the elliptically polarising undulator epu43p6gap11Heli

The Radia [3] magnet model of the epu43p6gap11Heli ID is shown in Figure 92. The length of the magnet model is 366.067 mm. The magnetic material in the model is NdFeb with a remanence of 1.28 T, a material similar to VACODYM 776 TP from Vacuumschmelze. Blocks with vertical magnetisation are blue and blocks with horizontal magnetisation are yellow. The block size is 30.x30.x10.9 mm³ and there is a 5. mm cut-out in two of the corners of the blocks. The total length of the epu43p6gap11Heli ID is 3941.27 mm.

2.2.6 Analysis of the magnetic field of the epu43p6gap11Heli ID

The effective magnetic fields on axis and the fundamental photon energy of the epu43p6gap11Heli ID are shown in Table 17. The higher harmonic contents in the magnetic field of an elliptically polarising undulator made of permanent magnets is negligible and the effective field has about the same strength as the peak field.

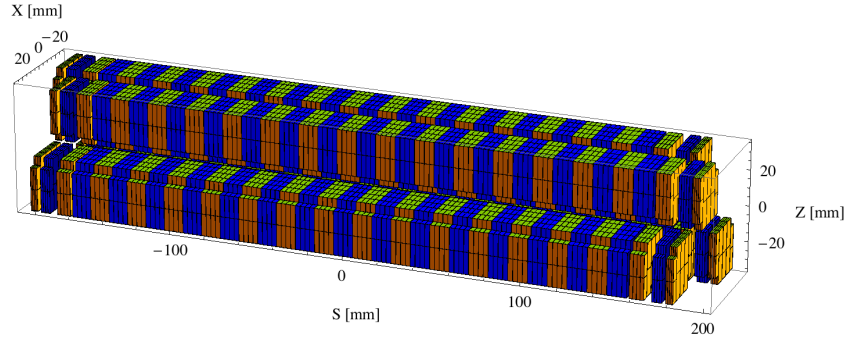


Figure 92: Magnetic model of the epu43p6gap11Heli ID. The ID has been modelled with Radia [3]

Table 17: Effective Fields on axis and Fundamental Photon Energy of the epu43p6gap11Heli ID

Undulator Period	43.6	mm
Undulator Gap	11	mm
Undulator Mode	Helical	
Undulator Phase	13.126	mm
Vertical Peak Field	0.544	T
Effective Vertical Field	0.546	T
K _x (from vert. field)	2.223	
Horizontal Peak Field:	0.548	T
Effective Horizontal Field	0.546	T
K _z (from hor. field)	2.223	
Photon Energy, Harm.1	0.330	keV
Emitted Power	6.690	kW
Total Length	3941.3	mm

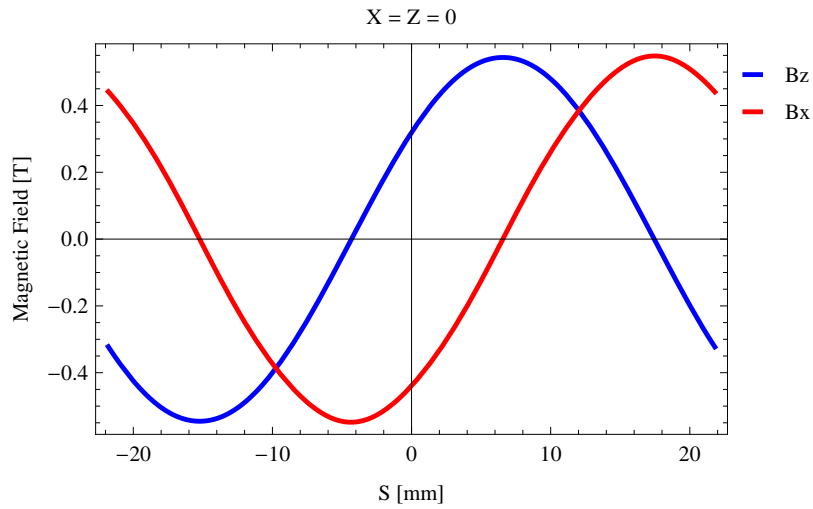


Figure 93: Vertical magnetic field in a central pole of the epu43p6gap11Heli ID along the ID axis, $X = Z = 0$

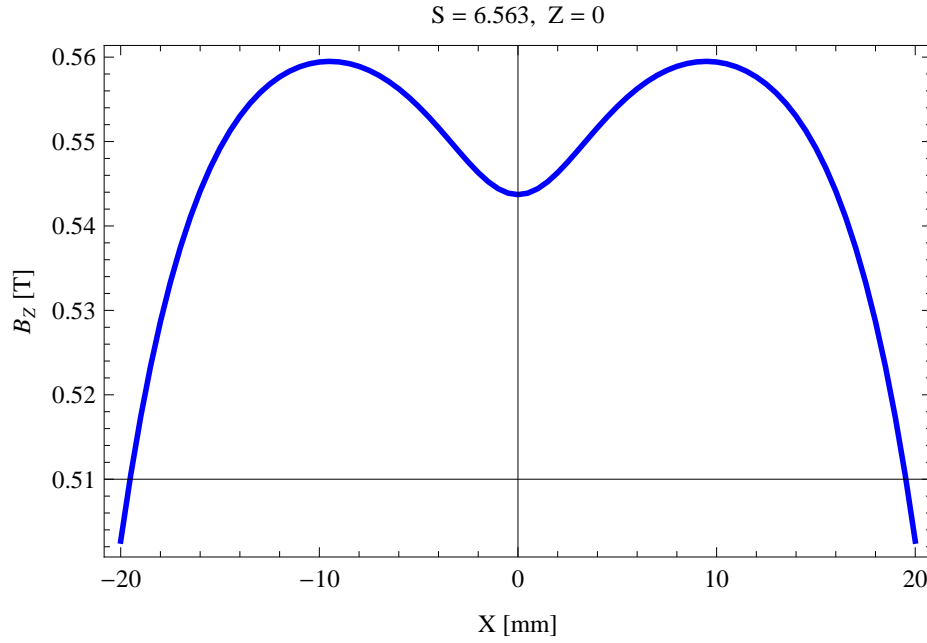


Figure 94: Vertical magnetic field in a central pole of the epu43p6gap11Heli ID along the horizontally transverse direction to the ID axis, $S = 6.563, Z = 0$

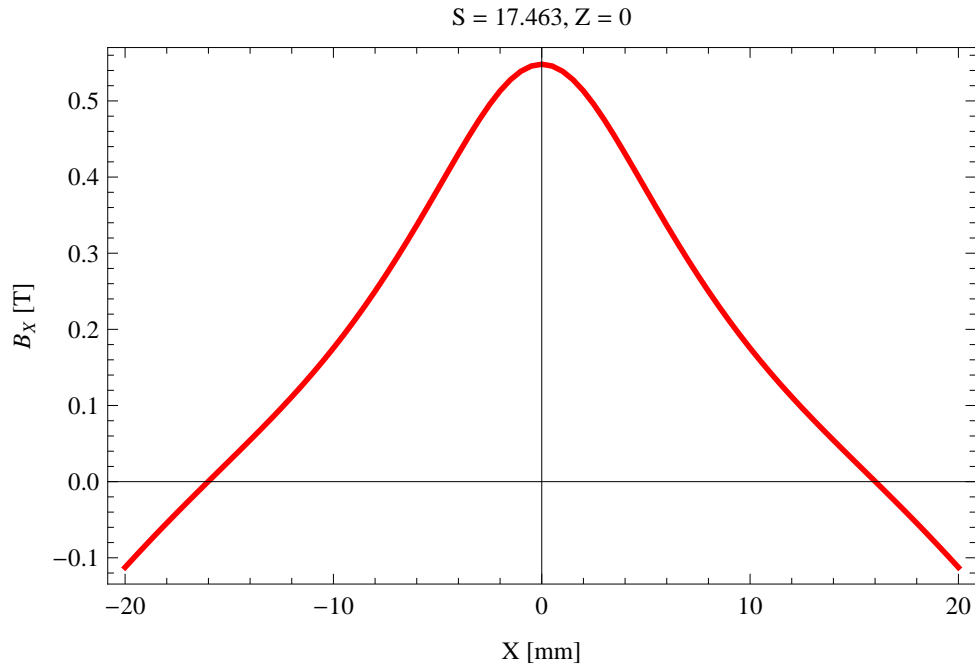


Figure 95: Horizontal magnetic field in a central pole of the epu43p6gap11Heli ID along the horizontally transverse direction to the ID axis, $S = 17.463, Z = 0$

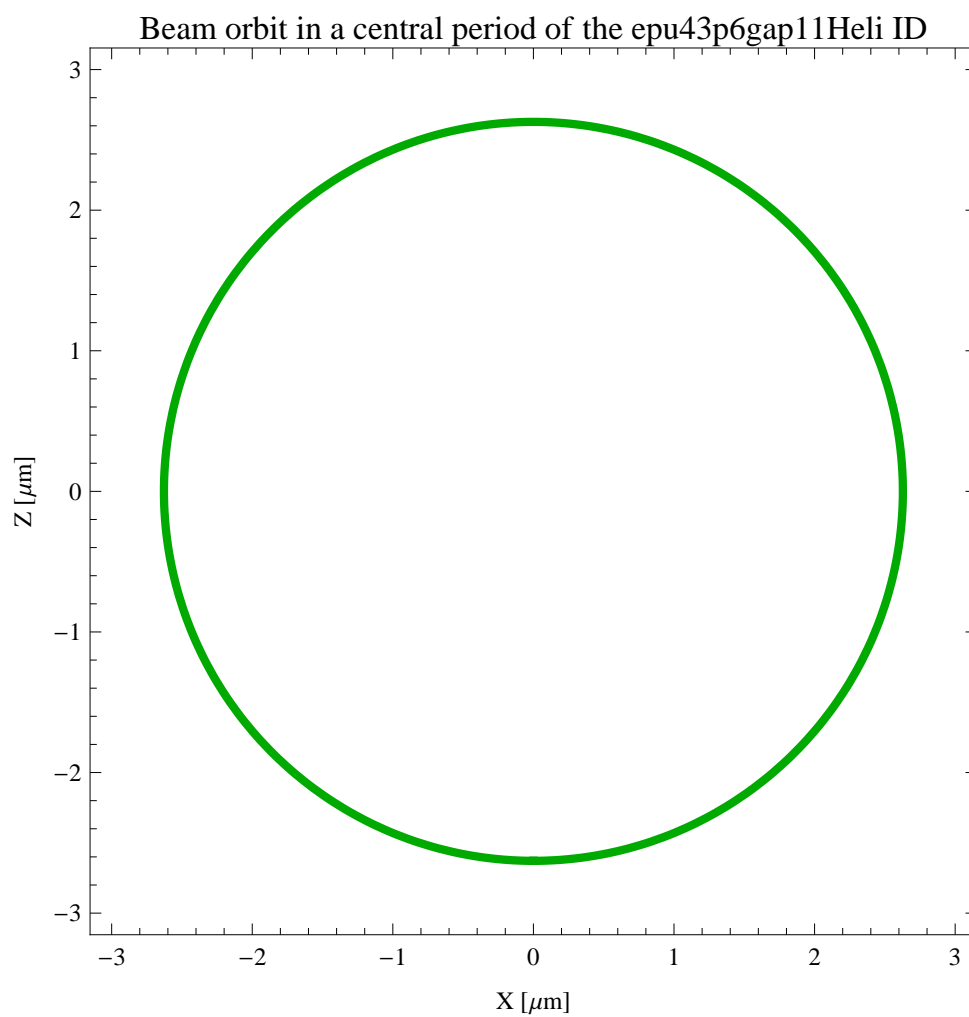


Figure 96: The beam orbit of the electron beam through a central period of the epu43p6gap11Heli ID

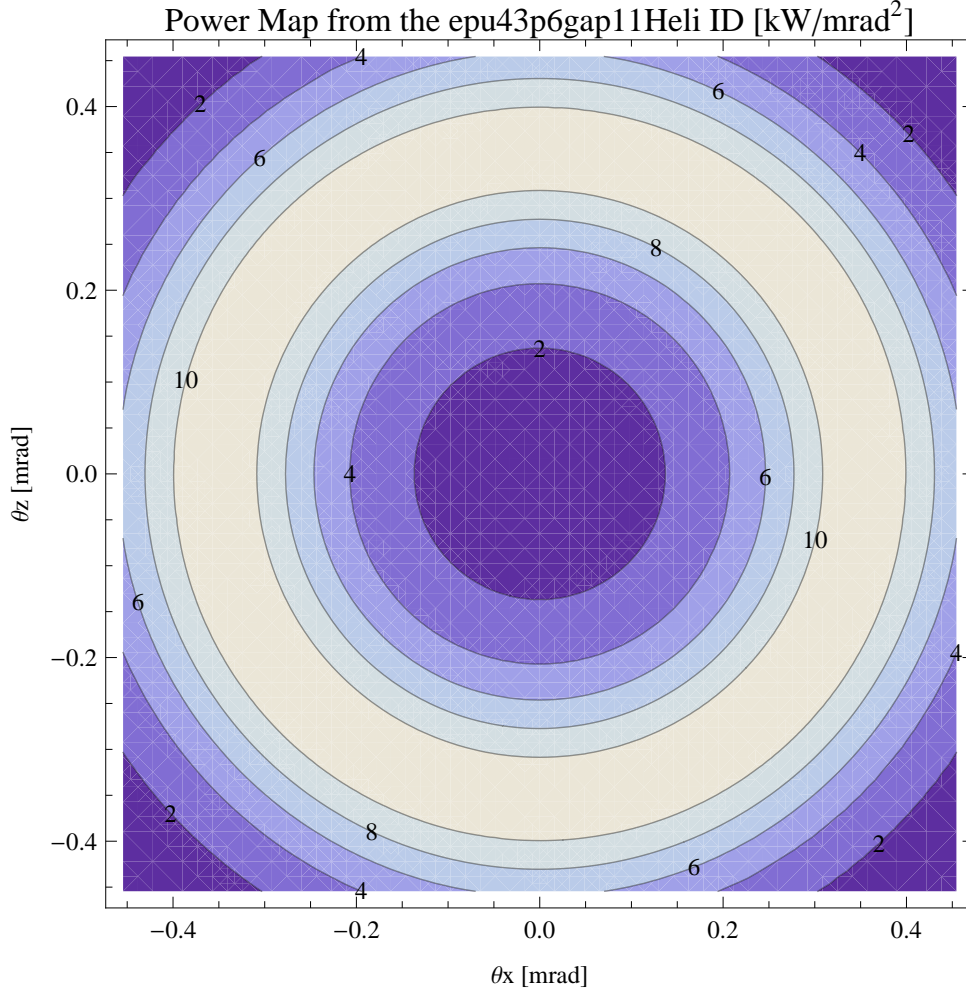


Figure 97: Map of the power distribution of the emitted synchrotron radiation by the epu43p6gap11Heli ID

2.2.7 Synchrotron radiation from the epu43p6gap11Heli ID

The power map of the emitted synchrotron radiation by the epu43p6gap11Heli ID, assuming a 0.5 A filament beam with an energy of 3 GeV and undulator properties of the synchrotron radiation, is shown in Figure 97. The on-axis power density is 1.033 kW/mrad²

A map of the degree of linear polarisation of the fundamental harmonic of the synchrotron radiation emitted by the epu43p6gap11Heli ID over the angle of observation is shown in Figure 98.

A map of the degree of 45 degree polarisation of the fundamental harmonic of the synchrotron radiation emitted by the epu43p6gap11Heli ID over the angle of observation is shown in Figure 99.

A map of the degree of circular polarisation of the fundamental harmonic of the synchrotron radiation emitted by the epu43p6gap11Heli ID over the angle of observation is shown in Figure 100.

The on axis brilliance at peak energy and the angular spectral flux from the epu43p6gap11Heli ID have been calculated with the given beam parameters, which are 0.5 A of stored current, $\beta_H = 9$ m, $\varepsilon_H = 0.263$ nmrad, $\beta_V = 4.8$ m, $\varepsilon_V = 8$. pmrad, and an energy spread of 0.001.

Degree of Linear Polarisation in Harm.1 from the epu43p6gap11Heli ID

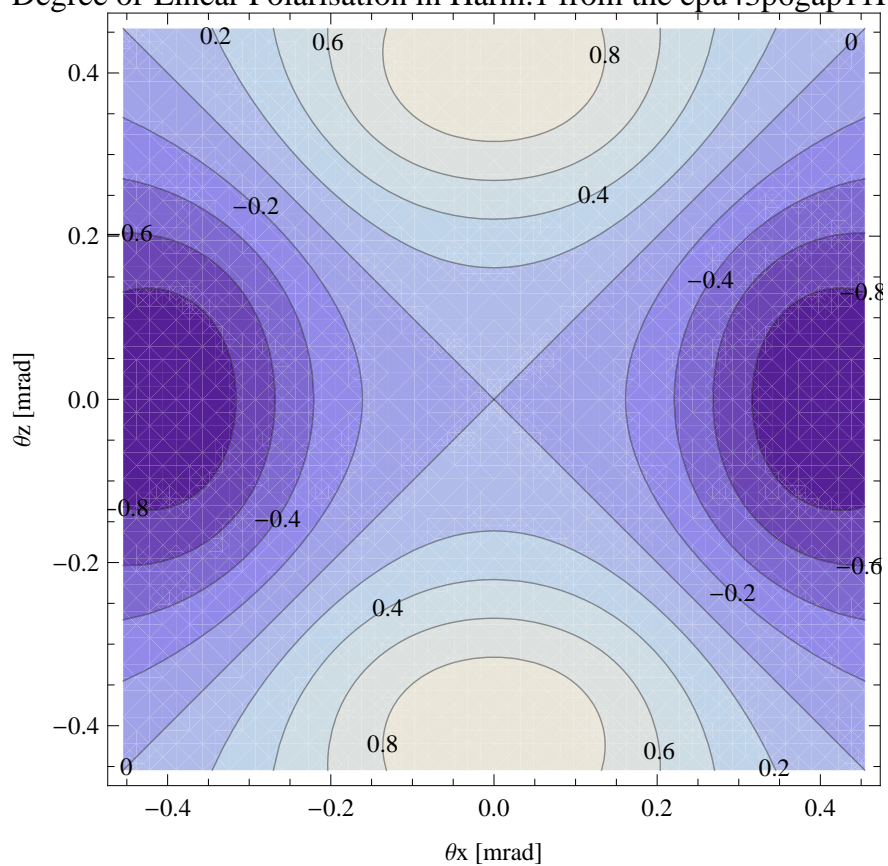


Figure 98: Map of linear polarisation in the fundamental harmonic of the synchrotron radiation emitted by the epu43p6gap11Heli ID

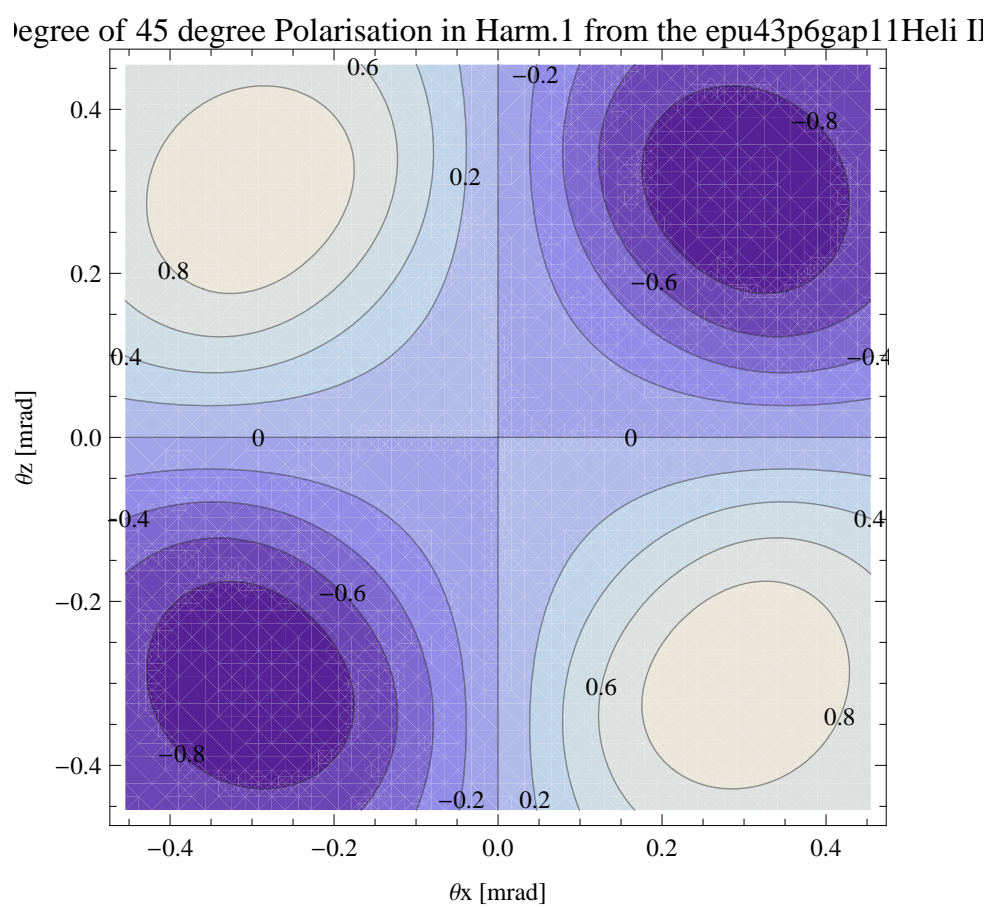


Figure 99: Map of 45 degree polarisation in the fundamental harmonic of the synchrotron radiation emitted by the epu43p6gap11Heli ID

Degree of Circular Polarisation in Harm.1 from the epu43p6gap11Heli ID

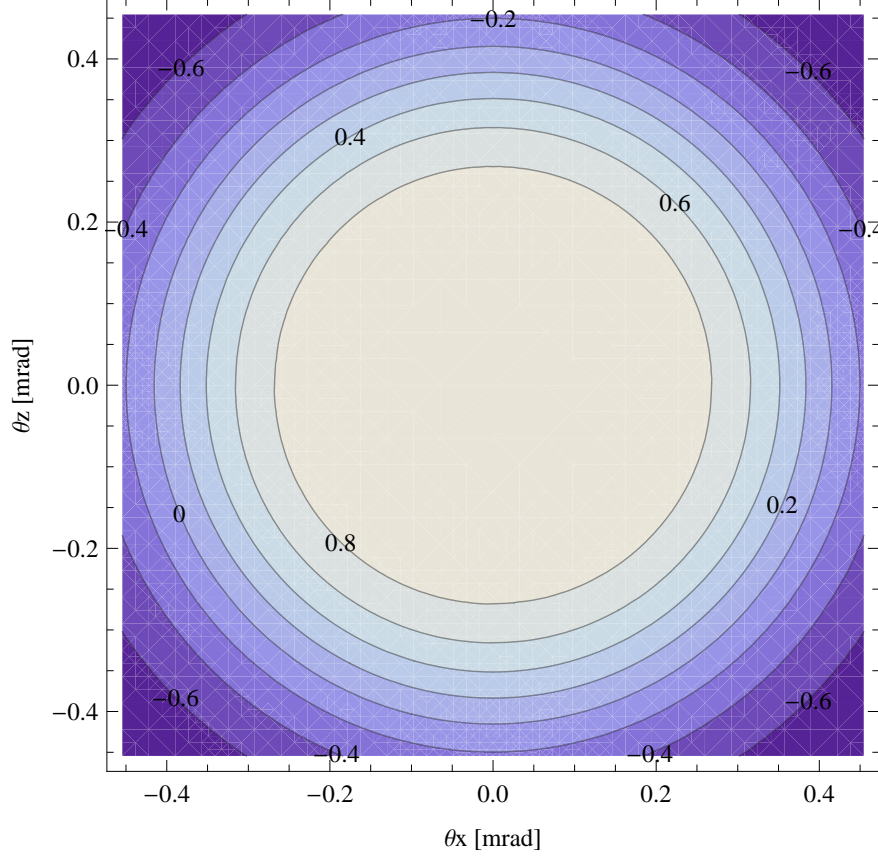


Figure 100: Map of circular polarisation in the fundamental harmonic of the synchrotron radiation emitted by the epu43p6gap11Heli ID

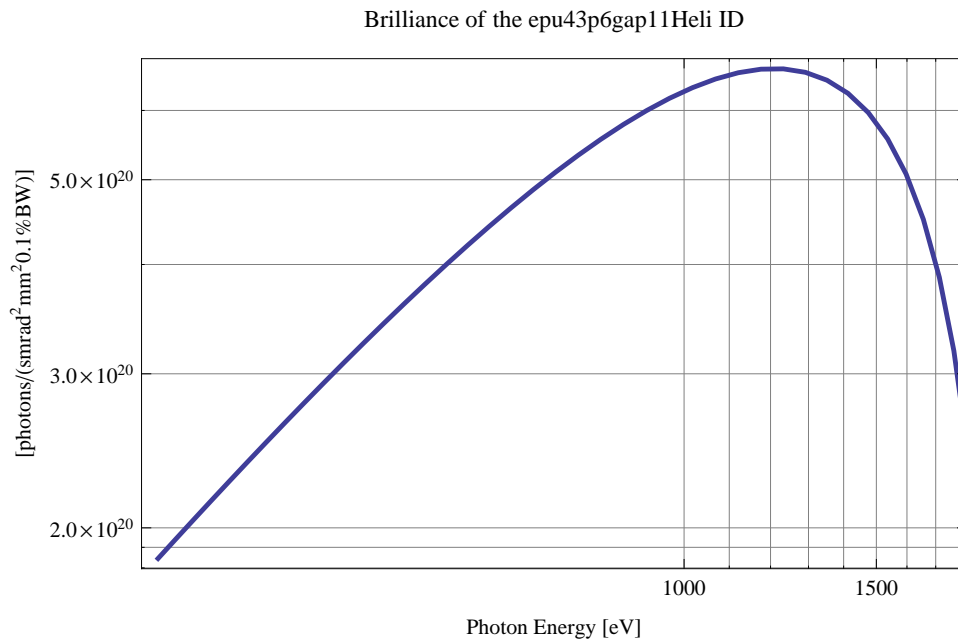


Figure 101: The brilliance at peak energy of the synchrotron radiation emitted by the epu43p6gap11Heli ID

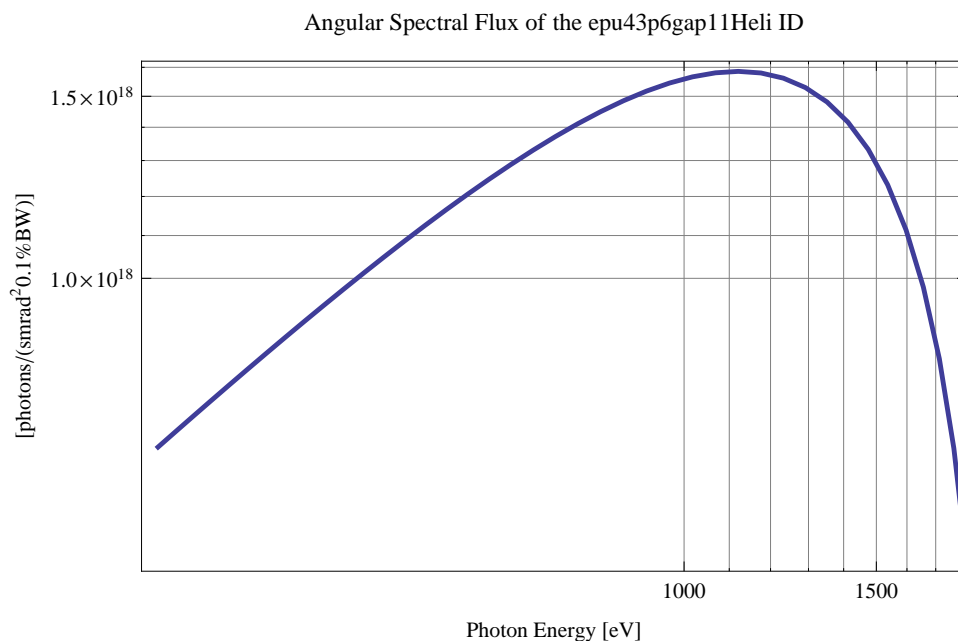


Figure 102: The angular spectral flux of the synchrotron radiation emitted by the epu43p6gap11Heli ID

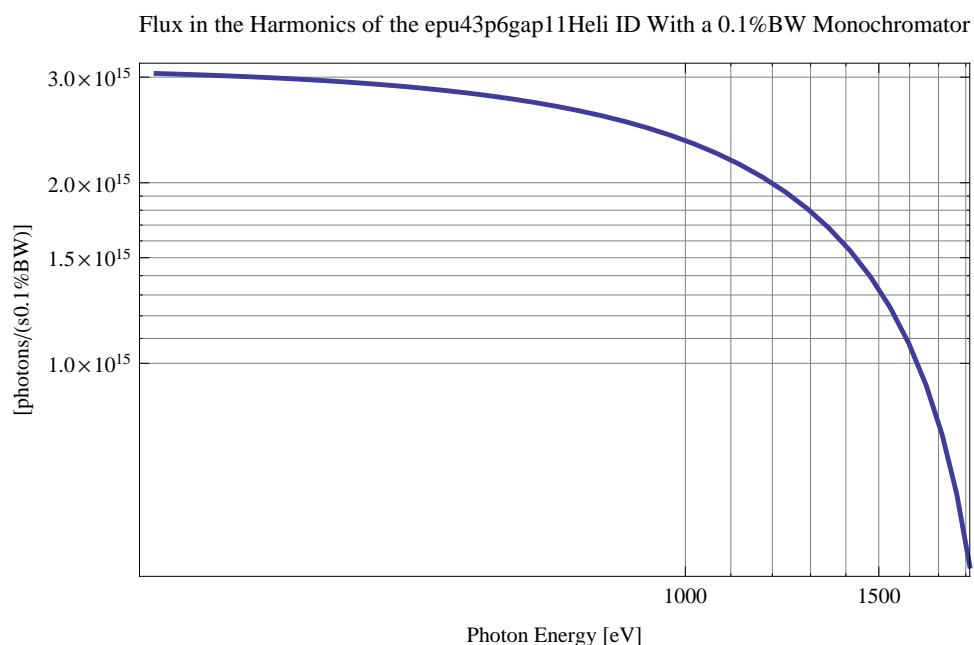


Figure 103: The flux of photons in the harmonics of the emitted synchrotron radiation from the epu43p6gap11Heli ID using a 0.1%BW monochromator

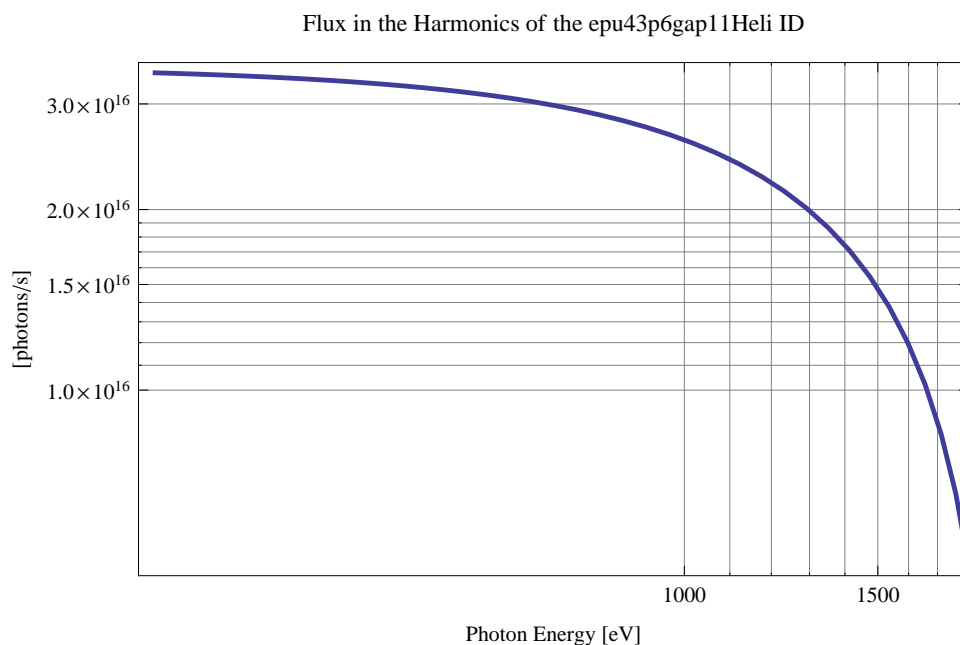


Figure 104: The flux of photons in the harmonics of the emitted synchrotron radiation from the epu43p6gap11Heli ID

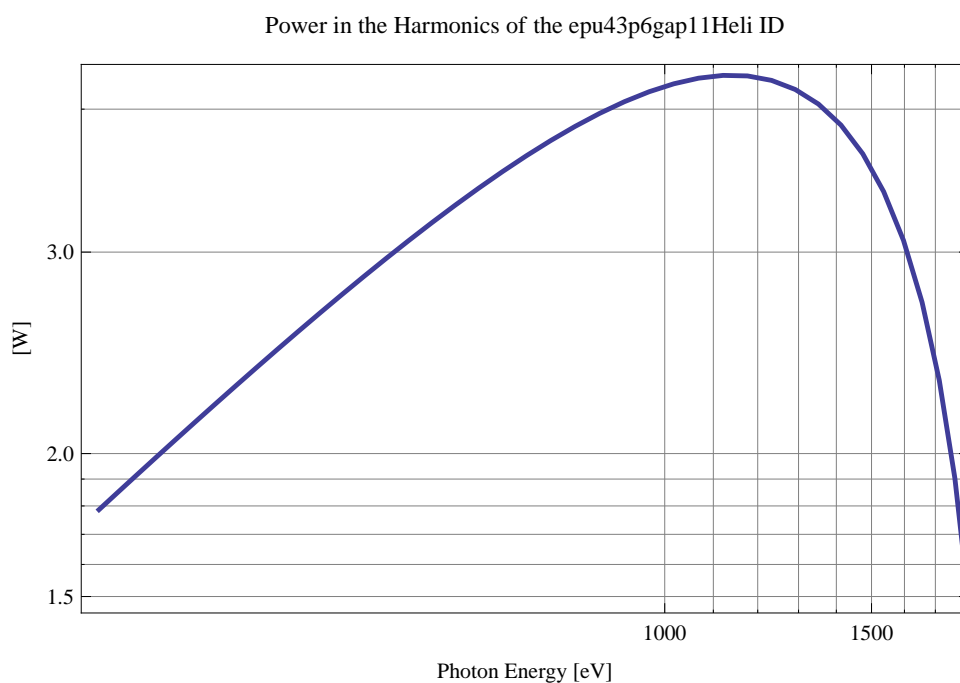


Figure 105: The power in the harmonics of the emitted synchrotron radiation from the epu43p6gap11Heli ID

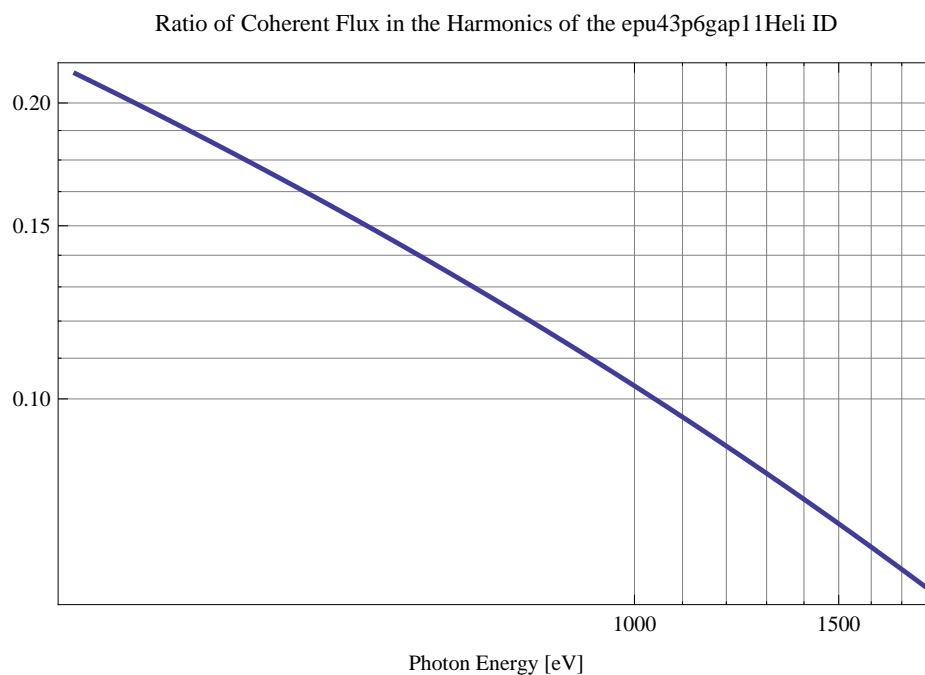


Figure 106: The ratio of coherent flux in the harmonics of the emitted synchrotron radiation from the epu43p6gap11Heli ID

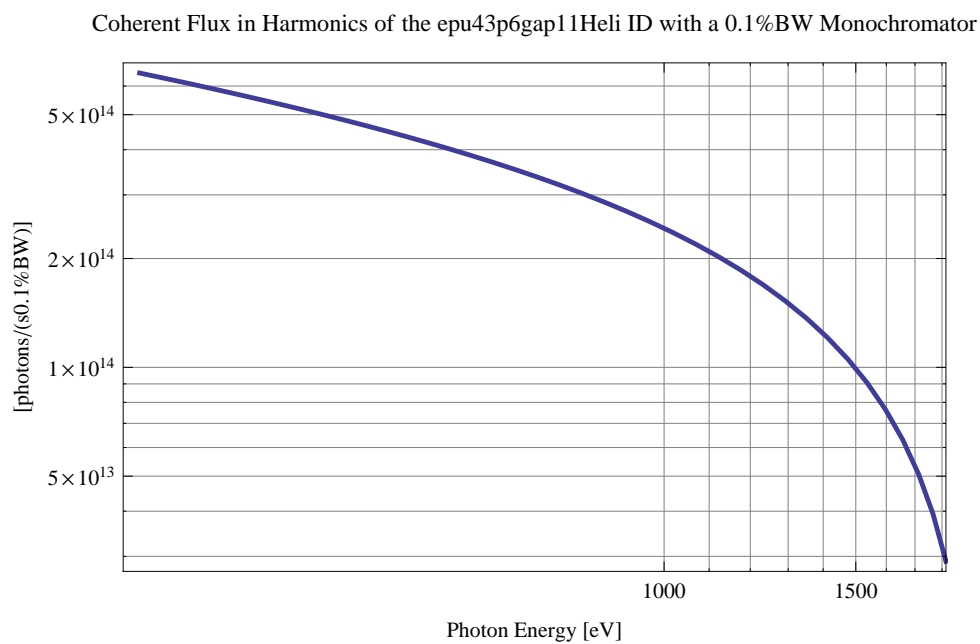


Figure 107: The coherent flux in the harmonics of the epu43p6gap11Heli ID using a 0.1%BW Monochromator

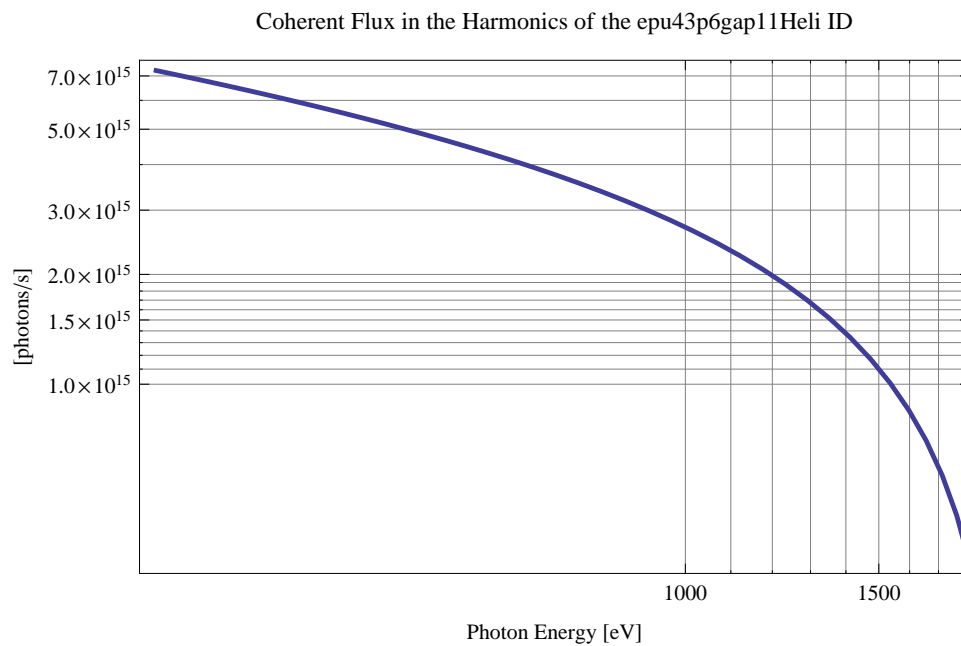


Figure 108: The coherent flux in the harmonics of the epu43p6gap11Heli ID

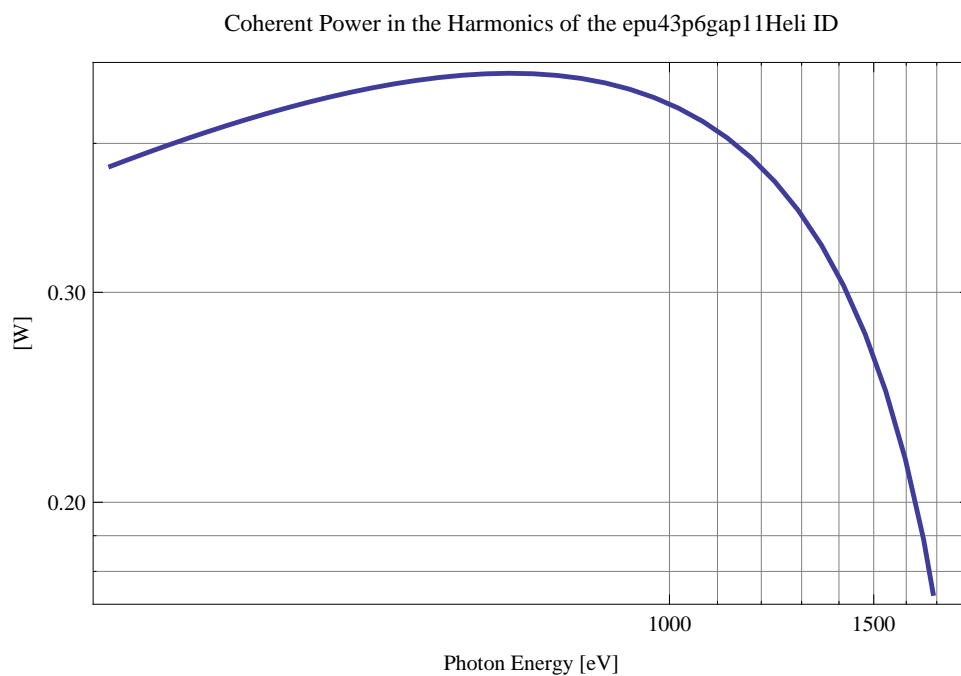


Figure 109: The power of coherent synchrotron radiation in the harmonics of the epu43p6gap11Heli ID

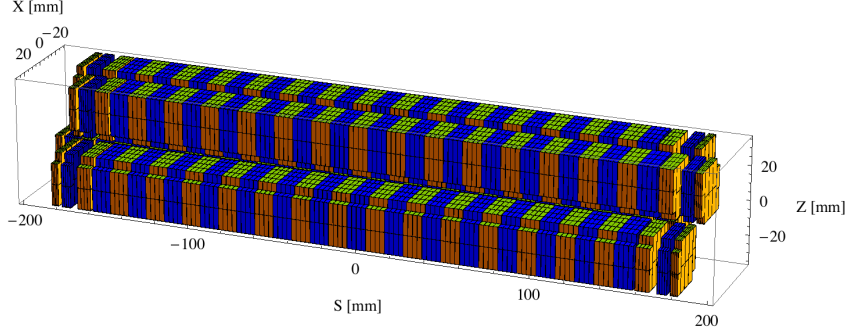


Figure 110: Magnetic model of the epu43p6gap11Incl ID. The ID has been modelled with Radia [3]

The brilliance at peak energy and the angular spectral flux density from the epu43p6gap11Heli ID for different harmonics at maximum K-value (3.144) are given in Table 18 and for minimum K-value (0.400) these values are given in Table 19.

Table 18: The brilliance at peak energy and the angular spectral flux density from the epu43p6gap11Heli ID for different harmonics at maximum K-value (3.144)

Harmonic	Photon Energy [eV]	Brilliance [Ph./((smrad ² mrad ² 0.1%BW))]	Angular Spectral Flux [Ph./((smrad ² 0.1%BW))]
1	329.806	1.84×10^{20}	6.87×10^{17}

Table 19: The brilliance at peak energy and the angular spectral flux density from the epu43p6gap11Heli ID for different harmonics at minimum K-value (0.4)

Harmonic	Photon Energy [eV]	Brilliance [Ph./((smrad ² mrad ² 0.1%BW))]	Angular Spectral Flux [Ph./((smrad ² 0.1%BW))]
1	1815.06	2.49×10^{20}	5.33×10^{17}

2.2.8 Magnet model of the elliptically polaraising undulator epu43p6gap11Incl

The Radia [3] magnet model of the epu43p6gap11Incl ID is shown in Figure 110. The length of the magnet model is 366.067 mm. The magnetic material in the model is NdFeb with a remanence of 1.28 T, a meterial similar to VACODYM 776 TP from Vacuumschmelze. Blocks with vertical magnetisation are blue and blocks with horizontal magnetisation are yellow. The block size is 30.x30.x10.9 mm³ and there is a 5. mm cut-out in two of the corners of the blocks. The total length of the epu43p6gap11Incl ID is 3941.27 mm.

2.2.9 Analysis of the magnetic field of the epu43p6gap11Incl ID

The effective magnetic fields on axis and the fundamental photon energy of the epu43p6gap11Incl ID are shown in Table 20. The higher harmonic contents in the magnetic field of an elliptically

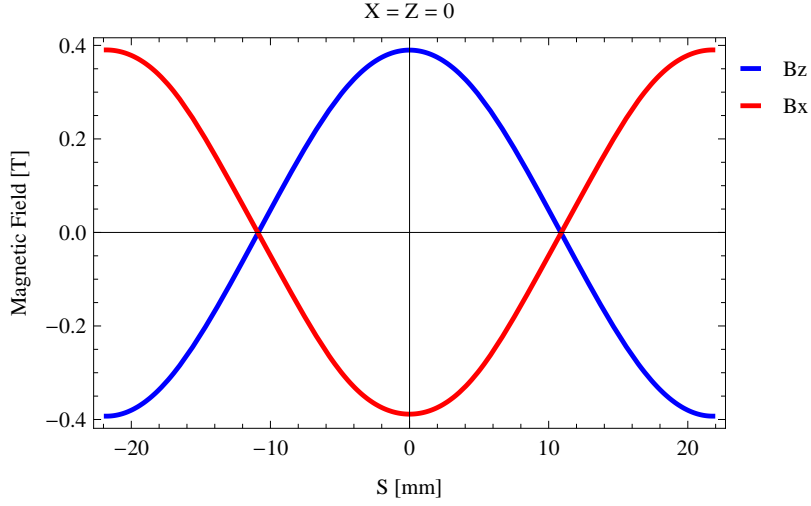


Figure 111: Vertical magnetic field in a central pole of the epu43p6gap11Incl ID along the ID axis, $X = Z = 0$

polarising undulator made of permanent magnets is negligible and the effective field has about the same strength as the peak field.

Table 20: Effective Fields on axis and Fundamental Photon Energy of the epu43p6gap11Incl ID

Undulator Period	43.6	mm
Undulator Gap	11	mm
Undulator Mode	Inclined	
Undulator Phase	12.027	mm
Vertical Peak Field	0.390	T
Effective Vertical Field	0.391	T
Kx (from vert. field)	1.592	
Horizontal Peak Field:	-0.389	T
Effective Horizontal Field	0.391	T
Kz (from hor. field)	1.592	
Photon Energy, Harm.1	0.555	keV
Emitted Power	3.431	kW
Total Length	3941.3	mm

2.2.10 Synchrotron radiation from the epu43p6gap11Incl ID

The power map of the emitted synchrotron radiation by the epu43p6gap11Incl ID, assuming a 0.5 A filament beam with an energy of 3 GeV and undulator properties of the synchrotron radiation, is shown in Figure 115. The on-axis power density is 21.288 kW/mrad²

A map of the degree of linear polarisation of the fundamental harmonic of the synchrotron radiation emitted by the epu43p6gap11Incl ID over the angle of observation is shown in Figure 116.

A map of the degree of 45 degree polarisation of the fundamental harmonic of the synchrotron radiation emitted by the epu43p6gap11Incl ID over the angle of observation is shown in Figure 117.

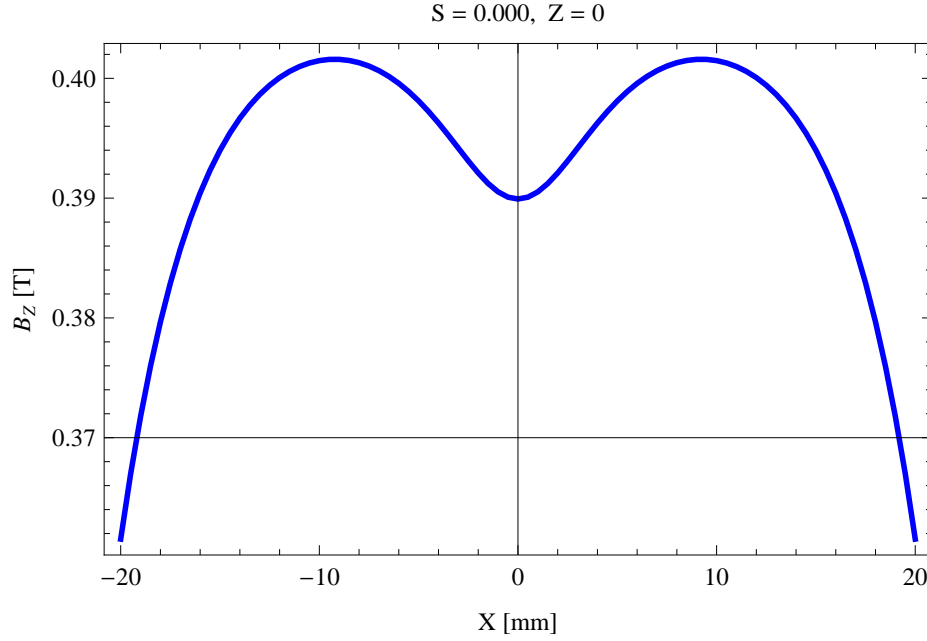


Figure 112: Vertical magnetic field in a central pole of the epu43p6gap11Incl ID along the horizontally transverse direction to the ID axis, $S = 0.000, Z = 0$

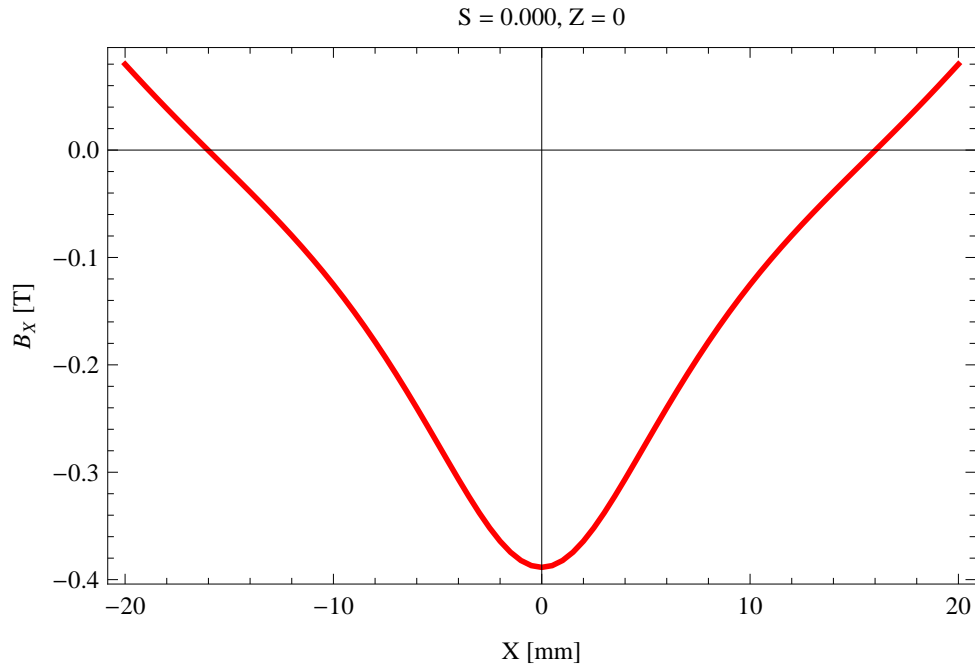


Figure 113: Horizontal magnetic field in a central pole of the epu43p6gap11Incl ID along the horizontally transverse direction to the ID axis, $S = 0.000, Z = 0$

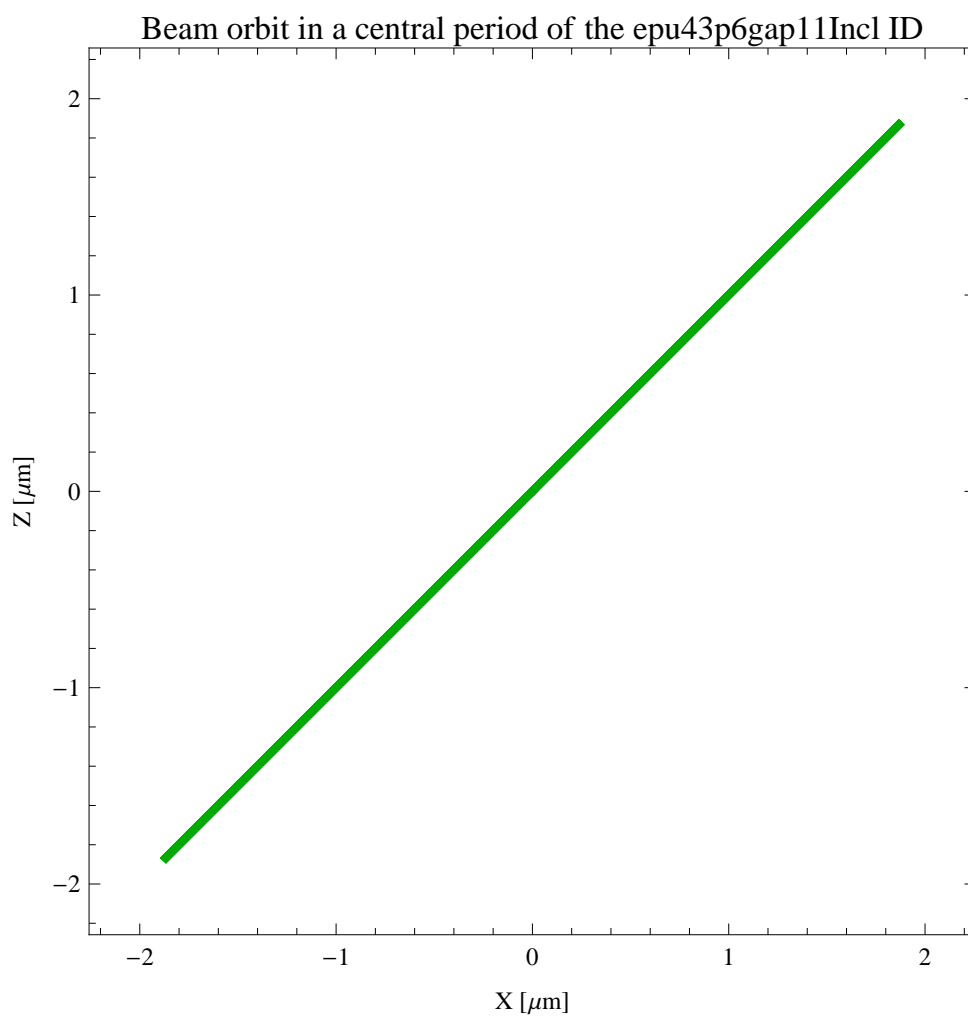


Figure 114: The beam orbit of the electron beam through a central period of the epu43p6gap11Incl ID

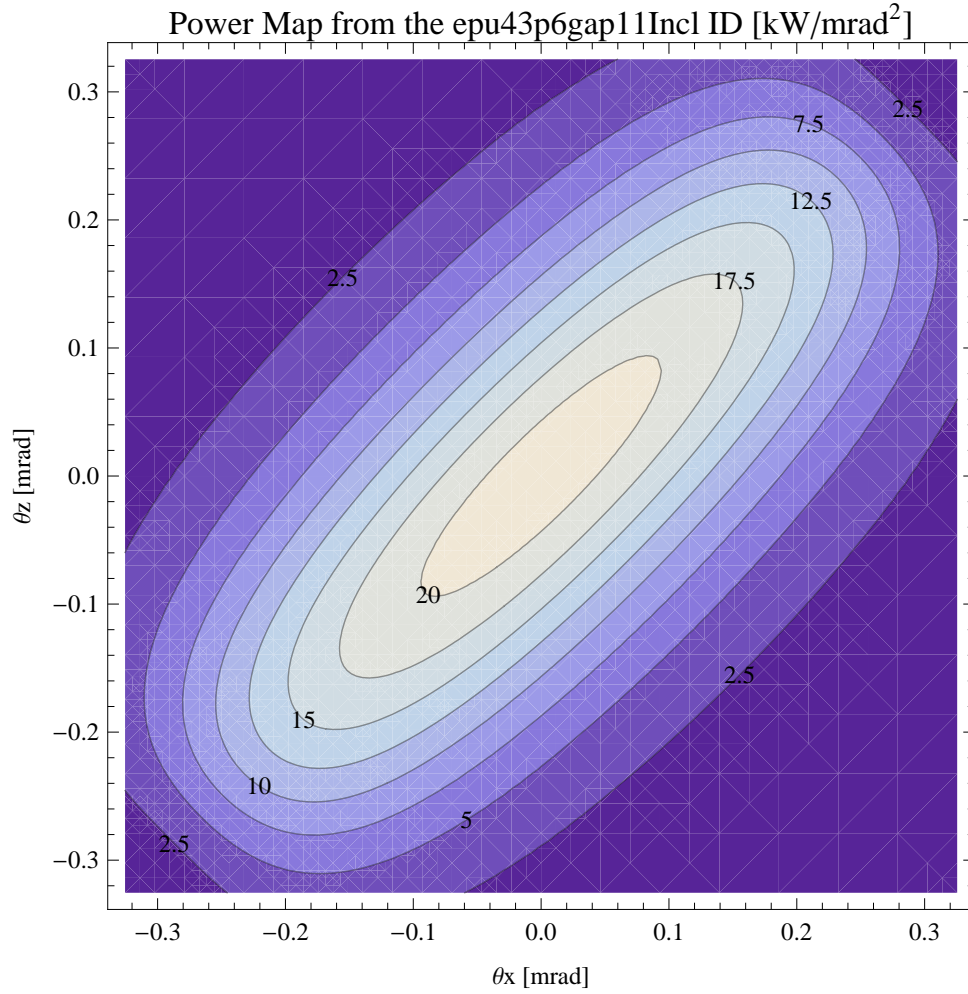


Figure 115: Map of the power distribution of the emitted synchrotron radiation by the epu43p6gap11Incl ID

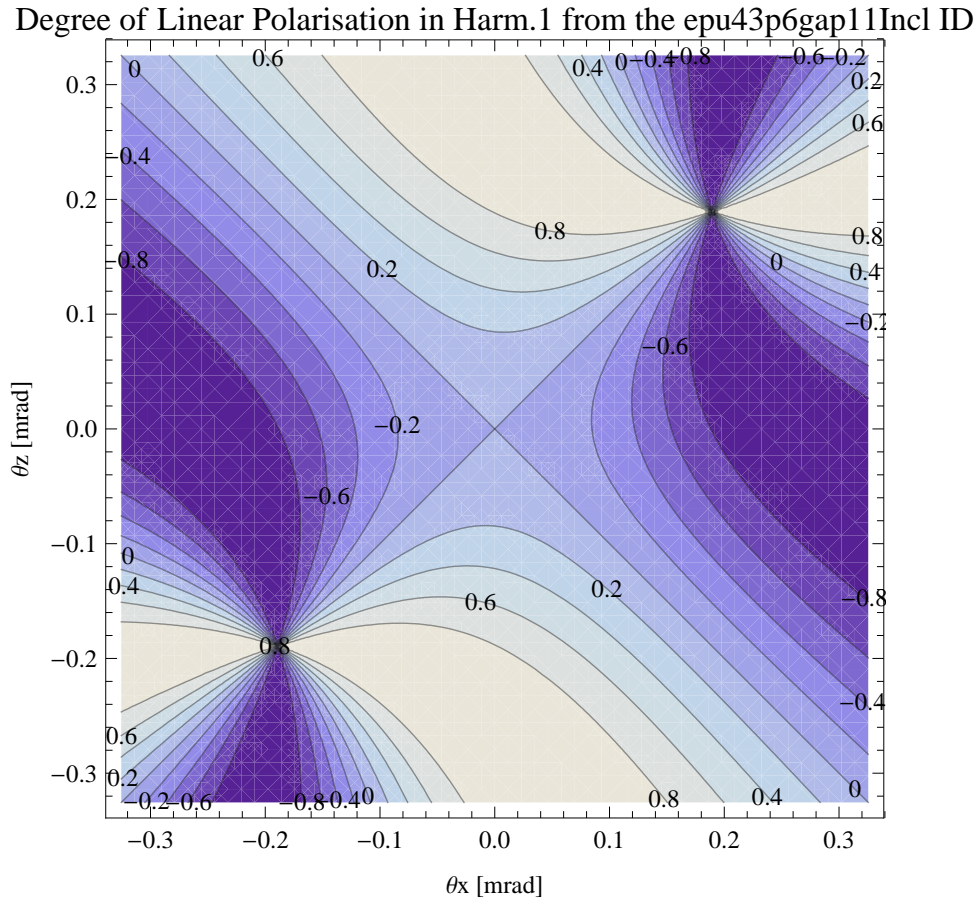


Figure 116: Map of linear polarisation in the fundamental harmonic of the synchrotron radiation emitted by the epu43p6gap11Incl ID

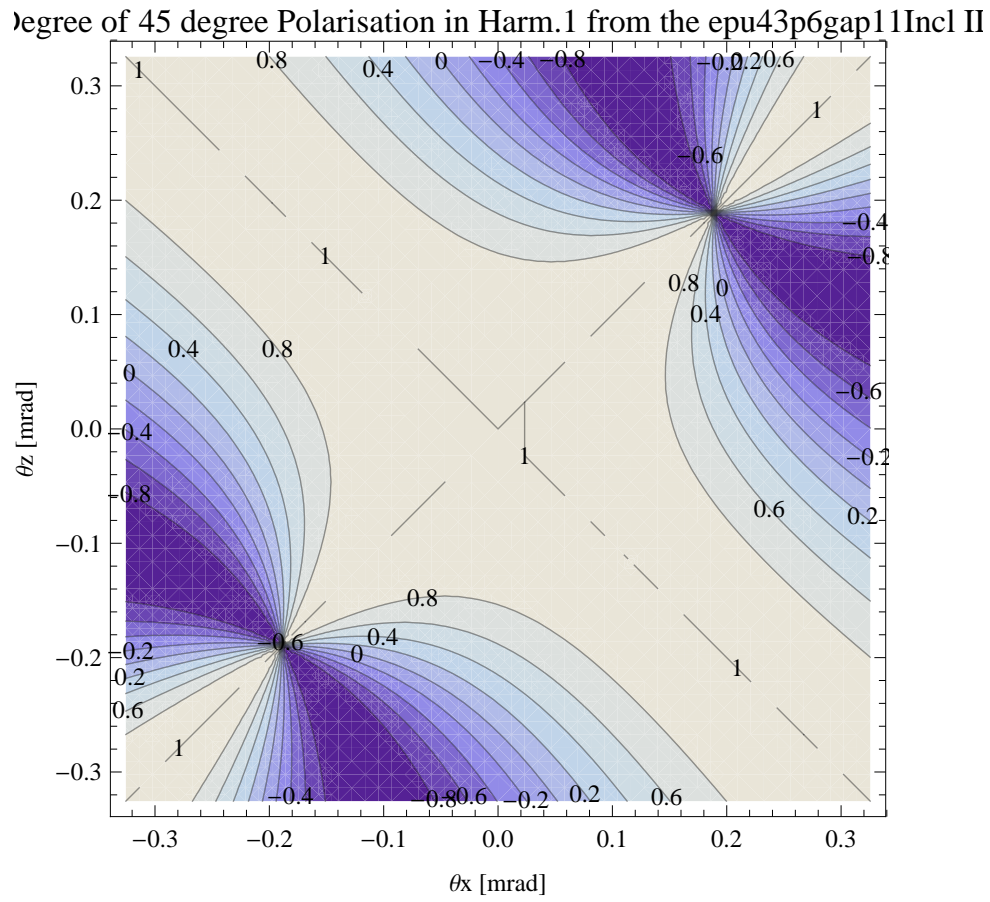


Figure 117: Map of 45 degree polarisation in the fundamental harmonic of the synchrotron radiation emitted by the epu43p6gap11Incl ID

Degree of Circular Polarisation in Harm.1 from the epu43p6gap11Incl ID

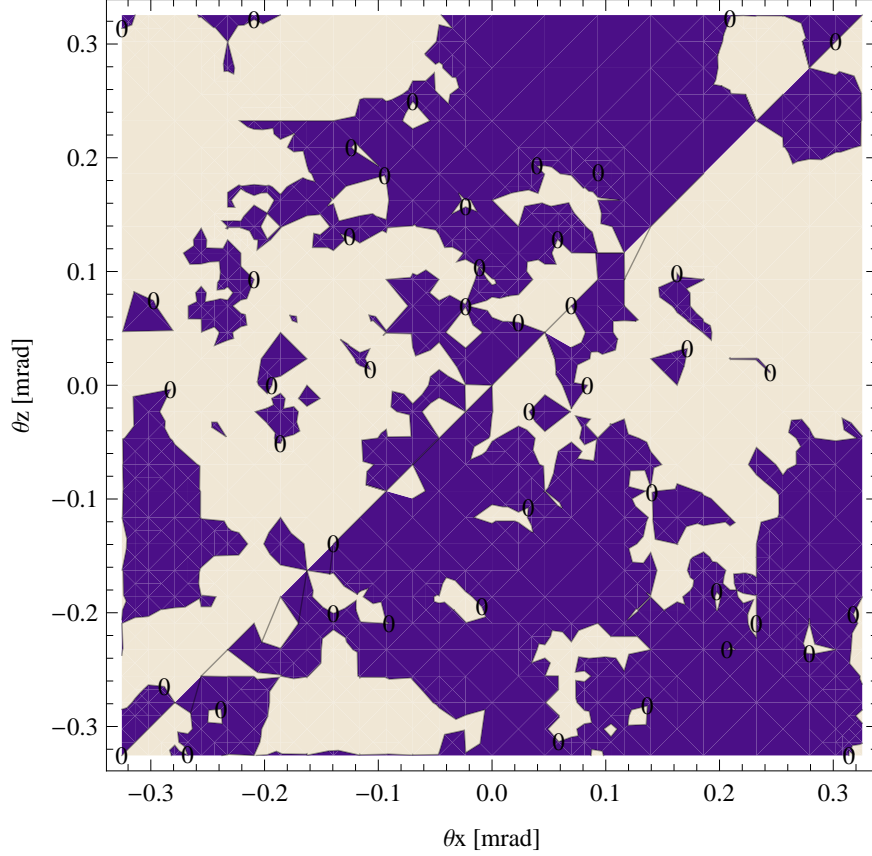


Figure 118: Map of circular polarisation in the fundamental harmonic of the synchrotron radiation emitted by the epu43p6gap11Incl ID

A map of the degree of circular polarisation of the fundamental harmonic of the synchrotron radiation emitted by the epu43p6gap11Incl ID over the angle of observation is shown in Figure 118.

The on axis brilliance at peak energy and the angular spectral flux from the epu43p6gap11Incl ID have been calculated with the given beam parameters, which are 0.5 A of stored current, $\beta_H = 9$ m, $\varepsilon_H = 0.263$ nmrad, $\beta_V = 4.8$ m, $\varepsilon_V = 8$. pmrad, and an energy spread of 0.001.

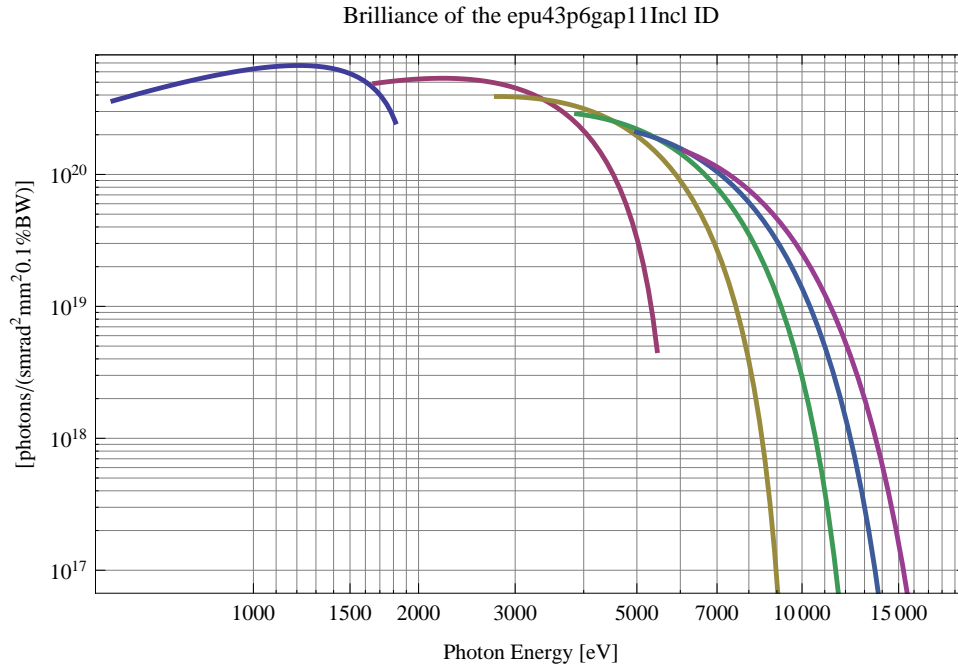


Figure 119: The brilliance at peak energy of the synchrotron radiation emitted by the epu43p6gap11Incl ID

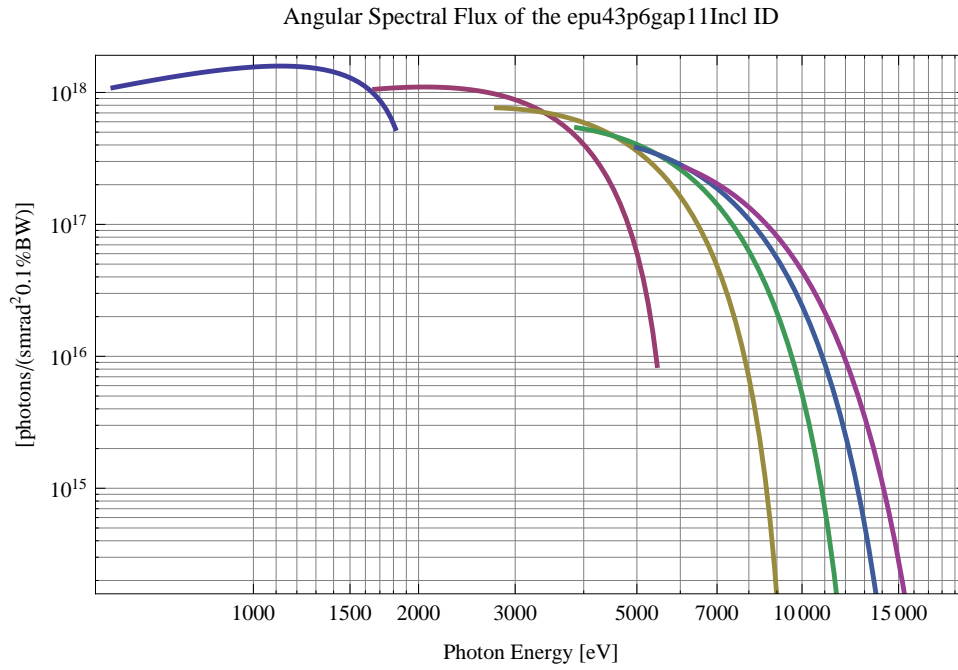


Figure 120: The angular spectral flux of the synchrotron radiation emitted by the epu43p6gap11Incl ID

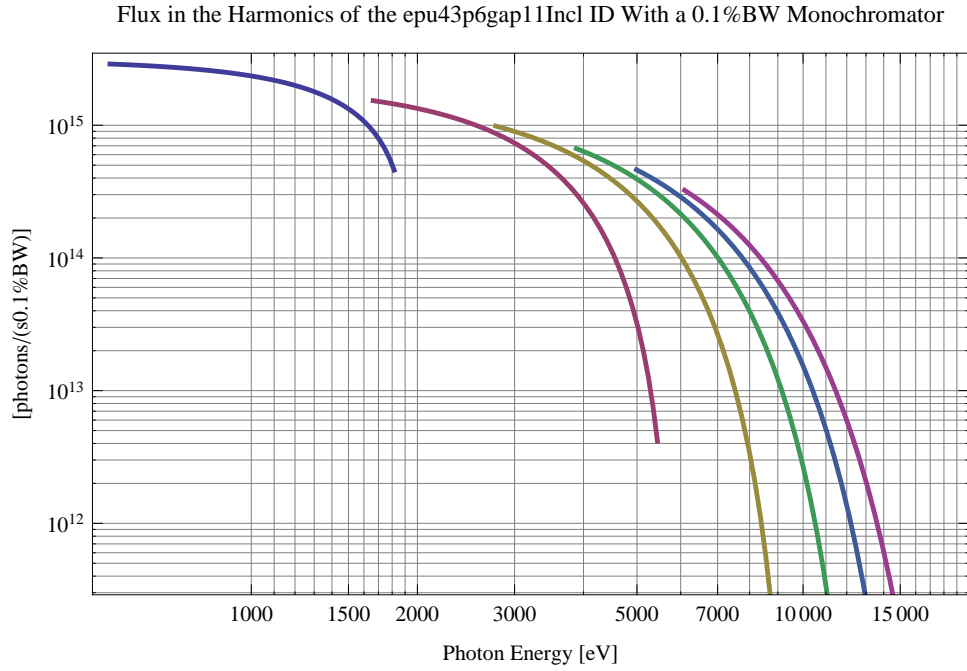


Figure 121: The flux of photons in the harmonics of the emitted synchrotron radiation from the epu43p6gap11Incl ID using a 0.1%BW monochromator

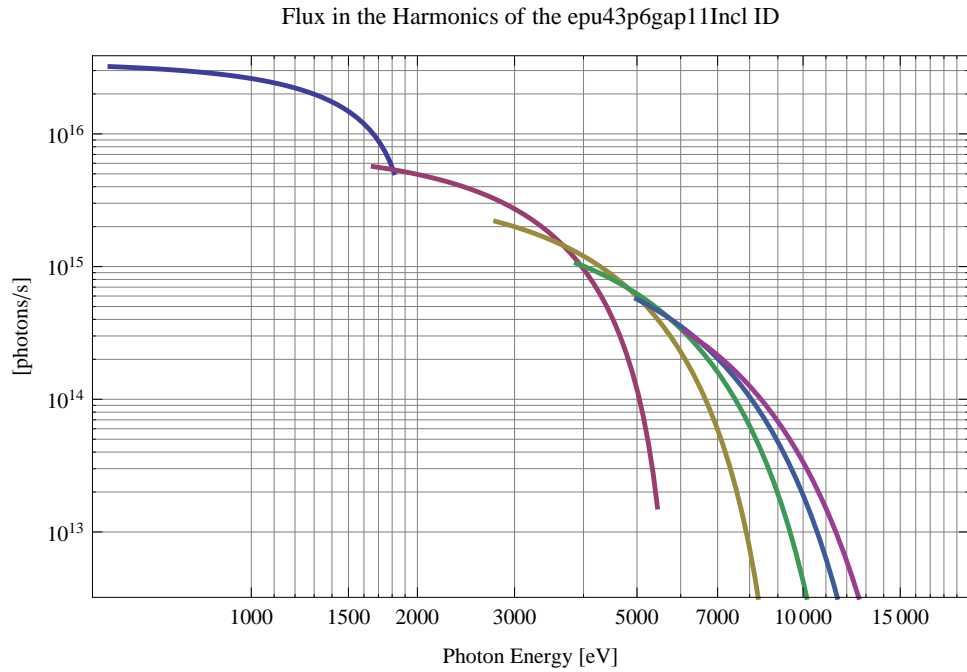


Figure 122: The flux of photons in the harmonics of the emitted synchrotron radiation from the epu43p6gap11Incl ID

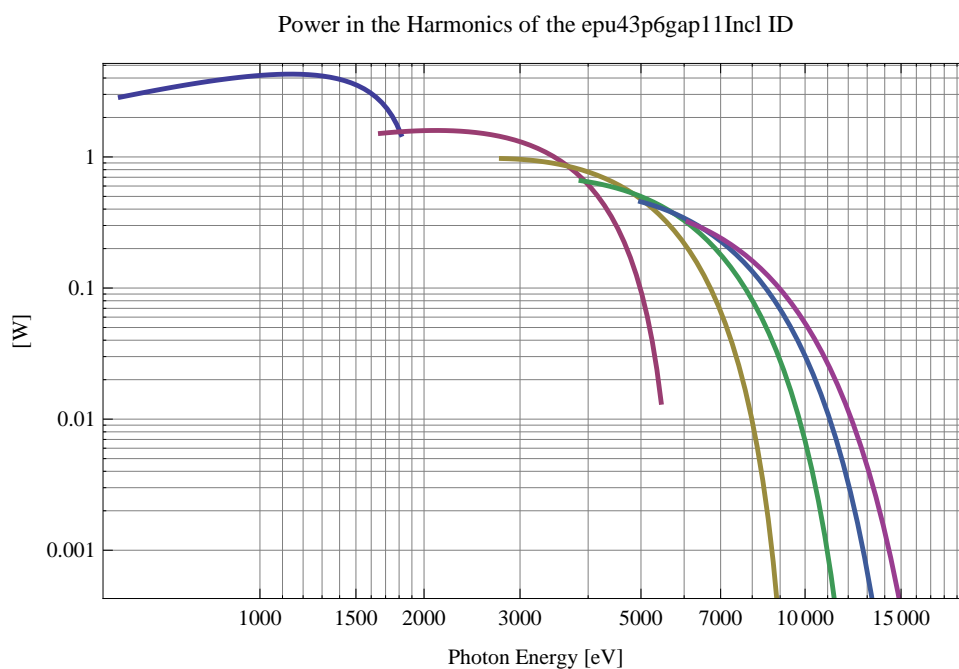


Figure 123: The power in the harmonics of the emitted synchrotron radiation from the epu43p6gap11Incl ID

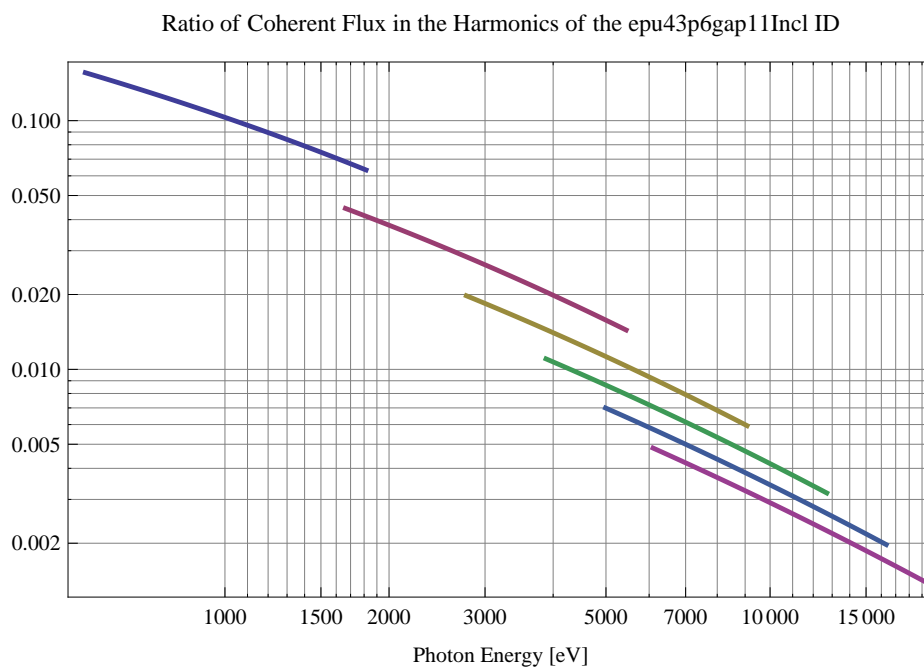


Figure 124: The ratio of coherent flux in the harmonics of the emitted synchrotron radiation from the epu43p6gap11Incl ID

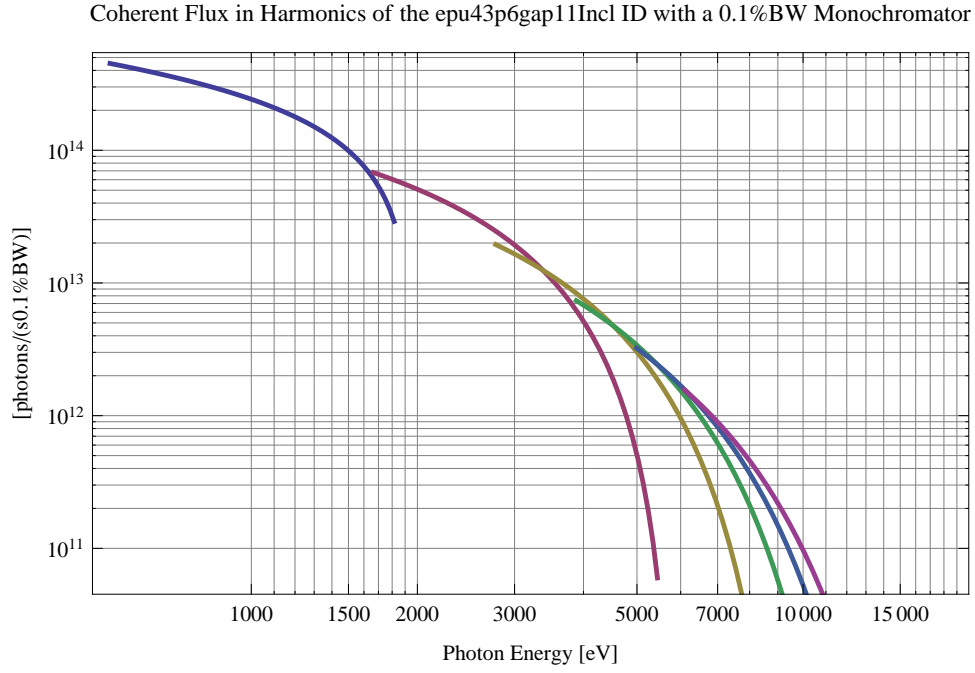


Figure 125: The coherent flux in the harmonics of the epu43p6gap11Incl ID using a 0.1%BW Monochromator

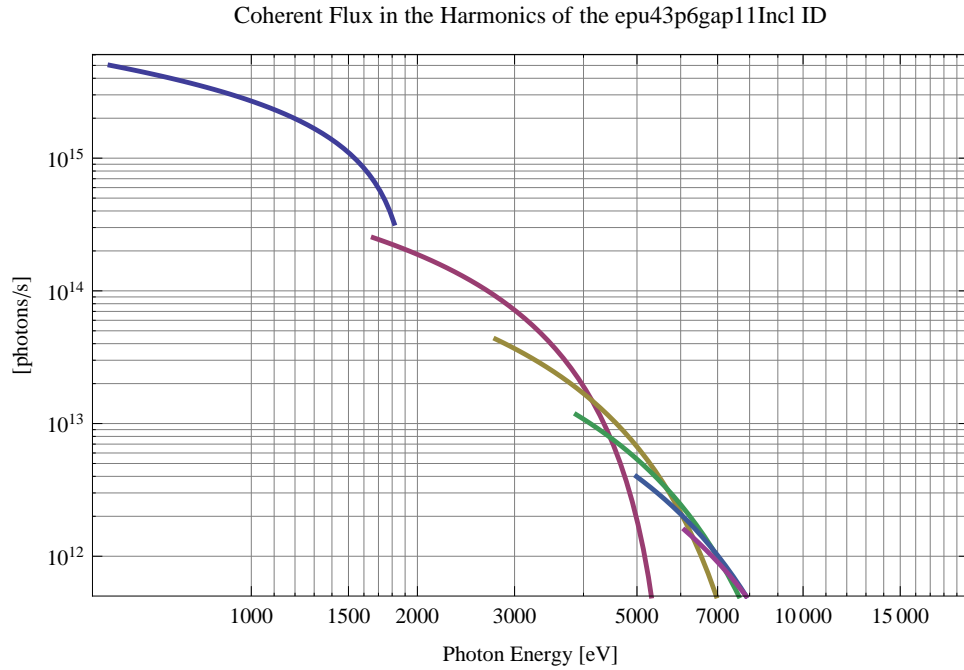


Figure 126: The coherent flux in the harmonics of the epu43p6gap11Incl ID

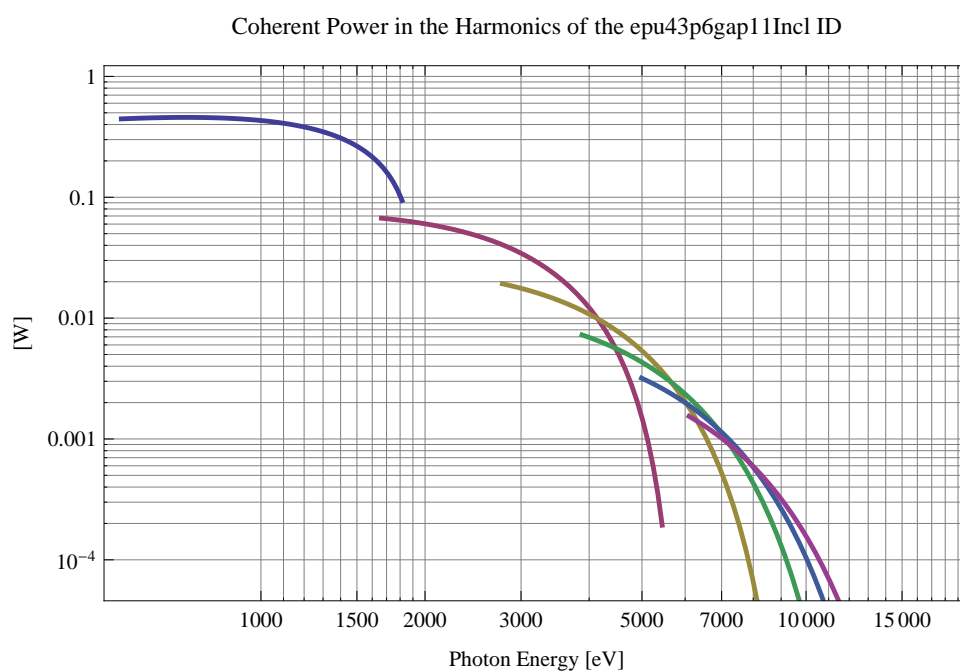


Figure 127: The power of coherent synchrotron radiation in the harmonics of the epu43p6gap11Incl ID

The brilliance at peak energy and the angular spectral flux density from the epu43p6gap11Incl ID for different harmonics at maximum K-value (2.252) are given in Table 21 and for minimum K-value (0.400) these values are given in Table 22.

Table 21: The brilliance at peak energy and the angular spectral flux density from the epu43p6gap11Incl ID for different harmonics at maximum K-value (2.252)

Harmonic	Photon Energy [eV]	Brilliance [Ph./((smrad ² mrads ² 0.1%BW))]	Angular Spectral Flux [Ph./((smrad ² 0.1%BW))]
1	554.492	3.61×10^{20}	1.09×10^{18}
3	1663.48	4.89×10^{20}	1.06×10^{18}
5	2772.46	3.9×10^{20}	7.65×10^{17}
7	3881.44	2.88×10^{20}	5.41×10^{17}
9	4990.43	2.09×10^{20}	3.83×10^{17}
11	6099.41	1.51×10^{20}	2.72×10^{17}

Table 22: The brilliance at peak energy and the angular spectral flux density from the epu43p6gap11Incl ID for different harmonics at minimum K-value (0.4)

Harmonic	Photon Energy [eV]	Brilliance [Ph./((smrad ² mrads ² 0.1%BW))]	Angular Spectral Flux [Ph./((smrad ² 0.1%BW))]
1	1815.06	2.49×10^{20}	5.33×10^{17}
3	5445.18	4.62×10^{18}	8.52×10^{15}
5	9075.31	5.21×10^{16}	9.34×10^{13}
7	12705.4	5.46×10^{14}	9.71×10^{11}
9	16335.5	5.62×10^{12}	9.94×10^9
11	19965.7	5.74×10^{10}	1.01×10^8

2.2.11 Magnet model of the elliptically polarising undulator epu43p6gap11Vert

The Radia [3] magnet model of the epu43p6gap11Vert ID is shown in Figure 128. The length of the magnet model is 366.067 mm. The magnetic material in the model is NdFeb with a remanence of 1.28 T, a material similar to VACODYM 776 TP from Vacuumschmelze. Blocks with vertical magnetisation are blue and blocks with horizontal magnetisation are yellow. The block size is 30.x30.x10.9 mm³ and there is a 5. mm cut-out in two of the corners of the blocks. The total length of the epu43p6gap11Vert ID is 3941.27 mm.

2.2.12 Analysis of the magnetic field of the epu43p6gap11Vert ID

The effective magnetic fields on axis and the fundamental photon energy of the epu43p6gap11Vert ID are shown in Table 23. The higher harmonic contents in the magnetic field of an elliptically polarising undulator made of permanent magnets is negligible and the effective field has about the same strength as the peak field.

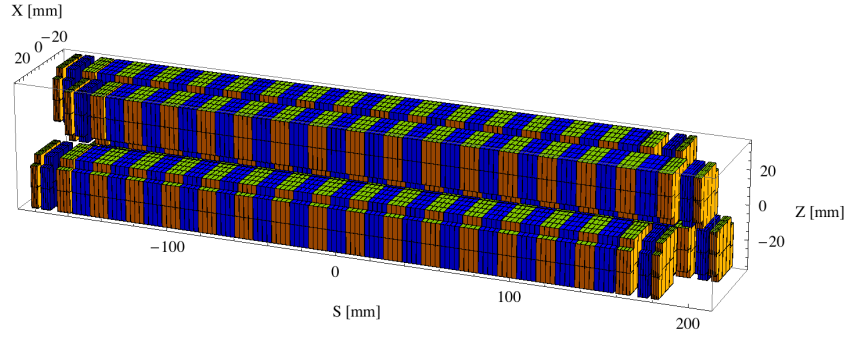


Figure 128: Magnetic model of the epu43p6gap11Vert ID. The ID has been modelled with Radia [3]

Table 23: Effective Fields on axis and Fundamental Photon Energy of the epu43p6gap11Vert ID

Undulator Period	43.6	mm
Undulator Gap	11	mm
Undulator Mode	Vertical	
Undulator Phase	21.800	mm
Vertical Peak Field	0.000	T
Effective Vertical Field	0.000	T
K _x (from vert. field)	0.000	
Horizontal Peak Field:	0.673	T
Effective Horizontal Field	0.673	T
K _z (from hor. field)	2.741	
Photon Energy, Harm.1	0.412	keV
Emitted Power	5.082	kW
Total Length	3941.3	mm

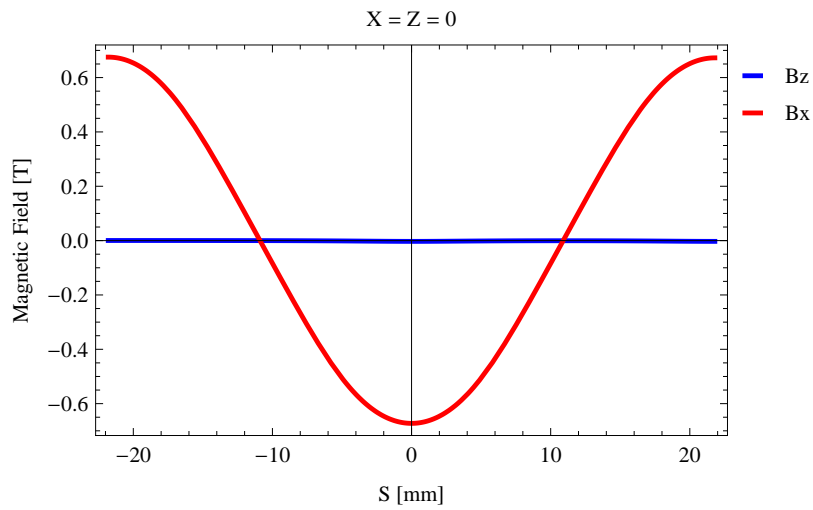


Figure 129: Vertical magnetic field in a central pole of the epu43p6gap11Vert ID along the ID axis, $X = Z = 0$

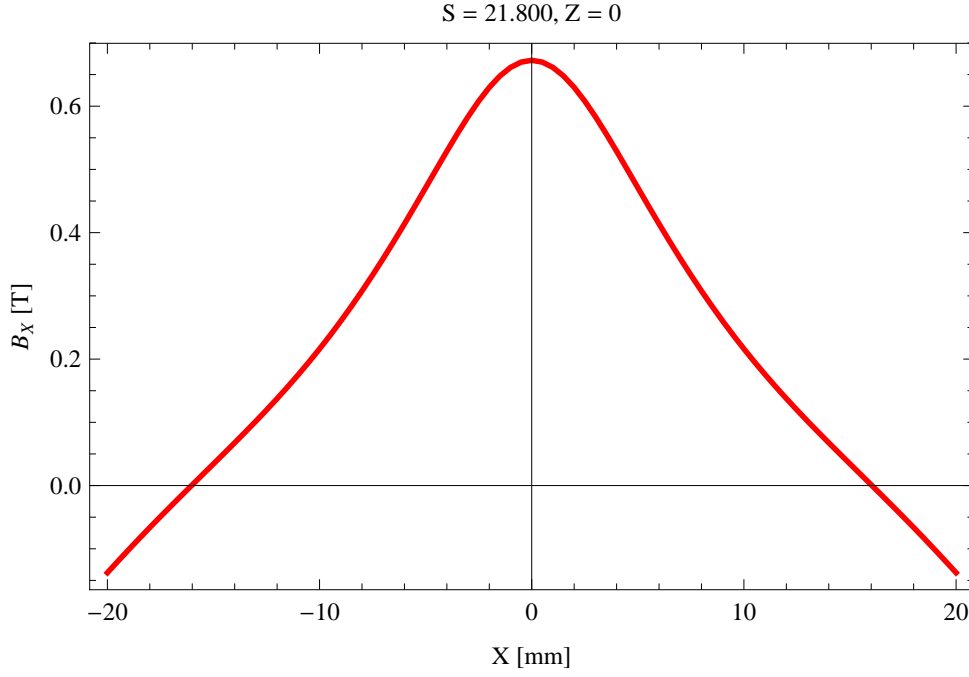


Figure 130: Horizontal magnetic field in a central pole of the epu43p6gap11Vert ID along the horizontally transverse direction to the ID axis, $S = 21.800$, $Z = 0$

2.2.13 Synchrotron radiation from the epu43p6gap11Vert ID

The power map of the emitted synchrotron radiation by the epu43p6gap11Vert ID, assuming a 0.5 A filament beam with an energy of 3 GeV and undulator properties of the synchrotron radiation, is shown in Figure 132. The on-axis power density is 26.035 kW/mrad^2

A map of the degree of linear polarisation of the fundamental harmonic of the synchrotron radiation emitted by the epu43p6gap11Vert ID over the angle of observation is shown in Figure 133.

A map of the degree of 45 degree polarisation of the fundamental harmonic of the synchrotron radiation emitted by the epu43p6gap11Vert ID over the angle of observation is shown in Figure 134.

A map of the degree of circular polarisation of the fundamental harmonic of the synchrotron radiation emitted by the epu43p6gap11Vert ID over the angle of observation is shown in Figure 135.

The on axis brilliance at peak energy and the angular spectral flux from the epu43p6gap11Vert ID have been calculated with the given beam parameters, which are 0.5 A of stored current, $\beta_H = 9 \text{ m}$, $\varepsilon_H = 0.263 \text{ nmrad}$, $\beta_V = 4.8 \text{ m}$, $\varepsilon_V = 8. \text{ pmrad}$, and an energy spread of 0.001.

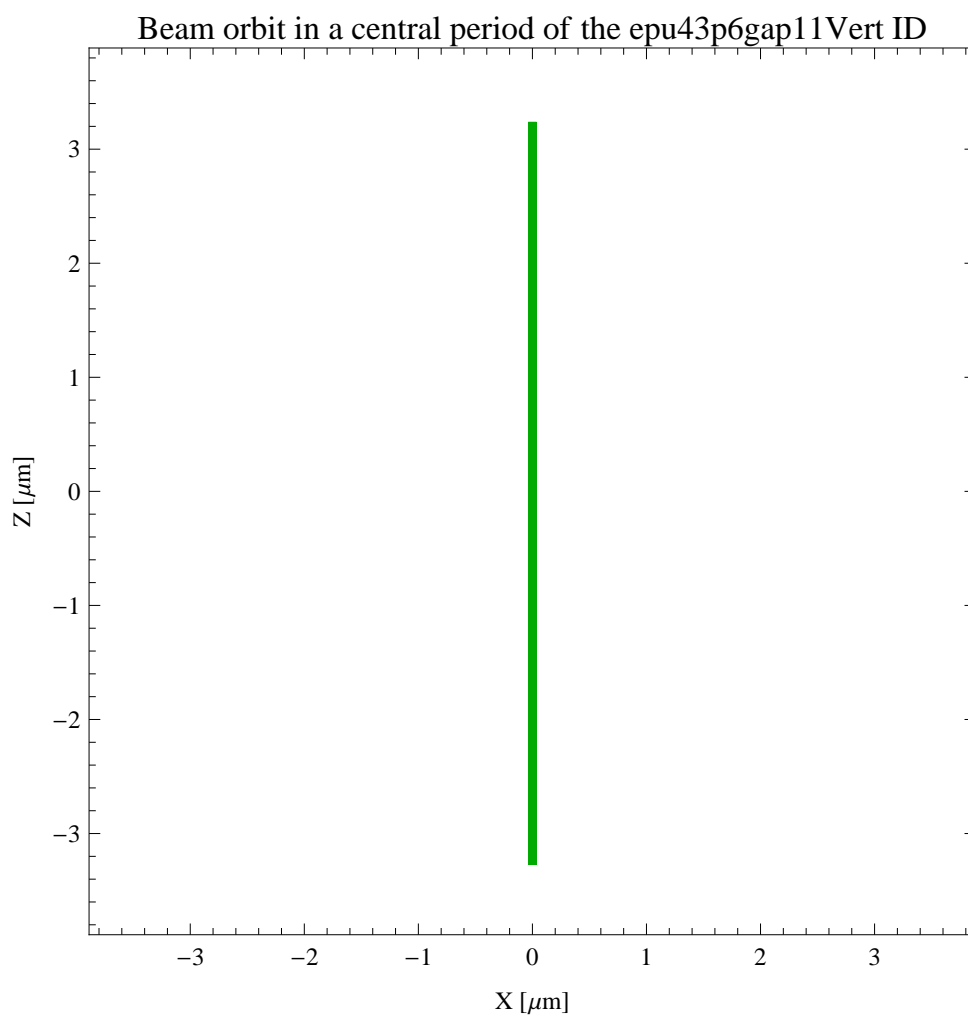


Figure 131: The beam orbit of the electron beam through a central period of the epu43p6gap11Vert ID

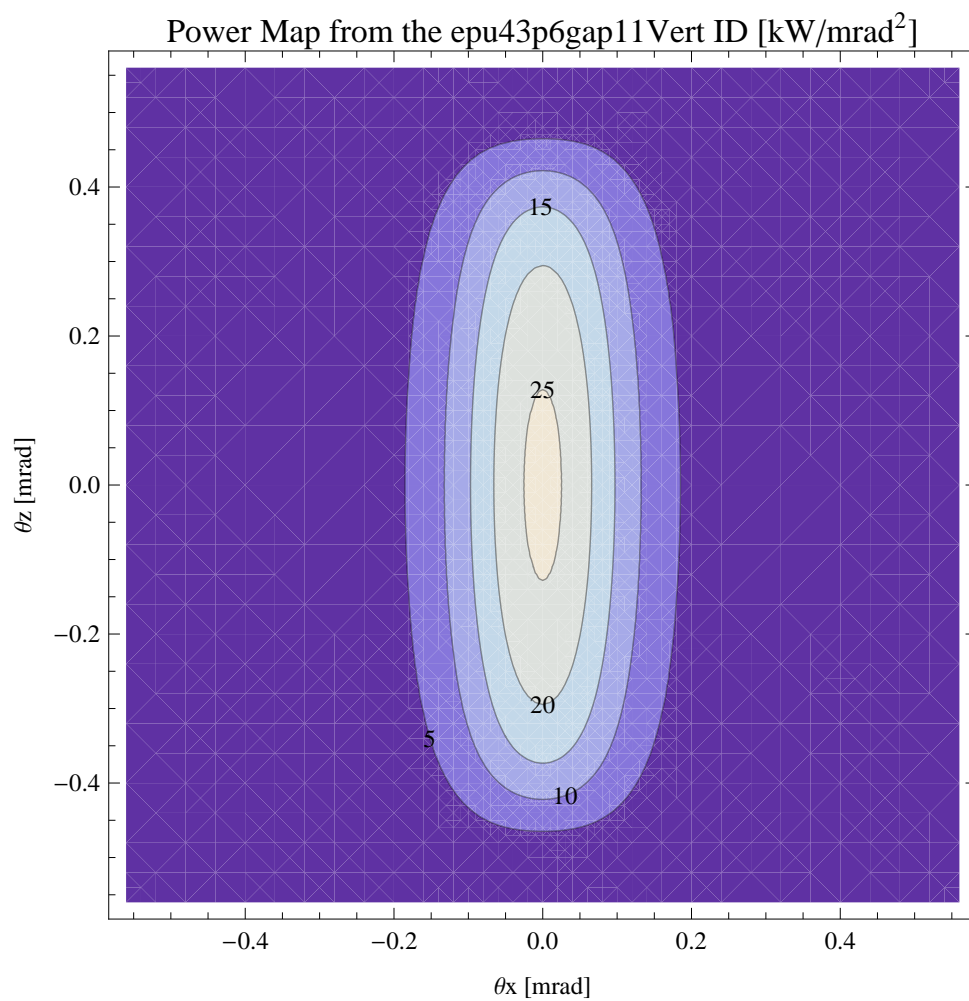


Figure 132: Map of the power distribution of the emitted synchrotron radiation by the epu43p6gap11Vert ID

Degree of Linear Polarisation in Harm.1 from the epu43p6gap11Vert ID

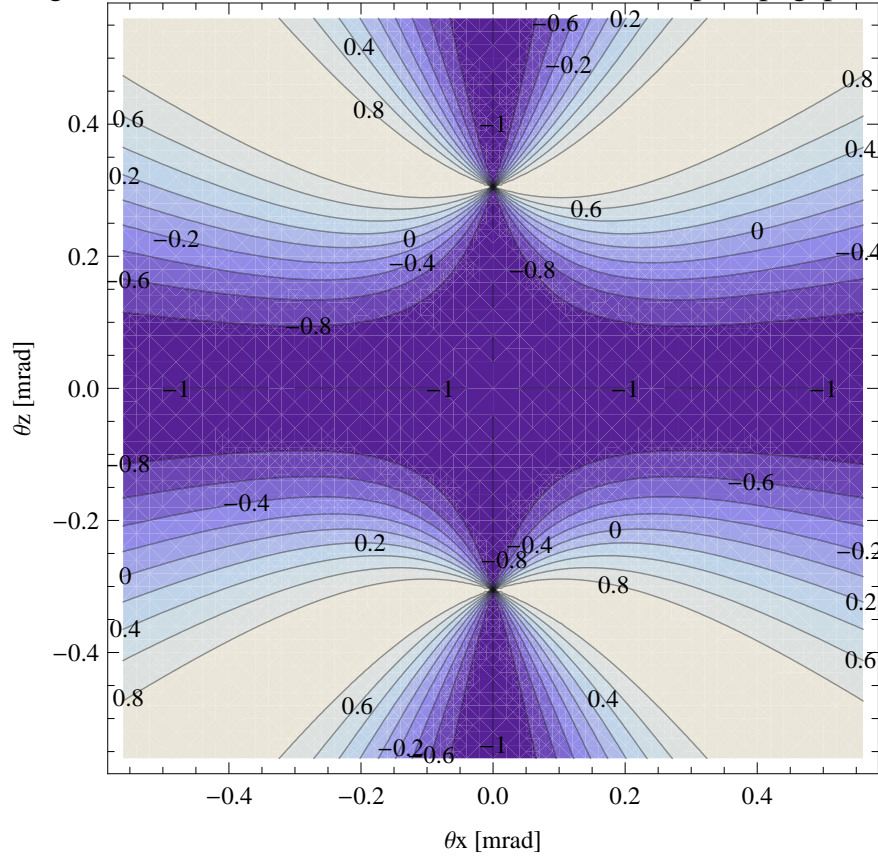


Figure 133: Map of linear polarisation in the fundamental harmonic of the synchrotron radiation emitted by the epu43p6gap11Vert ID

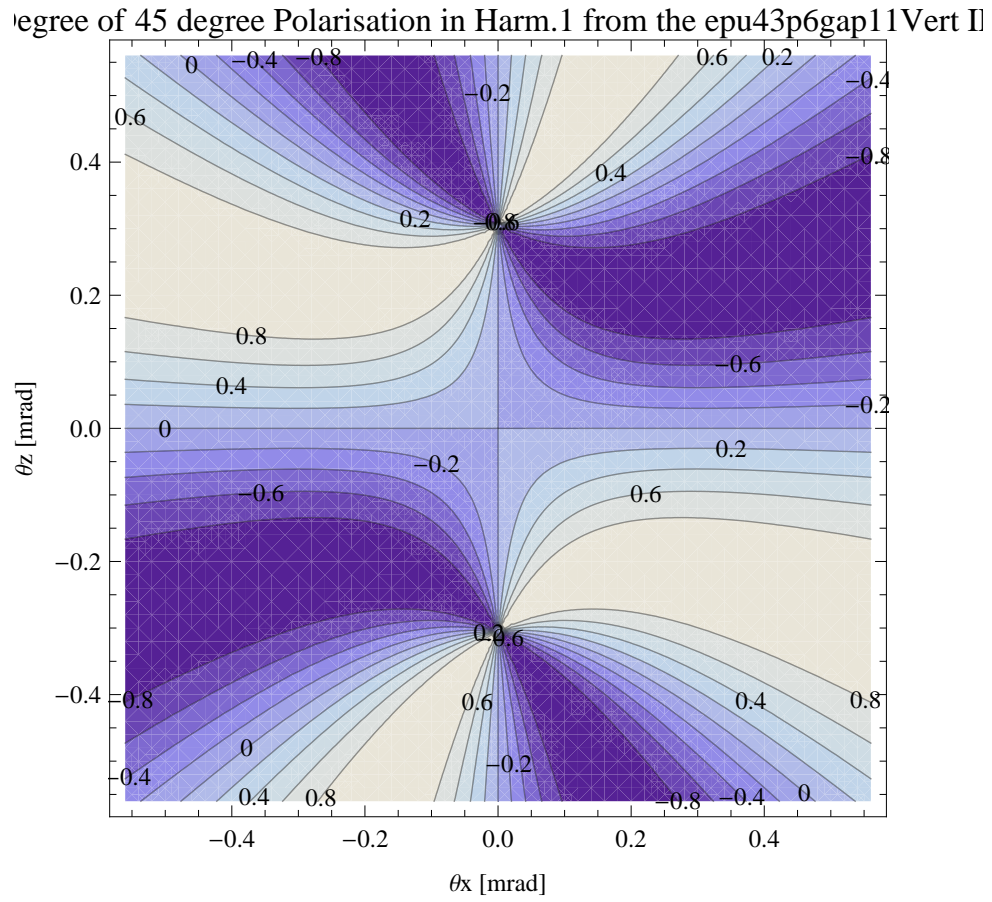


Figure 134: Map of 45 degree polarisation in the fundamental harmonic of the synchrotron radiation emitted by the epu43p6gap11Vert ID

Degree of Circular Polarisation in Harm.1 from the epu43p6gap11Vert II

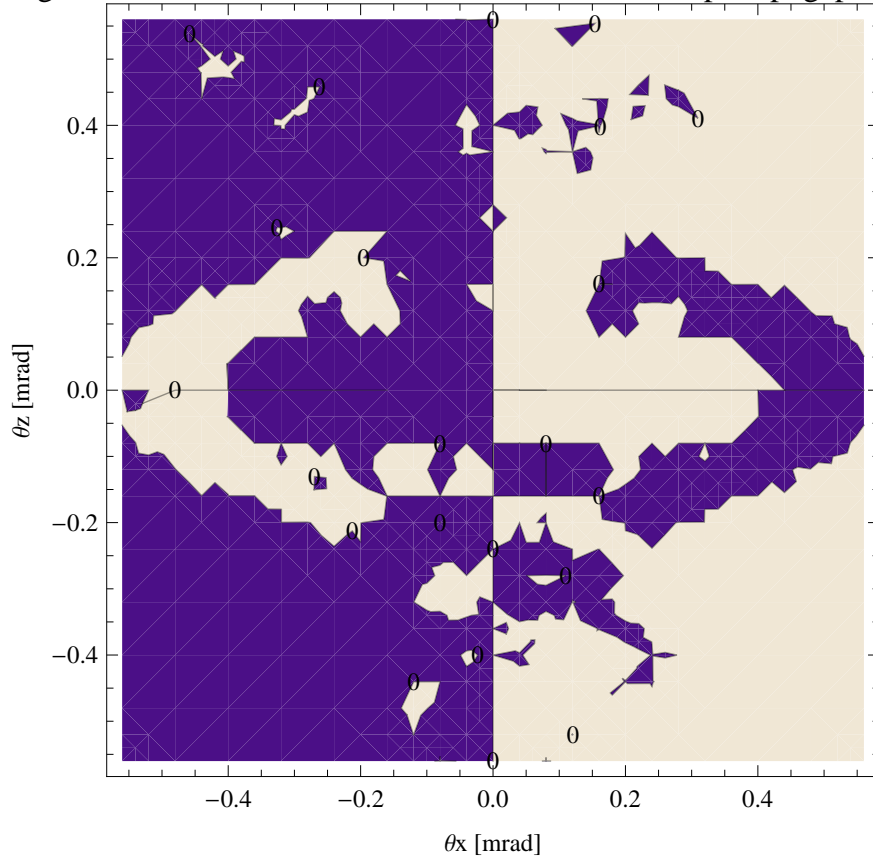


Figure 135: Map of circular polarisation in the fundamental harmonic of the synchrotron radiation emitted by the epu43p6gap11Vert ID

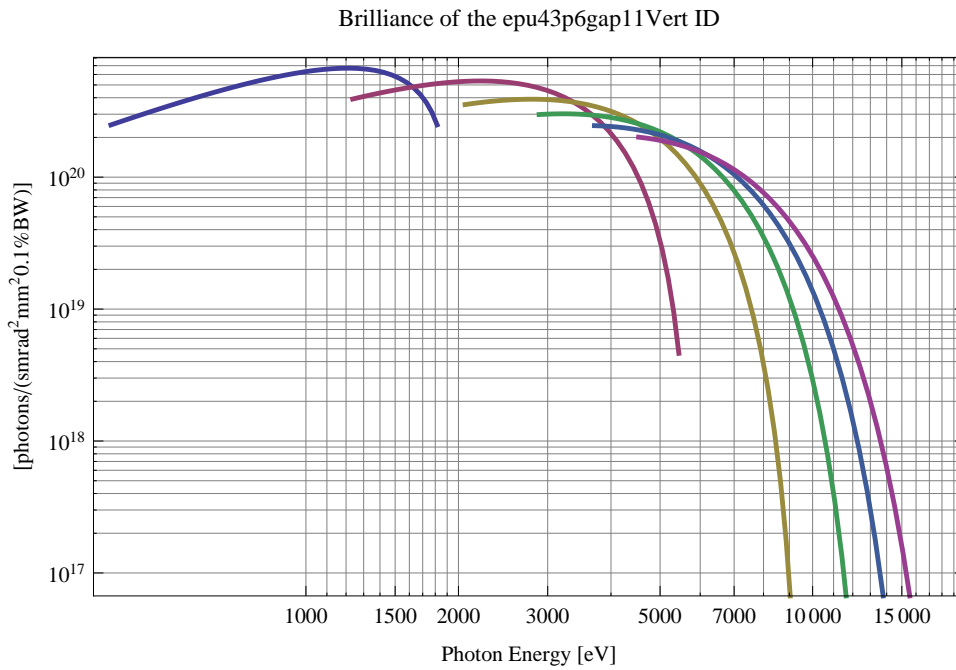


Figure 136: The brilliance at peak energy of the synchrotron radiation emitted by the epu43p6gap11Vert ID

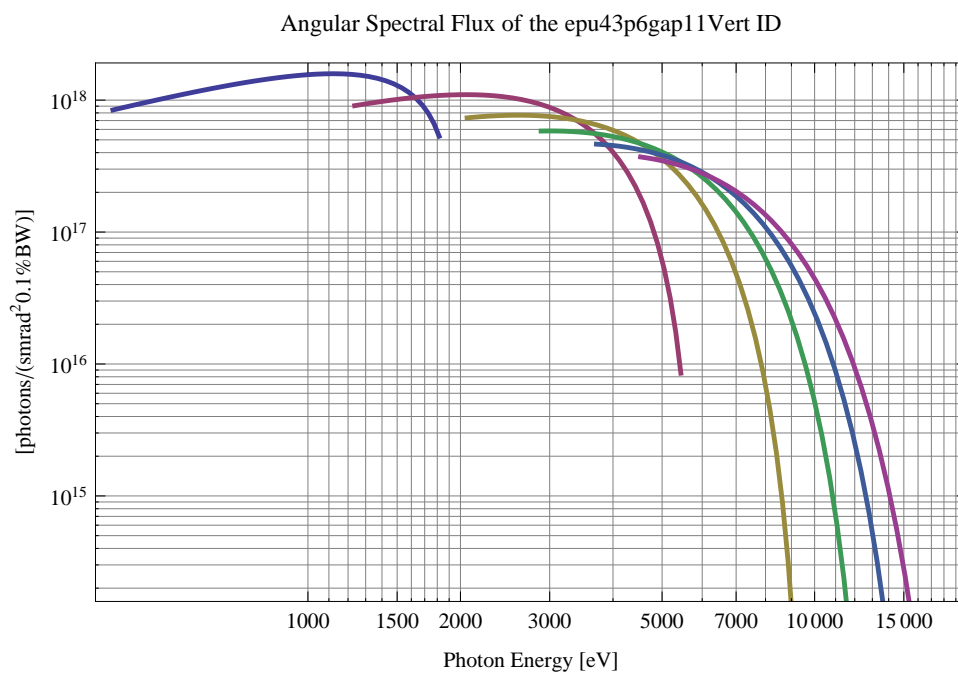


Figure 137: The angular spectral flux of the synchrotron radiation emitted by the epu43p6gap11Vert ID

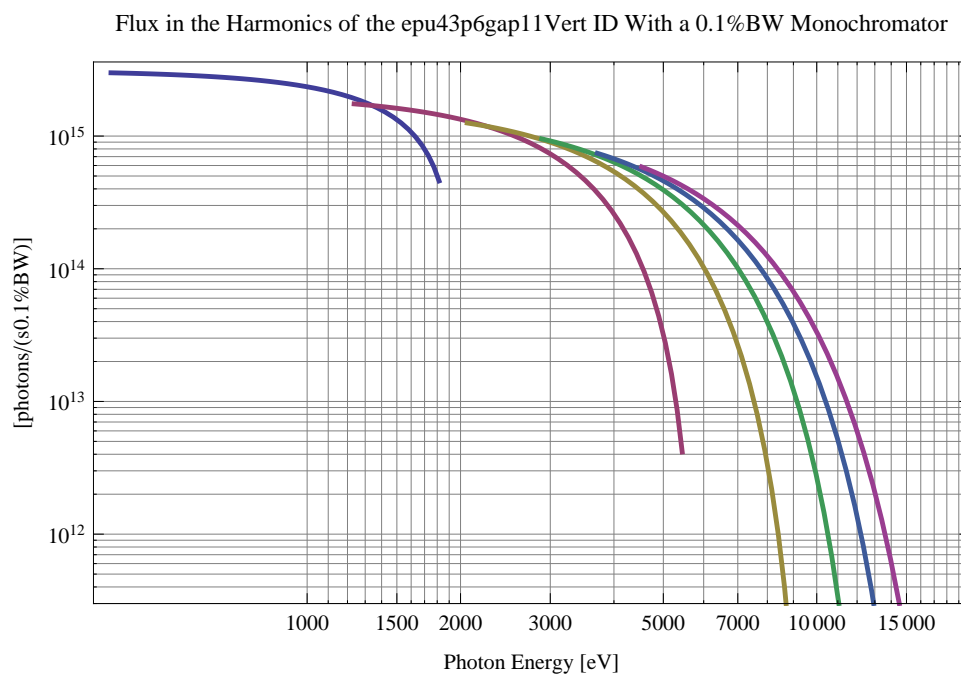


Figure 138: The flux of photons in the harmonics of the emitted synchrotron radiation from the epu43p6gap11Vert ID using a 0.1% BW monochromator

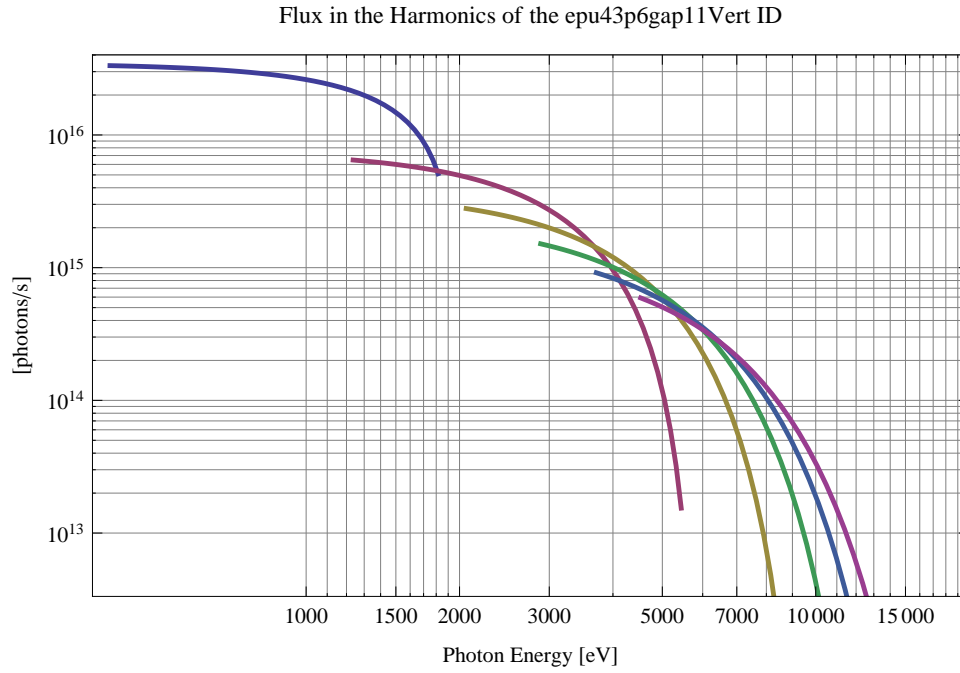


Figure 139: The flux of photons in the harmonics of the emitted synchrotron radiation from the epu43p6gap11Vert ID

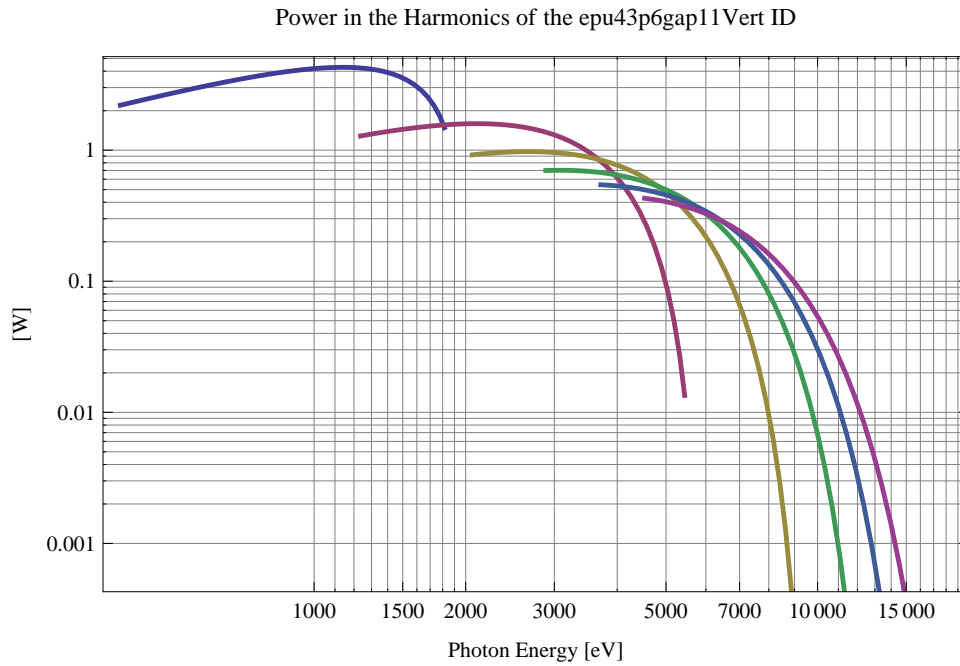


Figure 140: The power in the harmonics of the emitted synchrotron radiation from the epu43p6gap11Vert ID

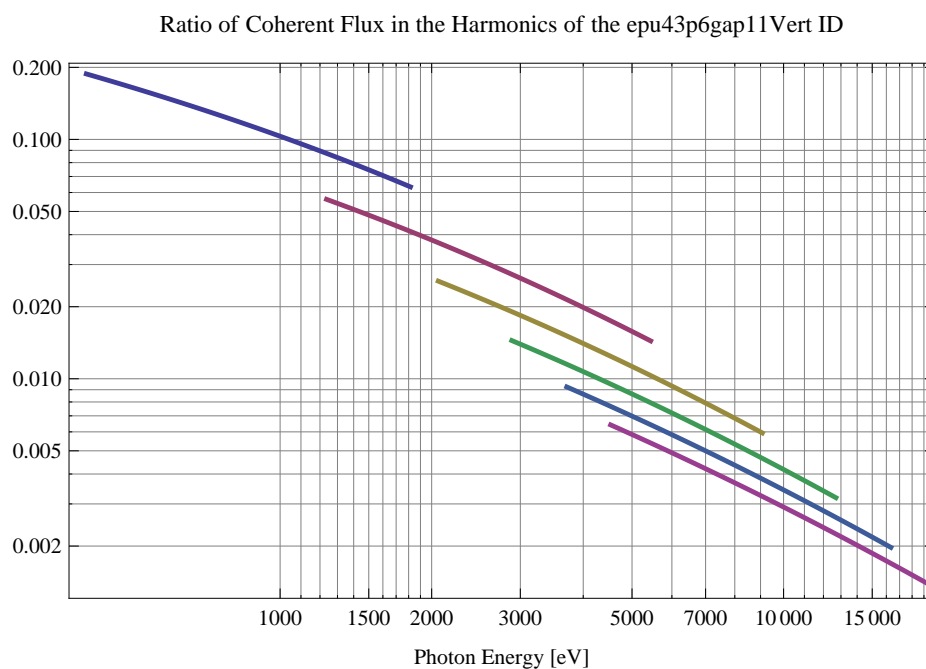


Figure 141: The ratio of coherent flux in the harmonics of the emitted synchrotron radiation from the epu43p6gap11Vert ID

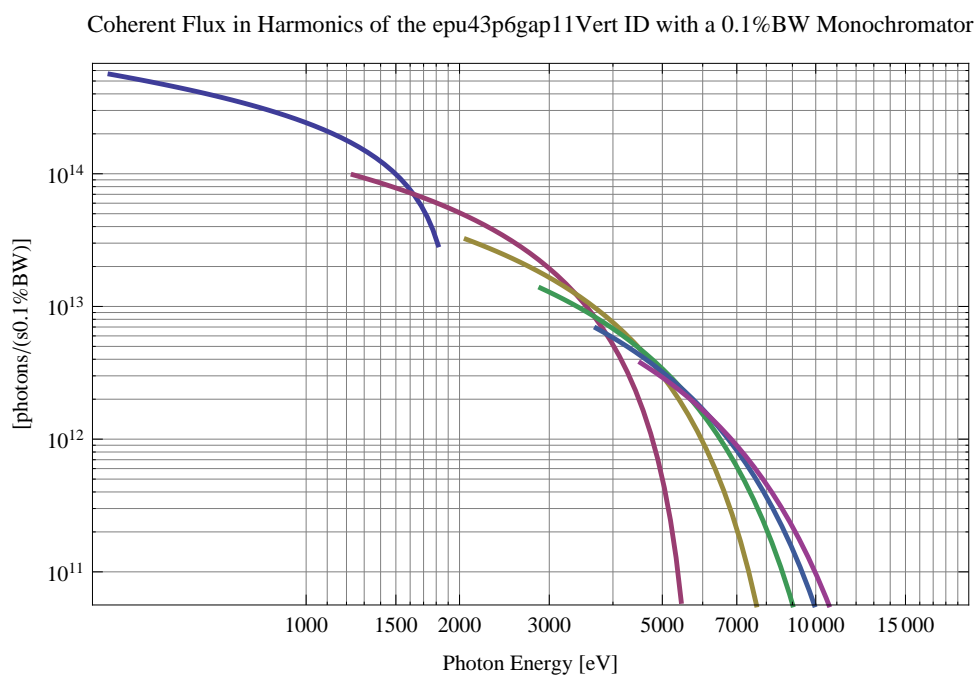


Figure 142: The coherent flux in the harmonics of the epu43p6gap11Vert ID using a 0.1%BW Monochromator

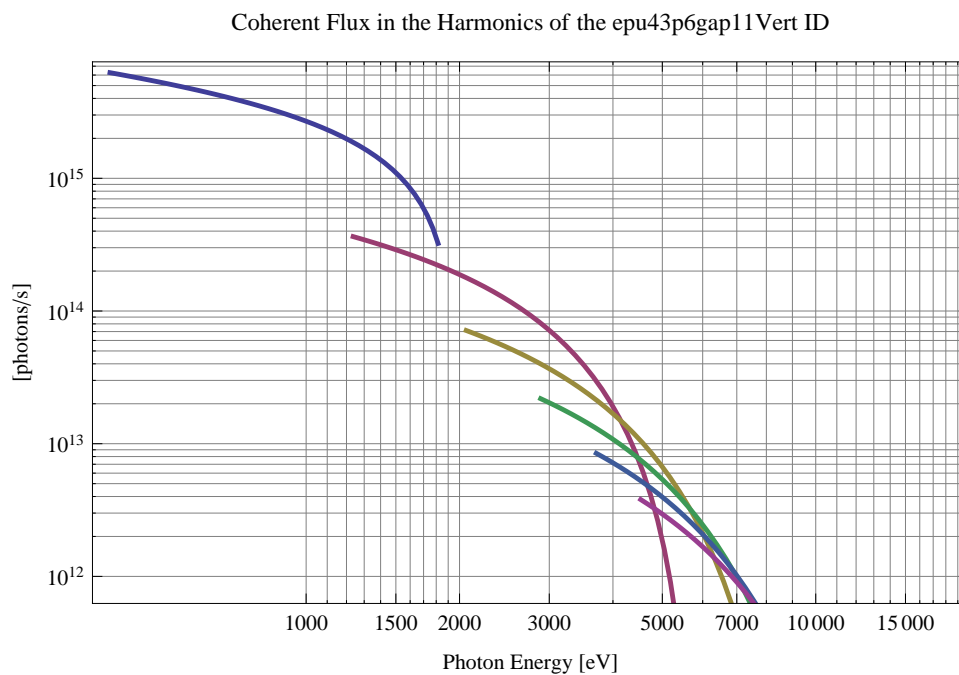


Figure 143: The coherent flux in the harmonics of the epu43p6gap11Vert ID

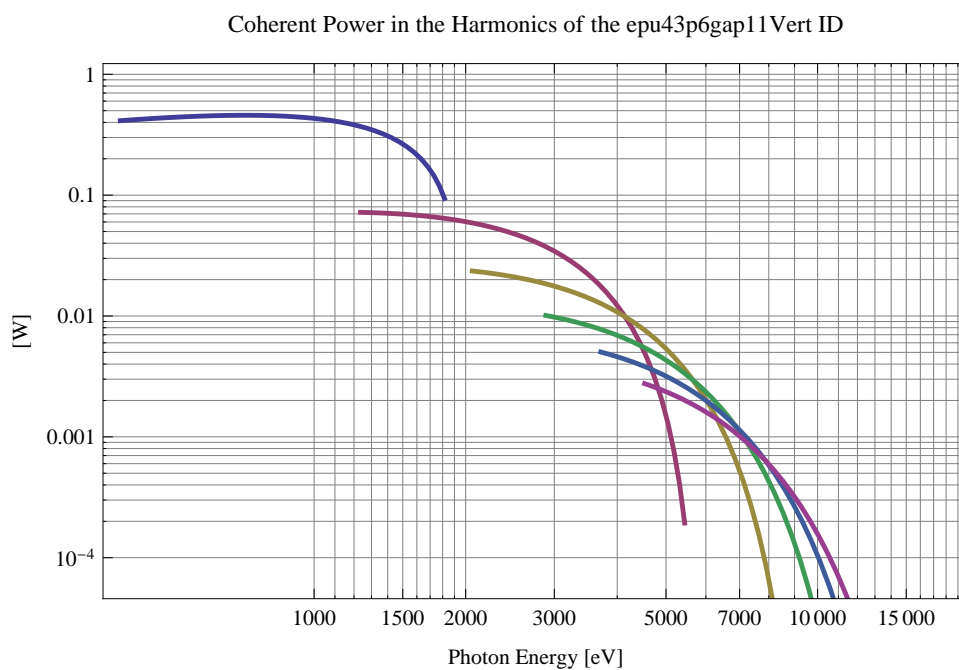


Figure 144: The power of coherent synchrotron radiation in the harmonics of the epu43p6gap11Vert ID

The brilliance at peak energy and the angular spectral flux density from the epu43p6gap11Vert ID for different harmonics at maximum K-value (2.741) are given in Table 24 and for minimum K-value (0.400) these values are given in Table 25.

Table 24: The brilliance at peak energy and the angular spectral flux density from the epu43p6gap11Vert ID for different harmonics at maximum K-value (2.741)

Harmonic	Photon Energy [eV]	Brilliance [Ph./($\text{smrad}^2\text{mrad}^20.1\%\text{BW}$)]	Angular Spectral Flux [Ph./($\text{smrad}^20.1\%\text{BW}$)]
1	412.211	2.49×10^{20}	8.42×10^{17}
3	1236.63	3.91×10^{20}	9.08×10^{17}
5	2061.05	3.55×10^{20}	7.34×10^{17}
7	2885.48	2.98×10^{20}	5.83×10^{17}
9	3709.9	2.46×10^{20}	4.64×10^{17}
11	4534.32	2.01×10^{20}	3.71×10^{17}

Table 25: The brilliance at peak energy and the angular spectral flux density from the epu43p6gap11Vert ID for different harmonics at minimum K-value (0.4)

Harmonic	Photon Energy [eV]	Brilliance [Ph./($\text{smrad}^2\text{mrad}^20.1\%\text{BW}$)]	Angular Spectral Flux [Ph./($\text{smrad}^20.1\%\text{BW}$)]
1	1815.06	2.49×10^{20}	5.33×10^{17}
3	5445.18	4.62×10^{18}	8.52×10^{15}
5	9075.31	5.21×10^{16}	9.34×10^{13}
7	12705.4	5.46×10^{14}	9.71×10^{11}
9	16335.5	5.62×10^{12}	9.94×10^9
11	19965.7	5.74×10^{10}	1.01×10^8

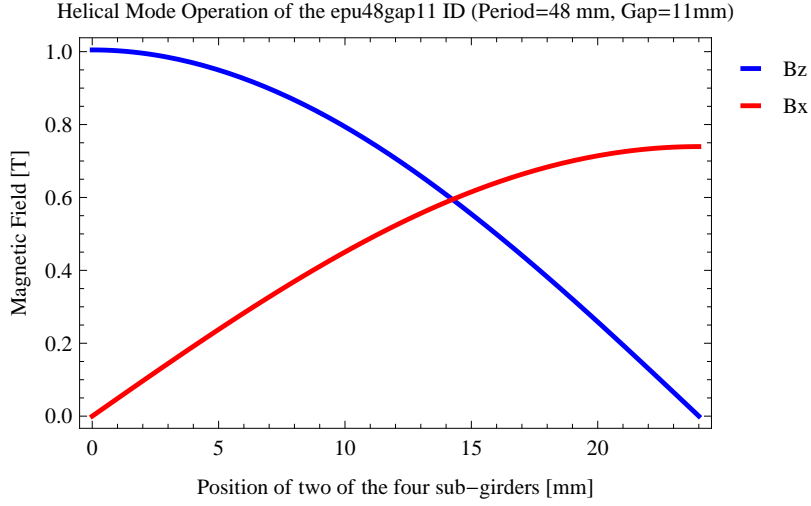


Figure 145: Vertical and horizontal magnetic field for the the epu48gap11 ID when operating in the helical mode for different positions for two of the four sub-girders

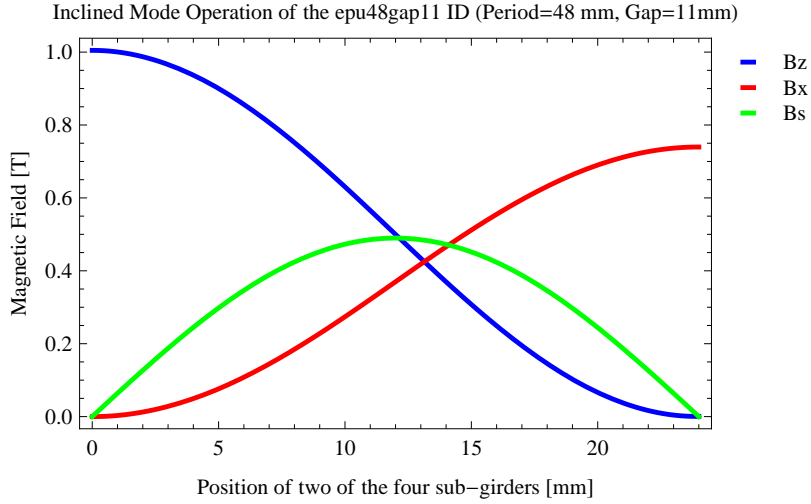


Figure 146: Vertical, horizontal, and longitudinal magnetic field for the the epu48gap11 ID when operating in the inclined mode for different positions for two of the four sub-girders

2.3 The elliptically polarising undulator epu48gap11

2.3.1 Modes of operation in the elliptically polarising undulator epu48gap11

Horizontal polarisation of the emitted synchrotron radiation from the epu48gap11 ID (Period=48 mm, Gap=11mm) is found in the planar mode when there is no movement of the sub-girders.

Circular polarisation is found in the elliptical mode of operation for a symmetric sub-grider movement of 14.2548 mm. Figure 145 shows the vertical and horizontal magnetic field for the epu48gap11 ID when operating in the helical mode.

45 degree polarisation is found in the inclined mode of operation for an assymetric sub-grider movement of 13.1396 mm. Figure 146 shows the vertical and horizontal magnetic field for the epu48gap11 ID when operating in the inclined mode.

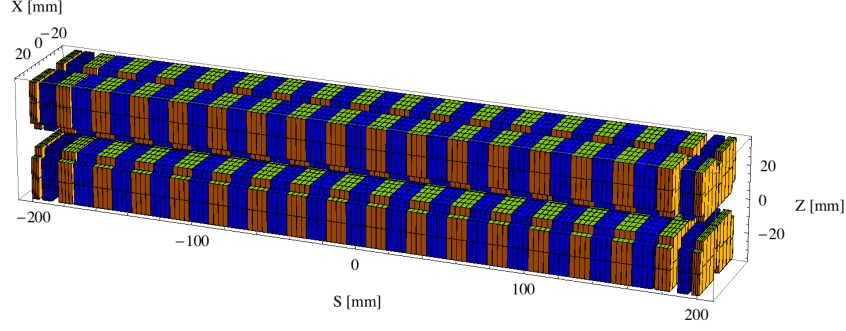


Figure 147: Magnetic model of the epu48gap11Plan ID. The ID has been modelled with Radia [3]

The following sub-sections will cover four different situations: The epu48gap11 operating in the planar mode for horizontal polarisation (epu48gap11Plan); The epu48gap11 operating in the helical mode for circular polarisation (epu48gap11Heli), the epu48gap11 operating in the inclined mode for 45 degree polarisation (epu48gap11Incl); and The epu48gap11 operating in the vertical mode for vertical polarisation (epu48gap11Vert).

2.3.2 Magnet model of the elliptically polarising undulator epu48gap11Plan

The Radia [3] magnet model of the epu48gap11Plan ID is shown in Figure 147. The length of the magnet model is 401.496 mm. The magnetic material in the model is NdFeb with a remanence of 1.28 T, a material similar to VACODYM 776 TP from Vacuumschmelze. Blocks with vertical magnetisation are blue and blocks with horizontal magnetisation are yellow. The block size is $30 \times 30 \times 12 \text{ mm}^3$ and there is a 5 mm cut-out in two of the corners of the blocks. The total length of the epu48gap11Plan ID is 3905.5 mm.

2.3.3 Analysis of the magnetic field of the epu48gap11Plan ID

The effective magnetic fields on axis and the fundamental photon energy of the epu48gap11Plan ID are shown in Table 26. The higher harmonic contents in the magnetic field of an elliptically polarising undulator made of permanent magnets is negligible and the effective field has about the same strength as the peak field.

2.3.4 Synchrotron radiation from the epu48gap11Plan ID

The power map of the emitted synchrotron radiation by the epu48gap11Plan ID, assuming a 0.5 A filament beam with an energy of 3 GeV and undulator properties of the synchrotron radiation, is shown in Figure 151. The on-axis power density is 35.179 kW/mrad^2

A map of the degree of linear polarisation of the fundamental harmonic of the synchrotron radiation emitted by the epu48gap11Plan ID over the angle of observation is shown in Figure 152.

A map of the degree of 45 degree polarisation of the fundamental harmonic of the synchrotron radiation emitted by the epu48gap11Plan ID over the angle of observation is shown in Figure 153.

Table 26: Effective Fields on axis and Fundamental Photon Energy of the epu48gap11Plan ID

Undulator Period	48	mm
Undulator Gap	11	mm
Undulator Mode	Planar	
Undulator Phase	0.000	mm
Vertical Peak Field	0.992	T
Effective Vertical Field	1.005	T
Kx (from vert. field)	4.506	
Horizontal Peak Field:	0.000	T
Effective Horizontal Field	0.000	T
Kz (from hor. field)	0.000	
Photon Energy, Harm.1	0.160	keV
Emitted Power	11.231	kW
Total Length	3905.5	mm

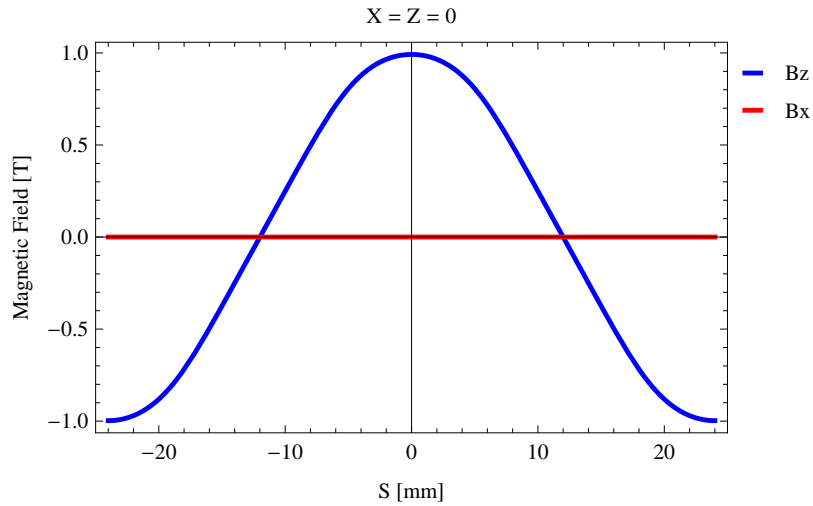


Figure 148: Vertical magnetic field in a central pole of the epu48gap11Plan ID along the ID axis, $X = Z = 0$

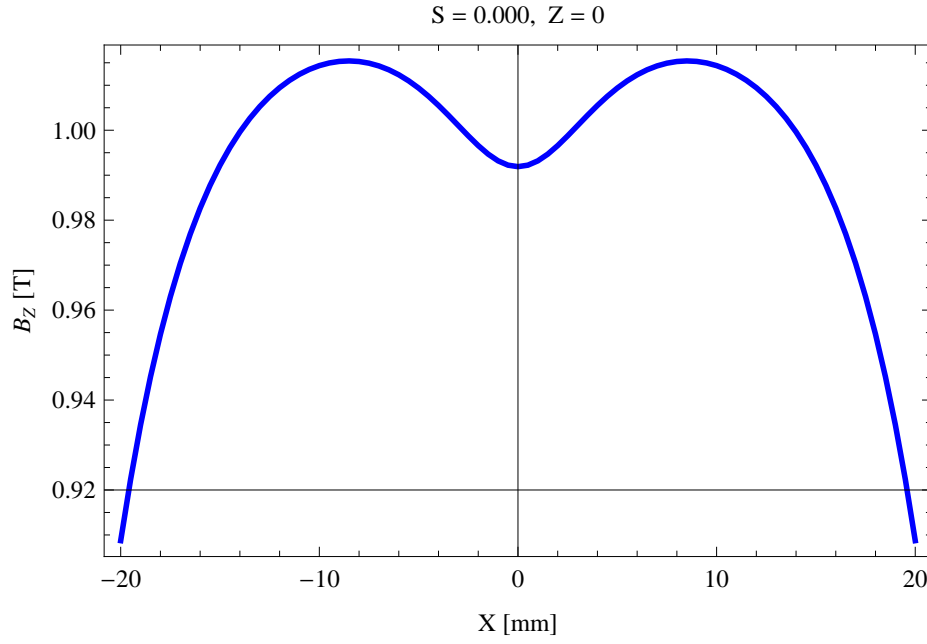


Figure 149: Vertical magnetic field in a central pole of the epu48gap11Plan ID along the horizontally transverse direction to the ID axis, $S = 0.000, Z = 0$

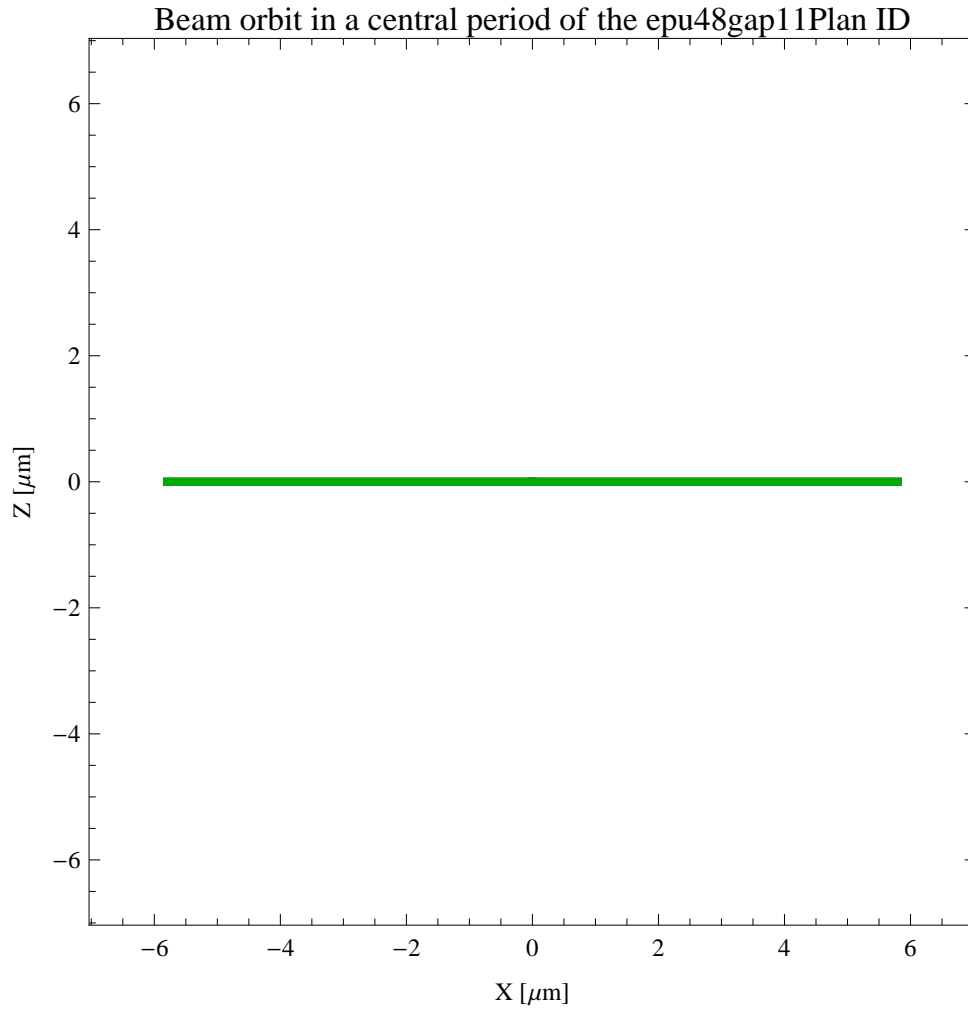


Figure 150: The beam orbit of the electron beam through a central period of the epu48gap11Plan ID

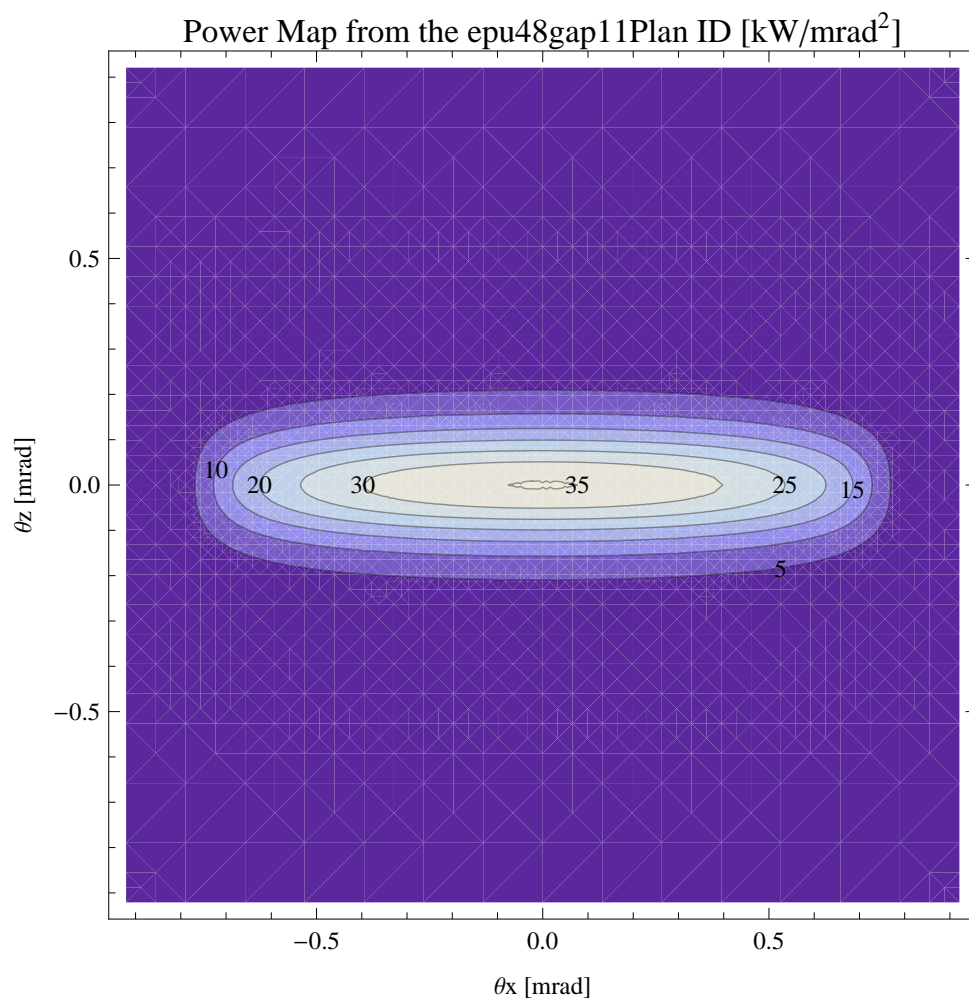


Figure 151: Map of the power distribution of the emitted synchrotron radiation by the epu48gap11Plan ID

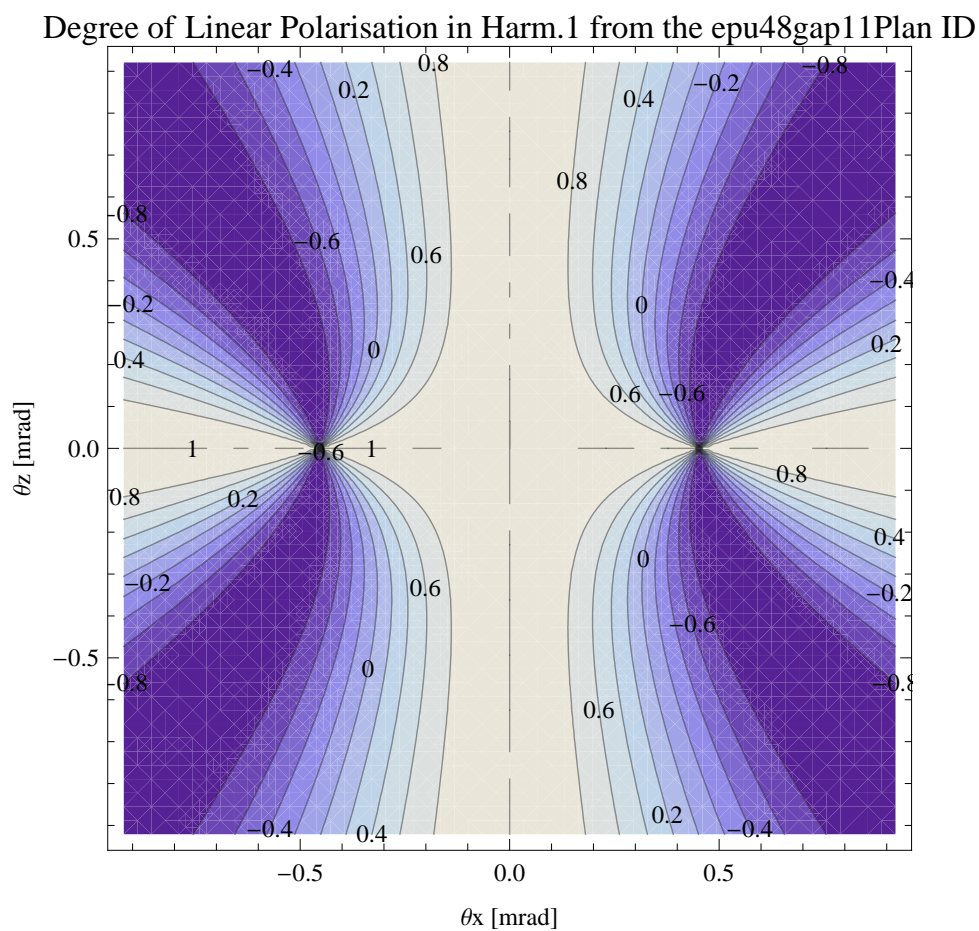


Figure 152: Map of linear polarisation in the fundamental harmonic of the synchrotron radiation emitted by the epu48gap11Plan ID

Degree of 45 degree Polarisation in Harm.1 from the epu48gap11Plan ID

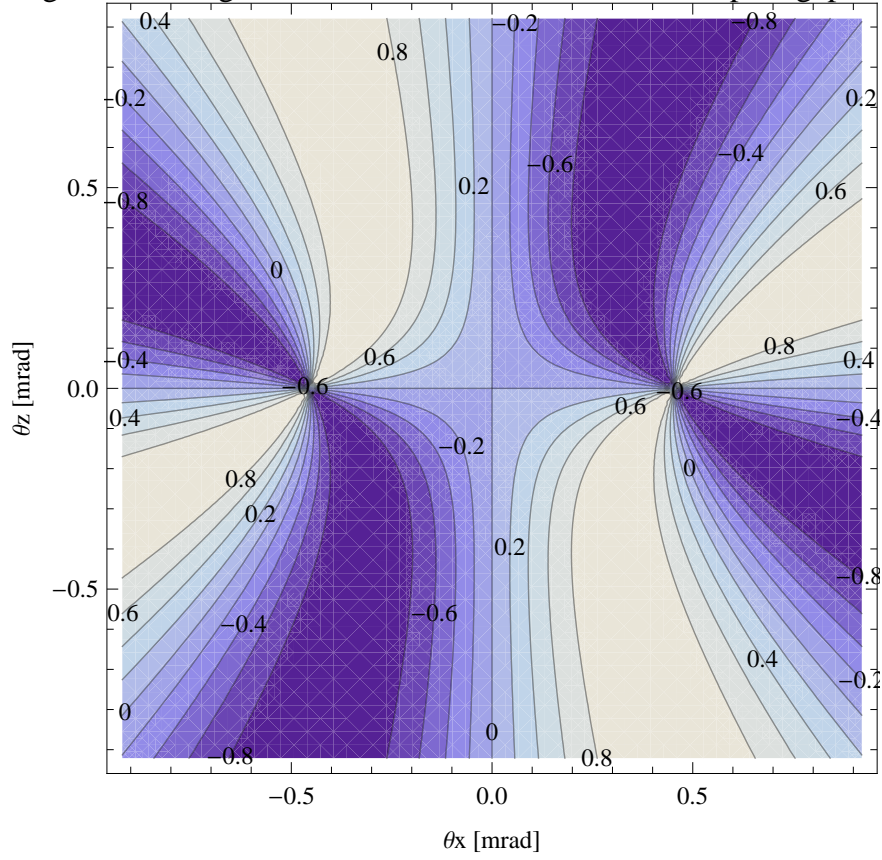


Figure 153: Map of 45 degree polarisation in the fundamental harmonic of the synchrotron radiation emitted by the epu48gap11Plan ID

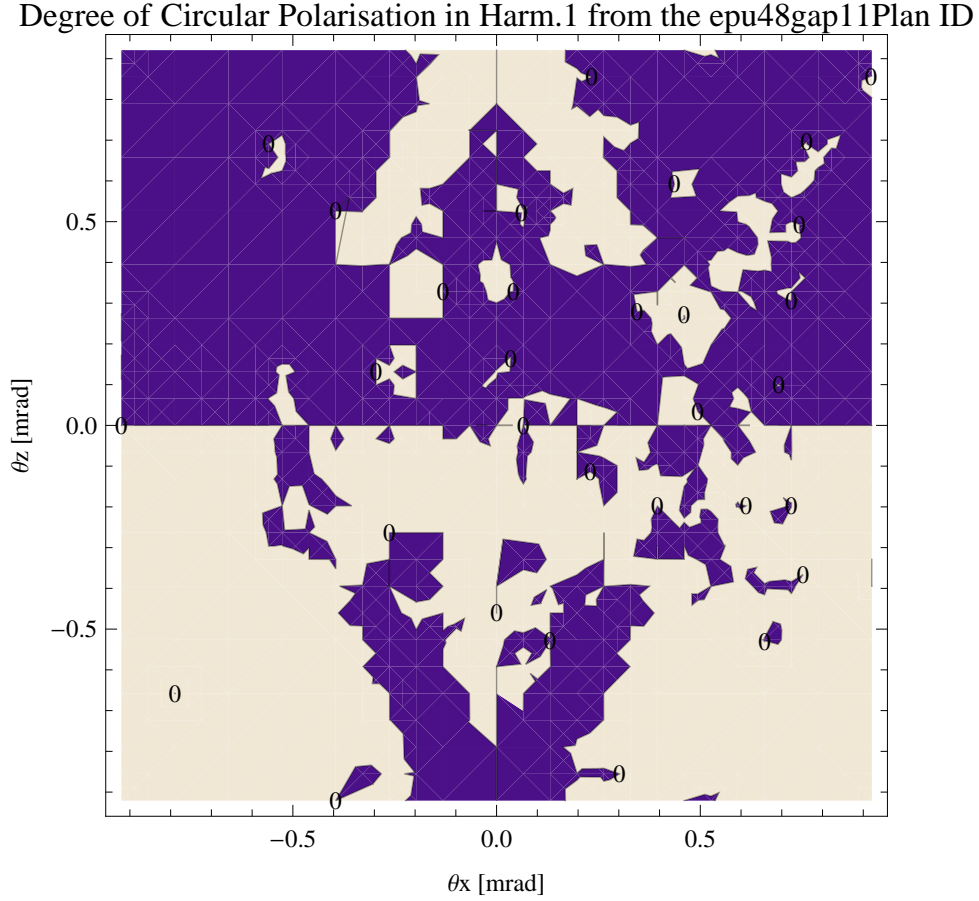


Figure 154: Map of circular polarisation in the fundamental harmonic of the synchrotron radiation emitted by the epu48gap11Plan ID

A map of the degree of circular polarisation of the fundamental harmonic of the synchrotron radiation emitted by the epu48gap11Plan ID over the angle of observation is shown in Figure 154.

The on axis brilliance at peak energy and the angular spectral flux from the epu48gap11Plan ID have been calculated with the given beam parameters, which are 0.5 A of stored current, $\beta_H = 9$ m, $\varepsilon_H = 0.263$ nmrad, $\beta_V = 4.8$ m, $\varepsilon_V = 8$. pmrad, and an energy spread of 0.001.

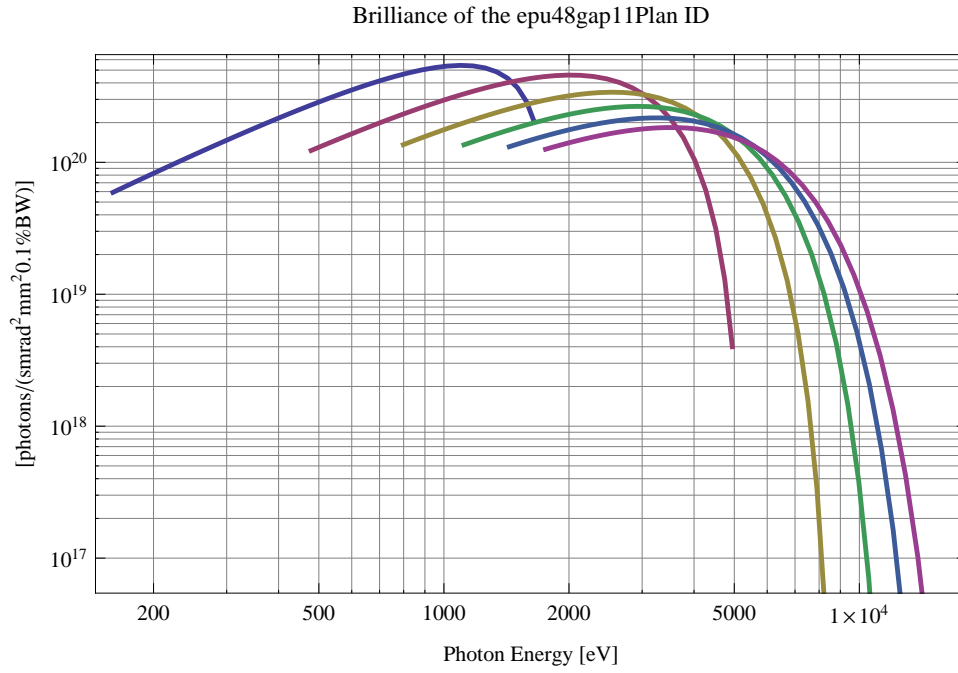


Figure 155: The brilliance at peak energy of the synchrotron radiation emitted by the epu48gap11Plan ID

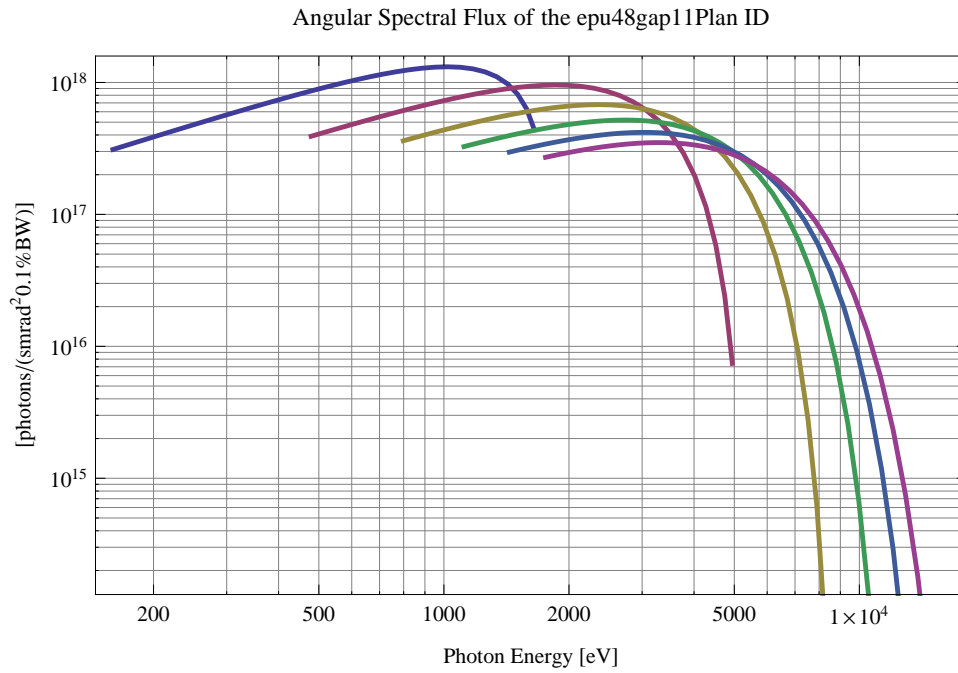


Figure 156: The angular spectral flux of the synchrotron radiation emitted by the epu48gap11Plan ID

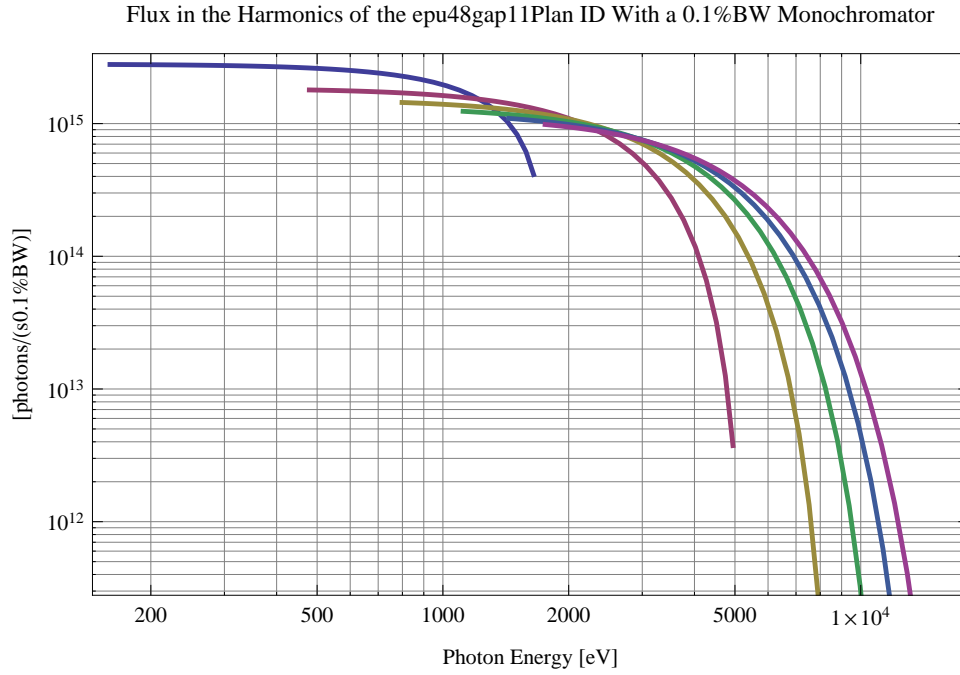


Figure 157: The flux of photons in the harmonics of the emitted synchrotron radiation from the epu48gap11Plan ID using a 0.1%BW monochromator

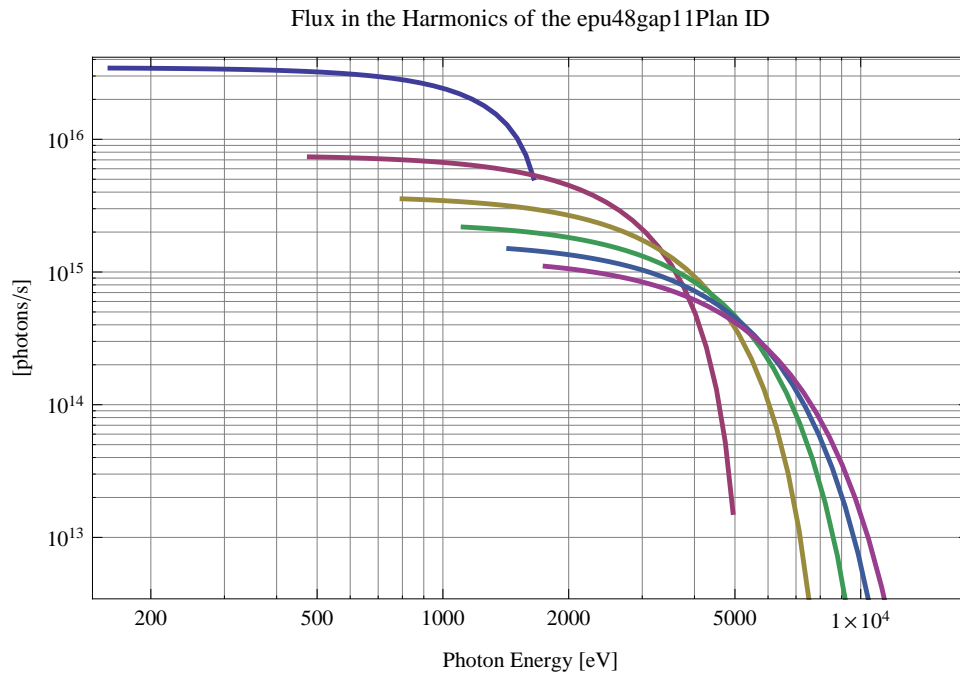


Figure 158: The flux of photons in the harmonics of the emitted synchrotron radiation from the epu48gap11Plan ID

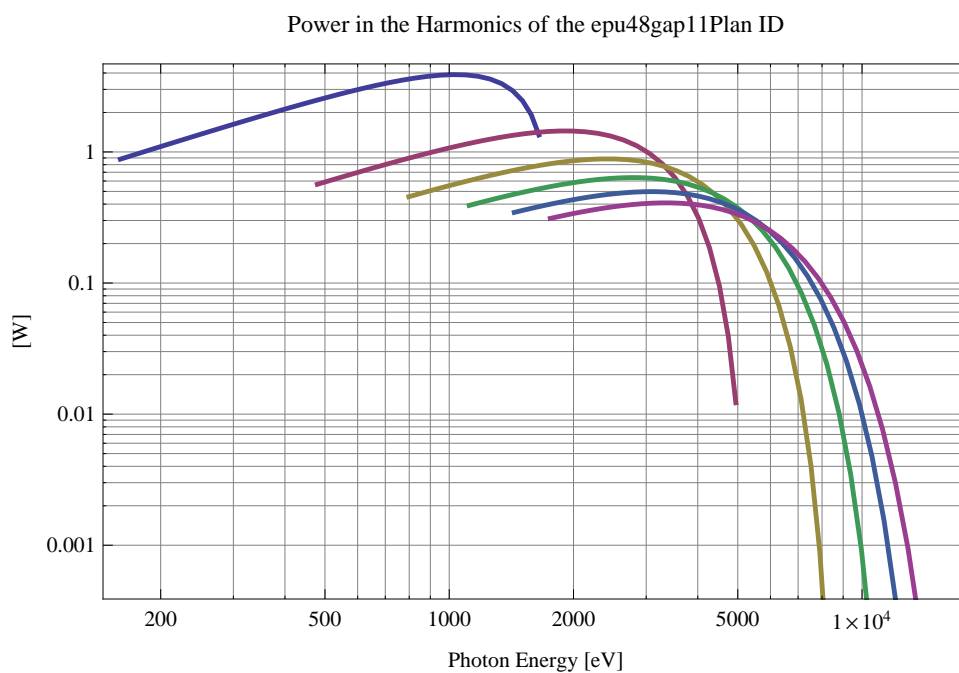


Figure 159: The power in the harmonics of the emitted synchrotron radiation from the epu48gap11Plan ID

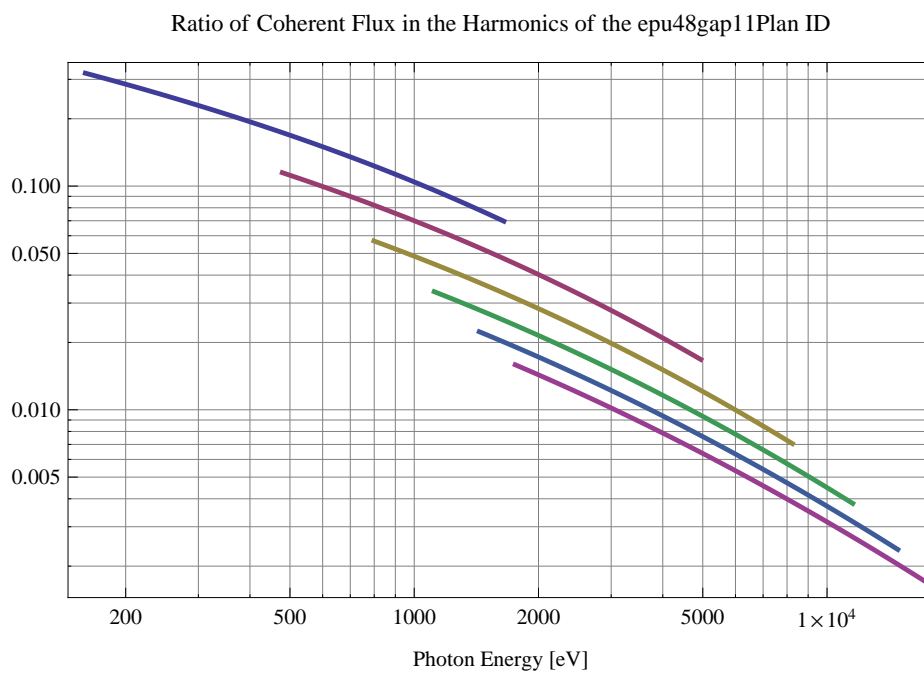


Figure 160: The ratio of coherent flux in the harmonics of the emitted synchrotron radiation from the epu48gap11Plan ID

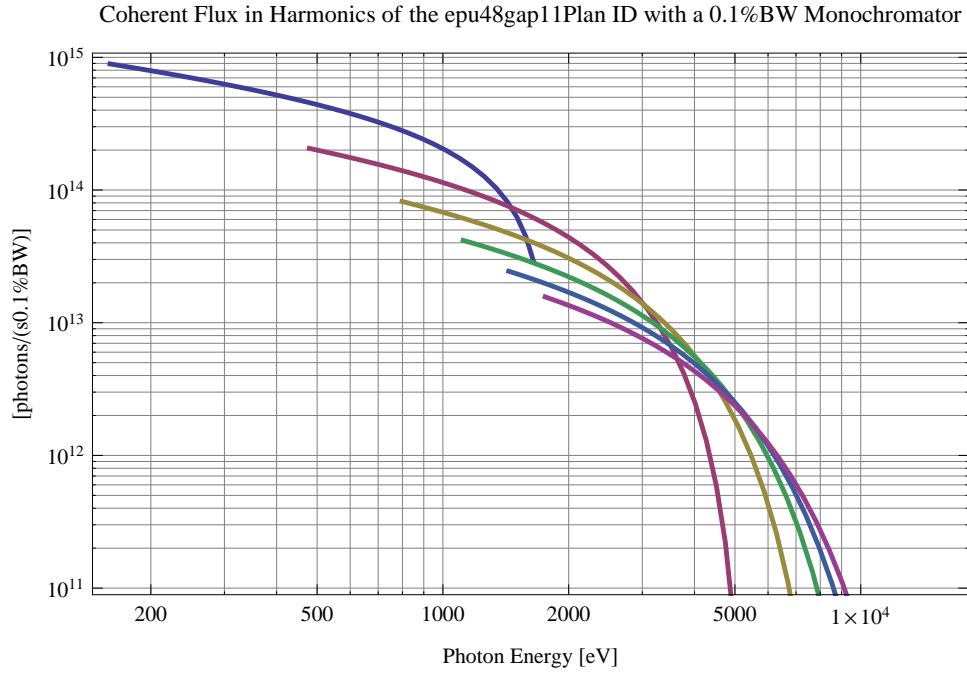


Figure 161: The coherent flux in the harmonics of the epu48gap11Plan ID using a 0.1%BW Monochromator

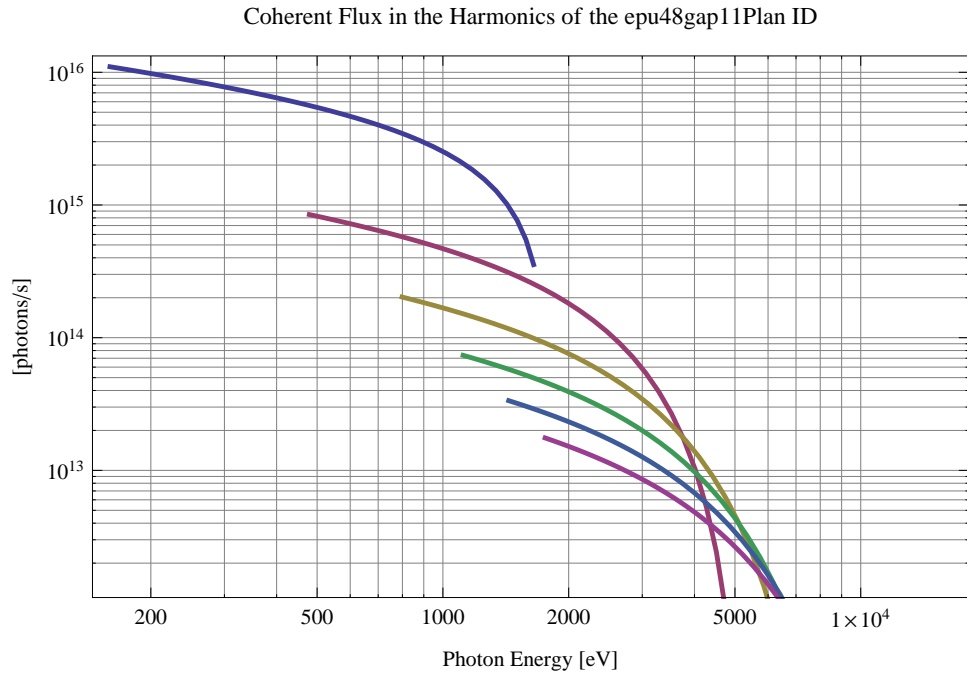


Figure 162: The coherent flux in the harmonics of the epu48gap11Plan ID

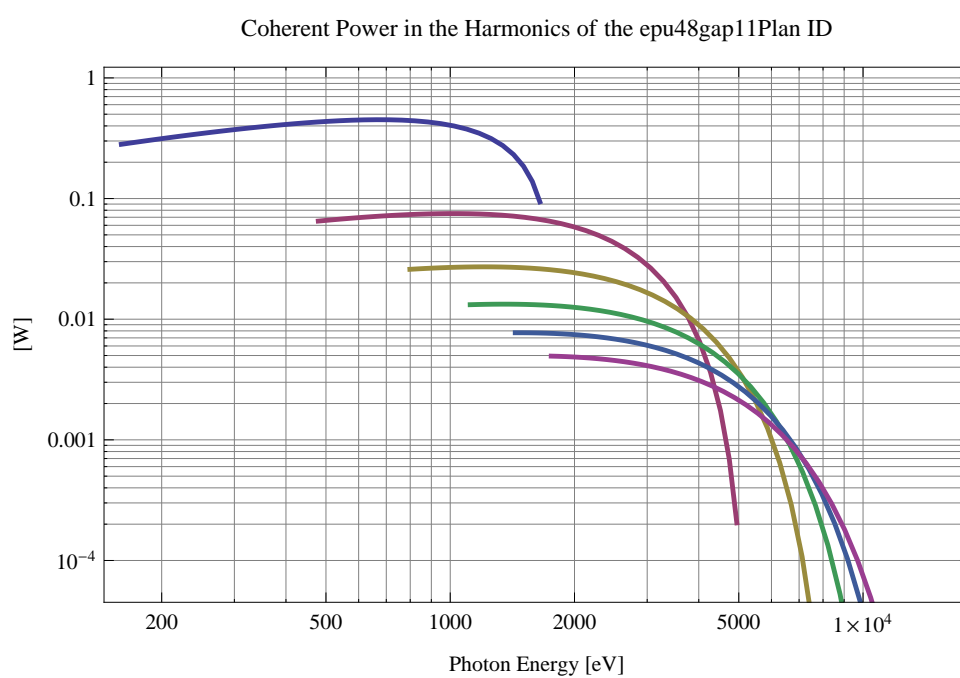


Figure 163: The power of coherent synchrotron radiation in the harmonics of the epu48gap11Plan ID

The brilliance at peak energy and the angular spectral flux density from the epu48gap11Plan ID for different harmonics at maximum K-value (4.506) are given in Table 27 and for minimum K-value (0.400) these values are given in Table 28.

Table 27: The brilliance at peak energy and the angular spectral flux density from the epu48gap11Plan ID for different harmonics at maximum K-value (4.506)

Harmonic	Photon Energy [eV]	Brilliance [Ph./ (smrad ² mrads ² 0.1%BW)]	Angular Spectral Flux [Ph./ (smrad ² 0.1%BW)]
1	159.689	5.92×10^{19}	3.1×10^{17}
3	479.066	1.23×10^{20}	3.91×10^{17}
5	798.443	1.36×10^{20}	3.61×10^{17}
7	1117.82	1.36×10^{20}	3.27×10^{17}
9	1437.2	1.31×10^{20}	2.96×10^{17}
11	1756.58	1.26×10^{20}	2.71×10^{17}

Table 28: The brilliance at peak energy and the angular spectral flux density from the epu48gap11Plan ID for different harmonics at minimum K-value (0.4)

Harmonic	Photon Energy [eV]	Brilliance [Ph./ (smrad ² mrads ² 0.1%BW)]	Angular Spectral Flux [Ph./ (smrad ² 0.1%BW)]
1	1648.68	2.04×10^{20}	4.43×10^{17}
3	4946.04	$4. \times 10^{18}$	7.43×10^{15}
5	8243.4	4.6×10^{16}	8.27×10^{13}
7	11540.8	4.86×10^{14}	8.64×10^{11}
9	14838.1	5.02×10^{12}	8.88×10^9
11	18135.5	5.13×10^{10}	9.06×10^7

2.3.5 Magnet model of the elliptically polarising undulator epu48gap11Heli

The Radia [3] magnet model of the epu48gap11Heli ID is shown in Figure 164. The length of the magnet model is 401.496 mm. The magnetic material in the model is NdFeb with a remanence of 1.28 T, a material similar to VACODYM 776 TP from Vacuumschmelze. Blocks with vertical magnetisation are blue and blocks with horizontal magnetisation are yellow. The block size is 30.x30.x12. mm³ and there is a 5. mm cut-out in two of the corners of the blocks. The total length of the epu48gap11Heli ID is 3905.5 mm.

2.3.6 Analysis of the magnetic field of the epu48gap11Heli ID

The effective magnetic fields on axis and the fundamental photon energy of the epu48gap11Heli ID are shown in Table 29. The higher harmonic contents in the magnetic field of an elliptically polarising undulator made of permanent magnets is negligible and the effective field has about the same strength as the peak field.

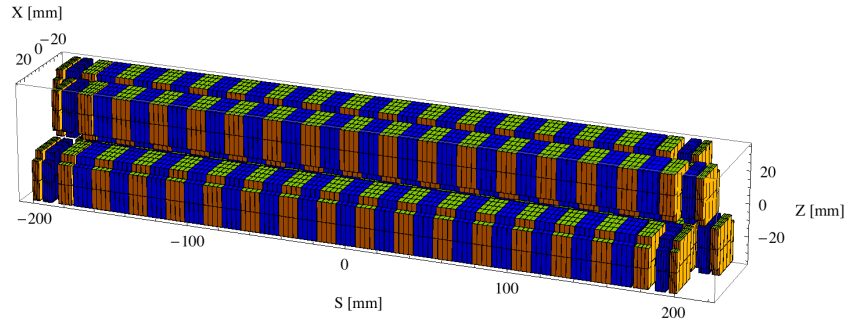


Figure 164: Magnetic model of the epu48gap11Heli ID. The ID has been modelled with Radia [3]

Table 29: Effective Fields on axis and Fundamental Photon Energy of the epu48gap11Heli ID

Undulator Period	48	mm
Undulator Gap	11	mm
Undulator Mode	Helical	
Undulator Phase	14.255	mm
Vertical Peak Field	0.592	T
Effective Vertical Field	0.595	T
Kx (from vert. field)	2.668	
Horizontal Peak Field:	0.598	T
Effective Horizontal Field	0.595	T
Kz (from hor. field)	2.668	
Photon Energy, Harm.1	0.219	keV
Emitted Power	7.873	kW
Total Length	3905.5	mm

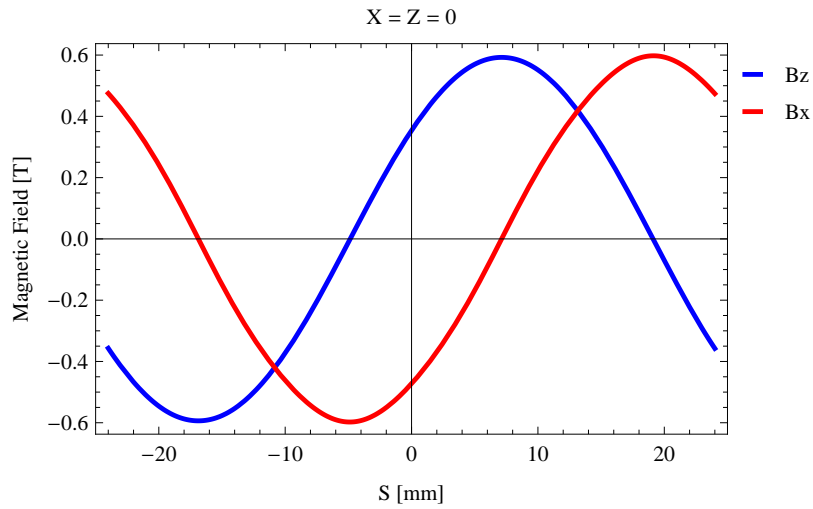


Figure 165: Vertical magnetic field in a central pole of the epu48gap11Heli ID along the ID axis, $X = Z = 0$

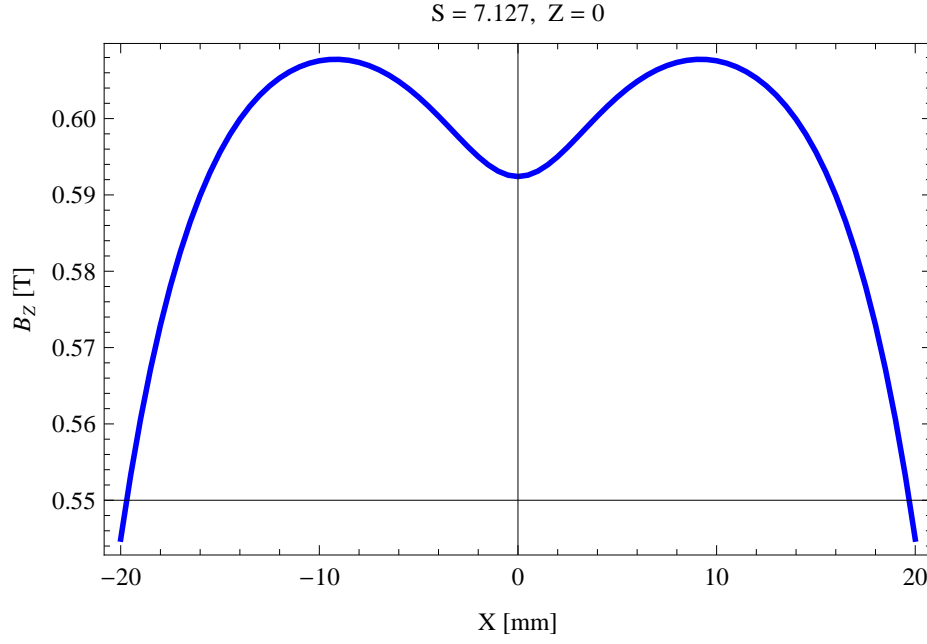


Figure 166: Vertical magnetic field in a central pole of the epu48gap11Heli ID along the horizontally transverse direction to the ID axis, $S = 7.127, Z = 0$

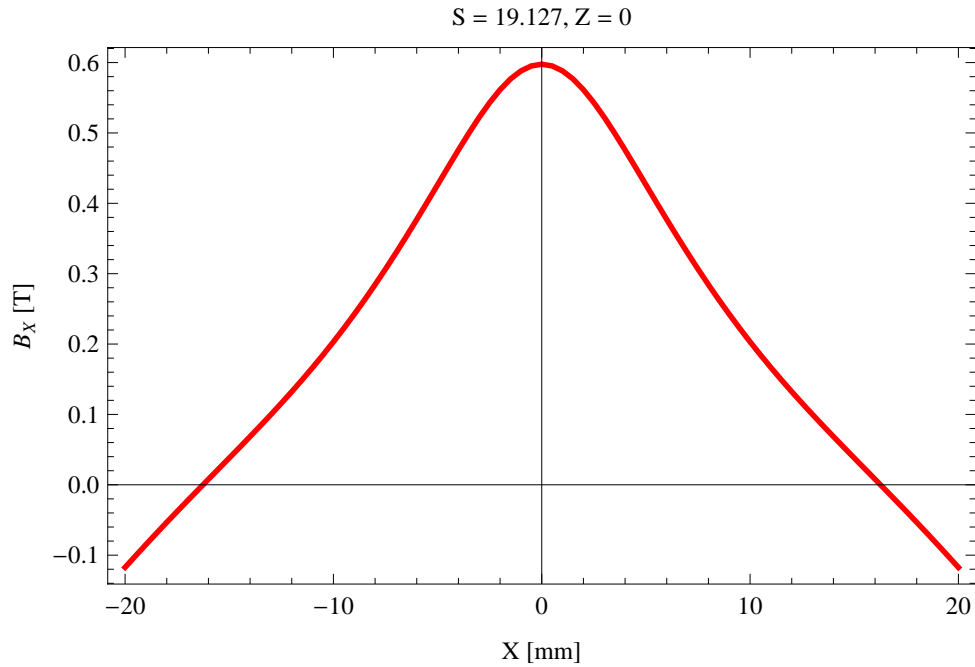


Figure 167: Horizontal magnetic field in a central pole of the epu48gap11Heli ID along the horizontally transverse direction to the ID axis, $S = 19.127, Z = 0$

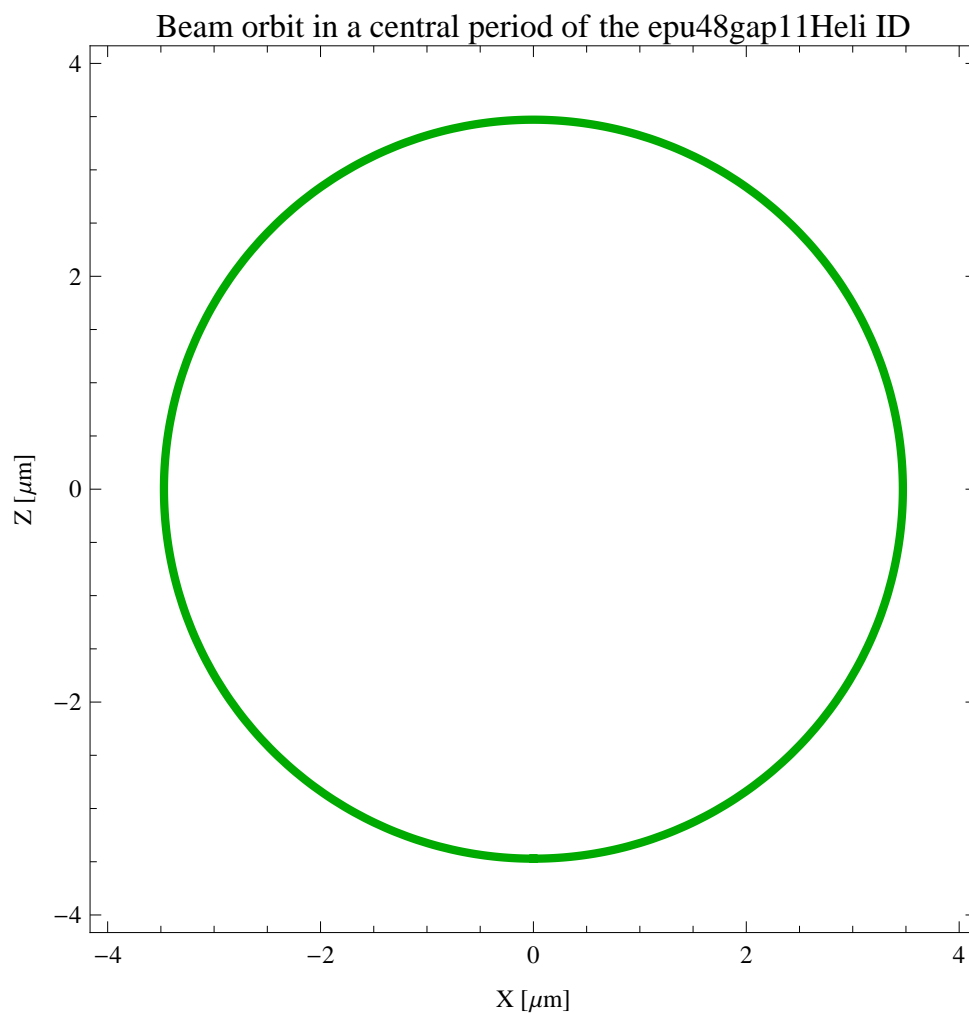


Figure 168: The beam orbit of the electron beam through a central period of the epu48gap11Heli ID

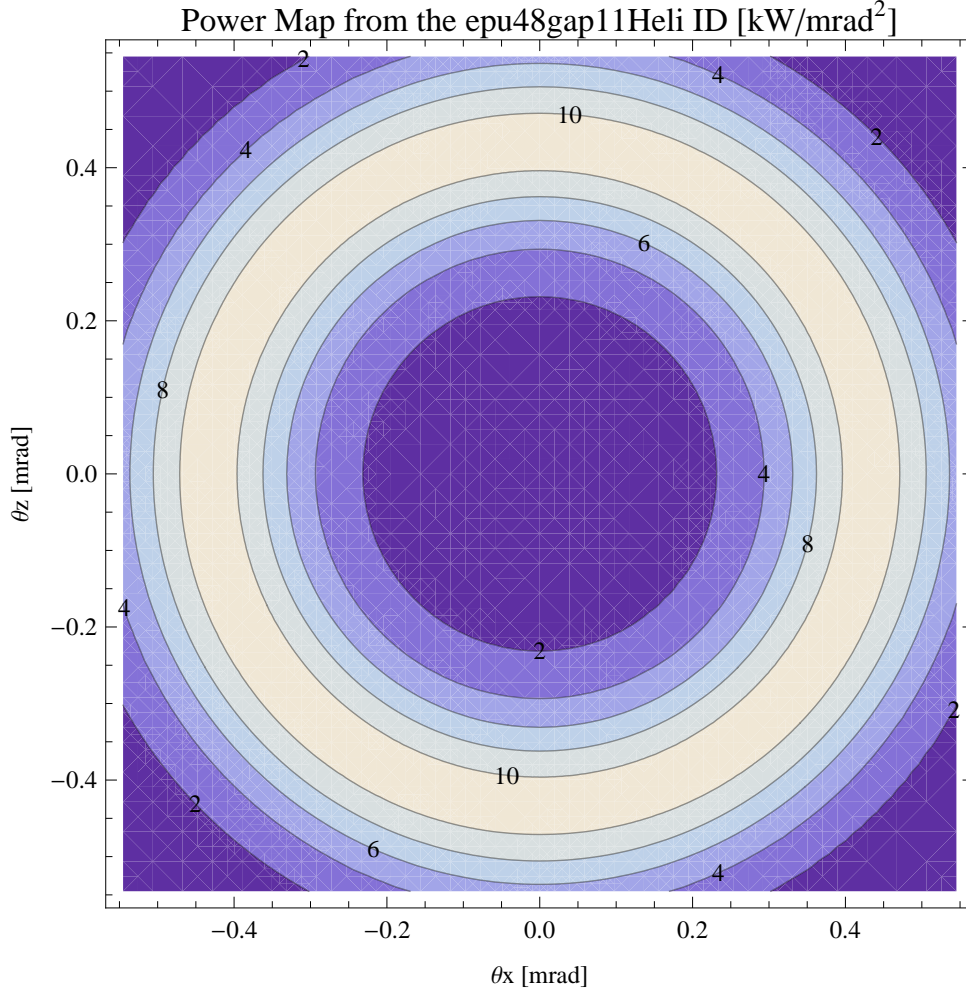


Figure 169: Map of the power distribution of the emitted synchrotron radiation by the epu48gap11Heli ID

2.3.7 Synchrotron radiation from the epu48gap11Heli ID

The power map of the emitted synchrotron radiation by the epu48gap11Heli ID, assuming a 0.5 A filament beam with an energy of 3 GeV and undulator properties of the synchrotron radiation, is shown in Figure 169. The on-axis power density is 0.477 kW/mrad^2

A map of the degree of linear polarisation of the fundamental harmonic of the synchrotron radiation emitted by the epu48gap11Heli ID over the angle of observation is shown in Figure 170.

A map of the degree of 45 degree polarisation of the fundamental harmonic of the synchrotron radiation emitted by the epu48gap11Heli ID over the angle of observation is shown in Figure 171.

A map of the degree of circular polarisation of the fundamental harmonic of the synchrotron radiation emitted by the epu48gap11Heli ID over the angle of observation is shown in Figure 172.

The on axis brilliance at peak energy and the angular spectral flux from the epu48gap11Heli ID have been calculated with the given beam parameters, which are 0.5 A of stored current, $\beta_H = 9 \text{ m}$, $\varepsilon_H = 0.263 \text{ nrad}$, $\beta_V = 4.8 \text{ m}$, $\varepsilon_V = 8. \text{ pmrad}$, and an energy spread of 0.001.

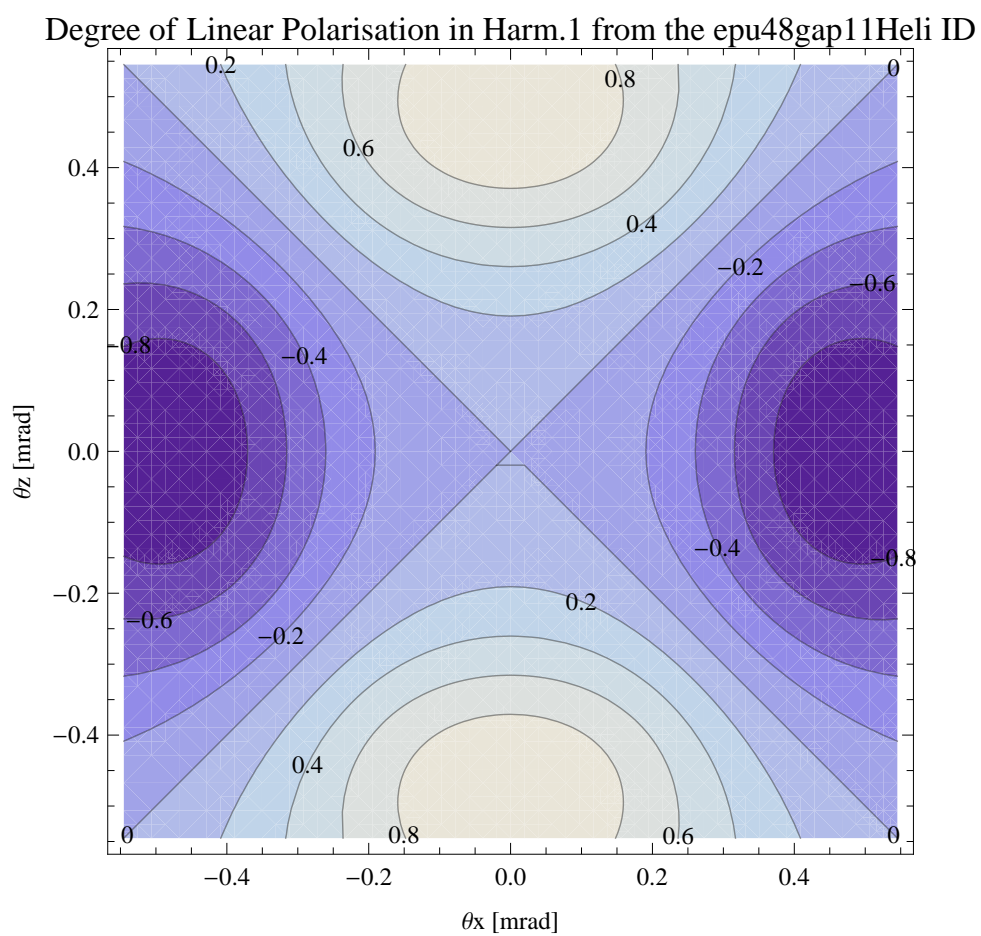


Figure 170: Map of linear polarisation in the fundamental harmonic of the synchrotron radiation emitted by the epu48gap11Heli ID

Degree of 45 degree Polarisation in Harm.1 from the epu48gap11Heli ID

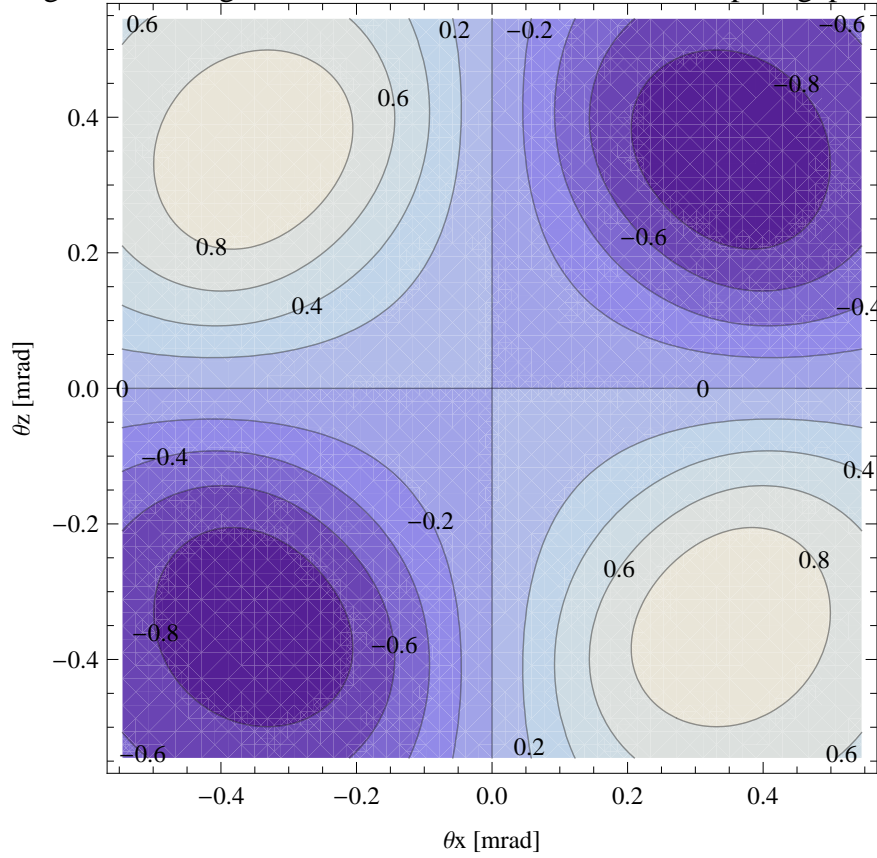


Figure 171: Map of 45 degree polarisation in the fundamental harmonic of the synchrotron radiation emitted by the epu48gap11Heli ID

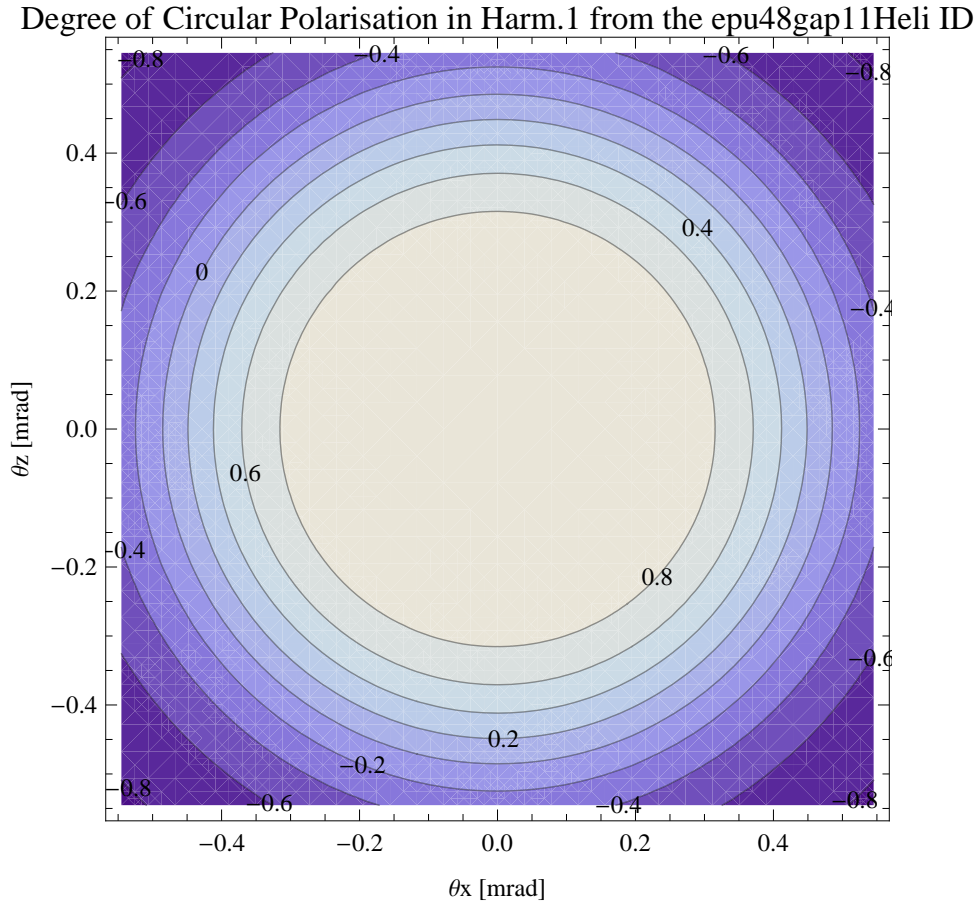


Figure 172: Map of circular polarisation in the fundamental harmonic of the synchrotron radiation emitted by the epu48gap11Heli ID

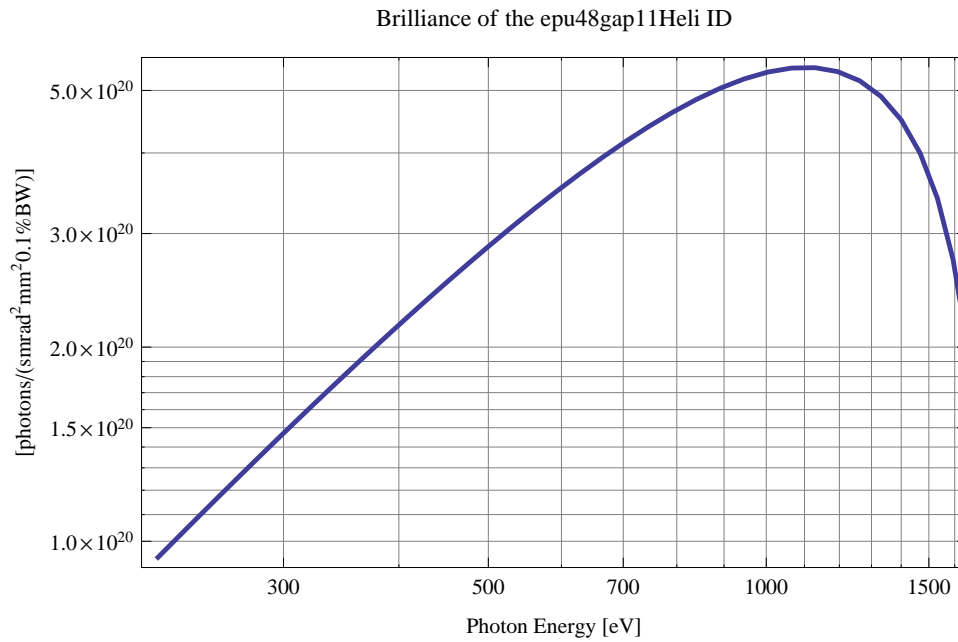


Figure 173: The brilliance at peak energy of the synchrotron radiation emitted by the epu48gap11Heli ID

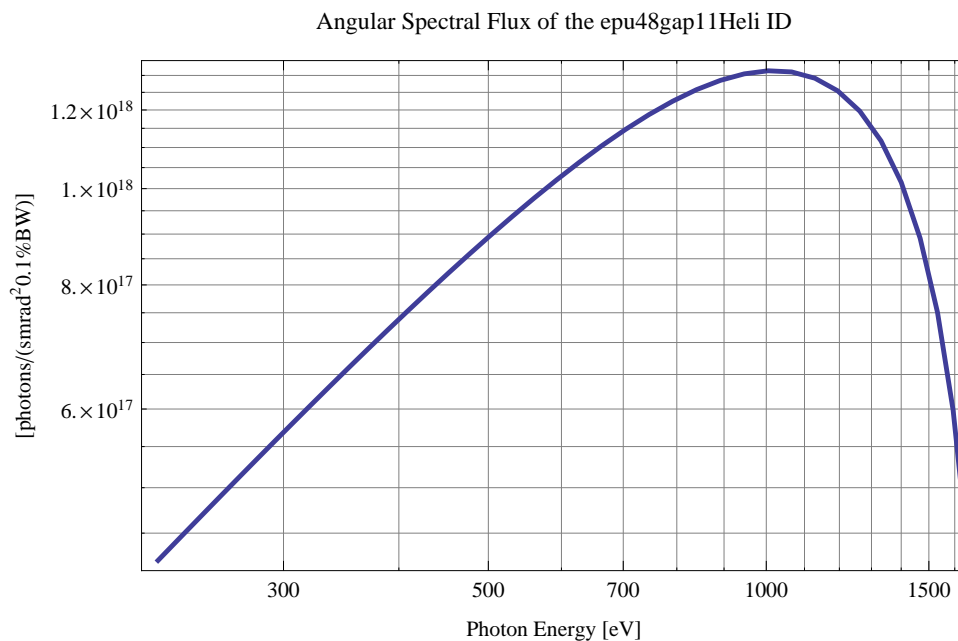


Figure 174: The angular spectral flux of the synchrotron radiation emitted by the epu48gap11Heli ID

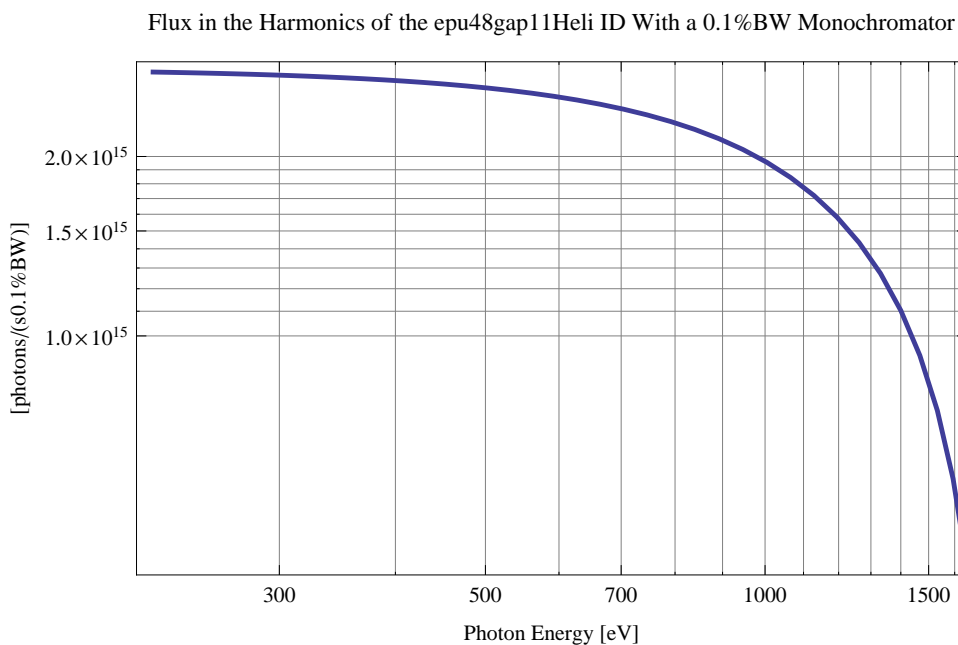


Figure 175: The flux of photons in the harmonics of the emitted synchrotron radiation from the epu48gap11Heli ID using a 0.1%BW monochromator

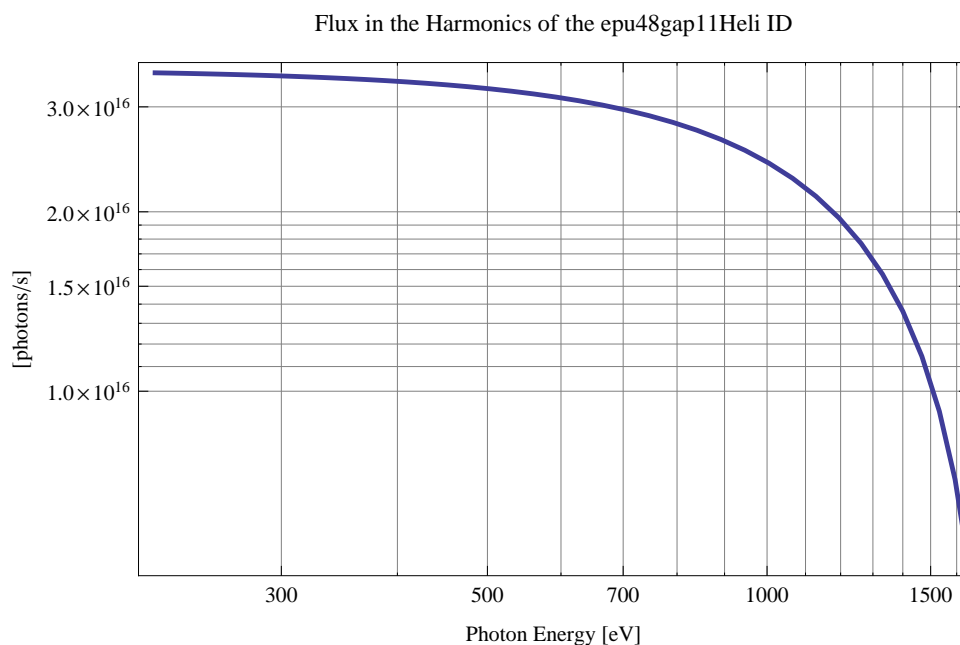


Figure 176: The flux of photons in the harmonics of the emitted synchrotron radiation from the epu48gap11Heli ID

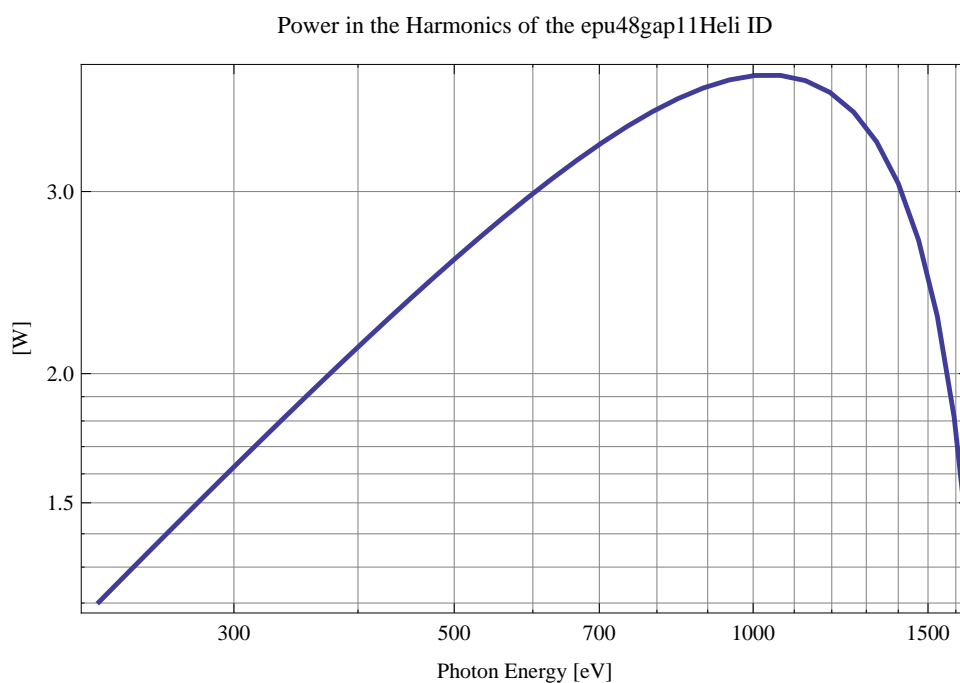


Figure 177: The power in the harmonics of the emitted synchrotron radiation from the epu48gap11Heli ID

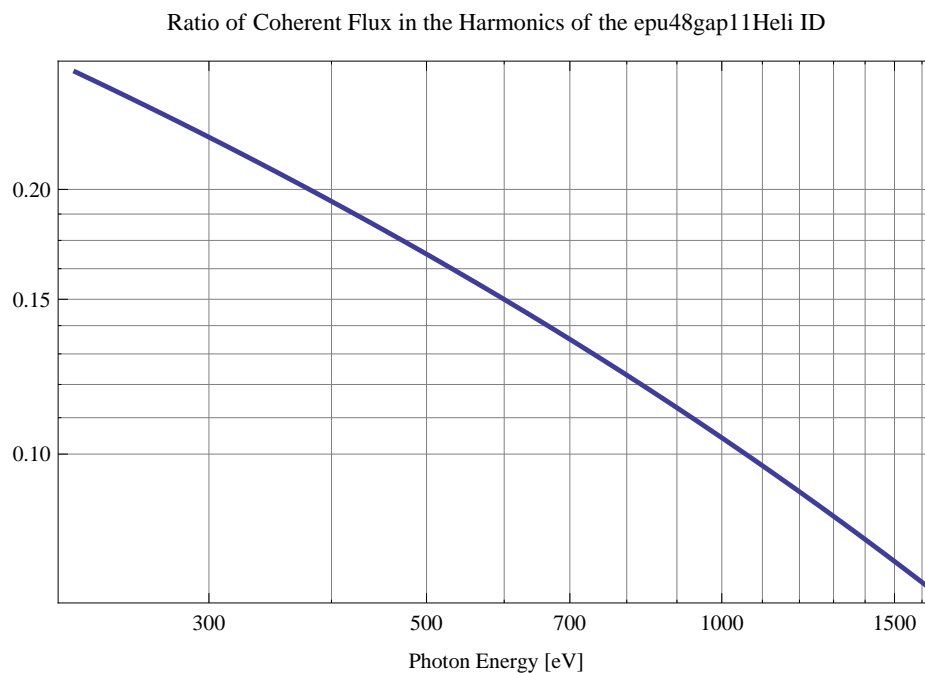


Figure 178: The ratio of coherent flux in the harmonics of the emitted synchrotron radiation from the epu48gap11Heli ID

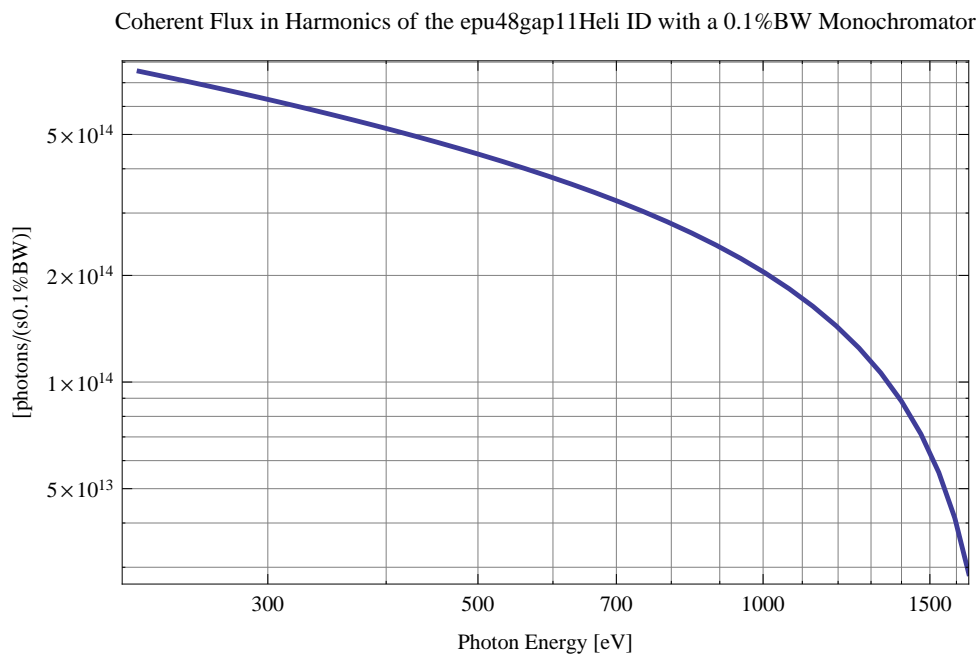


Figure 179: The coherent flux in the harmonics of the epu48gap11Heli ID using a 0.1%BW Monochromator

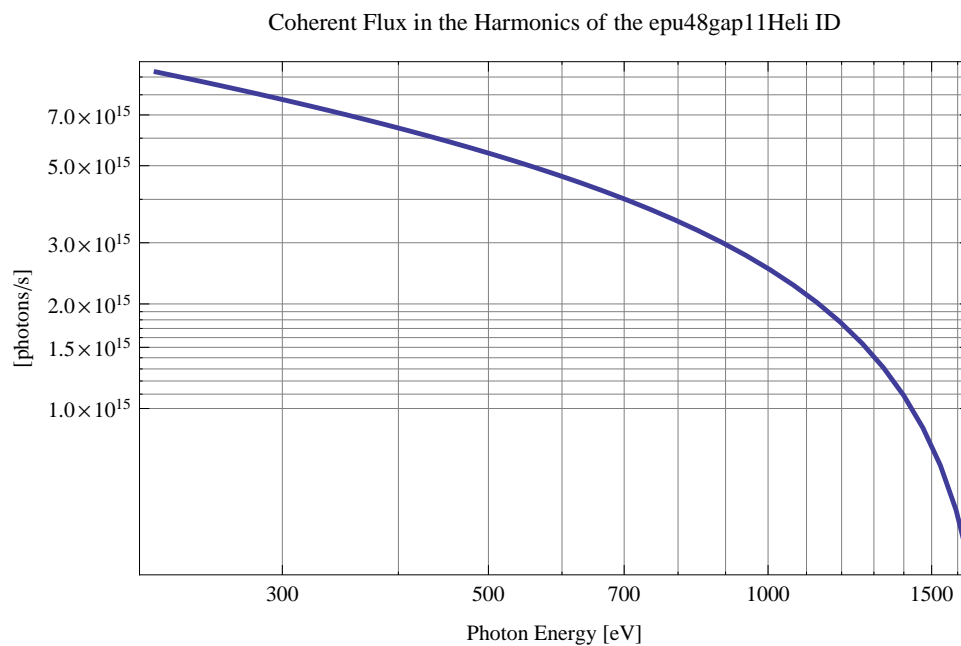


Figure 180: The coherent flux in the harmonics of the epu48gap11Heli ID

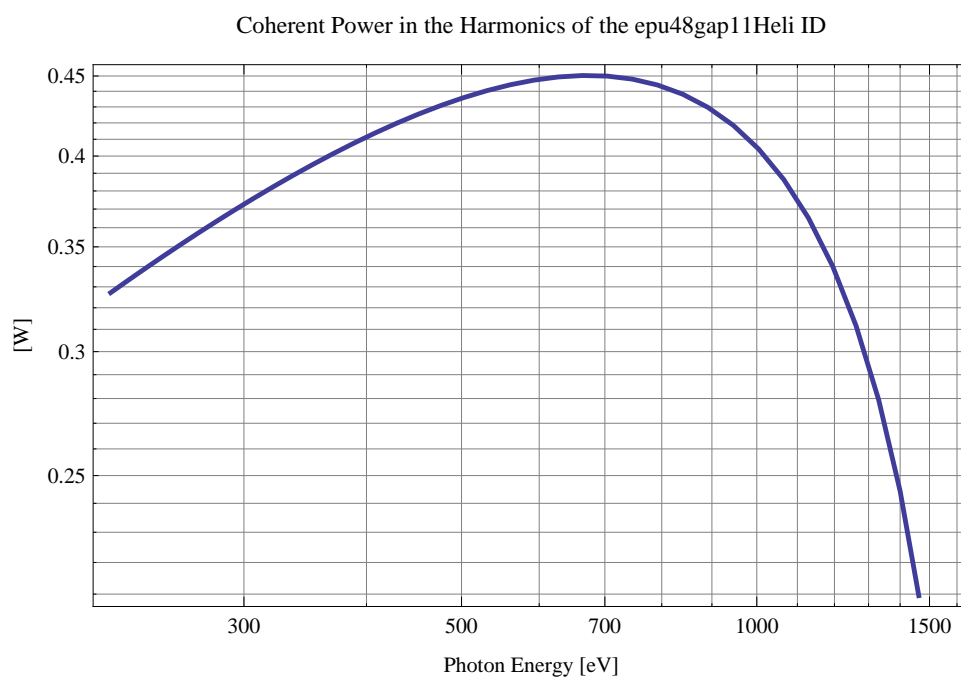


Figure 181: The power of coherent synchrotron radiation in the harmonics of the epu48gap11Heli ID

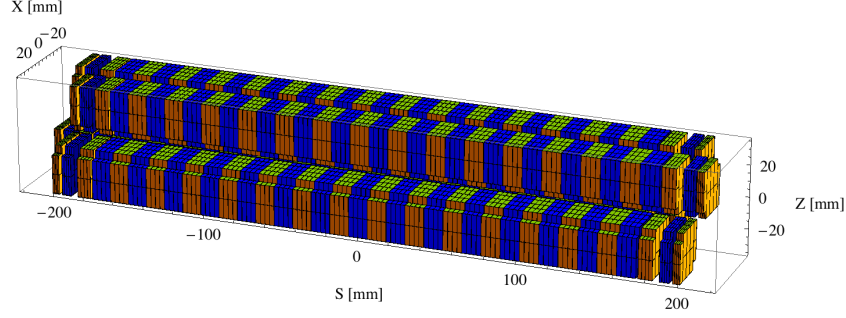


Figure 182: Magnetic model of the epu48gap11Incl ID. The ID has been modelled with Radia [3]

The brilliance at peak energy and the angular spectral flux density from the epu48gap11Heli ID for different harmonics at maximum K-value (3.772) are given in Table 30 and for minimum K-value (0.400) these values are given in Table 31.

Table 30: The brilliance at peak energy and the angular spectral flux density from the epu48gap11Heli ID for different harmonics at maximum K-value (3.772)

Harmonic	Photon Energy [eV]	Brilliance [Ph./((smrad ² mrad ² 0.1%BW))]	Angular Spectral Flux [Ph./((smrad ² 0.1%BW))]
1	219.402	9.44×10^{19}	4.22×10^{17}

Table 31: The brilliance at peak energy and the angular spectral flux density from the epu48gap11Heli ID for different harmonics at minimum K-value (0.4)

Harmonic	Photon Energy [eV]	Brilliance [Ph./((smrad ² mrad ² 0.1%BW))]	Angular Spectral Flux [Ph./((smrad ² 0.1%BW))]
1	1648.68	2.04×10^{20}	4.43×10^{17}

2.3.8 Magnet model of the elliptically polaraising undulator epu48gap11Incl

The Radia [3] magnet model of the epu48gap11Incl ID is shown in Figure 182. The length of the magnet model is 401.496 mm. The magnetic material in the model is NdFeb with a remanence of 1.28 T, a material similar to VACODYM 776 TP from Vacuumschmelze. Blocks with vertical magnetisation are blue and blocks with horizontal magnetisation are yellow. The block size is 30.x30.x12. mm³ and there is a 5. mm cut-out in two of the corners of the blocks. The total length of the epu48gap11Incl ID is 3905.5 mm.

2.3.9 Analysis of the magnetic field of the epu48gap11Incl ID

The effective magnetic fields on axis and the fundamental photon energy of the epu48gap11Incl ID are shown in Table 32. The higher harmonic contents in the magnetic field of an elliptically

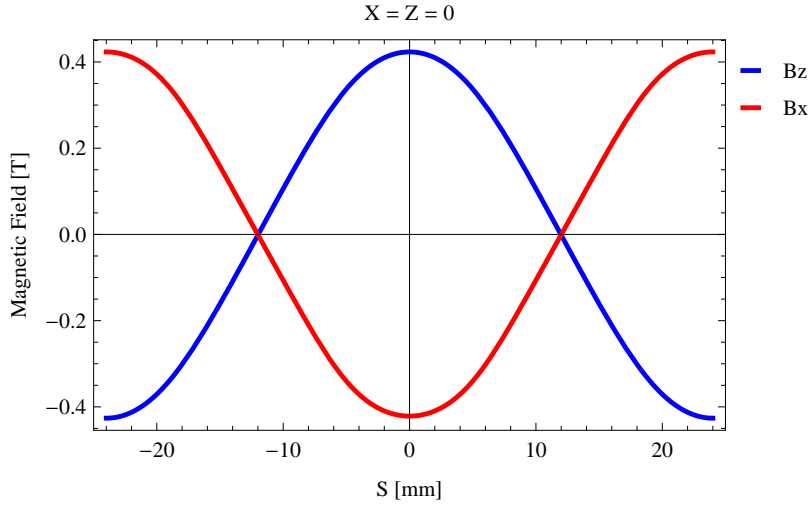


Figure 183: Vertical magnetic field in a central pole of the epu48gap11Incl ID along the ID axis, $X = Z = 0$

polarising undulator made of permanent magnets is negligible and the effective field has about the same strength as the peak field.

Table 32: Effective Fields on axis and Fundamental Photon Energy of the epu48gap11Incl ID

Undulator Period	48	mm
Undulator Gap	11	mm
Undulator Mode	Inclined	
Undulator Phase	13.140	mm
Vertical Peak Field	0.423	T
Effective Vertical Field	0.425	T
Kx (from vert. field)	1.905	
Horizontal Peak Field:	-0.421	T
Effective Horizontal Field	0.425	T
Kz (from hor. field)	1.905	
Photon Energy, Harm.1	0.385	keV
Emitted Power	4.017	kW
Total Length	3905.5	mm

2.3.10 Synchrotron radiation from the epu48gap11Incl ID

The power map of the emitted synchrotron radiation by the epu48gap11Incl ID, assuming a 0.5 A filament beam with an energy of 3 GeV and undulator properties of the synchrotron radiation, is shown in Figure 187. The on-axis power density is 20.892 kW/mrad²

A map of the degree of linear polarisation of the fundamental harmonic of the synchrotron radiation emitted by the epu48gap11Incl ID over the angle of observation is shown in Figure 188.

A map of the degree of 45 degree polarisation of the fundamental harmonic of the synchrotron radiation emitted by the epu48gap11Incl ID over the angle of observation is shown in Figure 189.

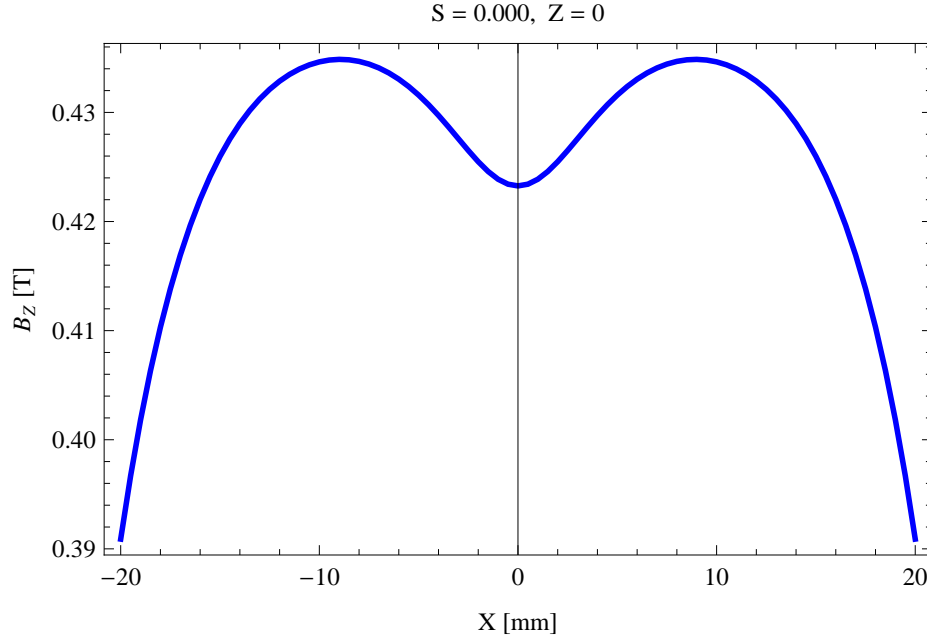


Figure 184: Vertical magnetic field in a central pole of the epu48gap11Incl ID along the horizontally transverse direction to the ID axis, $S = 0.000, Z = 0$

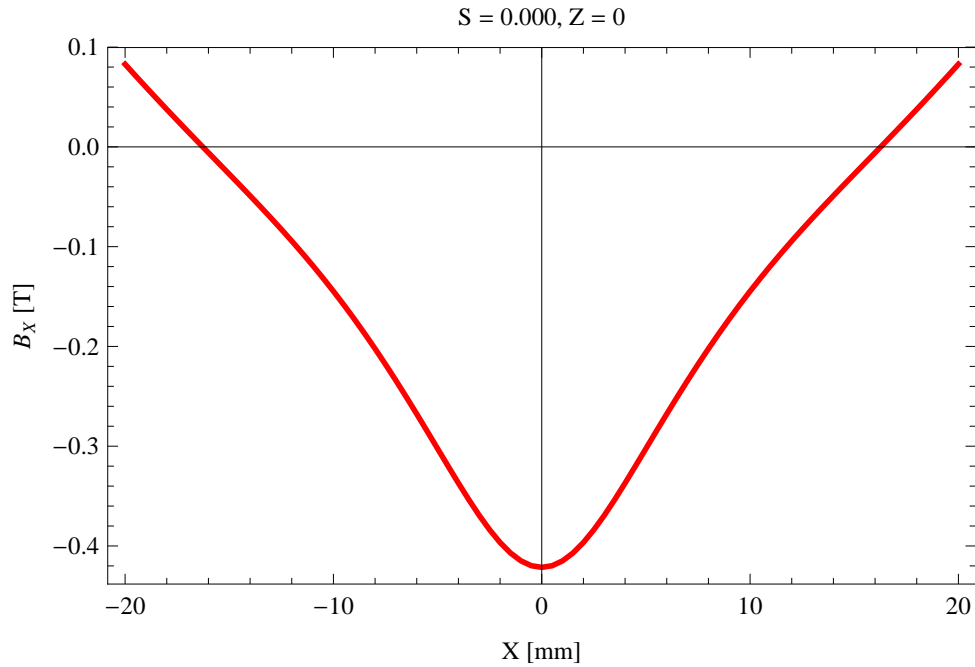


Figure 185: Horizontal magnetic field in a central pole of the epu48gap11Incl ID along the horizontally transverse direction to the ID axis, $S = 0.000, Z = 0$

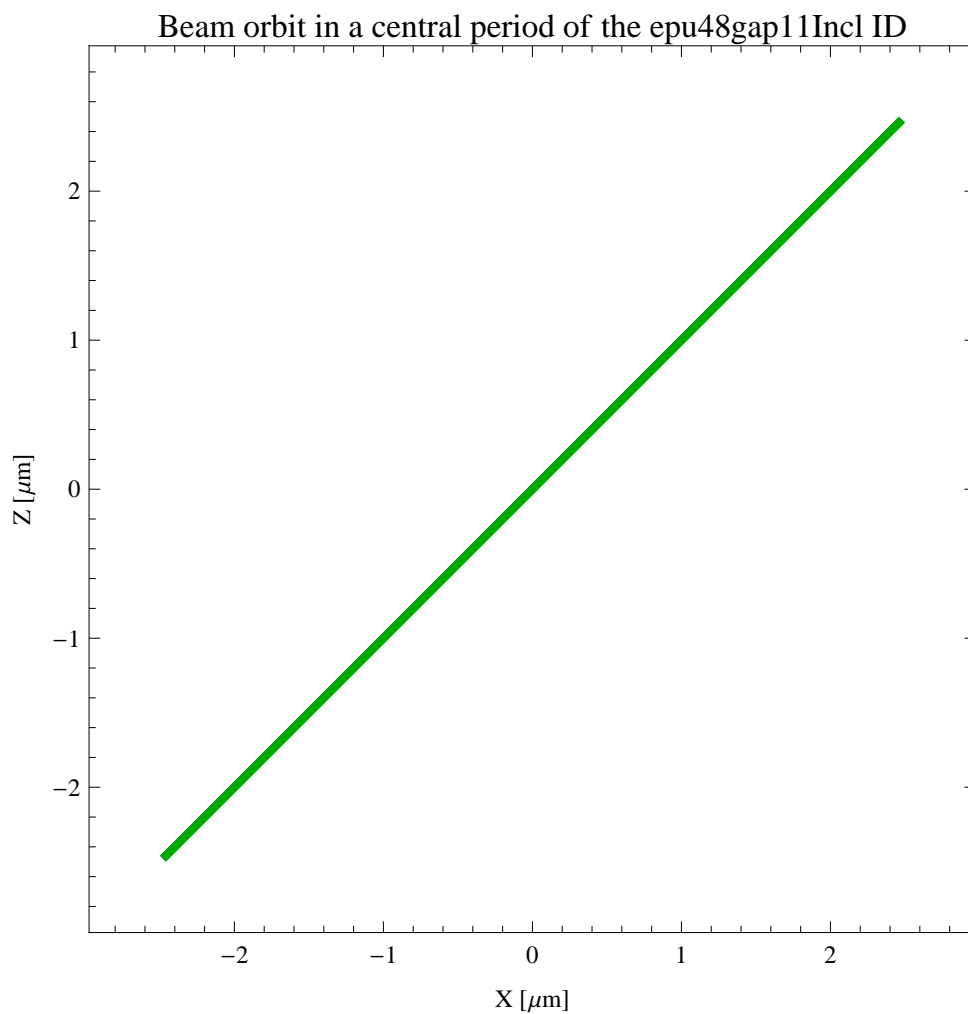


Figure 186: The beam orbit of the electron beam through a central period of the epu48gap11Incl ID

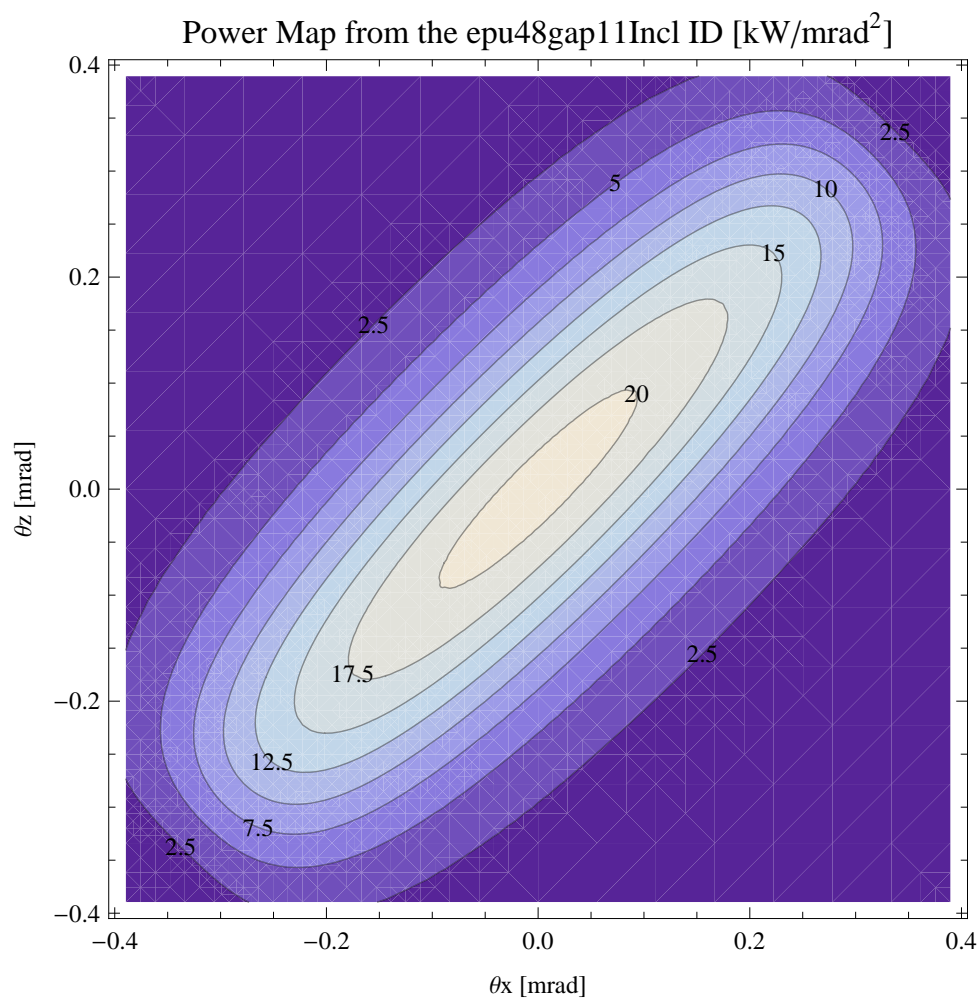


Figure 187: Map of the power distribution of the emitted synchrotron radiation by the epu48gap11Incl ID

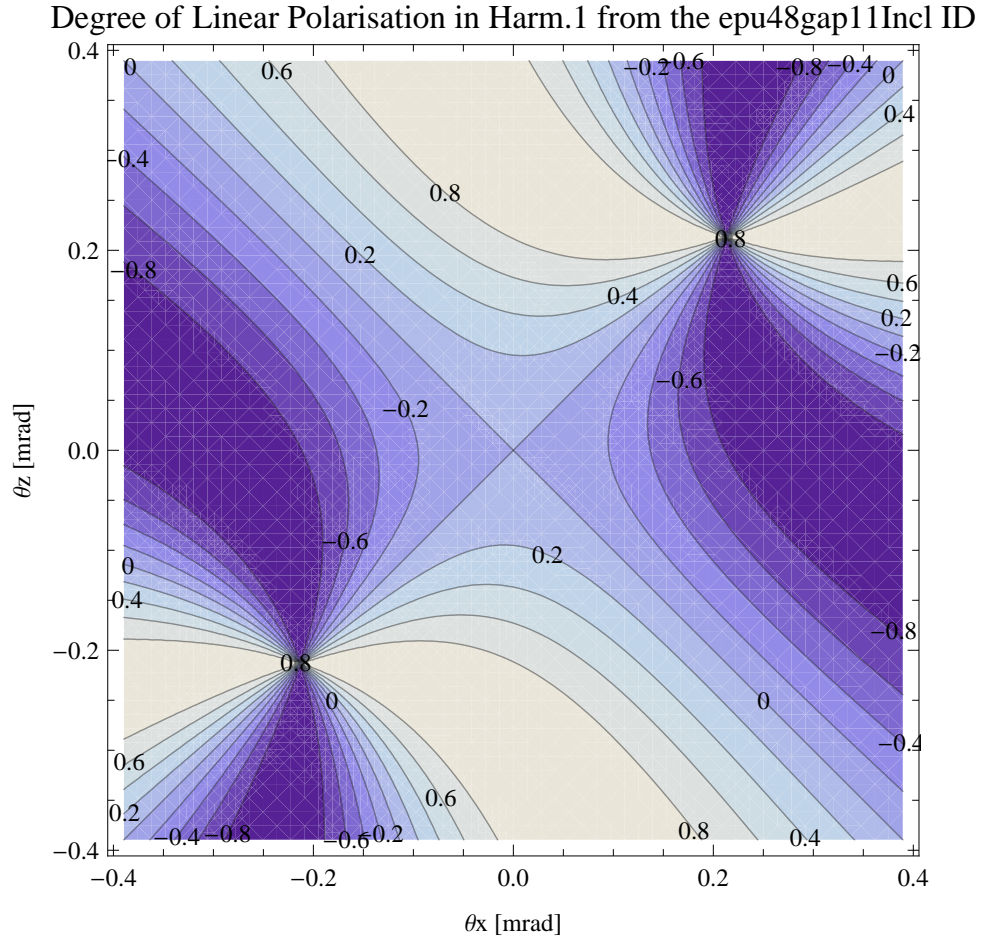


Figure 188: Map of linear polarisation in the fundamental harmonic of the synchrotron radiation emitted by the epu48gap11Incl ID

Degree of 45 degree Polarisation in Harm.1 from the epu48gap11Incl ID

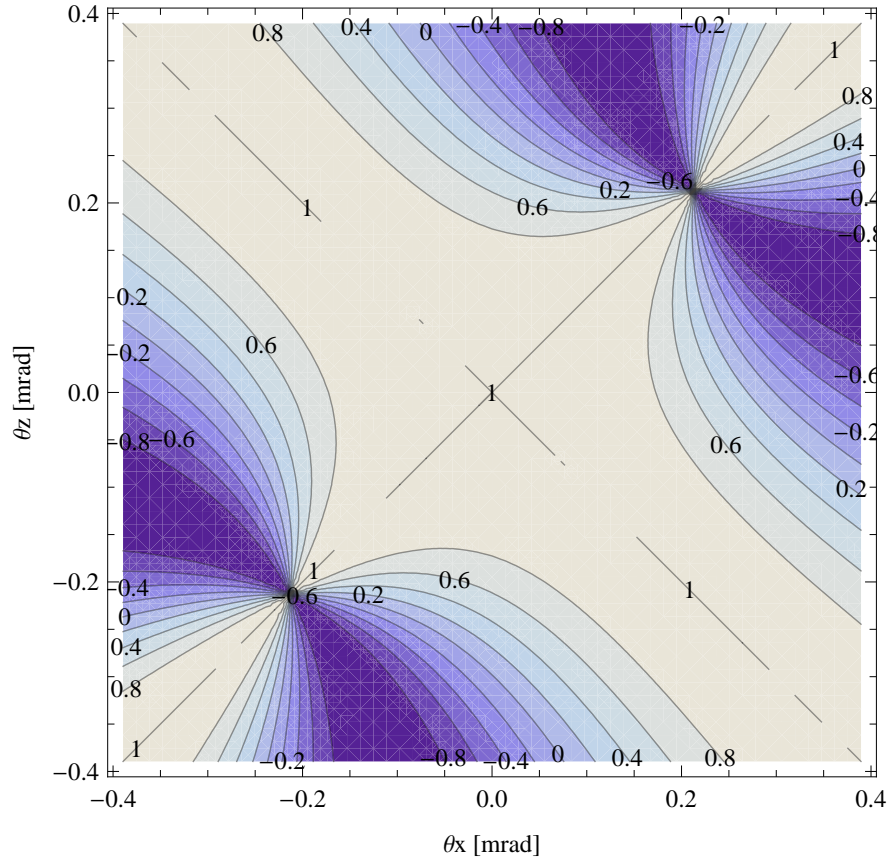


Figure 189: Map of 45 degree polarisation in the fundamental harmonic of the synchrotron radiation emitted by the epu48gap11Incl ID

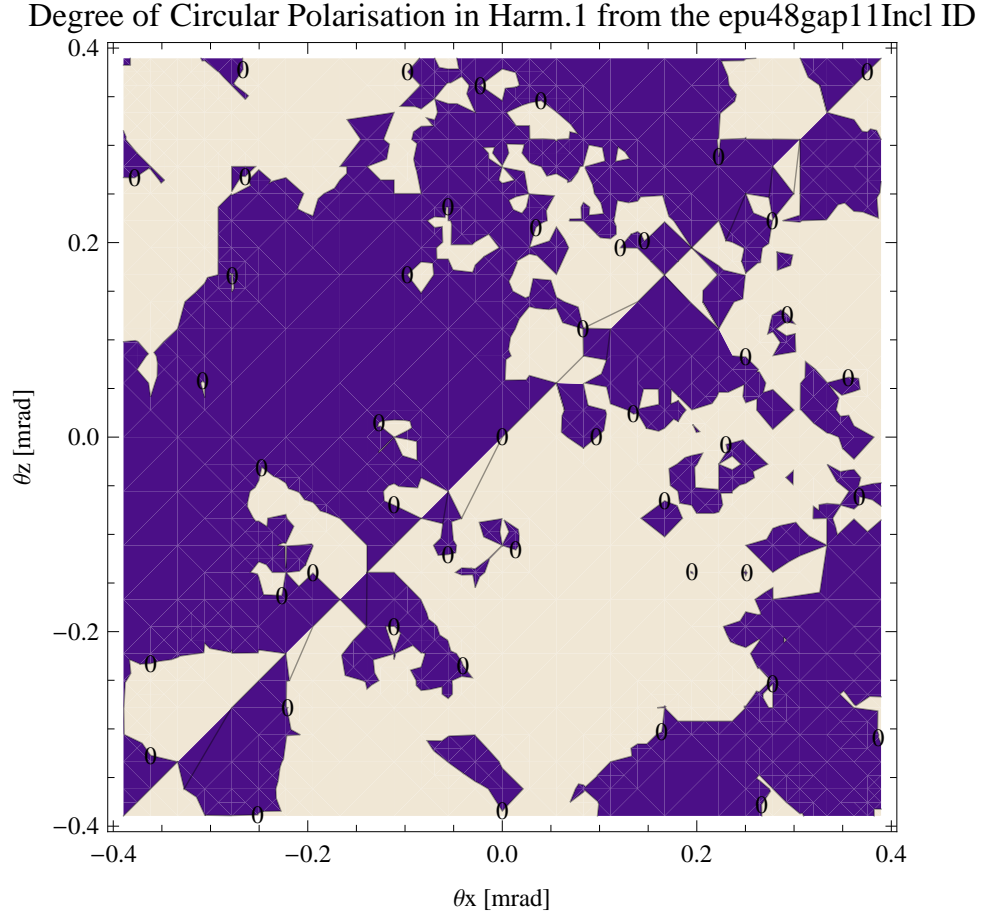


Figure 190: Map of circular polarisation in the fundamental harmonic of the synchrotron radiation emitted by the epu48gap11Incl ID

A map of the degree of circular polarisation of the fundamental harmonic of the synchrotron radiation emitted by the epu48gap11Incl ID over the angle of observation is shown in Figure 190.

The on axis brilliance at peak energy and the angular spectral flux from the epu48gap11Incl ID have been calculated with the given beam parameters, which are 0.5 A of stored current, $\beta_H = 9$ m, $\varepsilon_H = 0.263$ nmrad, $\beta_V = 4.8$ m, $\varepsilon_V = 8$. pmrad, and an energy spread of 0.001.

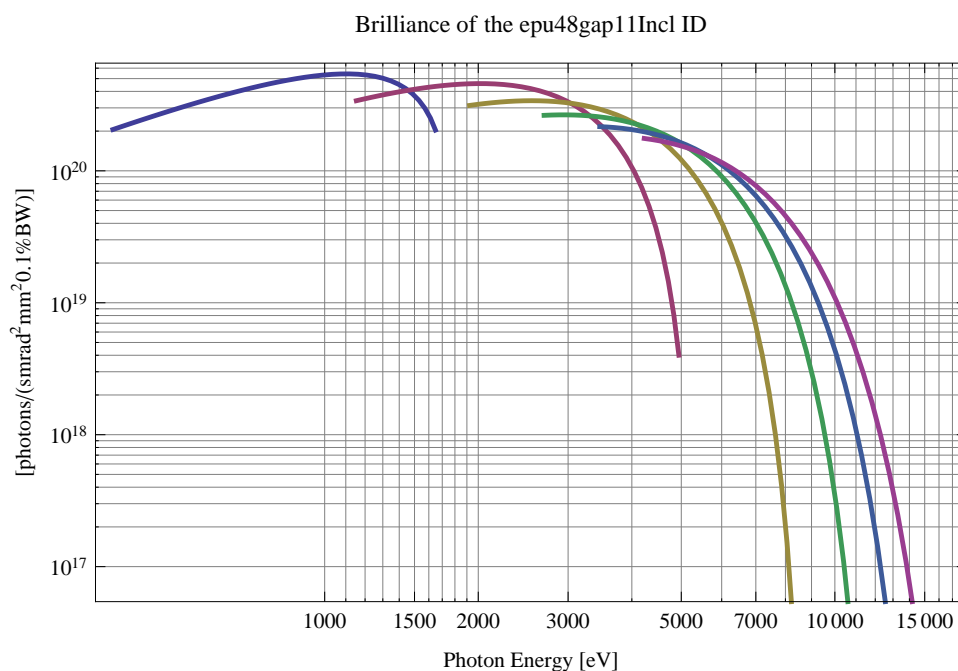


Figure 191: The brilliance at peak energy of the synchrotron radiation emitted by the epu48gap11Incl ID

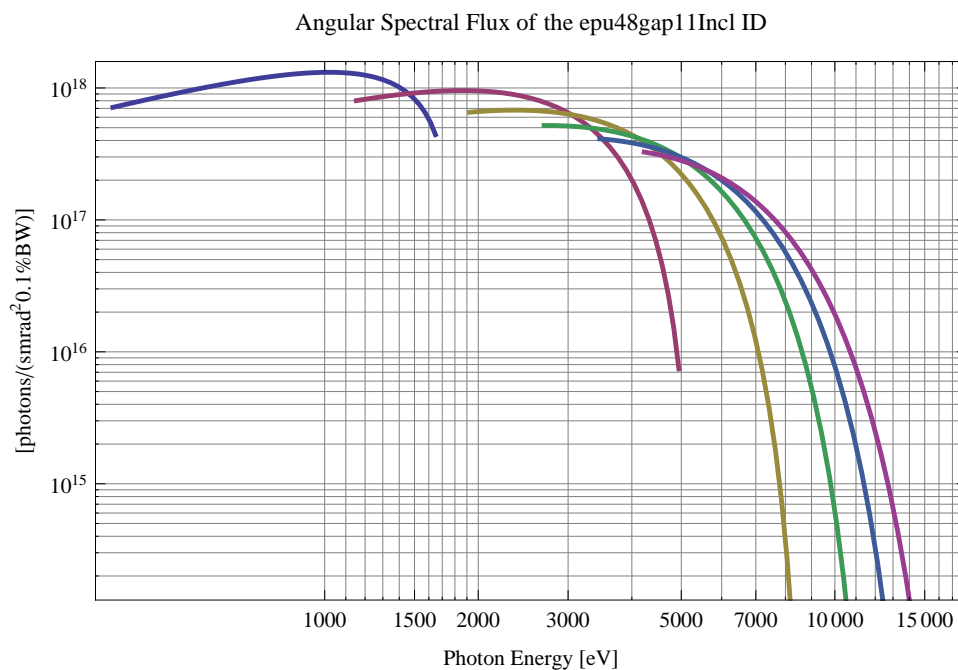


Figure 192: The angular spectral flux of the synchrotron radiation emitted by the epu48gap11Incl ID

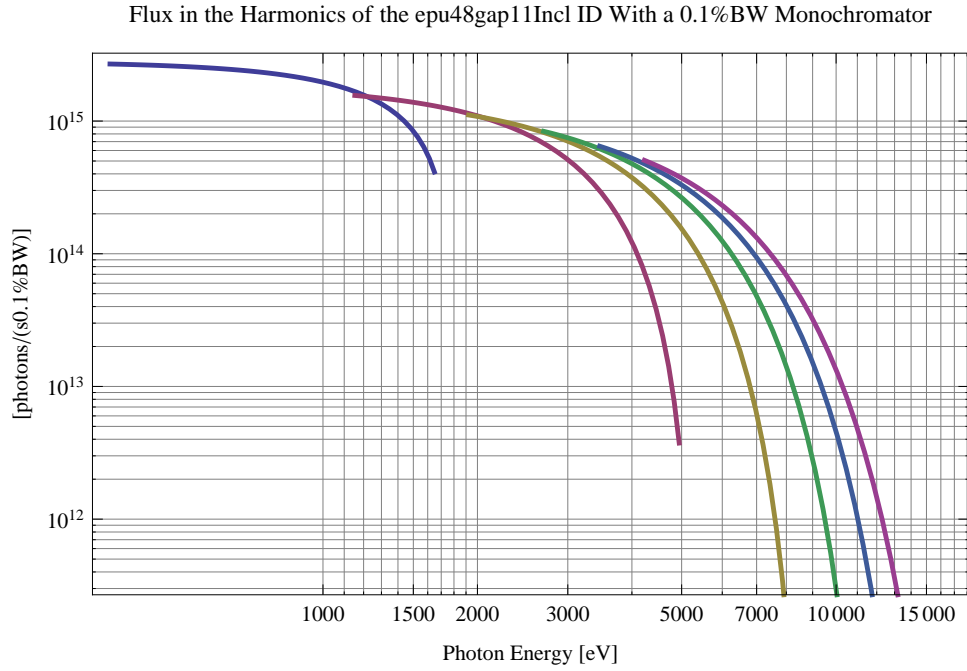


Figure 193: The flux of photons in the harmonics of the emitted synchrotron radiation from the epu48gap11Incl ID using a 0.1%BW monochromator

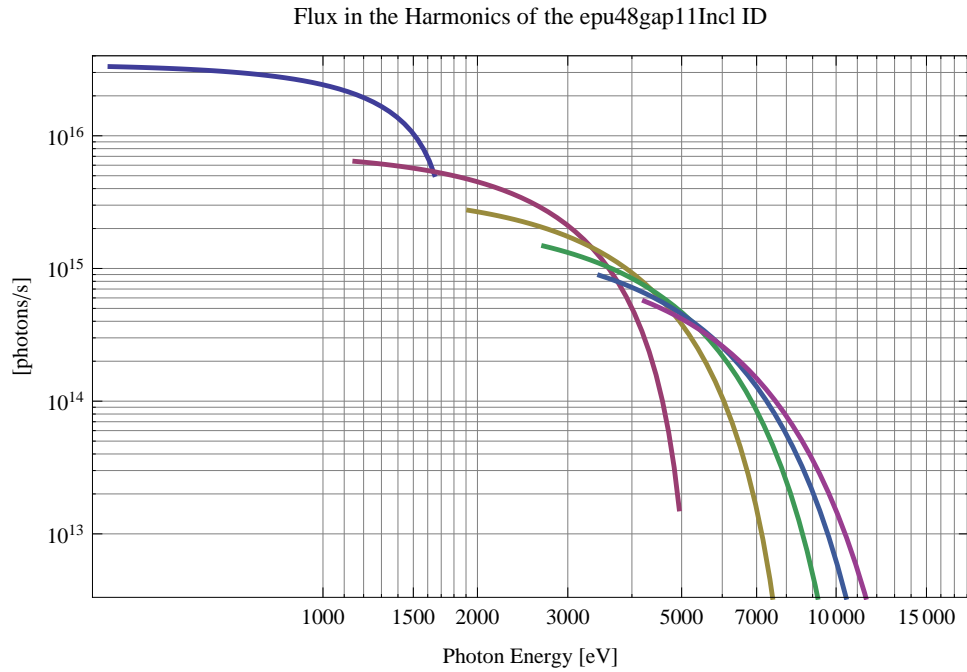


Figure 194: The flux of photons in the harmonics of the emitted synchrotron radiation from the epu48gap11Incl ID

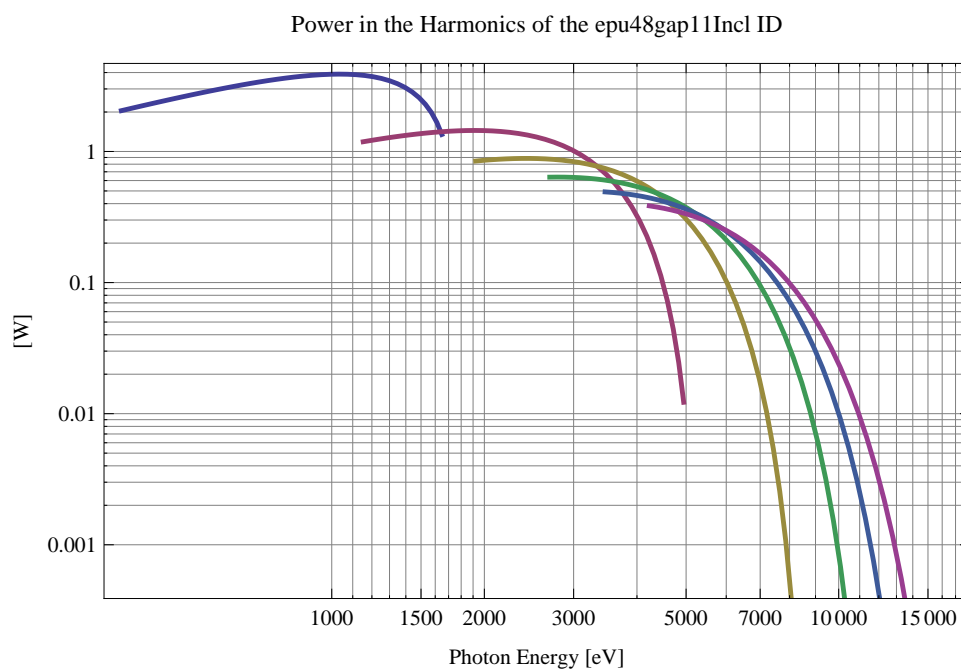


Figure 195: The power in the harmonics of the emitted synchrotron radiation from the epu48gap11Incl ID

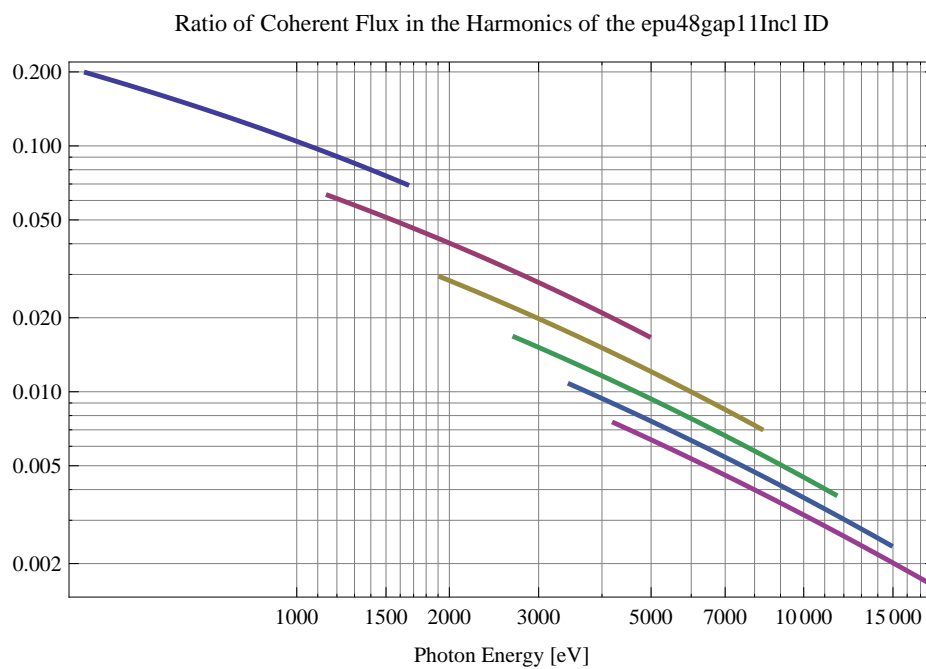


Figure 196: The ratio of coherent flux in the harmonics of the emitted synchrotron radiation from the epu48gap11Incl ID

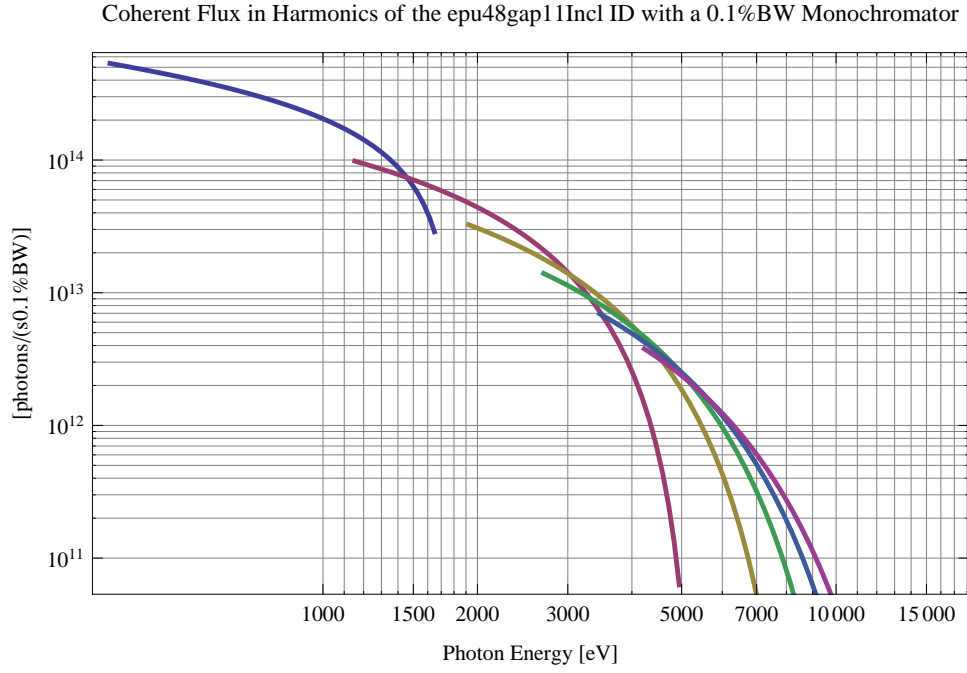


Figure 197: The coherent flux in the harmonics of the epu48gap11Incl ID using a 0.1%BW Monochromator

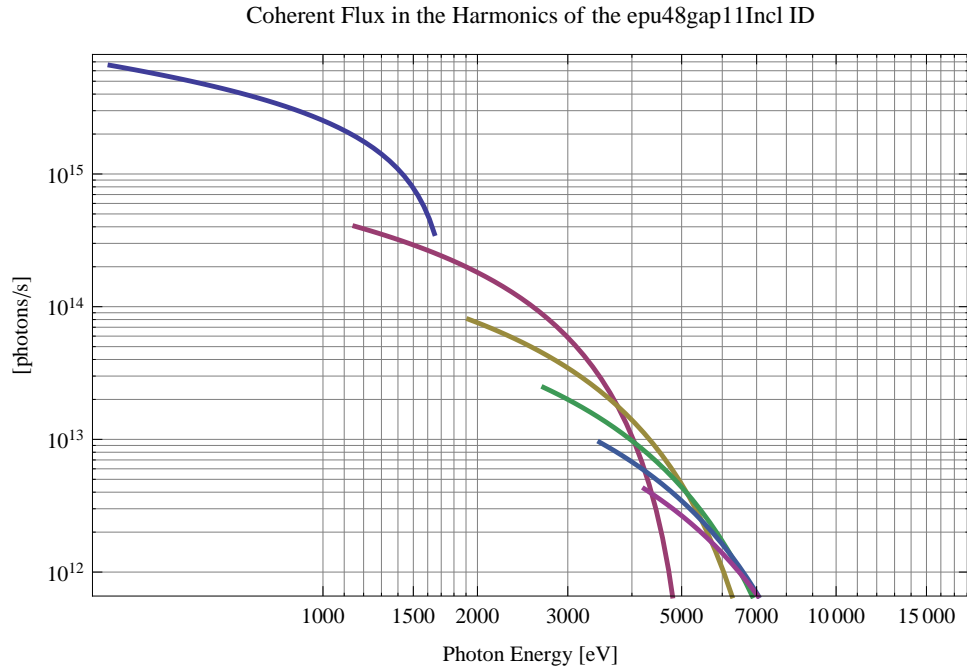


Figure 198: The coherent flux in the harmonics of the epu48gap11Incl ID

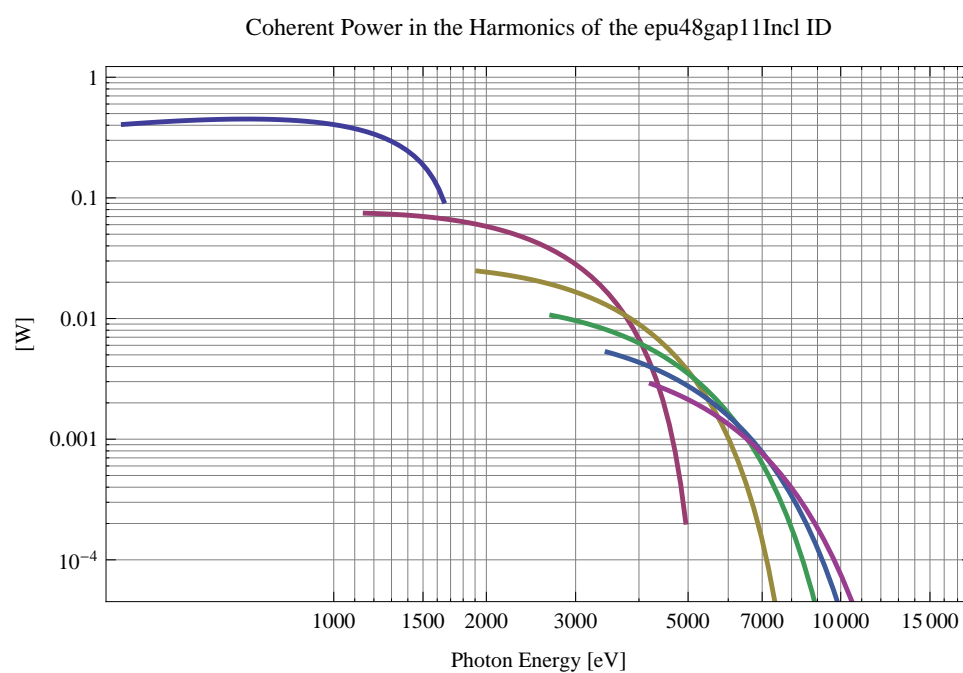


Figure 199: The power of coherent synchrotron radiation in the harmonics of the epu48gap11Incl ID

The brilliance at peak energy and the angular spectral flux density from the epu48gap11Incl ID for different harmonics at maximum K-value (2.695) are given in Table 33 and for minimum K-value (0.400) these values are given in Table 34.

Table 33: The brilliance at peak energy and the angular spectral flux density from the epu48gap11Incl ID for different harmonics at maximum K-value (2.695)

Harmonic	Photon Energy [eV]	Brilliance [Ph./ (smrad ² mrad ² 0.1% BW)]	Angular Spectral Flux [Ph./ (smrad ² 0.1% BW)]
1	384.54	2.06×10^{20}	7.13×10^{17}
3	1153.62	3.4×10^{20}	8.02×10^{17}
5	1922.7	3.13×10^{20}	6.55×10^{17}
7	2691.78	2.63×10^{20}	5.19×10^{17}
9	3460.86	2.16×10^{20}	4.11×10^{17}
11	4229.95	1.76×10^{20}	3.27×10^{17}

Table 34: The brilliance at peak energy and the angular spectral flux density from the epu48gap11Incl ID for different harmonics at minimum K-value (0.4)

Harmonic	Photon Energy [eV]	Brilliance [Ph./ (smrad ² mrad ² 0.1% BW)]	Angular Spectral Flux [Ph./ (smrad ² 0.1% BW)]
1	1648.68	2.04×10^{20}	4.43×10^{17}
3	4946.04	$4. \times 10^{18}$	7.43×10^{15}
5	8243.4	4.6×10^{16}	8.27×10^{13}
7	11540.8	4.86×10^{14}	8.64×10^{11}
9	14838.1	5.02×10^{12}	8.88×10^9
11	18135.5	5.13×10^{10}	9.06×10^7

2.3.11 Magnet model of the elliptically polarising undulator epu48gap11Vert

The Radia [3] magnet model of the epu48gap11Vert ID is shown in Figure 200. The length of the magnet model is 401.496 mm. The magnetic material in the model is NdFeb with a remanence of 1.28 T, a material similar to VACODYM 776 TP from Vacuumschmelze. Blocks with vertical magnetisation are blue and blocks with horizontal magnetisation are yellow. The block size is 30.x30.x12. mm³ and there is a 5. mm cut-out in two of the corners of the blocks. The total length of the epu48gap11Vert ID is 3905.5 mm.

2.3.12 Analysis of the magnetic field of the epu48gap11Vert ID

The effective magnetic fields on axis and the fundamental photon energy of the epu48gap11Vert ID are shown in Table 35. The higher harmonic contents in the magnetic field of an elliptically polarising undulator made of permanent magnets is negligible and the effective field has about the same strength as the peak field.

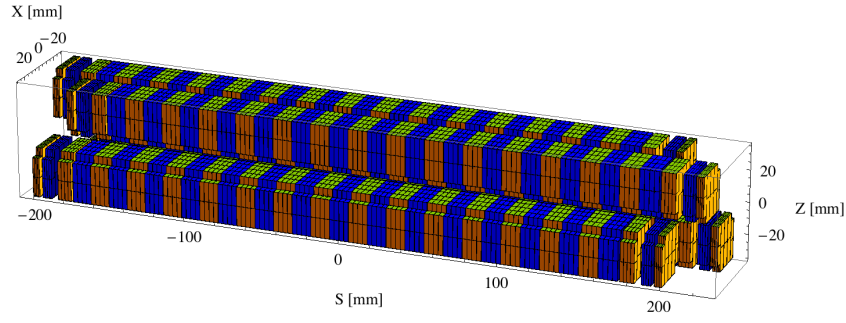


Figure 200: Magnetic model of the epu48gap11Vert ID. The ID has been modelled with Radia [3]

Table 35: Effective Fields on axis and Fundamental Photon Energy of the epu48gap11Vert ID

Undulator Period	48	mm
Undulator Gap	11	mm
Undulator Mode	Vertical	
Undulator Phase	24.000	mm
Vertical Peak Field	0.000	T
Effective Vertical Field	0.000	T
Kx (from vert. field)	0.000	
Horizontal Peak Field:	0.739	T
Effective Horizontal Field	0.740	T
Kz (from hor. field)	3.318	
Photon Energy, Harm.1	0.274	keV
Emitted Power	6.089	kW
Total Length	3905.5	mm

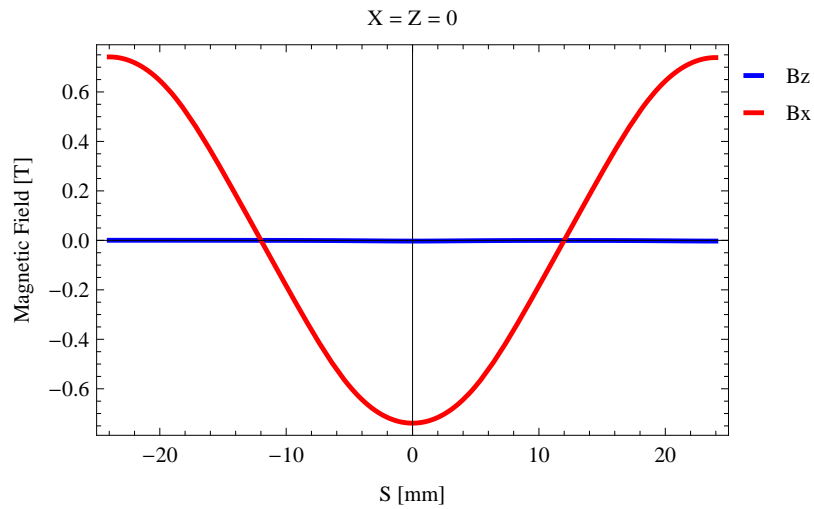


Figure 201: Vertical magnetic field in a central pole of the epu48gap11Vert ID along the ID axis, $X = Z = 0$

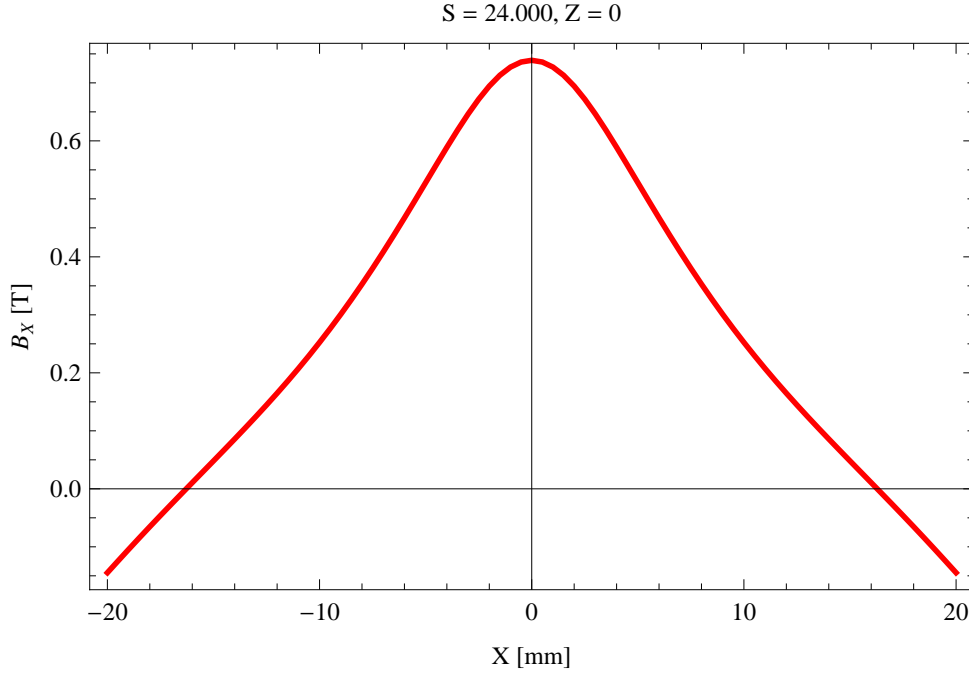


Figure 202: Horizontal magnetic field in a central pole of the epu48gap11Vert ID along the horizontally transverse direction to the ID axis, $S = 24.000$, $Z = 0$

2.3.13 Synchrotron radiation from the epu48gap11Vert ID

The power map of the emitted synchrotron radiation by the epu48gap11Vert ID, assuming a 0.5 A filament beam with an energy of 3 GeV and undulator properties of the synchrotron radiation, is shown in Figure 204. The on-axis power density is 25.818 kW/mrad²

A map of the degree of linear polarisation of the fundamental harmonic of the synchrotron radiation emitted by the epu48gap11Vert ID over the angle of observation is shown in Figure 205.

A map of the degree of 45 degree polarisation of the fundamental harmonic of the synchrotron radiation emitted by the epu48gap11Vert ID over the angle of observation is shown in Figure 206.

A map of the degree of circular polarisation of the fundamental harmonic of the synchrotron radiation emitted by the epu48gap11Vert ID over the angle of observation is shown in Figure 207.

The on axis brilliance at peak energy and the angular spectral flux from the epu48gap11Vert ID have been calculated with the given beam parameters, which are 0.5 A of stored current, $\beta_H = 9$ m, $\varepsilon_H = 0.263$ nmrad, $\beta_V = 4.8$ m, $\varepsilon_V = 8$. pmrad, and an energy spread of 0.001.

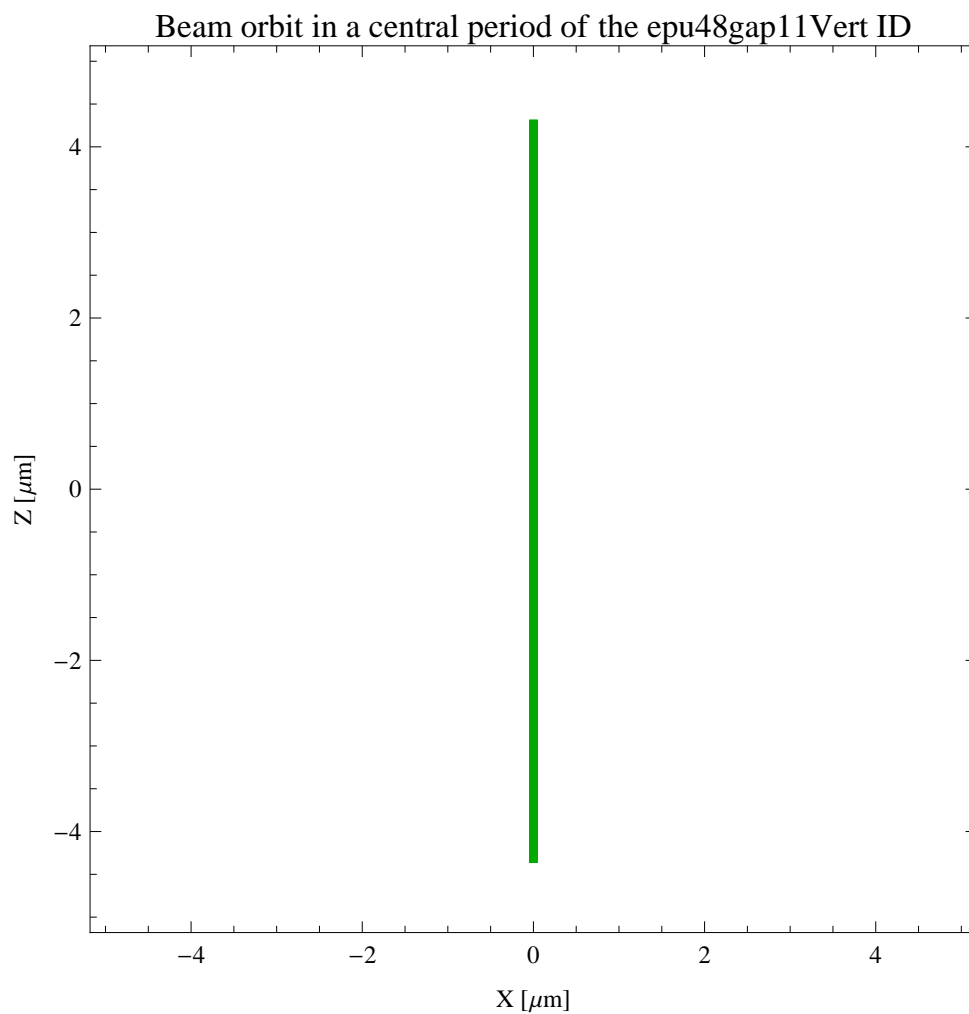


Figure 203: The beam orbit of the electron beam through a central period of the epu48gap11Vert ID

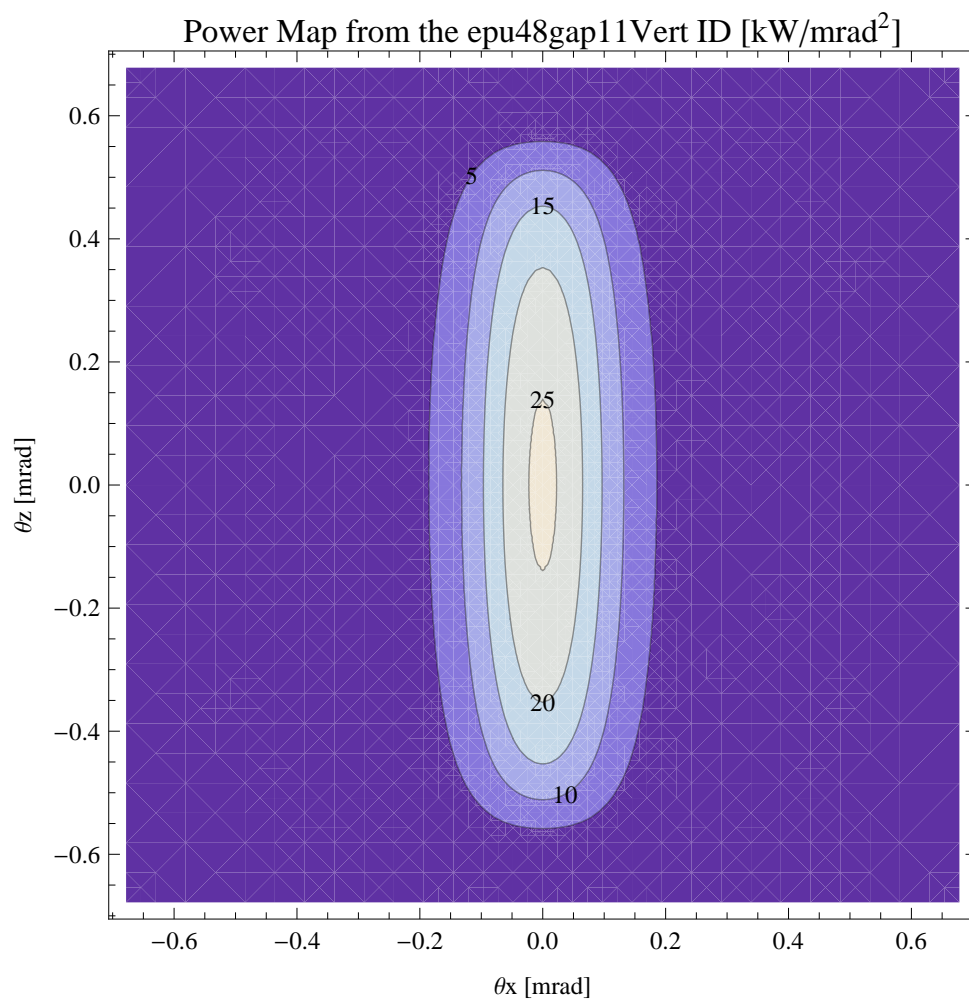


Figure 204: Map of the power distribution of the emitted synchrotron radiation by the epu48gap11Vert ID

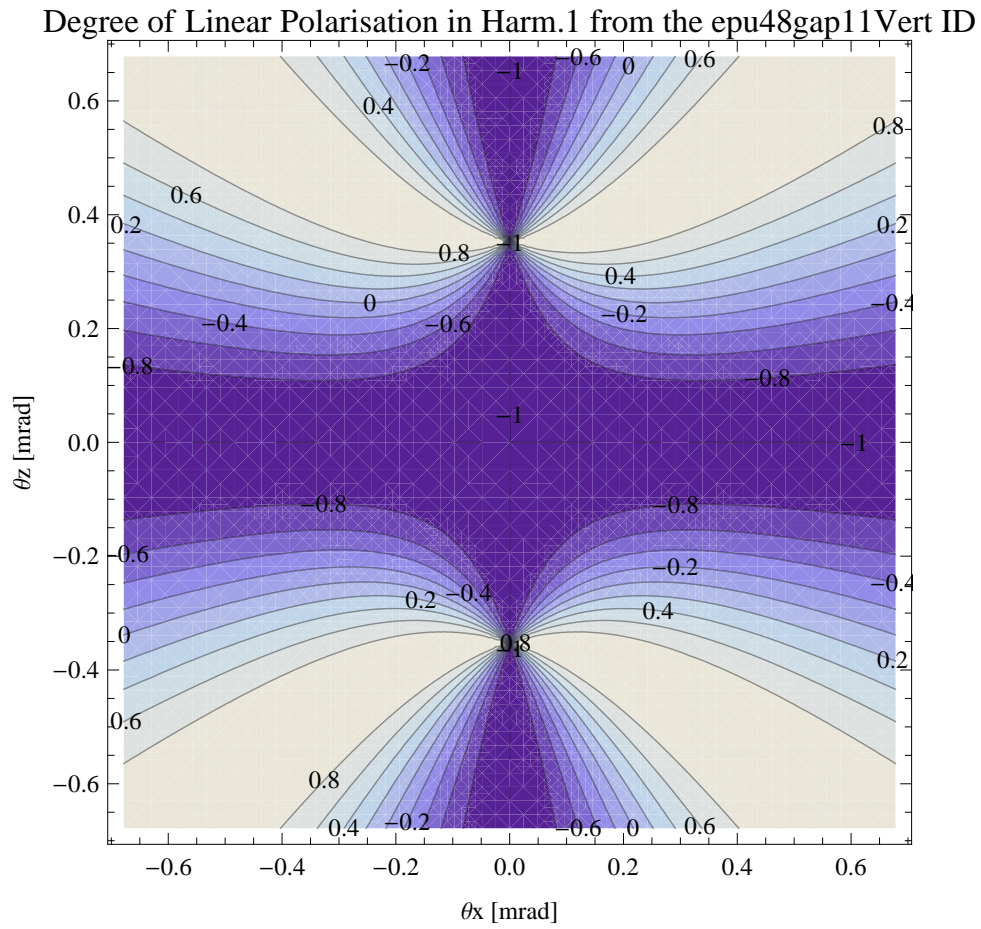


Figure 205: Map of linear polarisation in the fundamental harmonic of the synchrotron radiation emitted by the epu48gap11Vert ID

Degree of 45 degree Polarisation in Harm.1 from the epu48gap11Vert ID

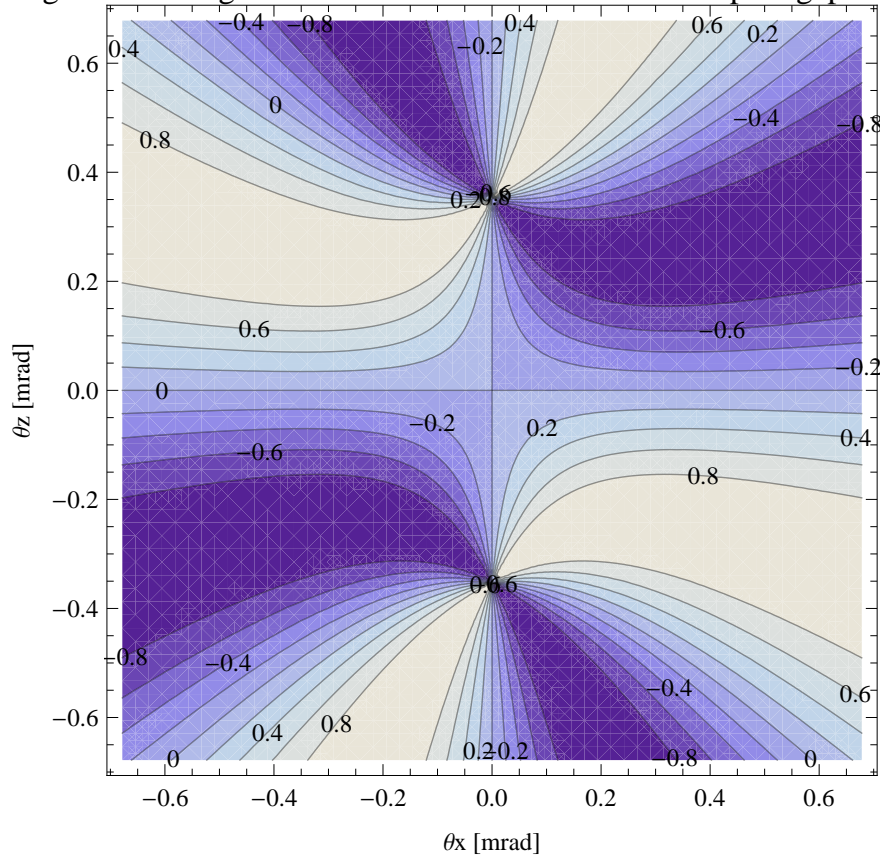


Figure 206: Map of 45 degree polarisation in the fundamental harmonic of the synchrotron radiation emitted by the epu48gap11Vert ID

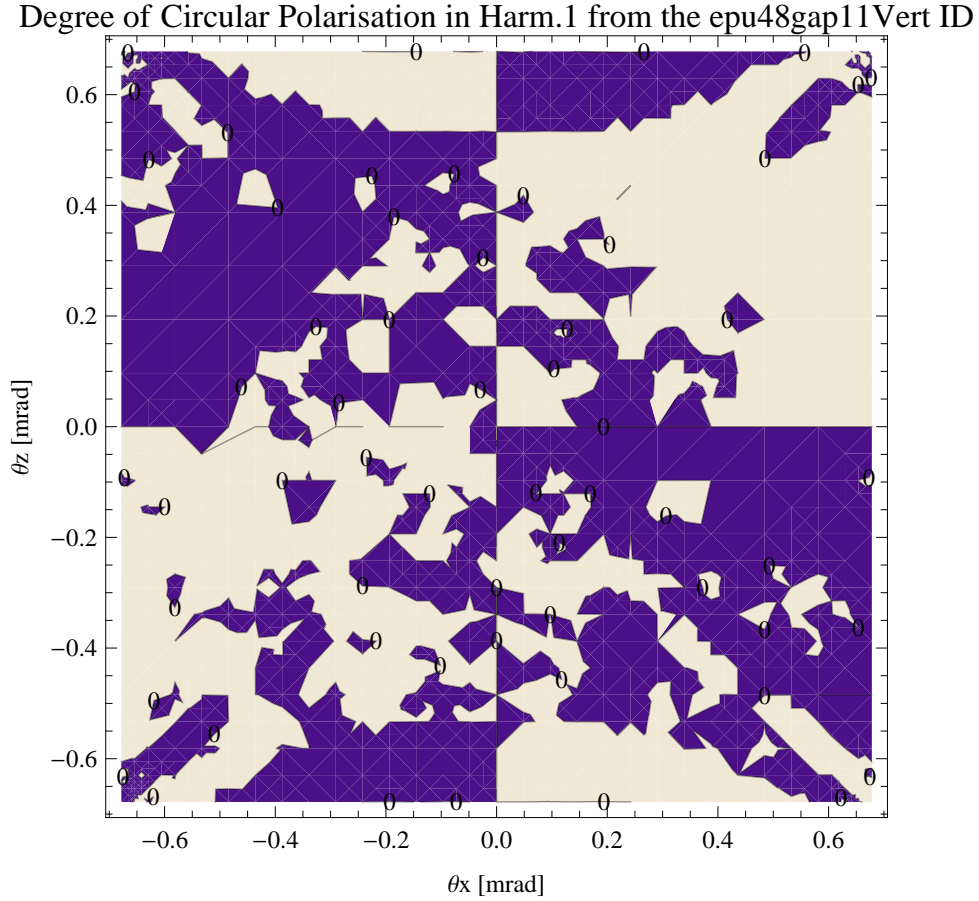


Figure 207: Map of circular polarisation in the fundamental harmonic of the synchrotron radiation emitted by the epu48gap11Vert ID

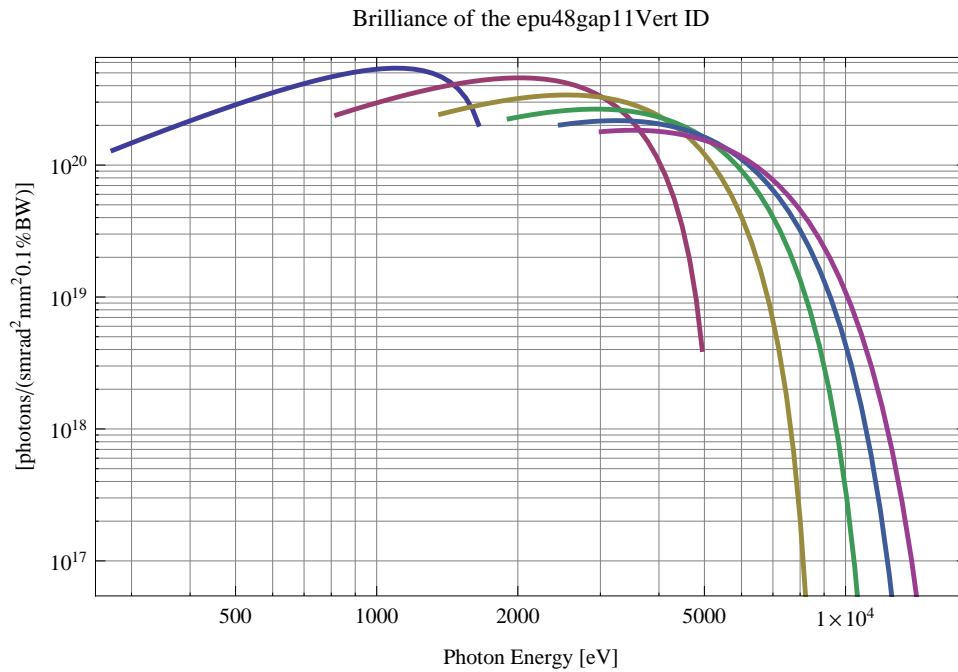


Figure 208: The brilliance at peak energy of the synchrotron radiation emitted by the epu48gap11Vert ID

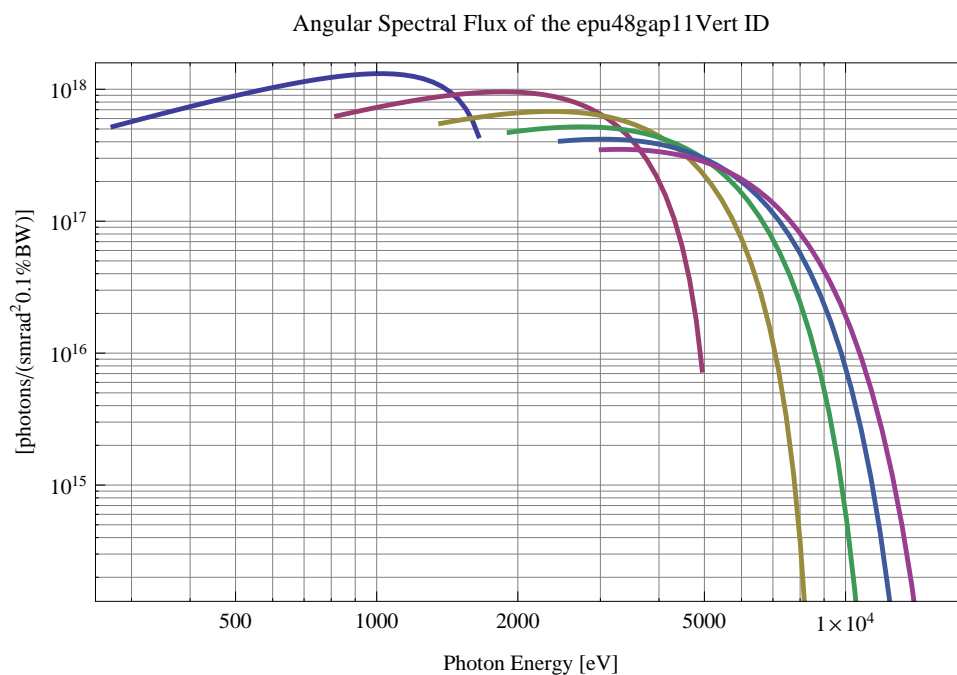


Figure 209: The angular spectral flux of the synchrotron radiation emitted by the epu48gap11Vert ID

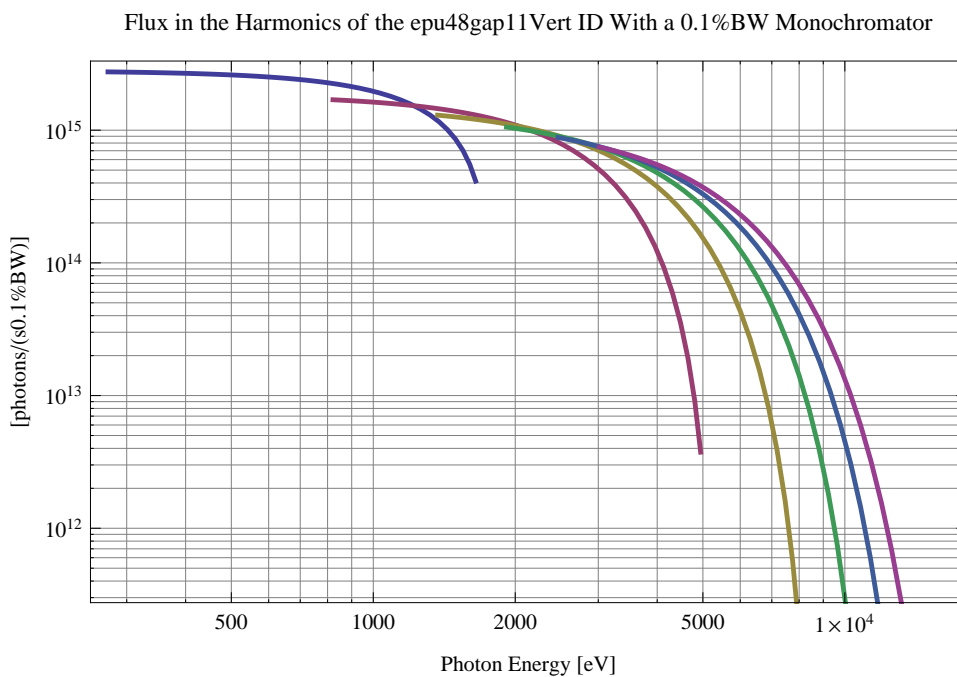


Figure 210: The flux of photons in the harmonics of the emitted synchrotron radiation from the epu48gap11Vert ID using a 0.1%BW monochromator

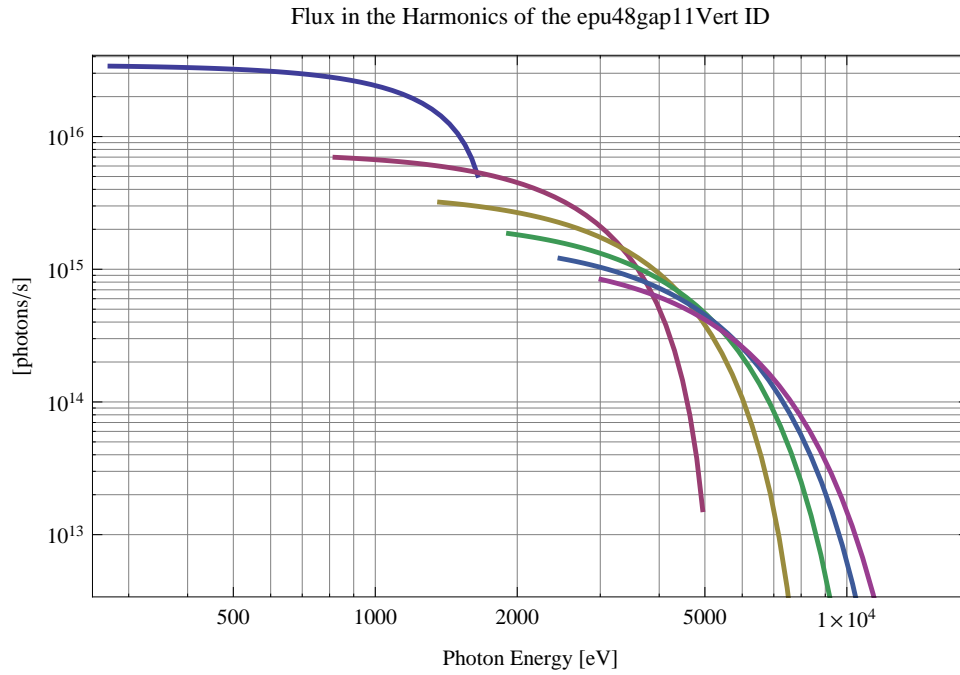


Figure 211: The flux of photons in the harmonics of the emitted synchrotron radiation from the epu48gap11Vert ID

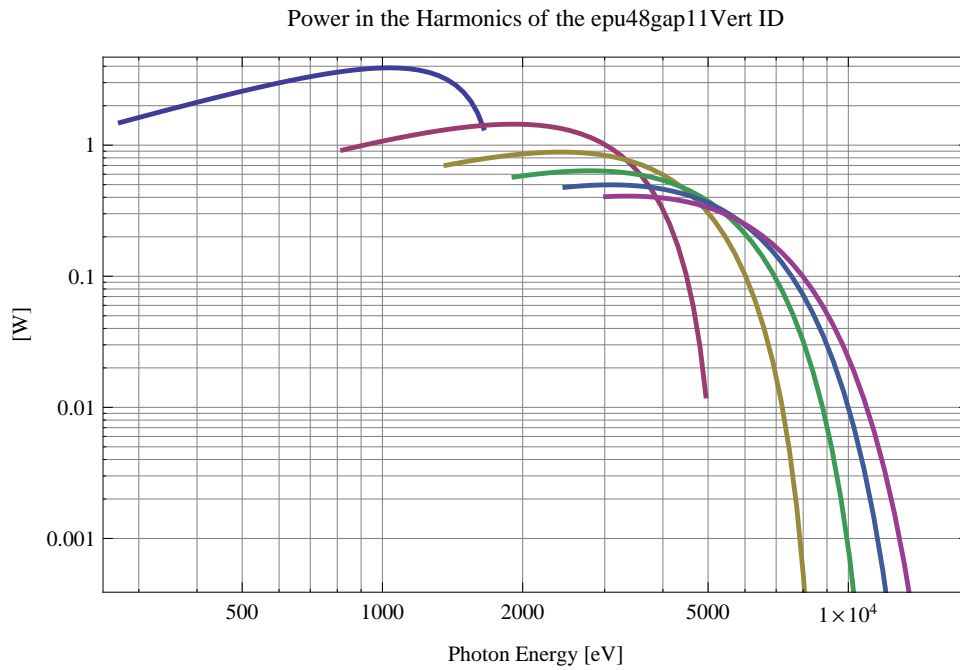


Figure 212: The power in the harmonics of the emitted synchrotron radiation from the epu48gap11Vert ID

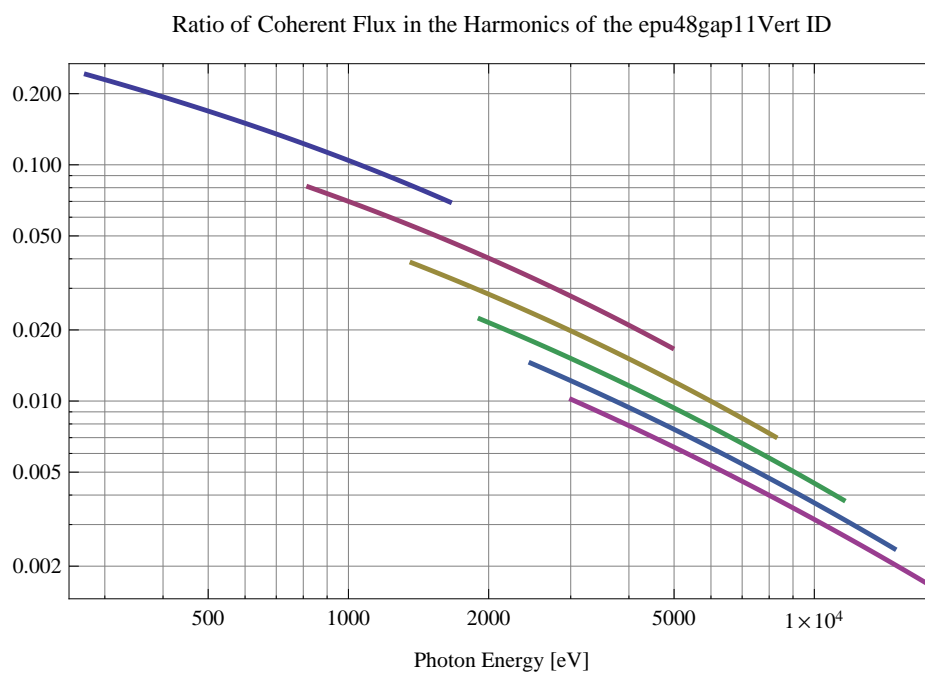


Figure 213: The ratio of coherent flux in the harmonics of the emitted synchrotron radiation from the epu48gap11Vert ID

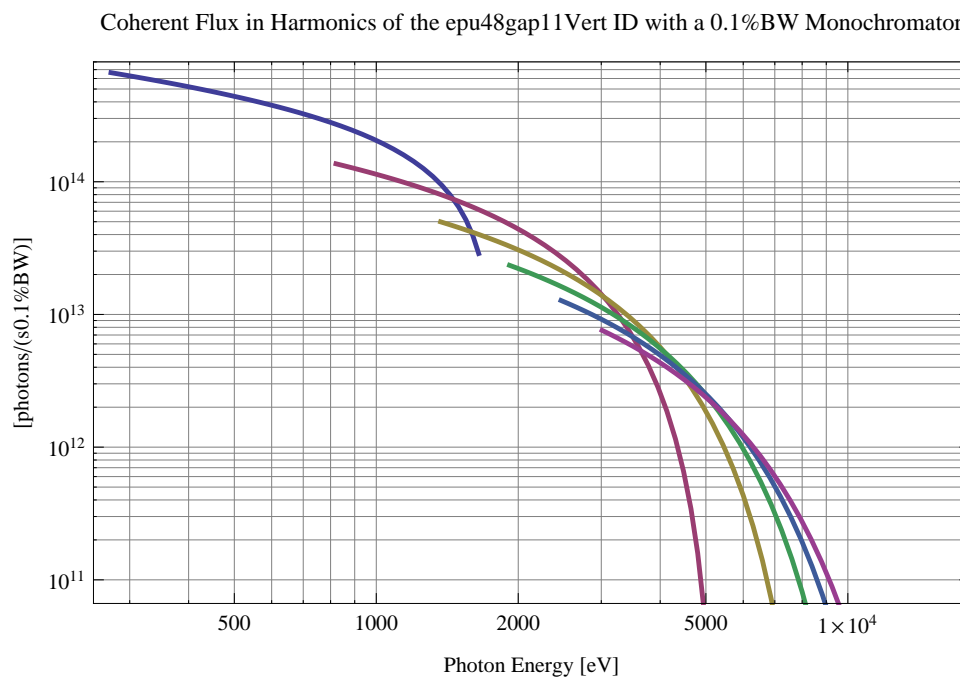


Figure 214: The coherent flux in the harmonics of the epu48gap11Vert ID using a 0.1%BW Monochromator

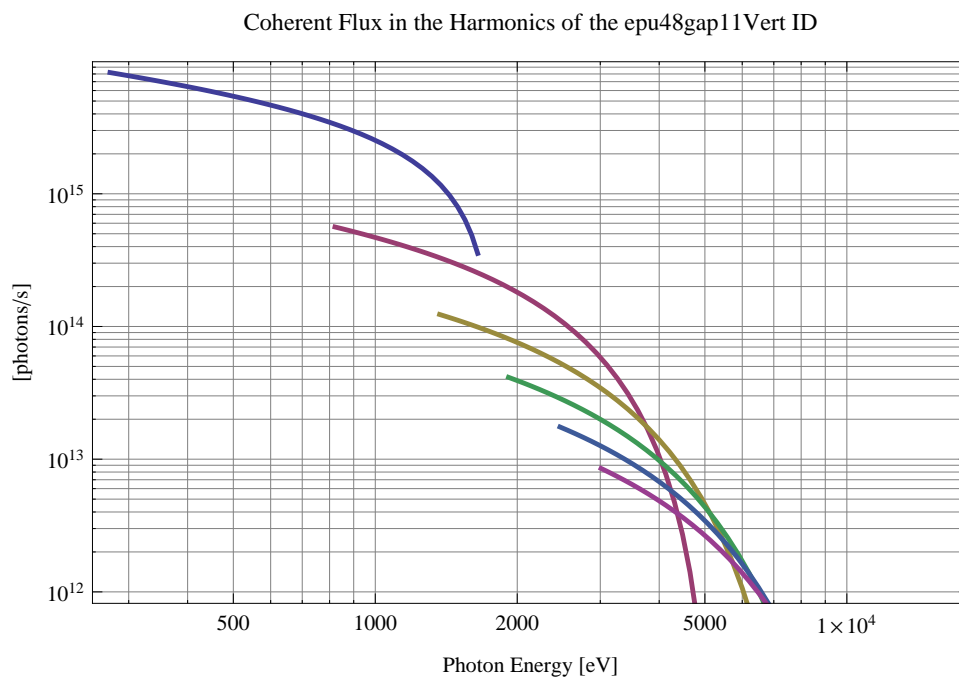


Figure 215: The coherent flux in the harmonics of the epu48gap11Vert ID

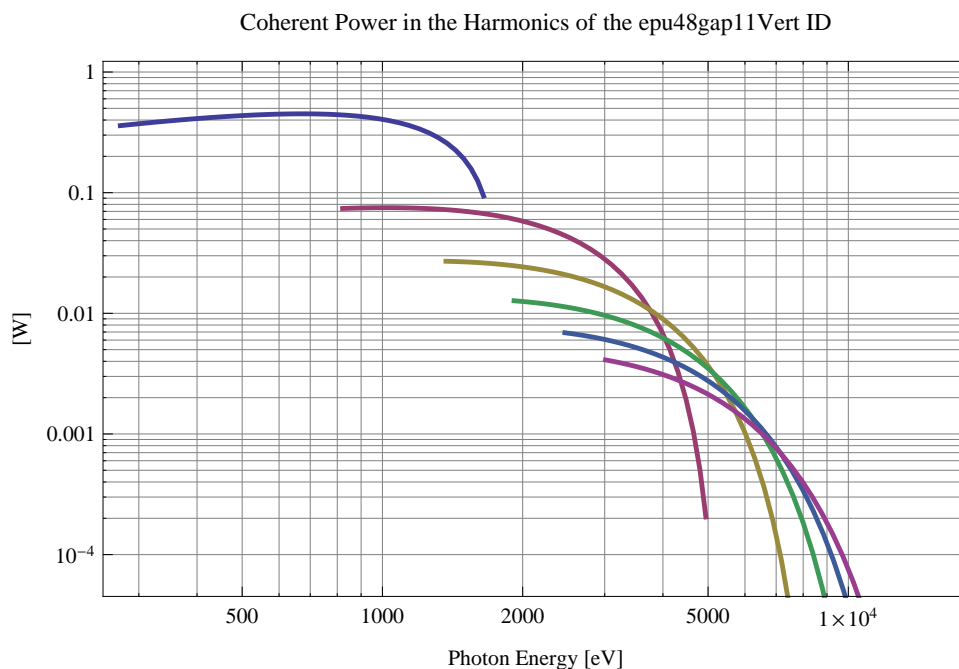


Figure 216: The power of coherent synchrotron radiation in the harmonics of the epu48gap11Vert ID

The brilliance at peak energy and the angular spectral flux density from the epu48gap11Vert ID for different harmonics at maximum K-value (3.318) are given in Table 36 and for minimum K-value (0.400) these values are given in Table 37.

Table 36: The brilliance at peak energy and the angular spectral flux density from the epu48gap11Vert ID for different harmonics at maximum K-value (3.318)

Harmonic	Photon Energy [eV]	Brilliance [Ph./($\text{smrad}^2\text{mrad}^20.1\%\text{BW}$)]	Angular Spectral Flux [Ph./($\text{smrad}^20.1\%\text{BW}$)]
1	273.803	1.29×10^{20}	5.22×10^{17}
3	821.408	2.4×10^{20}	6.27×10^{17}
5	1369.01	2.43×10^{20}	5.5×10^{17}
7	1916.62	2.24×10^{20}	4.71×10^{17}
9	2464.23	2.01×10^{20}	4.04×10^{17}
11	3011.83	1.79×10^{20}	3.48×10^{17}

Table 37: The brilliance at peak energy and the angular spectral flux density from the epu48gap11Vert ID for different harmonics at minimum K-value (0.4)

Harmonic	Photon Energy [eV]	Brilliance [Ph./($\text{smrad}^2\text{mrad}^20.1\%\text{BW}$)]	Angular Spectral Flux [Ph./($\text{smrad}^20.1\%\text{BW}$)]
1	1648.68	2.04×10^{20}	4.43×10^{17}
3	4946.04	$4. \times 10^{18}$	7.43×10^{15}
5	8243.4	4.6×10^{16}	8.27×10^{13}
7	11540.8	4.86×10^{14}	8.64×10^{11}
9	14838.1	5.02×10^{12}	8.88×10^9
11	18135.5	5.13×10^{10}	9.06×10^7

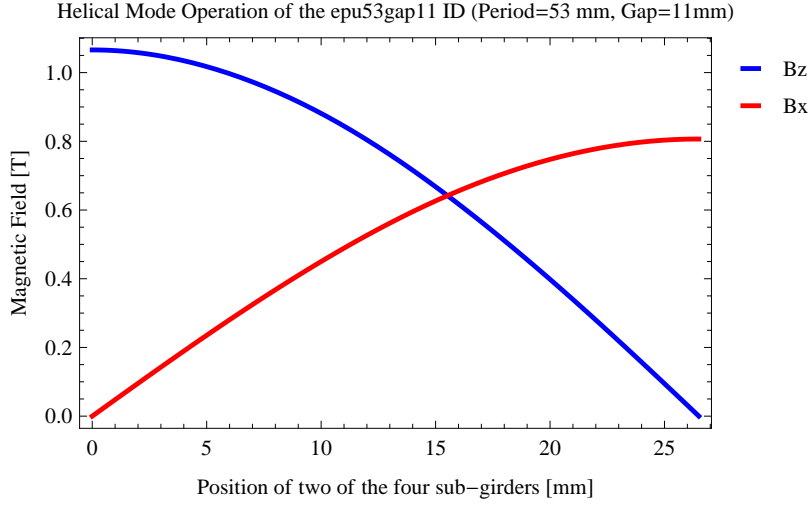


Figure 217: Vertical and horizontal magnetic field for the the epu53gap11 ID when operating in the helical mode for different positions for two of the four sub-girders

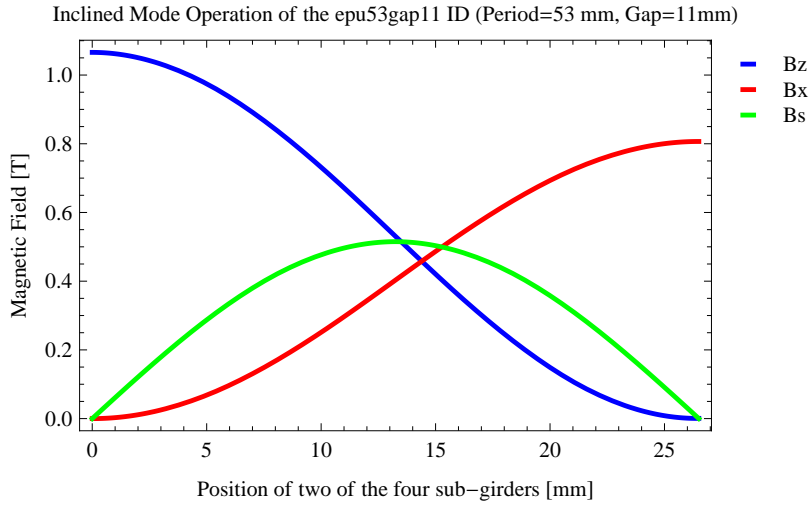


Figure 218: Vertical, horizontal, and longitudinal magnetic field for the the epu53gap11 ID when operating in the inclined mode for different positions for two of the four sub-girders

2.4 The elliptically polarising undulator epu53gap11

2.4.1 Modes of operation in the elliptically polarising undulator epu53gap11

Horizontal polarisation of the emitted synchrotron radiation from the epu53gap11 ID (Period=53 mm, Gap=11mm) is found in the planar mode when there is no movement of the sub-girders.

Circular polarisation is found in the elliptical mode of operation for a symmetric sub-grider movement of 15.5202 mm. Figure 217 shows the vertical and horizontal magnetic field for the epu53gap11 ID when operating in the helical mode.

45 degree polarisation is found in the inclined mode of operation for an assymetric sub-grider movement of 14.3962 mm. Figure 218 shows the vertical and horizontal magnetic field for the epu53gap11 ID when operating in the inclined mode.

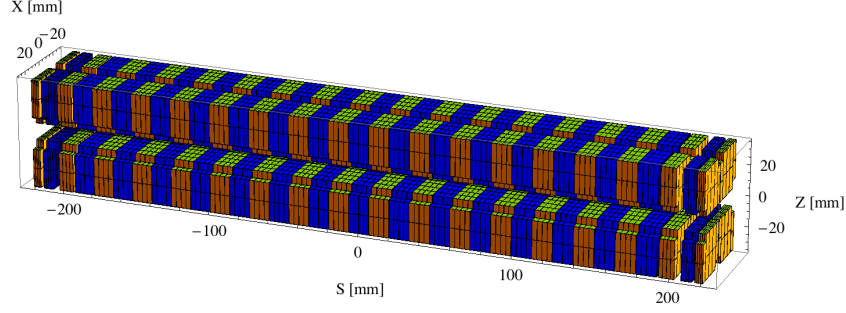


Figure 219: Magnetic model of the epu53gap11Plan ID. The ID has been modelled with Radia [3]

The following sub-sections will cover four different situations: The epu53gap11 operating in the planar mode for horizontal polarisation (epu53gap11Plan); The epu53gap11 operating in the helical mode for circular polarisation (epu53gap11Heli), the epu53gap11 operating in the inclined mode for 45 degree polarisation (epu53gap11Incl); and The epu53gap11 operating in the vertical mode for vertical polarisation (epu53gap11Vert).

2.4.2 Magnet model of the elliptically polarising undulator epu53gap11Plan

The Radia [3] magnet model of the epu53gap11Plan ID is shown in Figure 219. The length of the magnet model is 441.756 mm. The magnetic material in the model is NdFeb with a remanence of 1.28 T, a material similar to VACODYM 776 TP from Vacuumschmelze. Blocks with vertical magnetisation are blue and blocks with horizontal magnetisation are yellow. The block size is $30 \times 30 \times 13.25 \text{ mm}^3$ and there is a 5. mm cut-out in two of the corners of the blocks. The total length of the epu53gap11Plan ID is 3939.76 mm.

2.4.3 Analysis of the magnetic field of the epu53gap11Plan ID

The effective magnetic fields on axis and the fundamental photon energy of the epu53gap11Plan ID are shown in Table 38. The higher harmonic contents in the magnetic field of an elliptically polarising undulator made of permanent magnets is negligible and the effective field has about the same strength as the peak field.

2.4.4 Synchrotron radiation from the epu53gap11Plan ID

The power map of the emitted synchrotron radiation by the epu53gap11Plan ID, assuming a 0.5 A filament beam with an energy of 3 GeV and undulator properties of the synchrotron radiation, is shown in Figure 223. The on-axis power density is 34.085 kW/mrad^2

A map of the degree of linear polarisation of the fundamental harmonic of the synchrotron radiation emitted by the epu53gap11Plan ID over the angle of observation is shown in Figure 224.

A map of the degree of 45 degree polarisation of the fundamental harmonic of the synchrotron radiation emitted by the epu53gap11Plan ID over the angle of observation is shown in Figure 225.

Table 38: Effective Fields on axis and Fundamental Photon Energy of the epu53gap11Plan ID

Undulator Period	53	mm
Undulator Gap	11	mm
Undulator Mode	Planar	
Undulator Phase	0.000	mm
Vertical Peak Field	1.049	T
Effective Vertical Field	1.066	T
Kx (from vert. field)	5.277	
Horizontal Peak Field:	0.000	T
Effective Horizontal Field	0.000	T
Kz (from hor. field)	0.000	
Photon Energy, Harm.1	0.108	keV
Emitted Power	12.746	kW
Total Length	3939.8	mm

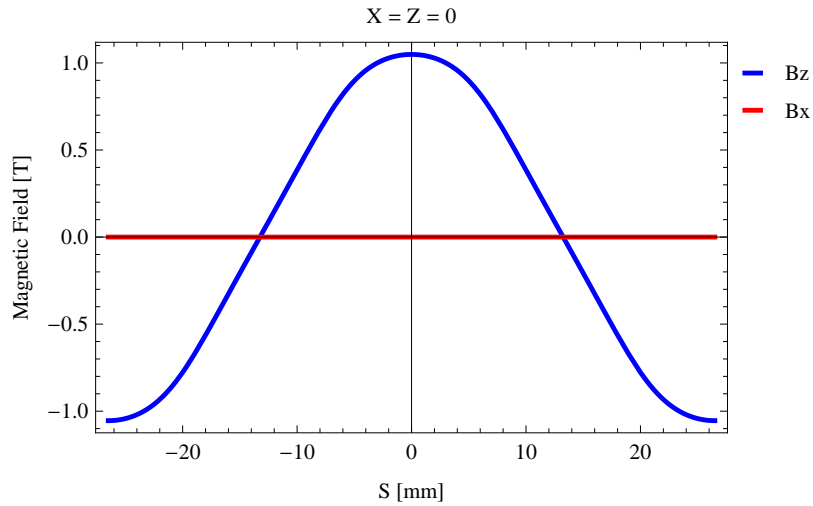


Figure 220: Vertical magnetic field in a central pole of the epu53gap11Plan ID along the ID axis, $X = Z = 0$

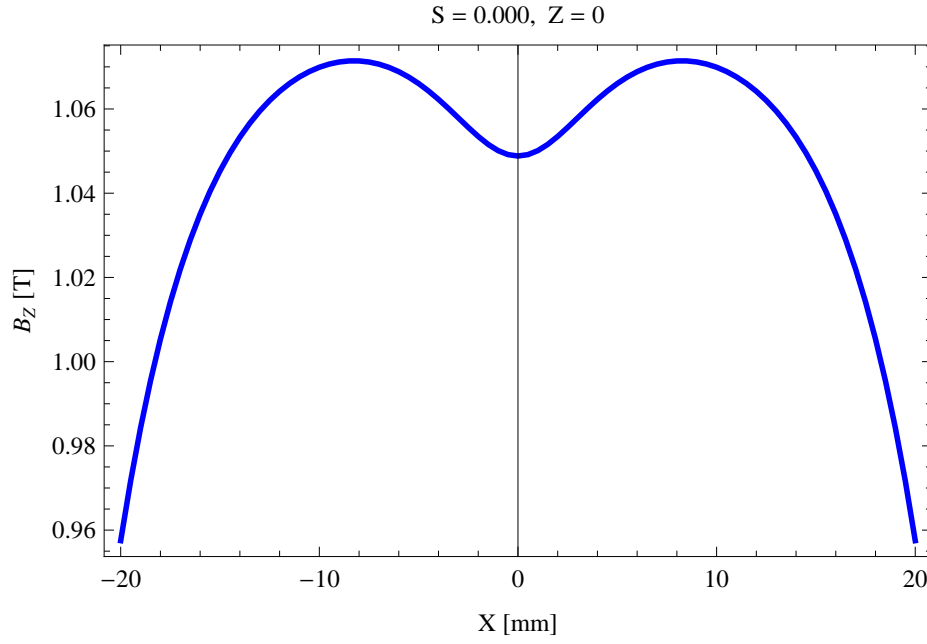


Figure 221: Vertical magnetic field in a central pole of the epu53gap11Plan ID along the horizontally transverse direction to the ID axis, $S = 0.000$, $Z = 0$

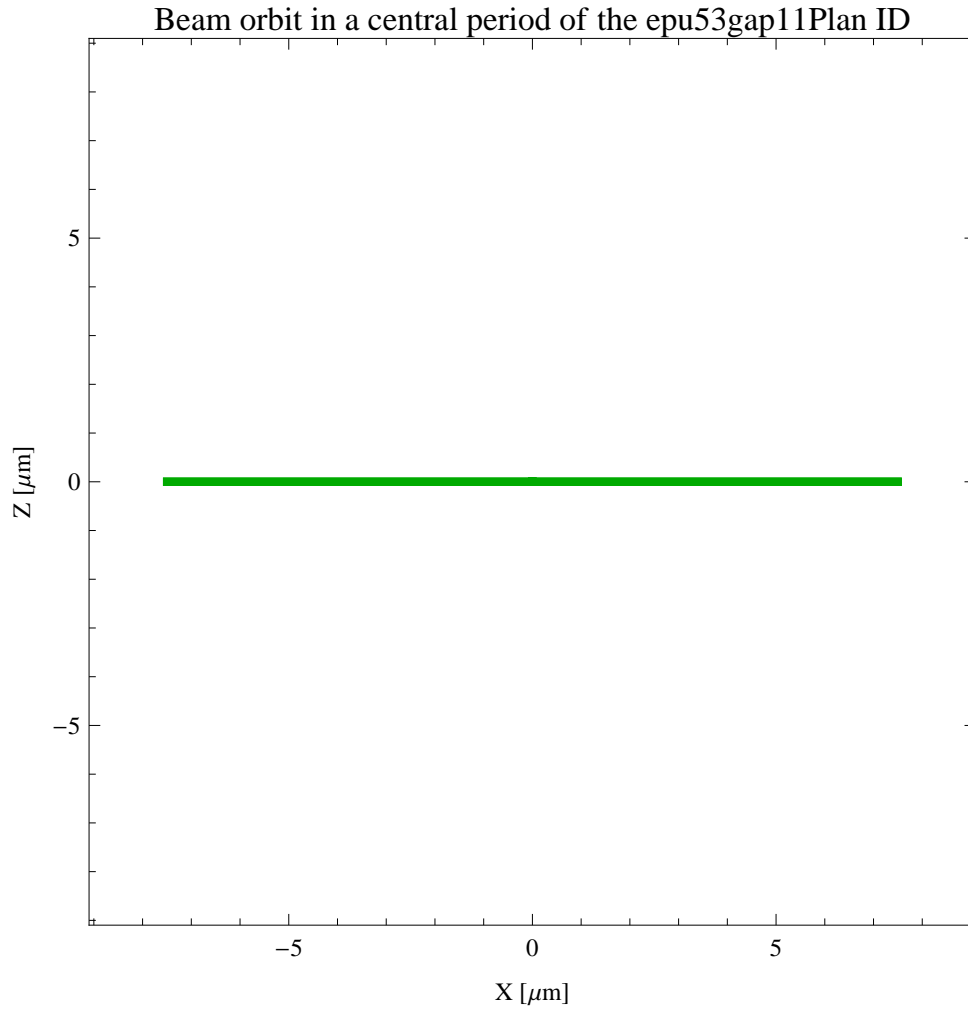


Figure 222: The beam orbit of the electron beam through a central period of the epu53gap11Plan ID

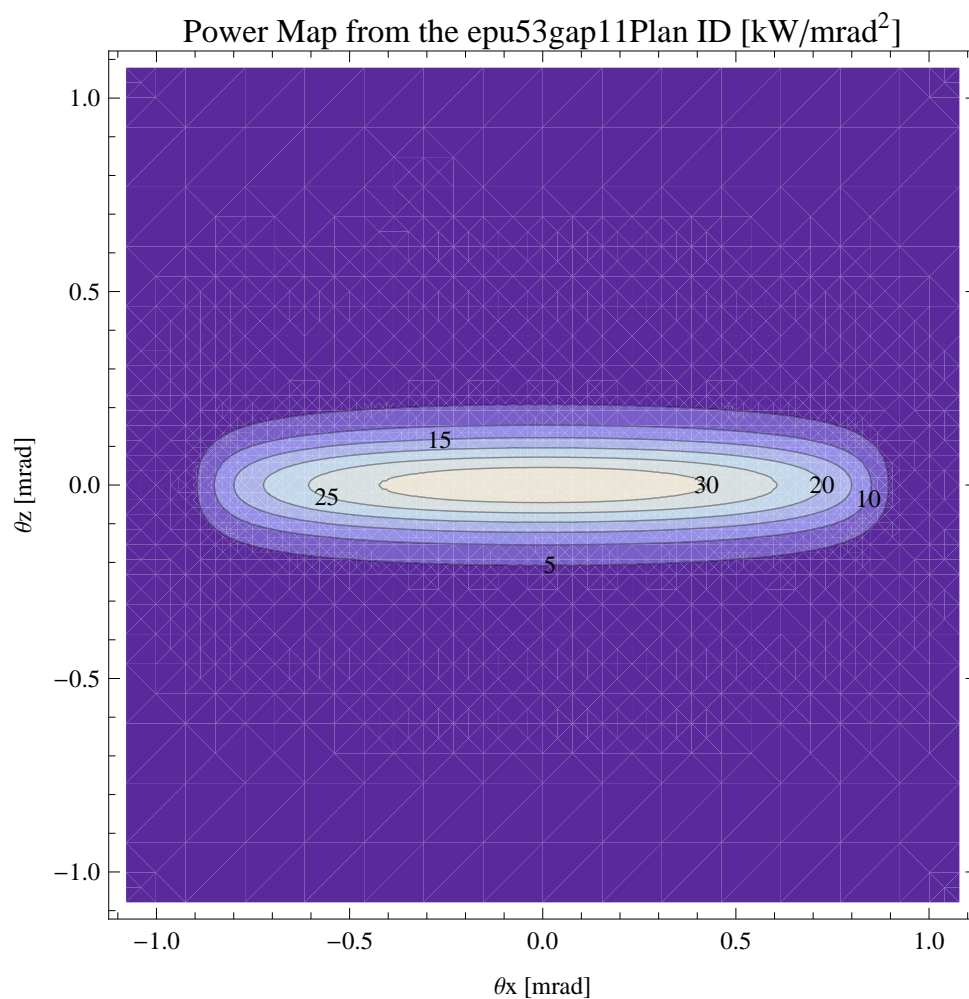


Figure 223: Map of the power distribution of the emitted synchrotron radiation by the epu53gap11Plan ID

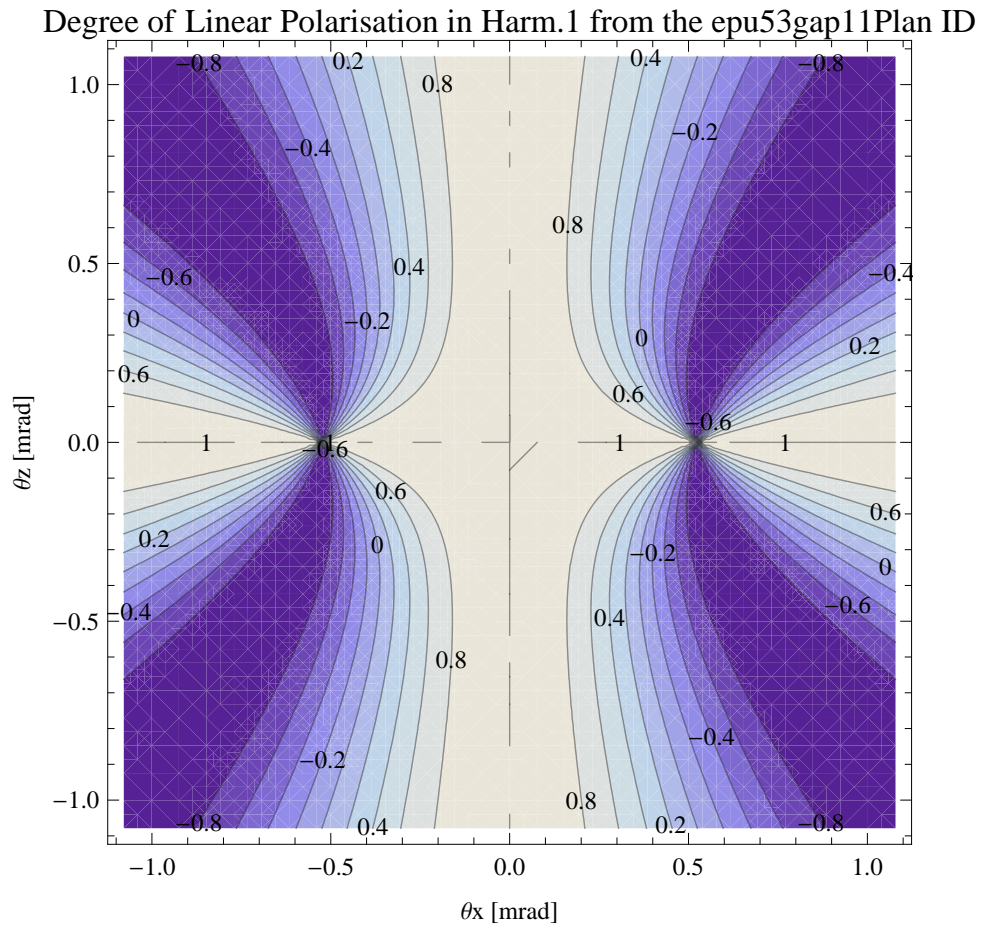


Figure 224: Map of linear polarisation in the fundamental harmonic of the synchrotron radiation emitted by the epu53gap11Plan ID

Degree of 45 degree Polarisation in Harm.1 from the epu53gap11Plan ID

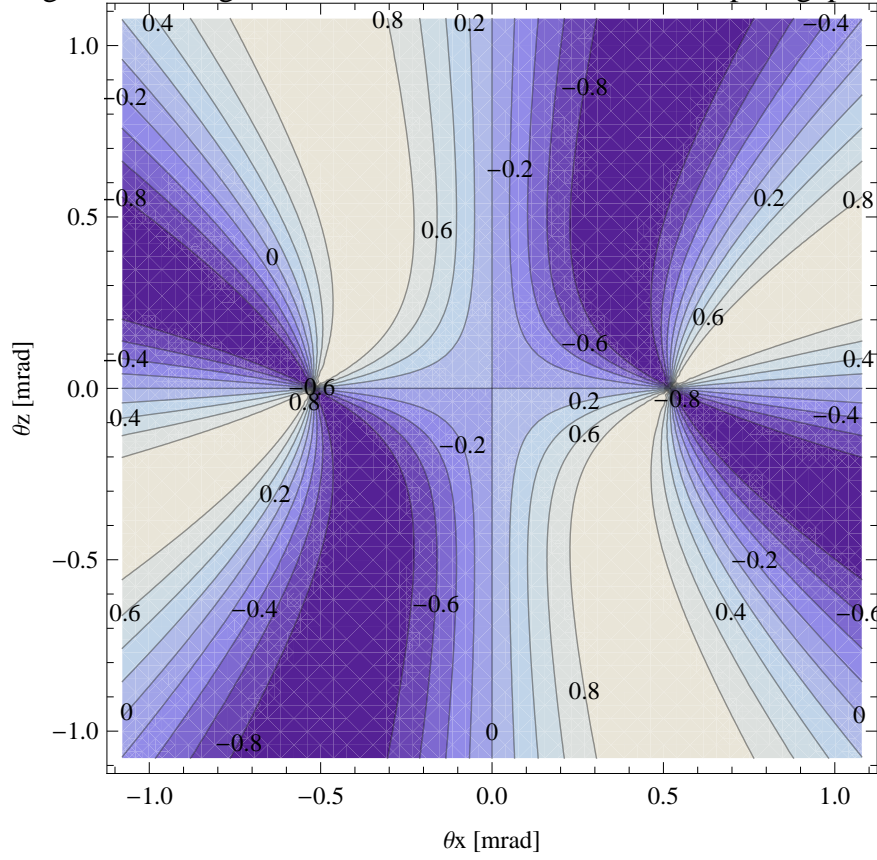


Figure 225: Map of 45 degree polarisation in the fundamental harmonic of the synchrotron radiation emitted by the epu53gap11Plan ID

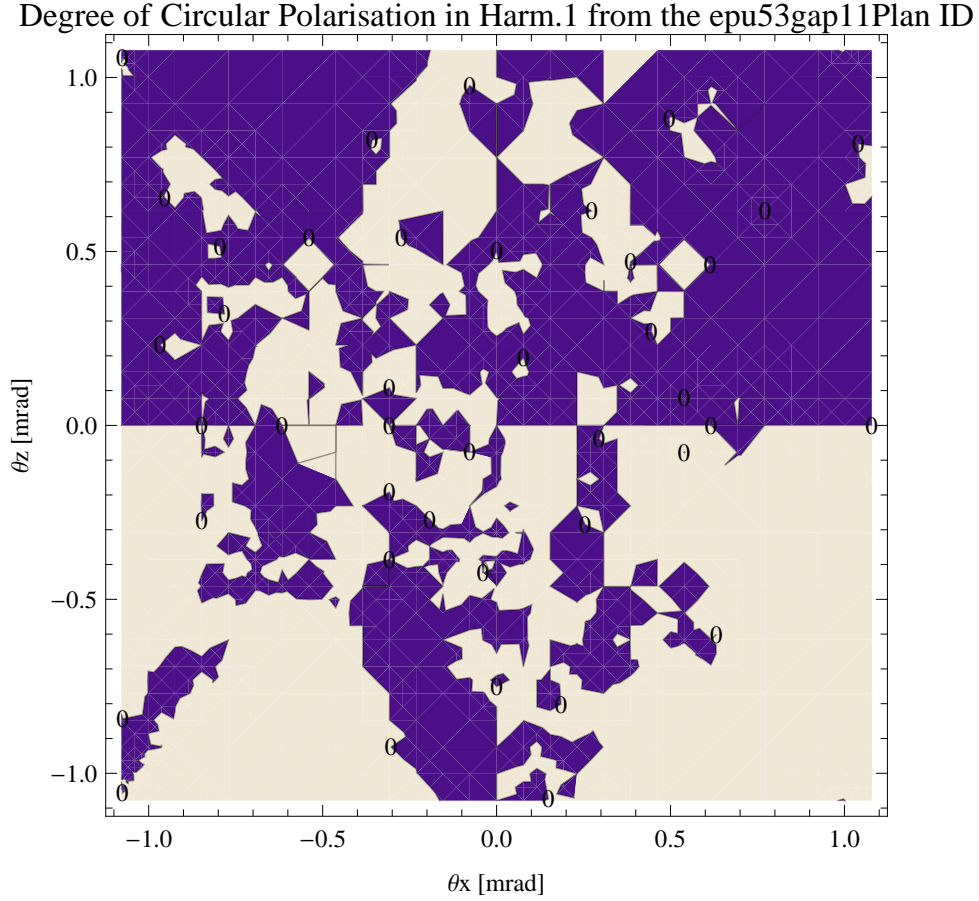


Figure 226: Map of circular polarisation in the fundamental harmonic of the synchrotron radiation emitted by the epu53gap11Plan ID

A map of the degree of circular polarisation of the fundamental harmonic of the synchrotron radiation emitted by the epu53gap11Plan ID over the angle of observation is shown in Figure 226.

The on axis brilliance at peak energy and the angular spectral flux from the epu53gap11Plan ID have been calculated with the given beam parameters, which are 0.5 A of stored current, $\beta_H = 9$ m, $\varepsilon_H = 0.263$ nmrad, $\beta_V = 4.8$ m, $\varepsilon_V = 8$. pmrad, and an energy spread of 0.001.

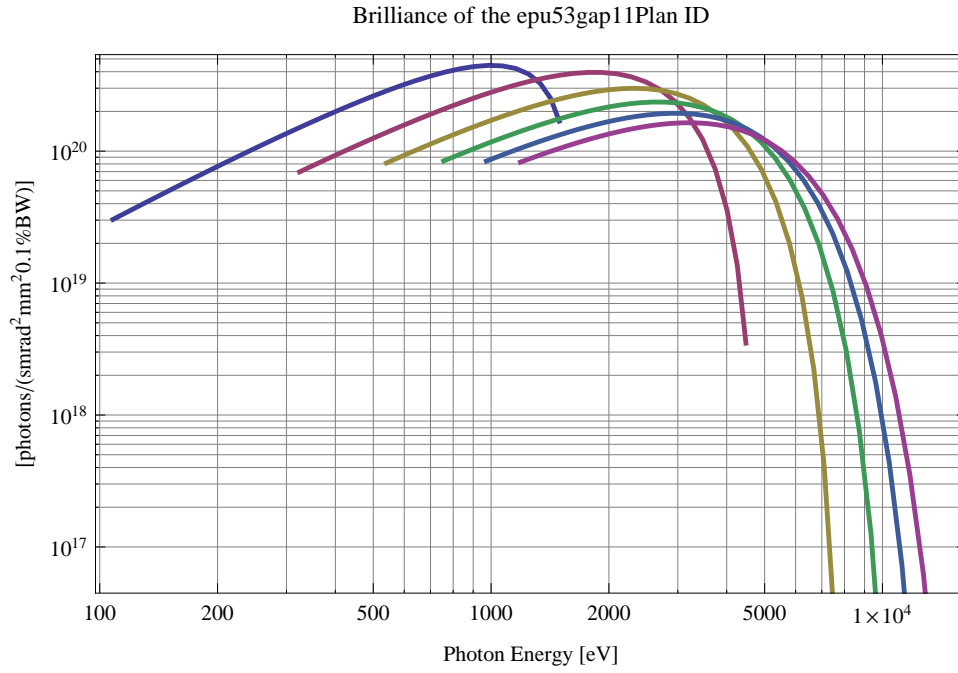


Figure 227: The brilliance at peak energy of the synchrotron radiation emitted by the epu53gap11Plan ID

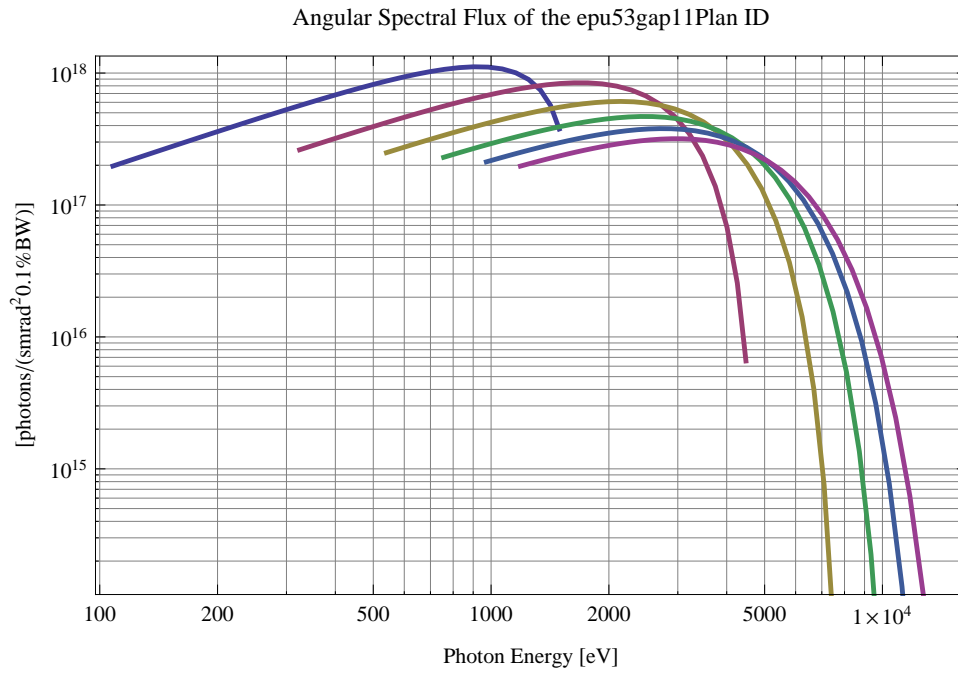


Figure 228: The angular spectral flux of the synchrotron radiation emitted by the epu53gap11Plan ID

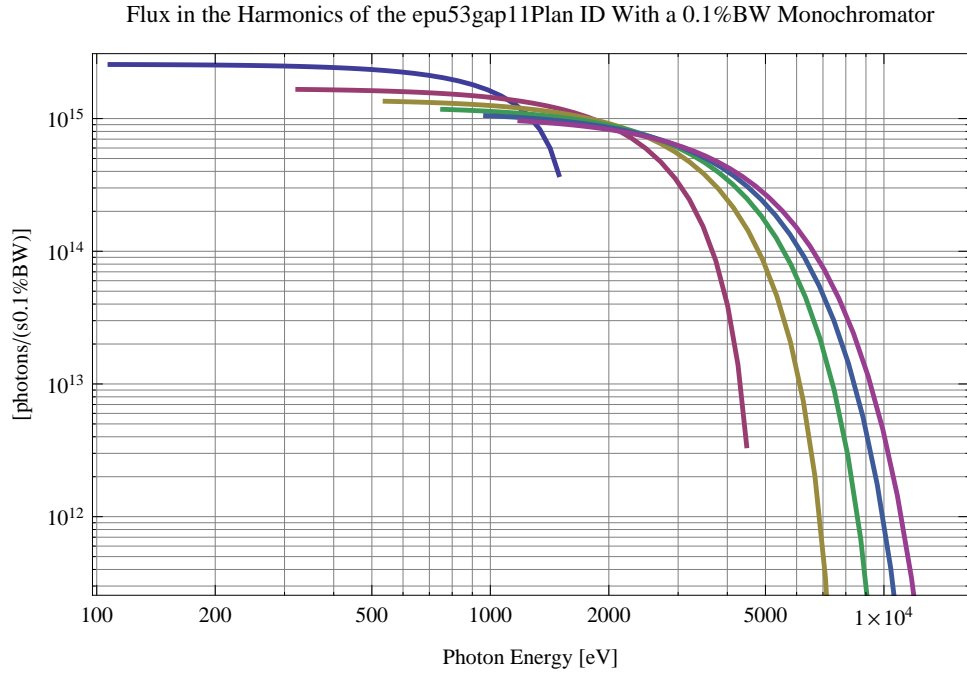


Figure 229: The flux of photons in the harmonics of the emitted synchrotron radiation from the epu53gap11Plan ID using a 0.1%BW monochromator

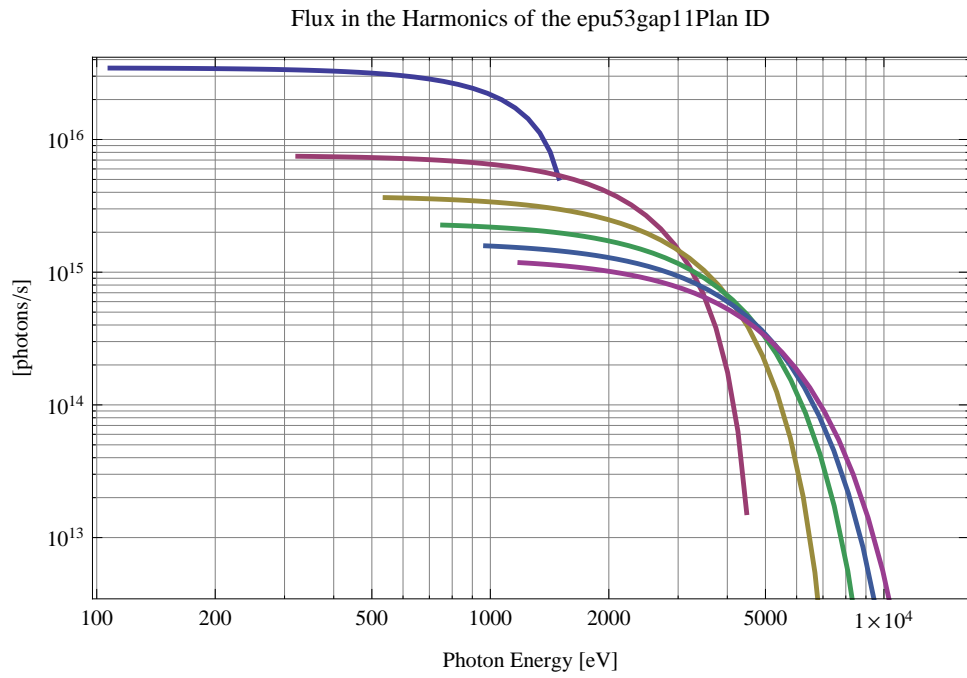


Figure 230: The flux of photons in the harmonics of the emitted synchrotron radiation from the epu53gap11Plan ID

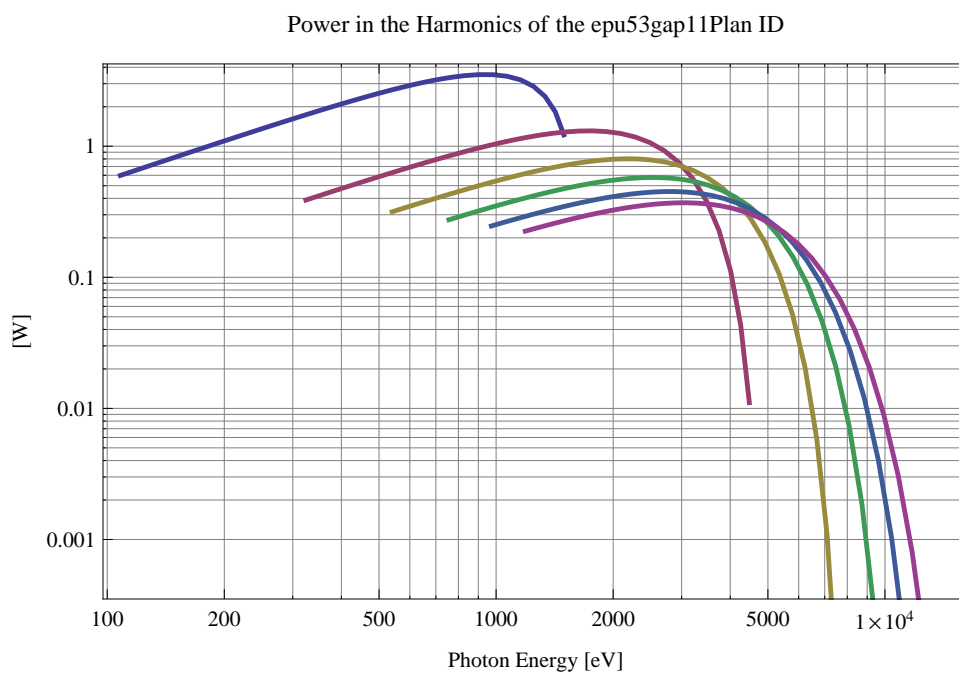


Figure 231: The power in the harmonics of the emitted synchrotron radiation from the epu53gap11Plan ID

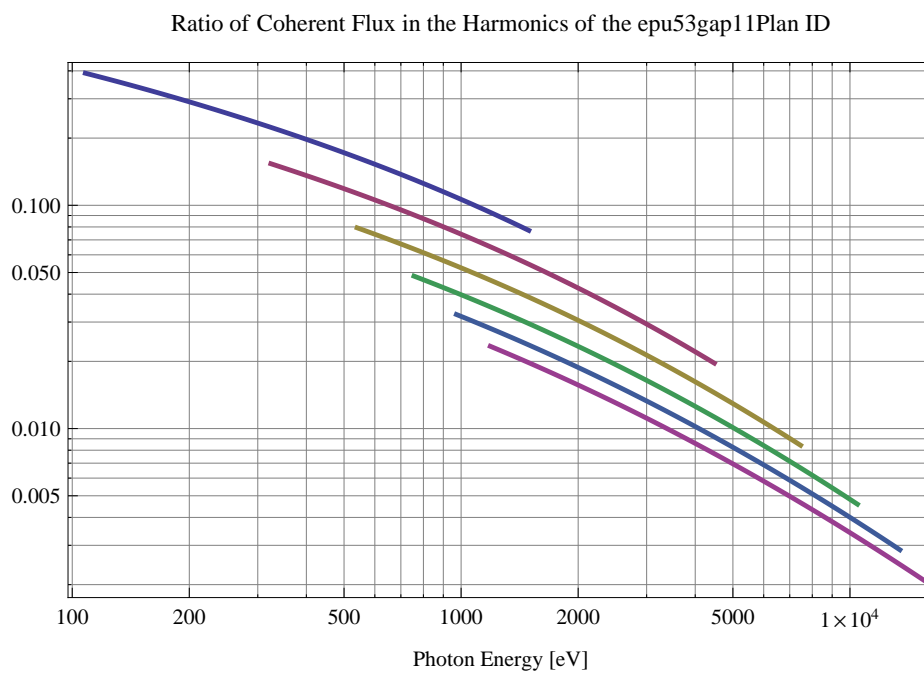


Figure 232: The ratio of coherent flux in the harmonics of the emitted synchrotron radiation from the epu53gap11Plan ID

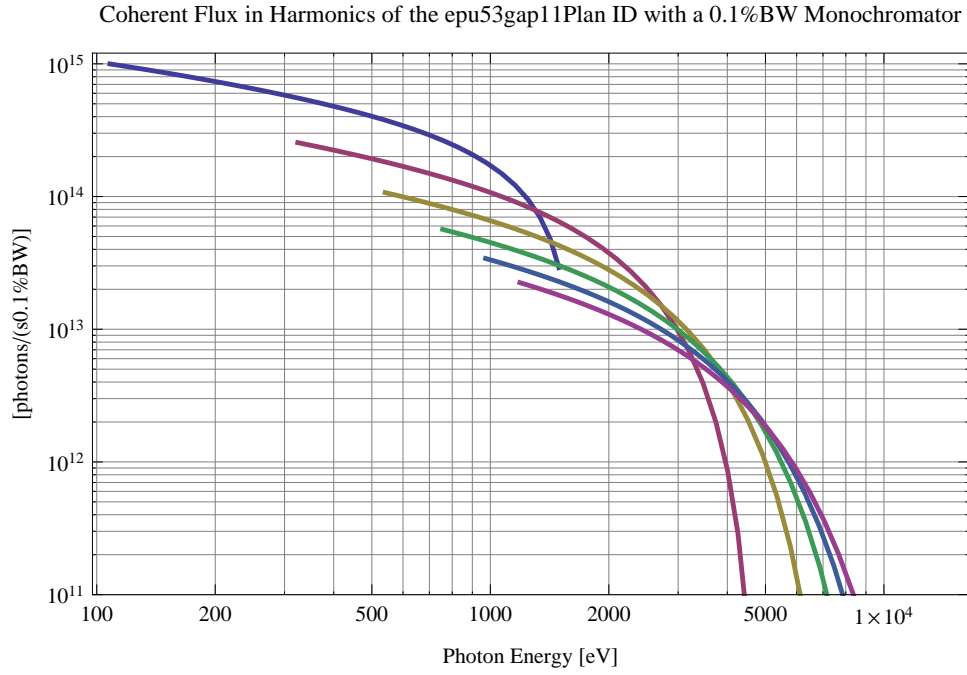


Figure 233: The coherent flux in the harmonics of the epu53gap11Plan ID using a 0.1%BW Monochromator

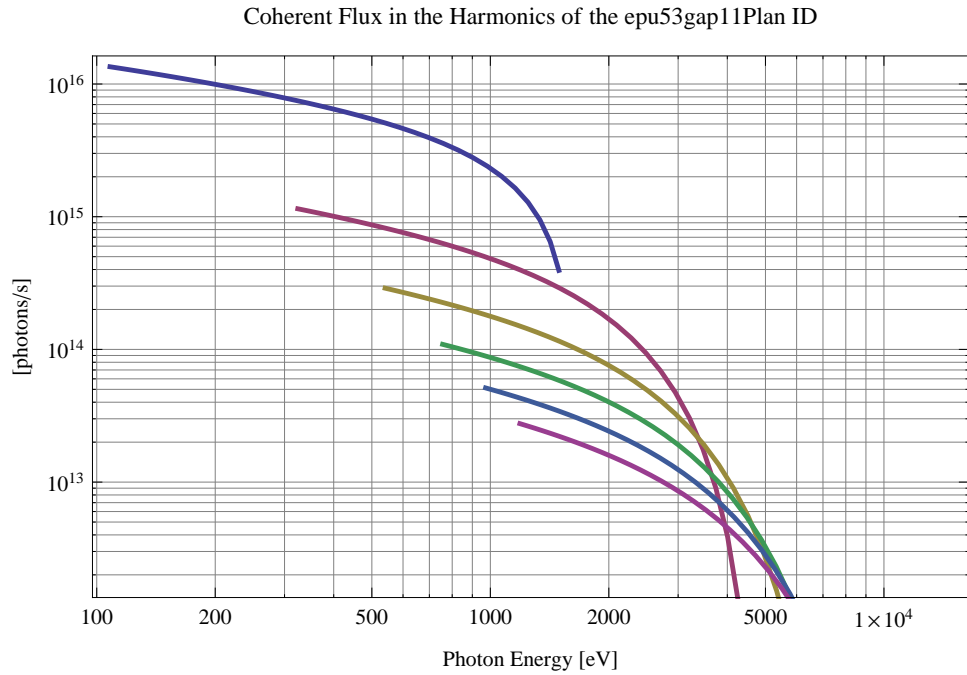


Figure 234: The coherent flux in the harmonics of the epu53gap11Plan ID

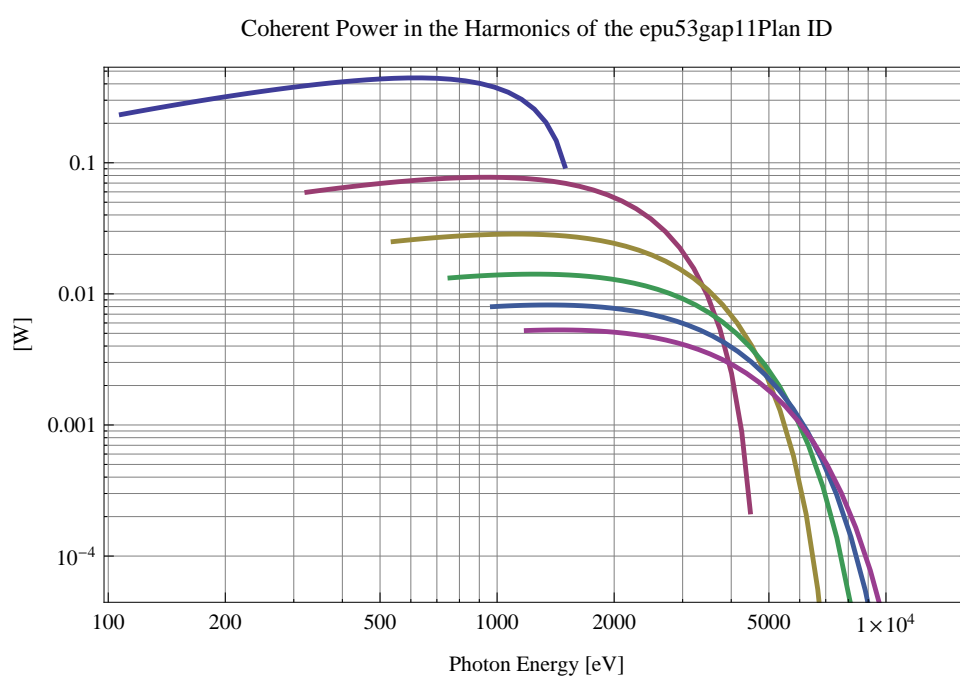


Figure 235: The power of coherent synchrotron radiation in the harmonics of the epu53gap11Plan ID

The brilliance at peak energy and the angular spectral flux density from the epu53gap11Plan ID for different harmonics at maximum K-value (5.277) are given in Table 39 and for minimum K-value (0.400) these values are given in Table 40.

Table 39: The brilliance at peak energy and the angular spectral flux density from the epu53gap11Plan ID for different harmonics at maximum K-value (5.277)

Harmonic	Photon Energy [eV]	Brilliance [Ph./ (smrad ² mrad ² 0.1% BW)]	Angular Spectral Flux [Ph./ (smrad ² 0.1% BW)]
1	108.062	3.03×10^{19}	1.97×10^{17}
3	324.185	6.97×10^{19}	2.62×10^{17}
5	540.309	8.13×10^{19}	2.49×10^{17}
7	756.433	8.42×10^{19}	2.3×10^{17}
9	972.556	8.4×10^{19}	2.12×10^{17}
11	1188.68	8.25×10^{19}	1.97×10^{17}

Table 40: The brilliance at peak energy and the angular spectral flux density from the epu53gap11Plan ID for different harmonics at minimum K-value (0.4)

Harmonic	Photon Energy [eV]	Brilliance [Ph./ (smrad ² mrad ² 0.1% BW)]	Angular Spectral Flux [Ph./ (smrad ² 0.1% BW)]
1	1493.14	1.69×10^{20}	3.77×10^{17}
3	4479.43	3.51×10^{18}	6.58×10^{15}
5	7465.72	4.11×10^{16}	7.43×10^{13}
7	10452.	4.38×10^{14}	7.82×10^{11}
9	13438.3	4.54×10^{12}	8.05×10^9
11	16424.6	4.65×10^{10}	8.23×10^7

2.4.5 Magnet model of the elliptically polarising undulator epu53gap11Heli

The Radia [3] magnet model of the epu53gap11Heli ID is shown in Figure 236. The length of the magnet model is 441.756 mm. The magnetic material in the model is NdFeb with a remanence of 1.28 T, a material similar to VACODYM 776 TP from Vacuumschmelze. Blocks with vertical magnetisation are blue and blocks with horizontal magnetisation are yellow. The block size is 30.x30.x13.25 mm³ and there is a 5. mm cut-out in two of the corners of the blocks. The total length of the epu53gap11Heli ID is 3939.76 mm.

2.4.6 Analysis of the magnetic field of the epu53gap11Heli ID

The effective magnetic fields on axis and the fundamental photon energy of the epu53gap11Heli ID are shown in Table 41. The higher harmonic contents in the magnetic field of an elliptically polarising undulator made of permanent magnets is negligible and the effective field has about the same strength as the peak field.

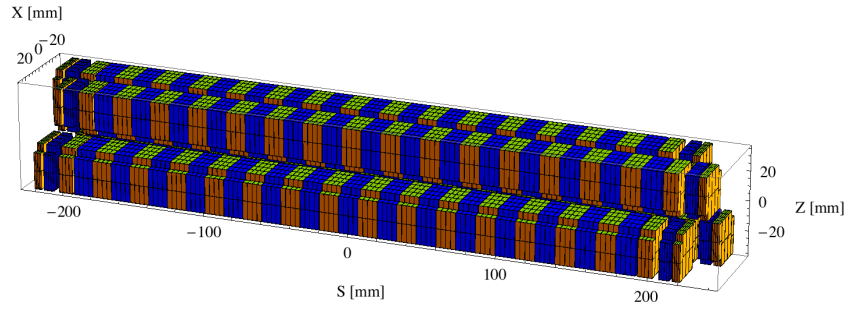


Figure 236: Magnetic model of the epu53gap11Heli ID. The ID has been modelled with Radia [3]

Table 41: Effective Fields on axis and Fundamental Photon Energy of the epu53gap11Heli ID

Undulator Period	53	mm
Undulator Gap	11	mm
Undulator Mode	Helical	
Undulator Phase	15.520	mm
Vertical Peak Field	0.641	T
Effective Vertical Field	0.642	T
Kx (from vert. field)	3.178	
Horizontal Peak Field:	0.647	T
Effective Horizontal Field	0.642	T
Kz (from hor. field)	3.178	
Photon Energy, Harm.1	0.145	keV
Emitted Power	9.246	kW
Total Length	3939.8	mm

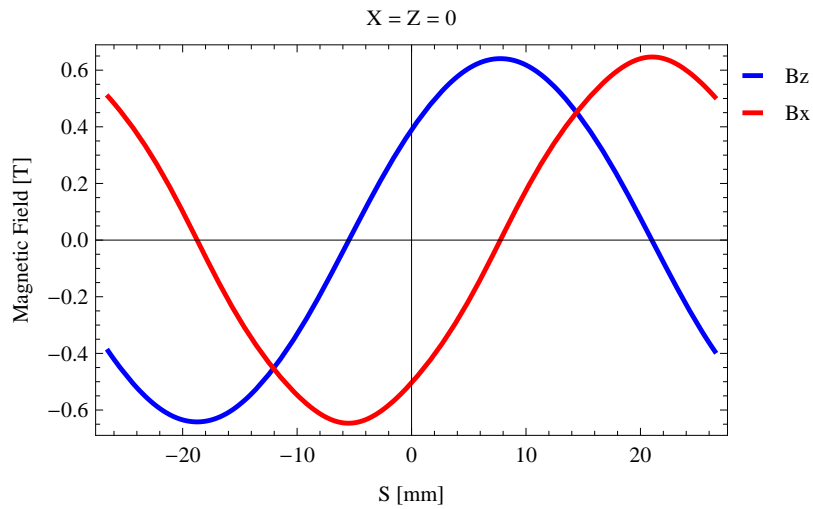


Figure 237: Vertical magnetic field in a central pole of the epu53gap11Heli ID along the ID axis, $X = Z = 0$

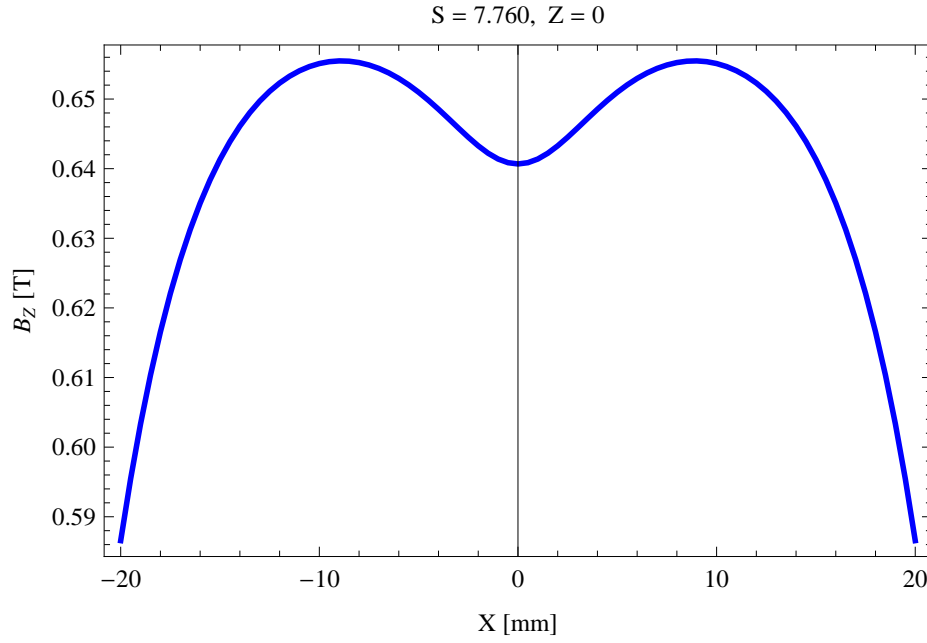


Figure 238: Vertical magnetic field in a central pole of the epu53gap11Heli ID along the horizontally transverse direction to the ID axis, $S = 7.760, Z = 0$

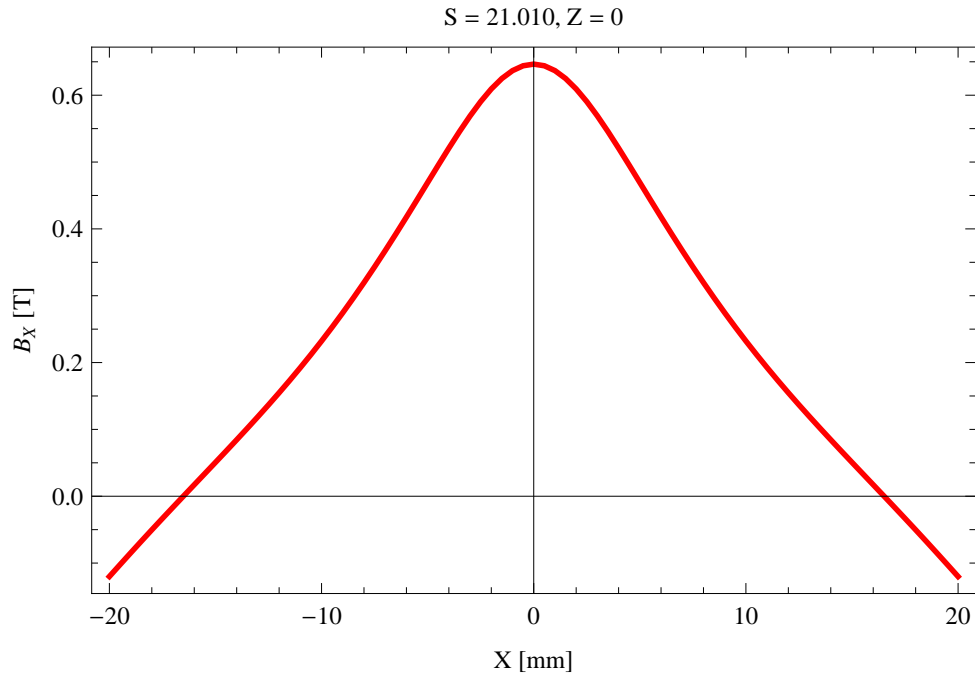


Figure 239: Horizontal magnetic field in a central pole of the epu53gap11Heli ID along the horizontally transverse direction to the ID axis, $S = 21.010, Z = 0$

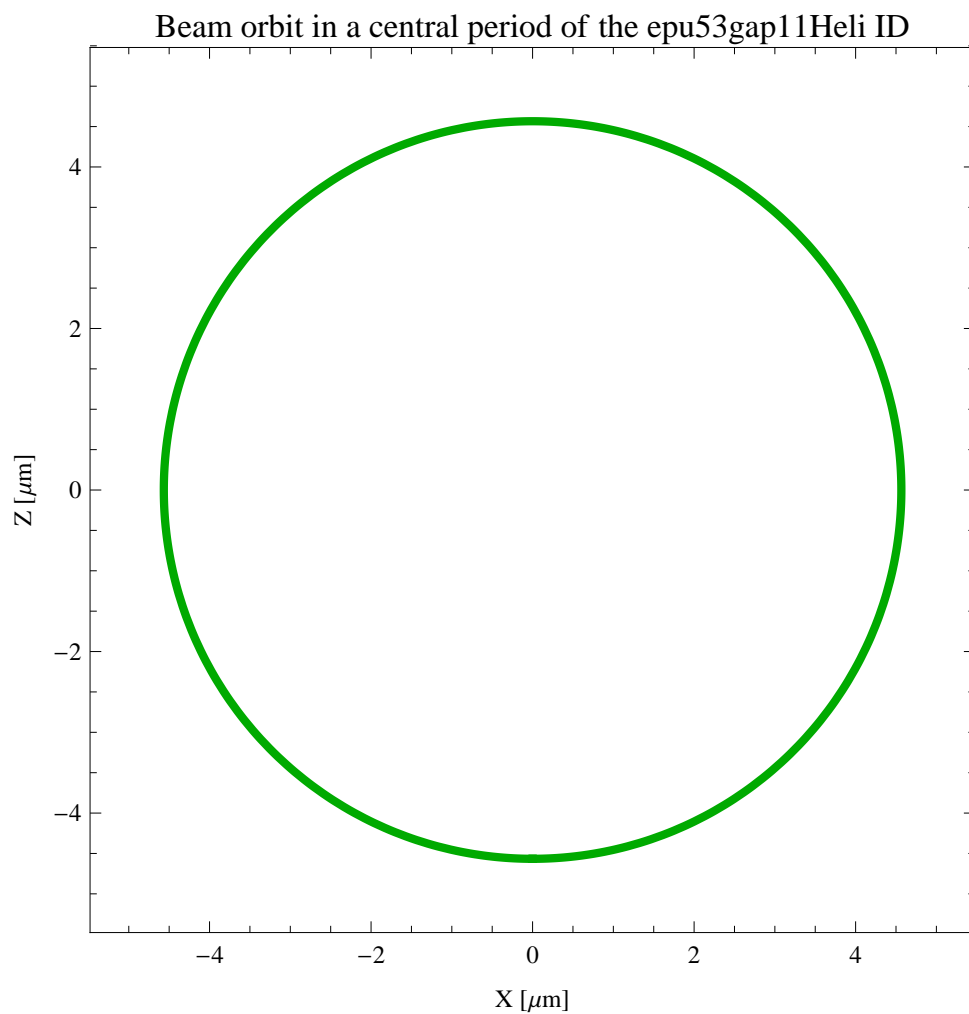


Figure 240: The beam orbit of the electron beam through a central period of the epu53gap11Heli ID

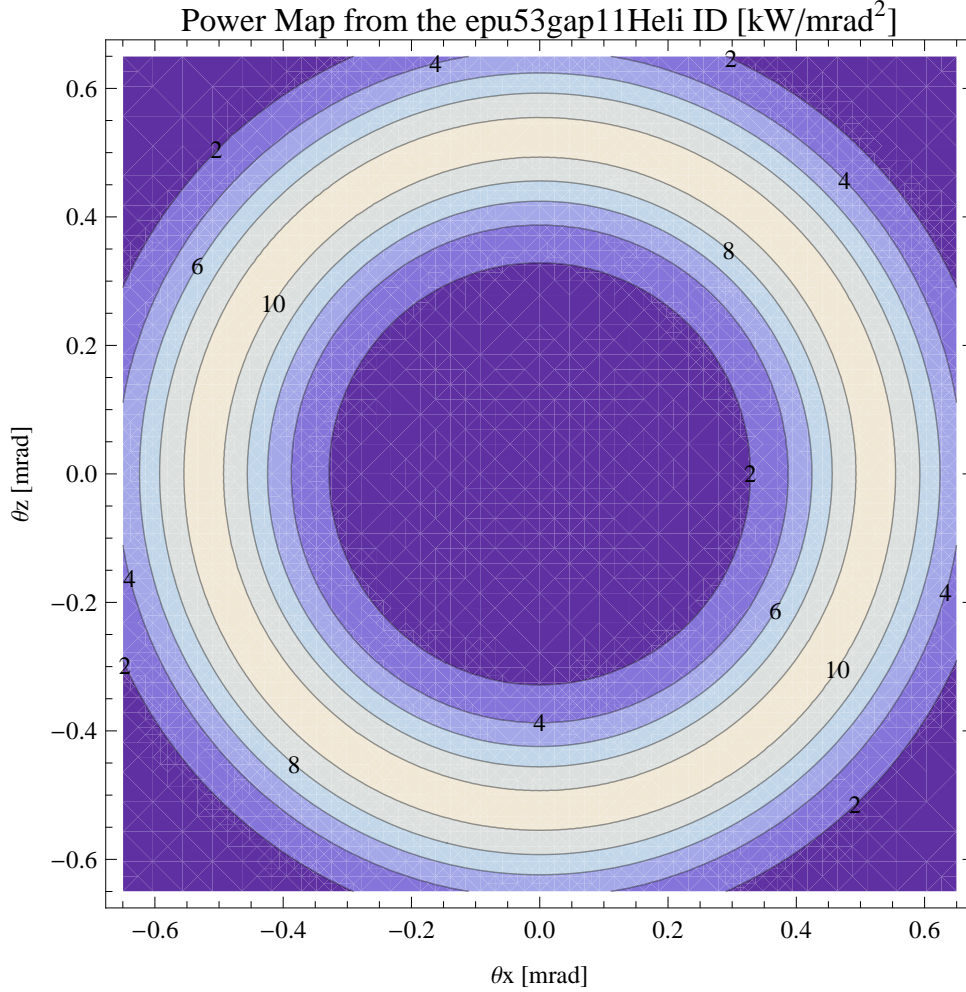


Figure 241: Map of the power distribution of the emitted synchrotron radiation by the epu53gap11Heli ID

2.4.7 Synchrotron radiation from the epu53gap11Heli ID

The power map of the emitted synchrotron radiation by the epu53gap11Heli ID, assuming a 0.5 A filament beam with an energy of 3 GeV and undulator properties of the synchrotron radiation, is shown in Figure 241. The on-axis power density is 0.219 kW/mrad²

A map of the degree of linear polarisation of the fundamental harmonic of the synchrotron radiation emitted by the epu53gap11Heli ID over the angle of observation is shown in Figure 242.

A map of the degree of 45 degree polarisation of the fundamental harmonic of the synchrotron radiation emitted by the epu53gap11Heli ID over the angle of observation is shown in Figure 243.

A map of the degree of circular polarisation of the fundamental harmonic of the synchrotron radiation emitted by the epu53gap11Heli ID over the angle of observation is shown in Figure 244.

The on axis brilliance at peak energy and the angular spectral flux from the epu53gap11Heli ID have been calculated with the given beam parameters, which are 0.5 A of stored current, $\beta_H = 9$ m, $\varepsilon_H = 0.263$ nmrad, $\beta_V = 4.8$ m, $\varepsilon_V = 8$. pmrad, and an energy spread of 0.001.

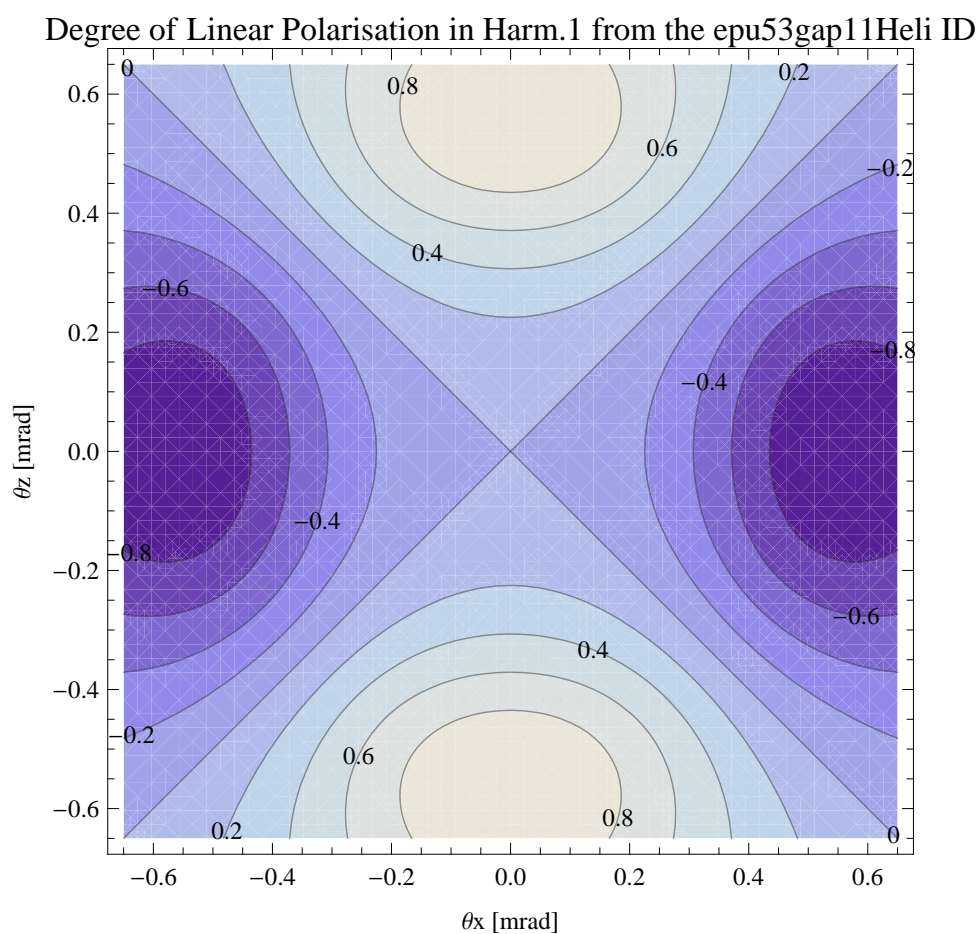


Figure 242: Map of linear polarisation in the fundamental harmonic of the synchrotron radiation emitted by the epu53gap11Heli ID

Degree of 45 degree Polarisation in Harm.1 from the epu53gap11Heli ID

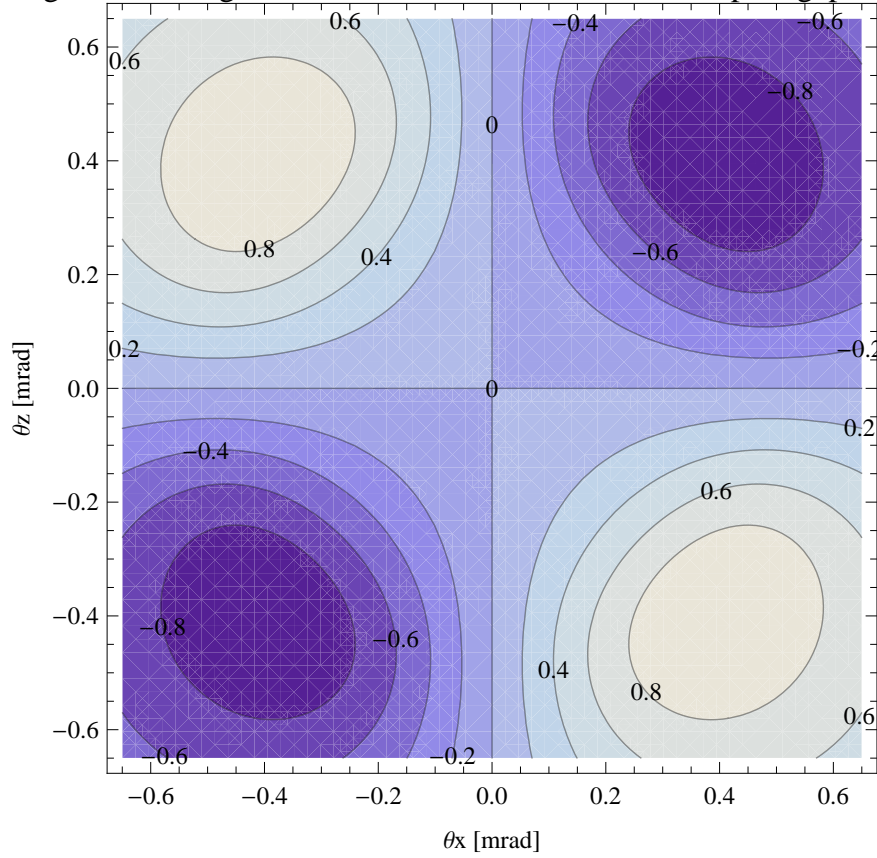


Figure 243: Map of 45 degree polarisation in the fundamental harmonic of the synchrotron radiation emitted by the epu53gap11Heli ID

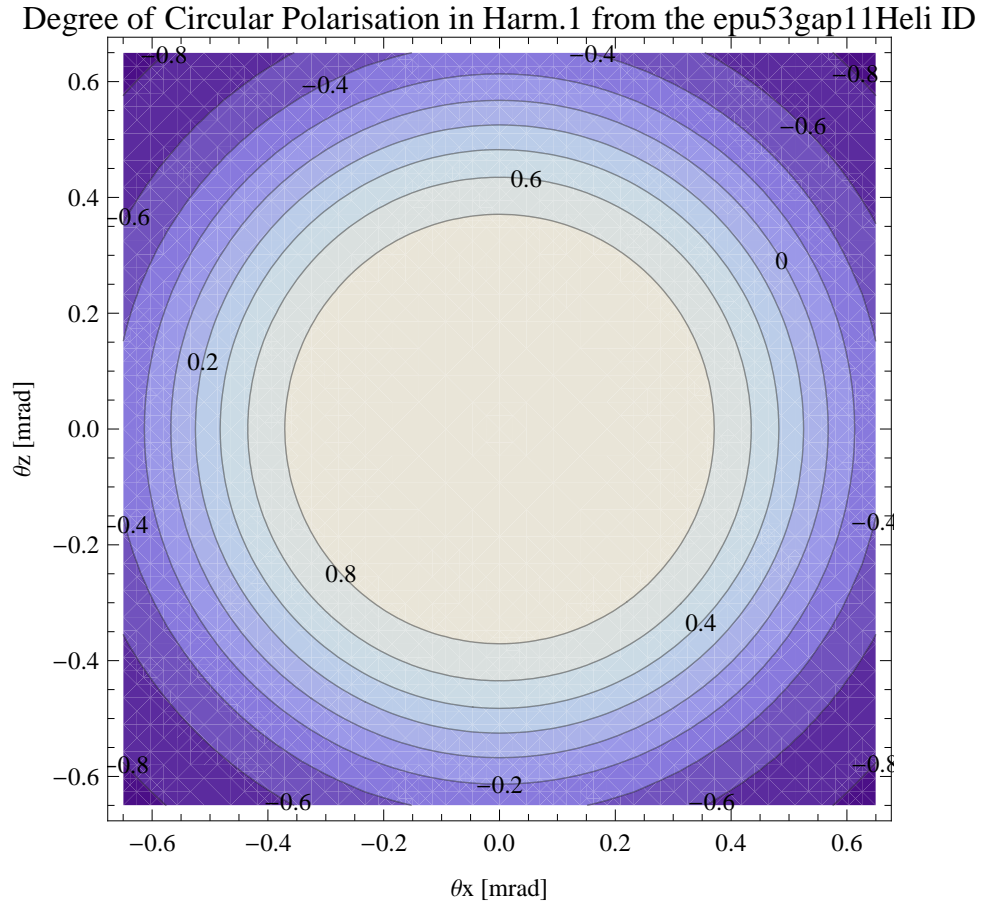


Figure 244: Map of circular polarisation in the fundamental harmonic of the synchrotron radiation emitted by the epu53gap11Heli ID

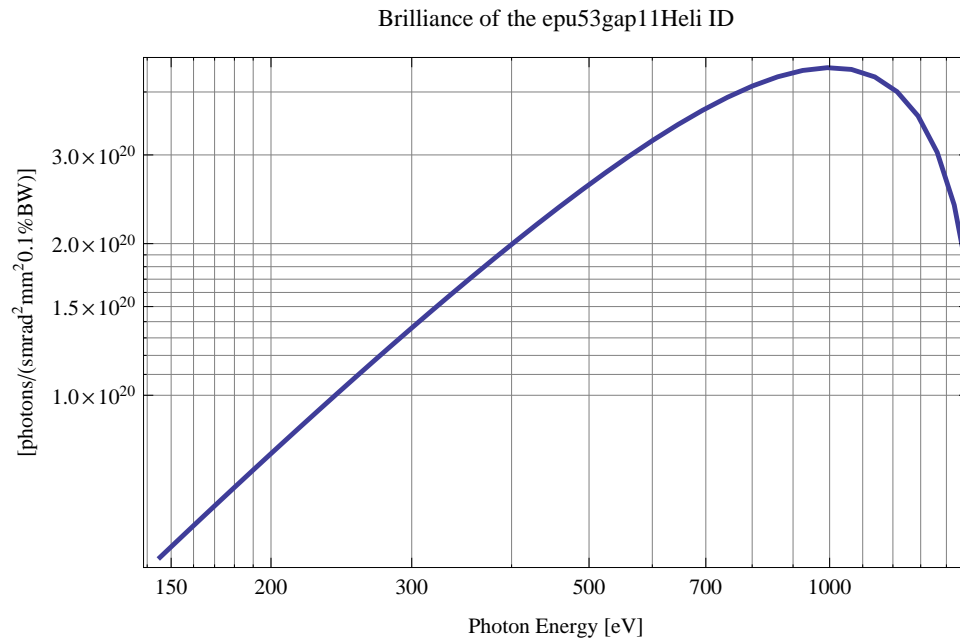


Figure 245: The brilliance at peak energy of the synchrotron radiation emitted by the epu53gap11Heli ID

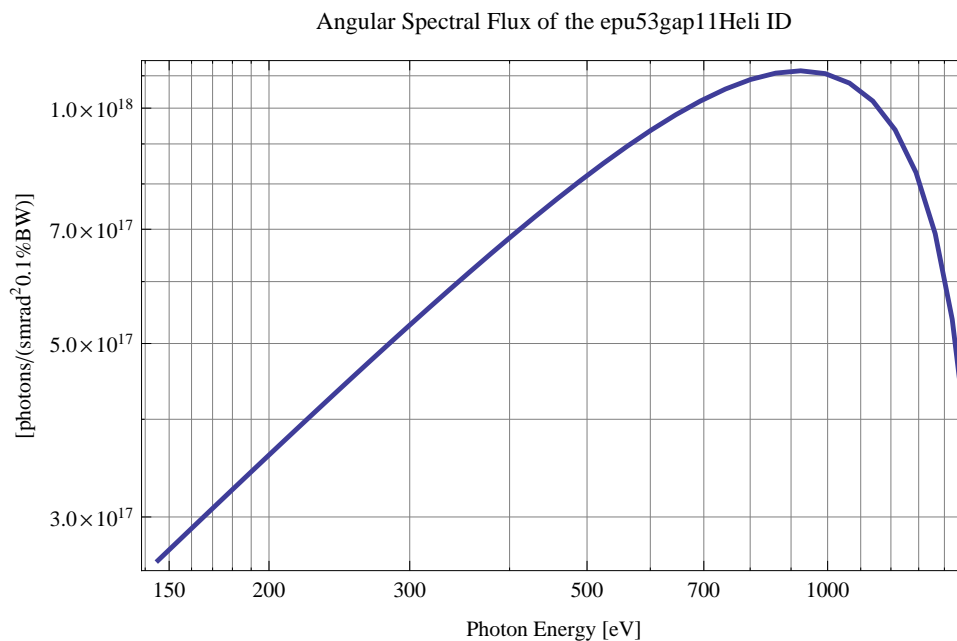


Figure 246: The angular spectral flux of the synchrotron radiation emitted by the epu53gap11Heli ID

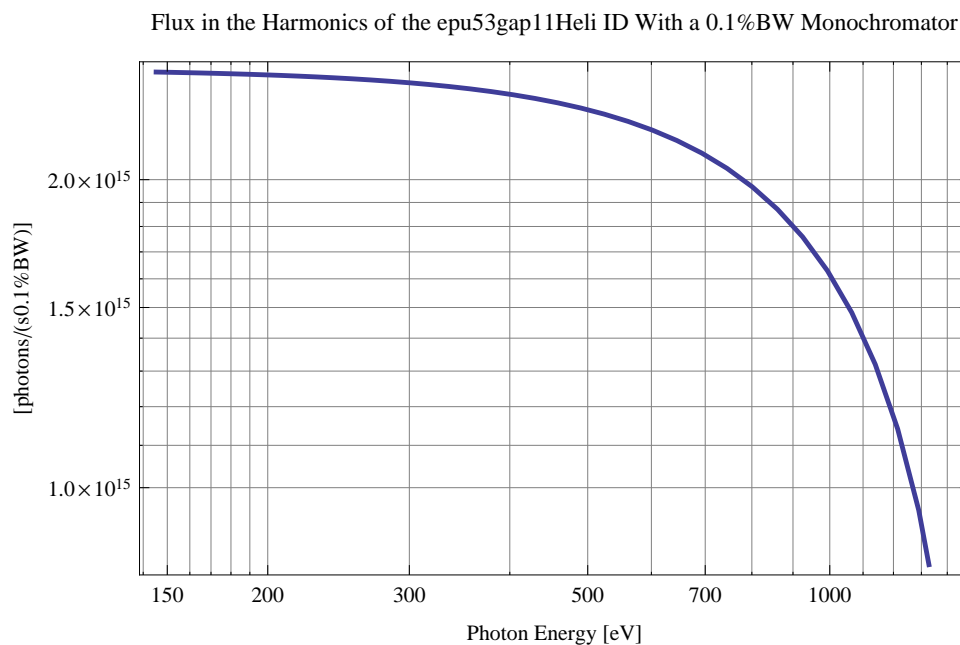


Figure 247: The flux of photons in the harmonics of the emitted synchrotron radiation from the epu53gap11Heli ID using a 0.1%BW monochromator

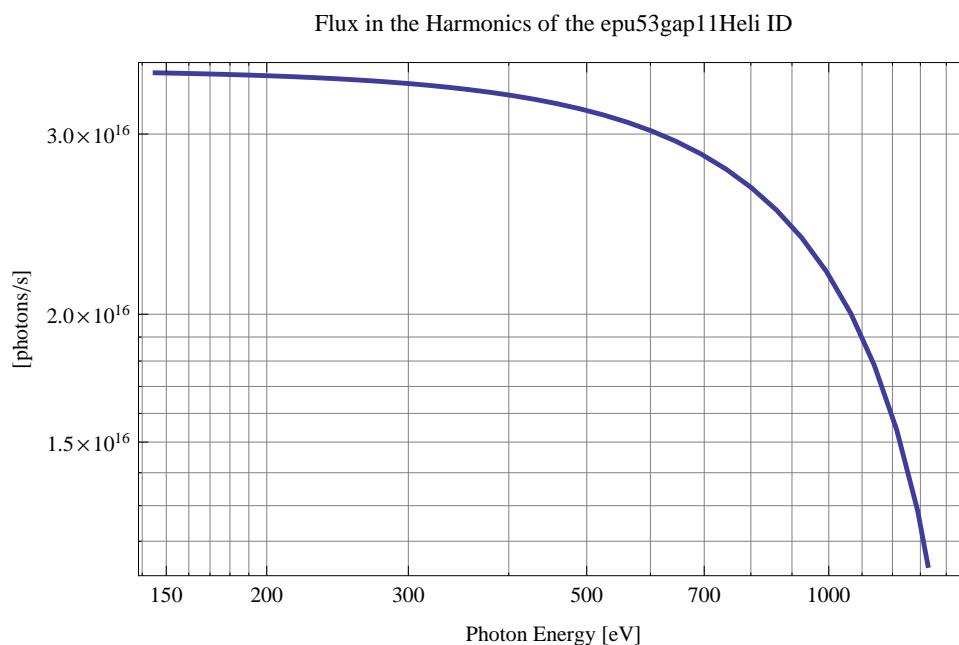


Figure 248: The flux of photons in the harmonics of the emitted synchrotron radiation from the epu53gap11Heli ID

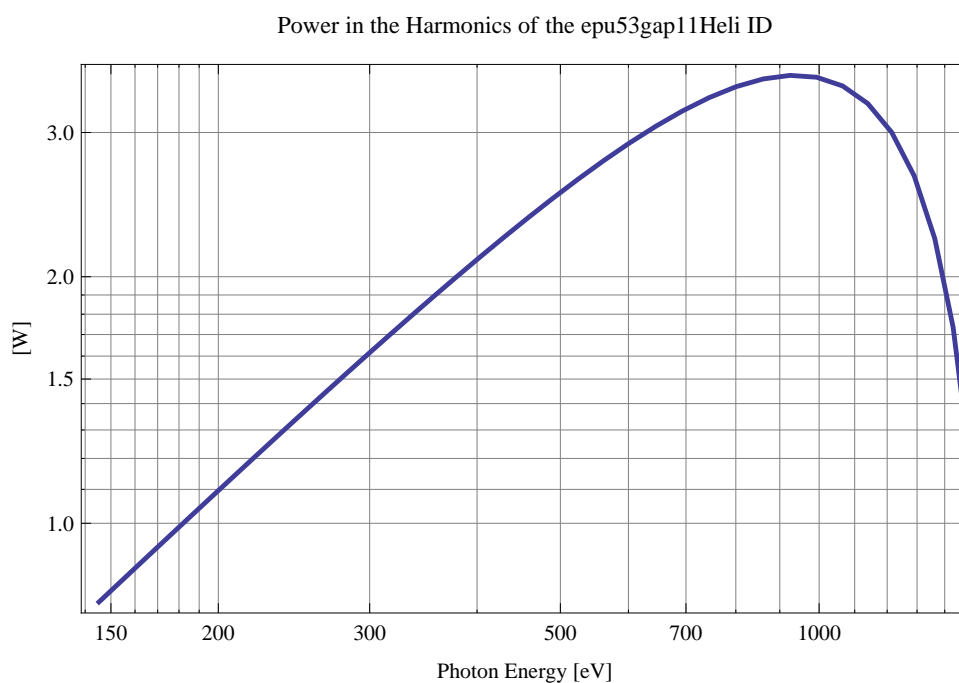


Figure 249: The power in the harmonics of the emitted synchrotron radiation from the epu53gap11Heli ID

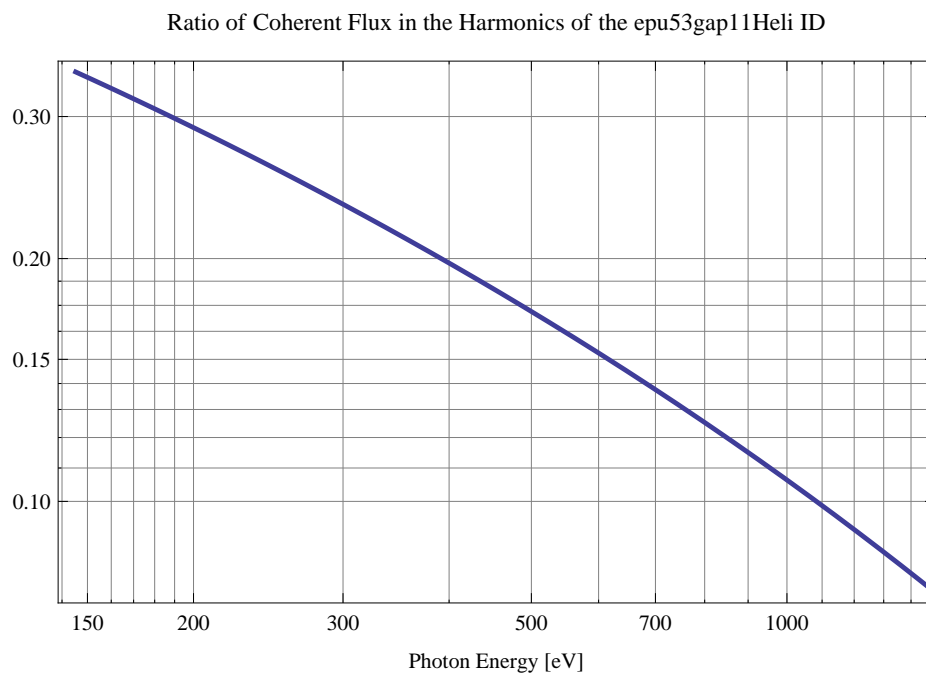


Figure 250: The ratio of coherent flux in the harmonics of the emitted synchrotron radiation from the epu53gap11Heli ID

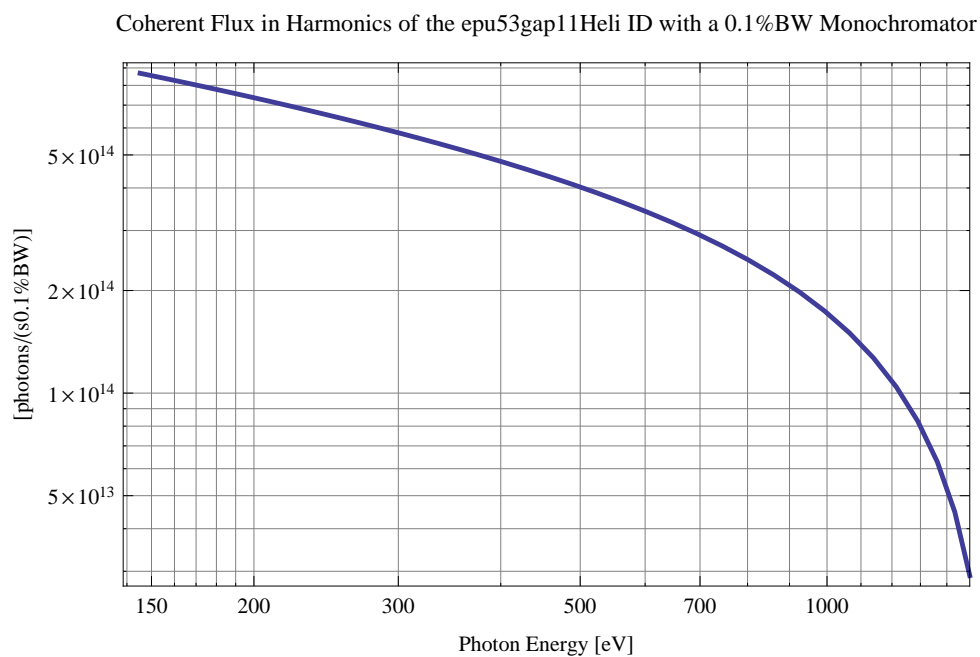


Figure 251: The coherent flux in the harmonics of the epu53gap11Heli ID using a 0.1%BW Monochromator

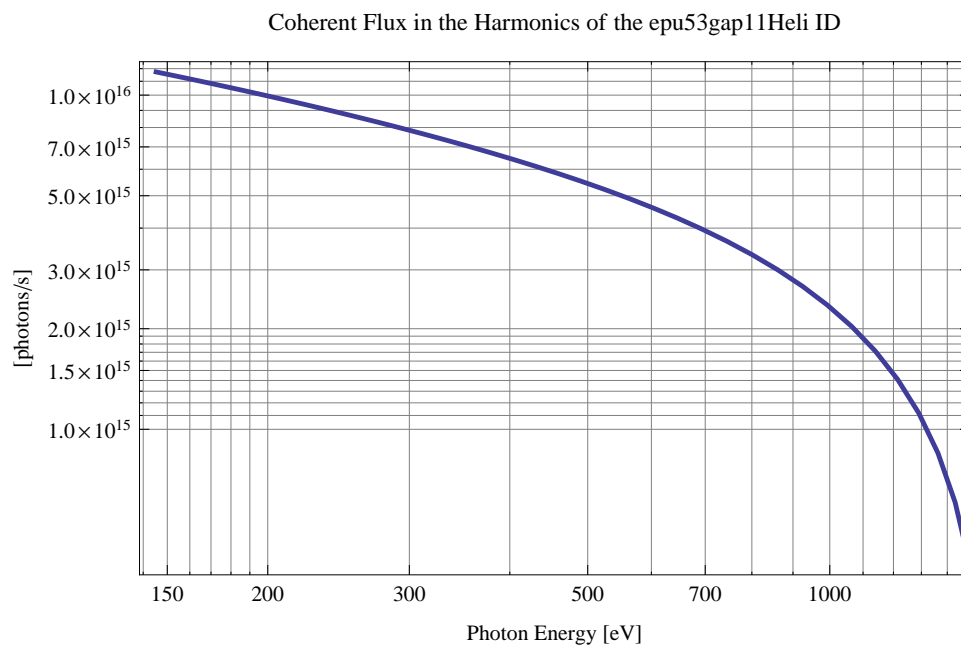


Figure 252: The coherent flux in the harmonics of the epu53gap11Heli ID

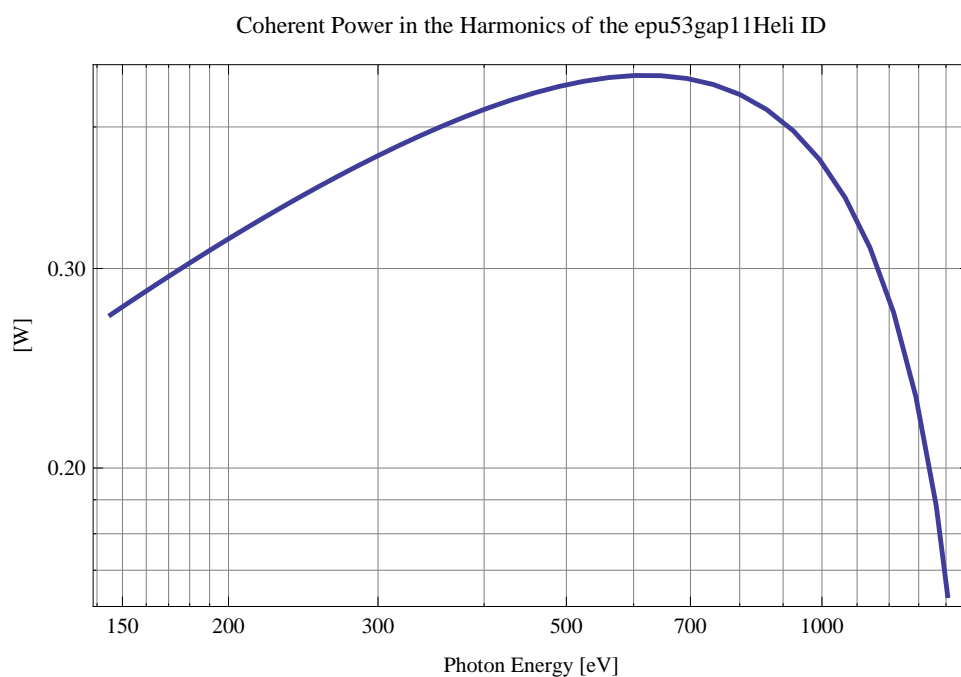


Figure 253: The power of coherent synchrotron radiation in the harmonics of the epu53gap11Heli ID

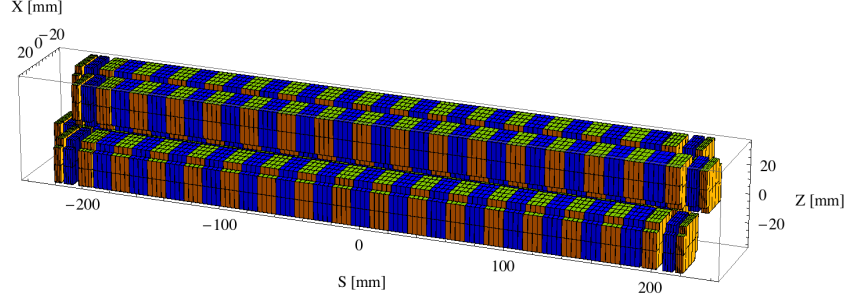


Figure 254: Magnetic model of the epu53gap11Incl ID. The ID has been modelled with Radia [3]

The brilliance at peak energy and the angular spectral flux density from the epu53gap11Heli ID for different harmonics at maximum K-value (4.494) are given in Table 42 and for minimum K-value (0.400) these values are given in Table 43.

Table 42: The brilliance at peak energy and the angular spectral flux density from the epu53gap11Heli ID for different harmonics at maximum K-value (4.494)

Harmonic	Photon Energy [eV]	Brilliance [Ph./((smrad ² mrad ² 0.1%BW))]	Angular Spectral Flux [Ph./((smrad ² 0.1%BW))]
1	145.281	4.77×10^{19}	2.64×10^{17}

Table 43: The brilliance at peak energy and the angular spectral flux density from the epu53gap11Heli ID for different harmonics at minimum K-value (0.4)

Harmonic	Photon Energy [eV]	Brilliance [Ph./((smrad ² mrad ² 0.1%BW))]	Angular Spectral Flux [Ph./((smrad ² 0.1%BW))]
1	1493.14	1.69×10^{20}	3.77×10^{17}

2.4.8 Magnet model of the elliptically polarising undulator epu53gap11Incl

The Radia [3] magnet model of the epu53gap11Incl ID is shown in Figure 254. The length of the magnet model is 441.756 mm. The magnetic material in the model is NdFeb with a remanence of 1.28 T, a material similar to VACODYM 776 TP from Vacuumschmelze. Blocks with vertical magnetisation are blue and blocks with horizontal magnetisation are yellow. The block size is 30.x30.x13.25 mm³ and there is a 5. mm cut-out in two of the corners of the blocks. The total length of the epu53gap11Incl ID is 3939.76 mm.

2.4.9 Analysis of the magnetic field of the epu53gap11Incl ID

The effective magnetic fields on axis and the fundamental photon energy of the epu53gap11Incl ID are shown in Table 44. The higher harmonic contents in the magnetic field of an elliptically

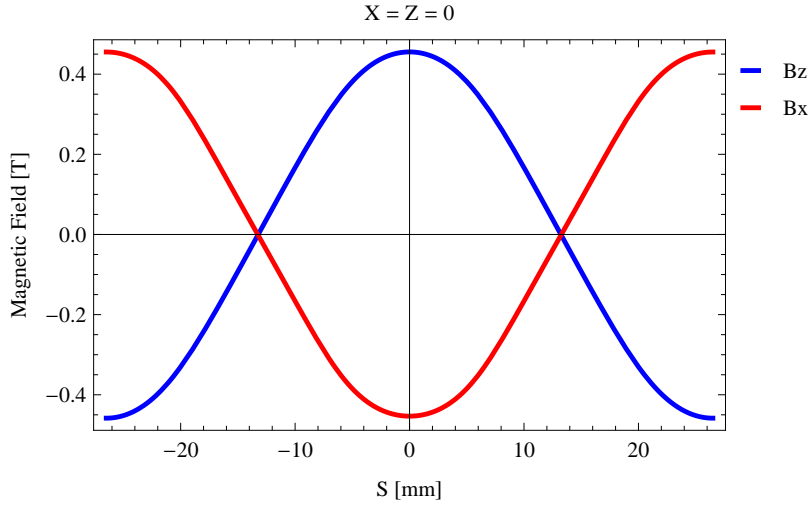


Figure 255: Vertical magnetic field in a central pole of the epu53gap11Incl ID along the ID axis, $X = Z = 0$

polarising undulator made of permanent magnets is negligible and the effective field has about the same strength as the peak field.

Table 44: Effective Fields on axis and Fundamental Photon Energy of the epu53gap11Incl ID

Undulator Period	53	mm
Undulator Gap	11	mm
Undulator Mode	Inclined	
Undulator Phase	14.396	mm
Vertical Peak Field	0.455	T
Effective Vertical Field	0.458	T
Kx (from vert. field)	2.267	
Horizontal Peak Field:	-0.453	T
Effective Horizontal Field	0.458	T
Kz (from hor. field)	2.267	
Photon Energy, Harm.1	0.263	keV
Emitted Power	4.706	kW
Total Length	3939.8	mm

2.4.10 Synchrotron radiation from the epu53gap11Incl ID

The power map of the emitted synchrotron radiation by the epu53gap11Incl ID, assuming a 0.5 A filament beam with an energy of 3 GeV and undulator properties of the synchrotron radiation, is shown in Figure 259. The on-axis power density is 20.610 kW/mrad²

A map of the degree of linear polarisation of the fundamental harmonic of the synchrotron radiation emitted by the epu53gap11Incl ID over the angle of observation is shown in Figure 260.

A map of the degree of 45 degree polarisation of the fundamental harmonic of the synchrotron radiation emitted by the epu53gap11Incl ID over the angle of observation is shown in Figure 261.

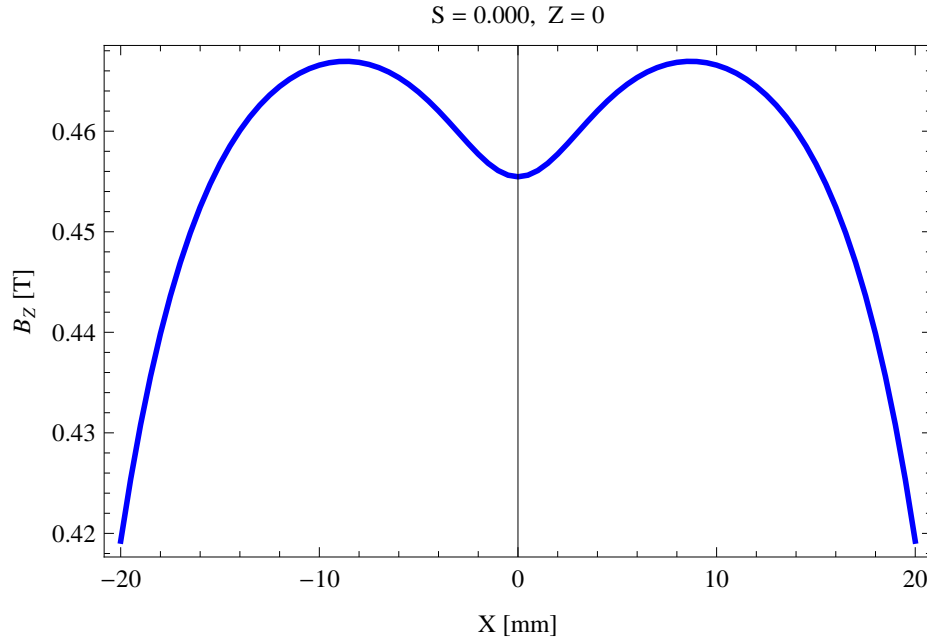


Figure 256: Vertical magnetic field in a central pole of the epu53gap11Incl ID along the horizontally transverse direction to the ID axis, $S = 0.000, Z = 0$

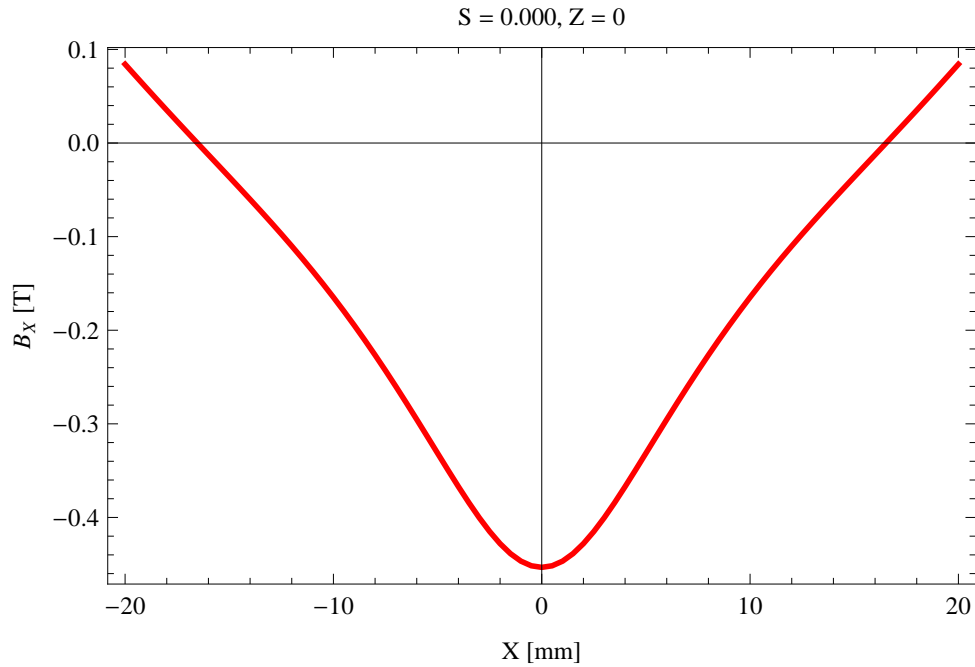


Figure 257: Horizontal magnetic field in a central pole of the epu53gap11Incl ID along the horizontally transverse direction to the ID axis, $S = 0.000, Z = 0$

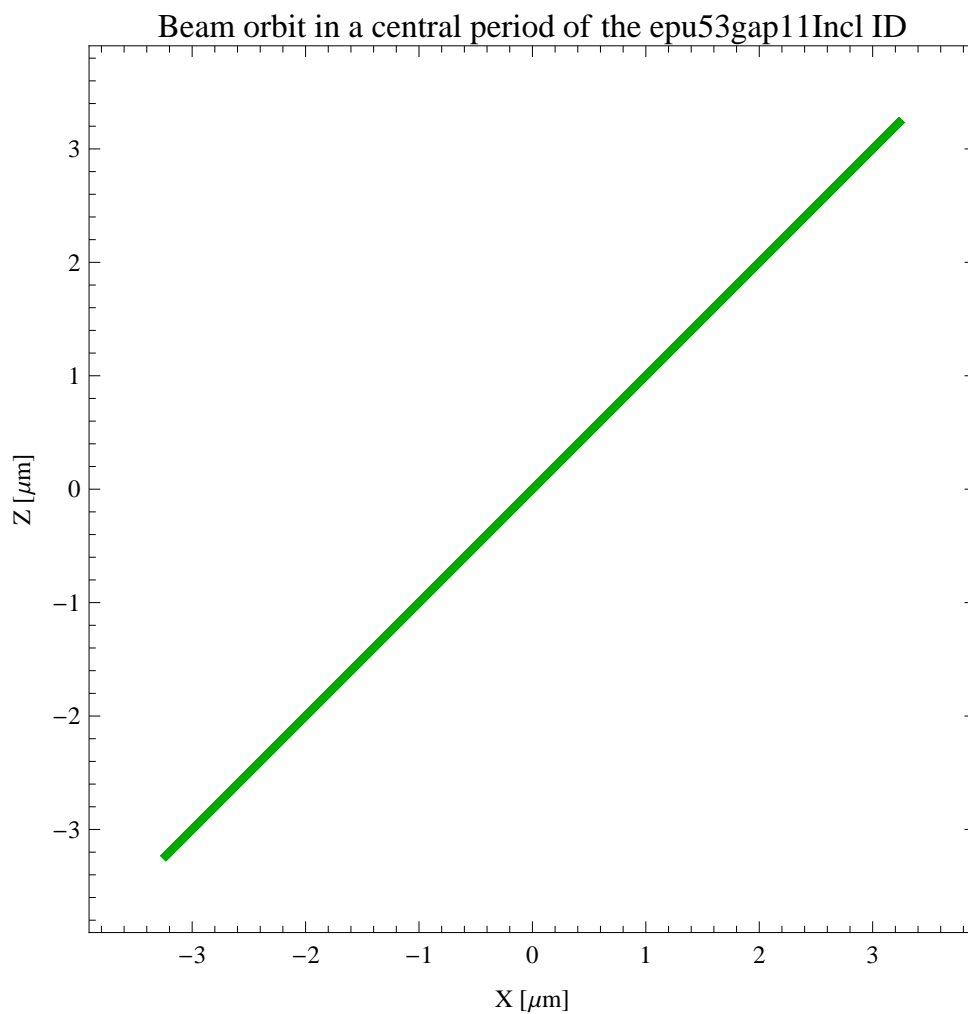


Figure 258: The beam orbit of the electron beam through a central period of the epu53gap11Incl ID

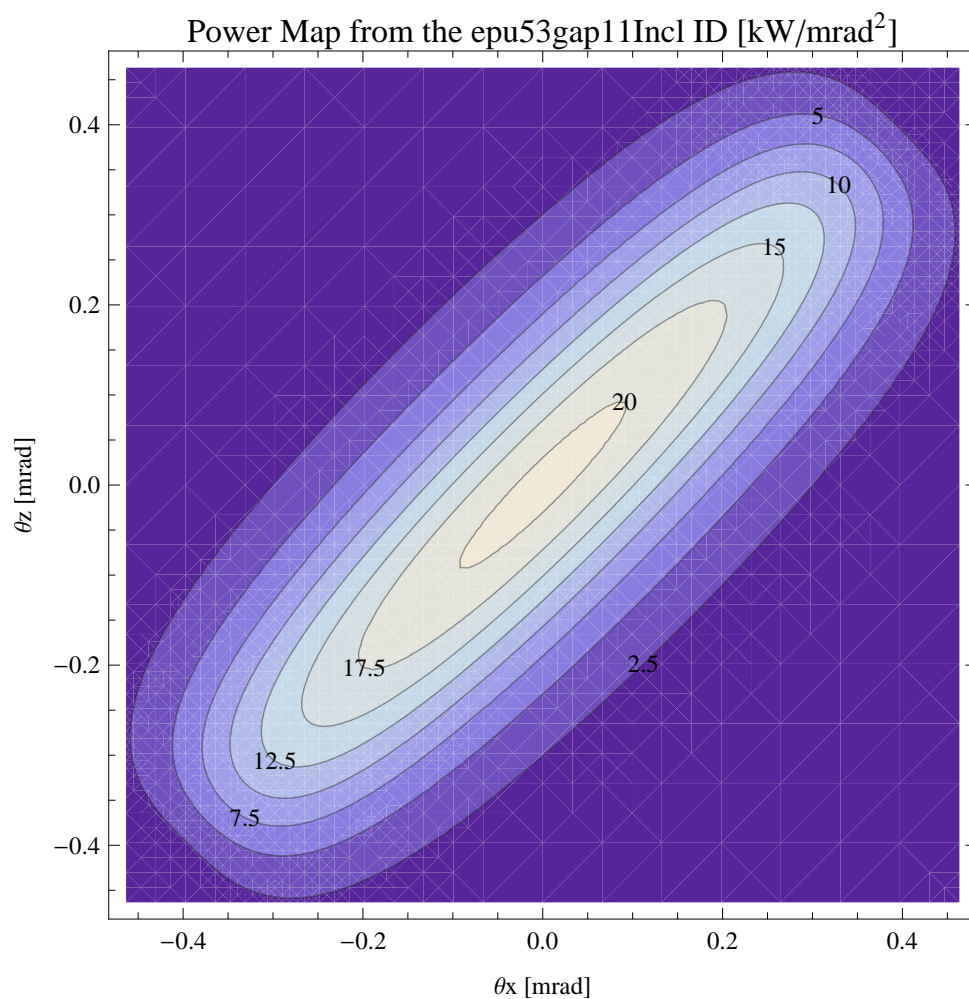


Figure 259: Map of the power distribution of the emitted synchrotron radiation by the epu53gap11Incl ID

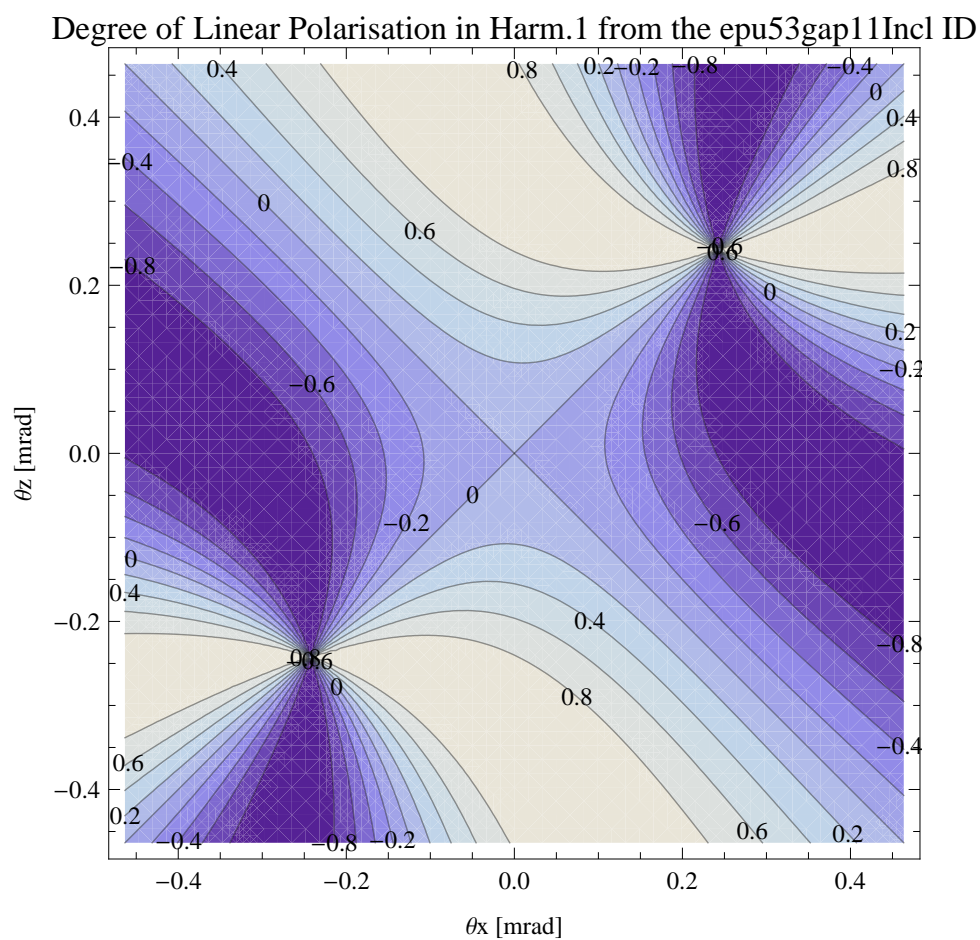


Figure 260: Map of linear polarisation in the fundamental harmonic of the synchrotron radiation emitted by the epu53gap11Incl ID

Degree of 45 degree Polarisation in Harm.1 from the epu53gap11Incl ID

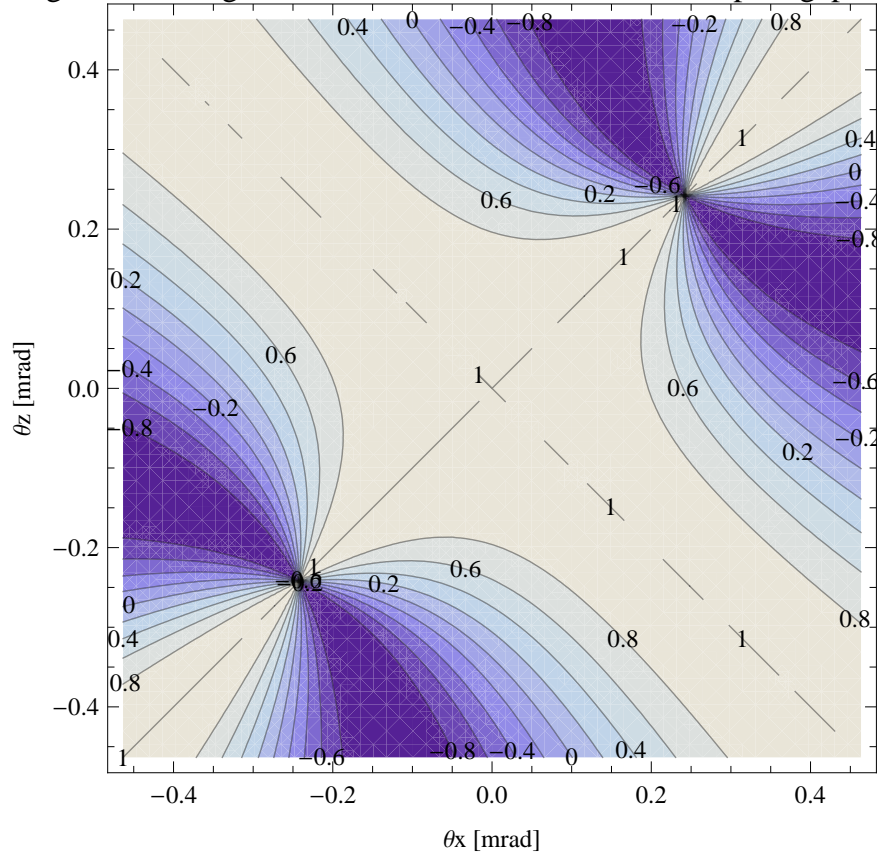


Figure 261: Map of 45 degree polarisation in the fundamental harmonic of the synchrotron radiation emitted by the epu53gap11Incl ID

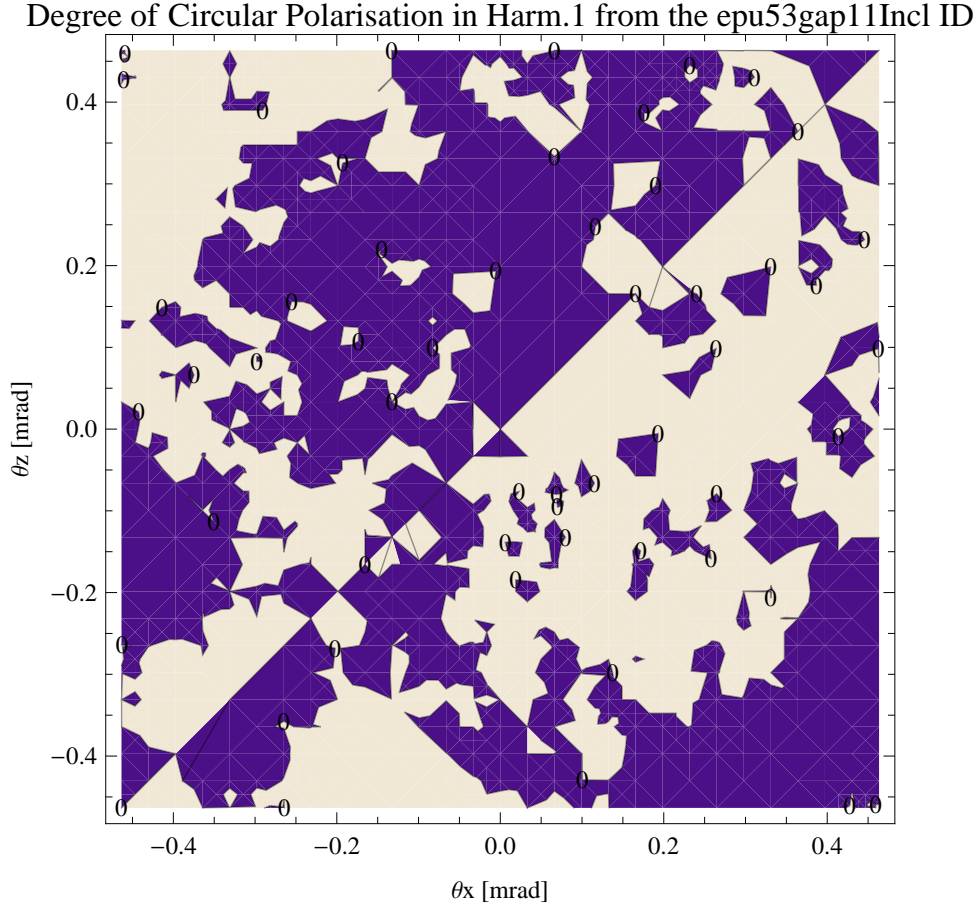


Figure 262: Map of circular polarisation in the fundamental harmonic of the synchrotron radiation emitted by the epu53gap11Incl ID

A map of the degree of circular polarisation of the fundamental harmonic of the synchrotron radiation emitted by the epu53gap11Incl ID over the angle of observation is shown in Figure 262.

The on axis brilliance at peak energy and the angular spectral flux from the epu53gap11Incl ID have been calculated with the given beam parameters, which are 0.5 A of stored current, $\beta_H = 9$ m, $\varepsilon_H = 0.263$ nmrad, $\beta_V = 4.8$ m, $\varepsilon_V = 8$. pmrad, and an energy spread of 0.001.

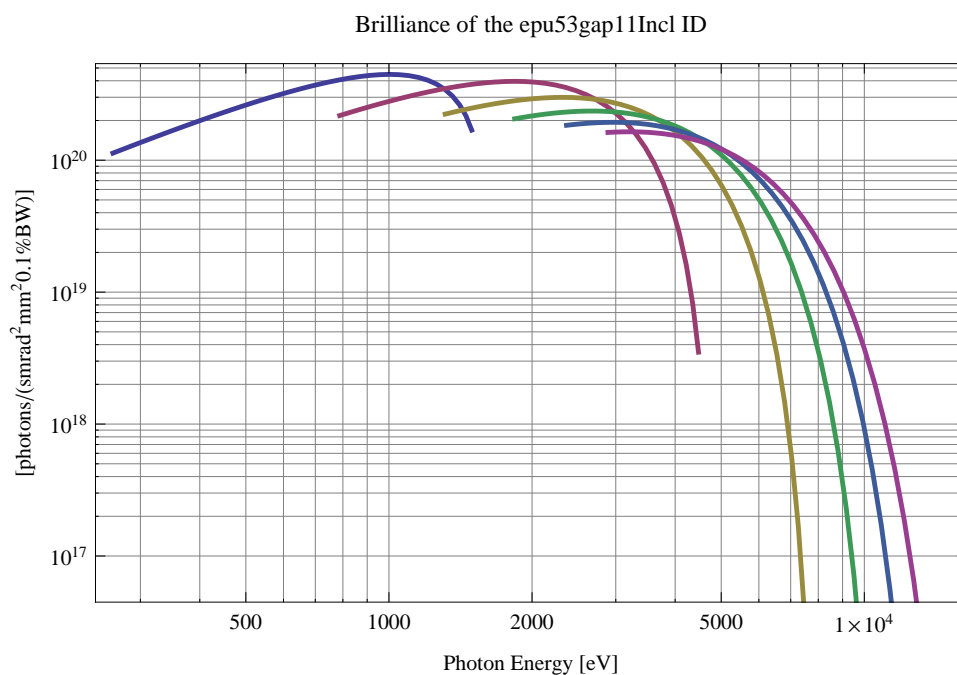


Figure 263: The brilliance at peak energy of the synchrotron radiation emitted by the epu53gap11Incl ID

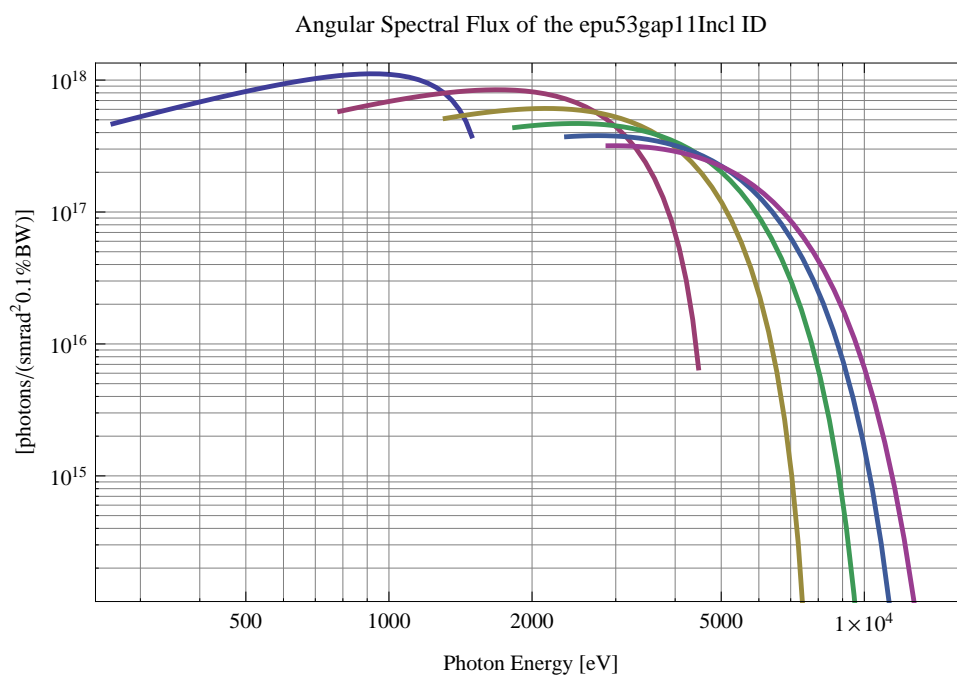


Figure 264: The angular spectral flux of the synchrotron radiation emitted by the epu53gap11Incl ID

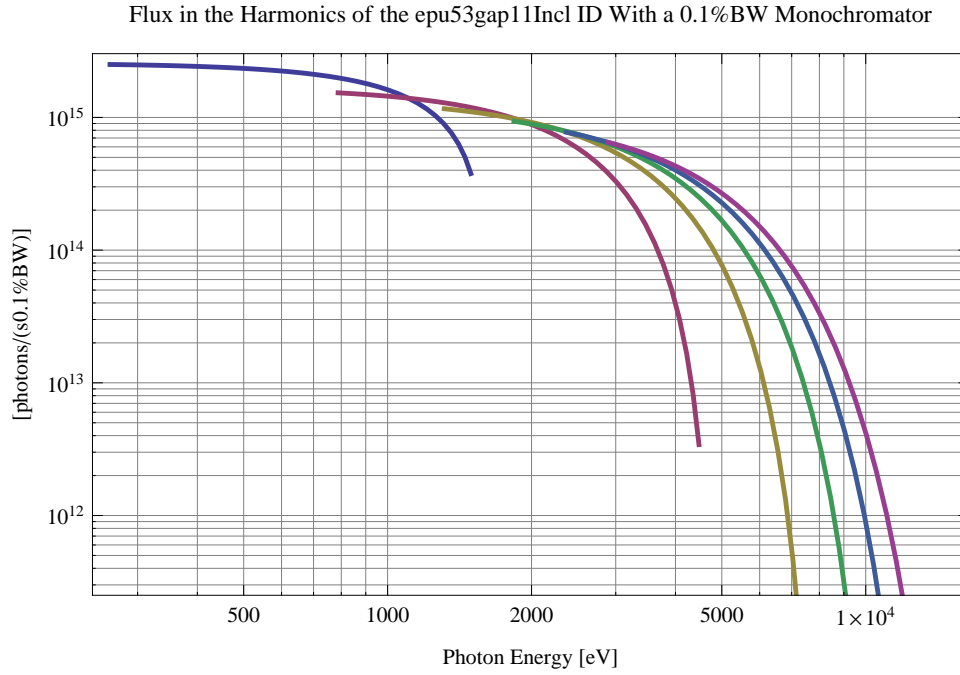


Figure 265: The flux of photons in the harmonics of the emitted synchrotron radiation from the epu53gap11Incl ID using a 0.1%BW monochromator

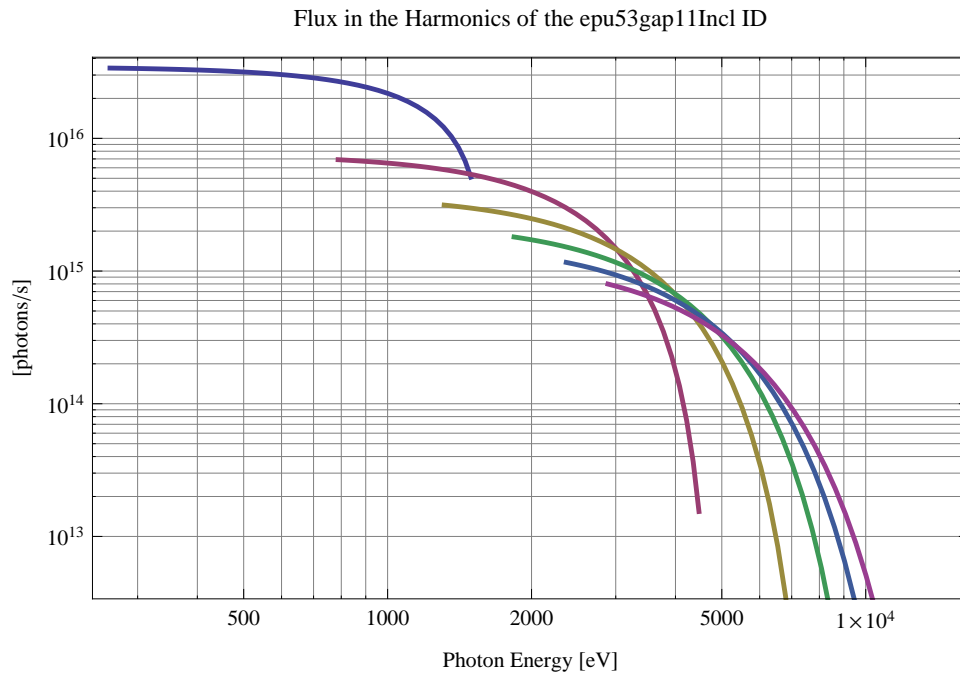


Figure 266: The flux of photons in the harmonics of the emitted synchrotron radiation from the epu53gap11Incl ID

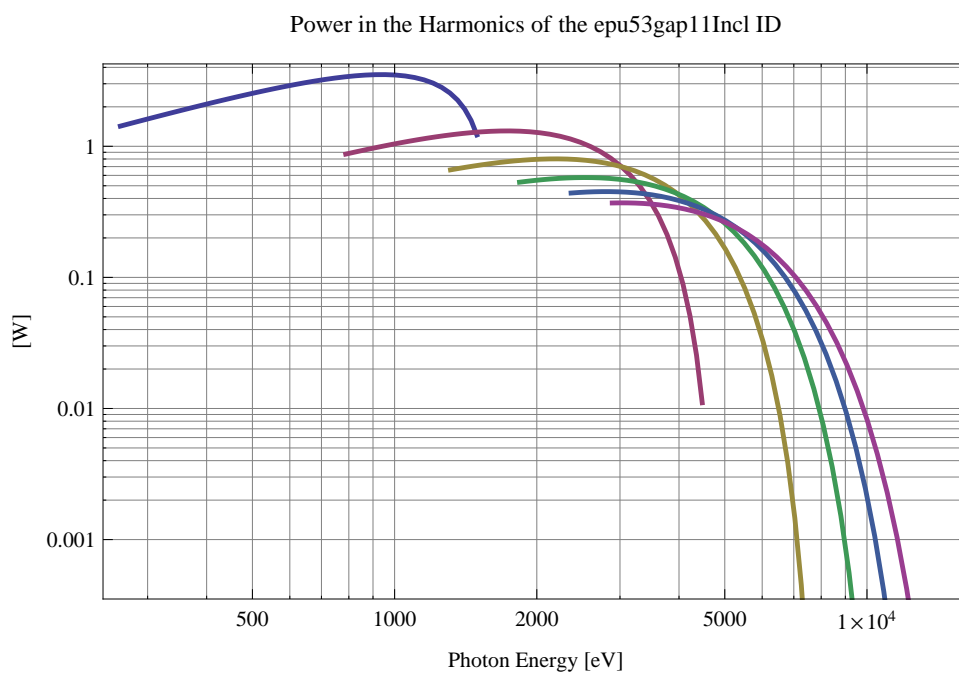


Figure 267: The power in the harmonics of the emitted synchrotron radiation from the epu53gap11Incl ID

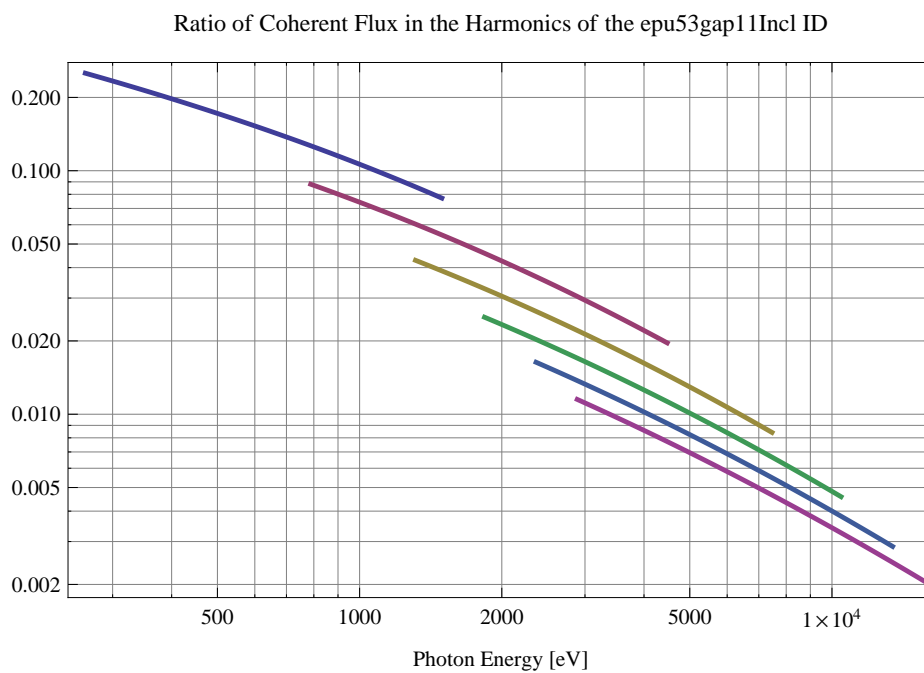


Figure 268: The ratio of coherent flux in the harmonics of the emitted synchrotron radiation from the epu53gap11Incl ID

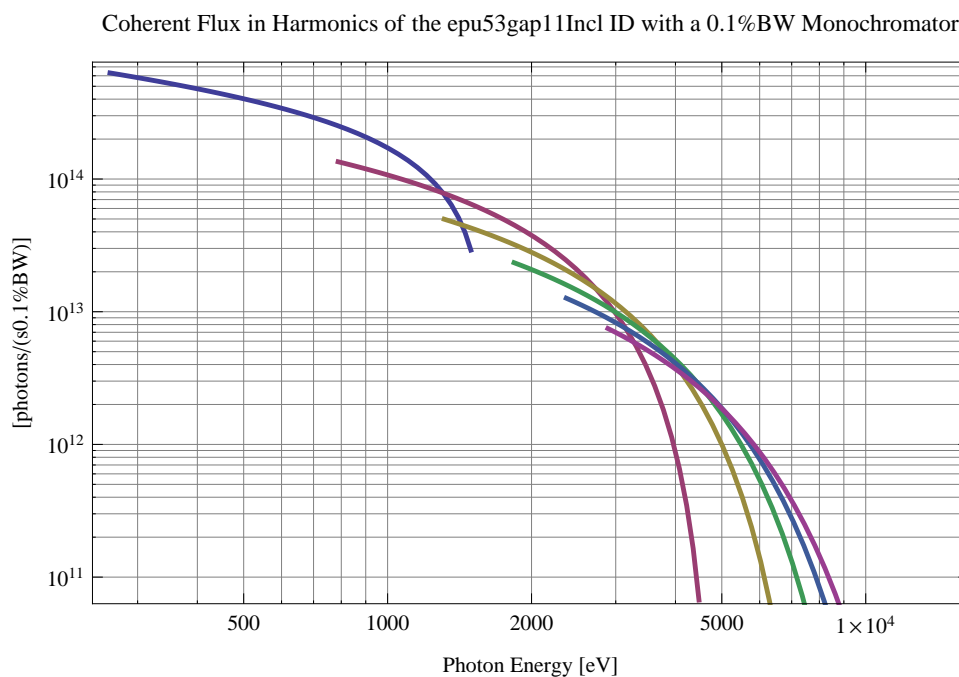


Figure 269: The coherent flux in the harmonics of the epu53gap11Incl ID using a 0.1%BW Monochromator

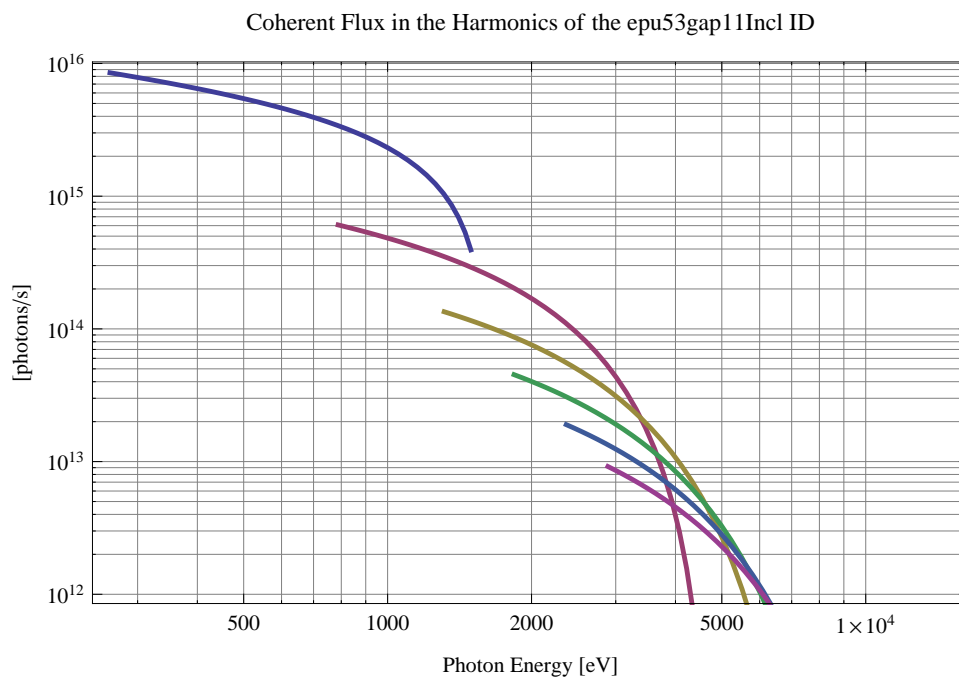


Figure 270: The coherent flux in the harmonics of the epu53gap11Incl ID

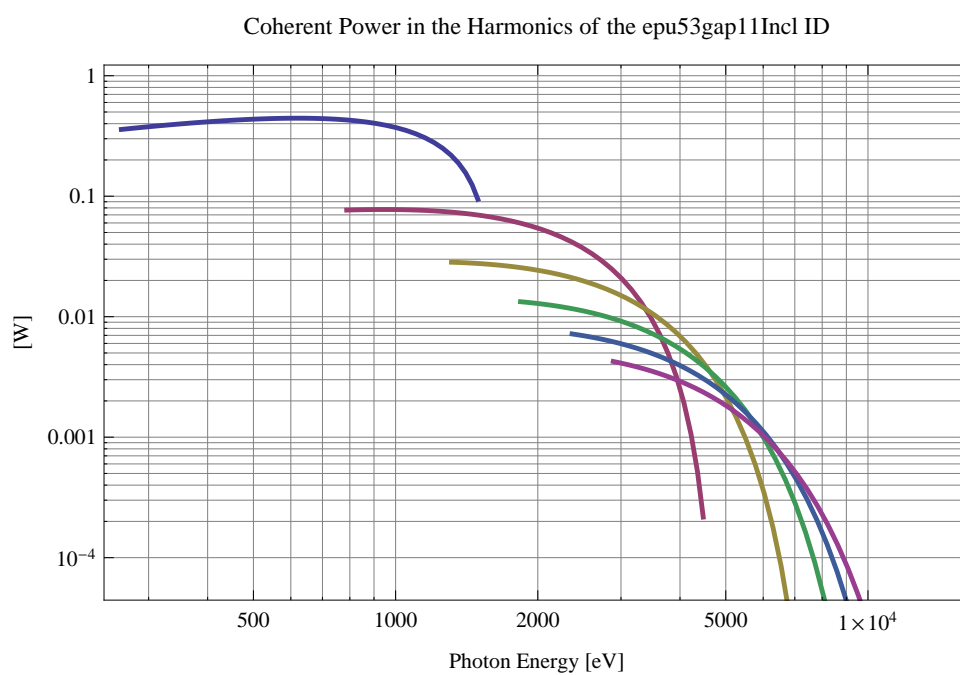


Figure 271: The power of coherent synchrotron radiation in the harmonics of the epu53gap11Incl ID

The brilliance at peak energy and the angular spectral flux density from the epu53gap11Incl ID for different harmonics at maximum K-value (3.206) are given in Table 45 and for minimum K-value (0.400) these values are given in Table 46.

Table 45: The brilliance at peak energy and the angular spectral flux density from the epu53gap11Incl ID for different harmonics at maximum K-value (3.206)

Harmonic	Photon Energy [eV]	Brilliance [Ph./ (smrad ² mrad ² 0.1% BW)]	Angular Spectral Flux [Ph./ (smrad ² 0.1% BW)]
1	262.631	1.13×10^{20}	4.66×10^{17}
3	787.893	2.18×10^{20}	5.79×10^{17}
5	1313.16	2.24×10^{20}	5.12×10^{17}
7	1838.42	2.06×10^{20}	4.37×10^{17}
9	2363.68	1.84×10^{20}	3.72×10^{17}
11	2888.94	1.62×10^{20}	3.18×10^{17}

Table 46: The brilliance at peak energy and the angular spectral flux density from the epu53gap11Incl ID for different harmonics at minimum K-value (0.4)

Harmonic	Photon Energy [eV]	Brilliance [Ph./ (smrad ² mrad ² 0.1% BW)]	Angular Spectral Flux [Ph./ (smrad ² 0.1% BW)]
1	1493.14	1.69×10^{20}	3.77×10^{17}
3	4479.43	3.51×10^{18}	6.58×10^{15}
5	7465.72	4.11×10^{16}	7.43×10^{13}
7	10452.	4.38×10^{14}	7.82×10^{11}
9	13438.3	4.54×10^{12}	8.05×10^9
11	16424.6	4.65×10^{10}	8.23×10^7

2.4.11 Magnet model of the elliptically polarising undulator epu53gap11Vert

The Radia [3] magnet model of the epu53gap11Vert ID is shown in Figure 272. The length of the magnet model is 441.756 mm. The magnetic material in the model is NdFeb with a remanence of 1.28 T, a material similar to VACODYM 776 TP from Vacuumschmelze. Blocks with vertical magnetisation are blue and blocks with horizontal magnetisation are yellow. The block size is 30.x30.x13.25 mm³ and there is a 5. mm cut-out in two of the corners of the blocks. The total length of the epu53gap11Vert ID is 3939.76 mm.

2.4.12 Analysis of the magnetic field of the epu53gap11Vert ID

The effective magnetic fields on axis and the fundamental photon energy of the epu53gap11Vert ID are shown in Table 47. The higher harmonic contents in the magnetic field of an elliptically polarising undulator made of permanent magnets is negligible and the effective field has about the same strength as the peak field.

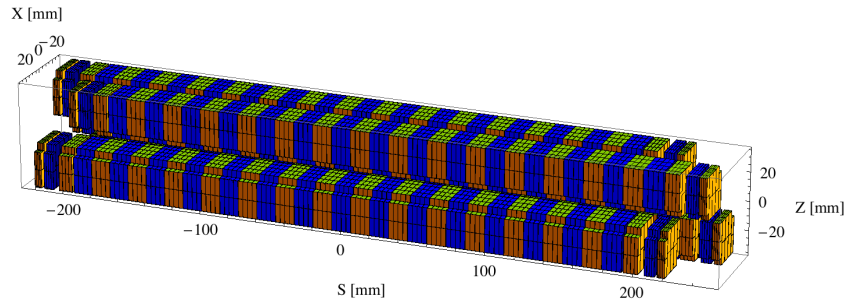


Figure 272: Magnetic model of the epu53gap11Vert ID. The ID has been modelled with Radia [3]

Table 47: Effective Fields on axis and Fundamental Photon Energy of the epu53gap11Vert ID

Undulator Period	53	mm
Undulator Gap	11	mm
Undulator Mode	Vertical	
Undulator Phase	26.500	mm
Vertical Peak Field	0.000	T
Effective Vertical Field	0.000	T
Kx (from vert. field)	0.000	
Horizontal Peak Field:	0.805	T
Effective Horizontal Field	0.807	T
Kz (from hor. field)	3.995	
Photon Energy, Harm.1	0.180	keV
Emitted Power	7.305	kW
Total Length	3939.8	mm

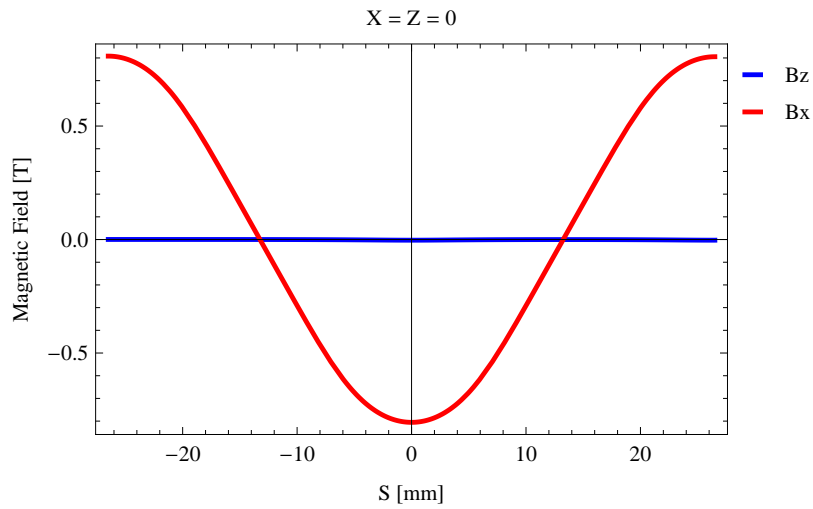


Figure 273: Vertical magnetic field in a central pole of the epu53gap11Vert ID along the ID axis, $X = Z = 0$

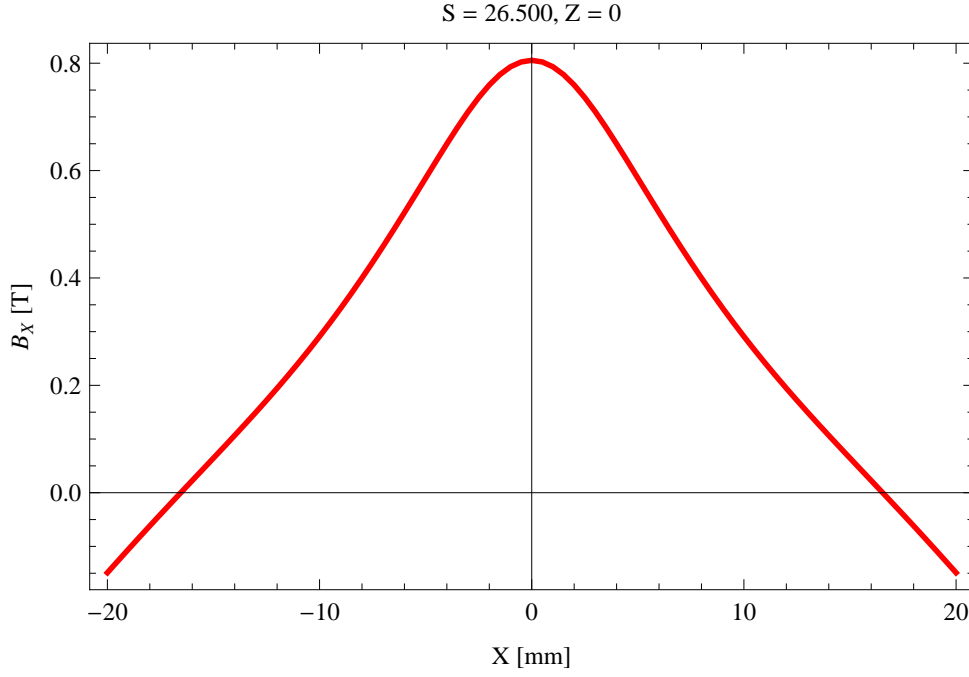


Figure 274: Horizontal magnetic field in a central pole of the epu53gap11Vert ID along the horizontally transverse direction to the ID axis, $S = 26.500$, $Z = 0$

2.4.13 Synchrotron radiation from the epu53gap11Vert ID

The power map of the emitted synchrotron radiation by the epu53gap11Vert ID, assuming a 0.5 A filament beam with an energy of 3 GeV and undulator properties of the synchrotron radiation, is shown in Figure 276. The on-axis power density is 25.749 kW/mrad²

A map of the degree of linear polarisation of the fundamental harmonic of the synchrotron radiation emitted by the epu53gap11Vert ID over the angle of observation is shown in Figure 277.

A map of the degree of 45 degree polarisation of the fundamental harmonic of the synchrotron radiation emitted by the epu53gap11Vert ID over the angle of observation is shown in Figure 278.

A map of the degree of circular polarisation of the fundamental harmonic of the synchrotron radiation emitted by the epu53gap11Vert ID over the angle of observation is shown in Figure 279.

The on axis brilliance at peak energy and the angular spectral flux from the epu53gap11Vert ID have been calculated with the given beam parameters, which are 0.5 A of stored current, $\beta_H = 9$ m, $\varepsilon_H = 0.263$ nmrad, $\beta_V = 4.8$ m, $\varepsilon_V = 8$. pmrad, and an energy spread of 0.001.

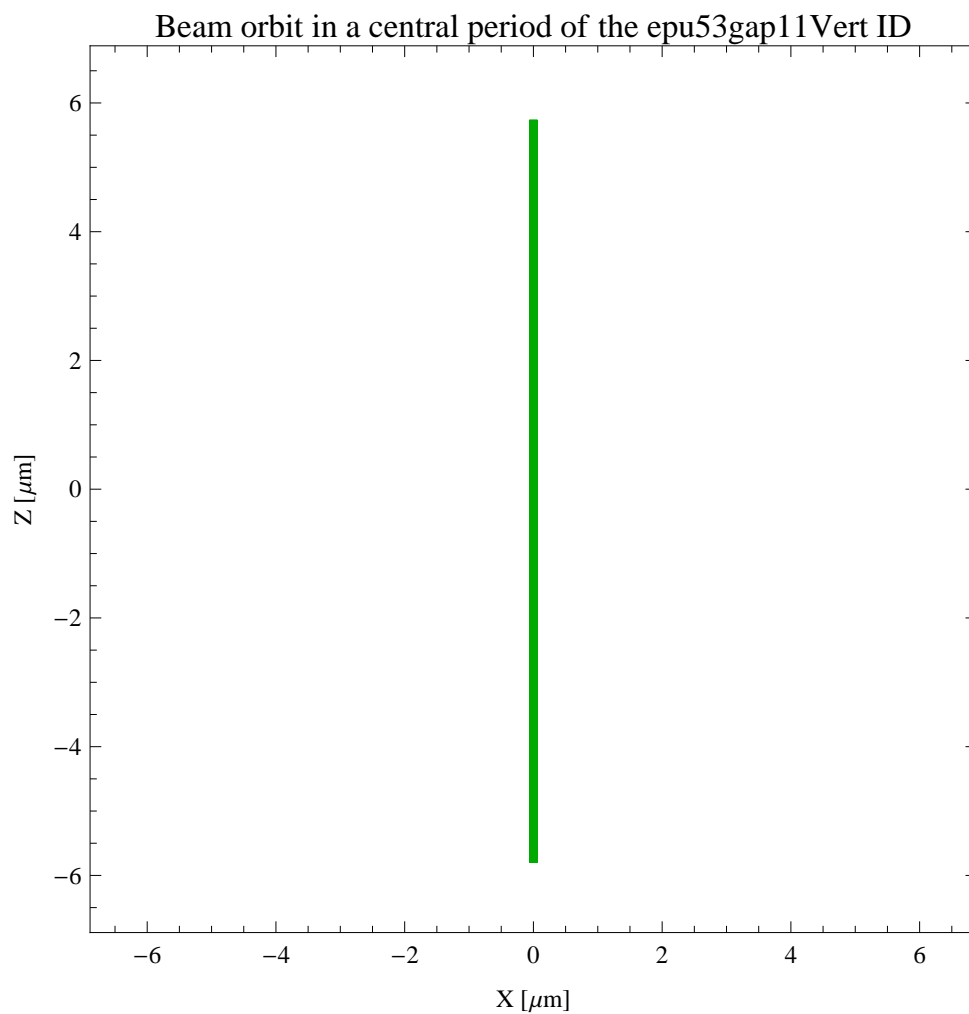


Figure 275: The beam orbit of the electron beam through a central period of the epu53gap11Vert ID

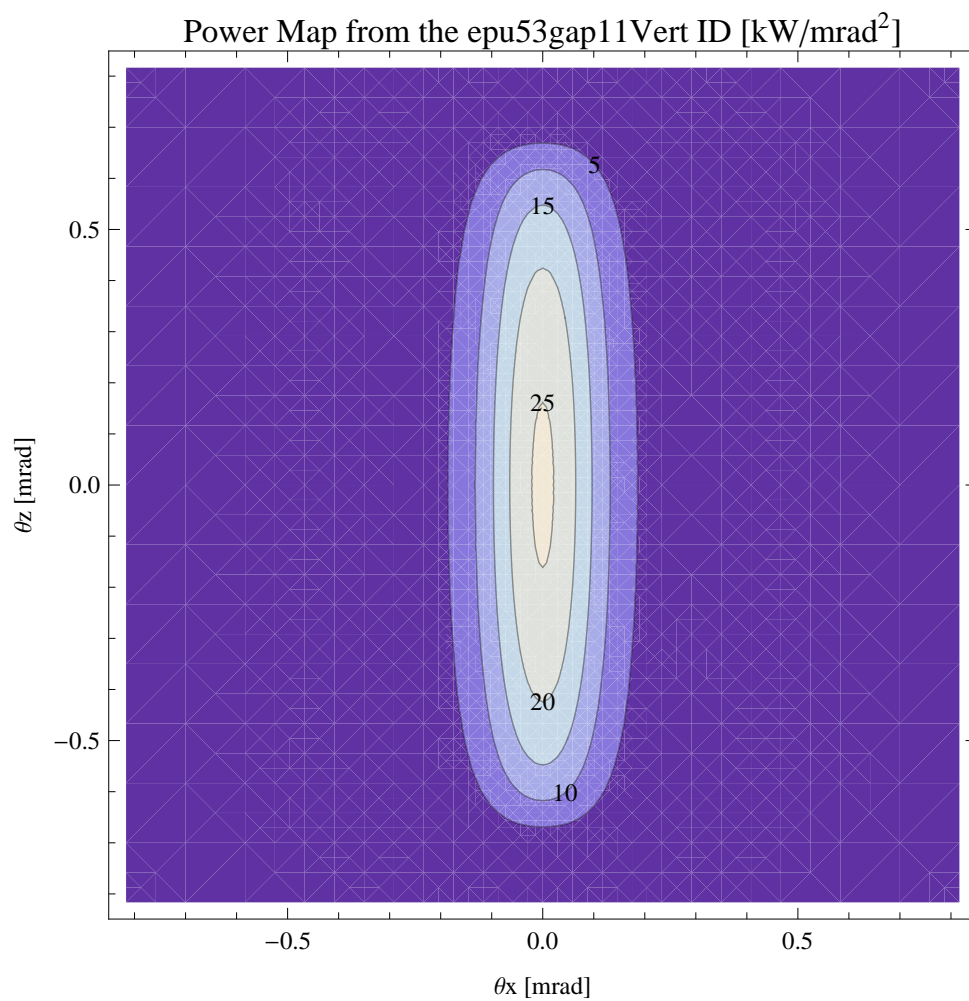


Figure 276: Map of the power distribution of the emitted synchrotron radiation by the epu53gap11Vert ID

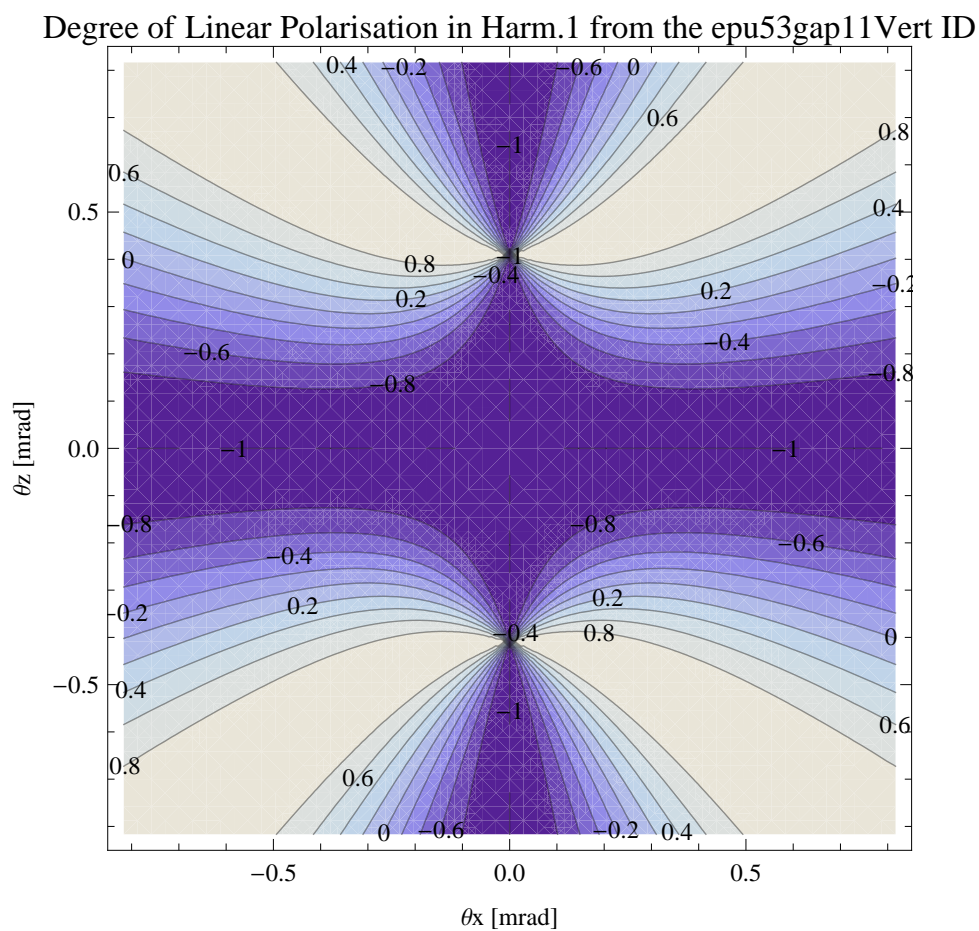


Figure 277: Map of linear polarisation in the fundamental harmonic of the synchrotron radiation emitted by the epu53gap11Vert ID

Degree of 45 degree Polarisation in Harm.1 from the epu53gap11Vert ID

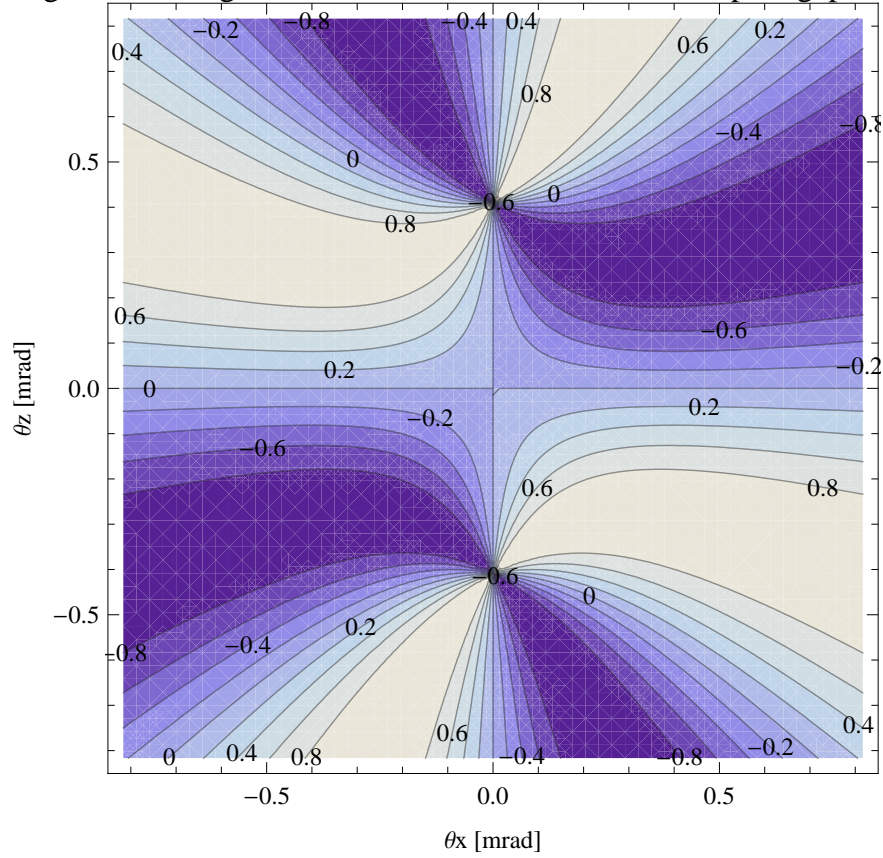


Figure 278: Map of 45 degree polarisation in the fundamental harmonic of the synchrotron radiation emitted by the epu53gap11Vert ID

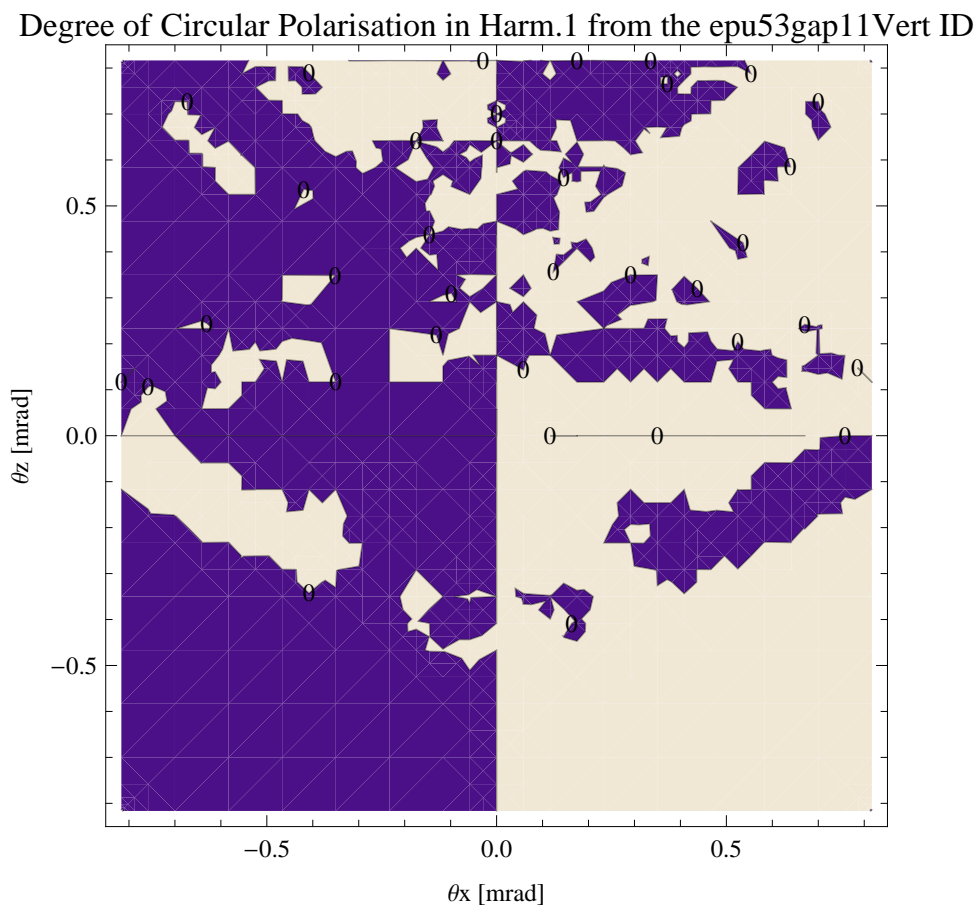


Figure 279: Map of circular polarisation in the fundamental harmonic of the synchrotron radiation emitted by the epu53gap11Vert ID

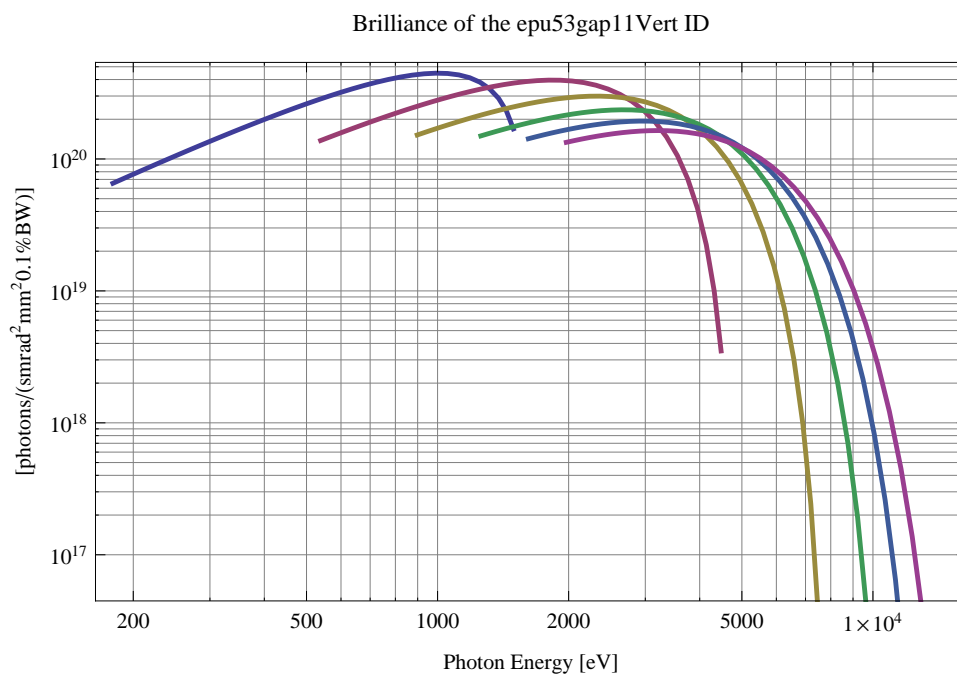


Figure 280: The brilliance at peak energy of the synchrotron radiation emitted by the epu53gap11Vert ID

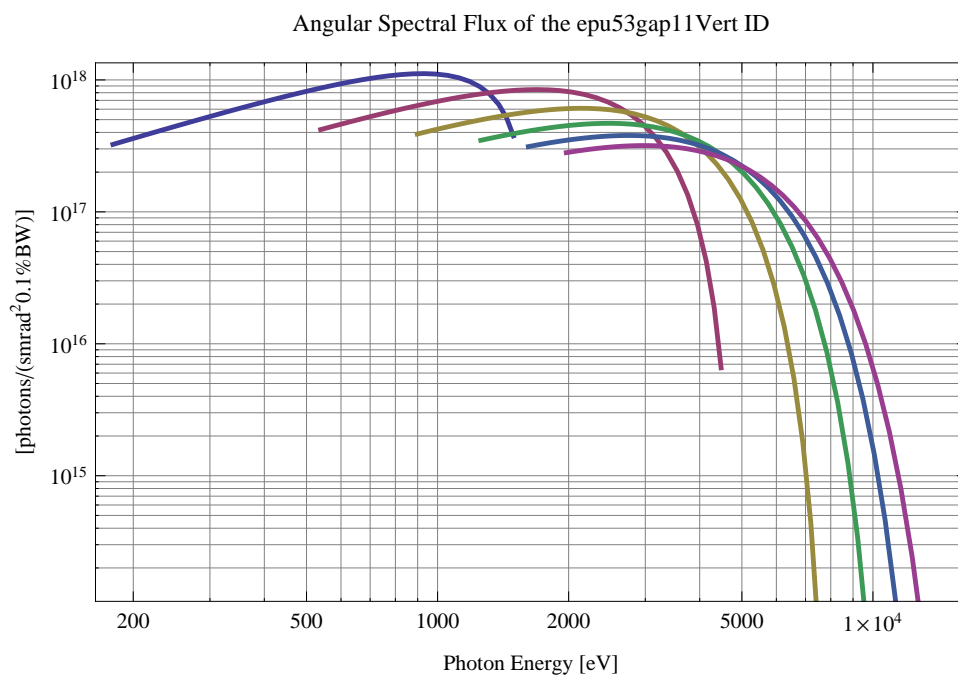


Figure 281: The angular spectral flux of the synchrotron radiation emitted by the epu53gap11Vert ID

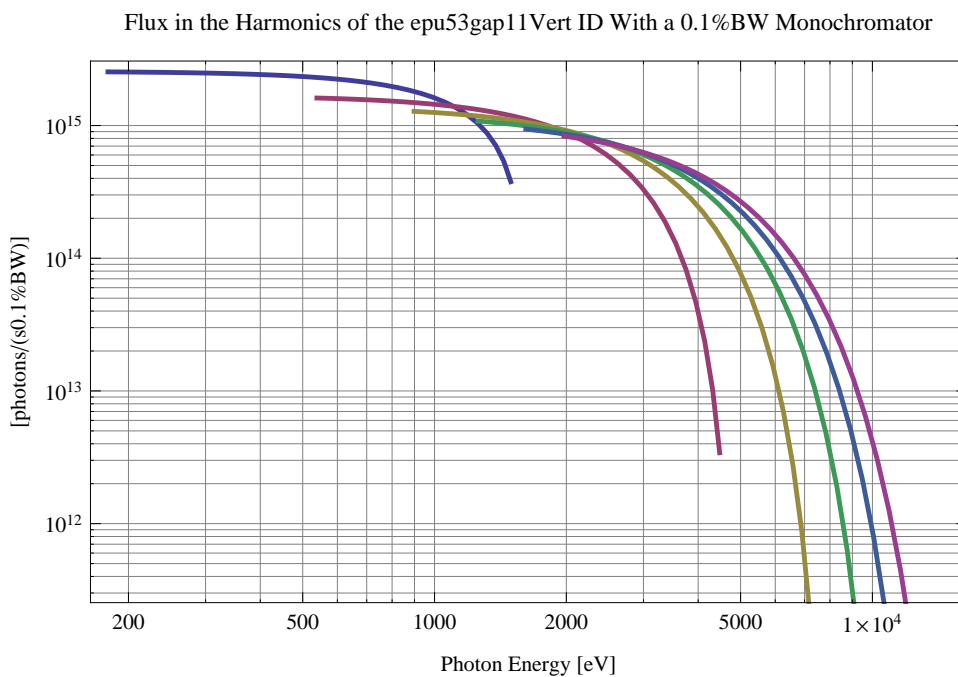


Figure 282: The flux of photons in the harmonics of the emitted synchrotron radiation from the epu53gap11Vert ID using a 0.1%BW monochromator

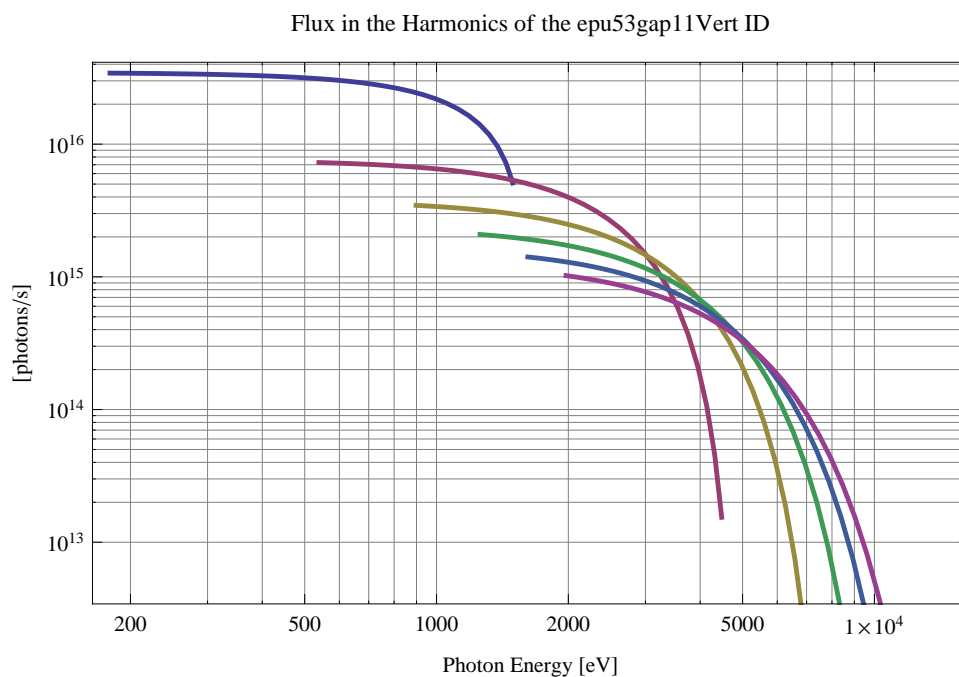


Figure 283: The flux of photons in the harmonics of the emitted synchrotron radiation from the epu53gap11Vert ID

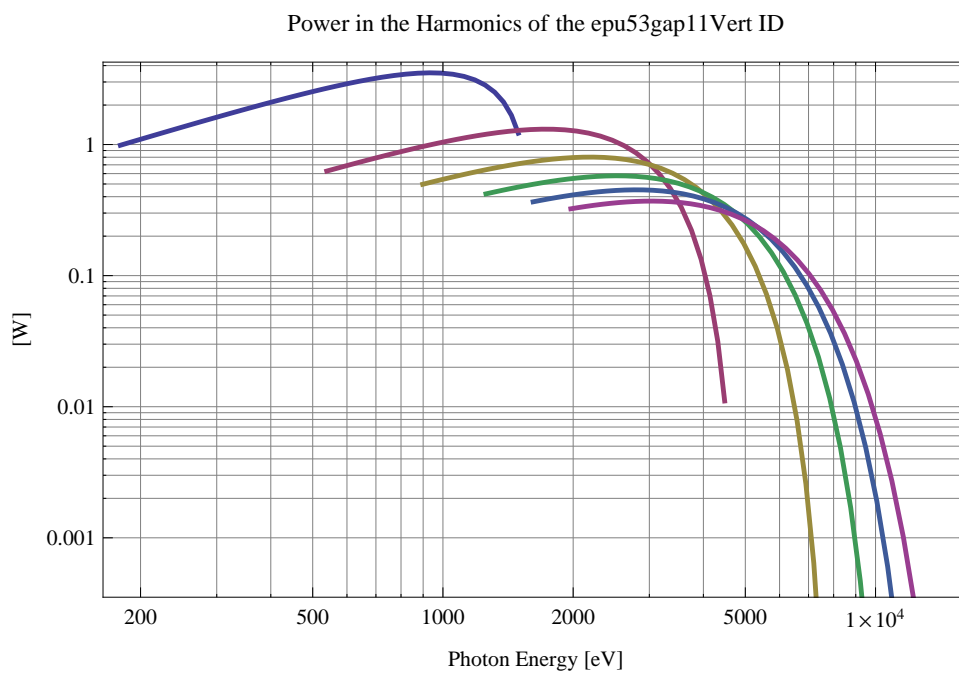


Figure 284: The power in the harmonics of the emitted synchrotron radiation from the epu53gap11Vert ID

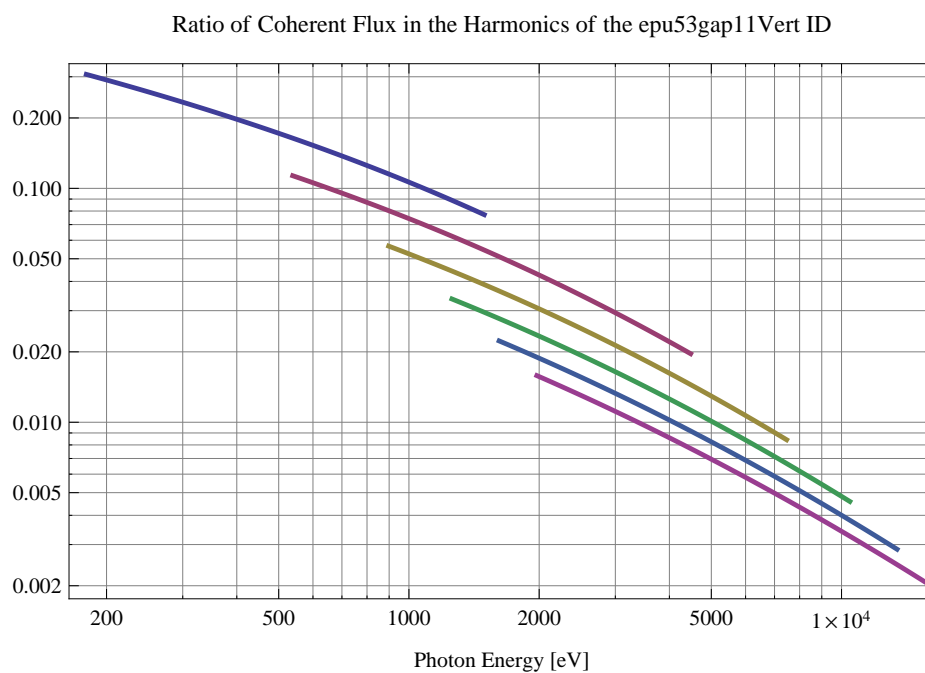


Figure 285: The ratio of coherent flux in the harmonics of the emitted synchrotron radiation from the epu53gap11Vert ID

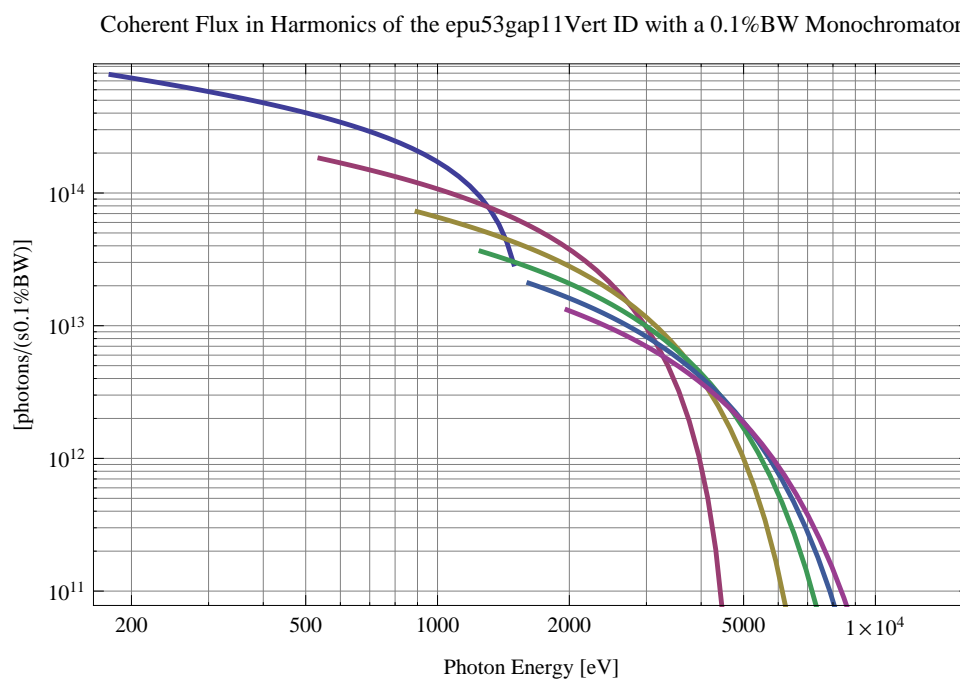


Figure 286: The coherent flux in the harmonics of the epu53gap11Vert ID using a 0.1%BW Monochromator

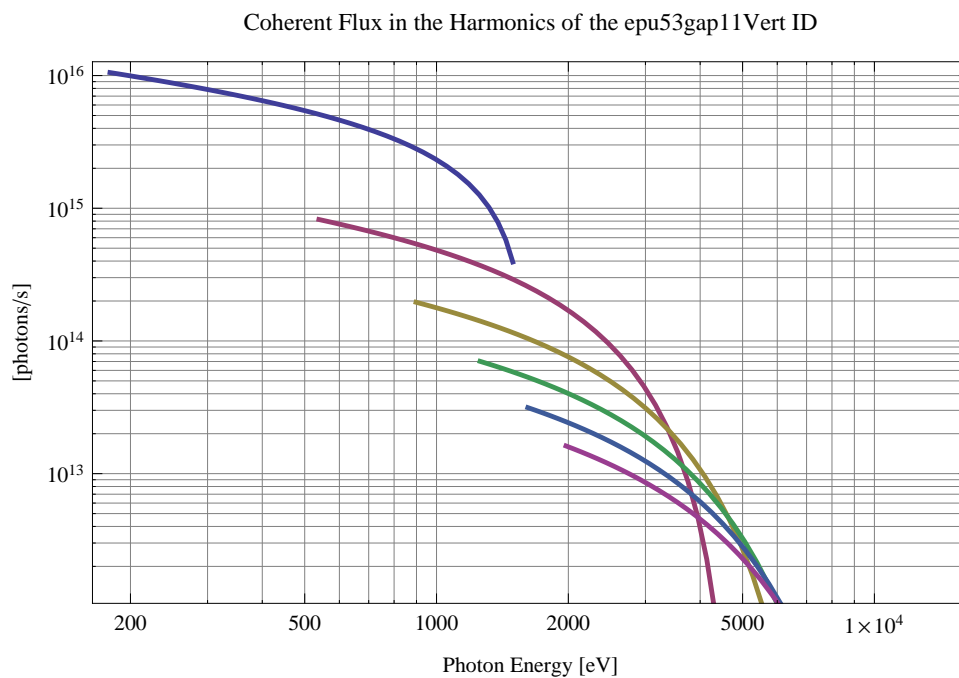


Figure 287: The coherent flux in the harmonics of the epu53gap11Vert ID

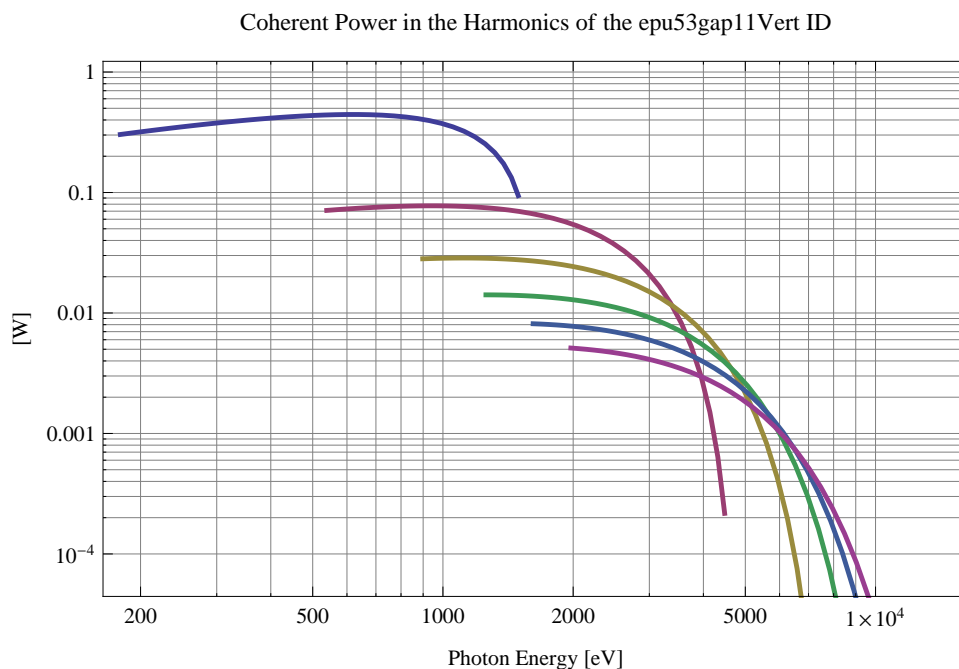


Figure 288: The power of coherent synchrotron radiation in the harmonics of the epu53gap11Vert ID

The brilliance at peak energy and the angular spectral flux density from the epu53gap11Vert ID for different harmonics at maximum K-value (3.995) are given in Table 48 and for minimum K-value (0.400) these values are given in Table 49.

Table 48: The brilliance at peak energy and the angular spectral flux density from the epu53gap11Vert ID for different harmonics at maximum K-value (3.995)

Harmonic	Photon Energy [eV]	Brilliance [Ph./($\text{smrad}^2\text{mrad}^20.1\%\text{BW}$)]	Angular Spectral Flux [Ph./($\text{smrad}^20.1\%\text{BW}$)]
1	179.591	6.54×10^{19}	3.24×10^{17}
3	538.774	1.38×10^{20}	4.2×10^{17}
5	897.956	1.52×10^{20}	3.89×10^{17}
7	1257.14	1.5×10^{20}	3.48×10^{17}
9	1616.32	1.42×10^{20}	3.12×10^{17}
11	1975.5	1.34×10^{20}	2.81×10^{17}

Table 49: The brilliance at peak energy and the angular spectral flux density from the epu53gap11Vert ID for different harmonics at minimum K-value (0.4)

Harmonic	Photon Energy [eV]	Brilliance [Ph./($\text{smrad}^2\text{mrad}^20.1\%\text{BW}$)]	Angular Spectral Flux [Ph./($\text{smrad}^20.1\%\text{BW}$)]
1	1493.14	1.69×10^{20}	3.77×10^{17}
3	4479.43	3.51×10^{18}	6.58×10^{15}
5	7465.72	4.11×10^{16}	7.43×10^{13}
7	10452.	4.38×10^{14}	7.82×10^{11}
9	13438.3	4.54×10^{12}	8.05×10^9
11	16424.6	4.65×10^{10}	8.23×10^7

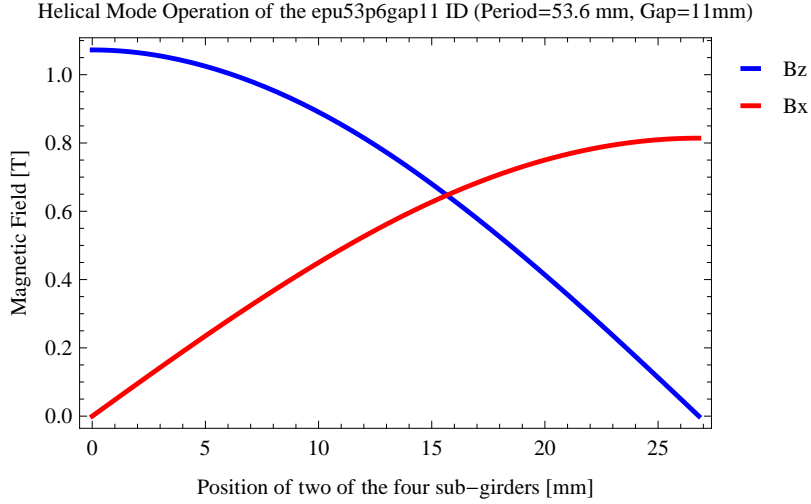


Figure 289: Vertical and horizontal magnetic field for the the epu53p6gap11 ID when operating in the helical mode for different positions for two of the four sub-girders

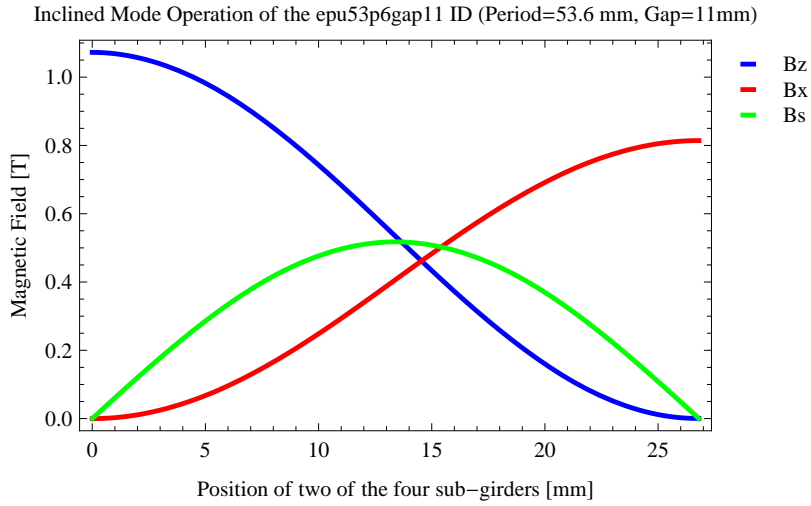


Figure 290: Vertical, horizontal, and longitudinal magnetic field for the the epu53p6gap11 ID when operating in the inclined mode for different positions for two of the four sub-girders

2.5 The elliptically polarising undulator epu53p6gap11

2.5.1 Modes of operation in the elliptically polarising undulator epu53p6gap11

Horizontal polarisation of the emitted synchrotron radiation from the epu53p6gap11 ID (Period=53.6 mm, Gap=11mm) is found in the planar mode when there is no movement of the sub-girders.

Circular polarisation is found in the elliptical mode of operation for a symmetric sub-grider movement of 15.6708 mm. Figure 289 shows the vertical and horizontal magnetic field for the epu53p6gap11 ID when operating in the helical mode.

45 degree polarisation is found in the inclined mode of operation for an assymetric sub-grider movement of 14.5465 mm. Figure 290 shows the vertical and horizontal magnetic field for the epu53p6gap11 ID when operating in the inclined mode.

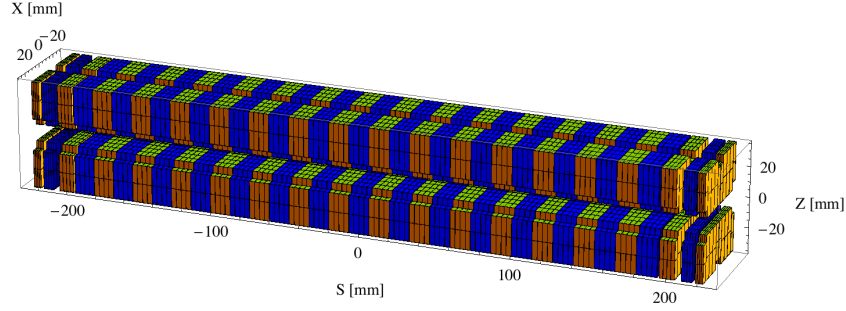


Figure 291: Magnetic model of the epu53p6gap11Plan ID. The ID has been modelled with Radia [3]

The following sub-sections will cover four different situations: The epu53p6gap11 operating in the planar mode for horizontal polarisation (epu53p6gap11Plan); The epu53p6gap11 operating in the helical mode for circular polarisation (epu53p6gap11Heli), the epu53p6gap11 operating in the inclined mode for 45 degree polarisation (epu53p6gap11Incl); and The epu53p6gap11 operating in the vertical mode for vertical polarisation (epu53p6gap11Vert).

2.5.2 Magnet model of the elliptically polarising undulator epu53p6gap11Plan

The Radia [3] magnet model of the epu53p6gap11Plan ID is shown in Figure 291. The length of the magnet model is 446.587 mm. The magnetic material in the model is NdFeb with a remanence of 1.28 T, a material similar to VACODYM 776 TP from Vacuumschmelze. Blocks with vertical magnetisation are blue and blocks with horizontal magnetisation are yellow. The block size is 30.x30.x13.4 mm³ and there is a 5. mm cut-out in two of the corners of the blocks. The total length of the epu53p6gap11Plan ID is 3930.59 mm.

2.5.3 Analysis of the magnetic field of the epu53p6gap11Plan ID

The effective magnetic fields on axis and the fundamental photon energy of the epu53p6gap11Plan ID are shown in Table 50. The higher harmonic contents in the magnetic field of an elliptically polarising undulator made of permanent magnets is negligible and the effective field has about the same strength as the peak field.

2.5.4 Synchrotron radiation from the epu53p6gap11Plan ID

The power map of the emitted synchrotron radiation by the epu53p6gap11Plan ID, assuming a 0.5 A filament beam with an energy of 3 GeV and undulator properties of the synchrotron radiation, is shown in Figure 295. The on-axis power density is 33.843 kW/mrad²

A map of the degree of linear polarisation of the fundamental harmonic of the synchrotron radiation emitted by the epu53p6gap11Plan ID over the angle of observation is shown in Figure 296.

A map of the degree of 45 degree polarisation of the fundamental harmonic of the synchrotron radiation emitted by the epu53p6gap11Plan ID over the angle of observation is shown in Figure 297.

Table 50: Effective Fields on axis and Fundamental Photon Energy of the epu53p6gap11Plan ID

Undulator Period	53.6	mm
Undulator Gap	11	mm
Undulator Mode	Planar	
Undulator Phase	0.000	mm
Vertical Peak Field	1.055	T
Effective Vertical Field	1.073	T
Kx (from vert. field)	5.372	
Horizontal Peak Field:	0.000	T
Effective Horizontal Field	0.000	T
Kz (from hor. field)	0.000	
Photon Energy, Harm.1	0.103	keV
Emitted Power	12.884	kW
Total Length	3930.6	mm

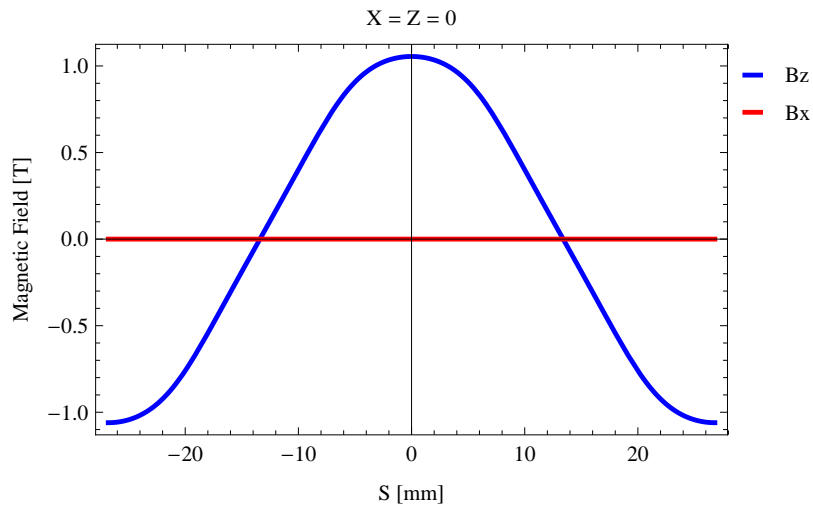


Figure 292: Vertical magnetic field in a central pole of the epu53p6gap11Plan ID along the ID axis, $X = Z = 0$

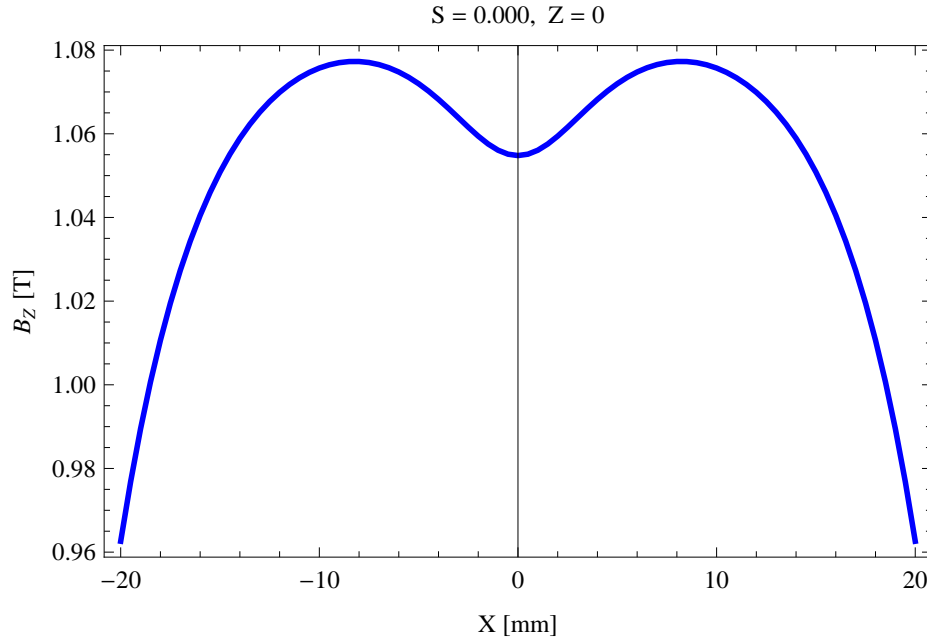


Figure 293: Vertical magnetic field in a central pole of the epu53p6gap11Plan ID along the horizontally transverse direction to the ID axis, $S = 0.000$, $Z = 0$

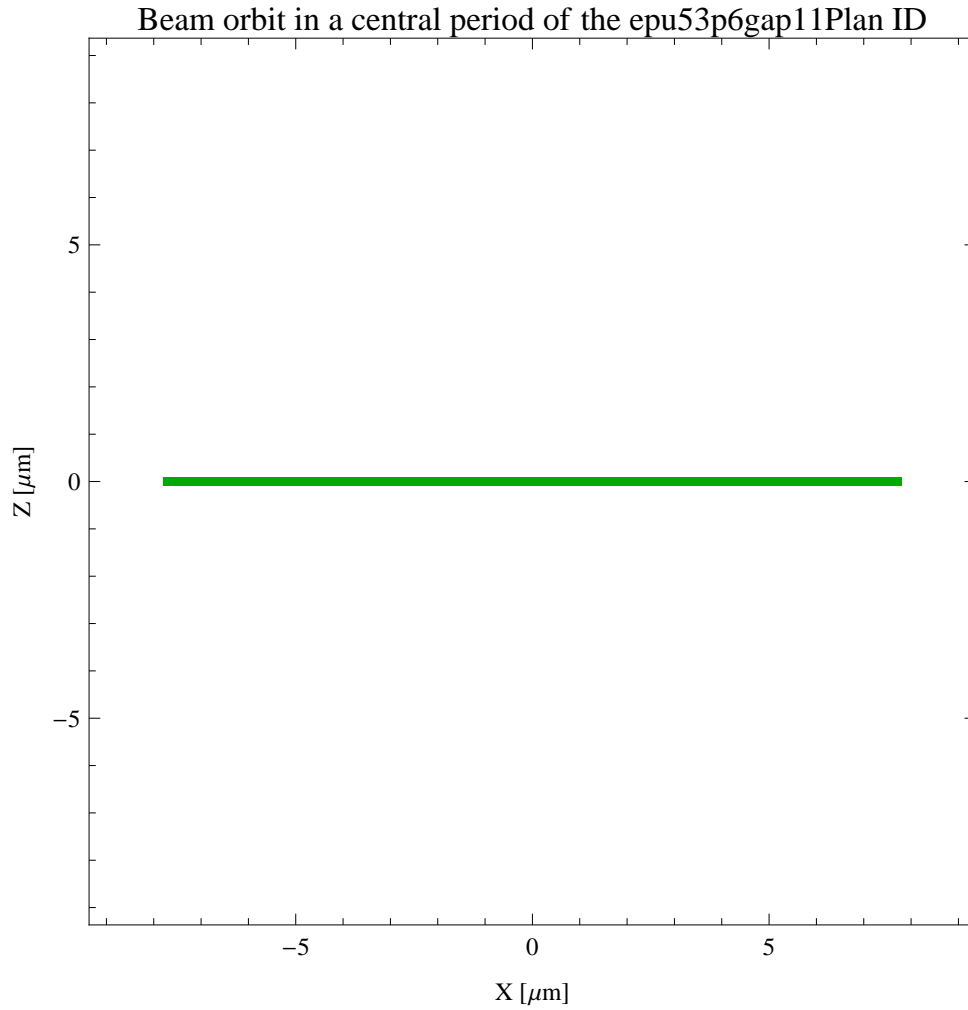


Figure 294: The beam orbit of the electron beam through a central period of the epu53p6gap11Plan ID

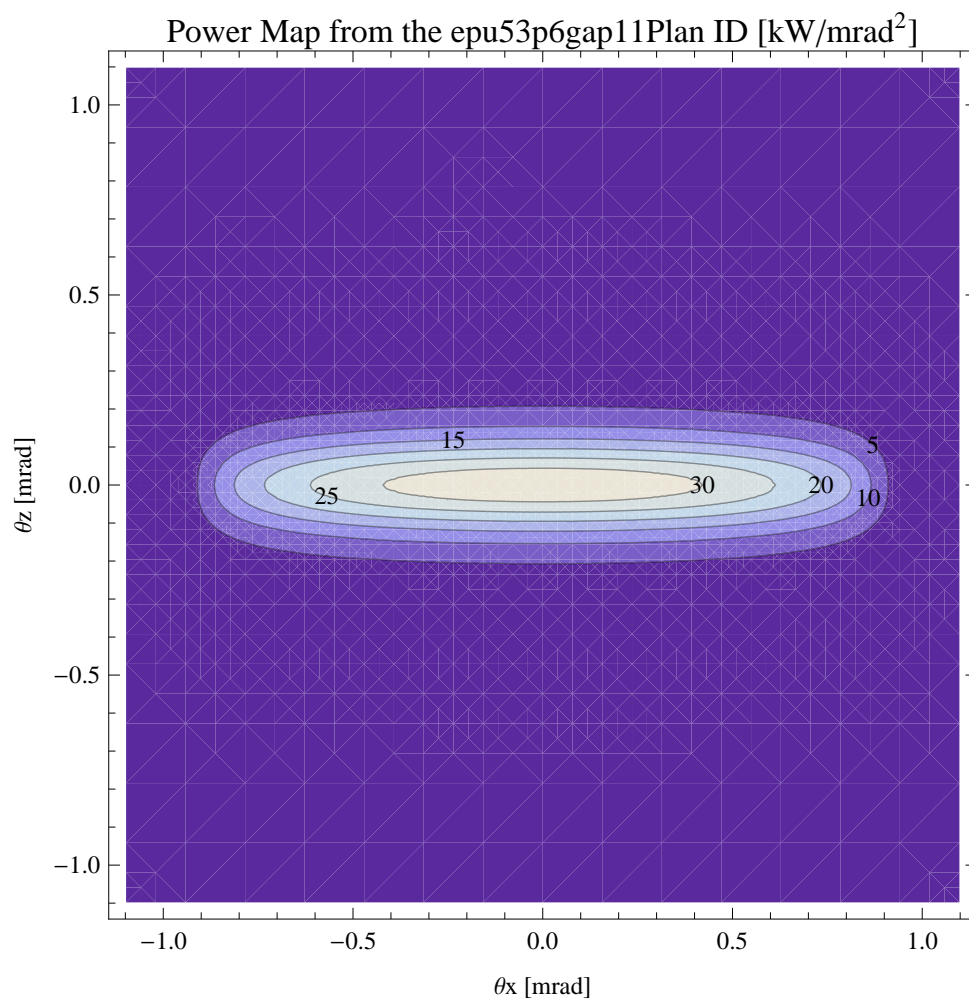


Figure 295: Map of the power distribution of the emitted synchrotron radiation by the epu53p6gap11Plan ID

Degree of Linear Polarisation in Harm.1 from the epu53p6gap11Plan ID

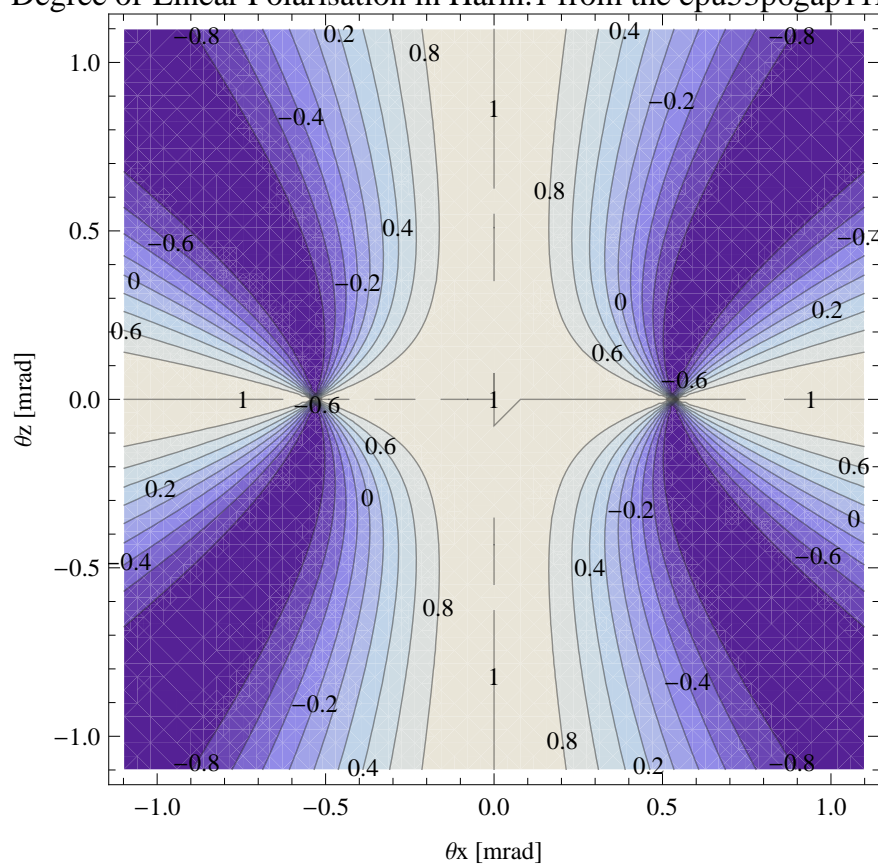


Figure 296: Map of linear polarisation in the fundamental harmonic of the synchrotron radiation emitted by the epu53p6gap11Plan ID

Degree of 45 degree Polarisation in Harm.1 from the epu53p6gap11Plan II

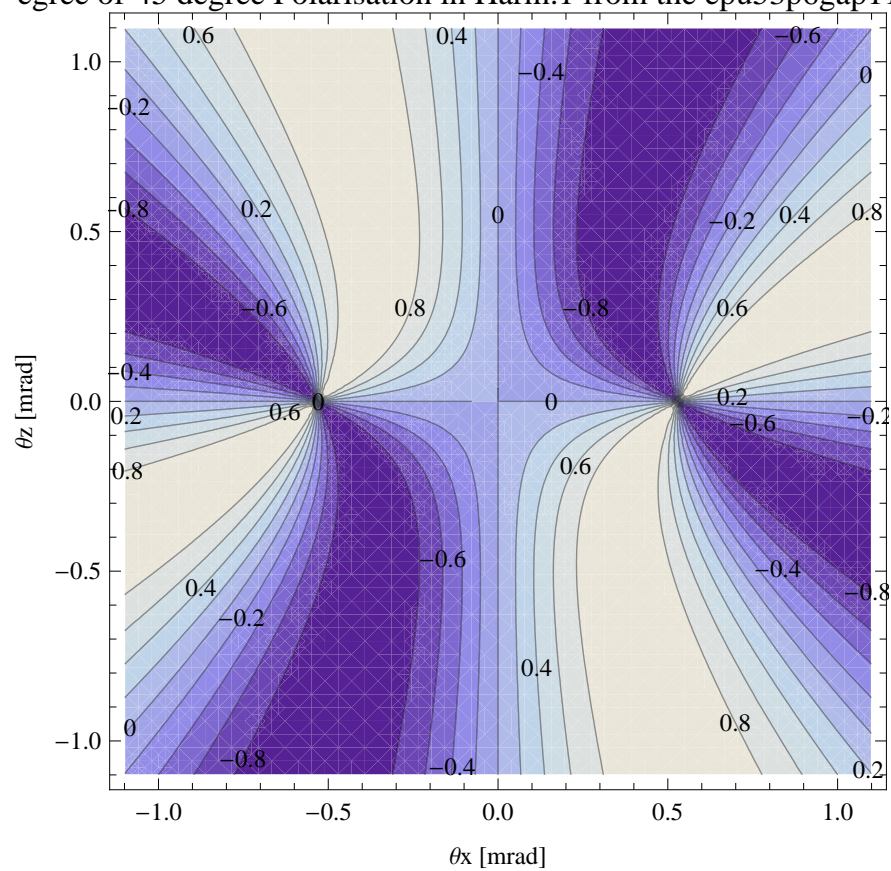


Figure 297: Map of 45 degree polarisation in the fundamental harmonic of the synchrotron radiation emitted by the epu53p6gap11Plan ID

Degree of Circular Polarisation in Harm.1 from the epu53p6gap11Plan II

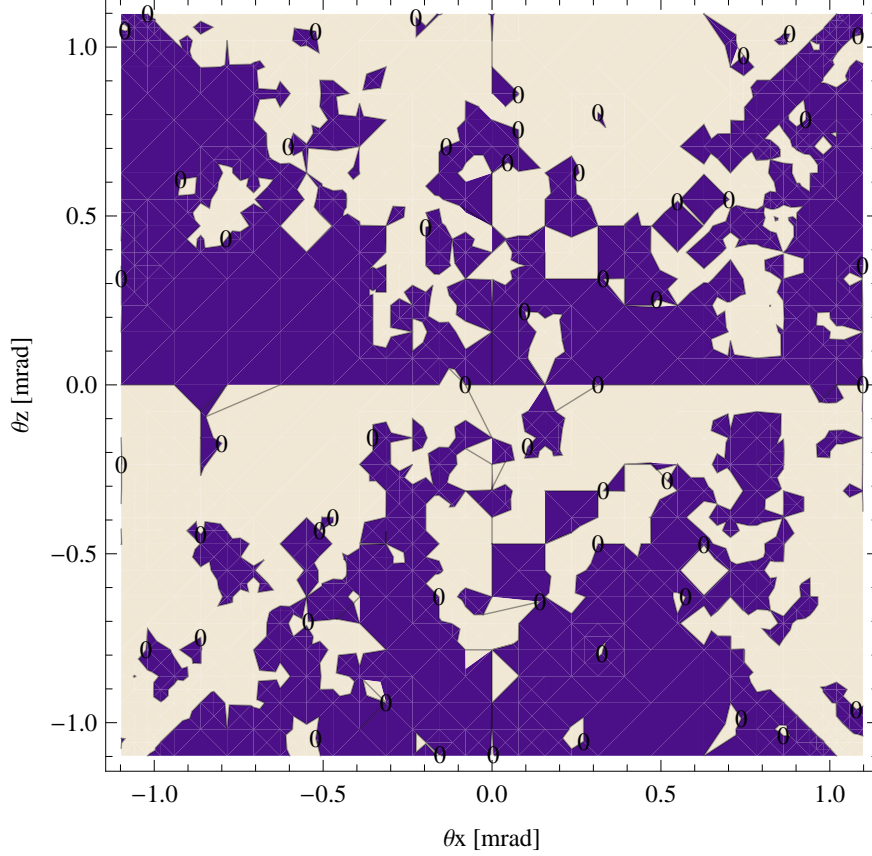


Figure 298: Map of circular polarisation in the fundamental harmonic of the synchrotron radiation emitted by the epu53p6gap11Plan ID

A map of the degree of circular polarisation of the fundamental harmonic of the synchrotron radiation emitted by the epu53p6gap11Plan ID over the angle of observation is shown in Figure 298.

The on axis brilliance at peak energy and the angular spectral flux from the epu53p6gap11Plan ID have been calculated with the given beam parameters, which are 0.5 A of stored current, $\beta_H = 9$ m, $\varepsilon_H = 0.263$ nmrad, $\beta_V = 4.8$ m, $\varepsilon_V = 8$. pmrad, and an energy spread of 0.001.

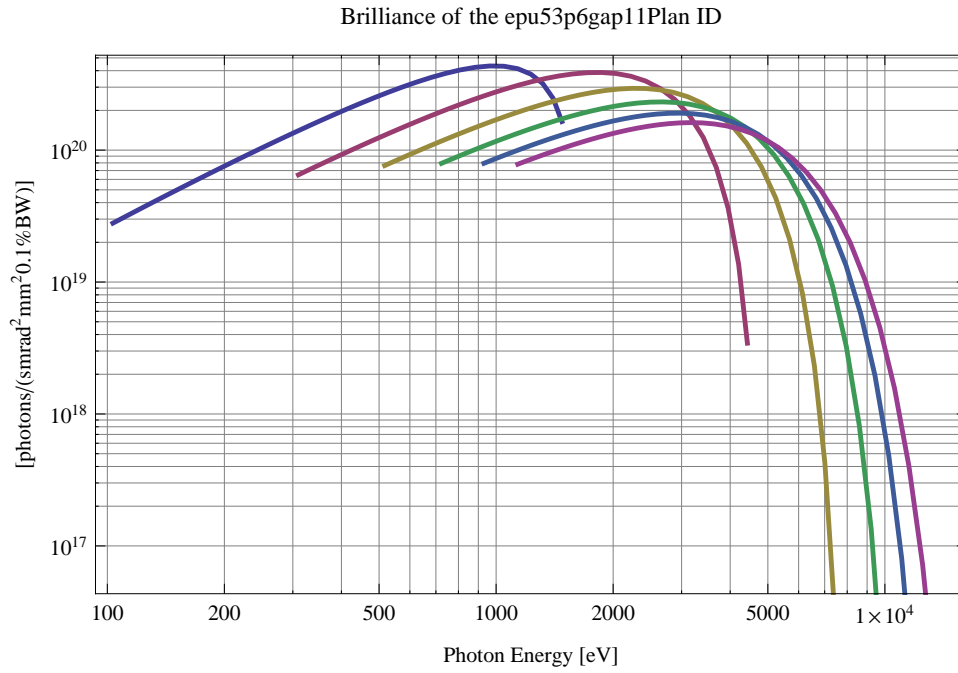


Figure 299: The brilliance at peak energy of the synchrotron radiation emitted by the epu53p6gap11Plan ID

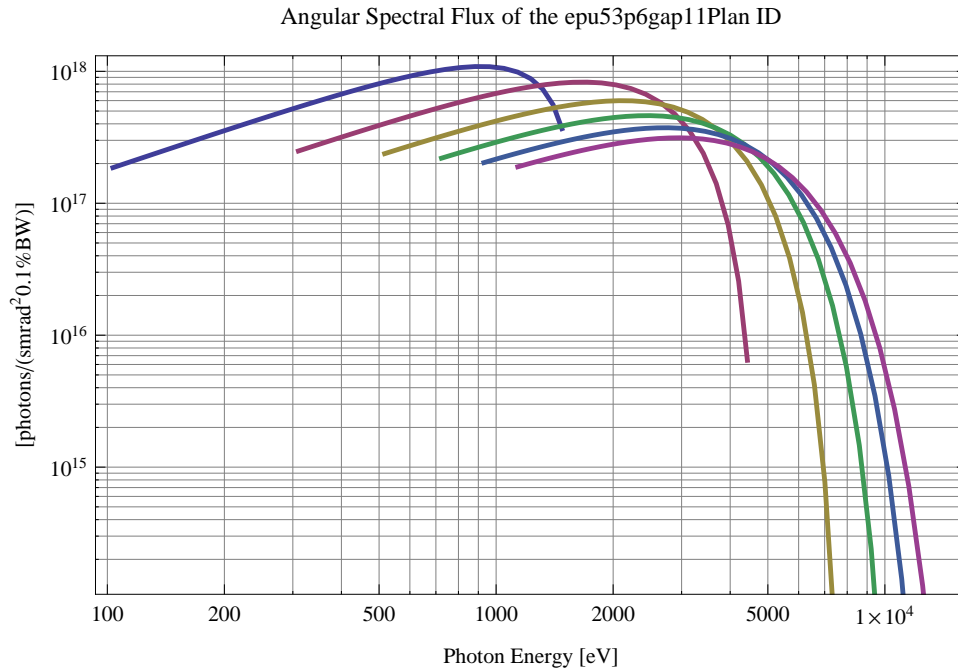


Figure 300: The angular spectral flux of the synchrotron radiation emitted by the epu53p6gap11Plan ID

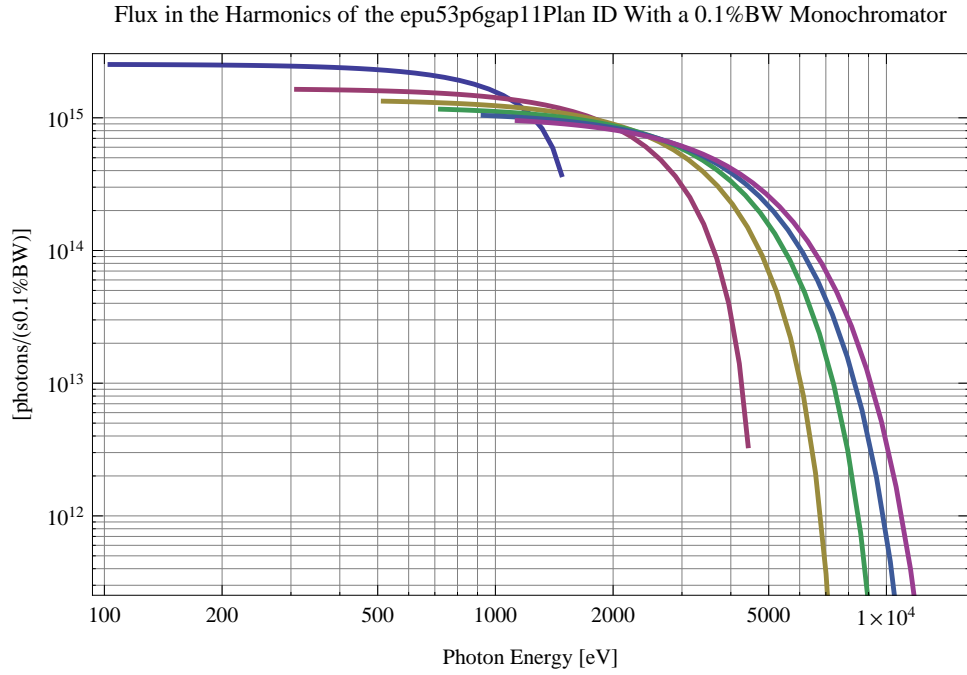


Figure 301: The flux of photons in the harmonics of the emitted synchrotron radiation from the epu53p6gap11Plan ID using a 0.1%BW monochromator

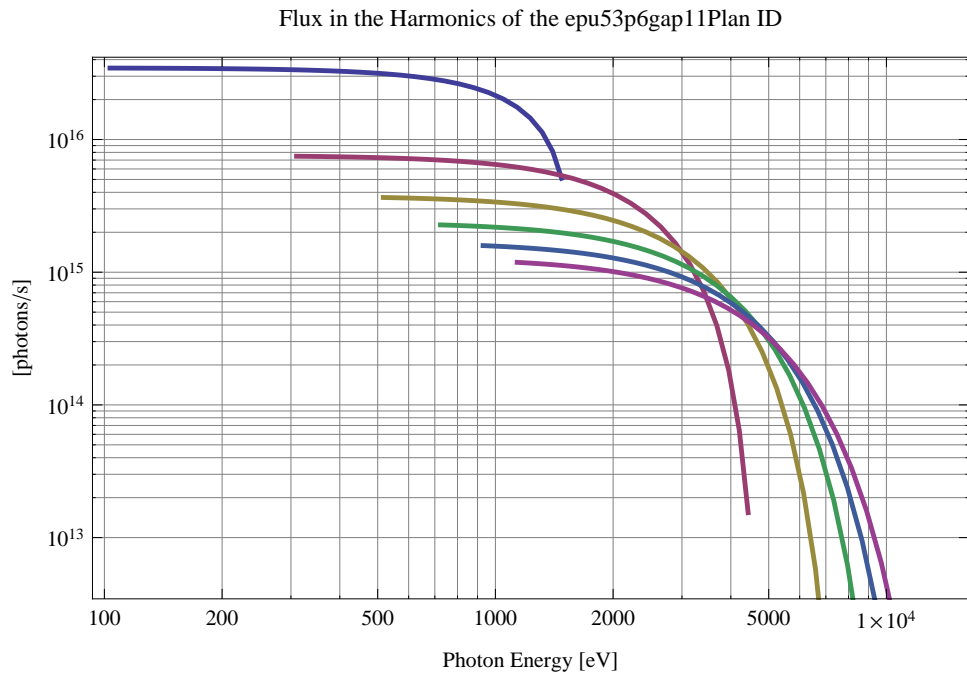


Figure 302: The flux of photons in the harmonics of the emitted synchrotron radiation from the epu53p6gap11Plan ID

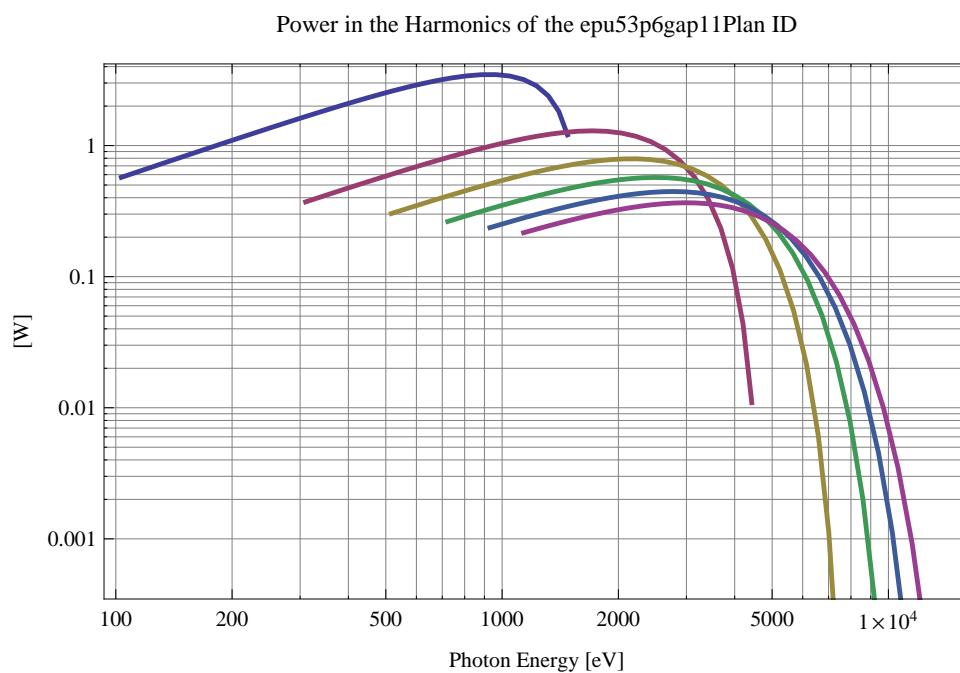


Figure 303: The power in the harmonics of the emitted synchrotron radiation from the epu53p6gap11Plan ID

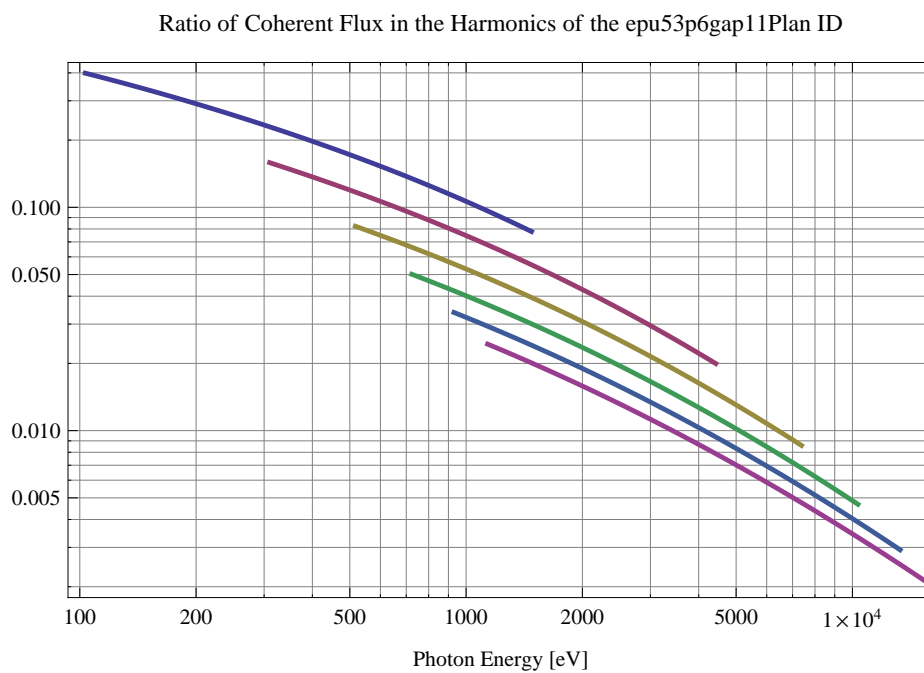


Figure 304: The ratio of coherent flux in the harmonics of the emitted synchrotron radiation from the epu53p6gap11Plan ID

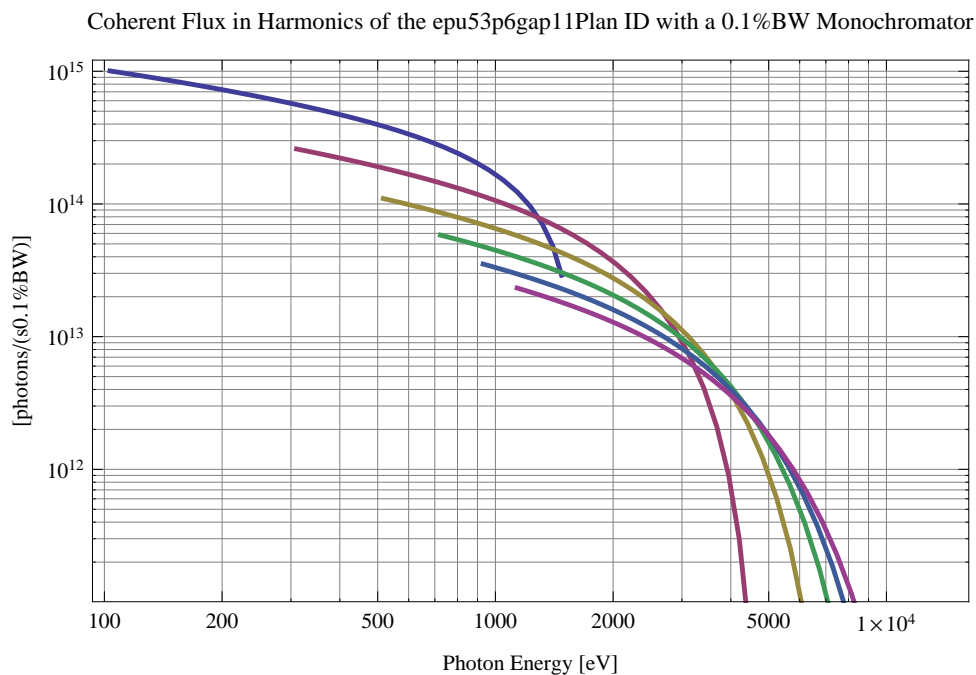


Figure 305: The coherent flux in the harmonics of the epu53p6gap11Plan ID using a 0.1%BW Monochromator

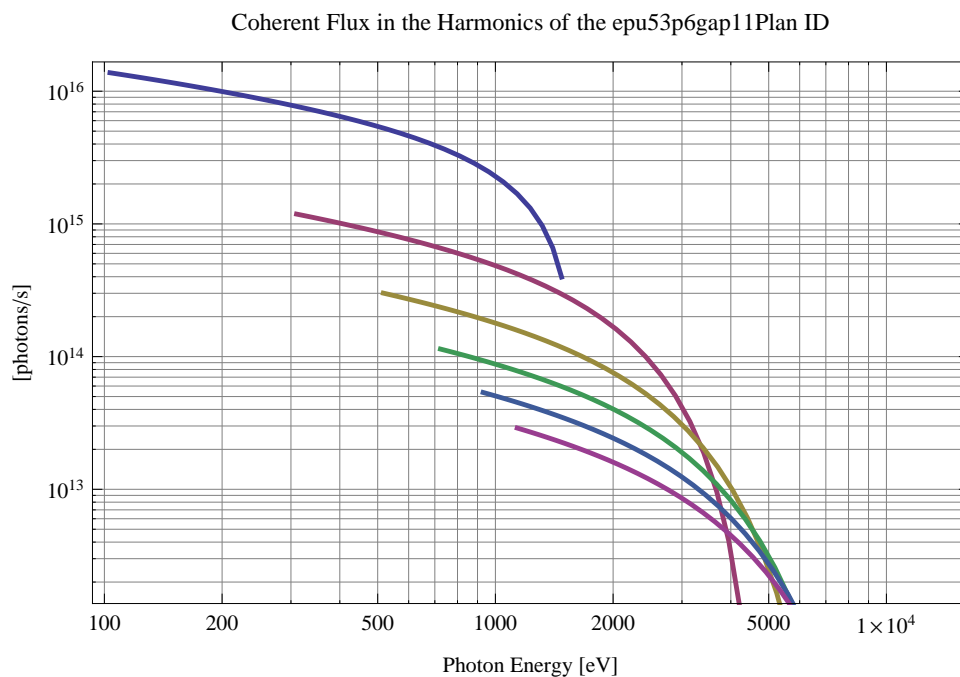


Figure 306: The coherent flux in the harmonics of the epu53p6gap11Plan ID

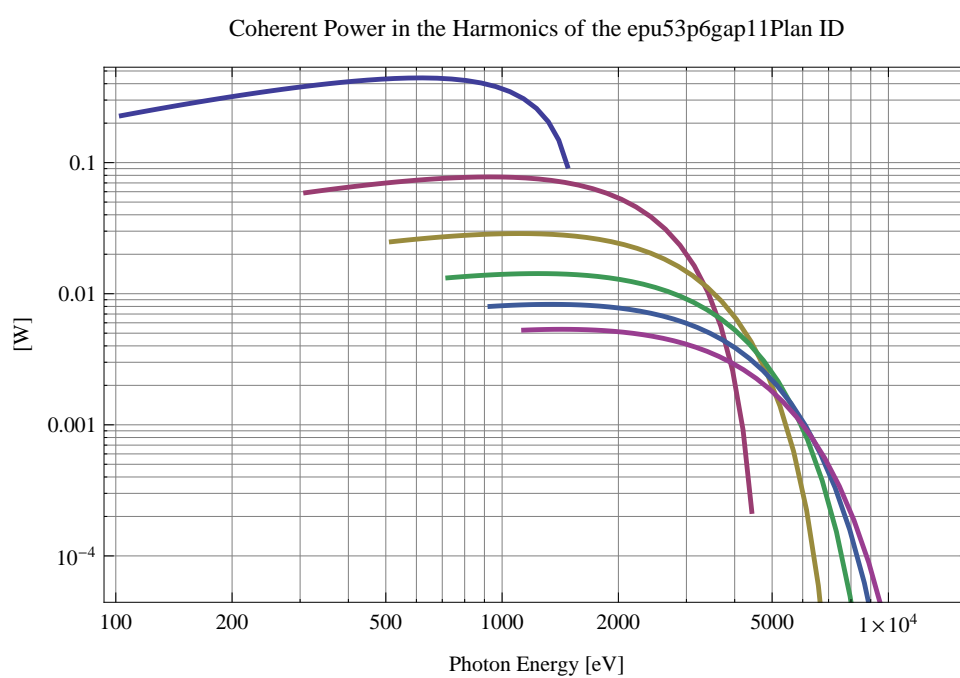


Figure 307: The power of coherent synchrotron radiation in the harmonics of the epu53p6gap11Plan ID

The brilliance at peak energy and the angular spectral flux density from the epu53p6gap11Plan ID for different harmonics at maximum K-value (5.372) are given in Table 51 and for minimum K-value (0.400) these values are given in Table 52.

Table 51: The brilliance at peak energy and the angular spectral flux density from the epu53p6gap11Plan ID for different harmonics at maximum K-value (5.372)

Harmonic	Photon Energy [eV]	Brilliance [Ph./((smrad ² mrads ² 0.1%BW))]	Angular Spectral Flux [Ph./((smrad ² 0.1%BW))]
1	103.357	2.8×10^{19}	1.86×10^{17}
3	310.071	6.5×10^{19}	2.49×10^{17}
5	516.785	7.63×10^{19}	2.38×10^{17}
7	723.498	7.93×10^{19}	2.2×10^{17}
9	930.212	7.94×10^{19}	2.03×10^{17}
11	1136.93	7.82×10^{19}	1.89×10^{17}

Table 52: The brilliance at peak energy and the angular spectral flux density from the epu53p6gap11Plan ID for different harmonics at minimum K-value (0.4)

Harmonic	Photon Energy [eV]	Brilliance [Ph./((smrad ² mrads ² 0.1%BW))]	Angular Spectral Flux [Ph./((smrad ² 0.1%BW))]
1	1476.43	1.65×10^{20}	3.68×10^{17}
3	4429.29	3.44×10^{18}	6.45×10^{15}
5	7382.15	4.04×10^{16}	7.31×10^{13}
7	10335.	4.31×10^{14}	7.7×10^{11}
9	13287.9	4.47×10^{12}	7.93×10^9
11	16240.7	4.59×10^{10}	8.11×10^7

2.5.5 Magnet model of the elliptically polarising undulator epu53p6gap11Heli

The Radia [3] magnet model of the epu53p6gap11Heli ID is shown in Figure 308. The length of the magnet model is 446.587 mm. The magnetic material in the model is NdFeb with a remanence of 1.28 T, a material similar to VACODYM 776 TP from Vacuumschmelze. Blocks with vertical magnetisation are blue and blocks with horizontal magnetisation are yellow. The block size is 30.x30.x13.4 mm³ and there is a 5. mm cut-out in two of the corners of the blocks. The total length of the epu53p6gap11Heli ID is 3930.59 mm.

2.5.6 Analysis of the magnetic field of the epu53p6gap11Heli ID

The effective magnetic fields on axis and the fundamental photon energy of the epu53p6gap11Heli ID are shown in Table 53. The higher harmonic contents in the magnetic field of an elliptically polarising undulator made of permanent magnets is negligible and the effective field has about the same strength as the peak field.

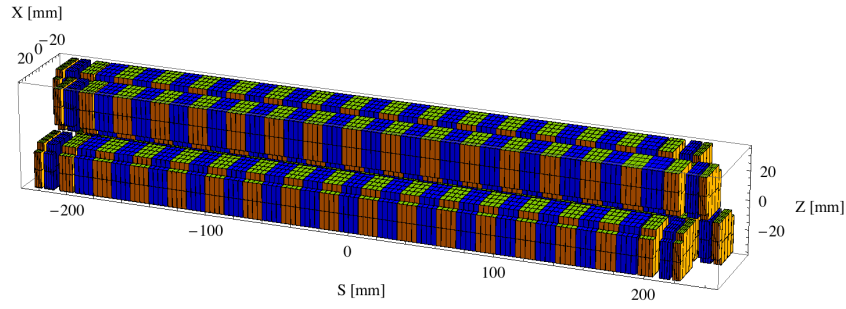


Figure 308: Magnetic model of the epu53p6gap11Heli ID. The ID has been modelled with Radia [3]

Table 53: Effective Fields on axis and Fundamental Photon Energy of the epu53p6gap11Heli ID

Undulator Period	53.6	mm
Undulator Gap	11	mm
Undulator Mode	Helical	
Undulator Phase	15.671	mm
Vertical Peak Field	0.646	T
Effective Vertical Field	0.647	T
K _x (from vert. field)	3.239	
Horizontal Peak Field:	0.652	T
Effective Horizontal Field	0.647	T
K _z (from hor. field)	3.239	
Photon Energy, Harm.1	0.139	keV
Emitted Power	9.369	kW
Total Length	3930.6	mm

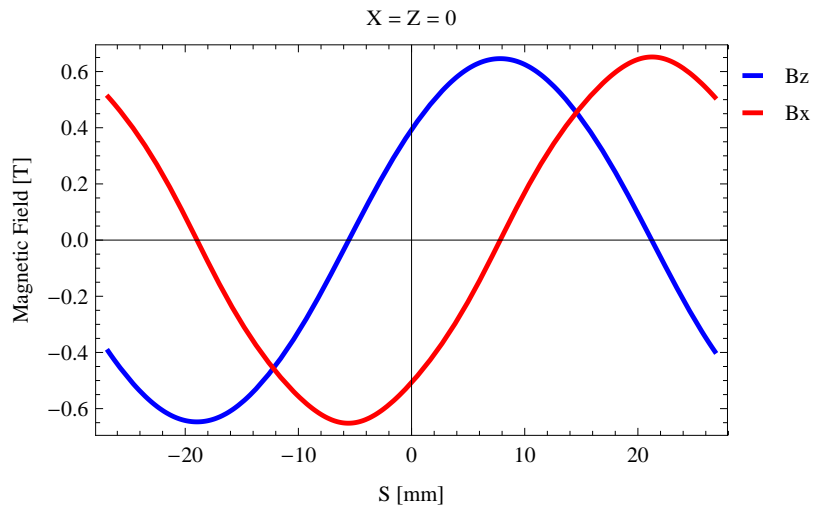


Figure 309: Vertical magnetic field in a central pole of the epu53p6gap11Heli ID along the ID axis, $X = Z = 0$

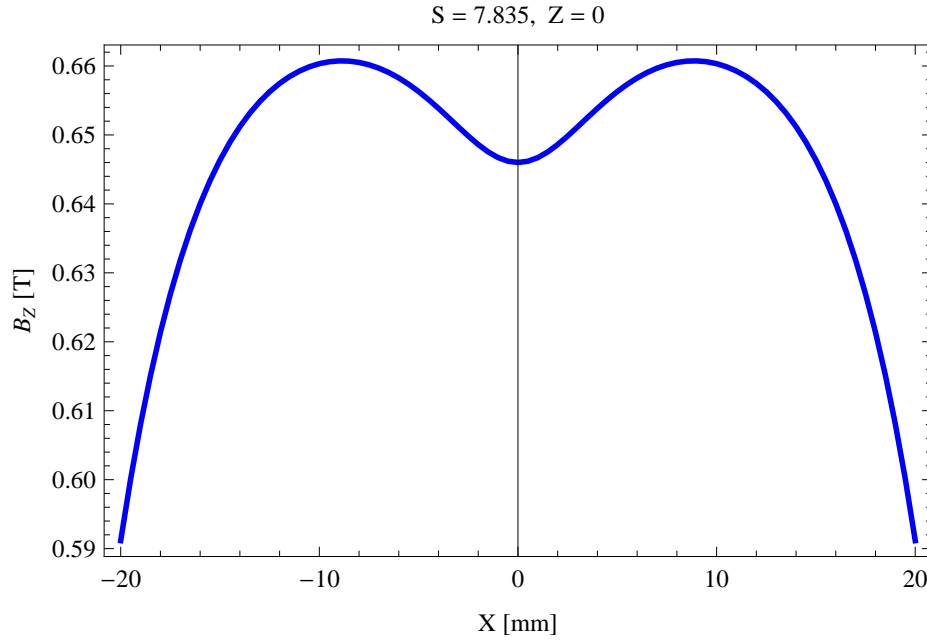


Figure 310: Vertical magnetic field in a central pole of the epu53p6gap11Heli ID along the horizontally transverse direction to the ID axis, $S = 7.835$, $Z = 0$

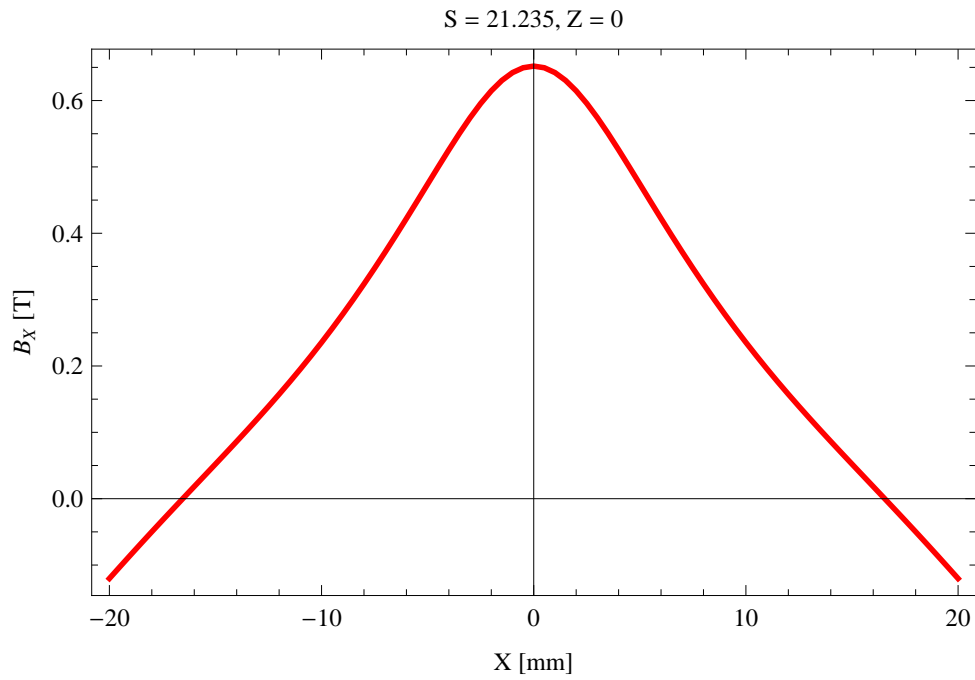


Figure 311: Horizontal magnetic field in a central pole of the epu53p6gap11Heli ID along the horizontally transverse direction to the ID axis, $S = 21.235$, $Z = 0$

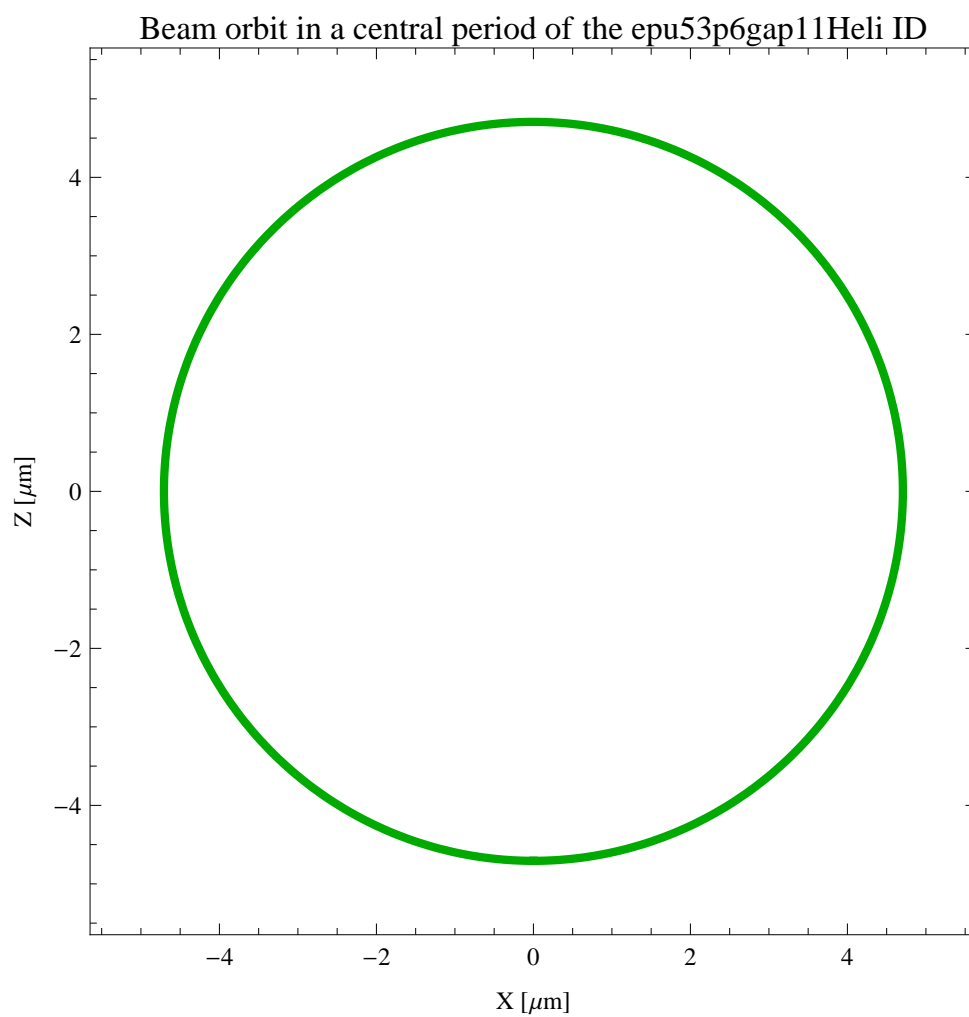


Figure 312: The beam orbit of the electron beam through a central period of the epu53p6gap11Heli ID

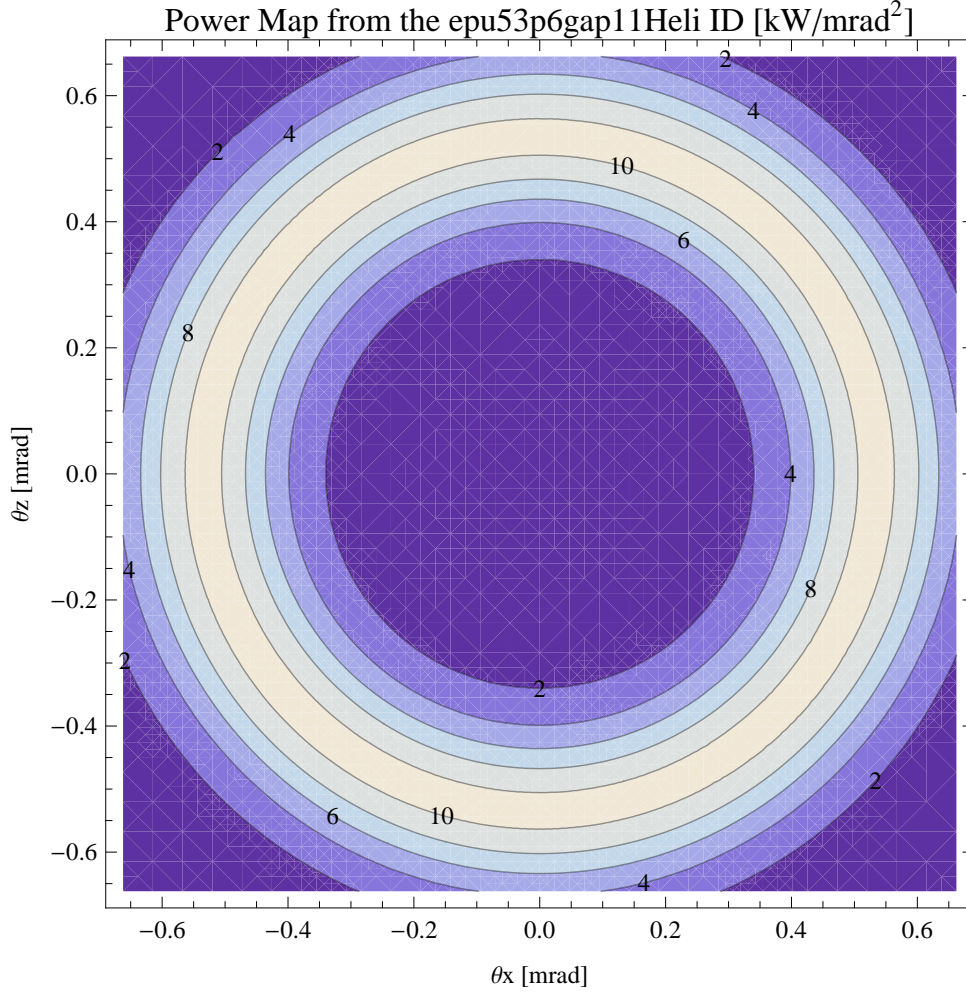


Figure 313: Map of the power distribution of the emitted synchrotron radiation by the epu53p6gap11Heli ID

2.5.7 Synchrotron radiation from the epu53p6gap11Heli ID

The power map of the emitted synchrotron radiation by the epu53p6gap11Heli ID, assuming a 0.5 A filament beam with an energy of 3 GeV and undulator properties of the synchrotron radiation, is shown in Figure 313. The on-axis power density is 0.200 kW/mrad²

A map of the degree of linear polarisation of the fundamental harmonic of the synchrotron radiation emitted by the epu53p6gap11Heli ID over the angle of observation is shown in Figure 314.

A map of the degree of 45 degree polarisation of the fundamental harmonic of the synchrotron radiation emitted by the epu53p6gap11Heli ID over the angle of observation is shown in Figure 315.

A map of the degree of circular polarisation of the fundamental harmonic of the synchrotron radiation emitted by the epu53p6gap11Heli ID over the angle of observation is shown in Figure 316.

The on axis brilliance at peak energy and the angular spectral flux from the epu53p6gap11Heli ID have been calculated with the given beam parameters, which are 0.5 A of stored current, $\beta_H = 9$ m, $\varepsilon_H = 0.263$ nmrad, $\beta_V = 4.8$ m, $\varepsilon_V = 8$. pmrad, and an energy spread of 0.001.

Degree of Linear Polarisation in Harm.1 from the epu53p6gap11Heli ID

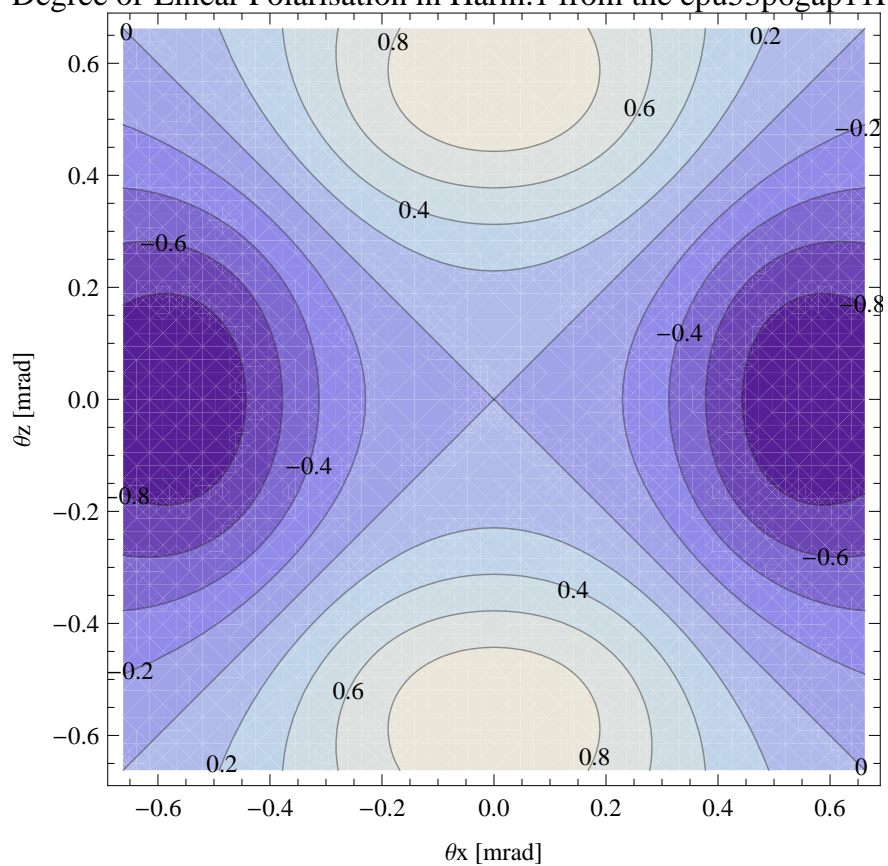


Figure 314: Map of linear polarisation in the fundamental harmonic of the synchrotron radiation emitted by the epu53p6gap11Heli ID

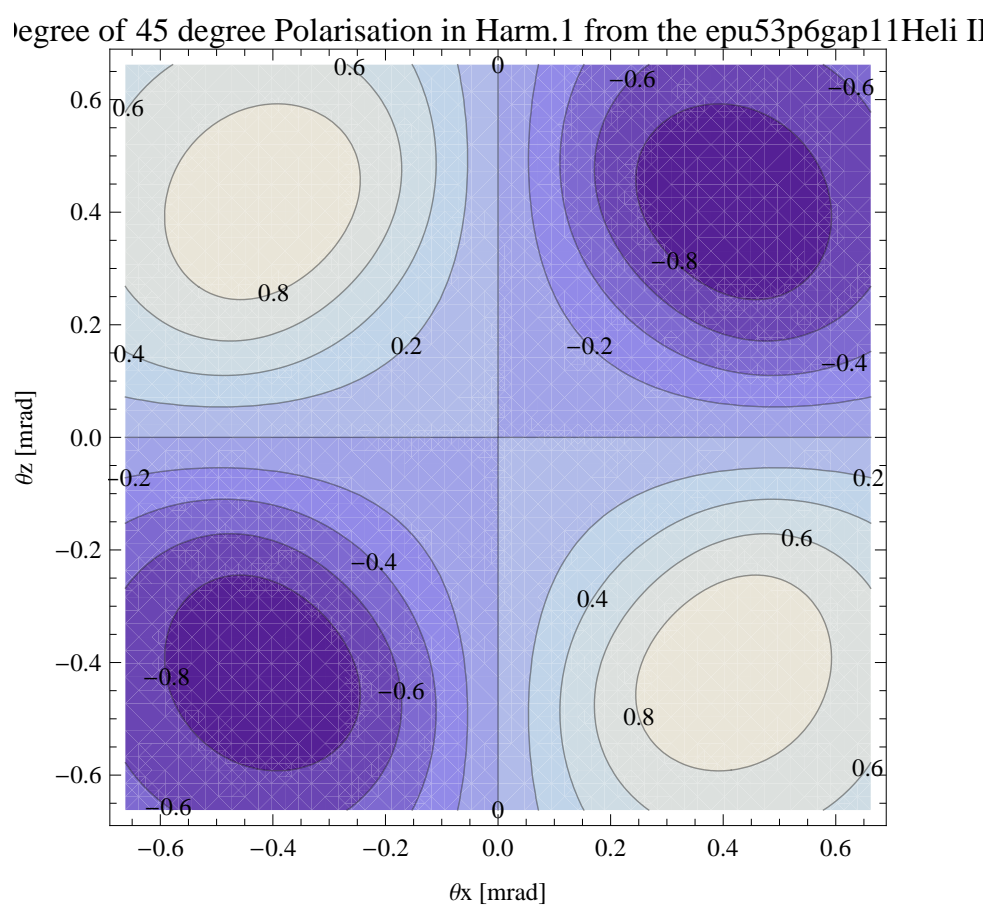


Figure 315: Map of 45 degree polarisation in the fundamental harmonic of the synchrotron radiation emitted by the epu53p6gap11Heli ID

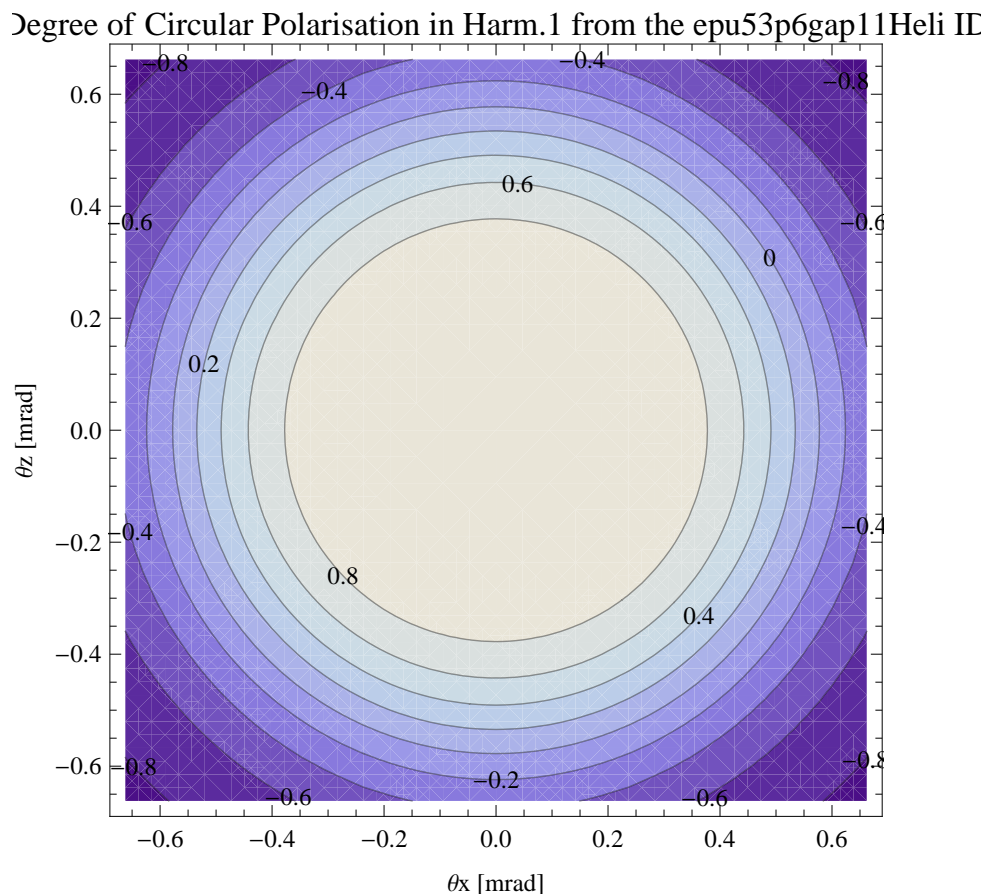


Figure 316: Map of circular polarisation in the fundamental harmonic of the synchrotron radiation emitted by the epu53p6gap11Heli ID

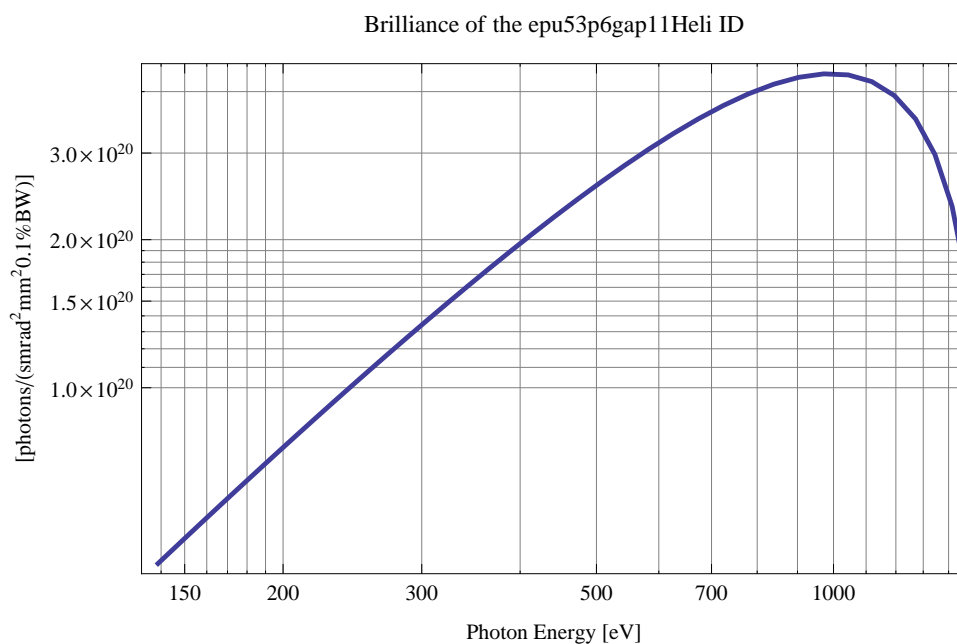


Figure 317: The brilliance at peak energy of the synchrotron radiation emitted by the epu53p6gap11Heli ID

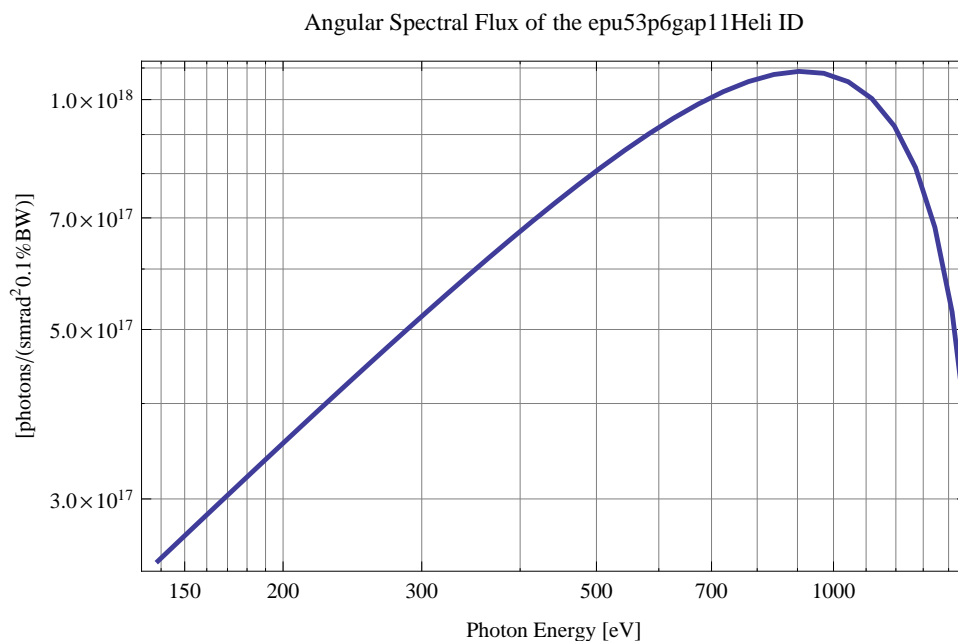


Figure 318: The angular spectral flux of the synchrotron radiation emitted by the epu53p6gap11Heli ID

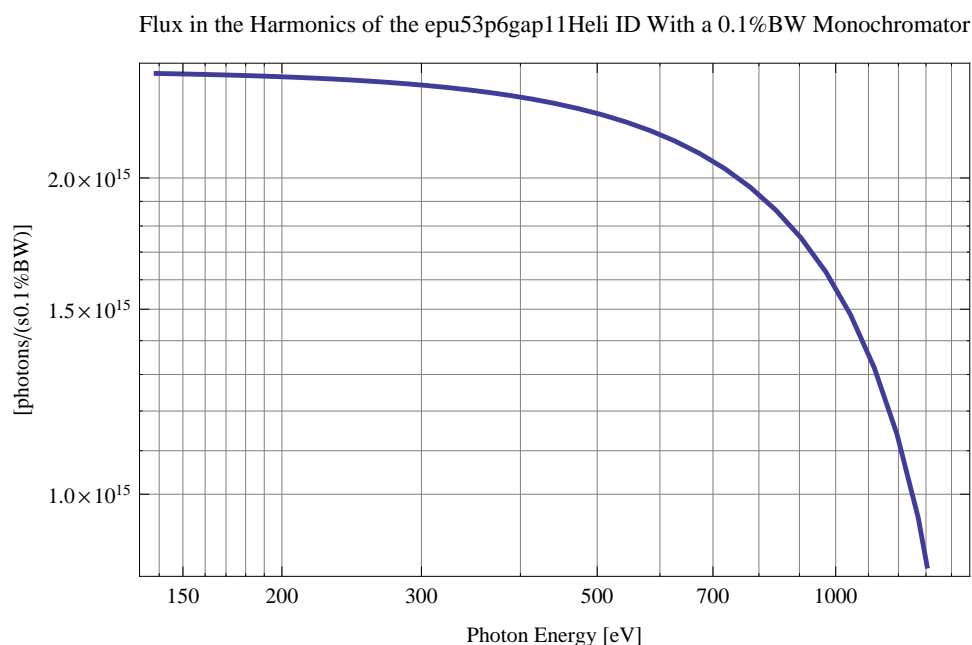


Figure 319: The flux of photons in the harmonics of the emitted synchrotron radiation from the epu53p6gap11Heli ID using a 0.1%BW monochromator

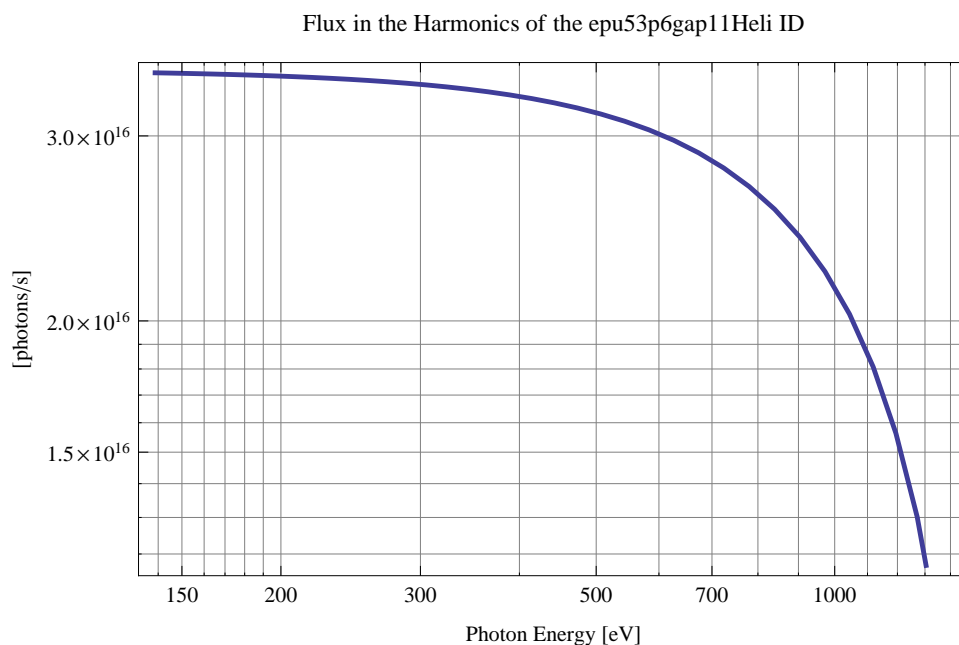


Figure 320: The flux of photons in the harmonics of the emitted synchrotron radiation from the epu53p6gap11Heli ID

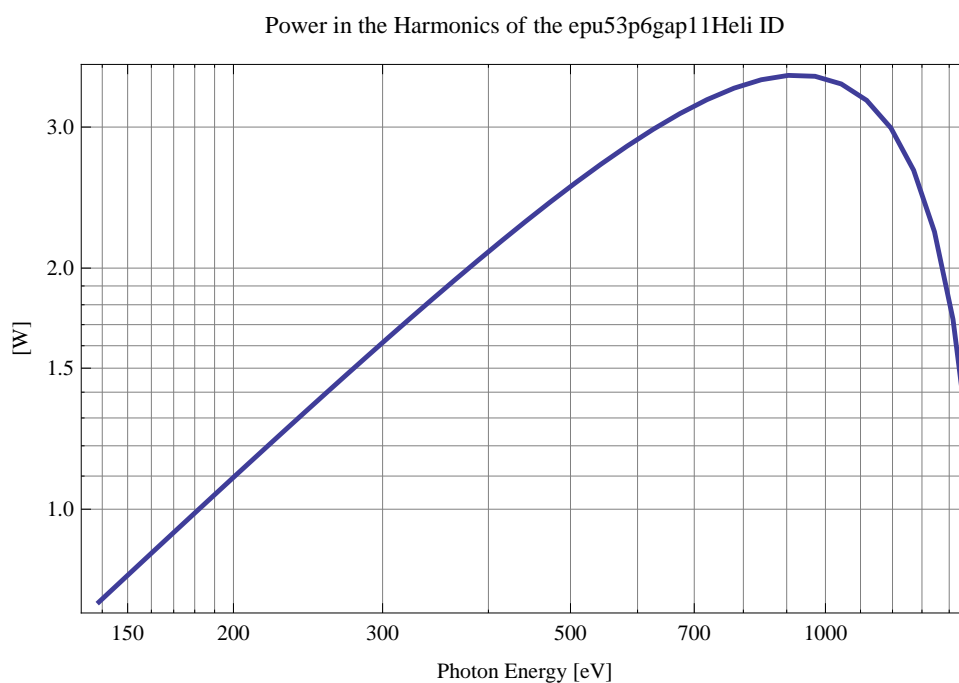


Figure 321: The power in the harmonics of the emitted synchrotron radiation from the epu53p6gap11Heli ID

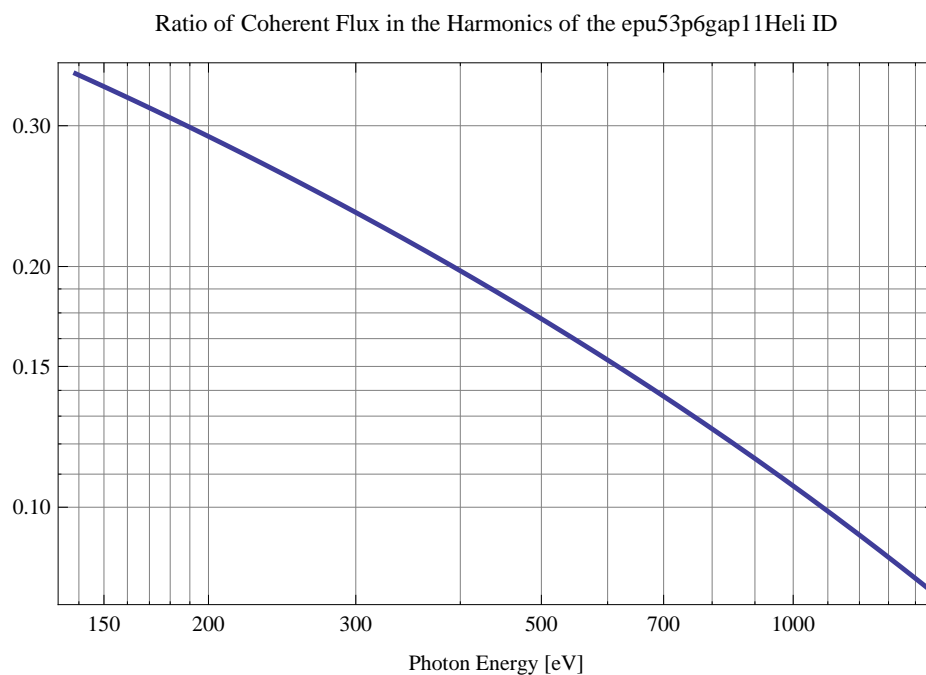


Figure 322: The ratio of coherent flux in the harmonics of the emitted synchrotron radiation from the epu53p6gap11Heli ID

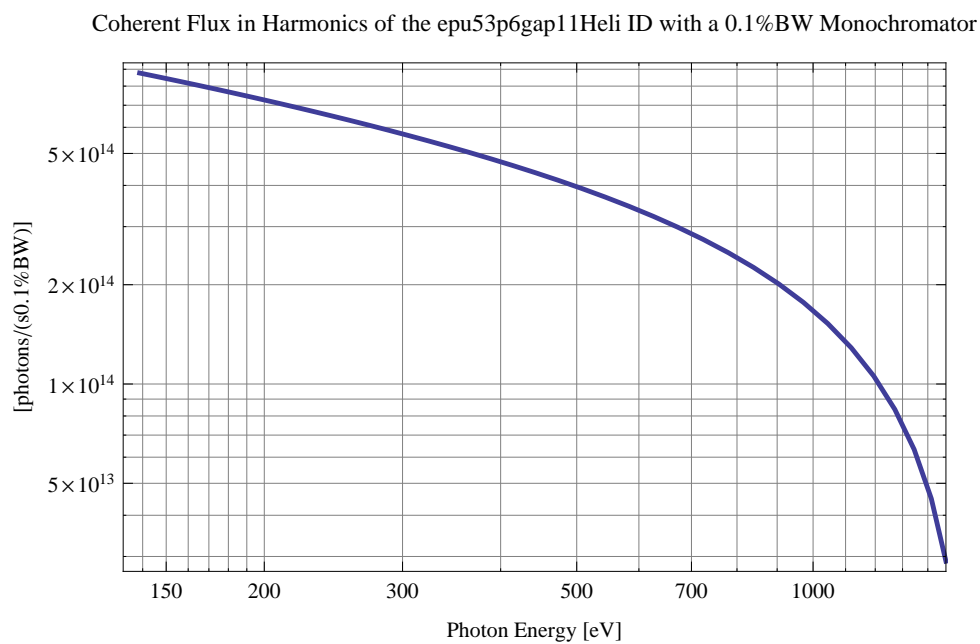


Figure 323: The coherent flux in the harmonics of the epu53p6gap11Heli ID using a 0.1%BW Monochromator

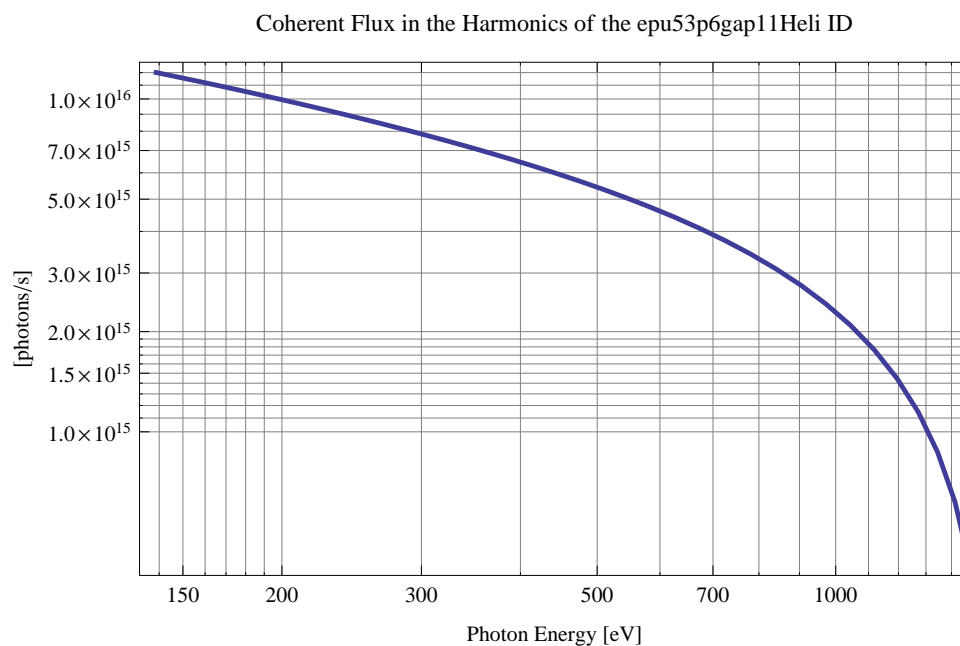


Figure 324: The coherent flux in the harmonics of the epu53p6gap11Heli ID

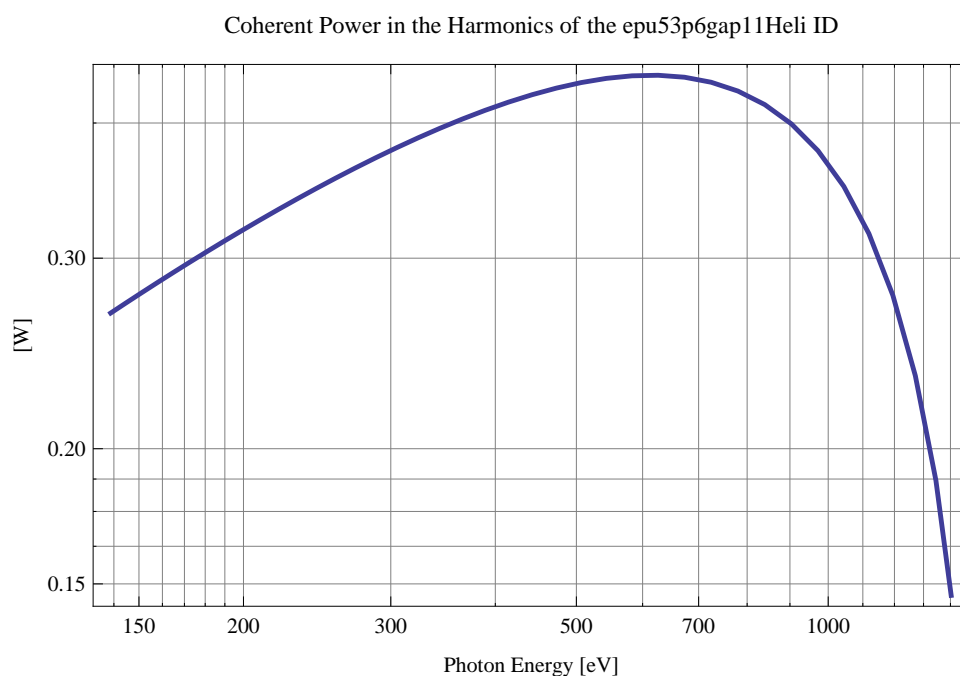


Figure 325: The power of coherent synchrotron radiation in the harmonics of the epu53p6gap11Heli ID

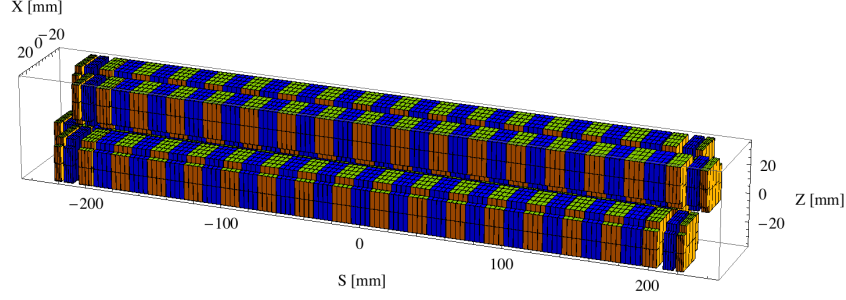


Figure 326: Magnetic model of the epu53p6gap11Incl ID. The ID has been modelled with Radia [3]

The brilliance at peak energy and the angular spectral flux density from the epu53p6gap11Heli ID for different harmonics at maximum K-value (4.581) are given in Table 54 and for minimum K-value (0.400) these values are given in Table 55.

Table 54: The brilliance at peak energy and the angular spectral flux density from the epu53p6gap11Heli ID for different harmonics at maximum K-value (4.581)

Harmonic	Photon Energy [eV]	Brilliance [Ph./ (smrad ² mrad ² 0.1%BW)]	Angular Spectral Flux [Ph./ (smrad ² 0.1%BW)]
1	138.76	4.39×10^{19}	2.49×10^{17}

Table 55: The brilliance at peak energy and the angular spectral flux density from the epu53p6gap11Heli ID for different harmonics at minimum K-value (0.4)

Harmonic	Photon Energy [eV]	Brilliance [Ph./ (smrad ² mrad ² 0.1%BW)]	Angular Spectral Flux [Ph./ (smrad ² 0.1%BW)]
1	1476.43	1.65×10^{20}	3.68×10^{17}

2.5.8 Magnet model of the elliptically polaraising undulator epu53p6gap11Incl

The Radia [3] magnet model of the epu53p6gap11Incl ID is shown in Figure 326. The length of the magnet model is 446.587 mm. The magnetic material in the model is NdFeb with a remanence of 1.28 T, a meterial similar to VACODYM 776 TP from Vacuumschmelze. Blocks with vertical magnetisation are blue and blocks with horizontal magnetisation are yellow. The block size is 30.x30.x13.4 mm³ and there is a 5. mm cut-out in two of the corners of the blocks. The total length of the epu53p6gap11Incl ID is 3930.59 mm.

2.5.9 Analysis of the magnetic field of the epu53p6gap11Incl ID

The effective magnetic fields on axis and the fundamental photon energy of the epu53p6gap11Incl ID are shown in Table 56. The higher harmonic contents in the magnetic field of an elliptically

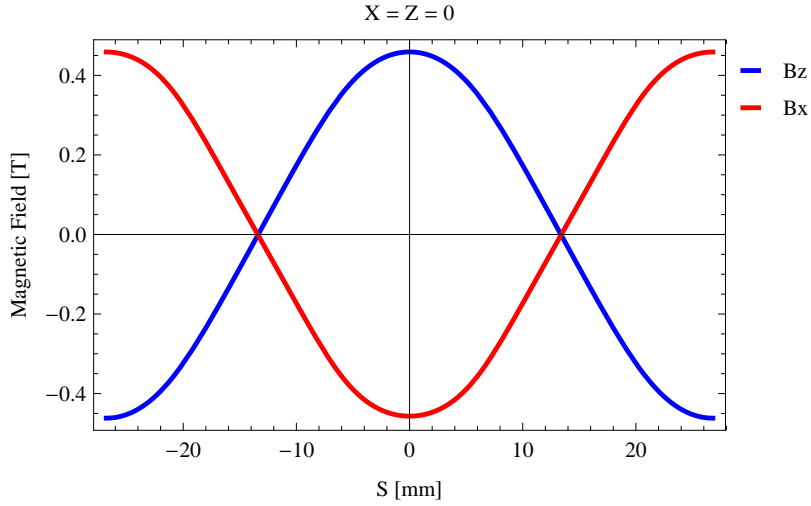


Figure 327: Vertical magnetic field in a central pole of the epu53p6gap11Incl ID along the ID axis, $X = Z = 0$

polarising undulator made of permanent magnets is negligible and the effective field has about the same strength as the peak field.

Table 56: Effective Fields on axis and Fundamental Photon Energy of the epu53p6gap11Incl ID

Undulator Period	53.6	mm
Undulator Gap	11	mm
Undulator Mode	Inclined	
Undulator Phase	14.546	mm
Vertical Peak Field	0.459	T
Effective Vertical Field	0.461	T
K _x (from vert. field)	2.308	
Horizontal Peak Field:	-0.457	T
Effective Horizontal Field	0.462	T
K _z (from hor. field)	2.313	
Photon Energy, Harm.1	0.252	keV
Emitted Power	4.767	kW
Total Length	3930.6	mm

2.5.10 Synchrotron radiation from the epu53p6gap11Incl ID

The power map of the emitted synchrotron radiation by the epu53p6gap11Incl ID, assuming a 0.5 A filament beam with an energy of 3 GeV and undulator properties of the synchrotron radiation, is shown in Figure 331. The on-axis power density is 20.489 kW/mrad²

A map of the degree of linear polarisation of the fundamental harmonic of the synchrotron radiation emitted by the epu53p6gap11Incl ID over the angle of observation is shown in Figure 332.

A map of the degree of 45 degree polarisation of the fundamental harmonic of the synchrotron radiation emitted by the epu53p6gap11Incl ID over the angle of observation is shown in Figure 333.

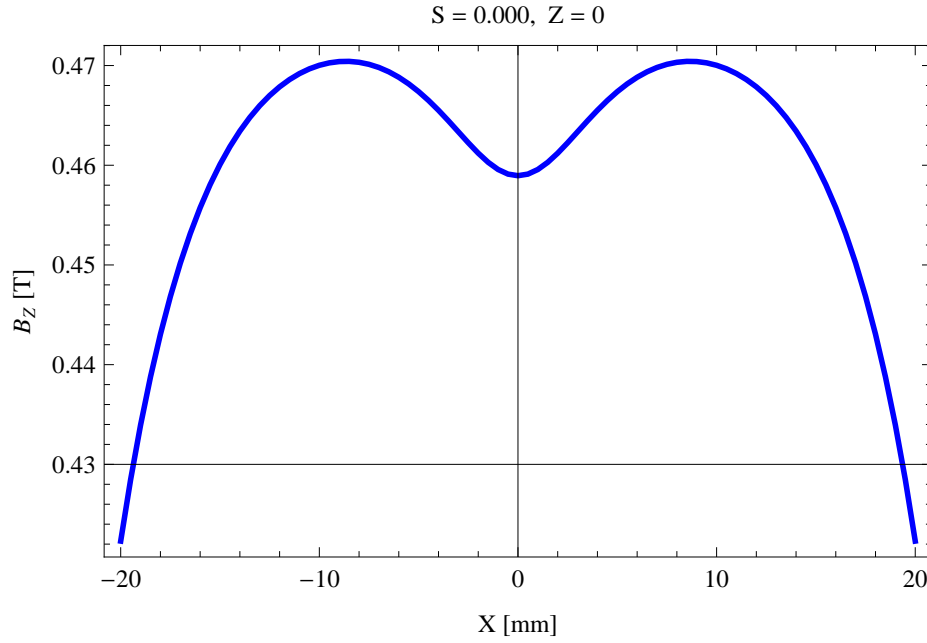


Figure 328: Vertical magnetic field in a central pole of the epu53p6gap11Incl ID along the horizontally transverse direction to the ID axis, $S = 0.000, Z = 0$

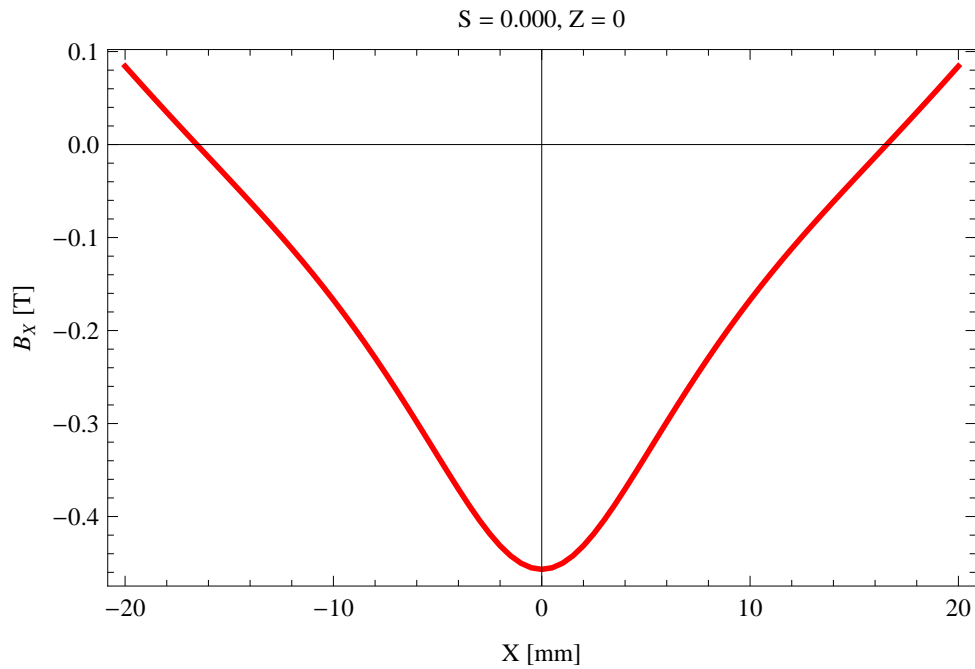


Figure 329: Horizontal magnetic field in a central pole of the epu53p6gap11Incl ID along the horizontally transverse direction to the ID axis, $S = 0.000, Z = 0$

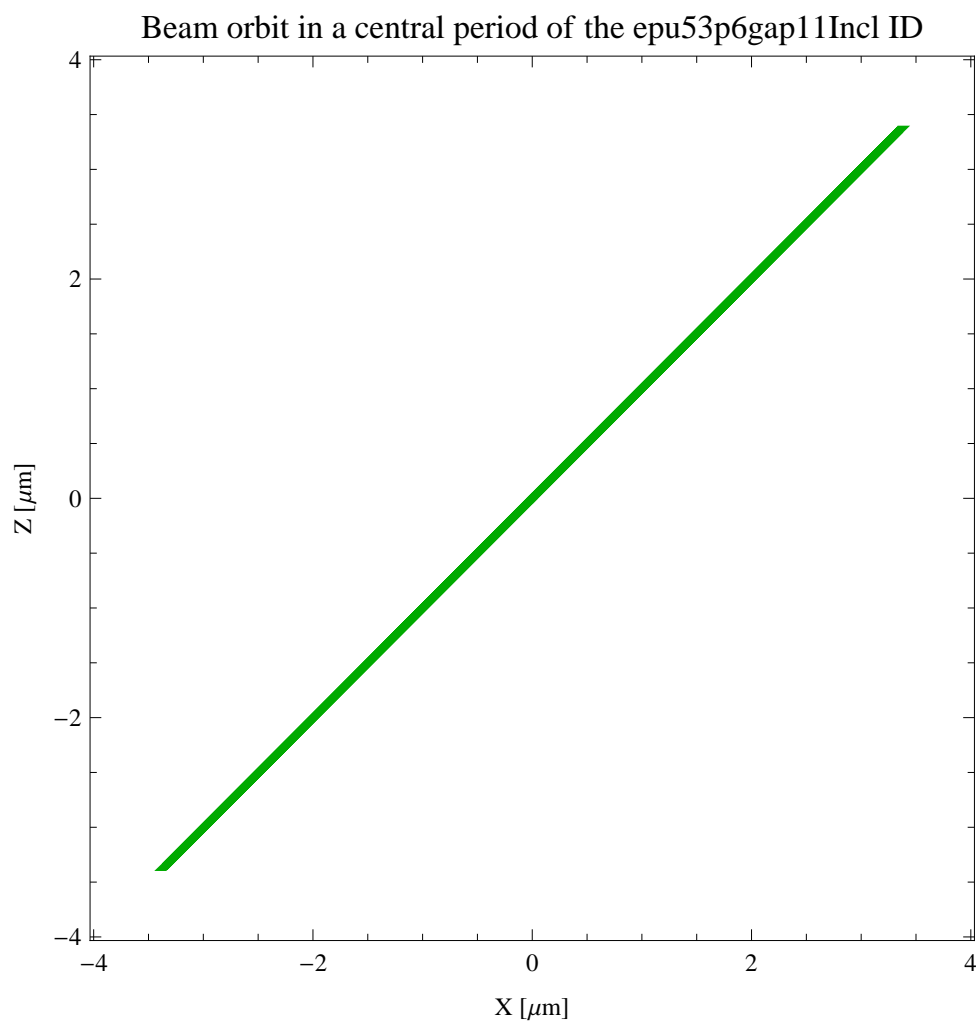


Figure 330: The beam orbit of the electron beam through a central period of the epu53p6gap11Incl ID

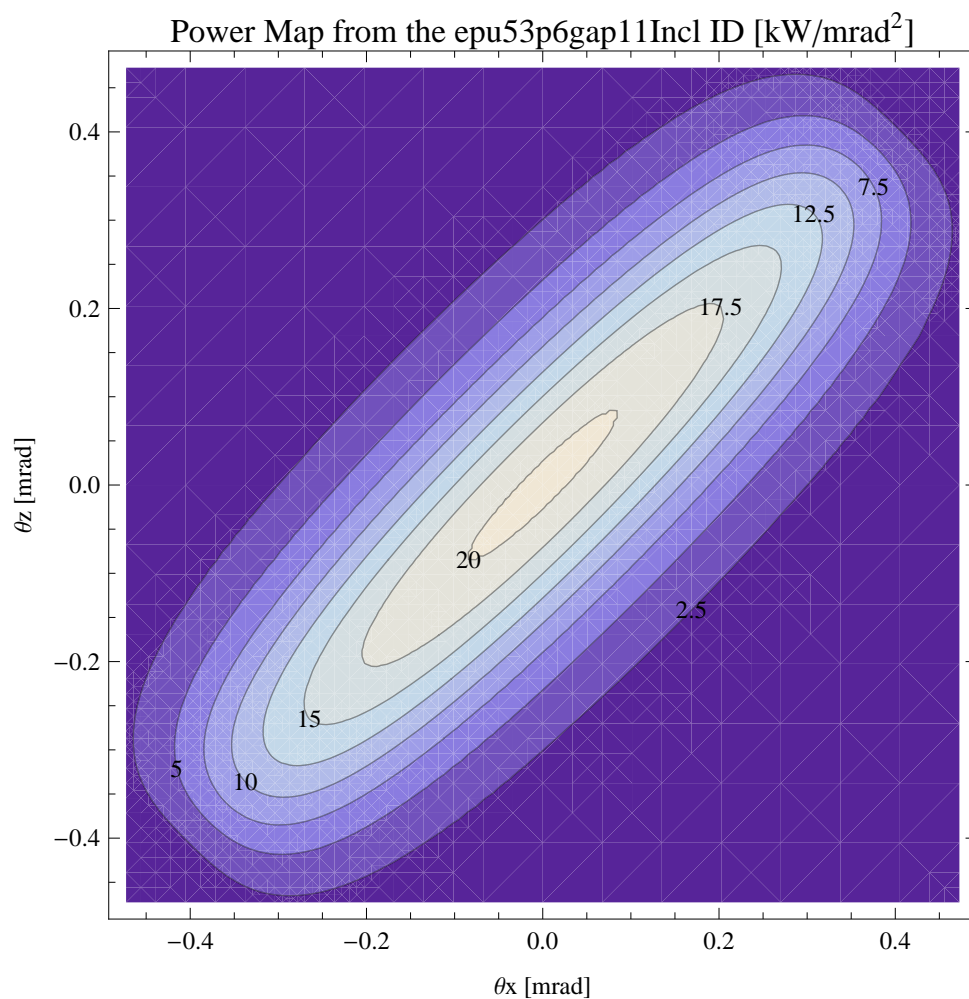


Figure 331: Map of the power distribution of the emitted synchrotron radiation by the epu53p6gap11Incl ID

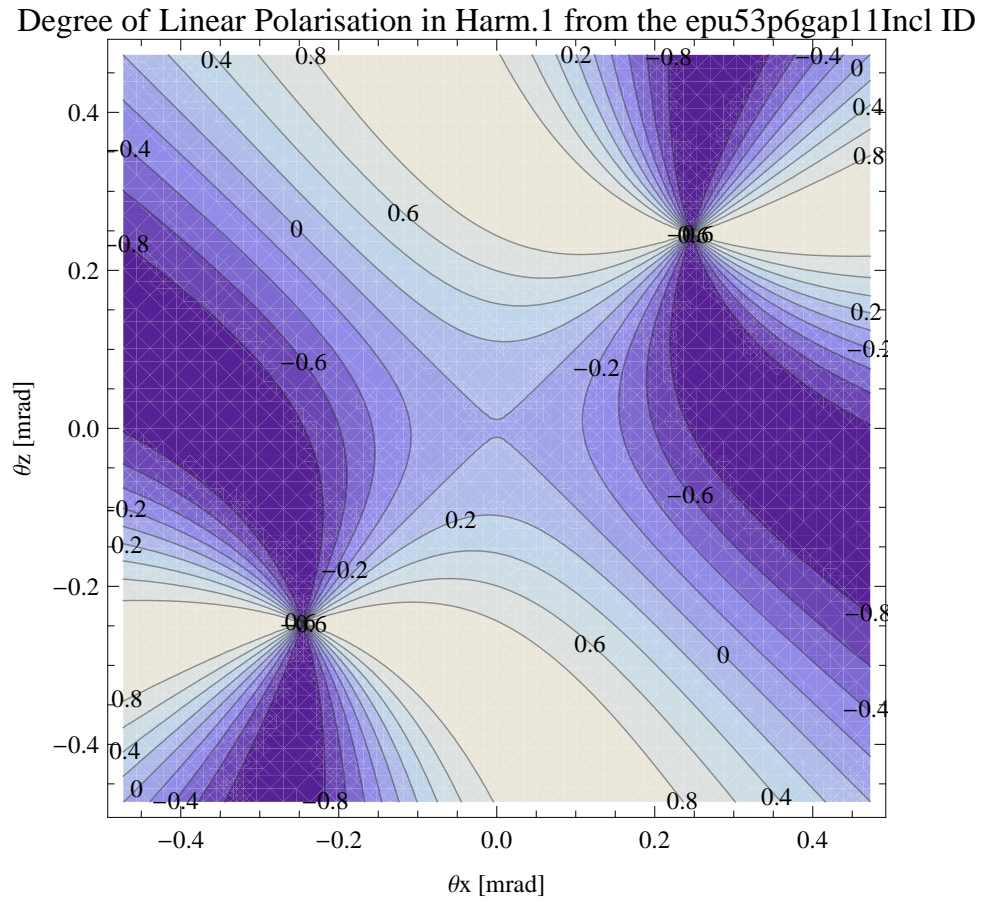


Figure 332: Map of linear polarisation in the fundamental harmonic of the synchrotron radiation emitted by the epu53p6gap11Incl ID

Degree of 45 degree Polarisation in Harm.1 from the epu53p6gap11Incl II

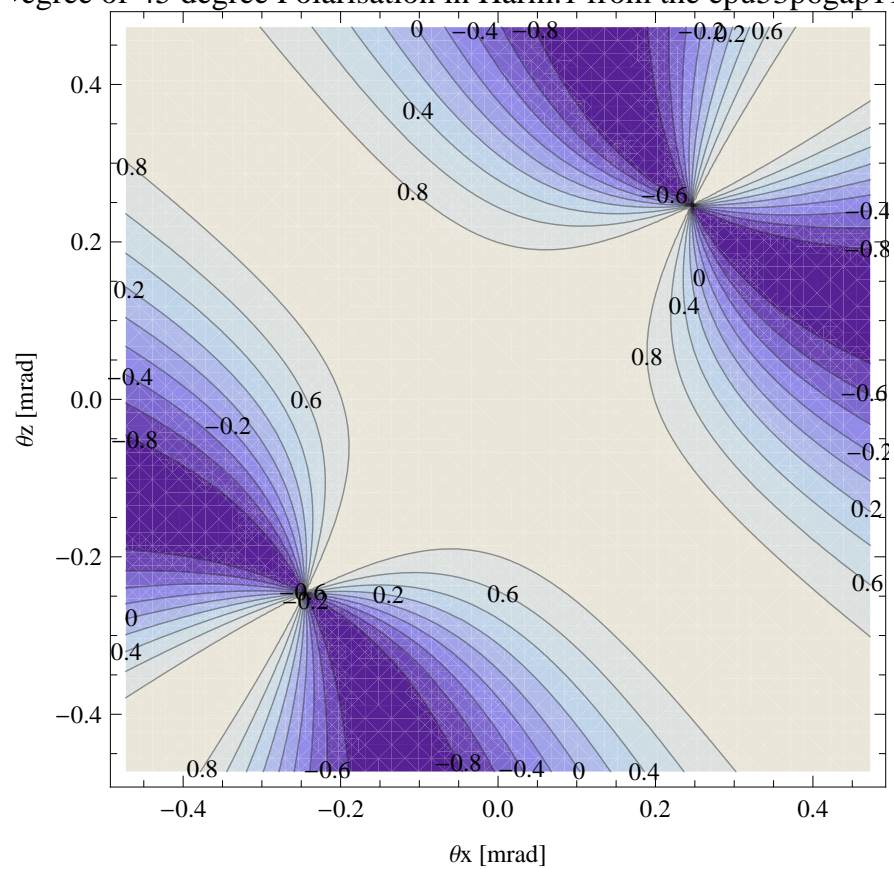


Figure 333: Map of 45 degree polarisation in the fundamental harmonic of the synchrotron radiation emitted by the epu53p6gap11Incl ID

Degree of Circular Polarisation in Harm.1 from the epu53p6gap11Incl ID

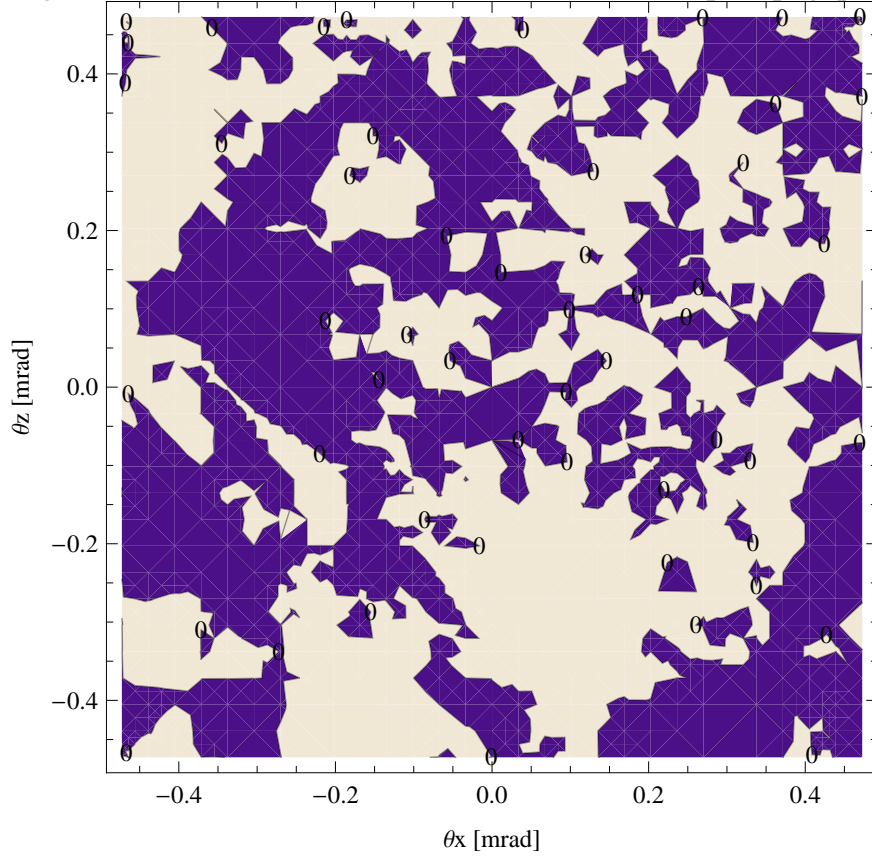


Figure 334: Map of circular polarisation in the fundamental harmonic of the synchrotron radiation emitted by the epu53p6gap11Incl ID

A map of the degree of circular polarisation of the fundamental harmonic of the synchrotron radiation emitted by the epu53p6gap11Incl ID over the angle of observation is shown in Figure 334.

The on axis brilliance at peak energy and the angular spectral flux from the epu53p6gap11Incl ID have been calculated with the given beam parameters, which are 0.5 A of stored current, $\beta_H = 9$ m, $\varepsilon_H = 0.263$ nmrad, $\beta_V = 4.8$ m, $\varepsilon_V = 8$. pmrad, and an energy spread of 0.001.

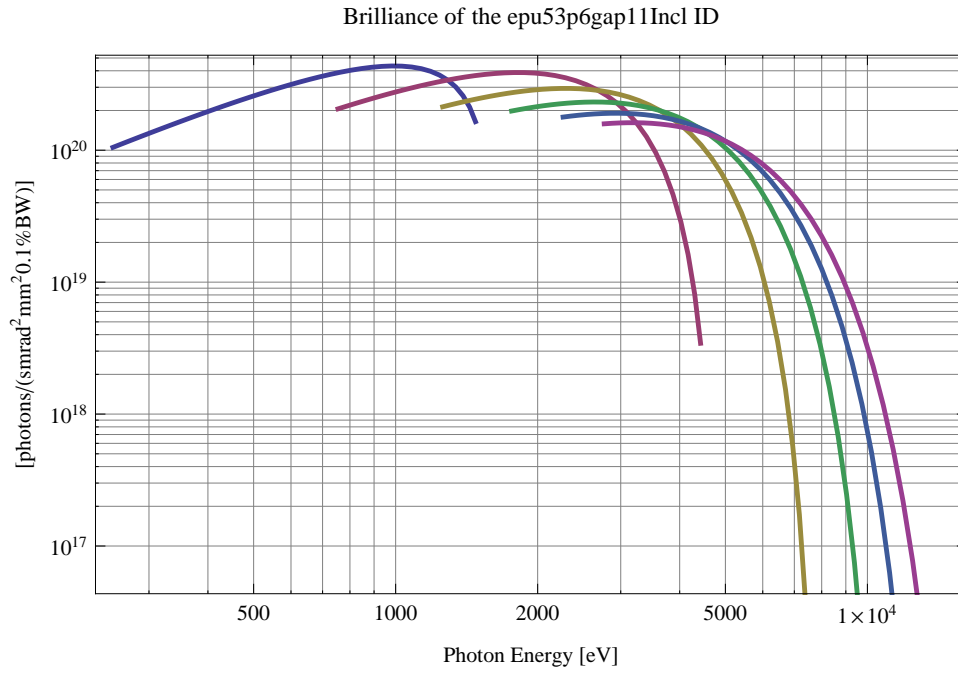


Figure 335: The brilliance at peak energy of the synchrotron radiation emitted by the epu53p6gap11Incl ID

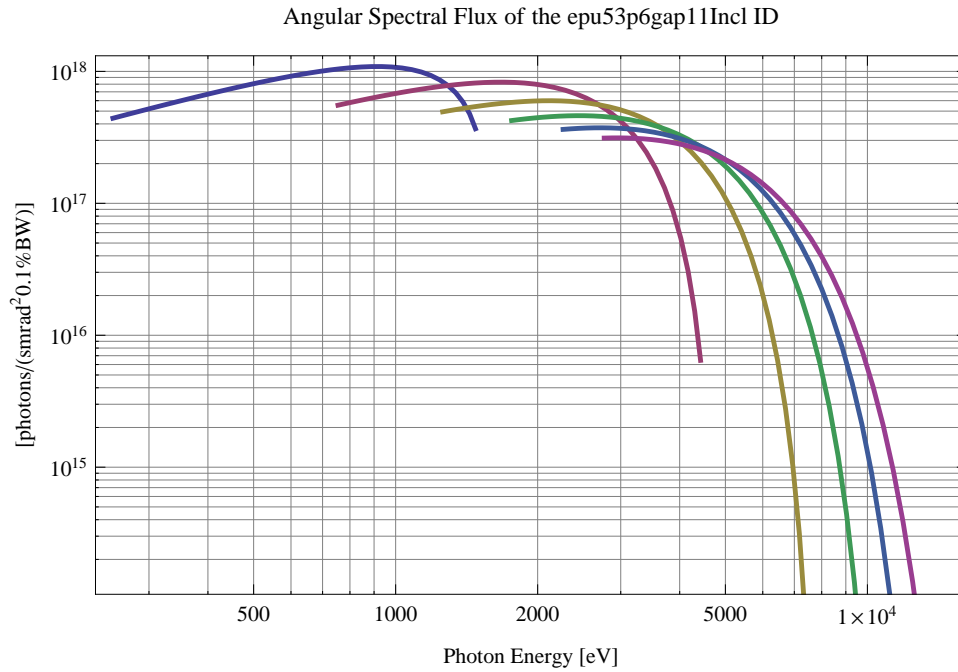


Figure 336: The angular spectral flux of the synchrotron radiation emitted by the epu53p6gap11Incl ID

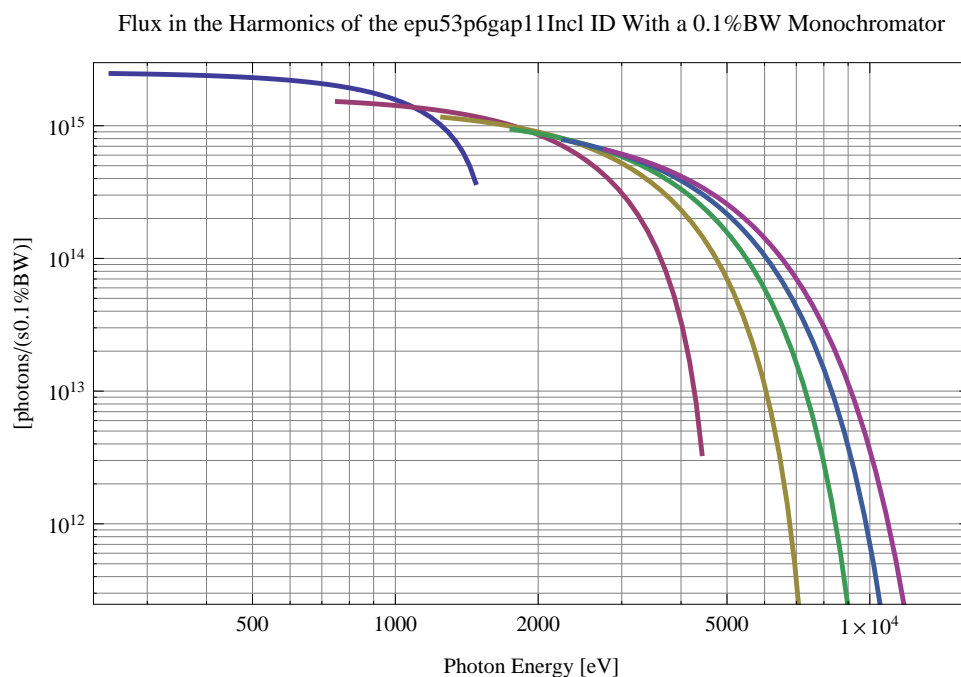


Figure 337: The flux of photons in the harmonics of the emitted synchrotron radiation from the epu53p6gap11Incl ID using a 0.1%BW monochromator

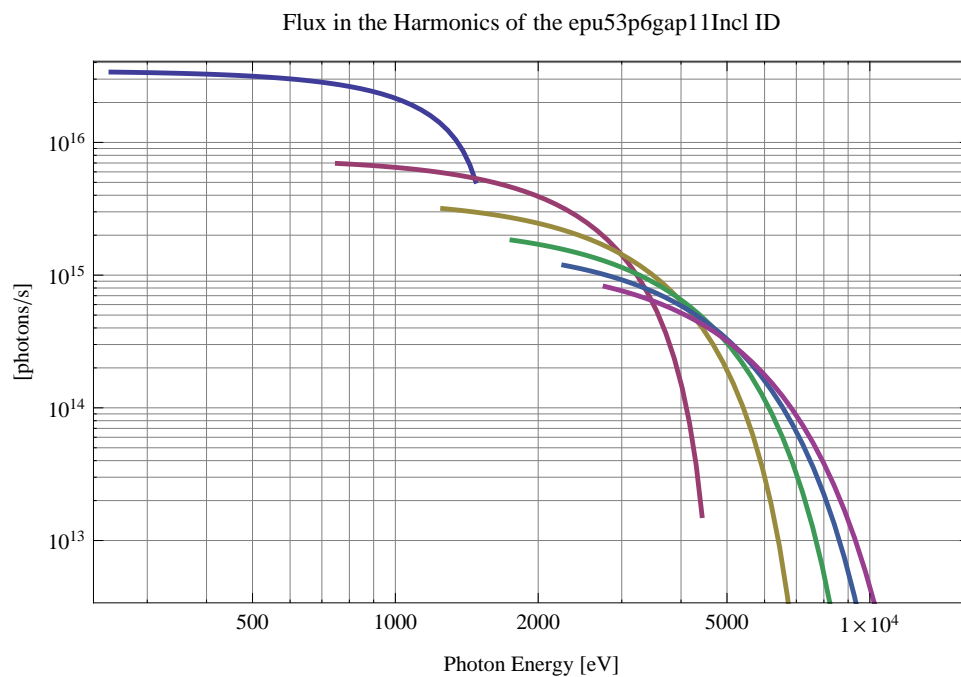


Figure 338: The flux of photons in the harmonics of the emitted synchrotron radiation from the epu53p6gap11Incl ID

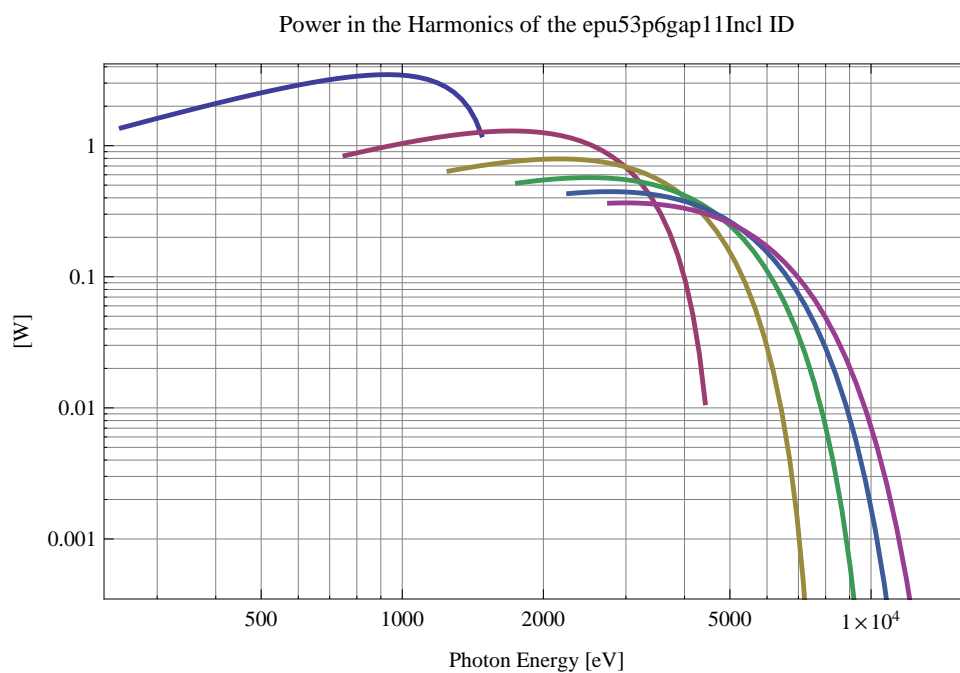


Figure 339: The power in the harmonics of the emitted synchrotron radiation from the epu53p6gap11Incl ID

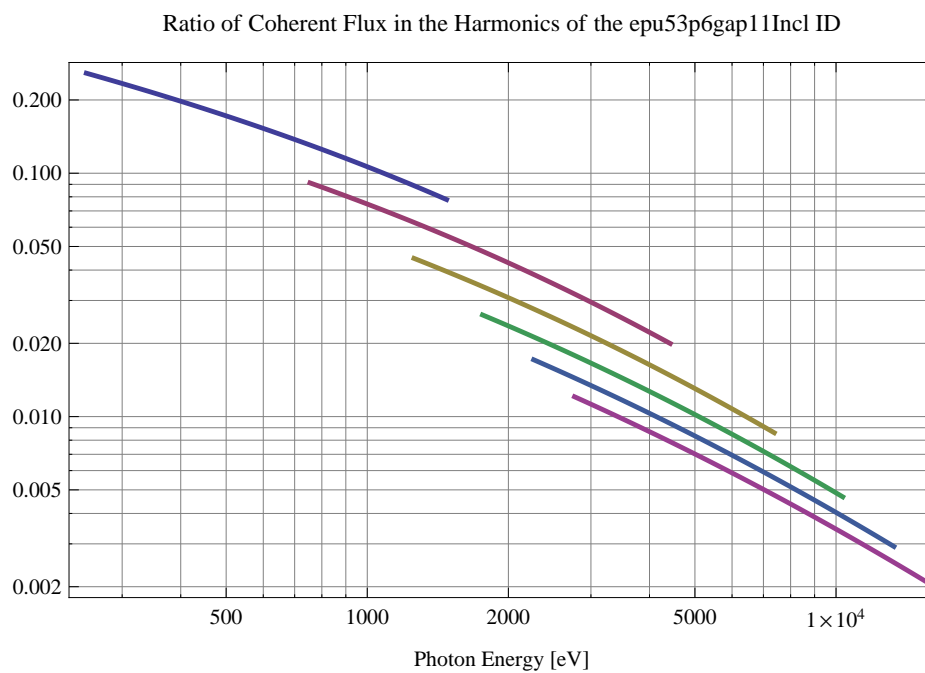


Figure 340: The ratio of coherent flux in the harmonics of the emitted synchrotron radiation from the epu53p6gap11Incl ID

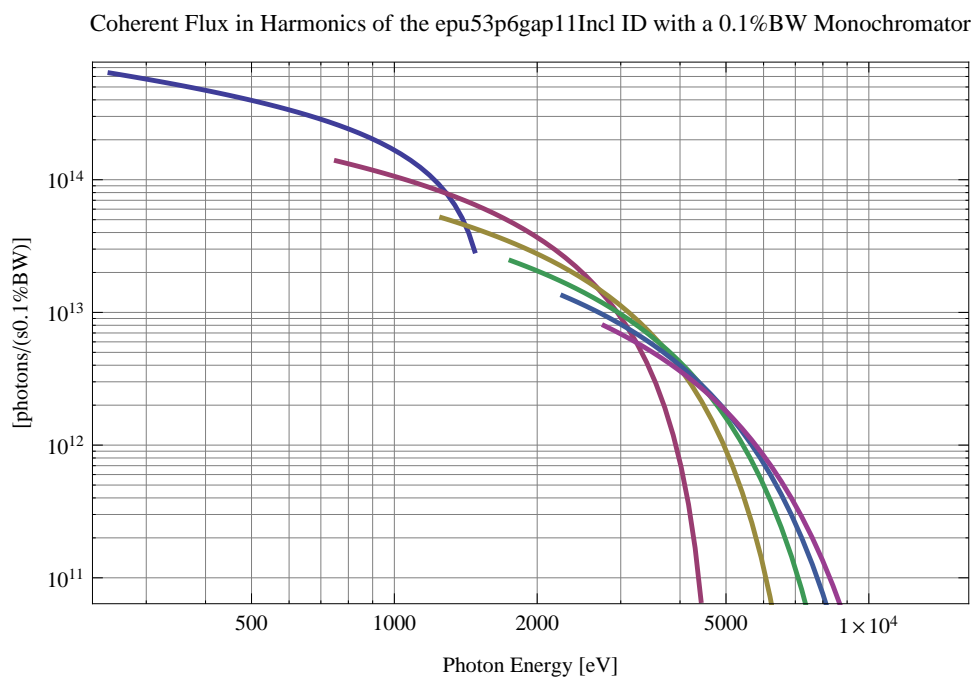


Figure 341: The coherent flux in the harmonics of the epu53p6gap11Incl ID using a 0.1%BW Monochromator

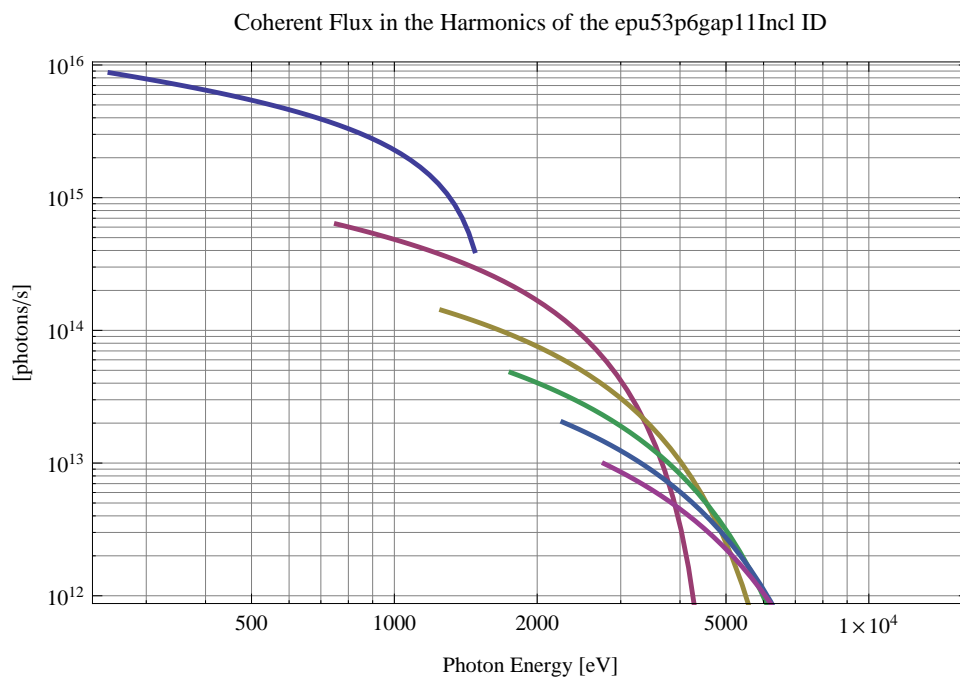


Figure 342: The coherent flux in the harmonics of the epu53p6gap11Incl ID

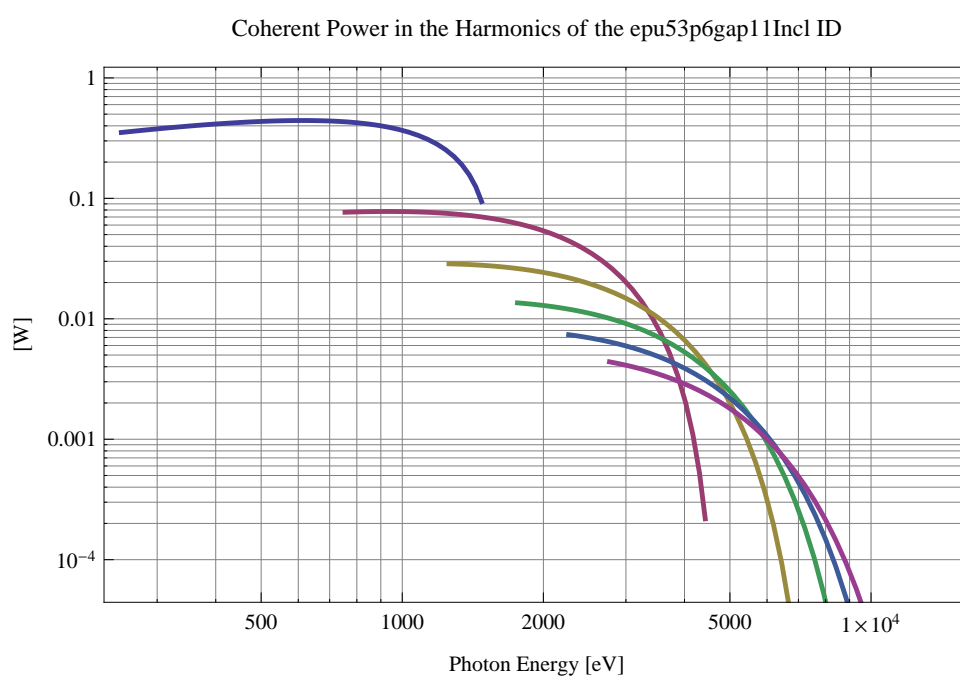


Figure 343: The power of coherent synchrotron radiation in the harmonics of the epu53p6gap11Incl ID

The brilliance at peak energy and the angular spectral flux density from the epu53p6gap11Incl ID for different harmonics at maximum K-value (3.267) are given in Table 57 and for minimum K-value (0.400) these values are given in Table 58.

Table 57: The brilliance at peak energy and the angular spectral flux density from the epu53p6gap11Incl ID for different harmonics at maximum K-value (3.267)

Harmonic	Photon Energy [eV]	Brilliance [Ph./ (smrad ² mrad ² 0.1% BW)]	Angular Spectral Flux [Ph./ (smrad ² 0.1% BW)]
1	251.59	1.05×10^{20}	4.42×10^{17}
3	754.771	2.06×10^{20}	5.54×10^{17}
5	1257.95	2.13×10^{20}	4.94×10^{17}
7	1761.13	1.98×10^{20}	4.24×10^{17}
9	2264.31	1.78×10^{20}	3.63×10^{17}
11	2767.49	1.59×10^{20}	3.12×10^{17}

Table 58: The brilliance at peak energy and the angular spectral flux density from the epu53p6gap11Incl ID for different harmonics at minimum K-value (0.4)

Harmonic	Photon Energy [eV]	Brilliance [Ph./ (smrad ² mrad ² 0.1% BW)]	Angular Spectral Flux [Ph./ (smrad ² 0.1% BW)]
1	1476.43	1.65×10^{20}	3.68×10^{17}
3	4429.29	3.44×10^{18}	6.45×10^{15}
5	7382.15	4.04×10^{16}	7.31×10^{13}
7	10335.	4.31×10^{14}	7.7×10^{11}
9	13287.9	4.47×10^{12}	7.93×10^9
11	16240.7	4.59×10^{10}	8.11×10^7

2.5.11 Magnet model of the elliptically polarising undulator epu53p6gap11Vert

The Radia [3] magnet model of the epu53p6gap11Vert ID is shown in Figure 344. The length of the magnet model is 446.587 mm. The magnetic material in the model is NdFeb with a remanence of 1.28 T, a material similar to VACODYM 776 TP from Vacuumschmelze. Blocks with vertical magnetisation are blue and blocks with horizontal magnetisation are yellow. The block size is 30.x30.x13.4 mm³ and there is a 5. mm cut-out in two of the corners of the blocks. The total length of the epu53p6gap11Vert ID is 3930.59 mm.

2.5.12 Analysis of the magnetic field of the epu53p6gap11Vert ID

The effective magnetic fields on axis and the fundamental photon energy of the epu53p6gap11Vert ID are shown in Table 59. The higher harmonic contents in the magnetic field of an elliptically polarising undulator made of permanent magnets is negligible and the effective field has about the same strength as the peak field.

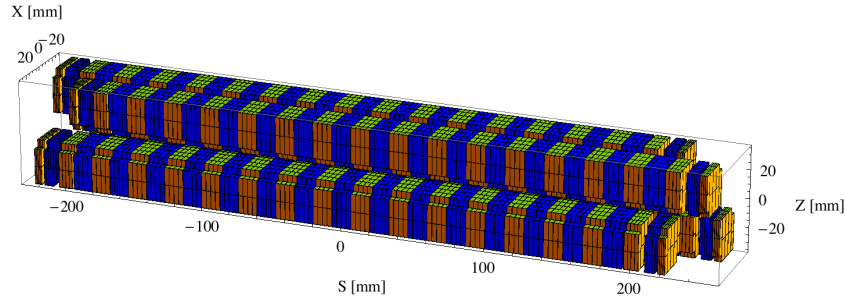


Figure 344: Magnetic model of the epu53p6gap11Vert ID. The ID has been modelled with Radia [3]

Table 59: Effective Fields on axis and Fundamental Photon Energy of the epu53p6gap11Vert ID

Undulator Period	53.6	mm
Undulator Gap	11	mm
Undulator Mode	Vertical	
Undulator Phase	26.800	mm
Vertical Peak Field	0.000	T
Effective Vertical Field	0.000	T
Kx (from vert. field)	0.000	
Horizontal Peak Field:	0.813	T
Effective Horizontal Field	0.814	T
Kz (from hor. field)	4.075	
Photon Energy, Harm.1	0.171	keV
Emitted Power	7.415	kW
Total Length	3930.6	mm

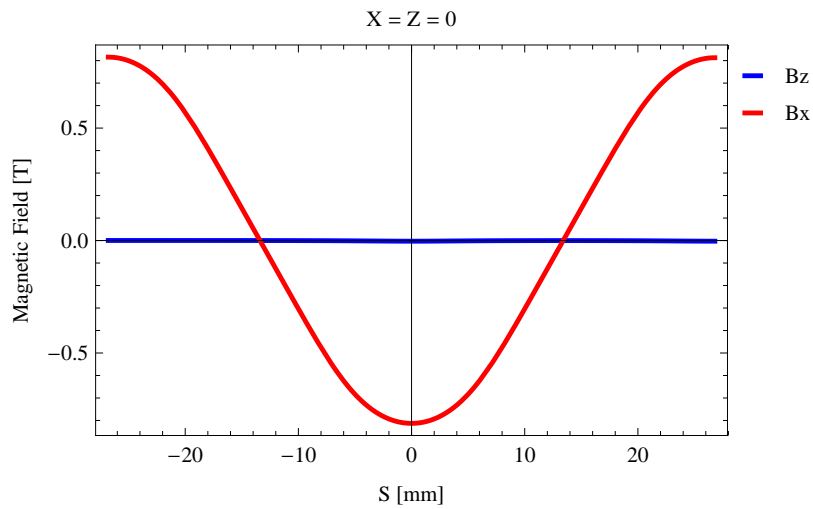


Figure 345: Vertical magnetic field in a central pole of the epu53p6gap11Vert ID along the ID axis, $X = Z = 0$

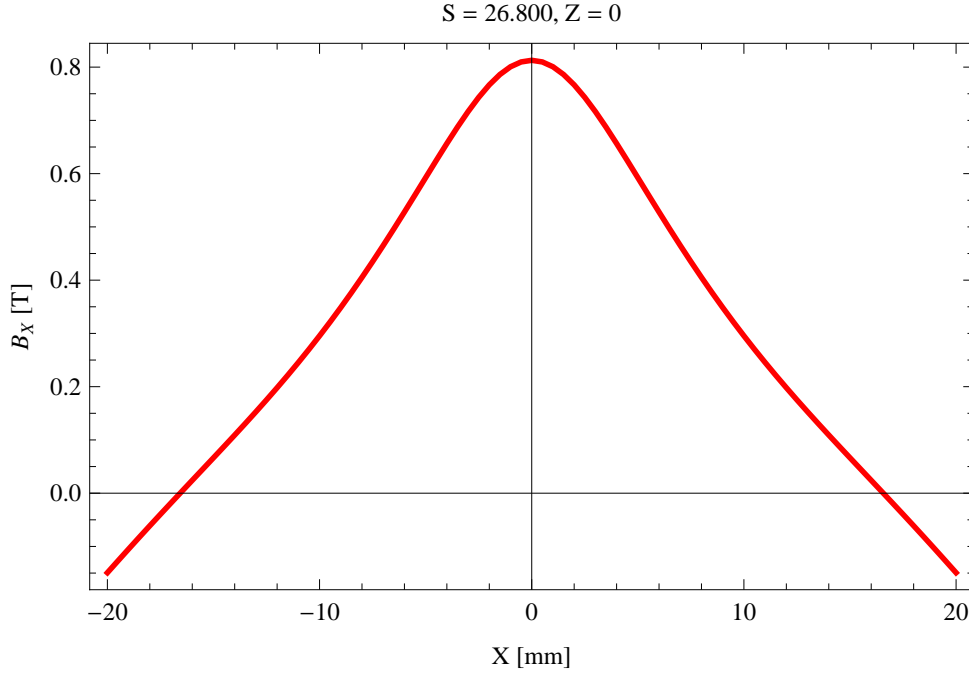


Figure 346: Horizontal magnetic field in a central pole of the epu53p6gap11Vert ID along the horizontally transverse direction to the ID axis, $S = 26.800$, $Z = 0$

2.5.13 Synchrotron radiation from the epu53p6gap11Vert ID

The power map of the emitted synchrotron radiation by the epu53p6gap11Vert ID, assuming a 0.5 A filament beam with an energy of 3 GeV and undulator properties of the synchrotron radiation, is shown in Figure 348. The on-axis power density is 25.622 kW/mrad^2

A map of the degree of linear polarisation of the fundamental harmonic of the synchrotron radiation emitted by the epu53p6gap11Vert ID over the angle of observation is shown in Figure 349.

A map of the degree of 45 degree polarisation of the fundamental harmonic of the synchrotron radiation emitted by the epu53p6gap11Vert ID over the angle of observation is shown in Figure 350.

A map of the degree of circular polarisation of the fundamental harmonic of the synchrotron radiation emitted by the epu53p6gap11Vert ID over the angle of observation is shown in Figure 351.

The on axis brilliance at peak energy and the angular spectral flux from the epu53p6gap11Vert ID have been calculated with the given beam parameters, which are 0.5 A of stored current, $\beta_H = 9 \text{ m}$, $\varepsilon_H = 0.263 \text{ nmrad}$, $\beta_V = 4.8 \text{ m}$, $\varepsilon_V = 8. \text{ pmrad}$, and an energy spread of 0.001.

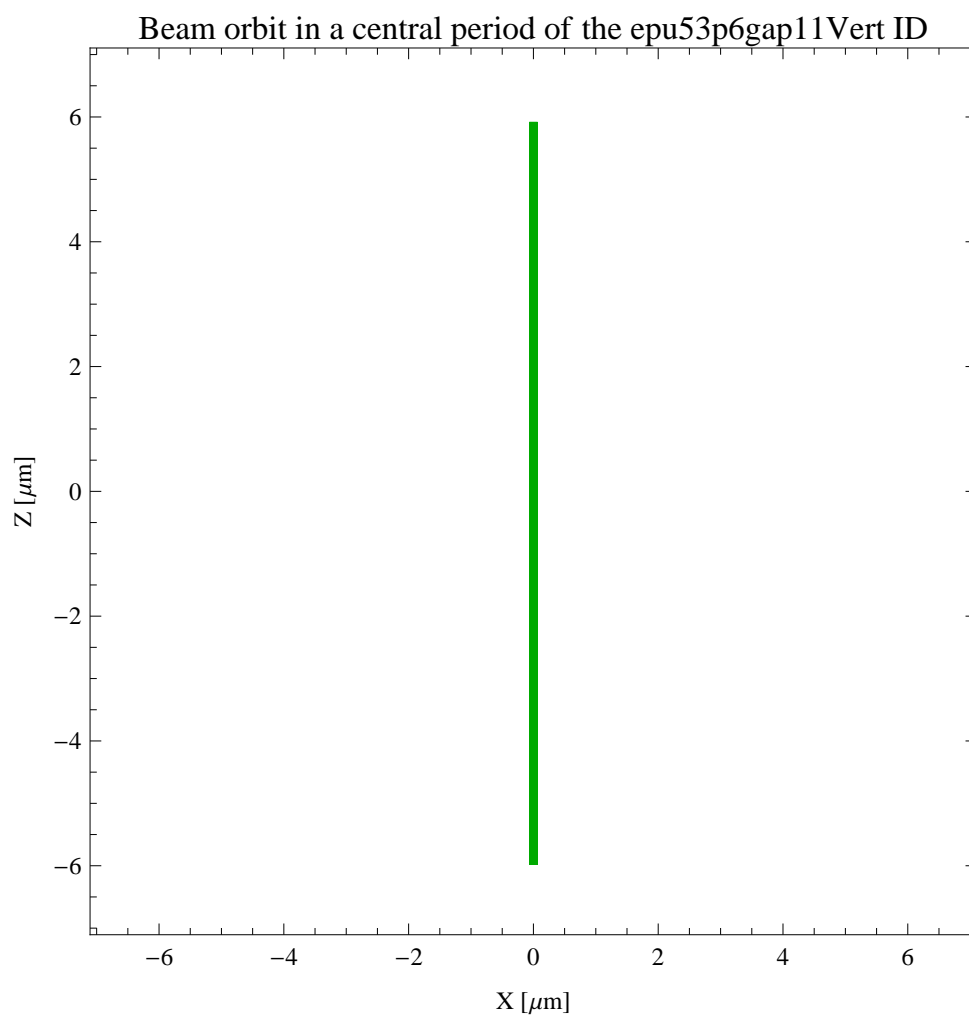


Figure 347: The beam orbit of the electron beam through a central period of the epu53p6gap11Vert ID

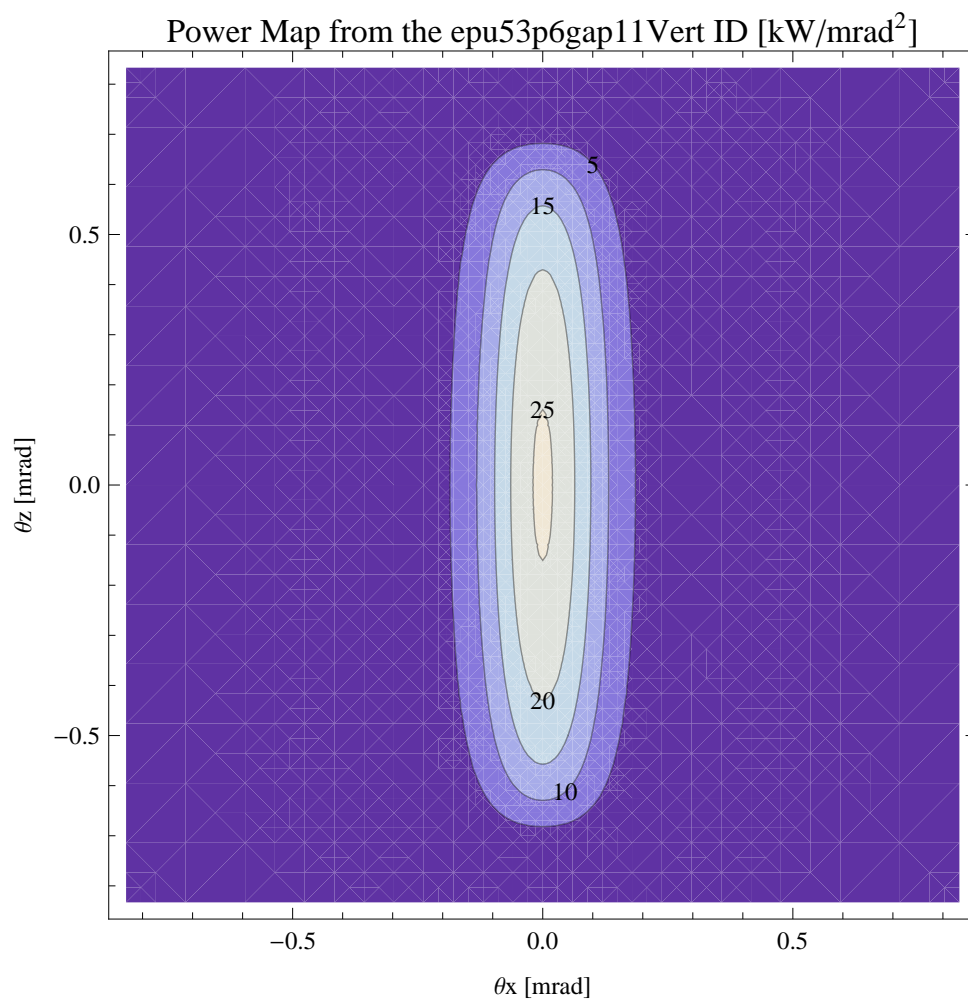


Figure 348: Map of the power distribution of the emitted synchrotron radiation by the epu53p6gap11Vert ID

Degree of Linear Polarisation in Harm.1 from the epu53p6gap11Vert ID

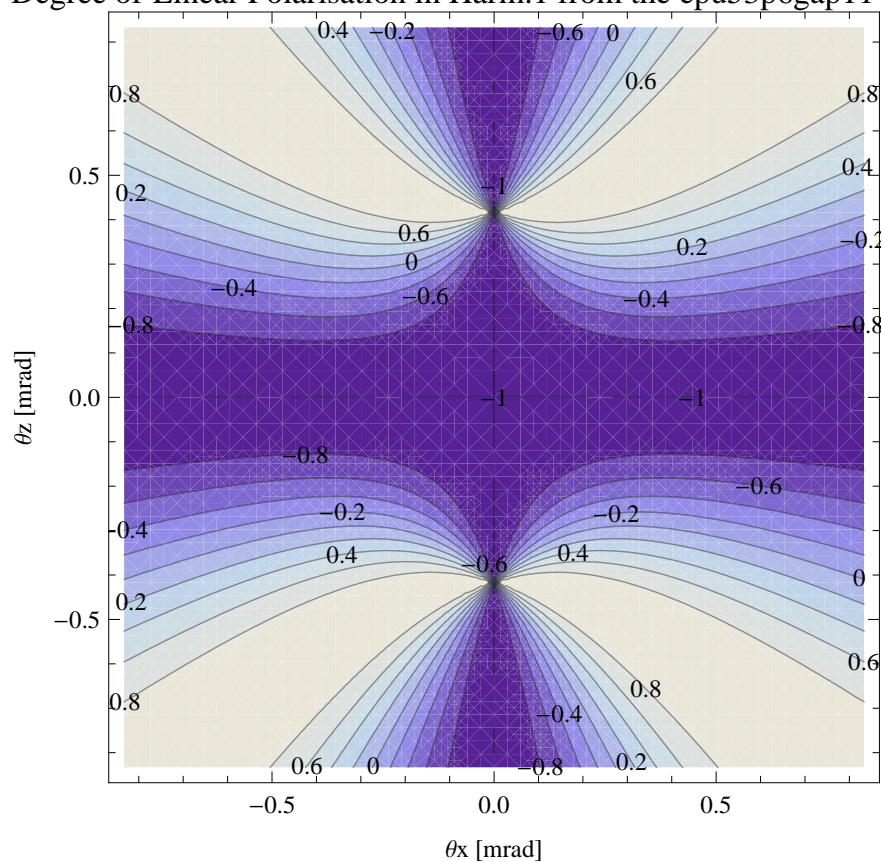


Figure 349: Map of linear polarisation in the fundamental harmonic of the synchrotron radiation emitted by the epu53p6gap11Vert ID

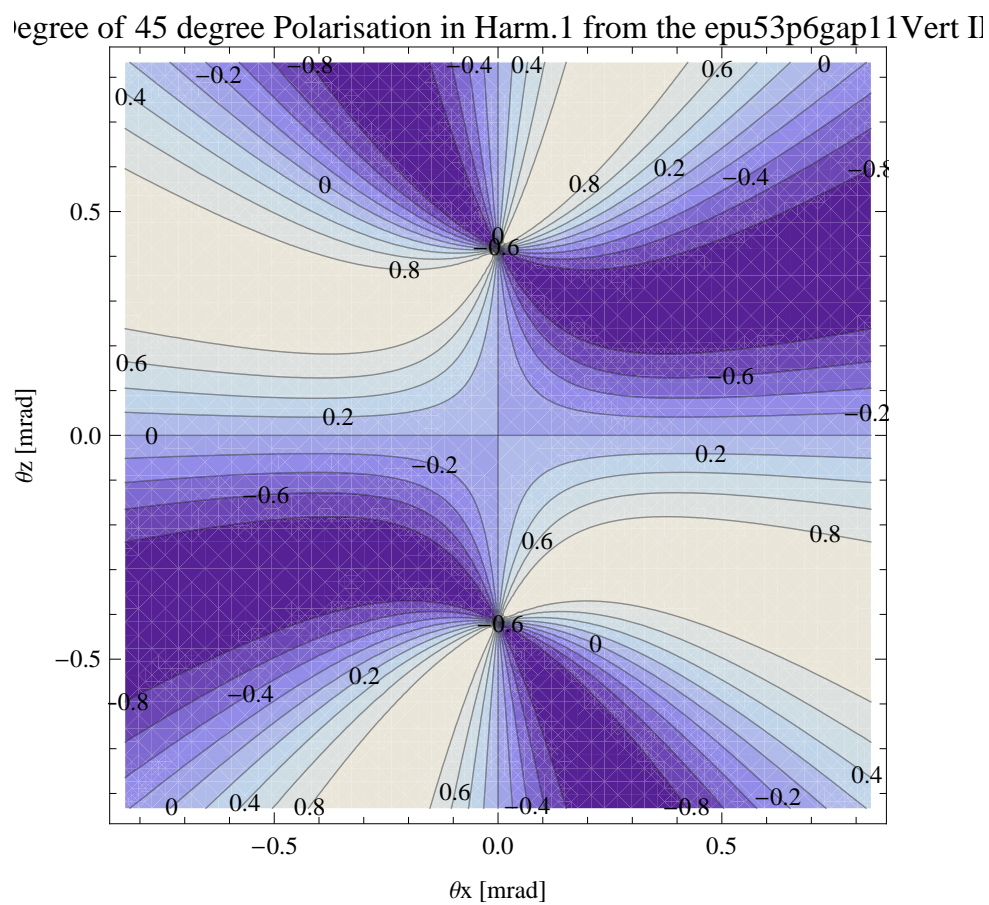


Figure 350: Map of 45 degree polarisation in the fundamental harmonic of the synchrotron radiation emitted by the epu53p6gap11Vert ID

Degree of Circular Polarisation in Harm.1 from the epu53p6gap11Vert II

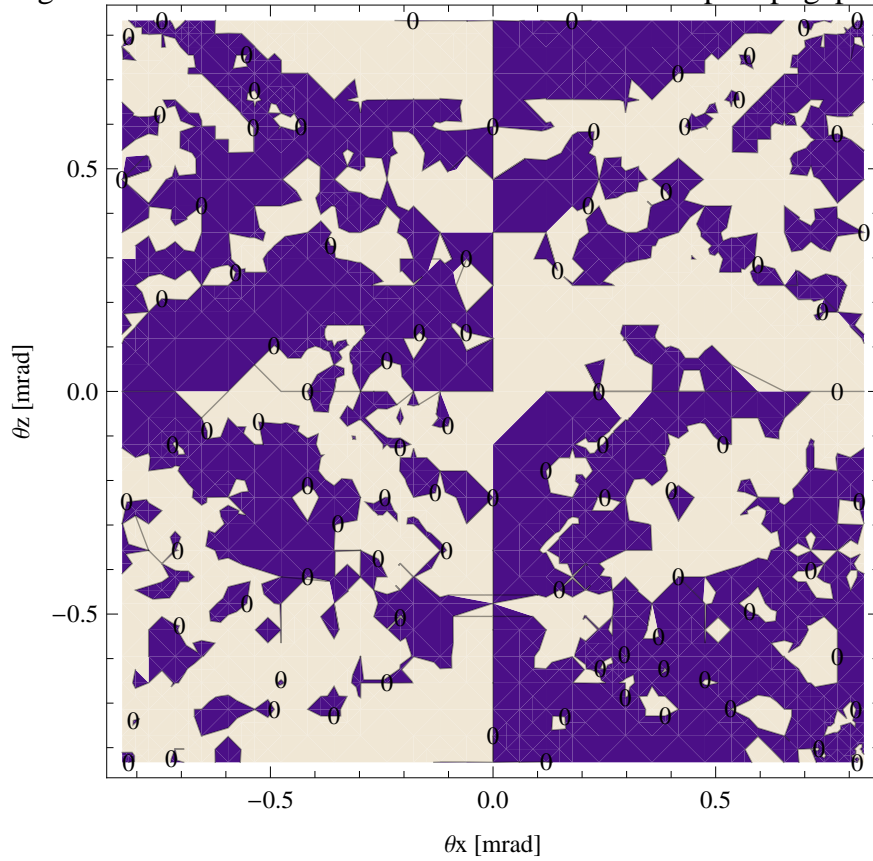


Figure 351: Map of circular polarisation in the fundamental harmonic of the synchrotron radiation emitted by the epu53p6gap11Vert ID

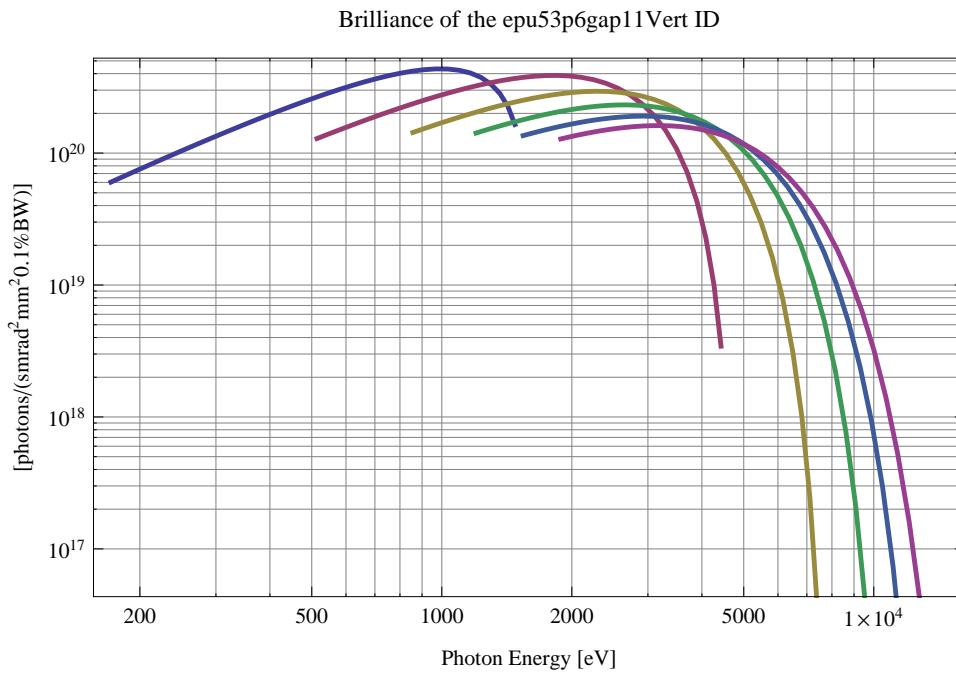


Figure 352: The brilliance at peak energy of the synchrotron radiation emitted by the epu53p6gap11Vert ID

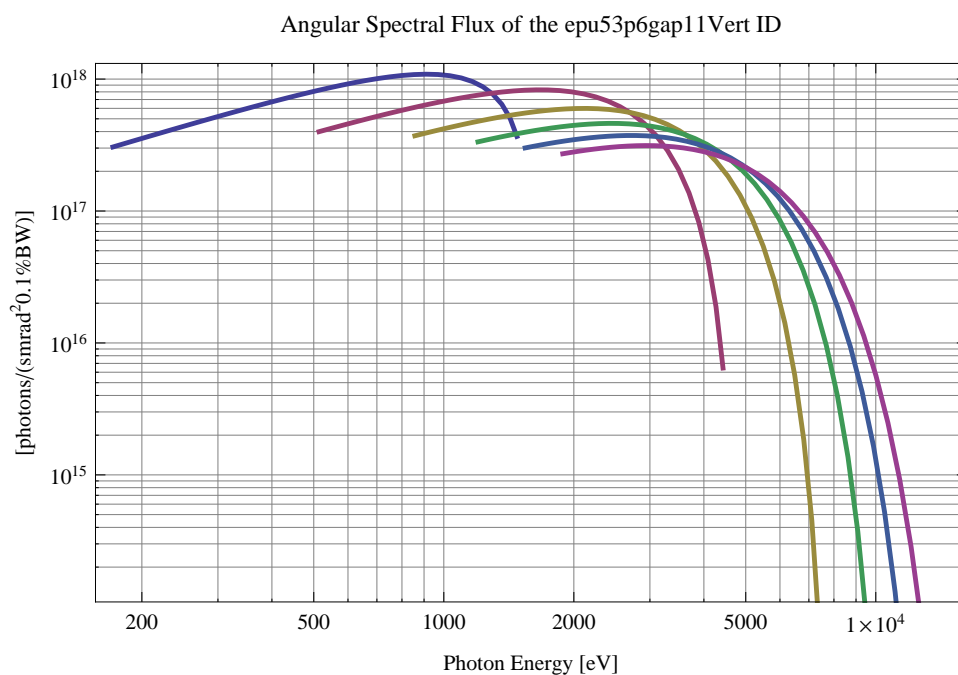


Figure 353: The angular spectral flux of the synchrotron radiation emitted by the epu53p6gap11Vert ID

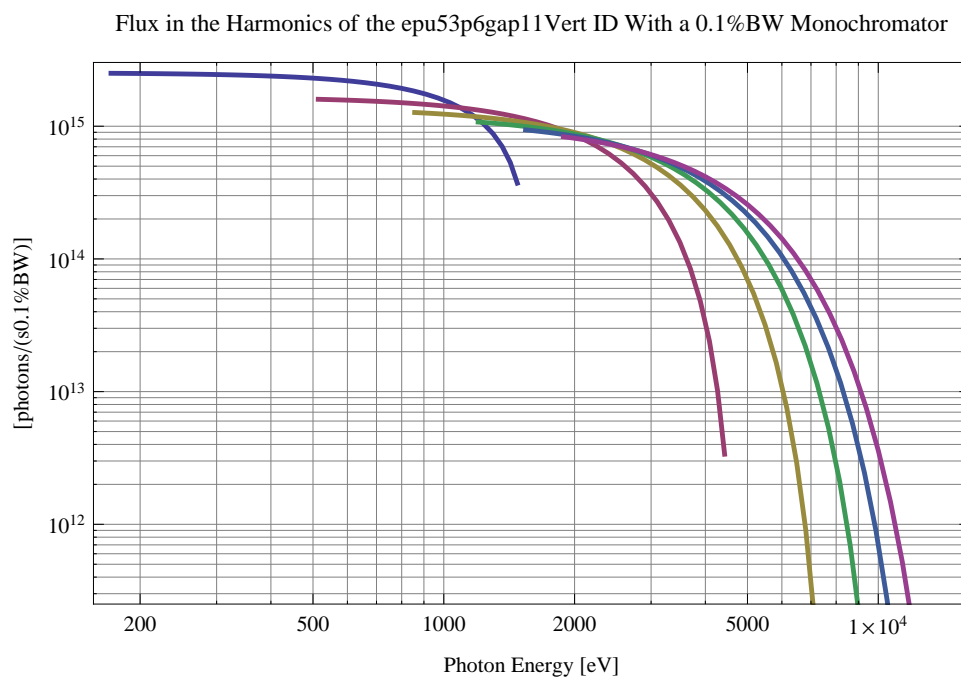


Figure 354: The flux of photons in the harmonics of the emitted synchrotron radiation from the epu53p6gap11Vert ID using a 0.1%BW monochromator

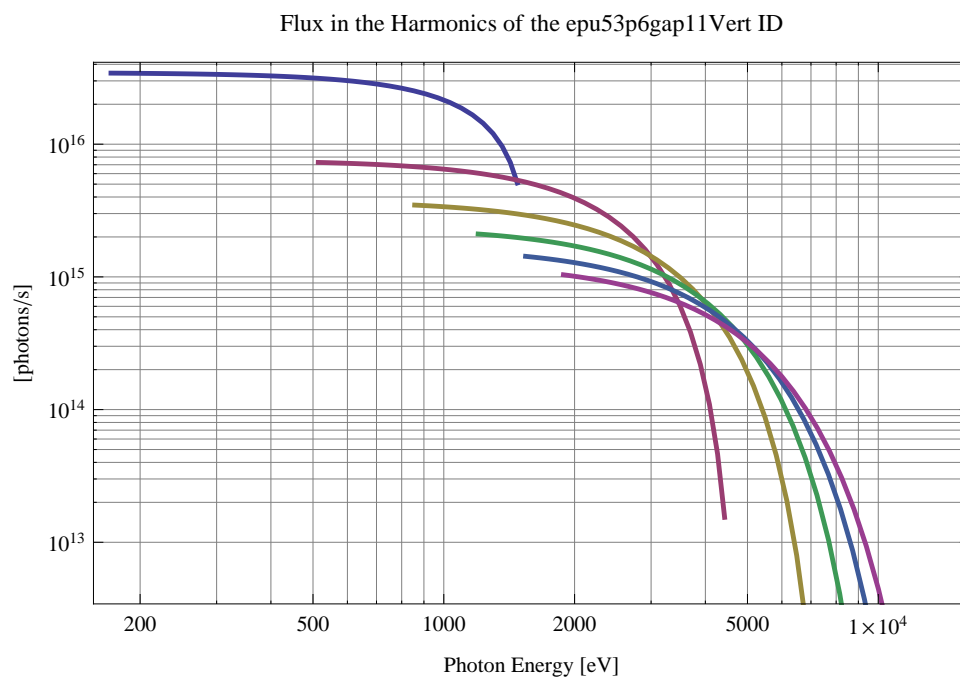


Figure 355: The flux of photons in the harmonics of the emitted synchrotron radiation from the epu53p6gap11Vert ID

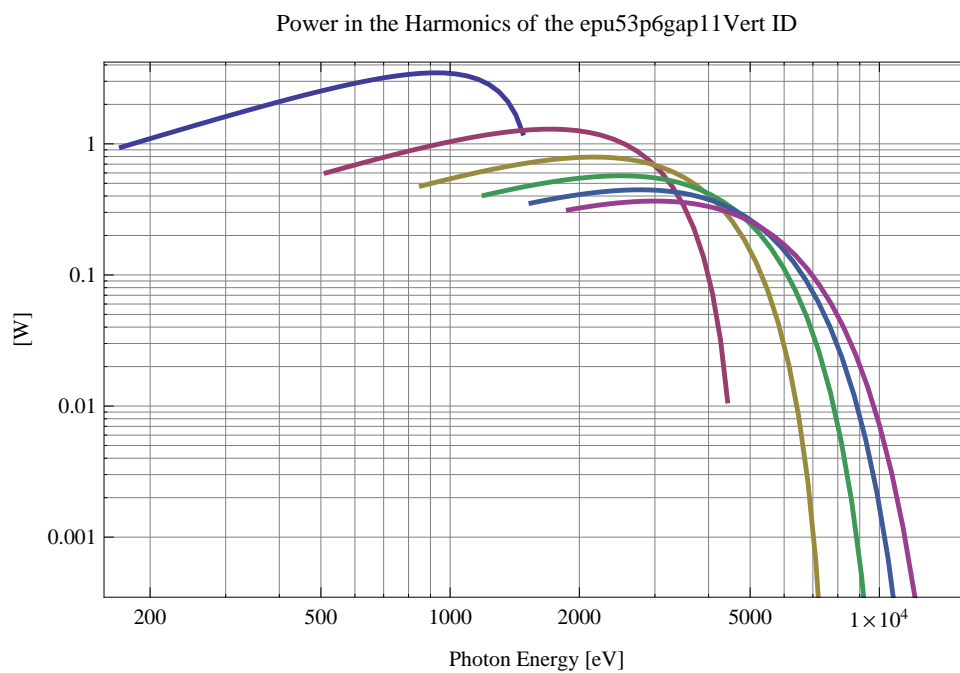


Figure 356: The power in the harmonics of the emitted synchrotron radiation from the epu53p6gap11Vert ID

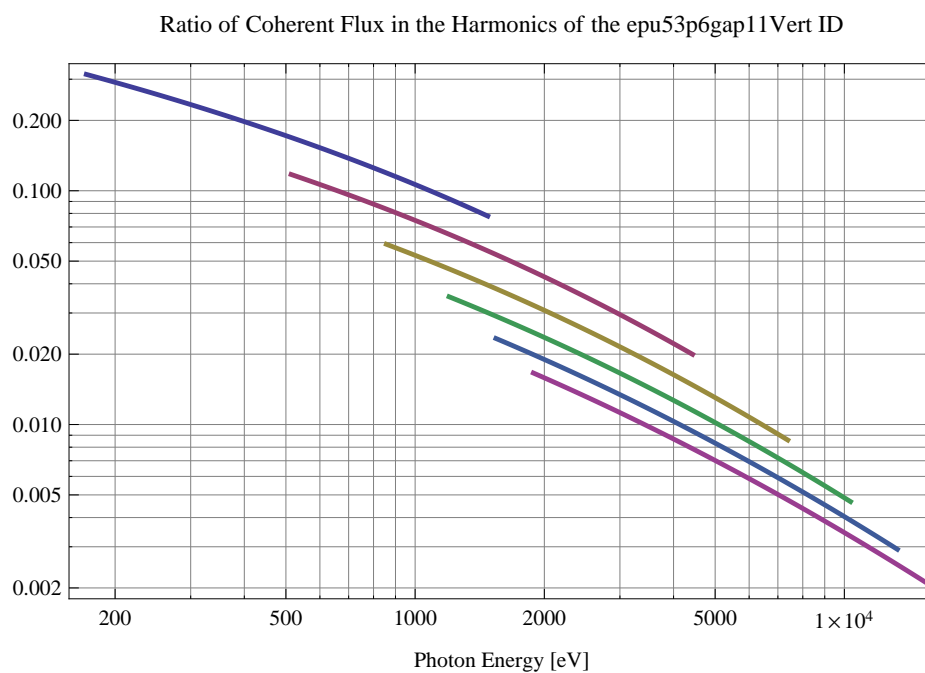


Figure 357: The ratio of coherent flux in the harmonics of the emitted synchrotron radiation from the epu53p6gap11Vert ID

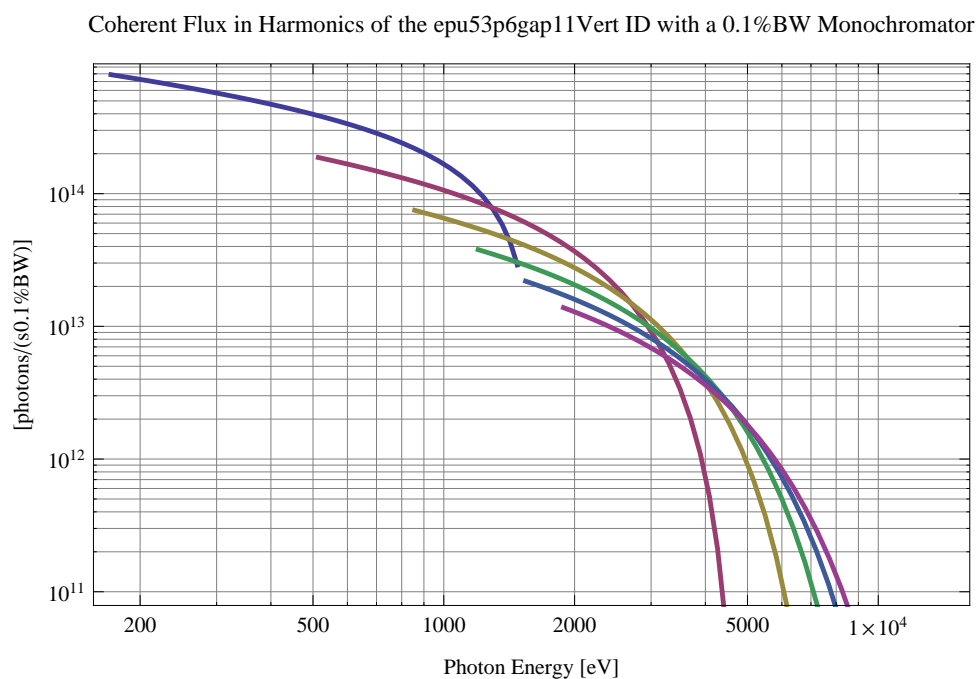


Figure 358: The coherent flux in the harmonics of the epu53p6gap11Vert ID using a 0.1%BW Monochromator

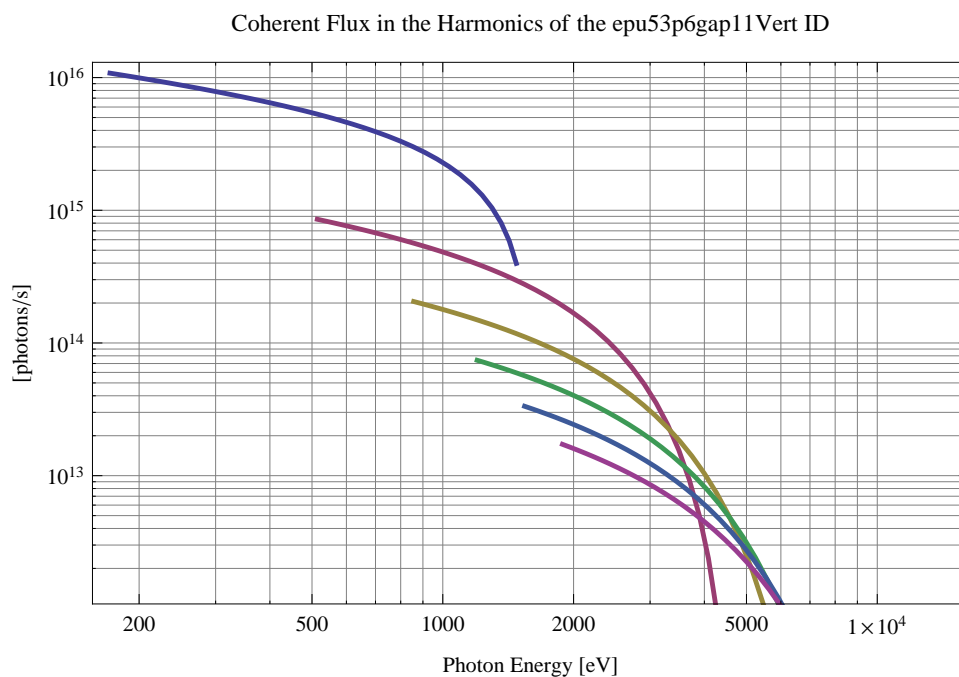


Figure 359: The coherent flux in the harmonics of the epu53p6gap11Vert ID

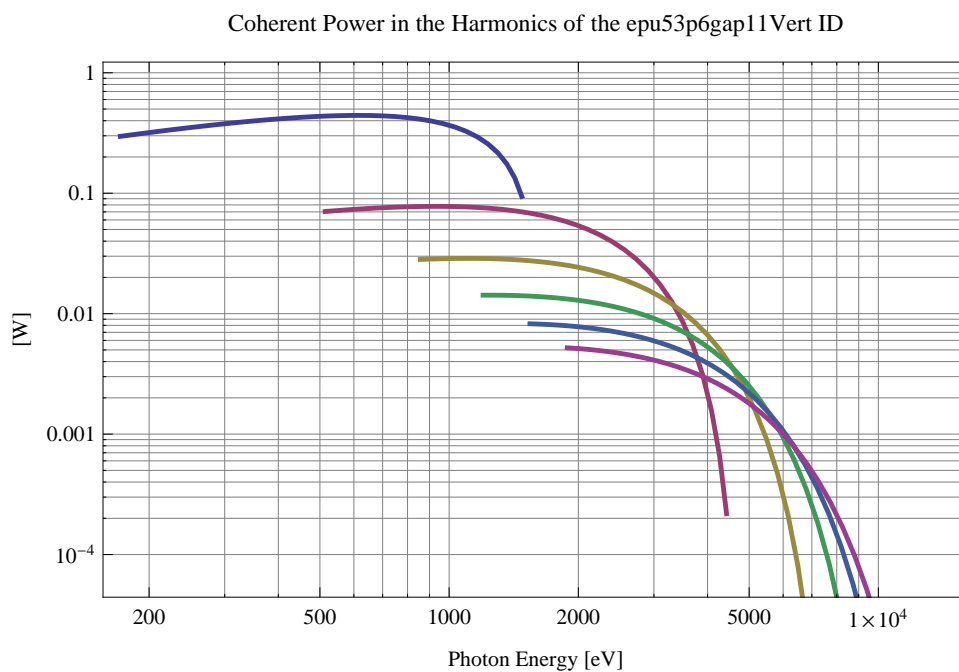


Figure 360: The power of coherent synchrotron radiation in the harmonics of the epu53p6gap11Vert ID

The brilliance at peak energy and the angular spectral flux density from the epu53p6gap11Vert ID for different harmonics at maximum K-value (4.075) are given in Table 60 and for minimum K-value (0.400) these values are given in Table 61.

Table 60: The brilliance at peak energy and the angular spectral flux density from the epu53p6gap11Vert ID for different harmonics at maximum K-value (4.075)

Harmonic	Photon Energy [eV]	Brilliance [Ph./($\text{smrad}^2\text{mrad}^20.1\%\text{BW}$)]	Angular Spectral Flux [Ph./($\text{smrad}^20.1\%\text{BW}$)]
1	171.399	6.03×10^{19}	3.06×10^{17}
3	514.196	1.29×10^{20}	3.99×10^{17}
5	856.993	1.43×10^{20}	3.72×10^{17}
7	1199.79	1.42×10^{20}	3.34×10^{17}
9	1542.59	1.36×10^{20}	3.01×10^{17}
11	1885.38	1.28×10^{20}	2.72×10^{17}

Table 61: The brilliance at peak energy and the angular spectral flux density from the epu53p6gap11Vert ID for different harmonics at minimum K-value (0.4)

Harmonic	Photon Energy [eV]	Brilliance [Ph./($\text{smrad}^2\text{mrad}^20.1\%\text{BW}$)]	Angular Spectral Flux [Ph./($\text{smrad}^20.1\%\text{BW}$)]
1	1476.43	1.65×10^{20}	3.68×10^{17}
3	4429.29	3.44×10^{18}	6.45×10^{15}
5	7382.15	4.04×10^{16}	7.31×10^{13}
7	10335.	4.31×10^{14}	7.7×10^{11}
9	13287.9	4.47×10^{12}	7.93×10^9
11	16240.7	4.59×10^{10}	8.11×10^7

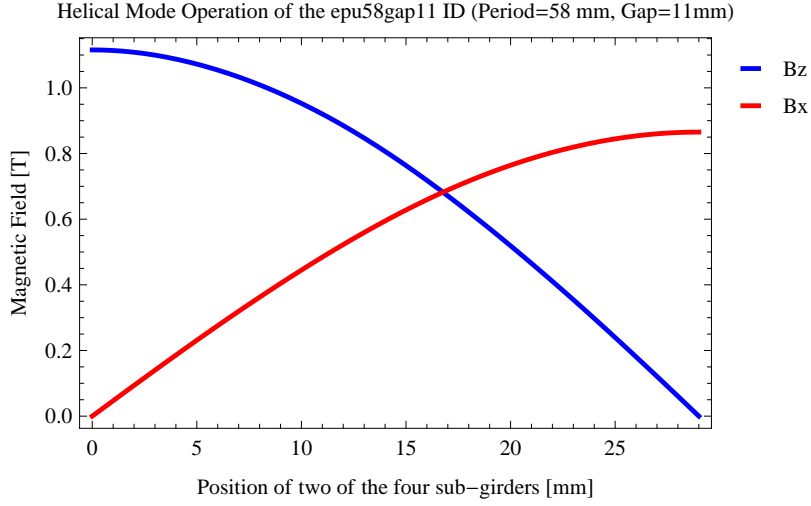


Figure 361: Vertical and horizontal magnetic field for the the epu58gap11 ID when operating in the helical mode for different positions for two of the four sub-girders

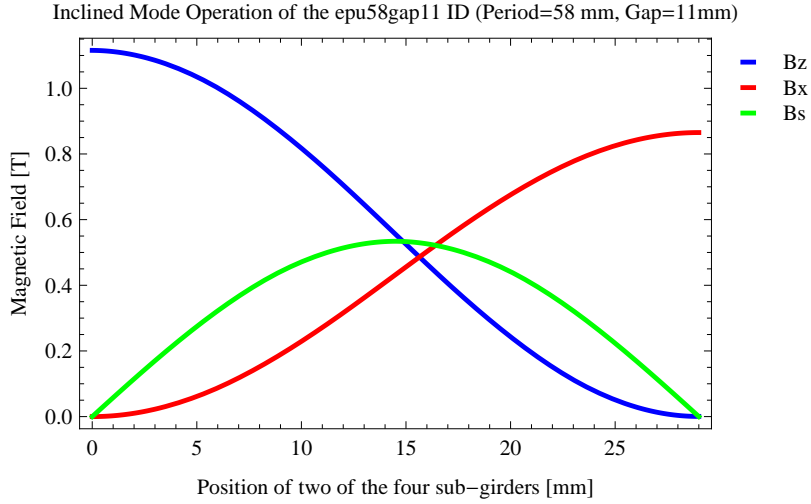


Figure 362: Vertical, horizontal, and longitudinal magnetic field for the the epu58gap11 ID when operating in the inclined mode for different positions for two of the four sub-girders

2.6 The elliptically polaraising undulator epu58gap11

2.6.1 Modes of operation in the elliptically polaraising undulator epu58gap11

Horizontal polarisation of the emitted synchrotron radiation from the epu58gap11 ID (Period=58 mm, Gap=11mm) is found in the planar mode when there is no movement of the sub-girders.

Circular polarisation is found in the elliptical mode of operation for a symmetric sub-grider movement of 16.7674 mm. Figure 361 shows the vertical and horizontal magnetic field for the epu58gap11 ID when operating in the helical mode.

45 degree polarisation is found in the inclined mode of operation for an assymetric sub-grider movement of 15.6446 mm. Figure 362 shows the vertical and horizontal magnetic field for the epu58gap11 ID when operating in the inclined mode.

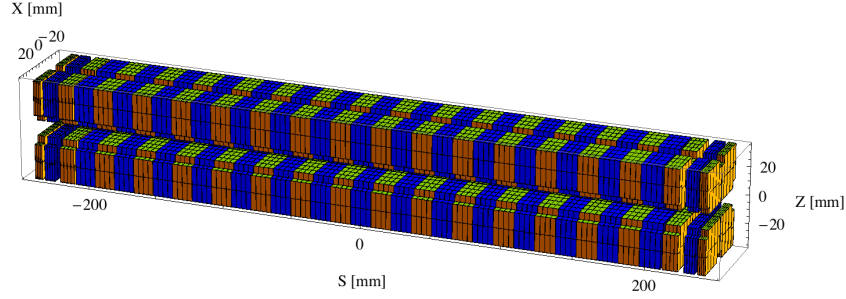


Figure 363: Magnetic model of the epu58gap11Plan ID. The ID has been modelled with Radia [3]

The following sub-sections will cover four different situations: The epu58gap11 operating in the planar mode for horizontal polarisation (epu58gap11Plan); The epu58gap11 operating in the helical mode for circular polarisation (epu58gap11Heli), the epu58gap11 operating in the inclined mode for 45 degree polarisation (epu58gap11Incl); and The epu58gap11 operating in the vertical mode for vertical polarisation (epu58gap11Vert).

2.6.2 Magnet model of the elliptically polarising undulator epu58gap11Plan

The Radia [3] magnet model of the epu58gap11Plan ID is shown in Figure 363. The length of the magnet model is 482.016 mm. The magnetic material in the model is NdFeb with a remanence of 1.28 T, a material similar to VACODYM 776 TP from Vacuumschmelze. Blocks with vertical magnetisation are blue and blocks with horizontal magnetisation are yellow. The block size is $30 \times 30 \times 14.5 \text{ mm}^3$ and there is a 5 mm cut-out in two of the corners of the blocks. The total length of the epu58gap11Plan ID is 3904.02 mm.

2.6.3 Analysis of the magnetic field of the epu58gap11Plan ID

The effective magnetic fields on axis and the fundamental photon energy of the epu58gap11Plan ID are shown in Table 62. The higher harmonic contents in the magnetic field of an elliptically polarising undulator made of permanent magnets is negligible and the effective field has about the same strength as the peak field.

2.6.4 Synchrotron radiation from the epu58gap11Plan ID

The power map of the emitted synchrotron radiation by the epu58gap11Plan ID, assuming a 0.5 A filament beam with an energy of 3 GeV and undulator properties of the synchrotron radiation, is shown in Figure 367. The on-axis power density is 32.284 kW/mrad^2

A map of the degree of linear polarisation of the fundamental harmonic of the synchrotron radiation emitted by the epu58gap11Plan ID over the angle of observation is shown in Figure 368.

A map of the degree of 45 degree polarisation of the fundamental harmonic of the synchrotron radiation emitted by the epu58gap11Plan ID over the angle of observation is shown in Figure 369.

Table 62: Effective Fields on axis and Fundamental Photon Energy of the epu58gap11Plan ID

Undulator Period	58	mm
Undulator Gap	11	mm
Undulator Mode	Planar	
Undulator Phase	0.000	mm
Vertical Peak Field	1.093	T
Effective Vertical Field	1.116	T
Kx (from vert. field)	6.046	
Horizontal Peak Field:	0.000	T
Effective Horizontal Field	0.000	T
Kz (from hor. field)	0.000	
Photon Energy, Harm.1	0.076	keV
Emitted Power	13.843	kW
Total Length	3904.0	mm

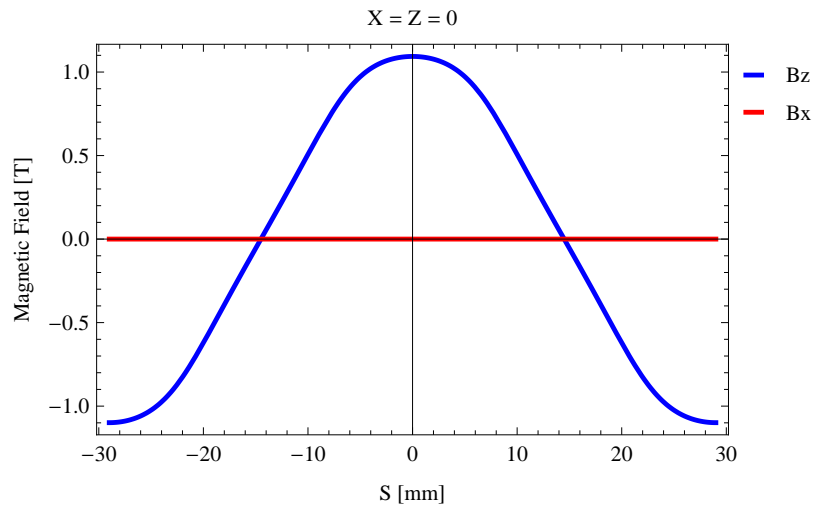


Figure 364: Vertical magnetic field in a central pole of the epu58gap11Plan ID along the ID axis, $X = Z = 0$

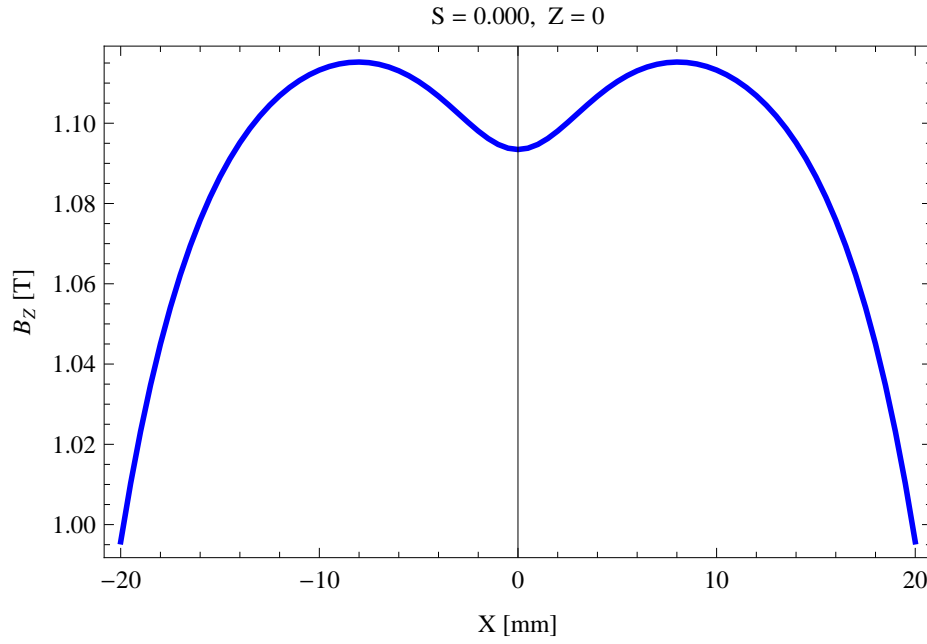


Figure 365: Vertical magnetic field in a central pole of the epu58gap11Plan ID along the horizontally transverse direction to the ID axis, $S = 0.000, Z = 0$

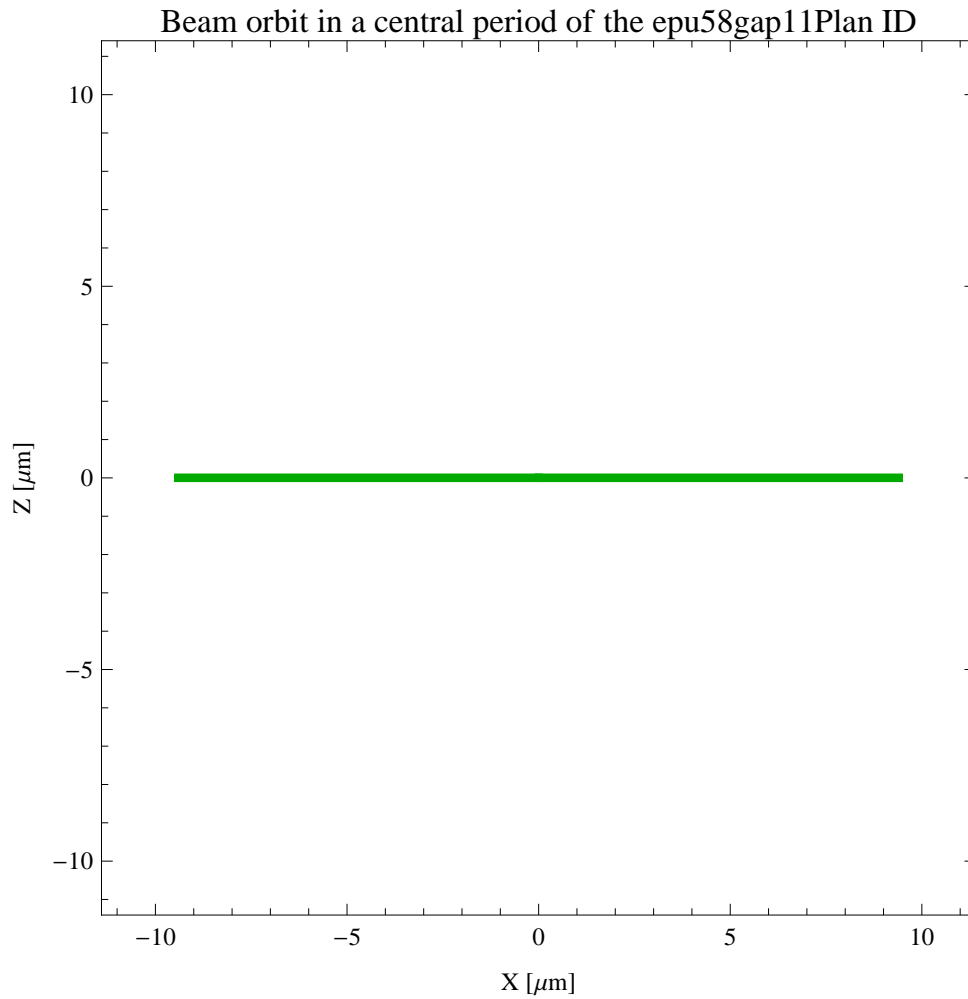


Figure 366: The beam orbit of the electron beam through a central period of the epu58gap11Plan ID

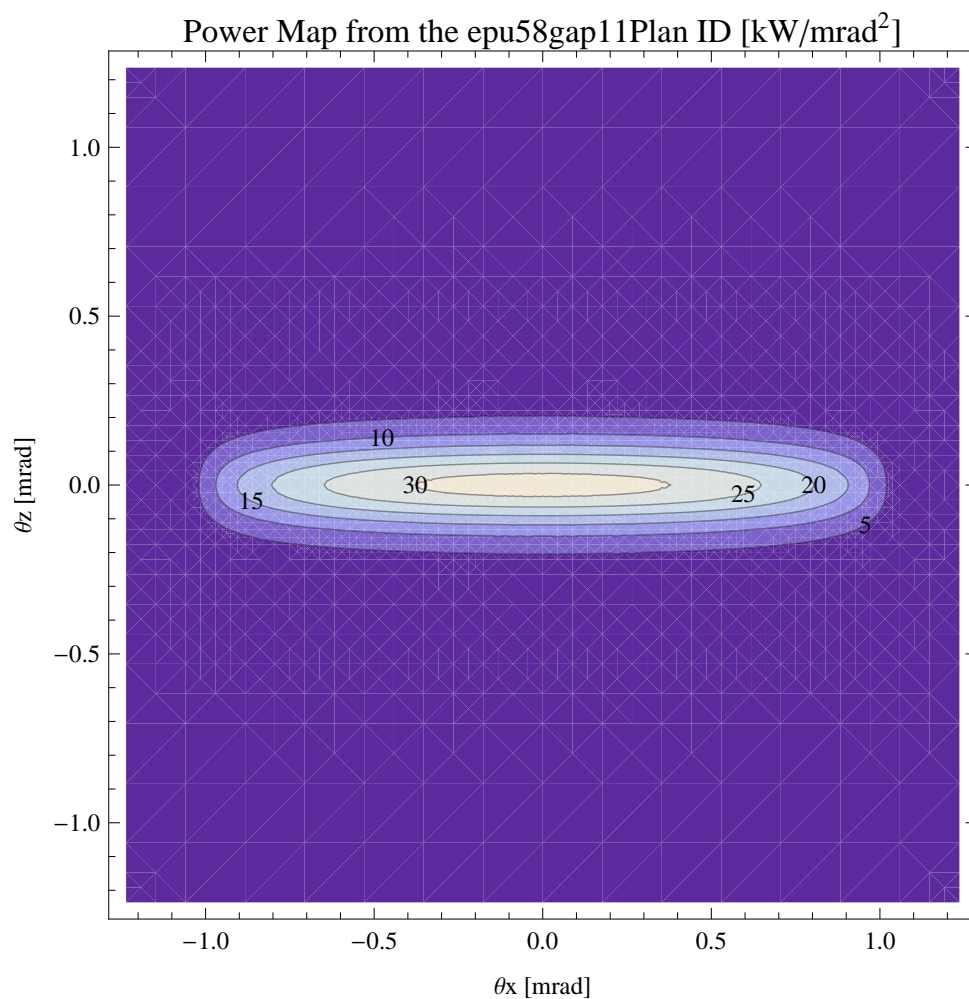


Figure 367: Map of the power distribution of the emitted synchrotron radiation by the epu58gap11Plan ID

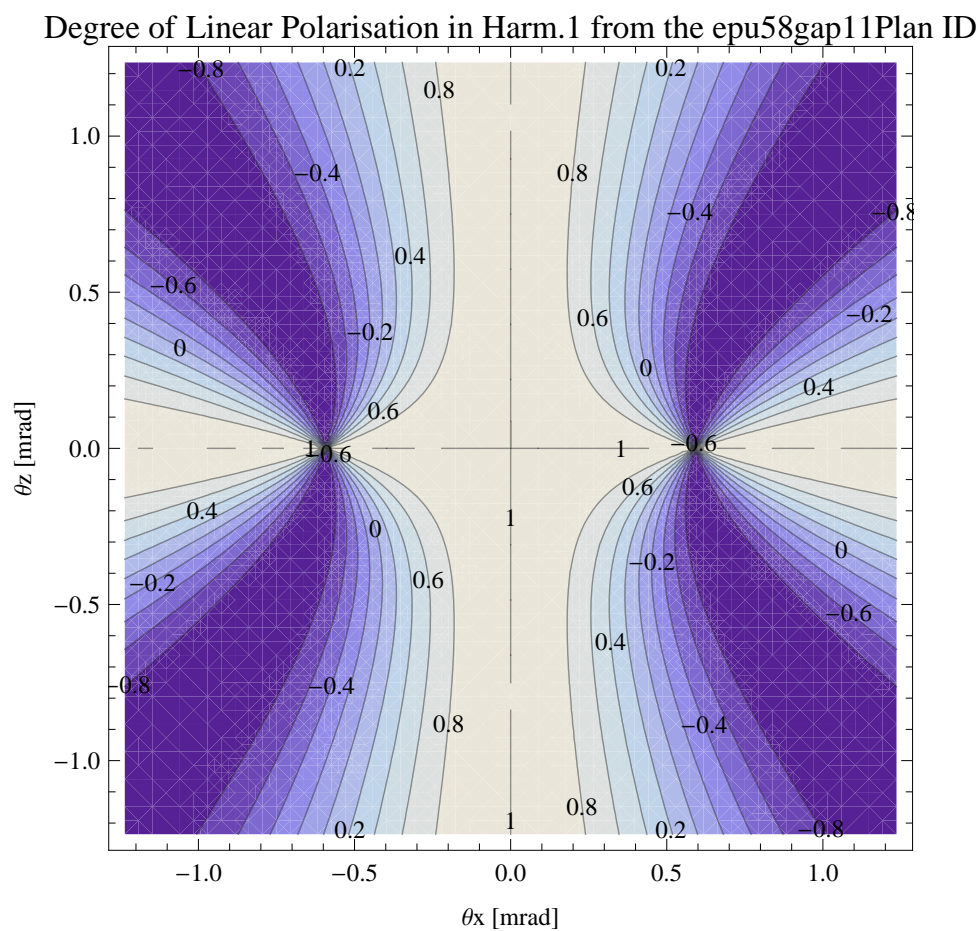


Figure 368: Map of linear polarisation in the fundamental harmonic of the synchrotron radiation emitted by the epu58gap11Plan ID

Degree of 45 degree Polarisation in Harm.1 from the epu58gap11Plan ID

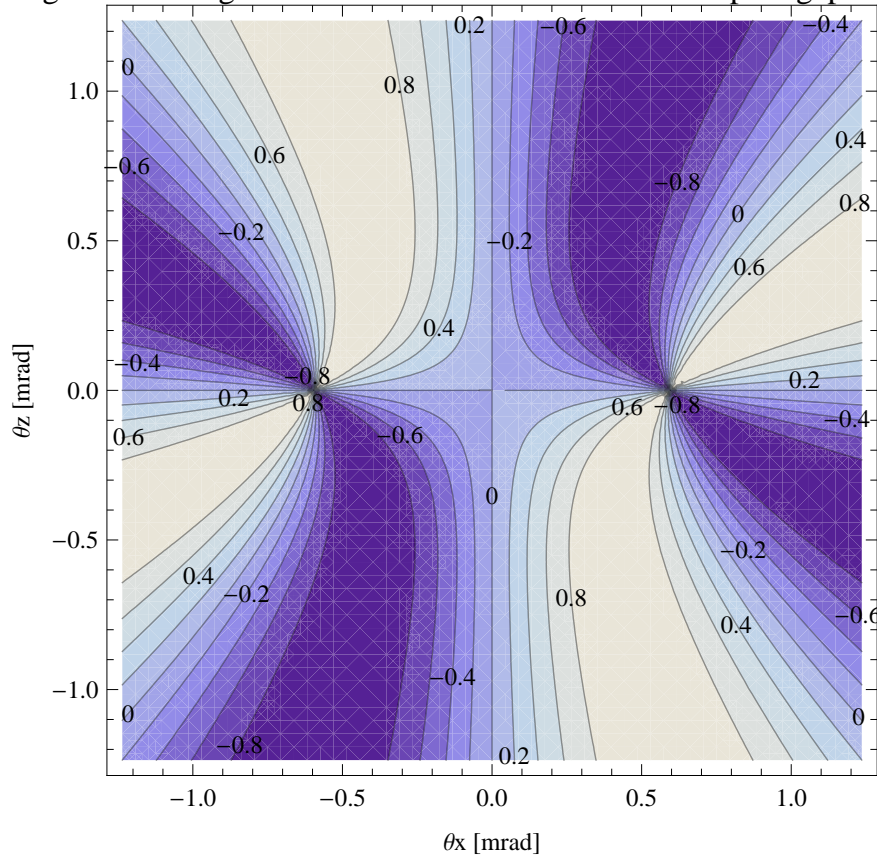


Figure 369: Map of 45 degree polarisation in the fundamental harmonic of the synchrotron radiation emitted by the epu58gap11Plan ID

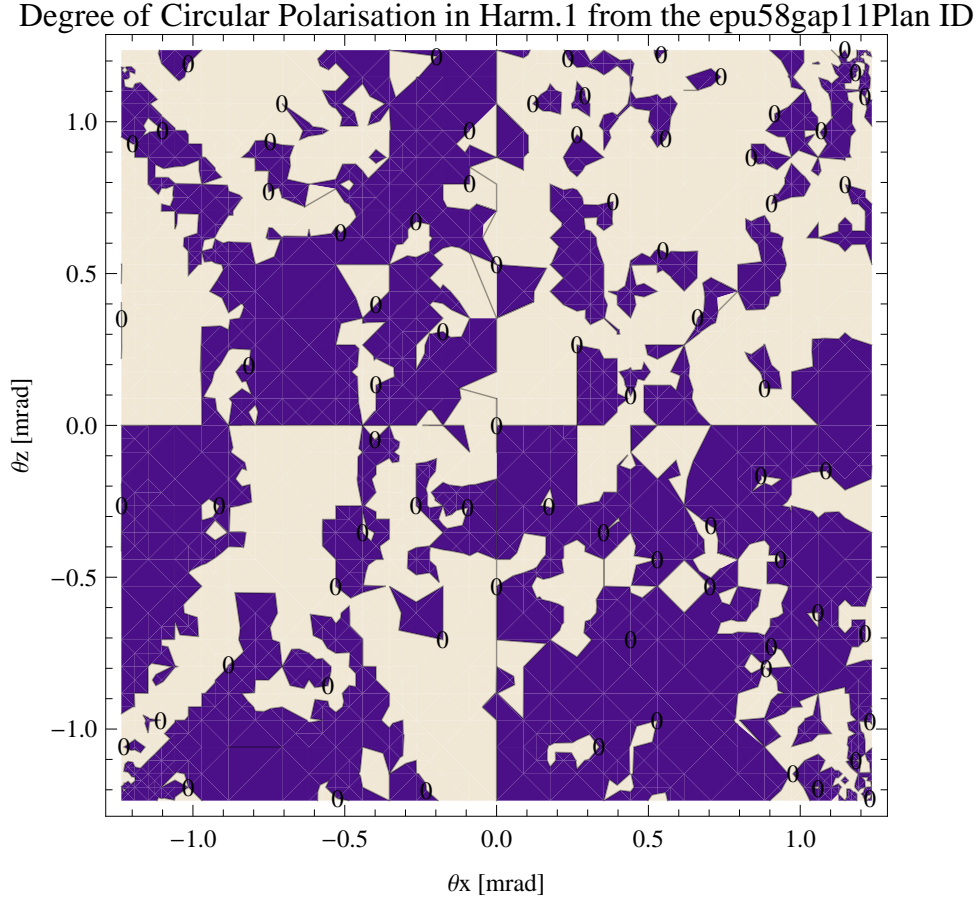


Figure 370: Map of circular polarisation in the fundamental harmonic of the synchrotron radiation emitted by the epu58gap11Plan ID

A map of the degree of circular polarisation of the fundamental harmonic of the synchrotron radiation emitted by the epu58gap11Plan ID over the angle of observation is shown in Figure 370.

The on axis brilliance at peak energy and the angular spectral flux from the epu58gap11Plan ID have been calculated with the given beam parameters, which are 0.5 A of stored current, $\beta_H = 9$ m, $\varepsilon_H = 0.263$ nmrad, $\beta_V = 4.8$ m, $\varepsilon_V = 8$. pmrad, and an energy spread of 0.001.

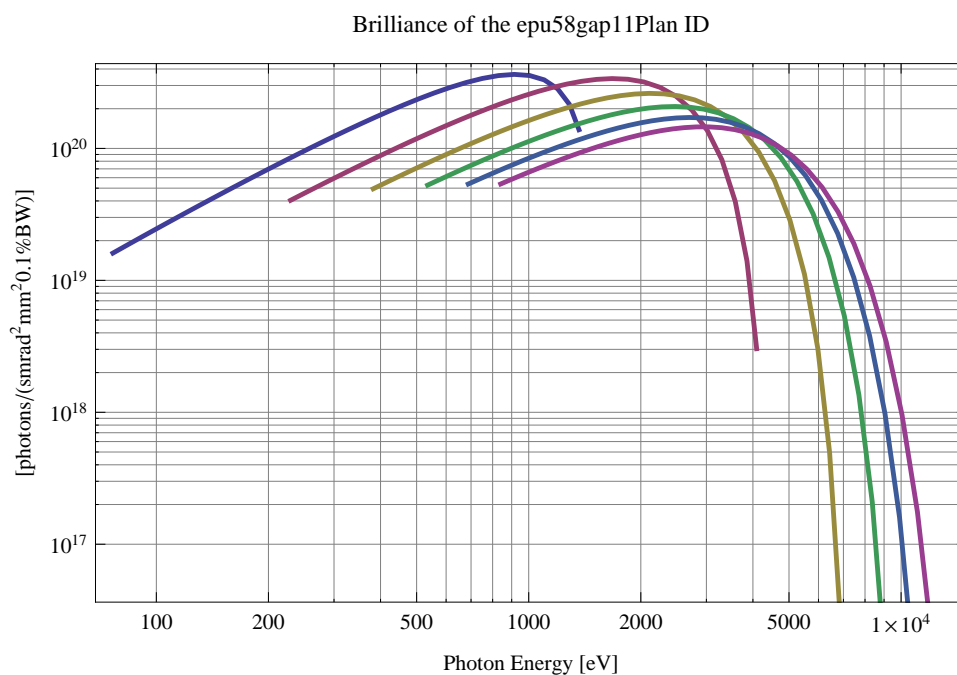


Figure 371: The brilliance at peak energy of the synchrotron radiation emitted by the epu58gap11Plan ID

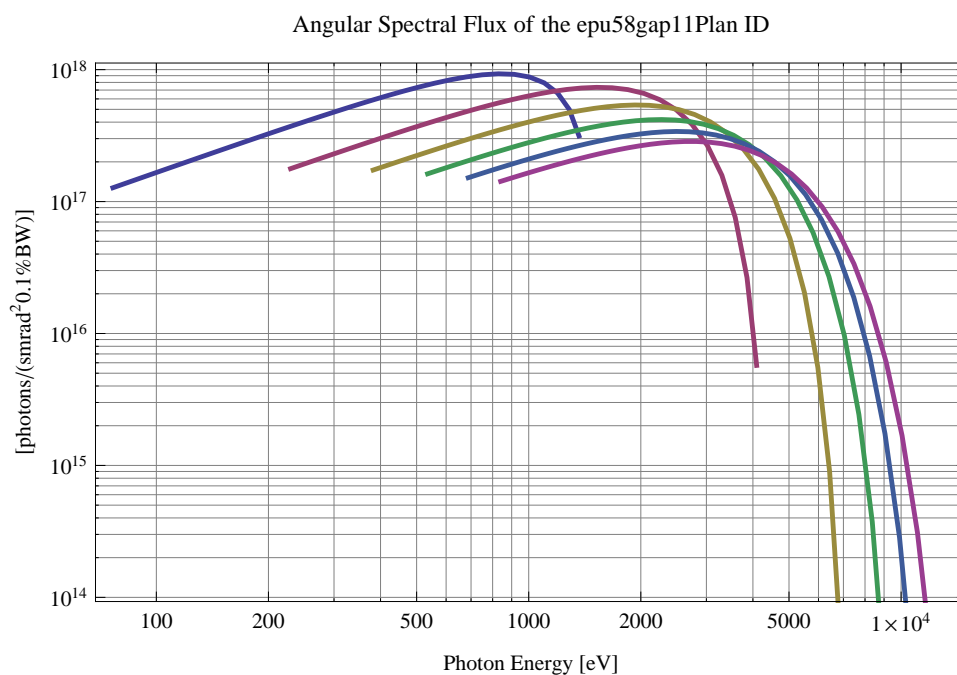


Figure 372: The angular spectral flux of the synchrotron radiation emitted by the epu58gap11Plan ID

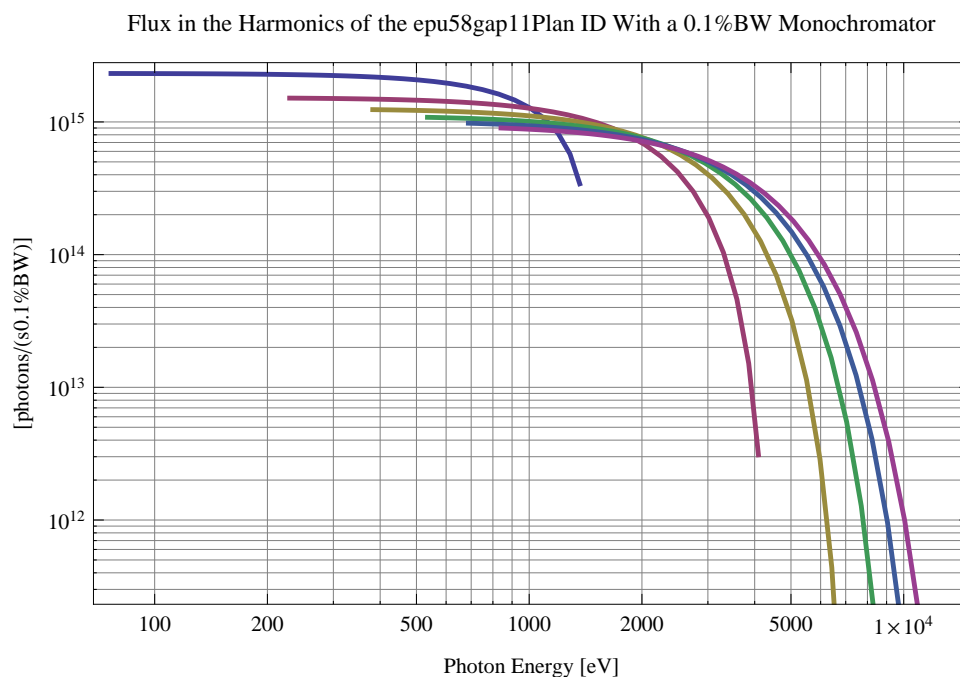


Figure 373: The flux of photons in the harmonics of the emitted synchrotron radiation from the epu58gap11Plan ID using a 0.1%BW monochromator

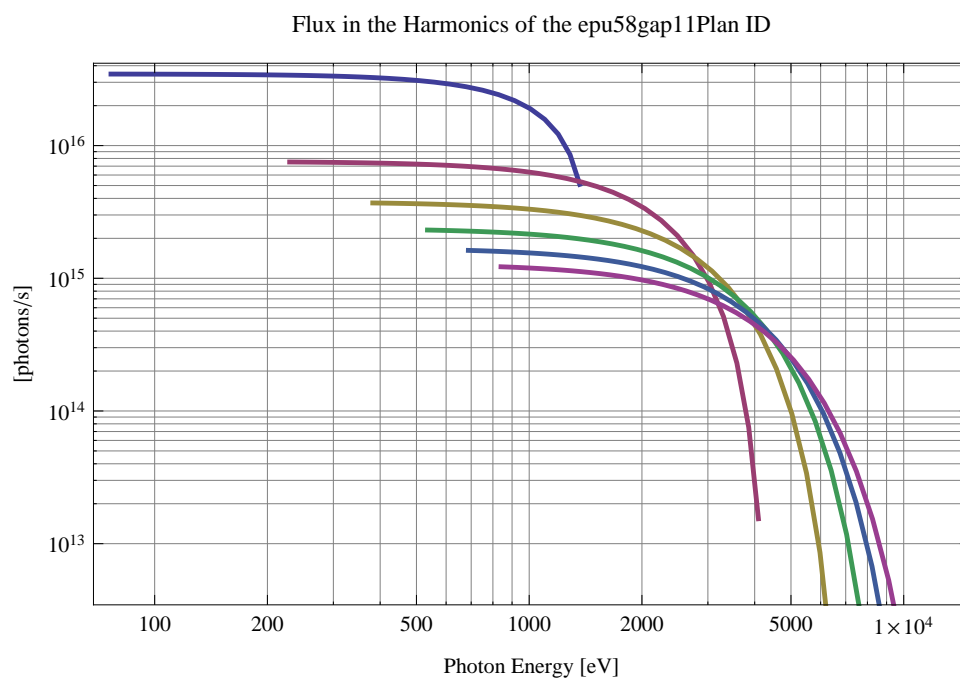


Figure 374: The flux of photons in the harmonics of the emitted synchrotron radiation from the epu58gap11Plan ID

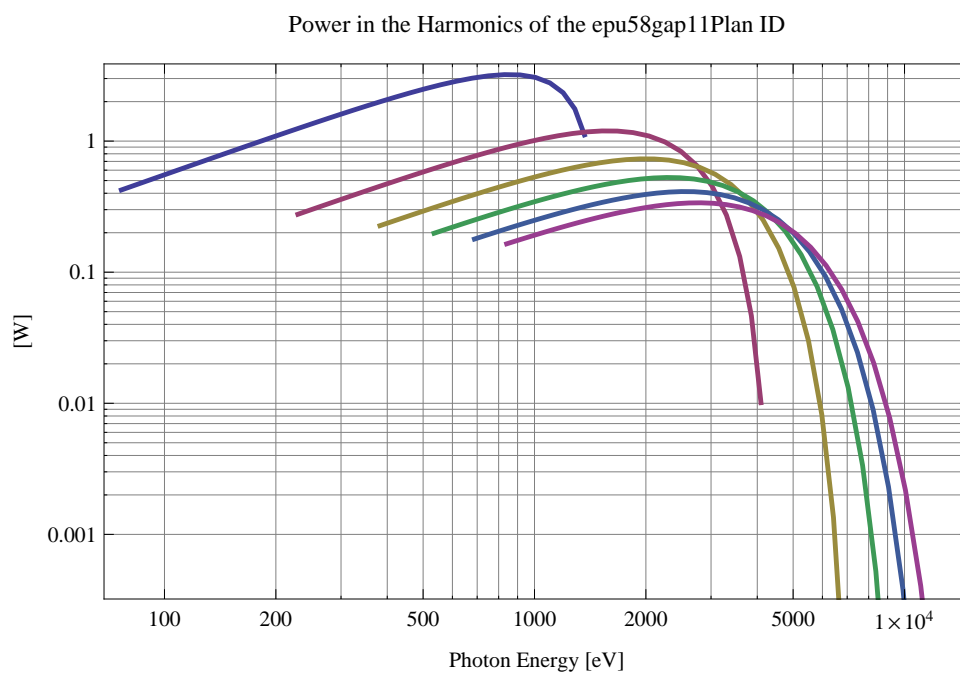


Figure 375: The power in the harmonics of the emitted synchrotron radiation from the epu58gap11Plan ID

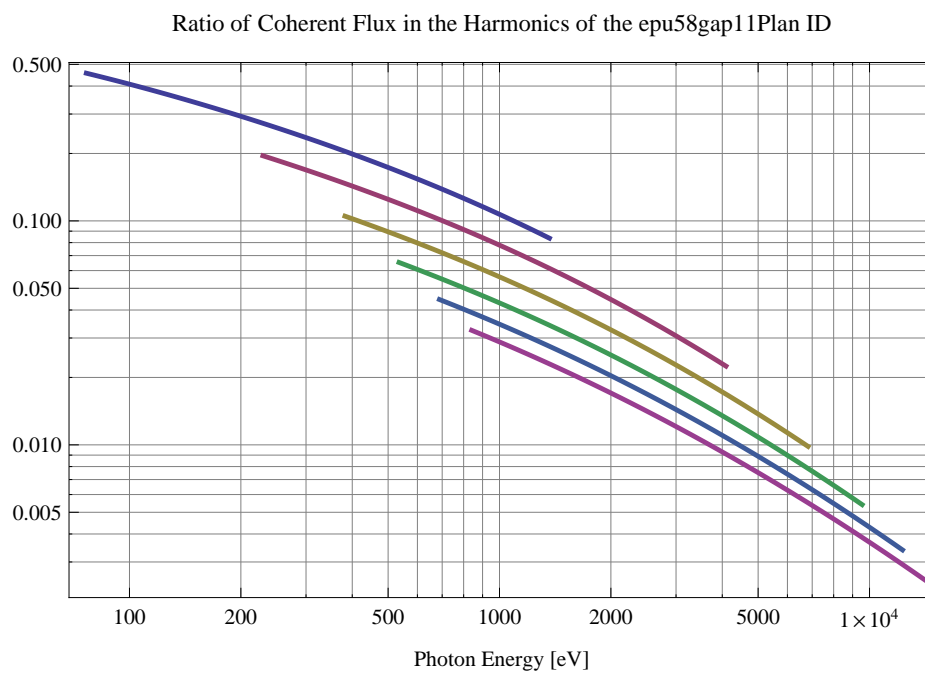


Figure 376: The ratio of coherent flux in the harmonics of the emitted synchrotron radiation from the epu58gap11Plan ID

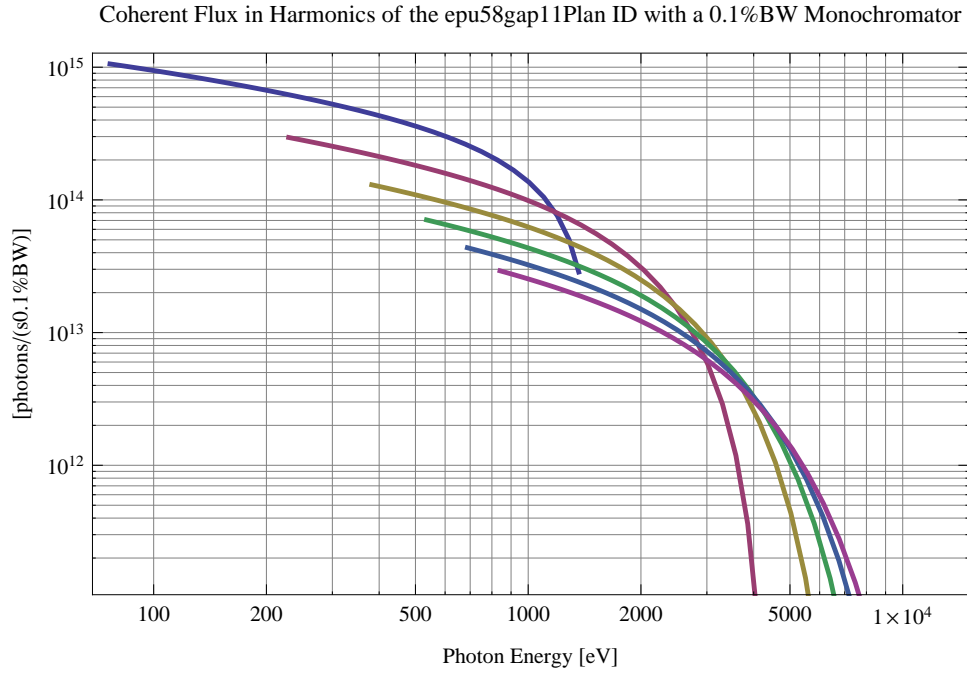


Figure 377: The coherent flux in the harmonics of the epu58gap11Plan ID using a 0.1%BW Monochromator

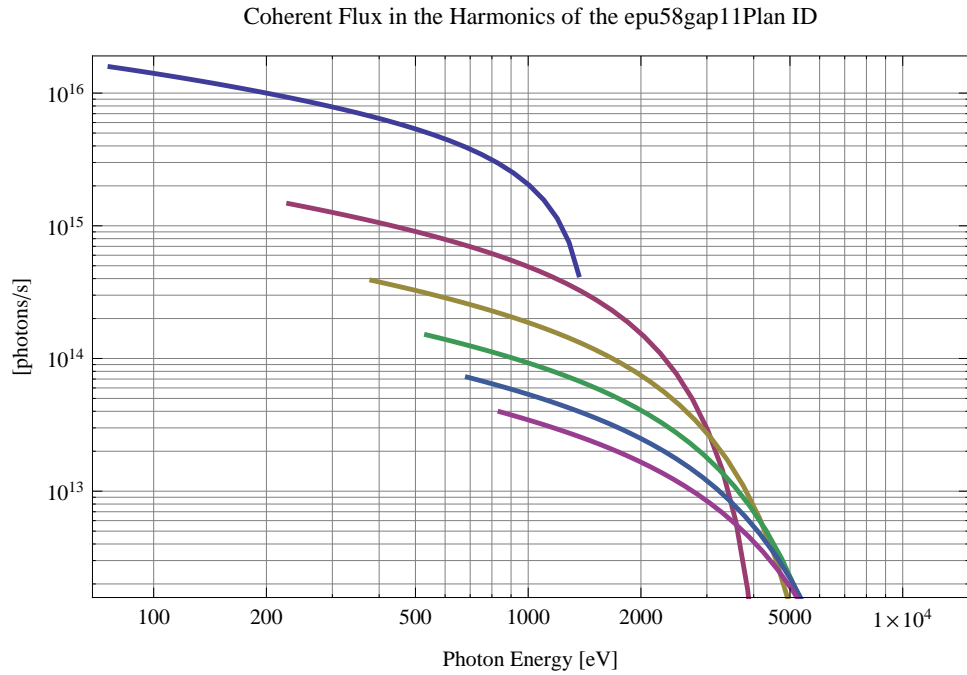


Figure 378: The coherent flux in the harmonics of the epu58gap11Plan ID

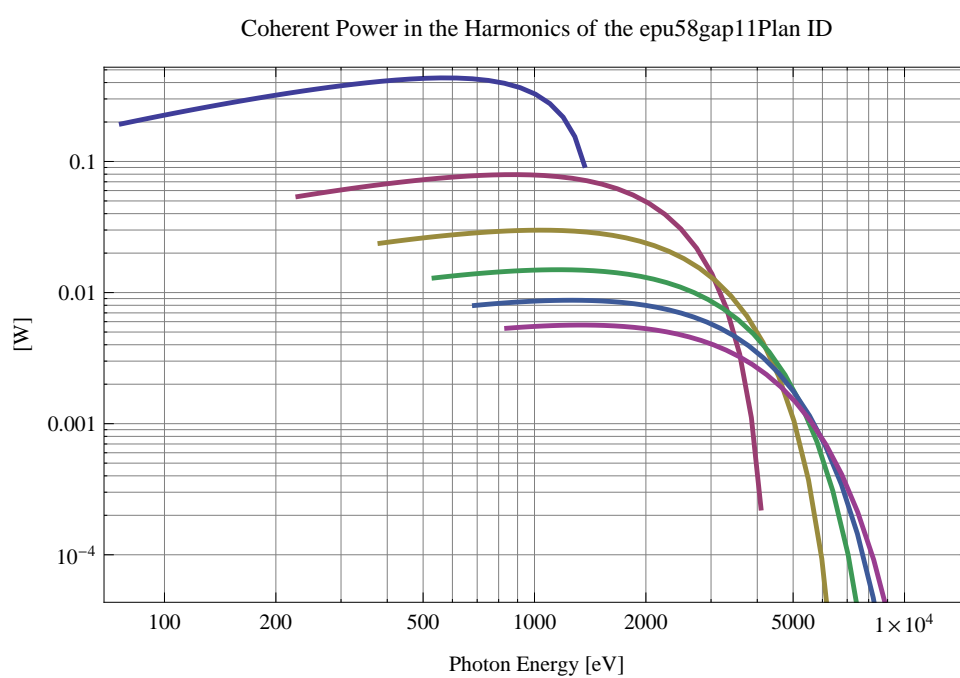


Figure 379: The power of coherent synchrotron radiation in the harmonics of the epu58gap11Plan ID

The brilliance at peak energy and the angular spectral flux density from the epu58gap11Plan ID for different harmonics at maximum K-value (6.046) are given in Table 63 and for minimum K-value (0.400) these values are given in Table 64.

Table 63: The brilliance at peak energy and the angular spectral flux density from the epu58gap11Plan ID for different harmonics at maximum K-value (6.046)

Harmonic	Photon Energy [eV]	Brilliance [Ph./($\text{smrad}^2\text{mrad}^2 0.1\% \text{BW}$)]	Angular Spectral Flux [Ph./($\text{smrad}^2 0.1\% \text{BW}$)]
1	76.4518	1.61×10^{19}	1.27×10^{17}
3	229.355	4.04×10^{19}	1.78×10^{17}
5	382.259	4.94×10^{19}	1.73×10^{17}
7	535.163	5.27×10^{19}	1.62×10^{17}
9	688.066	5.37×10^{19}	1.52×10^{17}
11	840.97	5.38×10^{19}	1.42×10^{17}

Table 64: The brilliance at peak energy and the angular spectral flux density from the epu58gap11Plan ID for different harmonics at minimum K-value (0.4)

Harmonic	Photon Energy [eV]	Brilliance [Ph./($\text{smrad}^2\text{mrad}^2 0.1\% \text{BW}$)]	Angular Spectral Flux [Ph./($\text{smrad}^2 0.1\% \text{BW}$)]
1	1364.43	1.39×10^{20}	3.15×10^{17}
3	4093.28	3.03×10^{18}	5.73×10^{15}
5	6822.13	3.63×10^{16}	6.59×10^{13}
7	9550.98	3.9×10^{14}	6.98×10^{11}
9	12279.8	4.07×10^{12}	7.22×10^9
11	15008.7	4.18×10^{10}	7.4×10^7

2.6.5 Magnet model of the elliptically polarising undulator epu58gap11Heli

The Radia [3] magnet model of the epu58gap11Heli ID is shown in Figure 380. The length of the magnet model is 482.016 mm. The magnetic material in the model is NdFeb with a remanence of 1.28 T, a material similar to VACODYM 776 TP from Vacuumschmelze. Blocks with vertical magnetisation are blue and blocks with horizontal magnetisation are yellow. The block size is $30 \times 30 \times 14.5 \text{ mm}^3$ and there is a 5. mm cut-out in two of the corners of the blocks. The total length of the epu58gap11Heli ID is 3904.02 mm.

2.6.6 Analysis of the magnetic field of the epu58gap11Heli ID

The effective magnetic fields on axis and the fundamental photon energy of the epu58gap11Heli ID are shown in Table 65. The higher harmonic contents in the magnetic field of an elliptically polarising undulator made of permanent magnets is negligible and the effective field has about the same strength as the peak field.

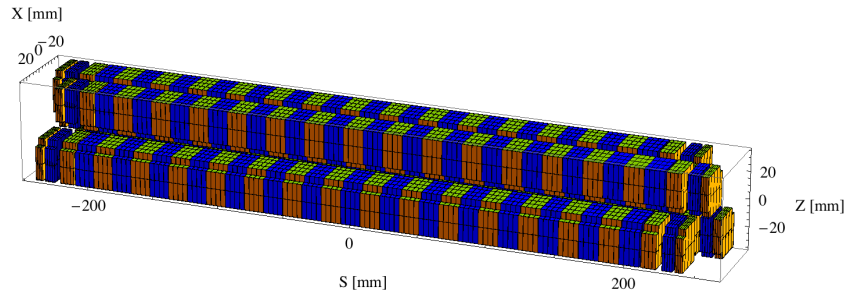


Figure 380: Magnetic model of the epu58gap11Heli ID. The ID has been modelled with Radia [3]

Table 65: Effective Fields on axis and Fundamental Photon Energy of the epu58gap11Heli ID

Undulator Period	58	mm
Undulator Gap	11	mm
Undulator Mode	Helical	
Undulator Phase	16.767	mm
Vertical Peak Field	0.682	T
Effective Vertical Field	0.682	T
K _x (from vert. field)	3.695	
Horizontal Peak Field:	0.688	T
Effective Horizontal Field	0.682	T
K _z (from hor. field)	3.695	
Photon Energy, Harm.1	0.101	keV
Emitted Power	10.340	kW
Total Length	3904.0	mm

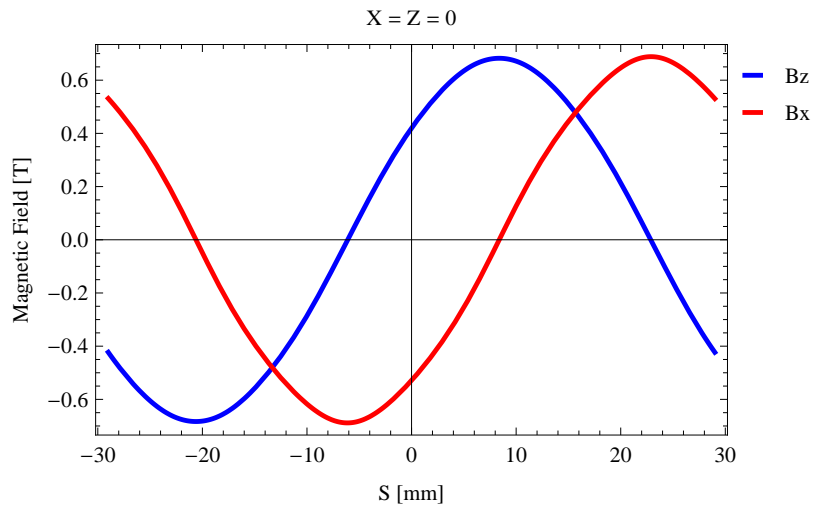


Figure 381: Vertical magnetic field in a central pole of the epu58gap11Heli ID along the ID axis, $X = Z = 0$

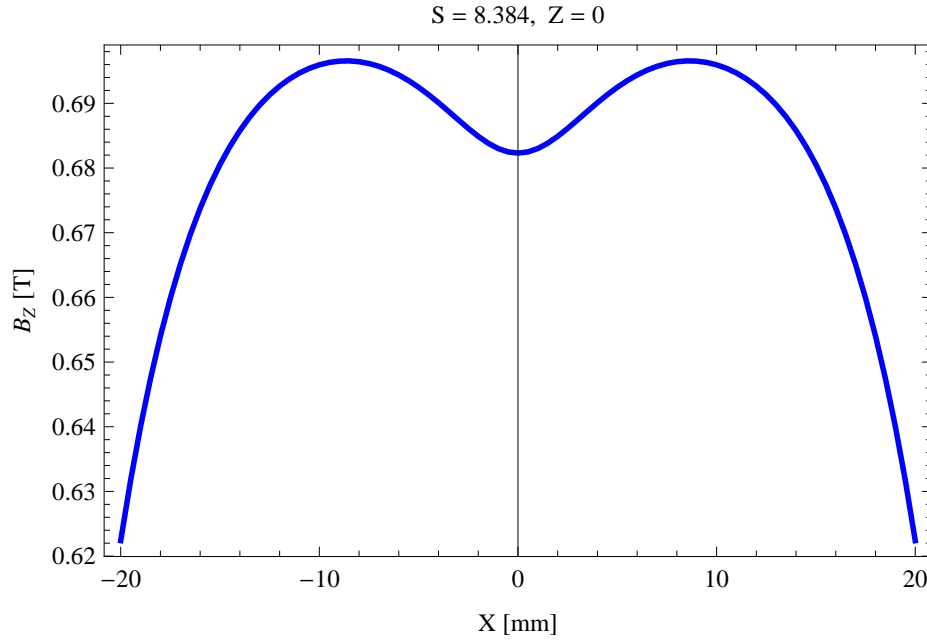


Figure 382: Vertical magnetic field in a central pole of the epu58gap11Heli ID along the horizontally transverse direction to the ID axis, $S = 8.384, Z = 0$

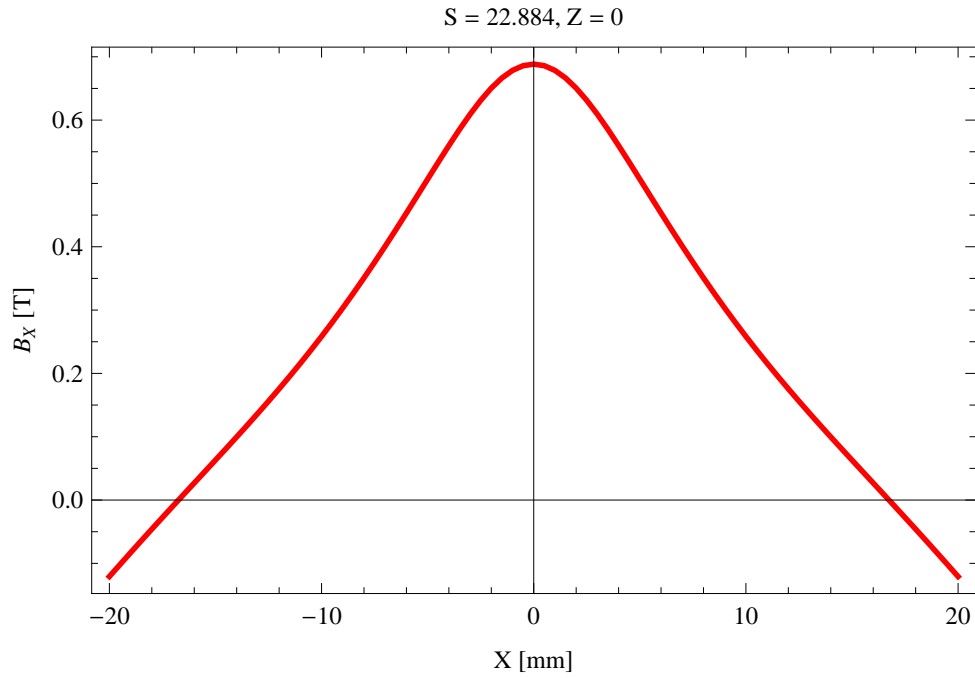


Figure 383: Horizontal magnetic field in a central pole of the epu58gap11Heli ID along the horizontally transverse direction to the ID axis, $S = 22.884, Z = 0$

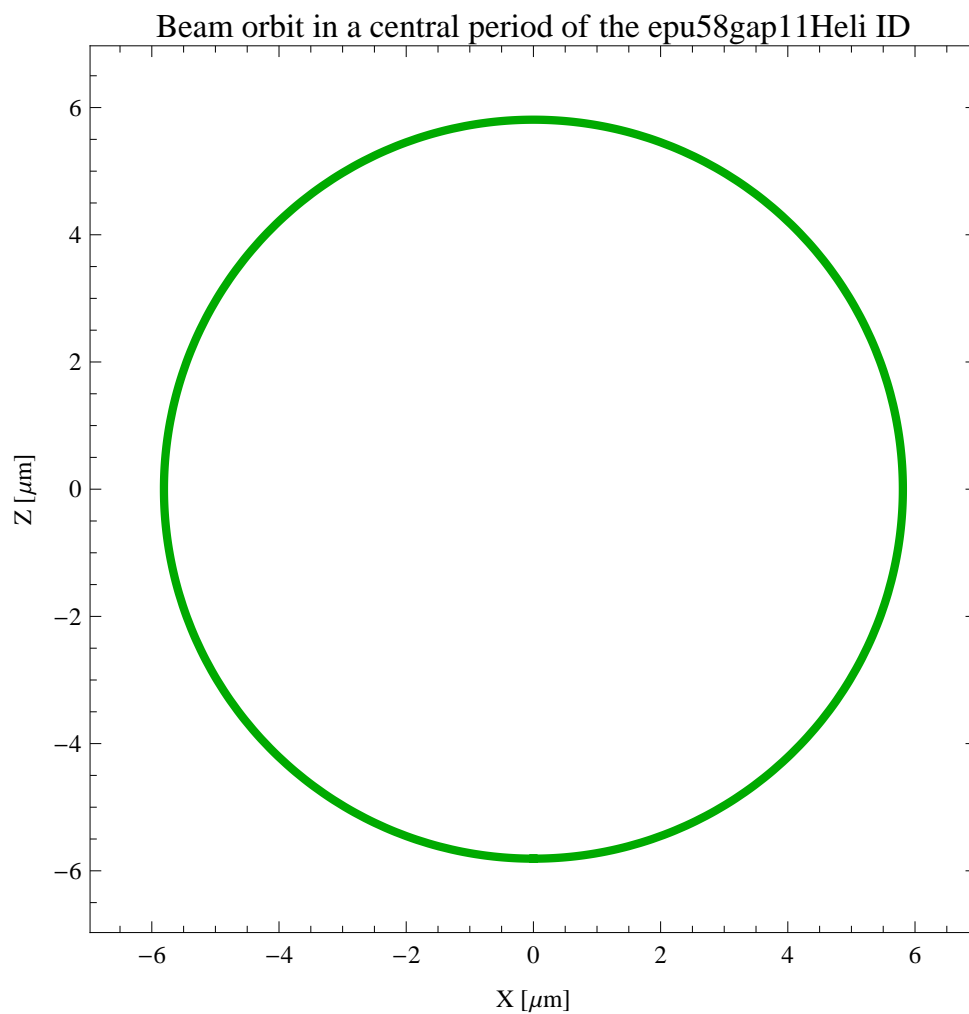


Figure 384: The beam orbit of the electron beam through a central period of the epu58gap11Heli ID

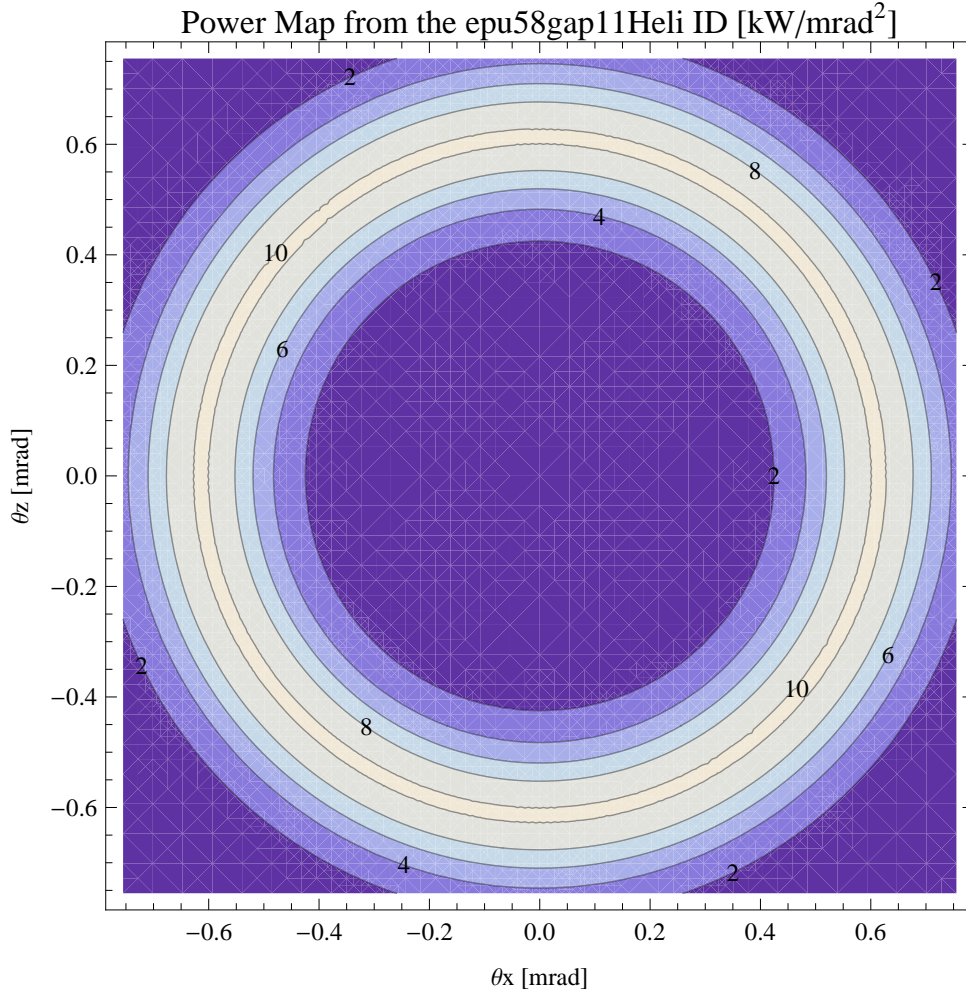


Figure 385: Map of the power distribution of the emitted synchrotron radiation by the epu58gap11Heli ID

2.6.7 Synchrotron radiation from the epu58gap11Heli ID

The power map of the emitted synchrotron radiation by the epu58gap11Heli ID, assuming a 0.5 A filament beam with an energy of 3 GeV and undulator properties of the synchrotron radiation, is shown in Figure 385. The on-axis power density is 0.106 kW/mrad²

A map of the degree of linear polarisation of the fundamental harmonic of the synchrotron radiation emitted by the epu58gap11Heli ID over the angle of observation is shown in Figure 386.

A map of the degree of 45 degree polarisation of the fundamental harmonic of the synchrotron radiation emitted by the epu58gap11Heli ID over the angle of observation is shown in Figure 387.

A map of the degree of circular polarisation of the fundamental harmonic of the synchrotron radiation emitted by the epu58gap11Heli ID over the angle of observation is shown in Figure 388.

The on axis brilliance at peak energy and the angular spectral flux from the epu58gap11Heli ID have been calculated with the given beam parameters, which are 0.5 A of stored current, $\beta_H = 9$ m, $\varepsilon_H = 0.263$ nrad, $\beta_V = 4.8$ m, $\varepsilon_V = 8$. pmrad, and an energy spread of 0.001.

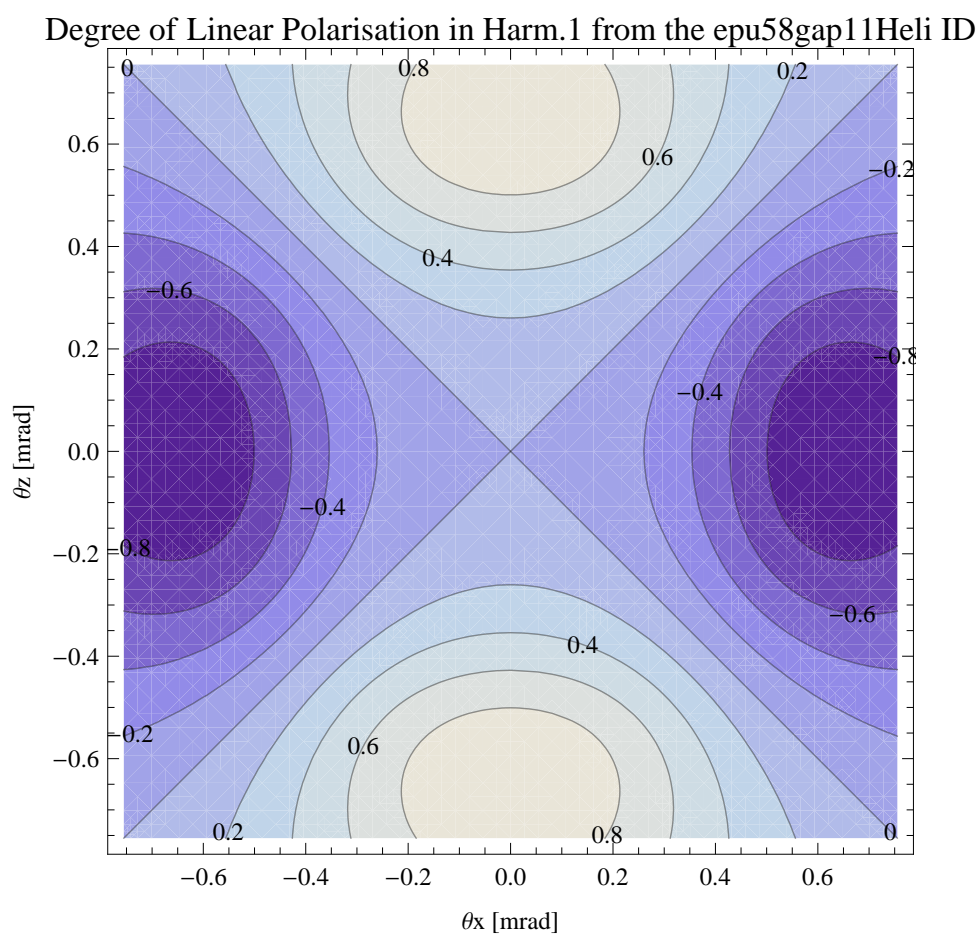


Figure 386: Map of linear polarisation in the fundamental harmonic of the synchrotron radiation emitted by the epu58gap11Heli ID

Degree of 45 degree Polarisation in Harm.1 from the epu58gap11Heli ID

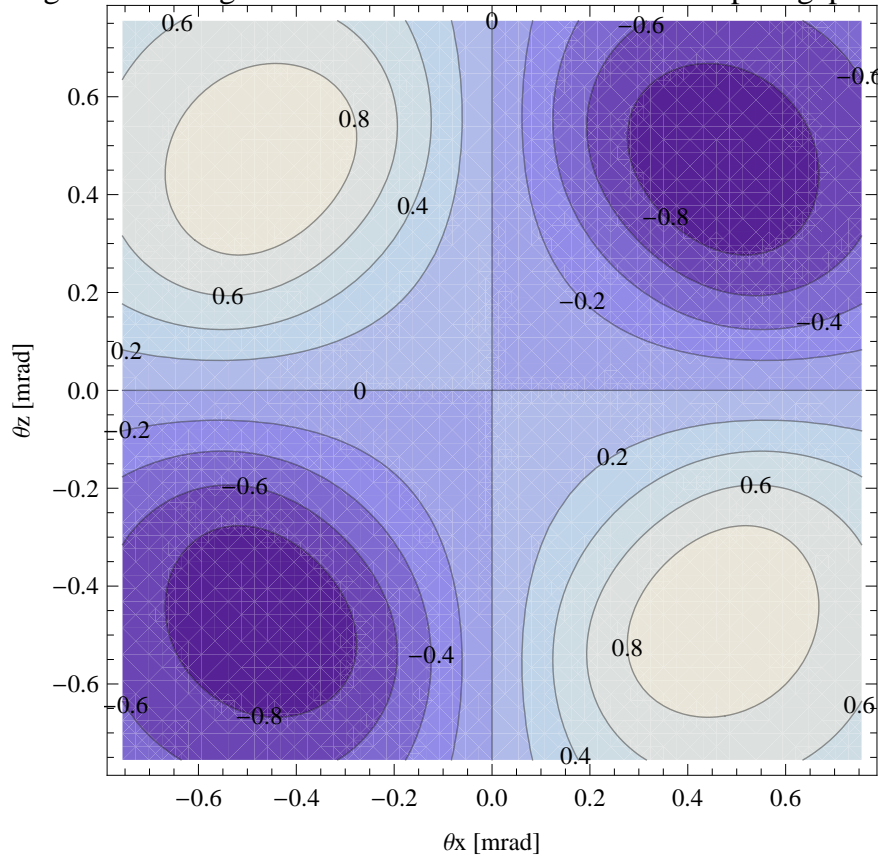


Figure 387: Map of 45 degree polarisation in the fundamental harmonic of the synchrotron radiation emitted by the epu58gap11Heli ID

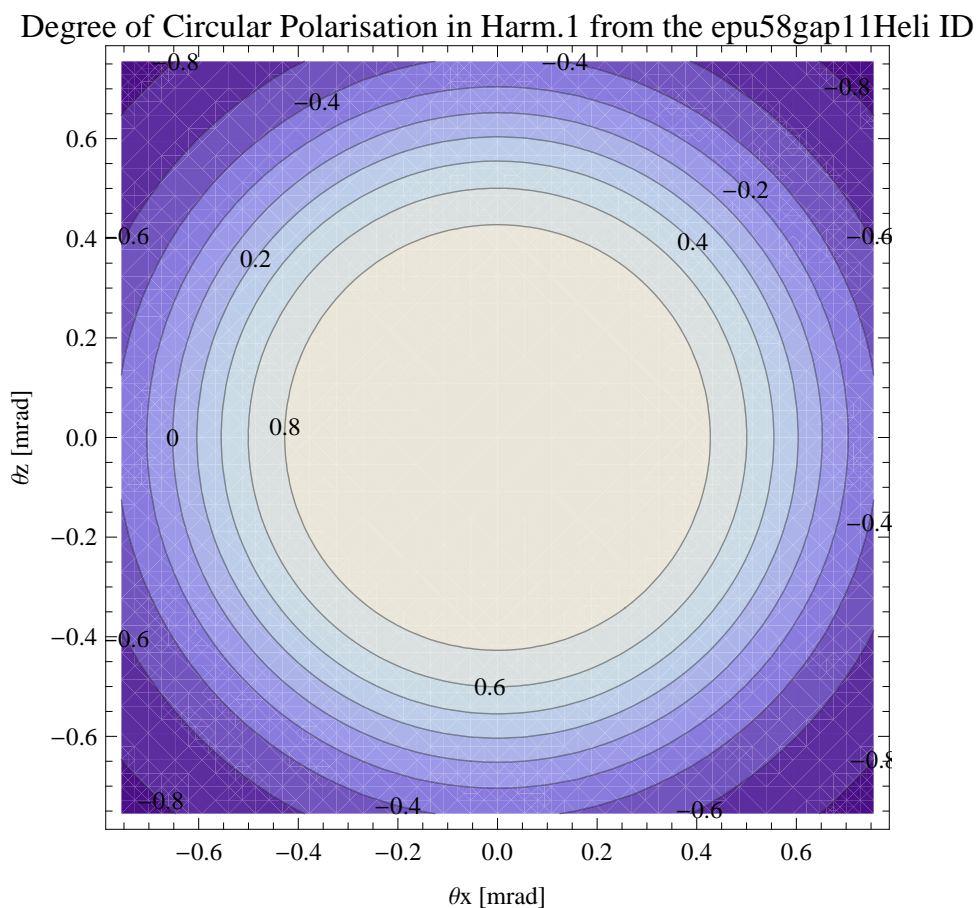


Figure 388: Map of circular polarisation in the fundamental harmonic of the synchrotron radiation emitted by the epu58gap11Heli ID

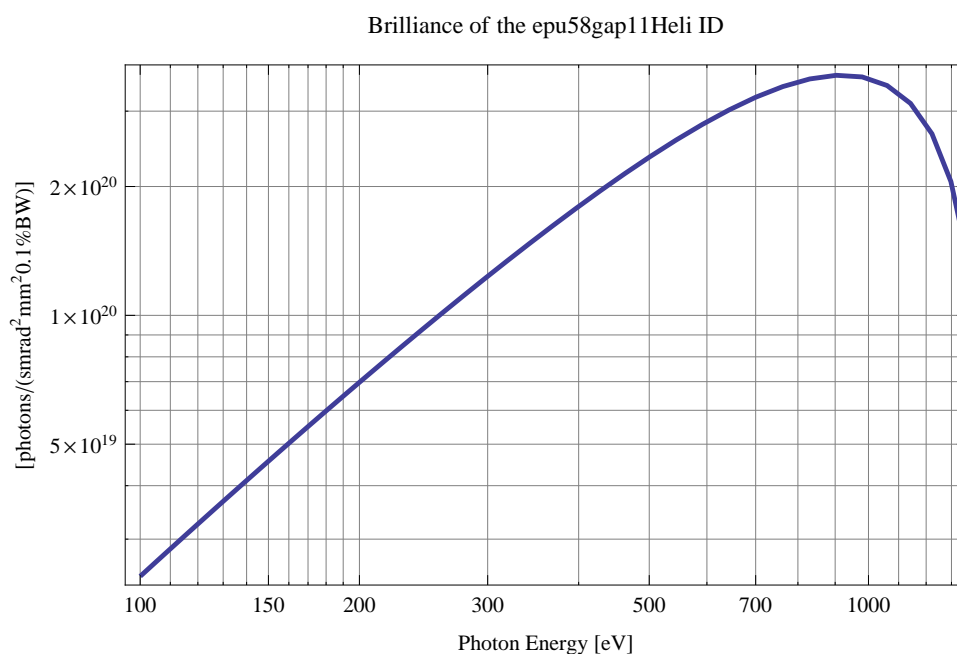


Figure 389: The brilliance at peak energy of the synchrotron radiation emitted by the epu58gap11Heli ID

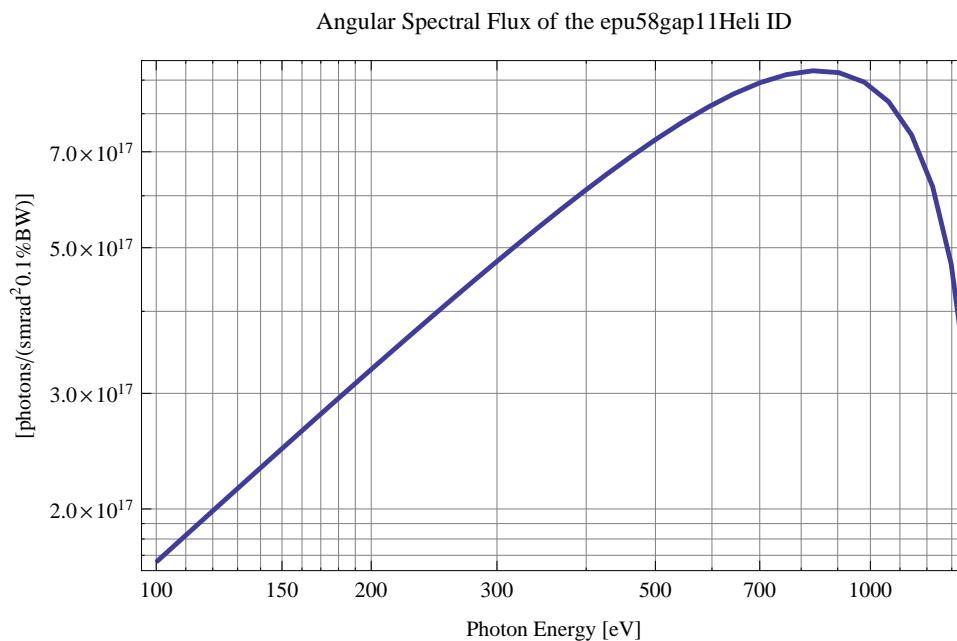


Figure 390: The angular spectral flux of the synchrotron radiation emitted by the epu58gap11Heli ID

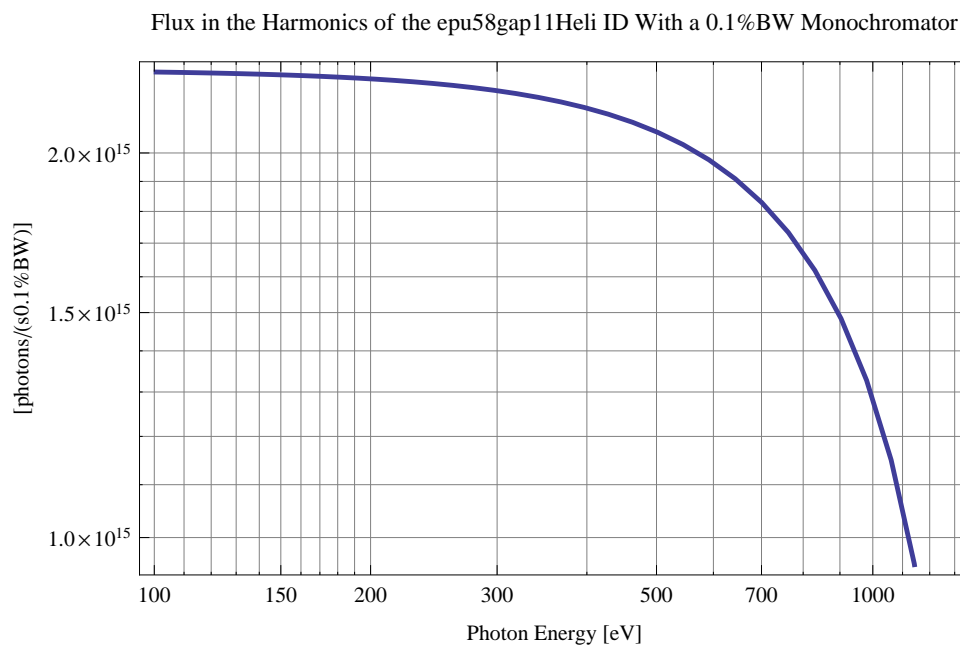


Figure 391: The flux of photons in the harmonics of the emitted synchrotron radiation from the epu58gap11Heli ID using a 0.1%BW monochromator

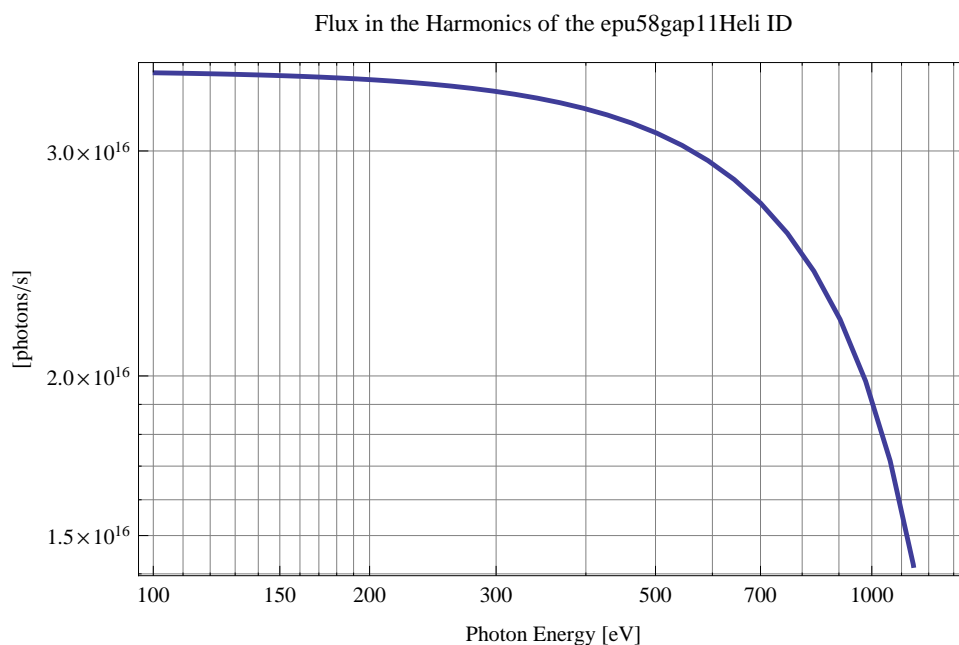


Figure 392: The flux of photons in the harmonics of the emitted synchrotron radiation from the epu58gap11Heli ID

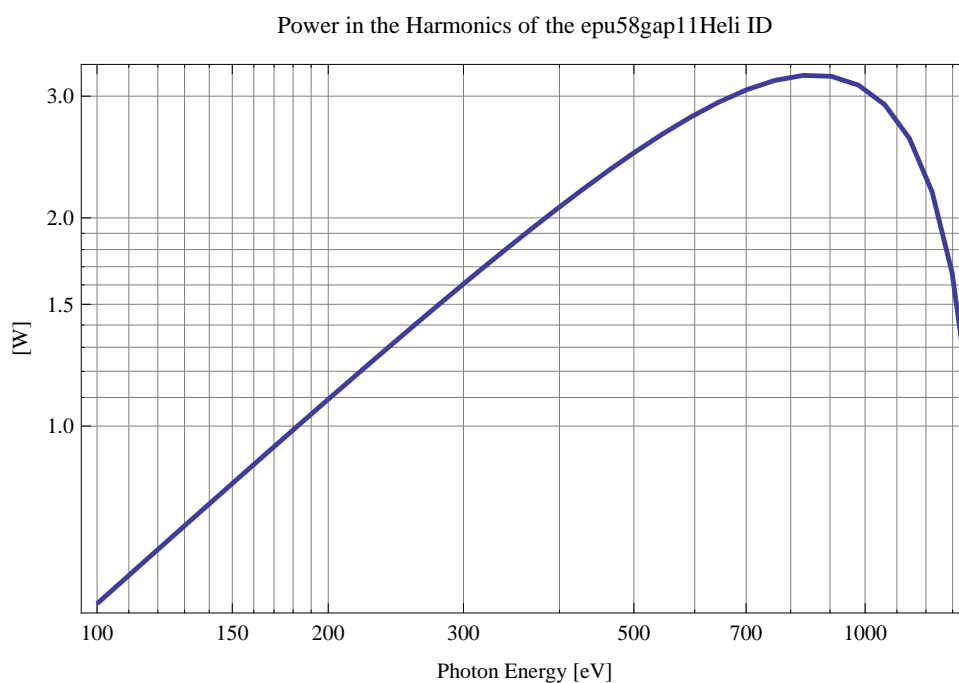


Figure 393: The power in the harmonics of the emitted synchrotron radiation from the epu58gap11Heli ID

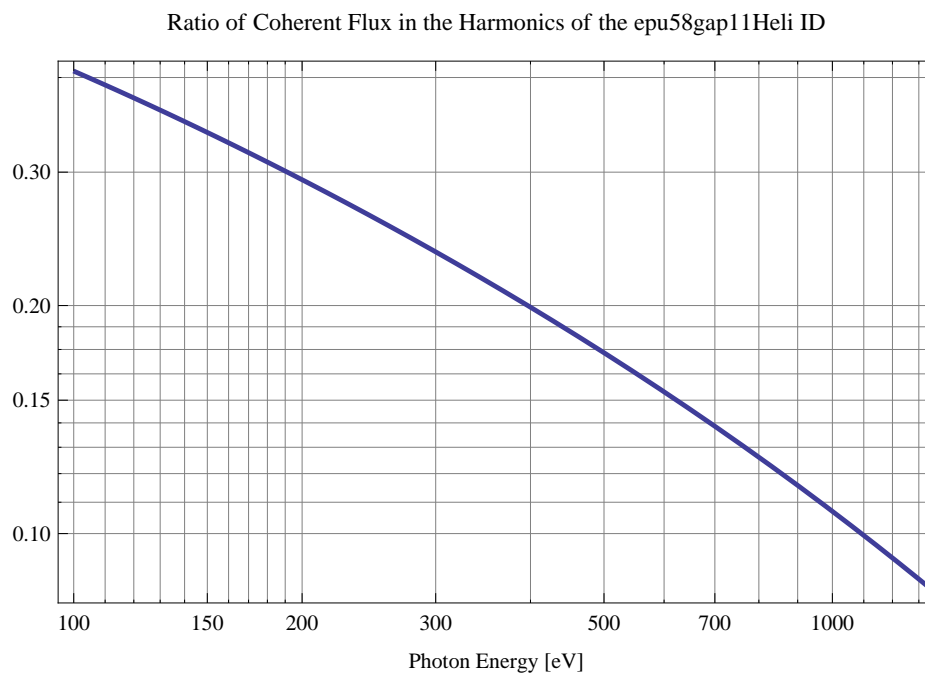


Figure 394: The ratio of coherent flux in the harmonics of the emitted synchrotron radiation from the epu58gap11Heli ID

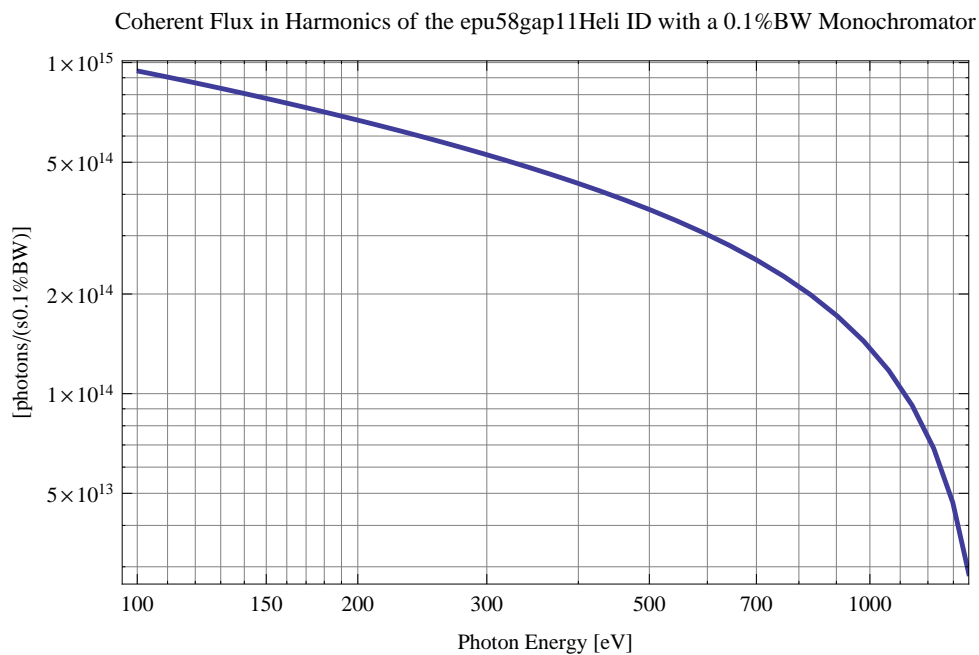


Figure 395: The coherent flux in the harmonics of the epu58gap11Heli ID using a 0.1%BW Monochromator

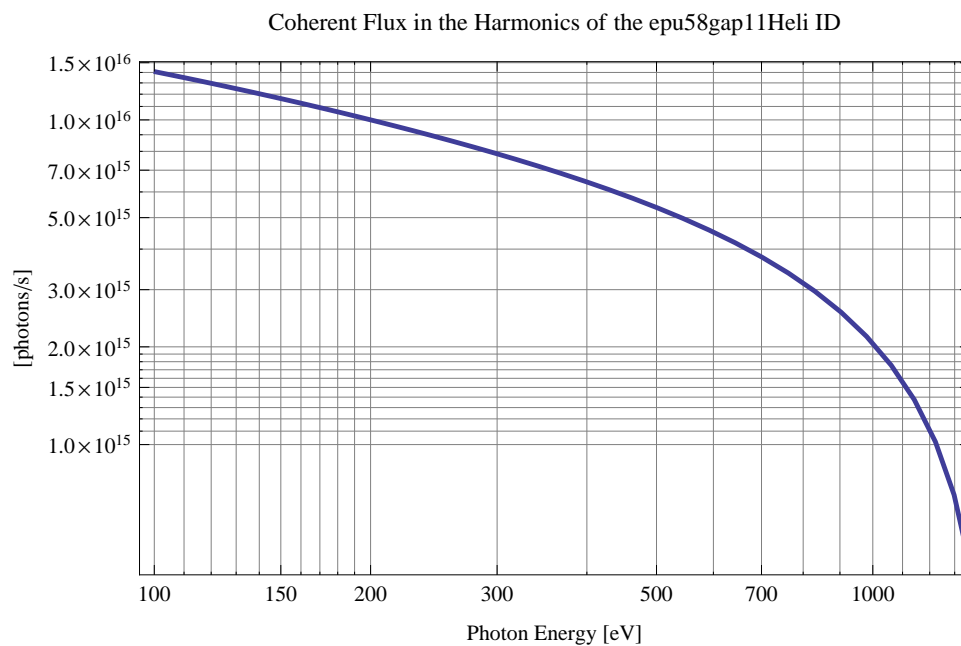


Figure 396: The coherent flux in the harmonics of the epu58gap11Heli ID

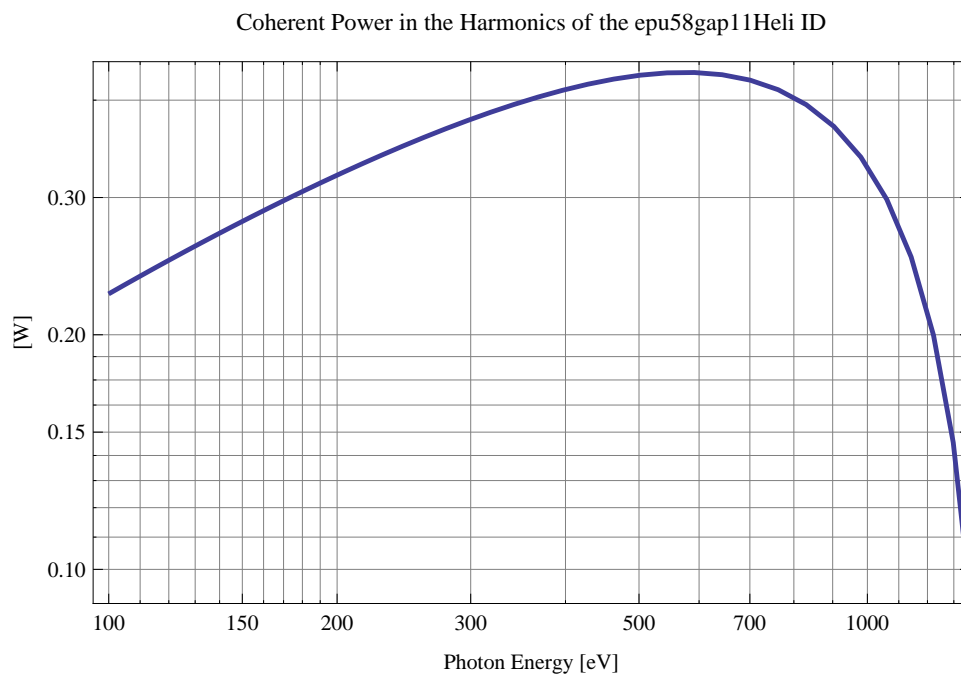


Figure 397: The power of coherent synchrotron radiation in the harmonics of the epu58gap11Heli ID

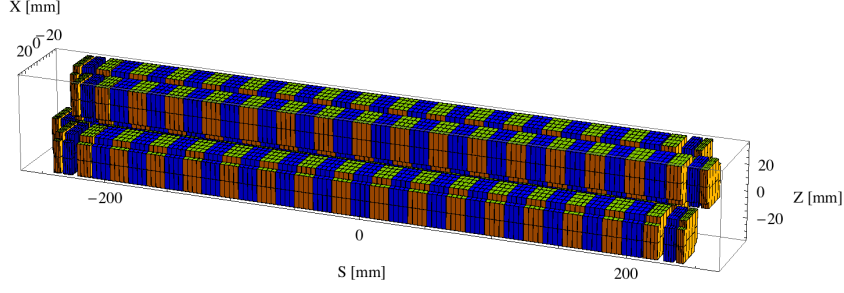


Figure 398: Magnetic model of the epu58gap11Incl ID. The ID has been modelled with Radia [3]

The brilliance at peak energy and the angular spectral flux density from the epu58gap11Heli ID for different harmonics at maximum K-value (5.225) are given in Table 66 and for minimum K-value (0.400) these values are given in Table 67.

Table 66: The brilliance at peak energy and the angular spectral flux density from the epu58gap11Heli ID for different harmonics at maximum K-value (5.225)

Harmonic	Photon Energy [eV]	Brilliance [Ph./((smrad ² mrad ² 0.1%BW))]	Angular Spectral Flux [Ph./((smrad ² 0.1%BW))]
1	100.589	2.48×10^{19}	1.67×10^{17}

Table 67: The brilliance at peak energy and the angular spectral flux density from the epu58gap11Heli ID for different harmonics at minimum K-value (0.4)

Harmonic	Photon Energy [eV]	Brilliance [Ph./((smrad ² mrad ² 0.1%BW))]	Angular Spectral Flux [Ph./((smrad ² 0.1%BW))]
1	1364.43	1.39×10^{20}	3.15×10^{17}

2.6.8 Magnet model of the elliptically polarising undulator epu58gap11Incl

The Radia [3] magnet model of the epu58gap11Incl ID is shown in Figure 398. The length of the magnet model is 482.016 mm. The magnetic material in the model is NdFeb with a remanence of 1.28 T, a material similar to VACODYM 776 TP from Vacuumschmelze. Blocks with vertical magnetisation are blue and blocks with horizontal magnetisation are yellow. The block size is 30.x30.x14.5 mm³ and there is a 5. mm cut-out in two of the corners of the blocks. The total length of the epu58gap11Incl ID is 3904.02 mm.

2.6.9 Analysis of the magnetic field of the epu58gap11Incl ID

The effective magnetic fields on axis and the fundamental photon energy of the epu58gap11Incl ID are shown in Table 68. The higher harmonic contents in the magnetic field of an elliptically polarising undulator made of permanent magnets is negligible and the effective field has about the same strength as the peak field.

Table 68: Effective Fields on axis and Fundamental Photon Energy of the epu58gap11Incl ID

Undulator Period	58	mm
Undulator Gap	11	mm
Undulator Mode	Inclined	
Undulator Phase	15.645	mm
Vertical Peak Field	0.482	T
Effective Vertical Field	0.486	T
K _x (from vert. field)	2.633	
Horizontal Peak Field:	−0.480	T
Effective Horizontal Field	0.486	T
K _z (from hor. field)	2.633	
Photon Energy, Harm.1	0.186	keV
Emitted Power	5.251	kW
Total Length	3904.0	mm

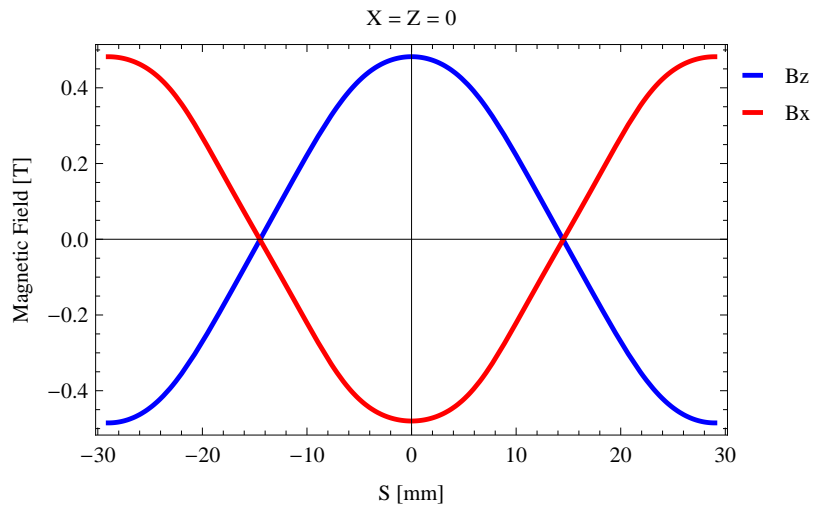


Figure 399: Vertical magnetic field in a central pole of the epu58gap11Incl ID along the ID axis, $X = Z = 0$

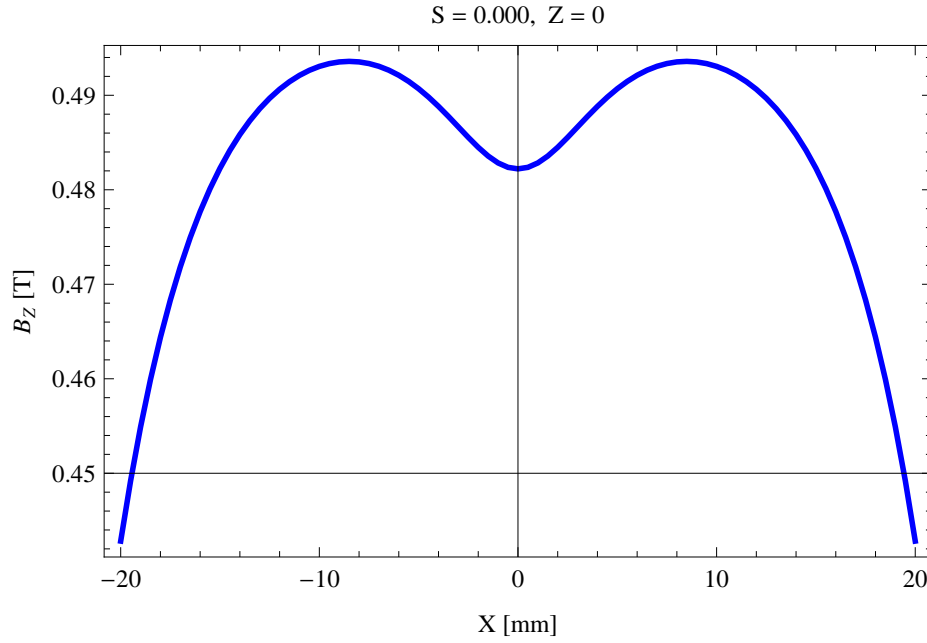


Figure 400: Vertical magnetic field in a central pole of the epu58gap11Incl ID along the horizontally transverse direction to the ID axis, $S = 0.000, Z = 0$

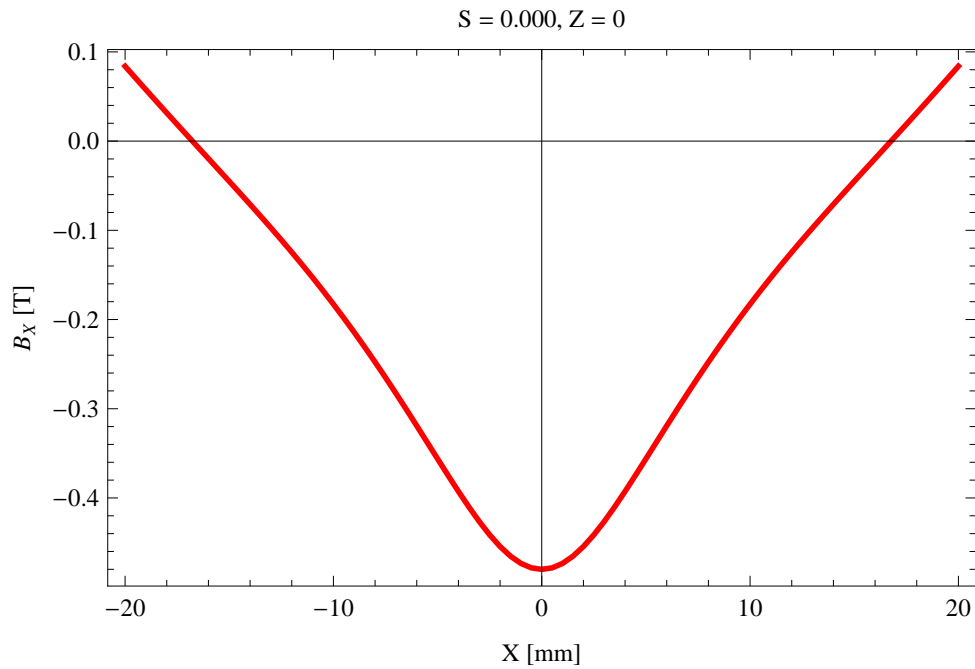


Figure 401: Horizontal magnetic field in a central pole of the epu58gap11Incl ID along the horizontally transverse direction to the ID axis, $S = 0.000, Z = 0$

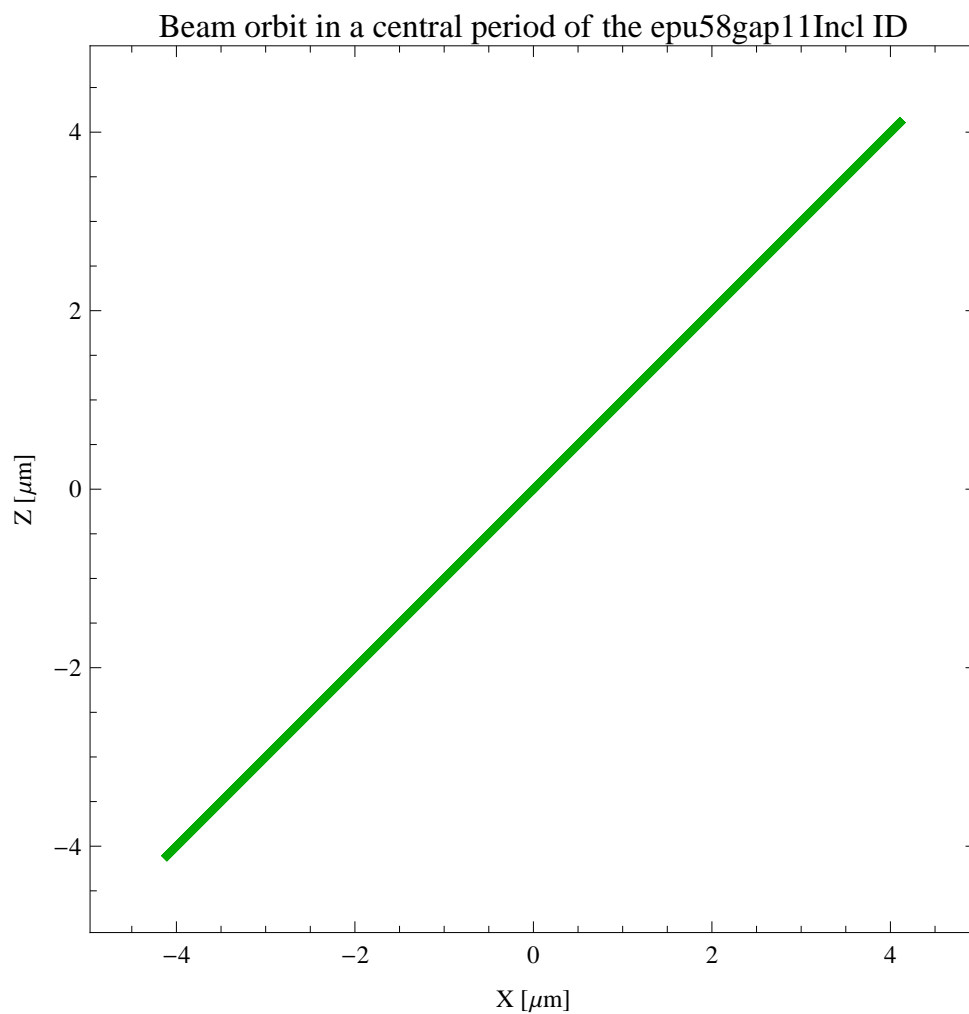


Figure 402: The beam orbit of the electron beam through a central period of the epu58gap11Incl ID

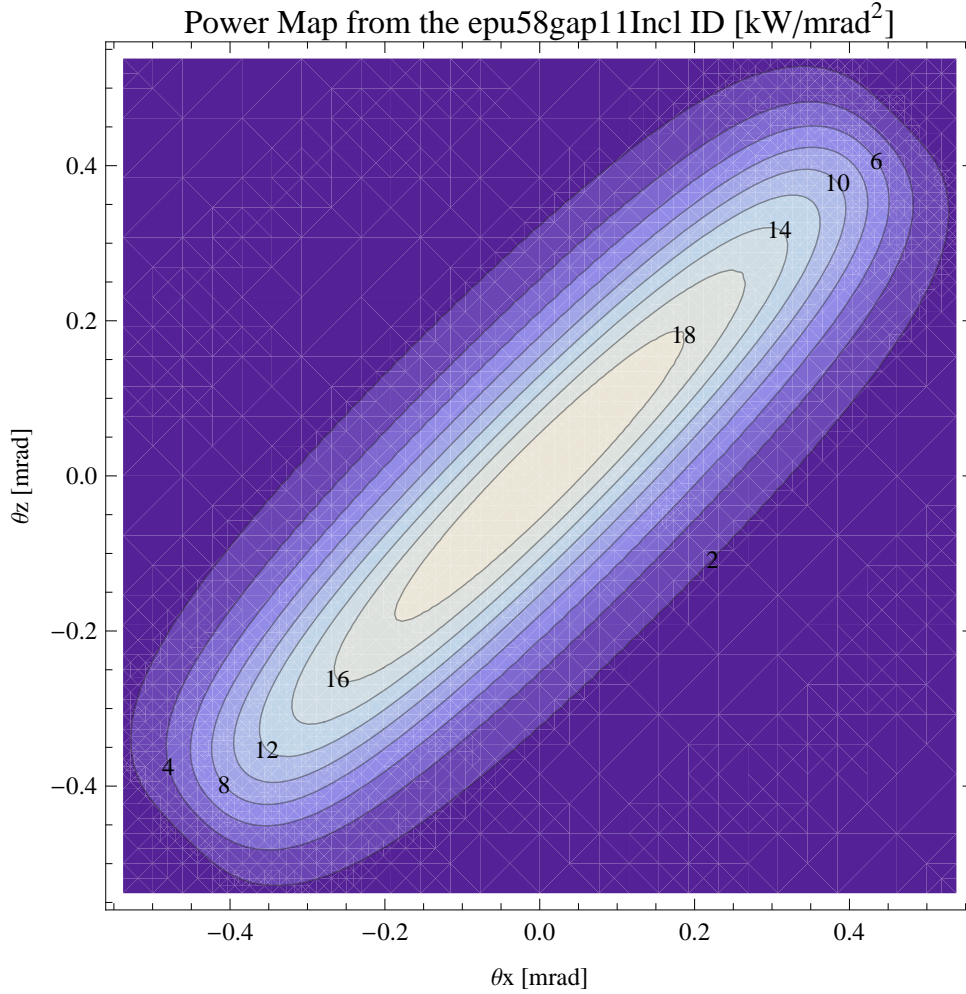


Figure 403: Map of the power distribution of the emitted synchrotron radiation by the epu58gap11Incl ID

2.6.10 Synchrotron radiation from the epu58gap11Incl ID

The power map of the emitted synchrotron radiation by the epu58gap11Incl ID, assuming a 0.5 A filament beam with an energy of 3 GeV and undulator properties of the synchrotron radiation, is shown in Figure 403. The on-axis power density is 19.812 kW/mrad²

A map of the degree of linear polarisation of the fundamental harmonic of the synchrotron radiation emitted by the epu58gap11Incl ID over the angle of observation is shown in Figure 404.

A map of the degree of 45 degree polarisation of the fundamental harmonic of the synchrotron radiation emitted by the epu58gap11Incl ID over the angle of observation is shown in Figure 405.

A map of the degree of circular polarisation of the fundamental harmonic of the synchrotron radiation emitted by the epu58gap11Incl ID over the angle of observation is shown in Figure 406.

The on axis brilliance at peak energy and the angular spectral flux from the epu58gap11Incl ID have been calculated with the given beam parameters, which are 0.5 A of stored current, $\beta_H = 9$ m, $\varepsilon_H = 0.263$ nrad, $\beta_V = 4.8$ m, $\varepsilon_V = 8$. pmrad, and an energy spread of 0.001.

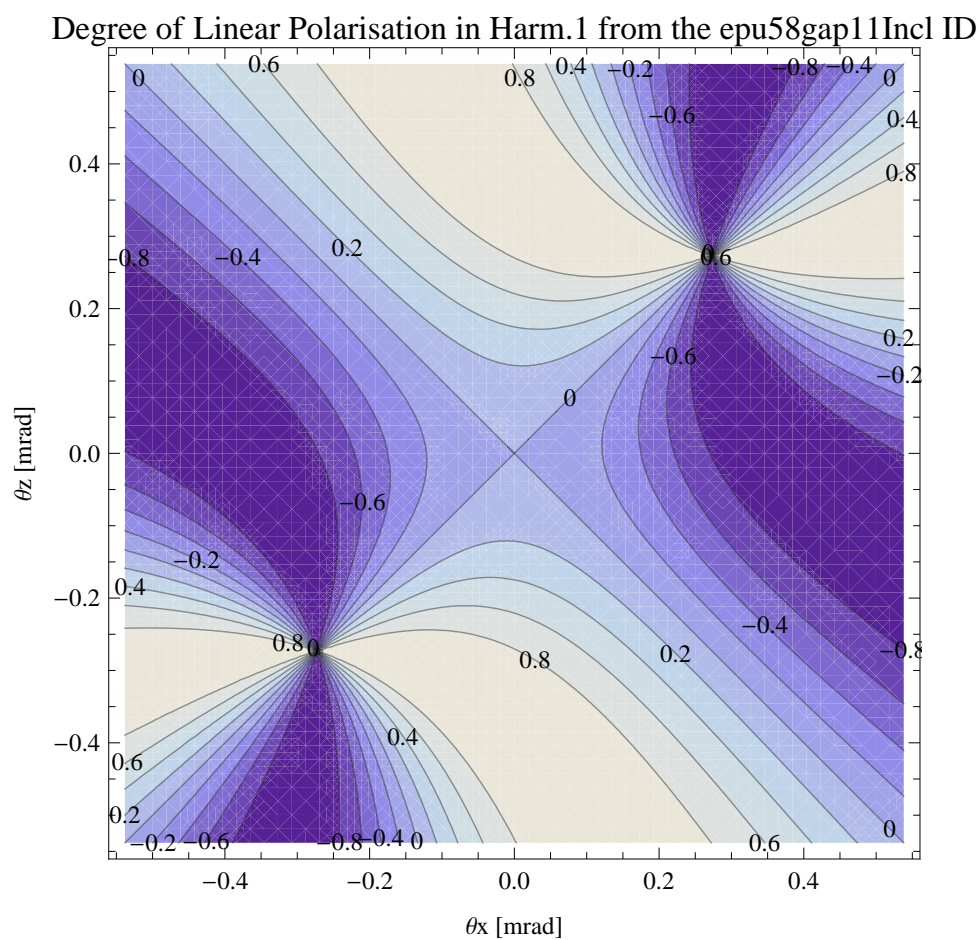


Figure 404: Map of linear polarisation in the fundamental harmonic of the synchrotron radiation emitted by the epu58gap11Incl ID

Degree of 45 degree Polarisation in Harm.1 from the epu58gap11Incl ID

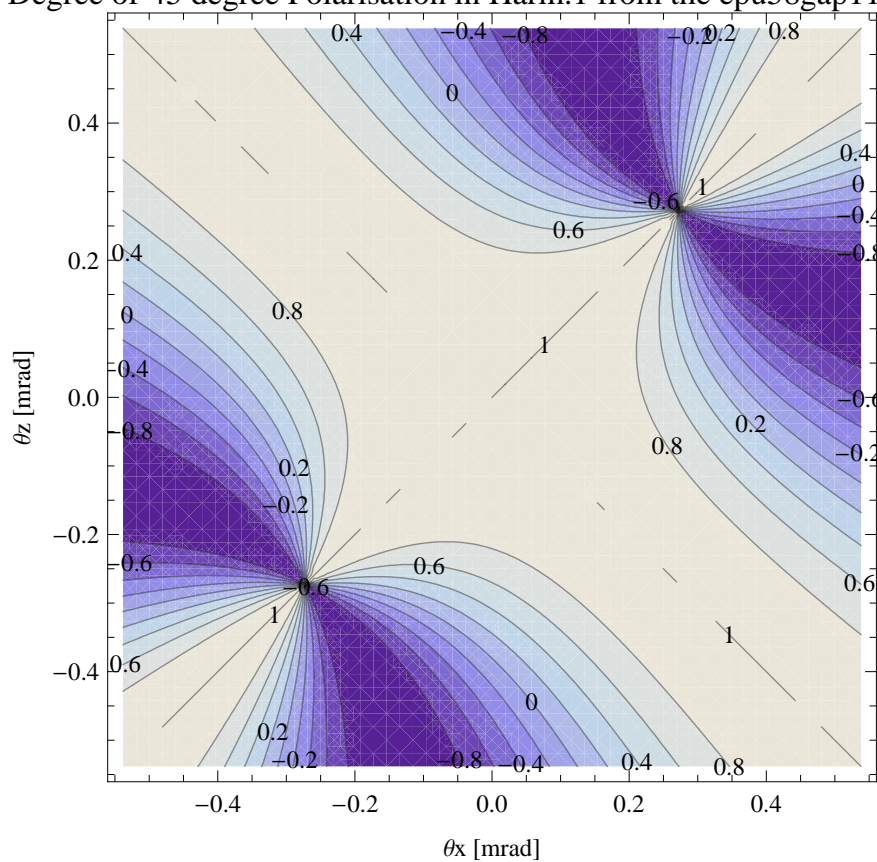


Figure 405: Map of 45 degree polarisation in the fundamental harmonic of the synchrotron radiation emitted by the epu58gap11Incl ID

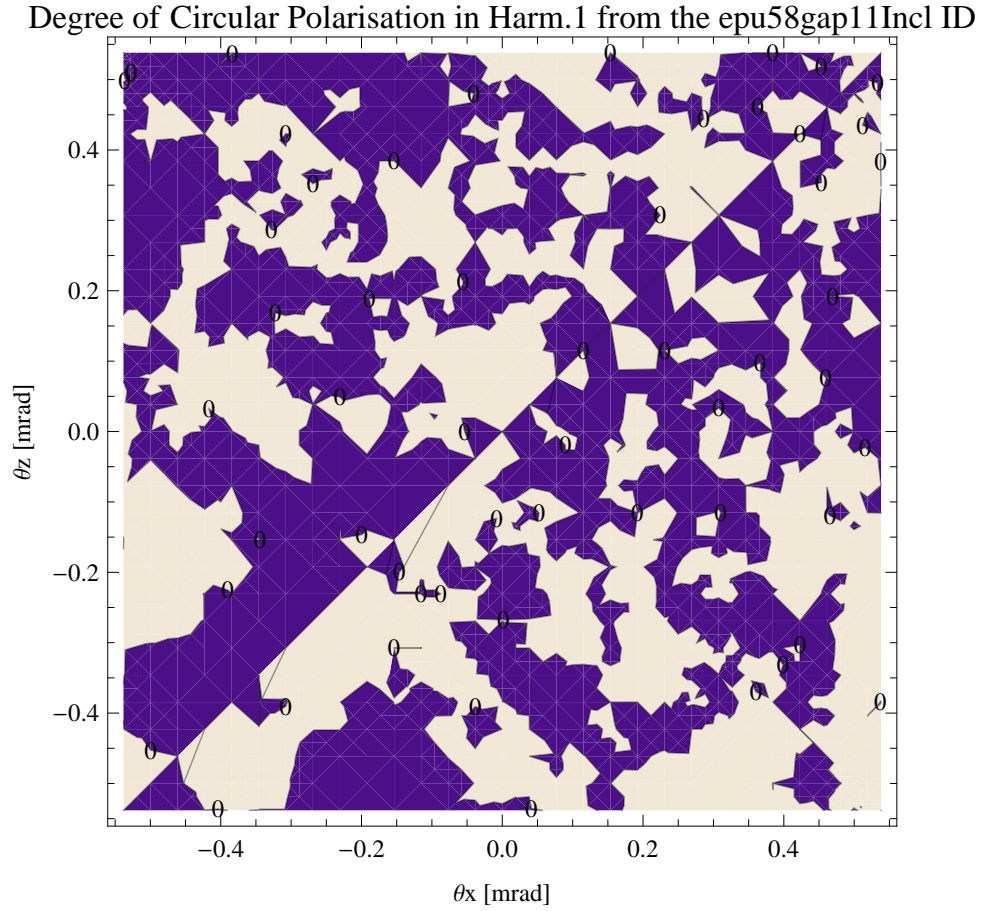


Figure 406: Map of circular polarisation in the fundamental harmonic of the synchrotron radiation emitted by the epu58gap11Incl ID

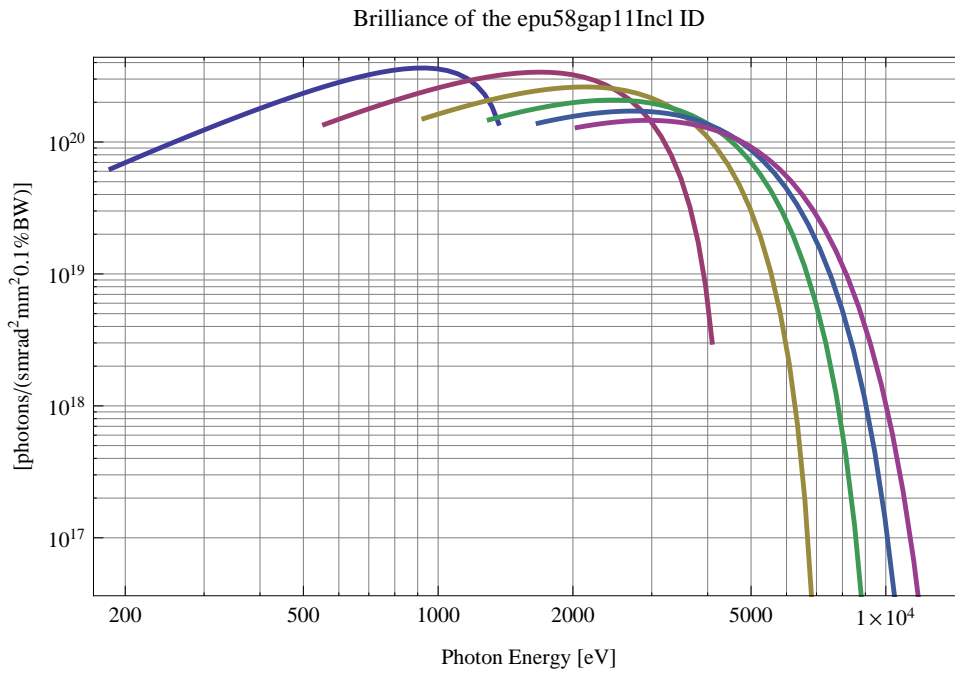


Figure 407: The brilliance at peak energy of the synchrotron radiation emitted by the epu58gap11Incl ID

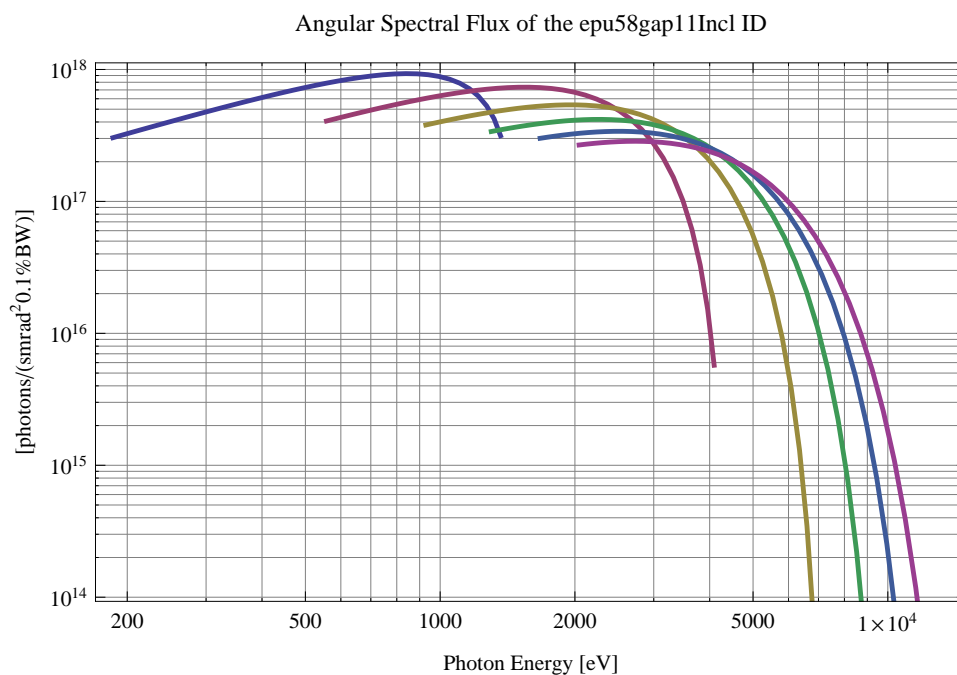


Figure 408: The angular spectral flux of the synchrotron radiation emitted by the epu58gap11Incl ID

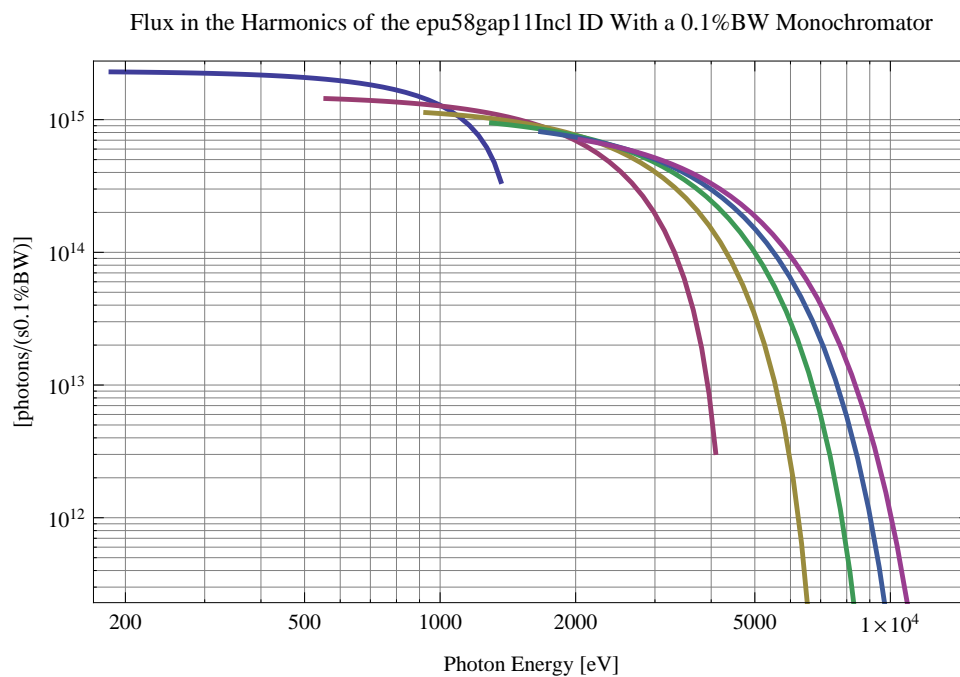


Figure 409: The flux of photons in the harmonics of the emitted synchrotron radiation from the epu58gap11Incl ID using a 0.1%BW monochromator

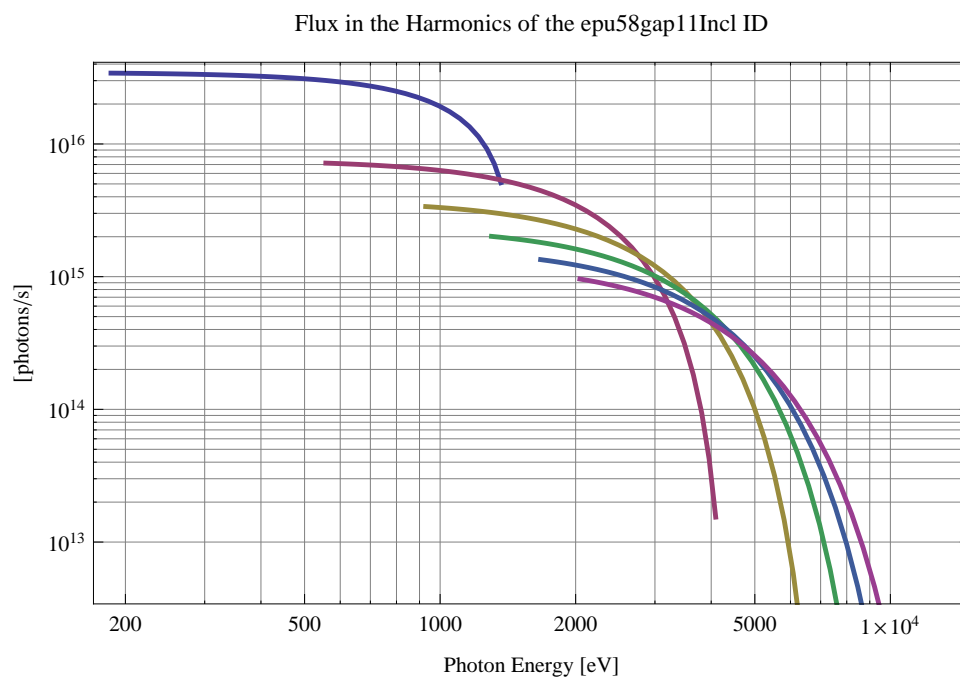


Figure 410: The flux of photons in the harmonics of the emitted synchrotron radiation from the epu58gap11Incl ID

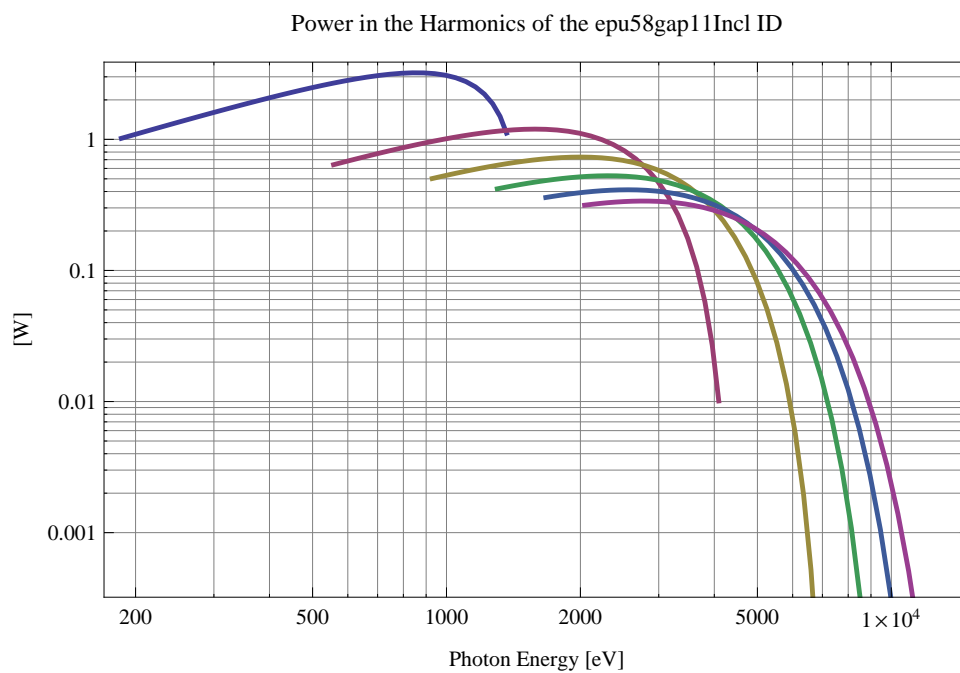


Figure 411: The power in the harmonics of the emitted synchrotron radiation from the epu58gap11Incl ID

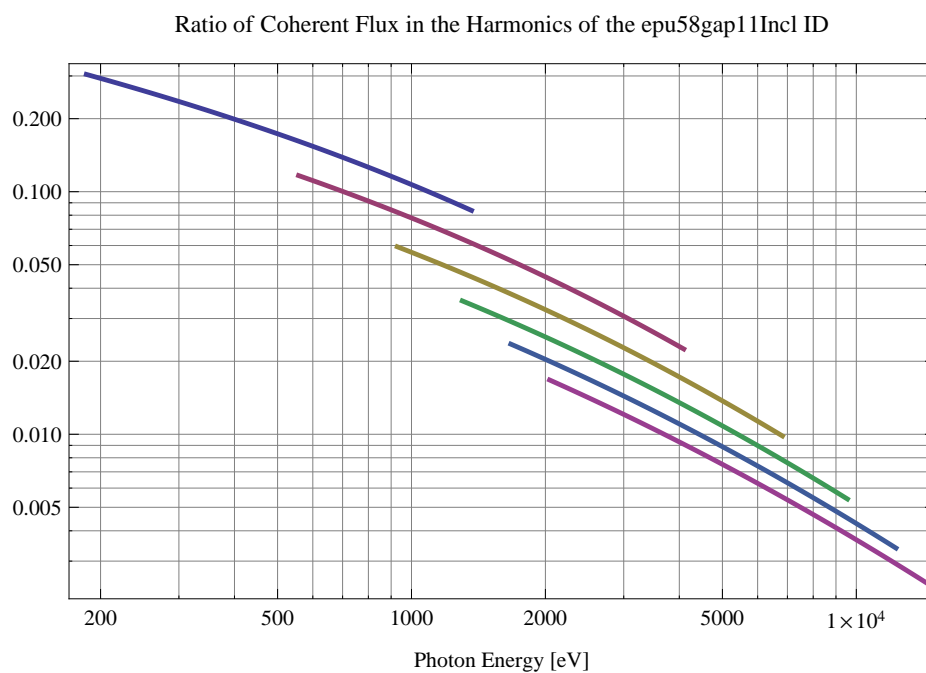


Figure 412: The ratio of coherent flux in the harmonics of the emitted synchrotron radiation from the epu58gap11Incl ID

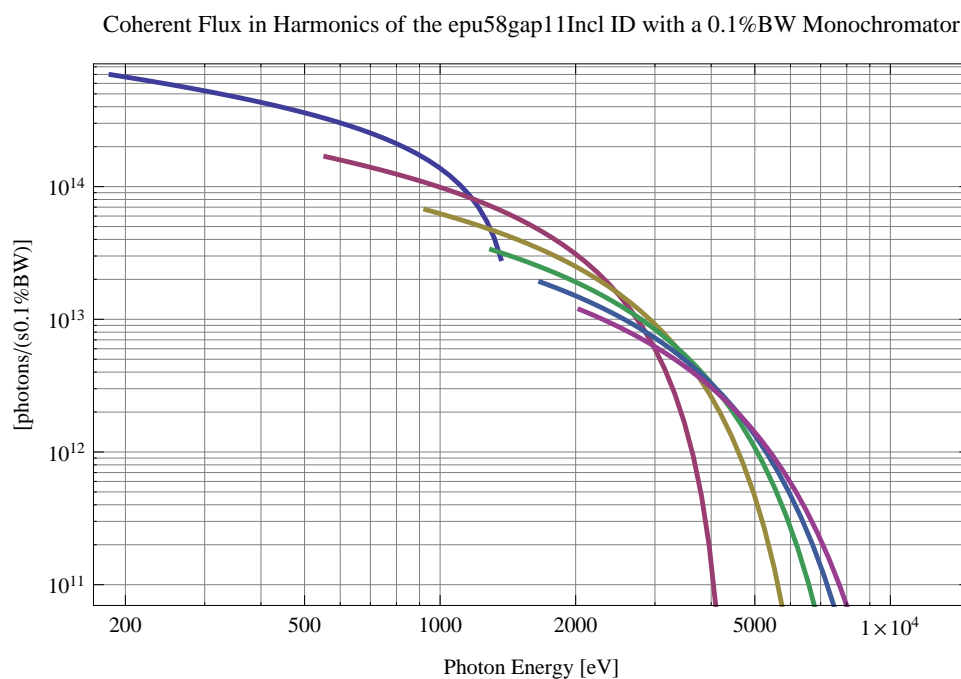


Figure 413: The coherent flux in the harmonics of the epu58gap11Incl ID using a 0.1%BW Monochromator

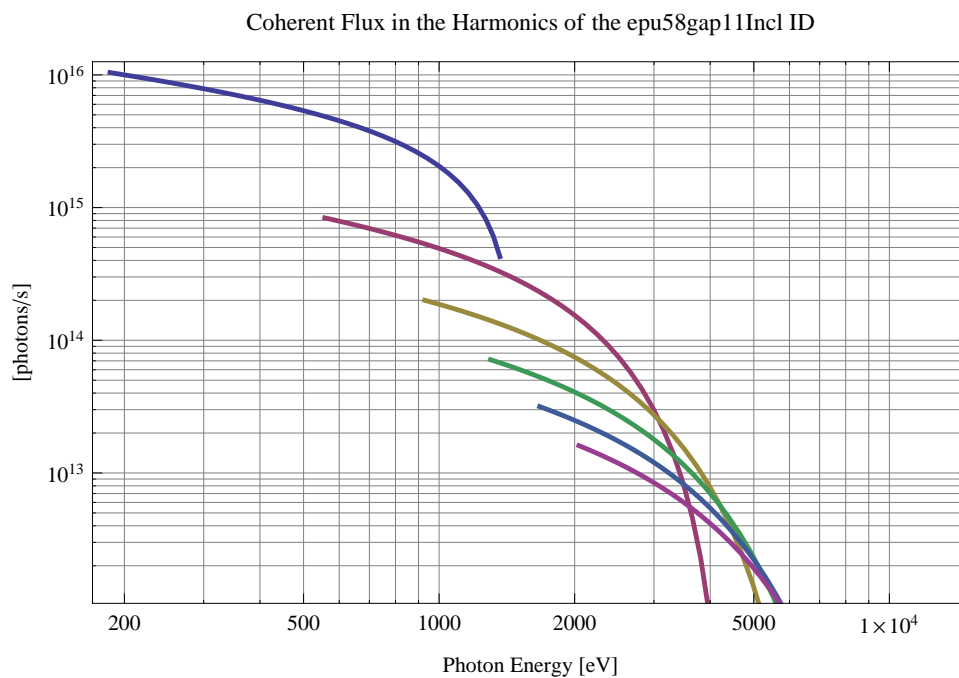


Figure 414: The coherent flux in the harmonics of the epu58gap11Incl ID

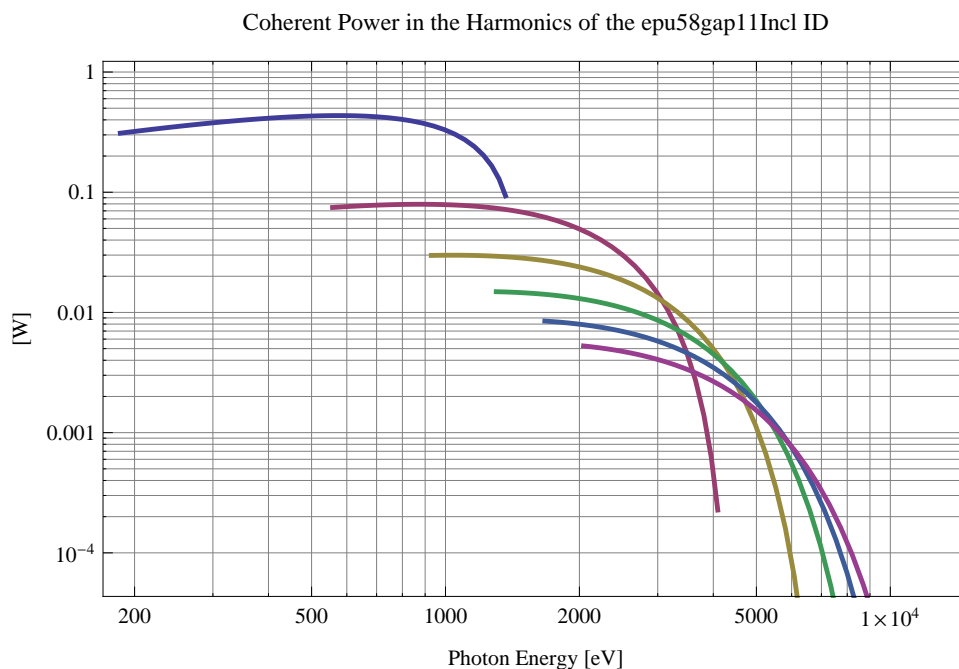


Figure 415: The power of coherent synchrotron radiation in the harmonics of the epu58gap11Incl ID

The brilliance at peak energy and the angular spectral flux density from the epu58gap11Incl ID for different harmonics at maximum K-value (3.723) are given in Table 69 and for minimum K-value (0.400) these values are given in Table 70.

Table 69: The brilliance at peak energy and the angular spectral flux density from the epu58gap11Incl ID for different harmonics at maximum K-value (3.723)

Harmonic	Photon Energy [eV]	Brilliance [Ph./ (smrad ² mrad ² 0.1% BW)]	Angular Spectral Flux [Ph./ (smrad ² 0.1% BW)]
1	185.79	6.26×10^{19}	3.04×10^{17}
3	557.37	1.36×10^{20}	4.07×10^{17}
5	928.95	1.51×10^{20}	3.8×10^{17}
7	1300.53	1.47×10^{20}	3.39×10^{17}
9	1672.11	1.39×10^{20}	3.01×10^{17}
11	2043.69	1.29×10^{20}	2.68×10^{17}

Table 70: The brilliance at peak energy and the angular spectral flux density from the epu58gap11Incl ID for different harmonics at minimum K-value (0.4)

Harmonic	Photon Energy [eV]	Brilliance [Ph./ (smrad ² mrad ² 0.1% BW)]	Angular Spectral Flux [Ph./ (smrad ² 0.1% BW)]
1	1364.43	1.39×10^{20}	3.15×10^{17}
3	4093.28	3.03×10^{18}	5.73×10^{15}
5	6822.13	3.63×10^{16}	6.59×10^{13}
7	9550.98	3.9×10^{14}	6.98×10^{11}
9	12279.8	4.07×10^{12}	7.22×10^9
11	15008.7	4.18×10^{10}	7.4×10^7

2.6.11 Magnet model of the elliptically polarising undulator epu58gap11Vert

The Radia [3] magnet model of the epu58gap11Vert ID is shown in Figure 416. The length of the magnet model is 482.016 mm. The magnetic material in the model is NdFeb with a remanence of 1.28 T, a material similar to VACODYM 776 TP from Vacuumschmelze. Blocks with vertical magnetisation are blue and blocks with horizontal magnetisation are yellow. The block size is 30.x30.x14.5 mm³ and there is a 5. mm cut-out in two of the corners of the blocks. The total length of the epu58gap11Vert ID is 3904.02 mm.

2.6.12 Analysis of the magnetic field of the epu58gap11Vert ID

The effective magnetic fields on axis and the fundamental photon energy of the epu58gap11Vert ID are shown in Table 71. The higher harmonic contents in the magnetic field of an elliptically polarising undulator made of permanent magnets is negligible and the effective field has about the same strength as the peak field.

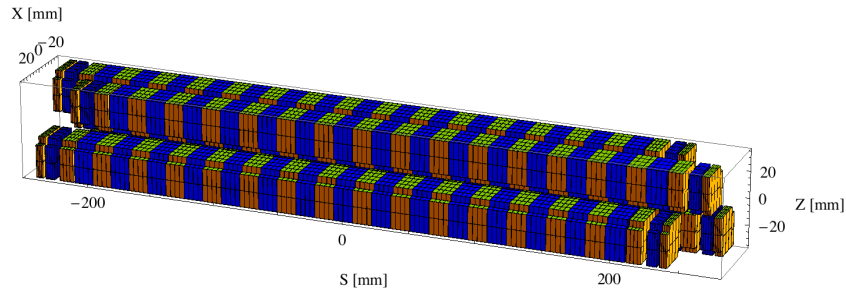


Figure 416: Magnetic model of the epu58gap11Vert ID. The ID has been modelled with Radia [3]

Table 71: Effective Fields on axis and Fundamental Photon Energy of the epu58gap11Vert ID

Undulator Period	58	mm
Undulator Gap	11	mm
Undulator Mode	Vertical	
Undulator Phase	29.000	mm
Vertical Peak Field	0.000	T
Effective Vertical Field	0.000	T
Kx (from vert. field)	0.000	
Horizontal Peak Field:	0.863	T
Effective Horizontal Field	0.865	T
Kz (from hor. field)	4.686	
Photon Energy, Harm.1	0.123	keV
Emitted Power	8.317	kW
Total Length	3904.0	mm

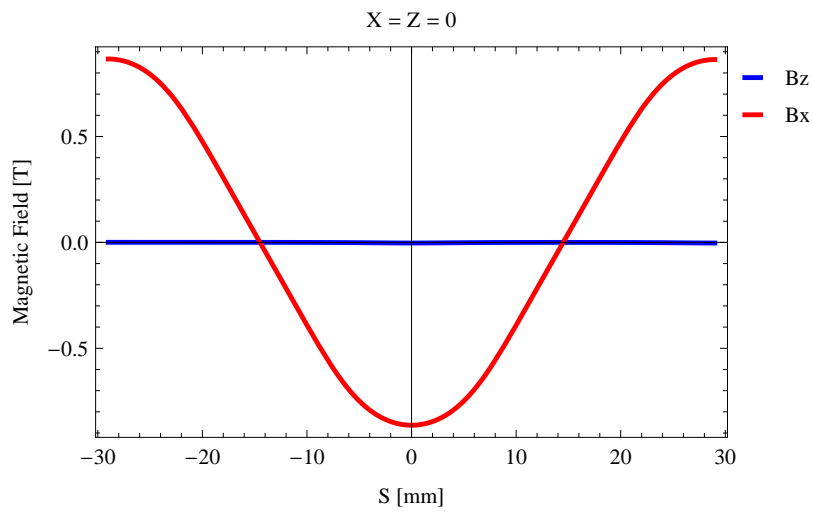


Figure 417: Vertical magnetic field in a central pole of the epu58gap11Vert ID along the ID axis, $X = Z = 0$

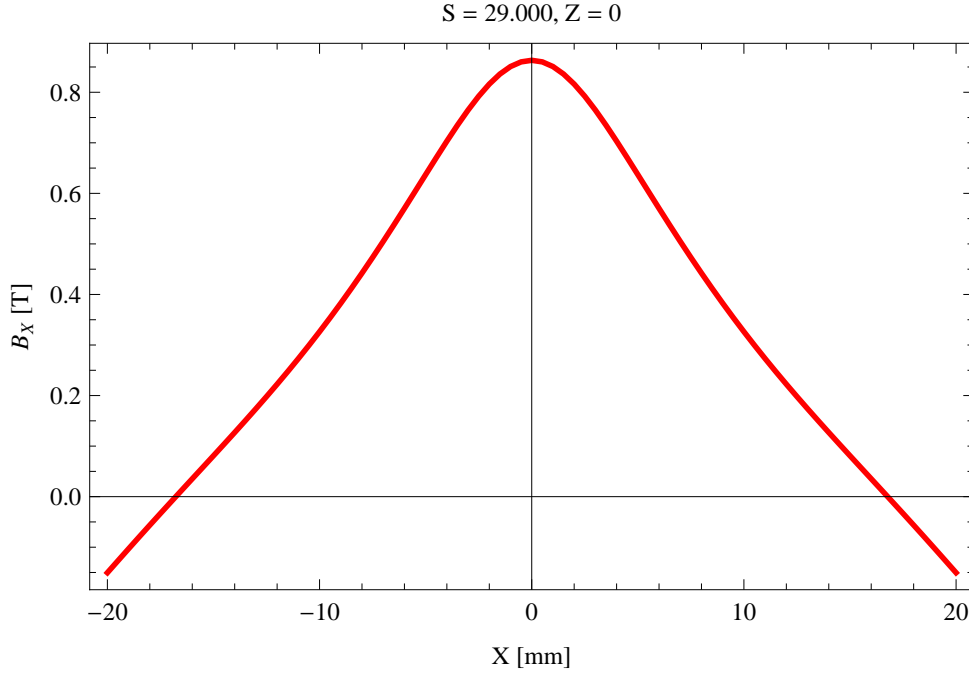


Figure 418: Horizontal magnetic field in a central pole of the epu58gap11Vert ID along the horizontally transverse direction to the ID axis, $S = 29.000$, $Z = 0$

2.6.13 Synchrotron radiation from the epu58gap11Vert ID

The power map of the emitted synchrotron radiation by the epu58gap11Vert ID, assuming a 0.5 A filament beam with an energy of 3 GeV and undulator properties of the synchrotron radiation, is shown in Figure 420. The on-axis power density is 24.987 kW/mrad²

A map of the degree of linear polarisation of the fundamental harmonic of the synchrotron radiation emitted by the epu58gap11Vert ID over the angle of observation is shown in Figure 421.

A map of the degree of 45 degree polarisation of the fundamental harmonic of the synchrotron radiation emitted by the epu58gap11Vert ID over the angle of observation is shown in Figure 422.

A map of the degree of circular polarisation of the fundamental harmonic of the synchrotron radiation emitted by the epu58gap11Vert ID over the angle of observation is shown in Figure 423.

The on axis brilliance at peak energy and the angular spectral flux from the epu58gap11Vert ID have been calculated with the given beam parameters, which are 0.5 A of stored current, $\beta_H = 9$ m, $\varepsilon_H = 0.263$ nmrad, $\beta_V = 4.8$ m, $\varepsilon_V = 8$ pmrad, and an energy spread of 0.001.

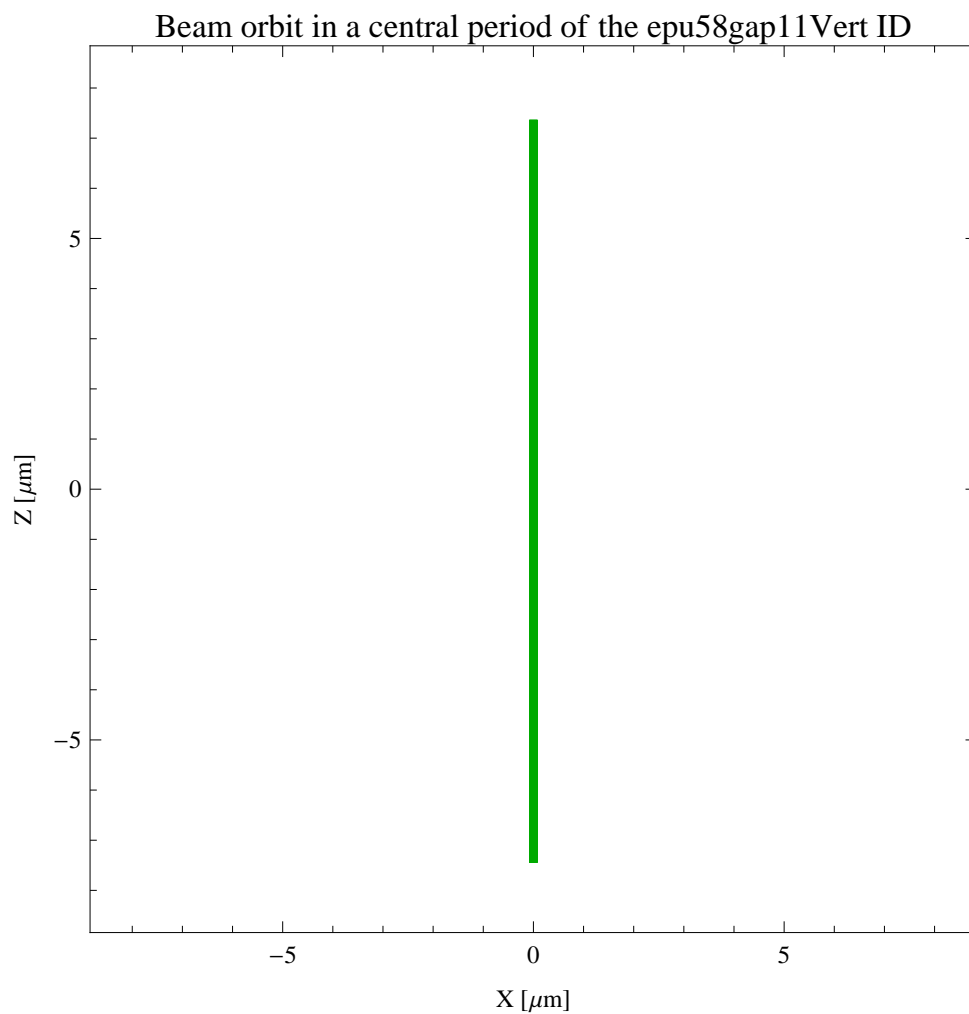


Figure 419: The beam orbit of the electron beam through a central period of the epu58gap11Vert ID

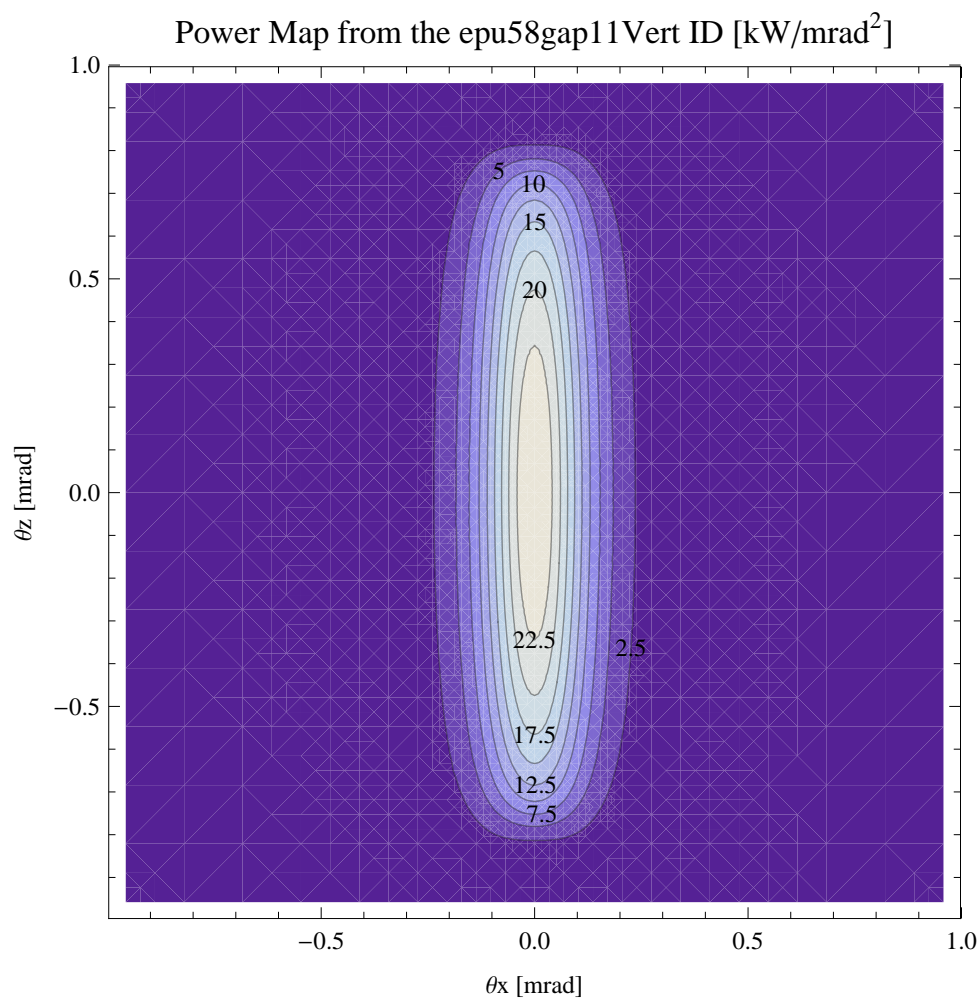


Figure 420: Map of the power distribution of the emitted synchrotron radiation by the epu58gap11Vert ID

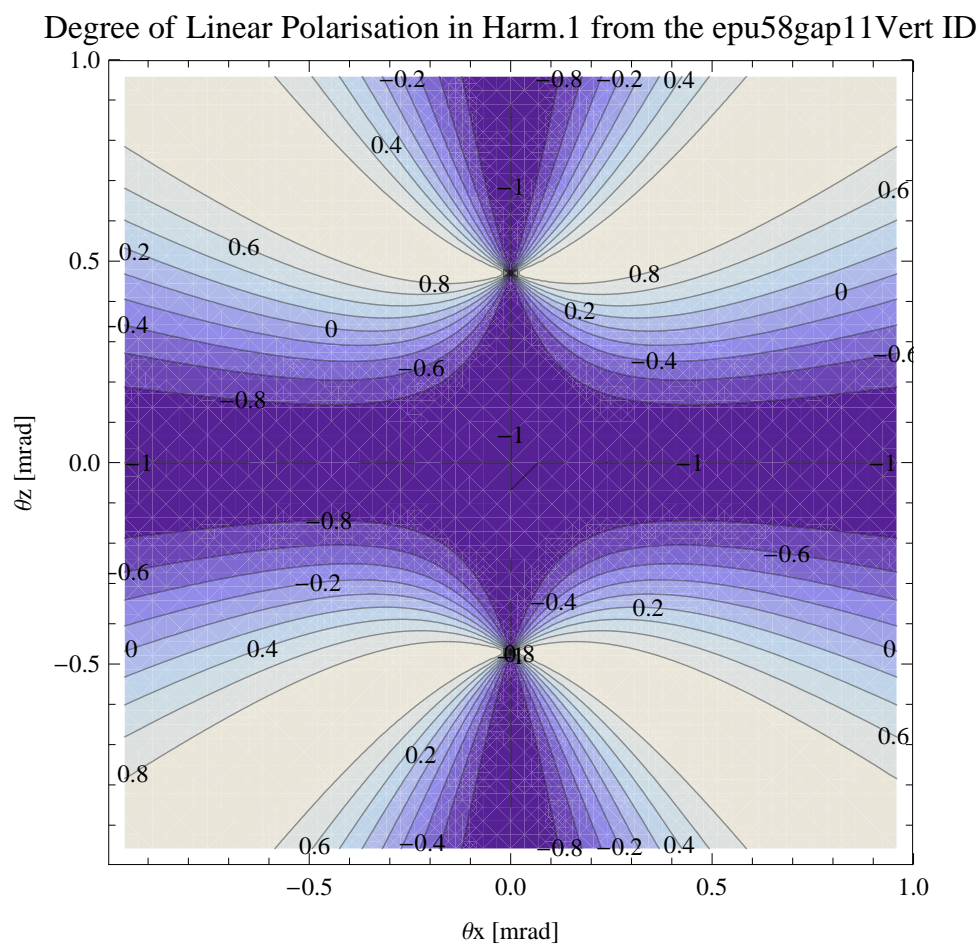


Figure 421: Map of linear polarisation in the fundamental harmonic of the synchrotron radiation emitted by the epu58gap11Vert ID

Degree of 45 degree Polarisation in Harm.1 from the epu58gap11Vert ID

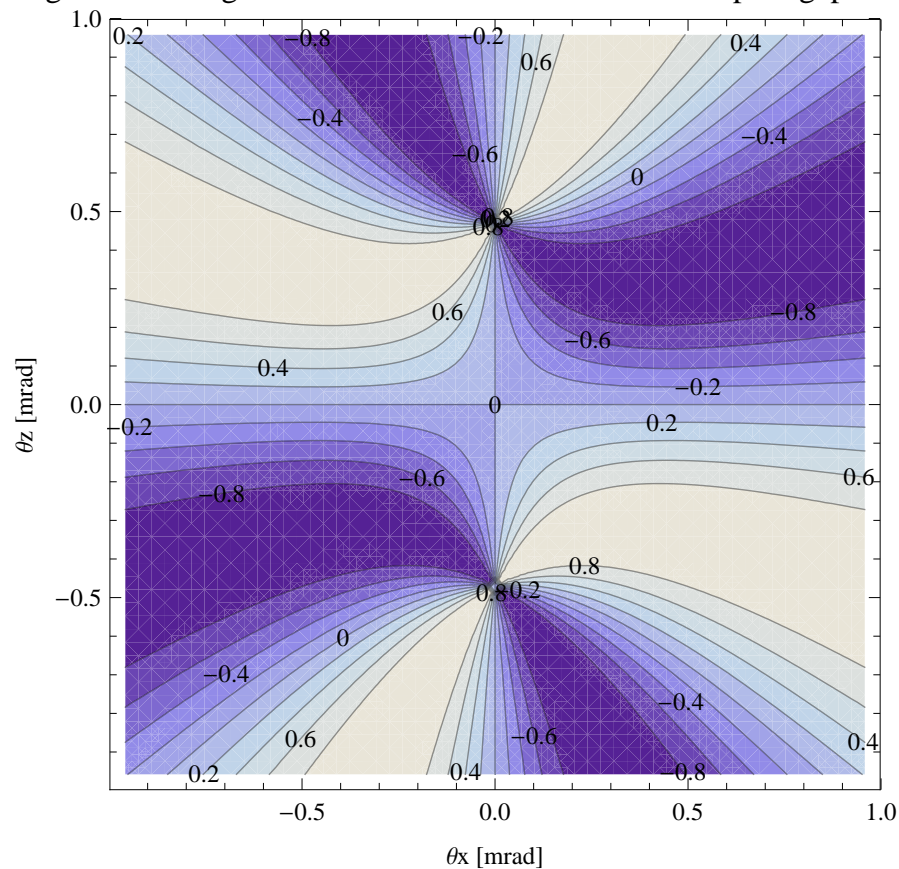


Figure 422: Map of 45 degree polarisation in the fundamental harmonic of the synchrotron radiation emitted by the epu58gap11Vert ID

Degree of Circular Polarisation in Harm.1 from the epu58gap11Vert ID

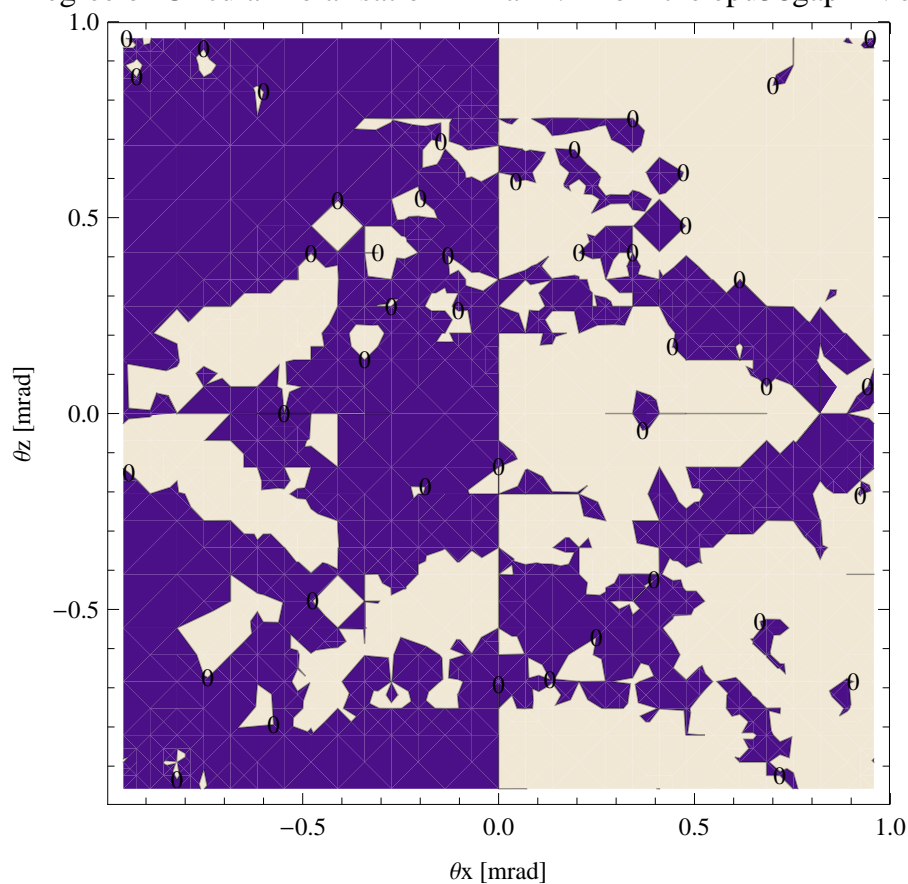


Figure 423: Map of circular polarisation in the fundamental harmonic of the synchrotron radiation emitted by the epu58gap11Vert ID

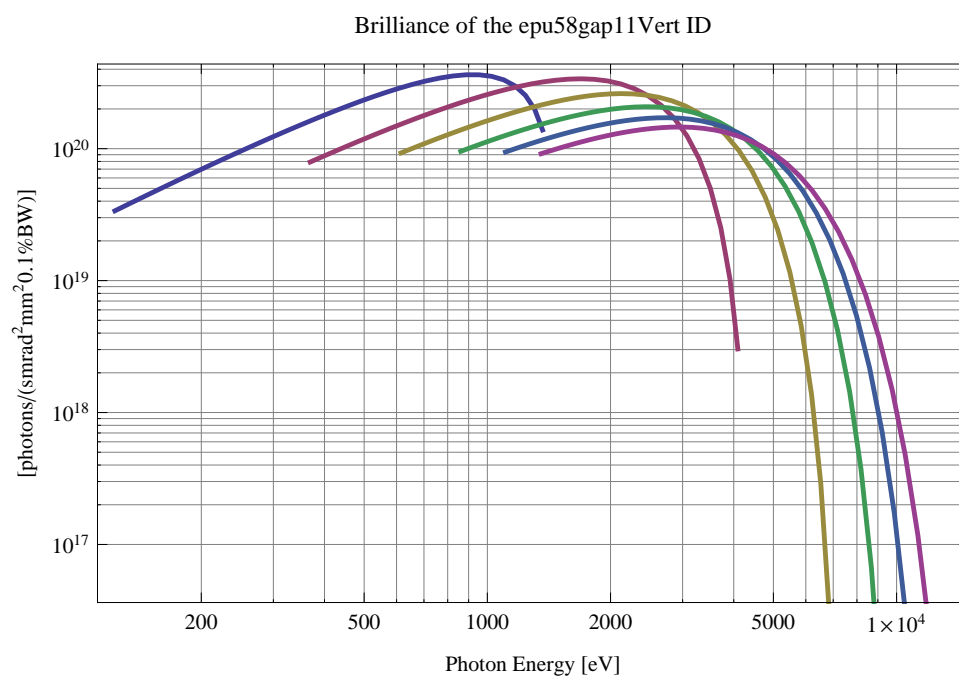


Figure 424: The brilliance at peak energy of the synchrotron radiation emitted by the epu58gap11Vert ID

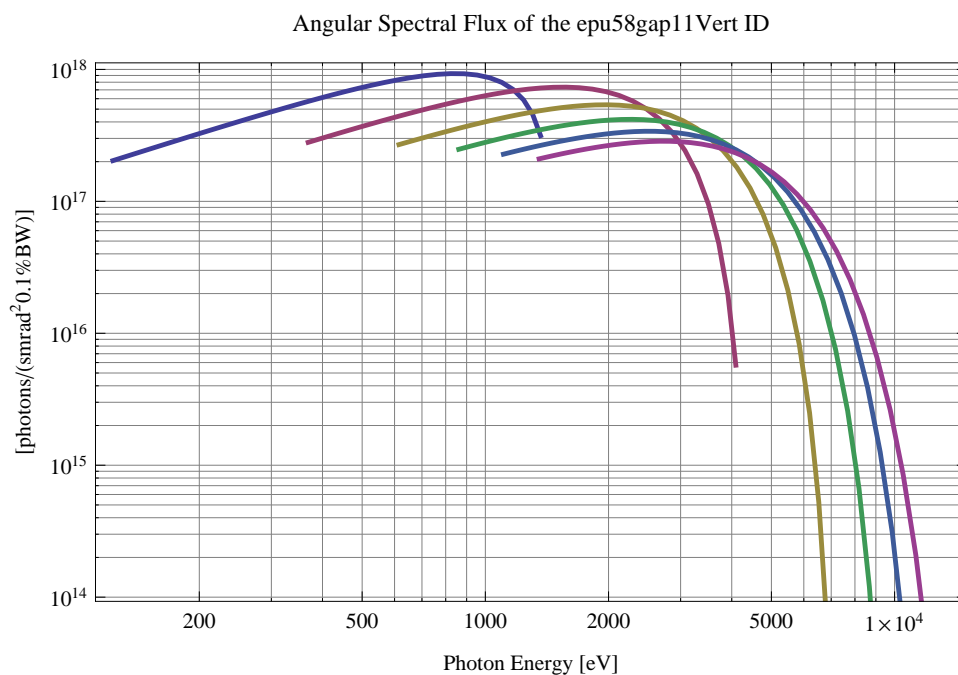


Figure 425: The angular spectral flux of the synchrotron radiation emitted by the epu58gap11Vert ID

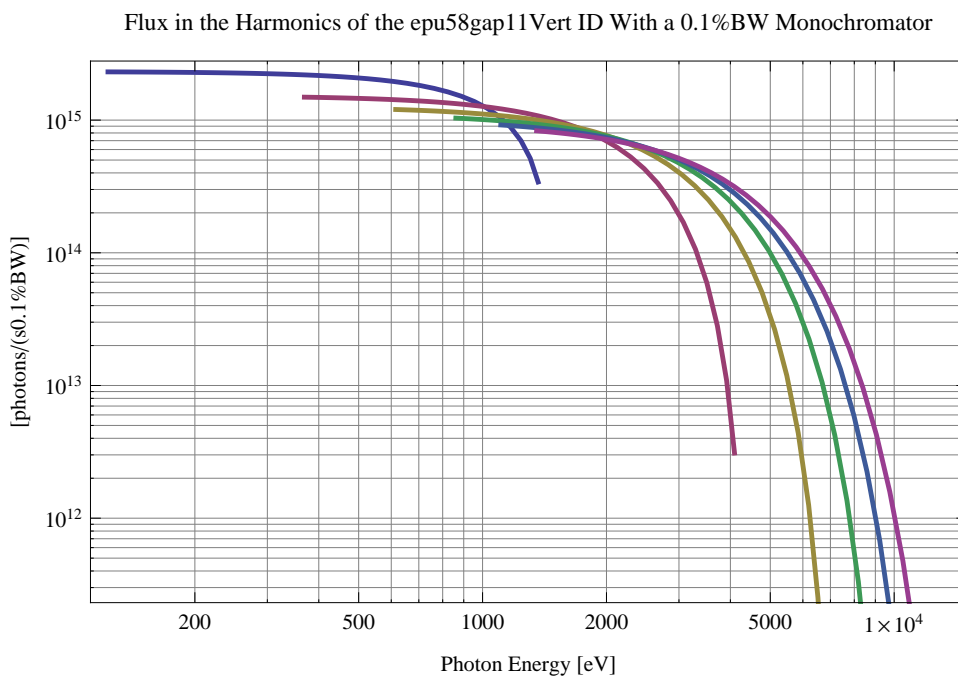


Figure 426: The flux of photons in the harmonics of the emitted synchrotron radiation from the epu58gap11Vert ID using a 0.1%BW monochromator

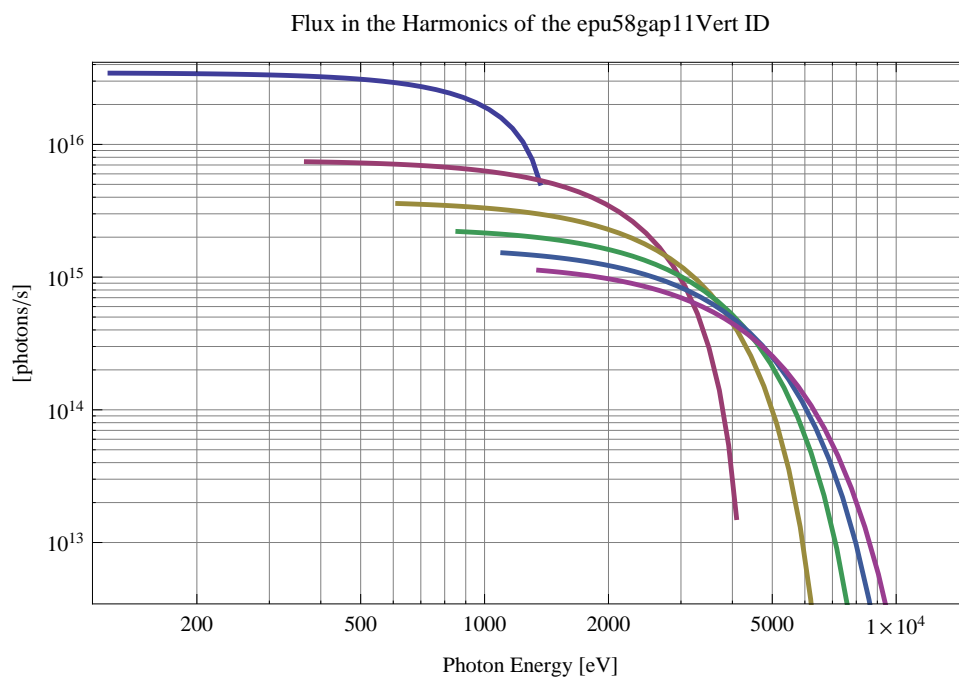


Figure 427: The flux of photons in the harmonics of the emitted synchrotron radiation from the epu58gap11Vert ID

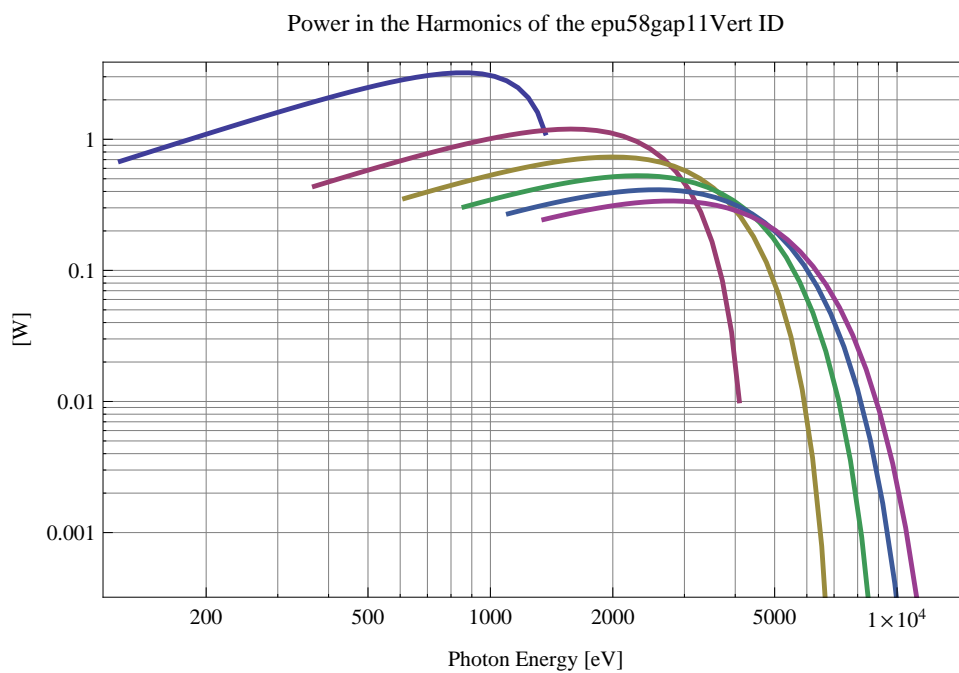


Figure 428: The power in the harmonics of the emitted synchrotron radiation from the epu58gap11Vert ID

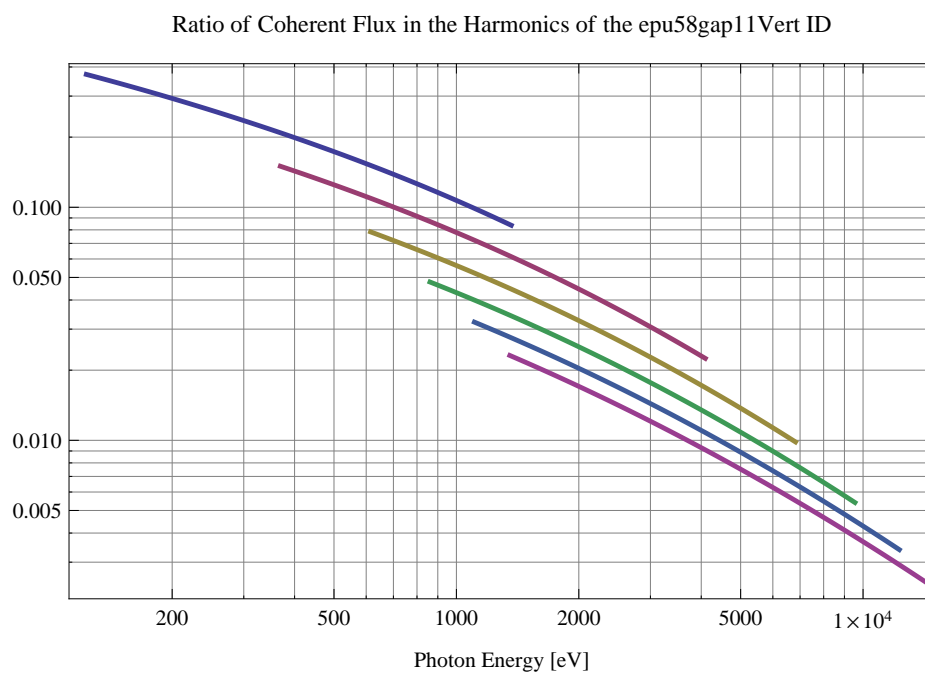


Figure 429: The ratio of coherent flux in the harmonics of the emitted synchrotron radiation from the epu58gap11Vert ID

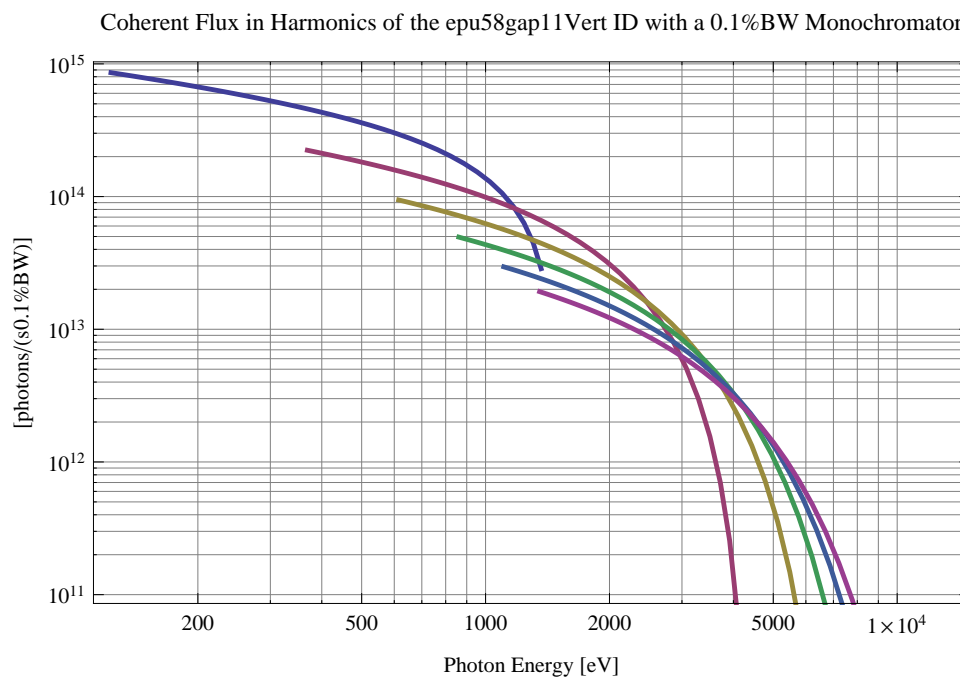


Figure 430: The coherent flux in the harmonics of the epu58gap11Vert ID using a 0.1%BW Monochromator

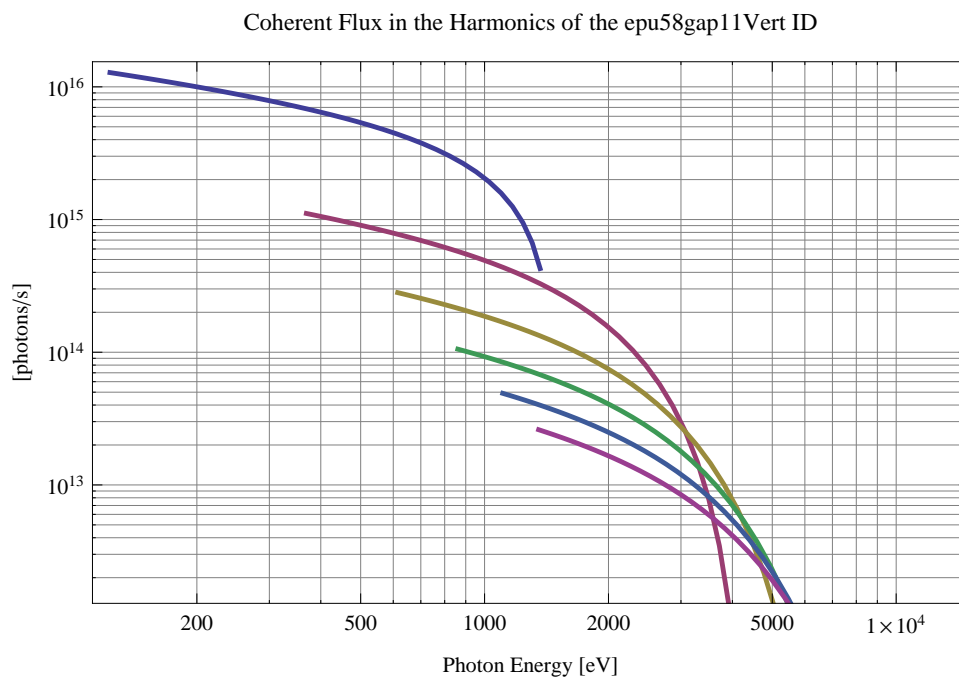


Figure 431: The coherent flux in the harmonics of the epu58gap11Vert ID

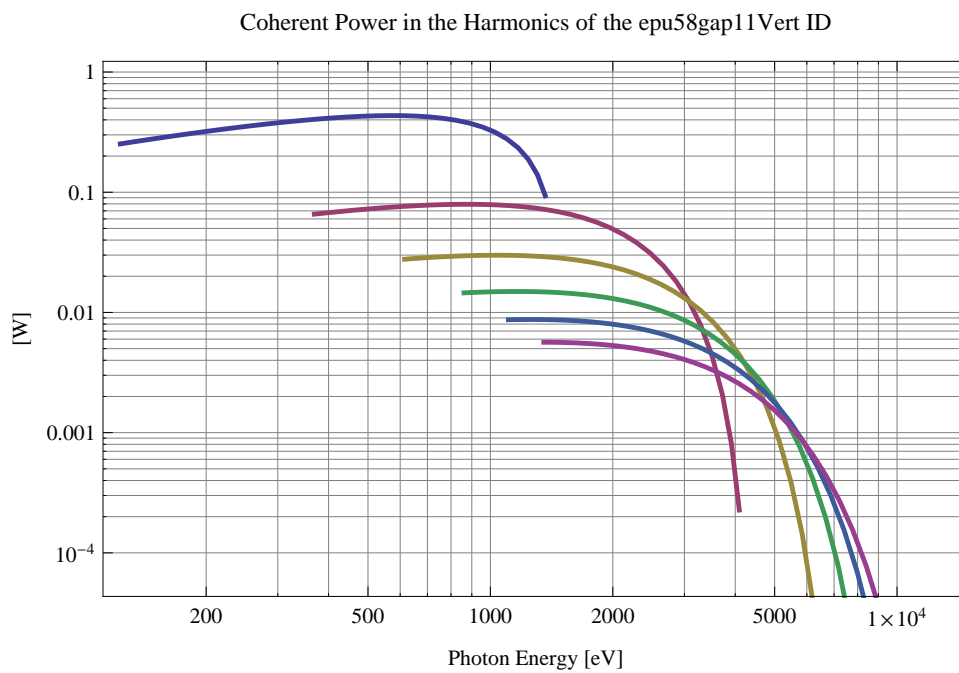


Figure 432: The power of coherent synchrotron radiation in the harmonics of the epu58gap11Vert ID

The brilliance at peak energy and the angular spectral flux density from the epu58gap11Vert ID for different harmonics at maximum K-value (4.686) are given in Table 72 and for minimum K-value (0.400) these values are given in Table 73.

Table 72: The brilliance at peak energy and the angular spectral flux density from the epu58gap11Vert ID for different harmonics at maximum K-value (4.686)

Harmonic	Photon Energy [eV]	Brilliance [Ph./ (smrad ² mrads ² 0.1%BW)]	Angular Spectral Flux [Ph./ (smrad ² 0.1%BW)]
1	123.016	3.38×10^{19}	2.04×10^{17}
3	369.049	7.92×10^{19}	2.8×10^{17}
5	615.082	9.28×10^{19}	2.69×10^{17}
7	861.114	9.55×10^{19}	2.48×10^{17}
9	1107.15	9.43×10^{19}	2.28×10^{17}
11	1353.18	9.16×10^{19}	2.1×10^{17}

Table 73: The brilliance at peak energy and the angular spectral flux density from the epu58gap11Vert ID for different harmonics at minimum K-value (0.4)

Harmonic	Photon Energy [eV]	Brilliance [Ph./ (smrad ² mrads ² 0.1%BW)]	Angular Spectral Flux [Ph./ (smrad ² 0.1%BW)]
1	1364.43	1.39×10^{20}	3.15×10^{17}
3	4093.28	3.03×10^{18}	5.73×10^{15}
5	6822.13	3.63×10^{16}	6.59×10^{13}
7	9550.98	3.9×10^{14}	6.98×10^{11}
9	12279.8	4.07×10^{12}	7.22×10^9
11	15008.7	4.18×10^{10}	7.4×10^7

References

- [1] S. C. Leemann, Å. Andersson, M. Eriksson, L.-J. Lindgren, E. Wallén, J. Bengtsson, and A. Streun. Beam dynamics for the MAX IV 3 GeV storage ring. *Phys. Rev. ST Accel. Beams*, 12:120701, 2009.
- [2] <http://www.maxlab.lu.se/local/UndWeb/UndWeb.html>.
- [3] O. Chubar, P. Elleaume and J. Chavanne. *Journal of Synchrotron Radiation*, 5:481, 1998.

List of Tables

1	Beam parameters in the middle of the straight sections of the MAX IV 3 GeV Ring [1]	4
2	Effective Fields on axis and Fundamental Photon Energy of the epu38gap11Plan ID	7
3	The brilliance at peak energy and the angular spectral flux density from the epu38gap11Plan ID for different harmonics at maximum K-value (2.978)	18

4	The brilliance at peak energy and the angular spectral flux density from the epu38gap11Plan ID for different harmonics at minimum K-value (0.4)	18
5	Effective Fields on axis and Fundamental Photon Energy of the epu38gap11Heli ID	19
6	The brilliance at peak energy and the angular spectral flux density from the epu38gap11Heli ID for different harmonics at maximum K-value (2.384)	30
7	The brilliance at peak energy and the angular spectral flux density from the epu38gap11Heli ID for different harmonics at minimum K-value (0.4)	30
8	Effective Fields on axis and Fundamental Photon Energy of the epu38gap11Incl ID	31
9	The brilliance at peak energy and the angular spectral flux density from the epu38gap11Incl ID for different harmonics at maximum K-value (1.712)	43
10	The brilliance at peak energy and the angular spectral flux density from the epu38gap11Incl ID for different harmonics at minimum K-value (0.4)	43
11	Effective Fields on axis and Fundamental Photon Energy of the epu38gap11Vert ID	44
12	The brilliance at peak energy and the angular spectral flux density from the epu38gap11Vert ID for different harmonics at maximum K-value (2.048)	55
13	The brilliance at peak energy and the angular spectral flux density from the epu38gap11Vert ID for different harmonics at minimum K-value (0.4)	55
14	Effective Fields on axis and Fundamental Photon Energy of the epu43p6gap11Plan ID	58
15	The brilliance at peak energy and the angular spectral flux density from the epu43p6gap11Plan ID for different harmonics at maximum K-value (3.828) . . .	69
16	The brilliance at peak energy and the angular spectral flux density from the epu43p6gap11Plan ID for different harmonics at minimum K-value (0.4)	69
17	Effective Fields on axis and Fundamental Photon Energy of the epu43p6gap11Heli ID	70
18	The brilliance at peak energy and the angular spectral flux density from the epu43p6gap11Heli ID for different harmonics at maximum K-value (3.144)	81
19	The brilliance at peak energy and the angular spectral flux density from the epu43p6gap11Heli ID for different harmonics at minimum K-value (0.4)	81
20	Effective Fields on axis and Fundamental Photon Energy of the epu43p6gap11Incl ID	82
21	The brilliance at peak energy and the angular spectral flux density from the epu43p6gap11Incl ID for different harmonics at maximum K-value (2.252)	94
22	The brilliance at peak energy and the angular spectral flux density from the epu43p6gap11Incl ID for different harmonics at minimum K-value (0.4)	94
23	Effective Fields on axis and Fundamental Photon Energy of the epu43p6gap11Vert ID	95
24	The brilliance at peak energy and the angular spectral flux density from the epu43p6gap11Vert ID for different harmonics at maximum K-value (2.741)	106
25	The brilliance at peak energy and the angular spectral flux density from the epu43p6gap11Vert ID for different harmonics at minimum K-value (0.4)	106
26	Effective Fields on axis and Fundamental Photon Energy of the epu48gap11Plan ID	109
27	The brilliance at peak energy and the angular spectral flux density from the epu48gap11Plan ID for different harmonics at maximum K-value (4.506)	120
28	The brilliance at peak energy and the angular spectral flux density from the epu48gap11Plan ID for different harmonics at minimum K-value (0.4)	120
29	Effective Fields on axis and Fundamental Photon Energy of the epu48gap11Heli ID	121
30	The brilliance at peak energy and the angular spectral flux density from the epu48gap11Heli ID for different harmonics at maximum K-value (3.772)	132

31	The brilliance at peak energy and the angular spectral flux density from the epu48gap11Heli ID for different harmonics at minimum K-value (0.4)	132
32	Effective Fields on axis and Fundamental Photon Energy of the epu48gap11Incl ID	133
33	The brilliance at peak energy and the angular spectral flux density from the epu48gap11Incl ID for different harmonics at maximum K-value (2.695)	145
34	The brilliance at peak energy and the angular spectral flux density from the epu48gap11Incl ID for different harmonics at minimum K-value (0.4)	145
35	Effective Fields on axis and Fundamental Photon Energy of the epu48gap11Vert ID	146
36	The brilliance at peak energy and the angular spectral flux density from the epu48gap11Vert ID for different harmonics at maximum K-value (3.318)	157
37	The brilliance at peak energy and the angular spectral flux density from the epu48gap11Vert ID for different harmonics at minimum K-value (0.4)	157
38	Effective Fields on axis and Fundamental Photon Energy of the epu53gap11Plan ID	160
39	The brilliance at peak energy and the angular spectral flux density from the epu53gap11Plan ID for different harmonics at maximum K-value (5.277)	171
40	The brilliance at peak energy and the angular spectral flux density from the epu53gap11Plan ID for different harmonics at minimum K-value (0.4)	171
41	Effective Fields on axis and Fundamental Photon Energy of the epu53gap11Heli ID	172
42	The brilliance at peak energy and the angular spectral flux density from the epu53gap11Heli ID for different harmonics at maximum K-value (4.494)	183
43	The brilliance at peak energy and the angular spectral flux density from the epu53gap11Heli ID for different harmonics at minimum K-value (0.4)	183
44	Effective Fields on axis and Fundamental Photon Energy of the epu53gap11Incl ID	184
45	The brilliance at peak energy and the angular spectral flux density from the epu53gap11Incl ID for different harmonics at maximum K-value (3.206)	196
46	The brilliance at peak energy and the angular spectral flux density from the epu53gap11Incl ID for different harmonics at minimum K-value (0.4)	196
47	Effective Fields on axis and Fundamental Photon Energy of the epu53gap11Vert ID	197
48	The brilliance at peak energy and the angular spectral flux density from the epu53gap11Vert ID for different harmonics at maximum K-value (3.995)	208
49	The brilliance at peak energy and the angular spectral flux density from the epu53gap11Vert ID for different harmonics at minimum K-value (0.4)	208
50	Effective Fields on axis and Fundamental Photon Energy of the epu53p6gap11Plan ID	211
51	The brilliance at peak energy and the angular spectral flux density from the epu53p6gap11Plan ID for different harmonics at maximum K-value (5.372)	222
52	The brilliance at peak energy and the angular spectral flux density from the epu53p6gap11Plan ID for different harmonics at minimum K-value (0.4)	222
53	Effective Fields on axis and Fundamental Photon Energy of the epu53p6gap11Heli ID	223
54	The brilliance at peak energy and the angular spectral flux density from the epu53p6gap11Heli ID for different harmonics at maximum K-value (4.581)	234
55	The brilliance at peak energy and the angular spectral flux density from the epu53p6gap11Heli ID for different harmonics at minimum K-value (0.4)	234
56	Effective Fields on axis and Fundamental Photon Energy of the epu53p6gap11Incl ID	235
57	The brilliance at peak energy and the angular spectral flux density from the epu53p6gap11Incl ID for different harmonics at maximum K-value (3.267)	247

58	The brilliance at peak energy and the angular spectral flux density from the epu53p6gap11Incl ID for different harmonics at minimum K-value (0.4)	247
59	Effective Fields on axis and Fundamental Photon Energy of the epu53p6gap11Vert ID	248
60	The brilliance at peak energy and the angular spectral flux density from the epu53p6gap11Vert ID for different harmonics at maximum K-value (4.075)	259
61	The brilliance at peak energy and the angular spectral flux density from the epu53p6gap11Vert ID for different harmonics at minimum K-value (0.4)	259
62	Effective Fields on axis and Fundamental Photon Energy of the epu58gap11Plan ID	262
63	The brilliance at peak energy and the angular spectral flux density from the epu58gap11Plan ID for different harmonics at maximum K-value (6.046)	273
64	The brilliance at peak energy and the angular spectral flux density from the epu58gap11Plan ID for different harmonics at minimum K-value (0.4)	273
65	Effective Fields on axis and Fundamental Photon Energy of the epu58gap11Heli ID	274
66	The brilliance at peak energy and the angular spectral flux density from the epu58gap11Heli ID for different harmonics at maximum K-value (5.225)	285
67	The brilliance at peak energy and the angular spectral flux density from the epu58gap11Heli ID for different harmonics at minimum K-value (0.4)	285
68	Effective Fields on axis and Fundamental Photon Energy of the epu58gap11Incl ID	286
69	The brilliance at peak energy and the angular spectral flux density from the epu58gap11Incl ID for different harmonics at maximum K-value (3.723)	297
70	The brilliance at peak energy and the angular spectral flux density from the epu58gap11Incl ID for different harmonics at minimum K-value (0.4)	297
71	Effective Fields on axis and Fundamental Photon Energy of the epu58gap11Vert ID	298
72	The brilliance at peak energy and the angular spectral flux density from the epu58gap11Vert ID for different harmonics at maximum K-value (4.686)	309
73	The brilliance at peak energy and the angular spectral flux density from the epu58gap11Vert ID for different harmonics at minimum K-value (0.4)	309

List of Figures

1	Vertical and horizontal magnetic field for the the epu38gap11 ID when operating in the helical mode for different positions for two of the four sub-girders	5
2	Vertical, horizontal, and longitudinal magnetic field for the the epu38gap11 ID when operating in the inclined mode for different positions for two of the four sub-girders	5
3	Magnetic model of the epu38gap11Plan ID. The ID has been modelled with Radia [3]	6
4	Vertical magnetic field in a central pole of the epu38gap11Plan ID along the ID axis, $X = Z = 0$	7
5	Vertical magnetic field in a central pole of the epu38gap11Plan ID along the horizontally transverse direction to the ID axis, $S = 0.000$, $Z = 0$	8
6	The beam orbit of the electron beam through a central period of the epu38gap11Plan ID	8
7	Map of the power distribution of the emitted synchrotron radiation by the epu38gap11Plan ID	9
8	Map of linear polarisation in the fundamental harmonic of the synchrotron radiation emitted by the epu38gap11Plan ID	10

9	Map of 45 degree polarisation in the fundamental harmonic of the synchrotron radiation emitted by the epu38gap11Plan ID	11
10	Map of circular polarisation in the fundamental harmonic of the synchrotron radiation emitted by the epu38gap11Plan ID	12
11	The brilliance at peak energy of the synchrotron radiation emitted by the epu38gap11Plan ID	13
12	The angular spectral flux of the synchrotron radiation emitted by the epu38gap11Plan ID	13
13	The flux of photons in the harmonics of the emitted synchrotron radiation from the epu38gap11Plan ID using a 0.1%BW monochromator	14
14	The flux of photons in the harmonics of the emitted synchrotron radiation from the epu38gap11Plan ID	14
15	The power in the harmonics of the emitted synchrotron radiation from the epu38gap11Plan ID	15
16	The ratio of coherent flux in the harmonics of the emitted synchrotron radiation from the epu38gap11Plan ID	15
17	The coherent flux in the harmonics of the epu38gap11Plan ID using a 0.1%BW Monochromator	16
18	The coherent flux in the harmonics of the epu38gap11Plan ID	16
19	The power of coherent synchrotron radiation in the harmonics of the epu38gap11Plan ID	17
20	Magnetic model of the epu38gap11Heli ID. The ID has been modelled with Radia [3]	19
21	Vertical magnetic field in a central pole of the epu38gap11Heli ID along the ID axis, $X = Z = 0$	19
22	Vertical magnetic field in a central pole of the epu38gap11Heli ID along the horizontally transverse direction to the ID axis, $S = 5.833, Z = 0$	20
23	Horizontal magnetic field in a central pole of the epu38gap11Heli ID along the horizontally transverse direction to the ID axis, $S = 15.333, Z = 0$	20
24	The beam orbit of the electron beam through a central period of the epu38gap11Heli ID	21
25	Map of the power distribution of the emitted synchrotron radiation by the epu38gap11Heli ID	22
26	Map of linear polarisation in the fundamental harmonic of the synchrotron radiation emitted by the epu38gap11Heli ID	23
27	Map of 45 degree polarisation in the fundamental harmonic of the synchrotron radiation emitted by the epu38gap11Heli ID	24
28	Map of circular polarisation in the fundamental harmonic of the synchrotron radiation emitted by the epu38gap11Heli ID	25
29	The brilliance at peak energy of the synchrotron radiation emitted by the epu38gap11Heli ID	25
30	The angular spectral flux of the synchrotron radiation emitted by the epu38gap11Heli ID	26
31	The flux of photons in the harmonics of the emitted synchrotron radiation from the epu38gap11Heli ID using a 0.1%BW monochromator	26
32	The flux of photons in the harmonics of the emitted synchrotron radiation from the epu38gap11Heli ID	27
33	The power in the harmonics of the emitted synchrotron radiation from the epu38gap11Heli ID	27
34	The ratio of coherent flux in the harmonics of the emitted synchrotron radiation from the epu38gap11Heli ID	28

35	The coherent flux in the harmonics of the epu38gap11Heli ID using a 0.1%BW Monochromator	28
36	The coherent flux in the harmonics of the epu38gap11Heli ID	29
37	The power of coherent synchrotron radiation in the harmonics of the epu38gap11Heli ID	29
38	Magnetic model of the epu38gap11Incl ID. The ID has been modelled with Radia [3]	30
39	Vertical magnetic field in a central pole of the epu38gap11Incl ID along the ID axis, $X = Z = 0$	31
40	Vertical magnetic field in a central pole of the epu38gap11Incl ID along the horizontally transverse direction to the ID axis, $S = 0.000$, $Z = 0$	32
41	Horizontal magnetic field in a central pole of the epu38gap11Incl ID along the horizontally transverse direction to the ID axis, $S = 0.000$, $Z = 0$	32
42	The beam orbit of the electron beam through a central period of the epu38gap11Incl ID	33
43	Map of the power distribution of the emitted synchrotron radiation by the epu38gap11Incl ID	34
44	Map of linear polarisation in the fundamental harmonic of the synchrotron radiation emitted by the epu38gap11Incl ID	35
45	Map of 45 degree polarisation in the fundamental harmonic of the synchrotron radiation emitted by the epu38gap11Incl ID	36
46	Map of circular polarisation in the fundamental harmonic of the synchrotron radiation emitted by the epu38gap11Incl ID	37
47	The brilliance at peak energy of the synchrotron radiation emitted by the epu38gap11Incl ID	38
48	The angular spectral flux of the synchrotron radiation emitted by the epu38gap11Incl ID	38
49	The flux of photons in the harmonics of the emitted synchrotron radiation from the epu38gap11Incl ID using a 0.1%BW monochromator	39
50	The flux of photons in the harmonics of the emitted synchrotron radiation from the epu38gap11Incl ID	39
51	The power in the harmonics of the emitted synchrotron radiation from the epu38gap11Incl ID	40
52	The ratio of coherent flux in the harmonics of the emitted synchrotron radiation from the epu38gap11Incl ID	40
53	The coherent flux in the harmonics of the epu38gap11Incl ID using a 0.1%BW Monochromator	41
54	The coherent flux in the harmonics of the epu38gap11Incl ID	41
55	The power of coherent synchrotron radiation in the harmonics of the epu38gap11Incl ID	42
56	Magnetic model of the epu38gap11Vert ID. The ID has been modelled with Radia [3]	44
57	Vertical magnetic field in a central pole of the epu38gap11Vert ID along the ID axis, $X = Z = 0$	44
58	Horizontal magnetic field in a central pole of the epu38gap11Vert ID along the horizontally transverse direction to the ID axis, $S = 19.000$, $Z = 0$	45
59	The beam orbit of the electron beam through a central period of the epu38gap11Vert ID	46
60	Map of the power distribution of the emitted synchrotron radiation by the epu38gap11Vert ID	47

61	Map of linear polarisation in the fundamental harmonic of the synchrotron radiation emitted by the epu38gap11Vert ID	48
62	Map of 45 degree polarisation in the fundamental harmonic of the synchrotron radiation emitted by the epu38gap11Vert ID	49
63	Map of circular polarisation in the fundamental harmonic of the synchrotron radiation emitted by the epu38gap11Vert ID	50
64	The brilliance at peak energy of the synchrotron radiation emitted by the epu38gap11Vert ID	50
65	The angular spectral flux of the synchrotron radiation emitted by the epu38gap11Vert ID	51
66	The flux of photons in the harmonics of the emitted synchrotron radiation from the epu38gap11Vert ID using a 0.1%BW monochromator	51
67	The flux of photons in the harmonics of the emitted synchrotron radiation from the epu38gap11Vert ID	52
68	The power in the harmonics of the emitted synchrotron radiation from the epu38gap11Vert ID	52
69	The ratio of coherent flux in the harmonics of the emitted synchrotron radiation from the epu38gap11Vert ID	53
70	The coherent flux in the harmonics of the epu38gap11Vert ID using a 0.1%BW Monochromator	53
71	The coherent flux in the harmonics of the epu38gap11Vert ID	54
72	The power of coherent synchrotron radiation in the harmonics of the epu38gap11Vert ID	54
73	Vertical and horizontal magnetic field for the the epu43p6gap11 ID when operating in the helical mode for different positions for two of the four sub-girders . . .	56
74	Vertical, horizontal, and longitudinal magnetic field for the the epu43p6gap11 ID when operating in the inclined mode for different positions for two of the four sub-girders	56
75	Magnetic model of the epu43p6gap11Plan ID. The ID has been modelled with Radia [3]	57
76	Vertical magnetic field in a central pole of the epu43p6gap11Plan ID along the ID axis, $X = Z = 0$	58
77	Vertical magnetic field in a central pole of the epu43p6gap11Plan ID along the horizontally transverse direction to the ID axis, $S = 0.000, Z = 0$	59
78	The beam orbit of the electron beam through a central period of the epu43p6gap11Plan ID	59
79	Map of the power distribution of the emitted synchrotron radiation by the epu43p6gap11Plan ID	60
80	Map of linear polarisation in the fundamental harmonic of the synchrotron radiation emitted by the epu43p6gap11Plan ID	61
81	Map of 45 degree polarisation in the fundamental harmonic of the synchrotron radiation emitted by the epu43p6gap11Plan ID	62
82	Map of circular polarisation in the fundamental harmonic of the synchrotron radiation emitted by the epu43p6gap11Plan ID	63
83	The brilliance at peak energy of the synchrotron radiation emitted by the epu43p6gap11Plan ID	64
84	The angular spectral flux of the synchrotron radiation emitted by the epu43p6gap11Plan ID	64
85	The flux of photons in the harmonics of the emitted synchrotron radiation from the epu43p6gap11Plan ID using a 0.1%BW monochromator	65

86	The flux of photons in the harmonics of the emitted synchrotron radiation from the epu43p6gap11Plan ID	65
87	The power in the harmonics of the emitted synchrotron radiation from the epu43p6gap11Plan ID	66
88	The ratio of coherent flux in the harmonics of the emitted synchrotron radiation from the epu43p6gap11Plan ID	66
89	The coherent flux in the harmonics of the epu43p6gap11Plan ID using a 0.1%BW Monochromator	67
90	The coherent flux in the harmonics of the epu43p6gap11Plan ID	67
91	The power of coherent synchrotron radiation in the harmonics of the epu43p6gap11Plan ID	68
92	Magnetic model of the epu43p6gap11Heli ID. The ID has been modelled with Radia [3]	70
93	Vertical magnetic field in a central pole of the epu43p6gap11Heli ID along the ID axis, $X = Z = 0$	70
94	Vertical magnetic field in a central pole of the epu43p6gap11Heli ID along the horizontally transverse direction to the ID axis, $S = 6.563$, $Z = 0$	71
95	Horizontal magnetic field in a central pole of the epu43p6gap11Heli ID along the horizontally transverse direction to the ID axis, $S = 17.463$, $Z = 0$	71
96	The beam orbit of the electron beam through a central period of the epu43p6gap11Heli ID	72
97	Map of the power distribution of the emitted synchrotron radiation by the epu43p6gap11Heli ID	73
98	Map of linear polarisation in the fundamental harmonic of the synchrotron radiation emitted by the epu43p6gap11Heli ID	74
99	Map of 45 degree polarisation in the fundamental harmonic of the synchrotron radiation emitted by the epu43p6gap11Heli ID	75
100	Map of circular polarisation in the fundamental harmonic of the synchrotron radiation emitted by the epu43p6gap11Heli ID	76
101	The brilliance at peak energy of the synchrotron radiation emitted by the epu43p6gap11Heli ID	76
102	The angular spectral flux of the synchrotron radiation emitted by the epu43p6gap11Heli ID	77
103	The flux of photons in the harmonics of the emitted synchrotron radiation from the epu43p6gap11Heli ID using a 0.1%BW monochromator	77
104	The flux of photons in the harmonics of the emitted synchrotron radiation from the epu43p6gap11Heli ID	78
105	The power in the harmonics of the emitted synchrotron radiation from the epu43p6gap11Heli ID	78
106	The ratio of coherent flux in the harmonics of the emitted synchrotron radiation from the epu43p6gap11Heli ID	79
107	The coherent flux in the harmonics of the epu43p6gap11Heli ID using a 0.1%BW Monochromator	79
108	The coherent flux in the harmonics of the epu43p6gap11Heli ID	80
109	The power of coherent synchrotron radiation in the harmonics of the epu43p6gap11Heli ID	80
110	Magnetic model of the epu43p6gap11Incl ID. The ID has been modelled with Radia [3]	81
111	Vertical magnetic field in a central pole of the epu43p6gap11Incl ID along the ID axis, $X = Z = 0$	82

112	Vertical magnetic field in a central pole of the epu43p6gap11Incl ID along the horizontally transverse direction to the ID axis, $S = 0.000$, $Z = 0$	83
113	Horizontal magnetic field in a central pole of the epu43p6gap11Incl ID along the horizontally transverse direction to the ID axis, $S = 0.000$, $Z = 0$	83
114	The beam orbit of the electron beam through a central period of the epu43p6gap11Incl ID	84
115	Map of the power distribution of the emitted synchrotron radiation by the epu43p6gap11Incl ID	85
116	Map of linear polarisation in the fundamental harmonic of the synchrotron radiation emitted by the epu43p6gap11Incl ID	86
117	Map of 45 degree polarisation in the fundamental harmonic of the synchrotron radiation emitted by the epu43p6gap11Incl ID	87
118	Map of circular polarisation in the fundamental harmonic of the synchrotron radiation emitted by the epu43p6gap11Incl ID	88
119	The brilliance at peak energy of the synchrotron radiation emitted by the epu43p6gap11Incl ID	89
120	The angular spectral flux of the synchrotron radiation emitted by the epu43p6gap11Incl ID	89
121	The flux of photons in the harmonics of the emitted synchrotron radiation from the epu43p6gap11Incl ID using a 0.1%BW monochromator	90
122	The flux of photons in the harmonics of the emitted synchrotron radiation from the epu43p6gap11Incl ID	90
123	The power in the harmonics of the emitted synchrotron radiation from the epu43p6gap11Incl ID	91
124	The ratio of coherent flux in the harmonics of the emitted synchrotron radiation from the epu43p6gap11Incl ID	91
125	The coherent flux in the harmonics of the epu43p6gap11Incl ID using a 0.1%BW Monochromator	92
126	The coherent flux in the harmonics of the epu43p6gap11Incl ID	92
127	The power of coherent synchrotron radiation in the harmonics of the epu43p6gap11Incl ID	93
128	Magnetic model of the epu43p6gap11Vert ID. The ID has been modelled with Radia [3]	95
129	Vertical magnetic field in a central pole of the epu43p6gap11Vert ID along the ID axis, $X = Z = 0$	95
130	Horizontal magnetic field in a central pole of the epu43p6gap11Vert ID along the horizontally transverse direction to the ID axis, $S = 21.800$, $Z = 0$	96
131	The beam orbit of the electron beam through a central period of the epu43p6gap11Vert ID	97
132	Map of the power distribution of the emitted synchrotron radiation by the epu43p6gap11Vert ID	98
133	Map of linear polarisation in the fundamental harmonic of the synchrotron radiation emitted by the epu43p6gap11Vert ID	99
134	Map of 45 degree polarisation in the fundamental harmonic of the synchrotron radiation emitted by the epu43p6gap11Vert ID	100
135	Map of circular polarisation in the fundamental harmonic of the synchrotron radiation emitted by the epu43p6gap11Vert ID	101
136	The brilliance at peak energy of the synchrotron radiation emitted by the epu43p6gap11Vert ID	101
137	The angular spectral flux of the synchrotron radiation emitted by the epu43p6gap11Vert ID	102

138	The flux of photons in the harmonics of the emitted synchrotron radiation from the epu43p6gap11Vert ID using a 0.1%BW monochromator	102
139	The flux of photons in the harmonics of the emitted synchrotron radiation from the epu43p6gap11Vert ID	103
140	The power in the harmonics of the emitted synchrotron radiation from the epu43p6gap11Vert ID	103
141	The ratio of coherent flux in the harmonics of the emitted synchrotron radiation from the epu43p6gap11Vert ID	104
142	The coherent flux in the harmonics of the epu43p6gap11Vert ID using a 0.1%BW Monochromator	104
143	The coherent flux in the harmonics of the epu43p6gap11Vert ID	105
144	The power of coherent synchrotron radiation in the harmonics of the epu43p6gap11Vert ID	105
145	Vertical and horizontal magnetic field for the the epu48gap11 ID when operating in the helical mode for different positions for two of the four sub-girders	107
146	Vertical, horizontal, and longitudinal magnetic field for the the epu48gap11 ID when operating in the inclined mode for different positions for two of the four sub-girders	107
147	Magnetic model of the epu48gap11Plan ID. The ID has been modelled with Radia [3]	108
148	Vertical magnetic field in a central pole of the epu48gap11Plan ID along the ID axis, $X = Z = 0$	109
149	Vertical magnetic field in a central pole of the epu48gap11Plan ID along the horizontally transverse direction to the ID axis, $S = 0.000$, $Z = 0$	110
150	The beam orbit of the electron beam through a central period of the epu48gap11Plan ID	110
151	Map of the power distribution of the emitted synchrotron radiation by the epu48gap11Plan ID	111
152	Map of linear polarisation in the fundamental harmonic of the synchrotron radiation emitted by the epu48gap11Plan ID	112
153	Map of 45 degree polarisation in the fundamental harmonic of the synchrotron radiation emitted by the epu48gap11Plan ID	113
154	Map of circular polarisation in the fundamental harmonic of the synchrotron radiation emitted by the epu48gap11Plan ID	114
155	The brilliance at peak energy of the synchrotron radiation emitted by the epu48gap11Plan ID	115
156	The angular spectral flux of the synchrotron radiation emitted by the epu48gap11Plan ID	115
157	The flux of photons in the harmonics of the emitted synchrotron radiation from the epu48gap11Plan ID using a 0.1%BW monochromator	116
158	The flux of photons in the harmonics of the emitted synchrotron radiation from the epu48gap11Plan ID	116
159	The power in the harmonics of the emitted synchrotron radiation from the epu48gap11Plan ID	117
160	The ratio of coherent flux in the harmonics of the emitted synchrotron radiation from the epu48gap11Plan ID	117
161	The coherent flux in the harmonics of the epu48gap11Plan ID using a 0.1%BW Monochromator	118
162	The coherent flux in the harmonics of the epu48gap11Plan ID	118
163	The power of coherent synchrotron radiation in the harmonics of the epu48gap11Plan ID	119

164	Magnetic model of the epu48gap11Heli ID. The ID has been modelled with Radia [3]	121
165	Vertical magnetic field in a central pole of the epu48gap11Heli ID along the ID axis, $X = Z = 0$	121
166	Vertical magnetic field in a central pole of the epu48gap11Heli ID along the horizontally transverse direction to the ID axis, $S = 7.127$, $Z = 0$	122
167	Horizontal magnetic field in a central pole of the epu48gap11Heli ID along the horizontally transverse direction to the ID axis, $S = 19.127$, $Z = 0$	122
168	The beam orbit of the electron beam through a central period of the epu48gap11Heli ID	123
169	Map of the power distribution of the emitted synchrotron radiation by the epu48gap11Heli ID	124
170	Map of linear polarisation in the fundamental harmonic of the synchrotron radiation emitted by the epu48gap11Heli ID	125
171	Map of 45 degree polarisation in the fundamental harmonic of the synchrotron radiation emitted by the epu48gap11Heli ID	126
172	Map of circular polarisation in the fundamental harmonic of the synchrotron radiation emitted by the epu48gap11Heli ID	127
173	The brilliance at peak energy of the synchrotron radiation emitted by the epu48gap11Heli ID	127
174	The angular spectral flux of the synchrotron radiation emitted by the epu48gap11Heli ID	128
175	The flux of photons in the harmonics of the emitted synchrotron radiation from the epu48gap11Heli ID using a 0.1%BW monochromator	128
176	The flux of photons in the harmonics of the emitted synchrotron radiation from the epu48gap11Heli ID	129
177	The power in the harmonics of the emitted synchrotron radiation from the epu48gap11Heli ID	129
178	The ratio of coherent flux in the harmonics of the emitted synchrotron radiation from the epu48gap11Heli ID	130
179	The coherent flux in the harmonics of the epu48gap11Heli ID using a 0.1%BW Monochromator	130
180	The coherent flux in the harmonics of the epu48gap11Heli ID	131
181	The power of coherent synchrotron radiation in the harmonics of the epu48gap11Heli ID	131
182	Magnetic model of the epu48gap11Incl ID. The ID has been modelled with Radia [3]	132
183	Vertical magnetic field in a central pole of the epu48gap11Incl ID along the ID axis, $X = Z = 0$	133
184	Vertical magnetic field in a central pole of the epu48gap11Incl ID along the horizontally transverse direction to the ID axis, $S = 0.000$, $Z = 0$	134
185	Horizontal magnetic field in a central pole of the epu48gap11Incl ID along the horizontally transverse direction to the ID axis, $S = 0.000$, $Z = 0$	134
186	The beam orbit of the electron beam through a central period of the epu48gap11Incl ID	135
187	Map of the power distribution of the emitted synchrotron radiation by the epu48gap11Incl ID	136
188	Map of linear polarisation in the fundamental harmonic of the synchrotron radiation emitted by the epu48gap11Incl ID	137
189	Map of 45 degree polarisation in the fundamental harmonic of the synchrotron radiation emitted by the epu48gap11Incl ID	138

190	Map of circular polarisation in the fundamental harmonic of the synchrotron radiation emitted by the epu48gap11Incl ID	139
191	The brilliance at peak energy of the synchrotron radiation emitted by the epu48gap11Incl ID	140
192	The angular spectral flux of the synchrotron radiation emitted by the epu48gap11Incl ID	140
193	The flux of photons in the harmonics of the emitted synchrotron radiation from the epu48gap11Incl ID using a 0.1%BW monochromator	141
194	The flux of photons in the harmonics of the emitted synchrotron radiation from the epu48gap11Incl ID	141
195	The power in the harmonics of the emitted synchrotron radiation from the epu48gap11Incl ID	142
196	The ratio of coherent flux in the harmonics of the emitted synchrotron radiation from the epu48gap11Incl ID	142
197	The coherent flux in the harmonics of the epu48gap11Incl ID using a 0.1%BW Monochromator	143
198	The coherent flux in the harmonics of the epu48gap11Incl ID	143
199	The power of coherent synchrotron radiation in the harmonics of the epu48gap11Incl ID	144
200	Magnetic model of the epu48gap11Vert ID. The ID has been modelled with Radia [3]	146
201	Vertical magnetic field in a central pole of the epu48gap11Vert ID along the ID axis, $X = Z = 0$	146
202	Horizontal magnetic field in a central pole of the epu48gap11Vert ID along the horizontally transverse direction to the ID axis, $S = 24.000, Z = 0$	147
203	The beam orbit of the electron beam through a central period of the epu48gap11Vert ID	148
204	Map of the power distribution of the emitted synchrotron radiation by the epu48gap11Vert ID	149
205	Map of linear polarisation in the fundamental harmonic of the synchrotron radiation emitted by the epu48gap11Vert ID	150
206	Map of 45 degree polarisation in the fundamental harmonic of the synchrotron radiation emitted by the epu48gap11Vert ID	151
207	Map of circular polarisation in the fundamental harmonic of the synchrotron radiation emitted by the epu48gap11Vert ID	152
208	The brilliance at peak energy of the synchrotron radiation emitted by the epu48gap11Vert ID	152
209	The angular spectral flux of the synchrotron radiation emitted by the epu48gap11Vert ID	153
210	The flux of photons in the harmonics of the emitted synchrotron radiation from the epu48gap11Vert ID using a 0.1%BW monochromator	153
211	The flux of photons in the harmonics of the emitted synchrotron radiation from the epu48gap11Vert ID	154
212	The power in the harmonics of the emitted synchrotron radiation from the epu48gap11Vert ID	154
213	The ratio of coherent flux in the harmonics of the emitted synchrotron radiation from the epu48gap11Vert ID	155
214	The coherent flux in the harmonics of the epu48gap11Vert ID using a 0.1%BW Monochromator	155
215	The coherent flux in the harmonics of the epu48gap11Vert ID	156

216	The power of coherent synchrotron radiation in the harmonics of the epu48gap11Vert ID	156
217	Vertical and horizontal magnetic field for the the epu53gap11 ID when operating in the helical mode for different positions for two of the four sub-girders	158
218	Vertical, horizontal, and longitudinal magnetic field for the the epu53gap11 ID when operating in the inclined mode for different positions for two of the four sub-girders	158
219	Magnetic model of the epu53gap11Plan ID. The ID has been modelled with Radia [3]	159
220	Vertical magnetic field in a central pole of the epu53gap11Plan ID along the ID axis, $X = Z = 0$	160
221	Vertical magnetic field in a central pole of the epu53gap11Plan ID along the horizontally transverse direction to the ID axis, $S = 0.000$, $Z = 0$	161
222	The beam orbit of the electron beam through a central period of the epu53gap11Plan ID	161
223	Map of the power distribution of the emitted synchrotron radiation by the epu53gap11Plan ID	162
224	Map of linear polarisation in the fundamental harmonic of the synchrotron radiation emitted by the epu53gap11Plan ID	163
225	Map of 45 degree polarisation in the fundamental harmonic of the synchrotron radiation emitted by the epu53gap11Plan ID	164
226	Map of circular polarisation in the fundamental harmonic of the synchrotron radiation emitted by the epu53gap11Plan ID	165
227	The brilliance at peak energy of the synchrotron radiation emitted by the epu53gap11Plan ID	166
228	The angular spectral flux of the synchrotron radiation emitted by the epu53gap11Plan ID	166
229	The flux of photons in the harmonics of the emitted synchrotron radiation from the epu53gap11Plan ID using a 0.1%BW monochromator	167
230	The flux of photons in the harmonics of the emitted synchrotron radiation from the epu53gap11Plan ID	167
231	The power in the harmonics of the emitted synchrotron radiation from the epu53gap11Plan ID	168
232	The ratio of coherent flux in the harmonics of the emitted synchrotron radiation from the epu53gap11Plan ID	168
233	The coherent flux in the harmonics of the epu53gap11Plan ID using a 0.1%BW Monochromator	169
234	The coherent flux in the harmonics of the epu53gap11Plan ID	169
235	The power of coherent synchrotron radiation in the harmonics of the epu53gap11Plan ID	170
236	Magnetic model of the epu53gap11Heli ID. The ID has been modelled with Radia [3]	172
237	Vertical magnetic field in a central pole of the epu53gap11Heli ID along the ID axis, $X = Z = 0$	172
238	Vertical magnetic field in a central pole of the epu53gap11Heli ID along the horizontally transverse direction to the ID axis, $S = 7.760$, $Z = 0$	173
239	Horizontal magnetic field in a central pole of the epu53gap11Heli ID along the horizontally transverse direction to the ID axis, $S = 21.010$, $Z = 0$	173
240	The beam orbit of the electron beam through a central period of the epu53gap11Heli ID	174

241	Map of the power distribution of the emitted synchrotron radiation by the epu53gap11Heli ID	175
242	Map of linear polarisation in the fundamental harmonic of the synchrotron radiation emitted by the epu53gap11Heli ID	176
243	Map of 45 degree polarisation in the fundamental harmonic of the synchrotron radiation emitted by the epu53gap11Heli ID	177
244	Map of circular polarisation in the fundamental harmonic of the synchrotron radiation emitted by the epu53gap11Heli ID	178
245	The brilliance at peak energy of the synchrotron radiation emitted by the epu53gap11Heli ID	178
246	The angular spectral flux of the synchrotron radiation emitted by the epu53gap11Heli ID	179
247	The flux of photons in the harmonics of the emitted synchrotron radiation from the epu53gap11Heli ID using a 0.1%BW monochromator	179
248	The flux of photons in the harmonics of the emitted synchrotron radiation from the epu53gap11Heli ID	180
249	The power in the harmonics of the emitted synchrotron radiation from the epu53gap11Heli ID	180
250	The ratio of coherent flux in the harmonics of the emitted synchrotron radiation from the epu53gap11Heli ID	181
251	The coherent flux in the harmonics of the epu53gap11Heli ID using a 0.1%BW Monochromator	181
252	The coherent flux in the harmonics of the epu53gap11Heli ID	182
253	The power of coherent synchrotron radiation in the harmonics of the epu53gap11Heli ID	182
254	Magnetic model of the epu53gap11Incl ID. The ID has been modelled with Radia [3]	183
255	Vertical magnetic field in a central pole of the epu53gap11Incl ID along the ID axis, $X = Z = 0$	184
256	Vertical magnetic field in a central pole of the epu53gap11Incl ID along the horizontally transverse direction to the ID axis, $S = 0.000$, $Z = 0$	185
257	Horizontal magnetic field in a central pole of the epu53gap11Incl ID along the horizontally transverse direction to the ID axis, $S = 0.000$, $Z = 0$	185
258	The beam orbit of the electron beam through a central period of the epu53gap11Incl ID	186
259	Map of the power distribution of the emitted synchrotron radiation by the epu53gap11Incl ID	187
260	Map of linear polarisation in the fundamental harmonic of the synchrotron radiation emitted by the epu53gap11Incl ID	188
261	Map of 45 degree polarisation in the fundamental harmonic of the synchrotron radiation emitted by the epu53gap11Incl ID	189
262	Map of circular polarisation in the fundamental harmonic of the synchrotron radiation emitted by the epu53gap11Incl ID	190
263	The brilliance at peak energy of the synchrotron radiation emitted by the epu53gap11Incl ID	191
264	The angular spectral flux of the synchrotron radiation emitted by the epu53gap11Incl ID	191
265	The flux of photons in the harmonics of the emitted synchrotron radiation from the epu53gap11Incl ID using a 0.1%BW monochromator	192
266	The flux of photons in the harmonics of the emitted synchrotron radiation from the epu53gap11Incl ID	192

267	The power in the harmonics of the emitted synchrotron radiation from the epu53gap11Incl ID	193
268	The ratio of coherent flux in the harmonics of the emitted synchrotron radiation from the epu53gap11Incl ID	193
269	The coherent flux in the harmonics of the epu53gap11Incl ID using a 0.1%BW Monochromator	194
270	The coherent flux in the harmonics of the epu53gap11Incl ID	194
271	The power of coherent synchrotron radiation in the harmonics of the epu53gap11Incl ID	195
272	Magnetic model of the epu53gap11Vert ID. The ID has been modelled with Radia [3]	197
273	Vertical magnetic field in a central pole of the epu53gap11Vert ID along the ID axis, $X = Z = 0$	197
274	Horizontal magnetic field in a central pole of the epu53gap11Vert ID along the horizontally transverse direction to the ID axis, $S = 26.500$, $Z = 0$	198
275	The beam orbit of the electron beam through a central period of the epu53gap11Vert ID	199
276	Map of the power distribution of the emitted synchrotron radiation by the epu53gap11Vert ID	200
277	Map of linear polarisation in the fundamental harmonic of the synchrotron radiation emitted by the epu53gap11Vert ID	201
278	Map of 45 degree polarisation in the fundamental harmonic of the synchrotron radiation emitted by the epu53gap11Vert ID	202
279	Map of circular polarisation in the fundamental harmonic of the synchrotron radiation emitted by the epu53gap11Vert ID	203
280	The brilliance at peak energy of the synchrotron radiation emitted by the epu53gap11Vert ID	203
281	The angular spectral flux of the synchrotron radiation emitted by the epu53gap11Vert ID	204
282	The flux of photons in the harmonics of the emitted synchrotron radiation from the epu53gap11Vert ID using a 0.1%BW monochromator	204
283	The flux of photons in the harmonics of the emitted synchrotron radiation from the epu53gap11Vert ID	205
284	The power in the harmonics of the emitted synchrotron radiation from the epu53gap11Vert ID	205
285	The ratio of coherent flux in the harmonics of the emitted synchrotron radiation from the epu53gap11Vert ID	206
286	The coherent flux in the harmonics of the epu53gap11Vert ID using a 0.1%BW Monochromator	206
287	The coherent flux in the harmonics of the epu53gap11Vert ID	207
288	The power of coherent synchrotron radiation in the harmonics of the epu53gap11Vert ID	207
289	Vertical and horizontal magnetic field for the the epu53p6gap11 ID when operating in the helical mode for different positions for two of the four sub-girders . . .	209
290	Vertical, horizontal, and longitudinal magnetic field for the the epu53p6gap11 ID when operating in the inclined mode for different positions for two of the four sub-girders	209
291	Magnetic model of the epu53p6gap11Plan ID. The ID has been modelled with Radia [3]	210
292	Vertical magnetic field in a central pole of the epu53p6gap11Plan ID along the ID axis, $X = Z = 0$	211

293	Vertical magnetic field in a central pole of the epu53p6gap11Plan ID along the horizontally transverse direction to the ID axis, $S = 0.000$, $Z = 0$	212
294	The beam orbit of the electron beam through a central period of the epu53p6gap11Plan ID	212
295	Map of the power distribution of the emitted synchrotron radiation by the epu53p6gap11Plan ID	213
296	Map of linear polarisation in the fundamental harmonic of the synchrotron radiation emitted by the epu53p6gap11Plan ID	214
297	Map of 45 degree polarisation in the fundamental harmonic of the synchrotron radiation emitted by the epu53p6gap11Plan ID	215
298	Map of circular polarisation in the fundamental harmonic of the synchrotron radiation emitted by the epu53p6gap11Plan ID	216
299	The brilliance at peak energy of the synchrotron radiation emitted by the epu53p6gap11Plan ID	217
300	The angular spectral flux of the synchrotron radiation emitted by the epu53p6gap11Plan ID	217
301	The flux of photons in the harmonics of the emitted synchrotron radiation from the epu53p6gap11Plan ID using a 0.1%BW monochromator	218
302	The flux of photons in the harmonics of the emitted synchrotron radiation from the epu53p6gap11Plan ID	218
303	The power in the harmonics of the emitted synchrotron radiation from the epu53p6gap11Plan ID	219
304	The ratio of coherent flux in the harmonics of the emitted synchrotron radiation from the epu53p6gap11Plan ID	219
305	The coherent flux in the harmonics of the epu53p6gap11Plan ID using a 0.1%BW Monochromator	220
306	The coherent flux in the harmonics of the epu53p6gap11Plan ID	220
307	The power of coherent synchrotron radiation in the harmonics of the epu53p6gap11Plan ID	221
308	Magnetic model of the epu53p6gap11Heli ID. The ID has been modelled with Radia [3]	223
309	Vertical magnetic field in a central pole of the epu53p6gap11Heli ID along the ID axis, $X = Z = 0$	223
310	Vertical magnetic field in a central pole of the epu53p6gap11Heli ID along the horizontally transverse direction to the ID axis, $S = 7.835$, $Z = 0$	224
311	Horizontal magnetic field in a central pole of the epu53p6gap11Heli ID along the horizontally transverse direction to the ID axis, $S = 21.235$, $Z = 0$	224
312	The beam orbit of the electron beam through a central period of the epu53p6gap11Heli ID	225
313	Map of the power distribution of the emitted synchrotron radiation by the epu53p6gap11Heli ID	226
314	Map of linear polarisation in the fundamental harmonic of the synchrotron radiation emitted by the epu53p6gap11Heli ID	227
315	Map of 45 degree polarisation in the fundamental harmonic of the synchrotron radiation emitted by the epu53p6gap11Heli ID	228
316	Map of circular polarisation in the fundamental harmonic of the synchrotron radiation emitted by the epu53p6gap11Heli ID	229
317	The brilliance at peak energy of the synchrotron radiation emitted by the epu53p6gap11Heli ID	229
318	The angular spectral flux of the synchrotron radiation emitted by the epu53p6gap11Heli ID	230

319	The flux of photons in the harmonics of the emitted synchrotron radiation from the epu53p6gap11Heli ID using a 0.1%BW monochromator	230
320	The flux of photons in the harmonics of the emitted synchrotron radiation from the epu53p6gap11Heli ID	231
321	The power in the harmonics of the emitted synchrotron radiation from the epu53p6gap11Heli ID	231
322	The ratio of coherent flux in the harmonics of the emitted synchrotron radiation from the epu53p6gap11Heli ID	232
323	The coherent flux in the harmonics of the epu53p6gap11Heli ID using a 0.1%BW Monochromator	232
324	The coherent flux in the harmonics of the epu53p6gap11Heli ID	233
325	The power of coherent synchrotron radiation in the harmonics of the epu53p6gap11Heli ID	233
326	Magnetic model of the epu53p6gap11Incl ID. The ID has been modelled with Radia [3]	234
327	Vertical magnetic field in a central pole of the epu53p6gap11Incl ID along the ID axis, $X = Z = 0$	235
328	Vertical magnetic field in a central pole of the epu53p6gap11Incl ID along the horizontally transverse direction to the ID axis, $S = 0.000, Z = 0$	236
329	Horizontal magnetic field in a central pole of the epu53p6gap11Incl ID along the horizontally transverse direction to the ID axis, $S = 0.000, Z = 0$	236
330	The beam orbit of the electron beam through a central period of the epu53p6gap11Incl ID	237
331	Map of the power distribution of the emitted synchrotron radiation by the epu53p6gap11Incl ID	238
332	Map of linear polarisation in the fundamental harmonic of the synchrotron radiation emitted by the epu53p6gap11Incl ID	239
333	Map of 45 degree polarisation in the fundamental harmonic of the synchrotron radiation emitted by the epu53p6gap11Incl ID	240
334	Map of circular polarisation in the fundamental harmonic of the synchrotron radiation emitted by the epu53p6gap11Incl ID	241
335	The brilliance at peak energy of the synchrotron radiation emitted by the epu53p6gap11Incl ID	242
336	The angular spectral flux of the synchrotron radiation emitted by the epu53p6gap11Incl ID	242
337	The flux of photons in the harmonics of the emitted synchrotron radiation from the epu53p6gap11Incl ID using a 0.1%BW monochromator	243
338	The flux of photons in the harmonics of the emitted synchrotron radiation from the epu53p6gap11Incl ID	243
339	The power in the harmonics of the emitted synchrotron radiation from the epu53p6gap11Incl ID	244
340	The ratio of coherent flux in the harmonics of the emitted synchrotron radiation from the epu53p6gap11Incl ID	244
341	The coherent flux in the harmonics of the epu53p6gap11Incl ID using a 0.1%BW Monochromator	245
342	The coherent flux in the harmonics of the epu53p6gap11Incl ID	245
343	The power of coherent synchrotron radiation in the harmonics of the epu53p6gap11Incl ID	246
344	Magnetic model of the epu53p6gap11Vert ID. The ID has been modelled with Radia [3]	248

345	Vertical magnetic field in a central pole of the epu53p6gap11Vert ID along the ID axis, $X = Z = 0$	248
346	Horizontal magnetic field in a central pole of the epu53p6gap11Vert ID along the horizontally transverse direction to the ID axis, $S = 26.800$, $Z = 0$	249
347	The beam orbit of the electron beam through a central period of the epu53p6gap11Vert ID	250
348	Map of the power distribution of the emitted synchrotron radiation by the epu53p6gap11Vert ID	251
349	Map of linear polarisation in the fundamental harmonic of the synchrotron radiation emitted by the epu53p6gap11Vert ID	252
350	Map of 45 degree polarisation in the fundamental harmonic of the synchrotron radiation emitted by the epu53p6gap11Vert ID	253
351	Map of circular polarisation in the fundamental harmonic of the synchrotron radiation emitted by the epu53p6gap11Vert ID	254
352	The brilliance at peak energy of the synchrotron radiation emitted by the epu53p6gap11Vert ID	254
353	The angular spectral flux of the synchrotron radiation emitted by the epu53p6gap11Vert ID	255
354	The flux of photons in the harmonics of the emitted synchrotron radiation from the epu53p6gap11Vert ID using a 0.1%BW monochromator	255
355	The flux of photons in the harmonics of the emitted synchrotron radiation from the epu53p6gap11Vert ID	256
356	The power in the harmonics of the emitted synchrotron radiation from the epu53p6gap11Vert ID	256
357	The ratio of coherent flux in the harmonics of the emitted synchrotron radiation from the epu53p6gap11Vert ID	257
358	The coherent flux in the harmonics of the epu53p6gap11Vert ID using a 0.1%BW Monochromator	257
359	The coherent flux in the harmonics of the epu53p6gap11Vert ID	258
360	The power of coherent synchrotron radiation in the harmonics of the epu53p6gap11Vert ID	258
361	Vertical and horizontal magnetic field for the the epu58gap11 ID when operating in the helical mode for different positions for two of the four sub-girders	260
362	Vertical, horizontal, and longitudinal magnetic field for the the epu58gap11 ID when operating in the inclined mode for different positions for two of the four sub-girders	260
363	Magnetic model of the epu58gap11Plan ID. The ID has been modelled with Radia [3]	261
364	Vertical magnetic field in a central pole of the epu58gap11Plan ID along the ID axis, $X = Z = 0$	262
365	Vertical magnetic field in a central pole of the epu58gap11Plan ID along the horizontally transverse direction to the ID axis, $S = 0.000$, $Z = 0$	263
366	The beam orbit of the electron beam through a central period of the epu58gap11Plan ID	263
367	Map of the power distribution of the emitted synchrotron radiation by the epu58gap11Plan ID	264
368	Map of linear polarisation in the fundamental harmonic of the synchrotron radiation emitted by the epu58gap11Plan ID	265
369	Map of 45 degree polarisation in the fundamental harmonic of the synchrotron radiation emitted by the epu58gap11Plan ID	266

370	Map of circular polarisation in the fundamental harmonic of the synchrotron radiation emitted by the epu58gap11Plan ID	267
371	The brilliance at peak energy of the synchrotron radiation emitted by the epu58gap11Plan ID	268
372	The angular spectral flux of the synchrotron radiation emitted by the epu58gap11Plan ID	268
373	The flux of photons in the harmonics of the emitted synchrotron radiation from the epu58gap11Plan ID using a 0.1%BW monochromator	269
374	The flux of photons in the harmonics of the emitted synchrotron radiation from the epu58gap11Plan ID	269
375	The power in the harmonics of the emitted synchrotron radiation from the epu58gap11Plan ID	270
376	The ratio of coherent flux in the harmonics of the emitted synchrotron radiation from the epu58gap11Plan ID	270
377	The coherent flux in the harmonics of the epu58gap11Plan ID using a 0.1%BW Monochromator	271
378	The coherent flux in the harmonics of the epu58gap11Plan ID	271
379	The power of coherent synchrotron radiation in the harmonics of the epu58gap11Plan ID	272
380	Magnetic model of the epu58gap11Heli ID. The ID has been modelled with Radia [3]	274
381	Vertical magnetic field in a central pole of the epu58gap11Heli ID along the ID axis, $X = Z = 0$	274
382	Vertical magnetic field in a central pole of the epu58gap11Heli ID along the horizontally transverse direction to the ID axis, $S = 8.384$, $Z = 0$	275
383	Horizontal magnetic field in a central pole of the epu58gap11Heli ID along the horizontally transverse direction to the ID axis, $S = 22.884$, $Z = 0$	275
384	The beam orbit of the electron beam through a central period of the epu58gap11Heli ID	276
385	Map of the power distribution of the emitted synchrotron radiation by the epu58gap11Heli ID	277
386	Map of linear polarisation in the fundamental harmonic of the synchrotron radiation emitted by the epu58gap11Heli ID	278
387	Map of 45 degree polarisation in the fundamental harmonic of the synchrotron radiation emitted by the epu58gap11Heli ID	279
388	Map of circular polarisation in the fundamental harmonic of the synchrotron radiation emitted by the epu58gap11Heli ID	280
389	The brilliance at peak energy of the synchrotron radiation emitted by the epu58gap11Heli ID	280
390	The angular spectral flux of the synchrotron radiation emitted by the epu58gap11Heli ID	281
391	The flux of photons in the harmonics of the emitted synchrotron radiation from the epu58gap11Heli ID using a 0.1%BW monochromator	281
392	The flux of photons in the harmonics of the emitted synchrotron radiation from the epu58gap11Heli ID	282
393	The power in the harmonics of the emitted synchrotron radiation from the epu58gap11Heli ID	282
394	The ratio of coherent flux in the harmonics of the emitted synchrotron radiation from the epu58gap11Heli ID	283
395	The coherent flux in the harmonics of the epu58gap11Heli ID using a 0.1%BW Monochromator	283

396	The coherent flux in the harmonics of the epu58gap11Heli ID	284
397	The power of coherent synchrotron radiation in the harmonics of the epu58gap11Heli ID	284
398	Magnetic model of the epu58gap11Incl ID. The ID has been modelled with Radia [3]	285
399	Vertical magnetic field in a central pole of the epu58gap11Incl ID along the ID axis, $X = Z = 0$	286
400	Vertical magnetic field in a central pole of the epu58gap11Incl ID along the horizontally transverse direction to the ID axis, $S = 0.000$, $Z = 0$	287
401	Horizontal magnetic field in a central pole of the epu58gap11Incl ID along the horizontally transverse direction to the ID axis, $S = 0.000$, $Z = 0$	287
402	The beam orbit of the electron beam through a central period of the epu58gap11Incl ID	288
403	Map of the power distribution of the emitted synchrotron radiation by the epu58gap11Incl ID	289
404	Map of linear polarisation in the fundamental harmonic of the synchrotron radiation emitted by the epu58gap11Incl ID	290
405	Map of 45 degree polarisation in the fundamental harmonic of the synchrotron radiation emitted by the epu58gap11Incl ID	291
406	Map of circular polarisation in the fundamental harmonic of the synchrotron radiation emitted by the epu58gap11Incl ID	292
407	The brilliance at peak energy of the synchrotron radiation emitted by the epu58gap11Incl ID	292
408	The angular spectral flux of the synchrotron radiation emitted by the epu58gap11Incl ID	293
409	The flux of photons in the harmonics of the emitted synchrotron radiation from the epu58gap11Incl ID using a 0.1%BW monochromator	293
410	The flux of photons in the harmonics of the emitted synchrotron radiation from the epu58gap11Incl ID	294
411	The power in the harmonics of the emitted synchrotron radiation from the epu58gap11Incl ID	294
412	The ratio of coherent flux in the harmonics of the emitted synchrotron radiation from the epu58gap11Incl ID	295
413	The coherent flux in the harmonics of the epu58gap11Incl ID using a 0.1%BW Monochromator	295
414	The coherent flux in the harmonics of the epu58gap11Incl ID	296
415	The power of coherent synchrotron radiation in the harmonics of the epu58gap11Incl ID	296
416	Magnetic model of the epu58gap11Vert ID. The ID has been modelled with Radia [3]	298
417	Vertical magnetic field in a central pole of the epu58gap11Vert ID along the ID axis, $X = Z = 0$	298
418	Horizontal magnetic field in a central pole of the epu58gap11Vert ID along the horizontally transverse direction to the ID axis, $S = 29.000$, $Z = 0$	299
419	The beam orbit of the electron beam through a central period of the epu58gap11Vert ID	300
420	Map of the power distribution of the emitted synchrotron radiation by the epu58gap11Vert ID	301
421	Map of linear polarisation in the fundamental harmonic of the synchrotron radiation emitted by the epu58gap11Vert ID	302

422	Map of 45 degree polarisation in the fundamental harmonic of the synchrotron radiation emitted by the epu58gap11Vert ID	303
423	Map of circular polarisation in the fundamental harmonic of the synchrotron radiation emitted by the epu58gap11Vert ID	304
424	The brilliance at peak energy of the synchrotron radiation emitted by the epu58gap11Vert ID	304
425	The angular spectral flux of the synchrotron radiation emitted by the epu58gap11Vert ID	305
426	The flux of photons in the harmonics of the emitted synchrotron radiation from the epu58gap11Vert ID using a 0.1%BW monochromator	305
427	The flux of photons in the harmonics of the emitted synchrotron radiation from the epu58gap11Vert ID	306
428	The power in the harmonics of the emitted synchrotron radiation from the epu58gap11Vert ID	306
429	The ratio of coherent flux in the harmonics of the emitted synchrotron radiation from the epu58gap11Vert ID	307
430	The coherent flux in the harmonics of the epu58gap11Vert ID using a 0.1%BW Monochromator	307
431	The coherent flux in the harmonics of the epu58gap11Vert ID	308
432	The power of coherent synchrotron radiation in the harmonics of the epu58gap11Vert ID	308